FUNCTIONALISATION OF POLYMERS: REACTIVE PROCESSING, STRUCTURE AND PERFORMANCE CHARACTERISTICS

EDDIYANTO

Doctor of Philosophy

Chemical Engineering & Applied Chemistry (CEAC)
School of Engineering and Applied Science
Aston University

October 2007

FUNCTIONALISATION OF POLYMERS: REACTIVE PROCESSING, STRUCTURE AND PERFORMANCE CHARACTERISTICS

EDDIYANTO

Doctor of Philosophy

ASTON UNIVERSITY

10 August 2007

ASTON UNIVERSITY

The Functionalisation of Polymers: Reactive Processing, Structure and Performance Characteristics

EDDIYANTO
Doctor of Philosophy

SUMMARY

The main aim of this work was to study the effect of two comonomers, trimethylolpropane trimethacrylate (TRIS) and divinylbenzene (DVB) on the nature and efficiency of grafting of two different monomers, glycidyl methacrylate (GMA) and maleic anhydride (MA), on polypropylene (PP) and on natural rubber (NR) using reactive processing methods. Four different peroxides benzoyl peroxide (BPO), dicumyl peroxide (DCP), 2,5-dimethyl-2,5-bis-(*tert*-butyl peroxy) hexane (T-101), and 1,1-di(*tert*-butylperoxy)-3,3,5-trimethyl cyclohexane (T-29B90) were examined as free radical initiators. An appropriate methodology was established and chemical composition and reactive processing parameters were examined and optimised. Procedures for purification of the reaction products were developed so that the extent of monomer grafting on the polymers can be characterised accurately, using mainly FTIR technique. The reaction mechanism of the functionalisation was also examined. It was found that in the absence of the coagents DVB and TRIS, the grafting degree of GMA and MA increased with increasing peroxide concentration, but the level of grafting was low and the homopolymerisation of GMA and the crosslinking of NR or chain scission of PP were identified as the main side reactions that competed with the desired grafting reaction in the polymers. At high concentrations of the peroxide T-101 (**>0.02 mr**) cross linking of NR and chain scission of PP became dominant and unacceptable. An attempt to add a reactive coagent, e.g. TRIS during grafting of GMA on natural rubber resulted in excessive crosslinking because of the very high reactivity of this comonomer with the C=C of the rubber. Therefore, the use of any multifunctional and highly reactive coagent such as TRIS, could not be applied in the grafting of GMA onto natural rubber. In the case of PP, however, the use of TRIS and DVB was shown to greatly enhance the grafting degree and reduce the chain scission with very little extent of monomer homopolymerisation taking place. The results showed that the grafting degree was increased with increasing GMA and MA concentrations. It was also found that T-101 was a suitable peroxide to initiate the grafting reaction of these monomers on NR and PP and the optimum temperature for this peroxide was $\geq 160^{\circ}C$. A very preliminary work was also conducted on the use of the functionalised-PP (*f*-PP) in the absence and presence of the two comonomers (*f*-PP-DVB or *f*-PP-TRIS) for the purpose of compatibilising PP-PBT blends through reactive blending. Examination of the morphology of the blends suggested that an effective compatibilisation has been achieved when using *f*-PP-DVB and *f*-PP-TRIS, however more work is required in this area.

Keywords: *coagent, comonomer, compatibilisation, functionalisation, melt blending natural rubber, polypropylene, radical initiator, reactive processing.*

ACKNOWLEDGEMENT

I wish to express my deepest gratitude to my supervisor, Dr. S. Al-Malaika for her guidance, patience, advice, and encouragement in carrying out this research and the preparation of the thesis.

My thanks are also due to Dr. H.H. Sheena, especially for his technical advice and discussion and to Prof. Dr. Basuki Wirjosentono for his encouragement, and to all members of the Polymer Processing and Performance (PPP) Group at Aston University, especially to Wei Kong, Mark Lay, Umar Daraz, and Azhar Ahmad for their friendship and useful discussions.

I would like to thank the Indonesian Government for providing part scholarship and to the Rector of State University of Medan for granting me a study leave.

Finally, I gratefully remember my parents, for their moral support, praying and blessing, and persistent encouragement throughout this work. This thesis would not have been possible without the encouragement, serenity and forbearance of my dear wife Neneng Z. Sundari, and my lovely daughters Humaira, Syafira, and Aisyah.

List of Contents

Chapter 3 Functionalisation of NR with GMA

Chapter 4 Functionalisation of PP with GMA

Chapter 5 Functionalisation of PP with MA, Compatibilisation of PBT/PP with GMA and MA

List of Schemes

List of Tables

List of Figures

Abbreviations and Symbols

AA	: Acrylic acid
ABS	: Acrylonitrile-butadiene-styrene terpolymer
ABS-*g*-GMA	: Glycidyl methacrylate grafted ABS
ABS-*g*-MA	: Maleic anhydride grafted ABS
AIBN	: α, α′-Azoisobutyronitrile
AMA	: allyl methacrylate
AM	: Acrylamide
AN	: Acrylonitrile
ATR	: Attenuated transmittance resonance
BBTCH	: 1,1-di(tert-butylperoxy)-3,3,5-trimethylcyclohexane
BPO	: Benzoyl peroxide
BR	: Polybutadiene rubber
BTB	: Brom thymol blue indicator
BTP	: bis[1-(tert-butylperoxy)-1-methylethyl]benzene
CBS	: N-cyclohexyl-2-benzothiazole sulphamide
CR	: Chlorinated Rubber
CNBR	: Chlorinated NBR
CTC	: Charge transfer complex
DBBA	: 3,5-di-ter-butyl-4hydoxy benzyl acrylate
DBPIPB	: 1,3-Bis (tert-butylperoxy-isopropyl) benzene
DCP	: dicumyl peroxide
DMAEMA	: 2-dimethylamino ethyl methacrylate
DHBP (DTBPH)	: 2,5-Di(t-butyl-peroxy)-2,5-dimethylhexane
DIPB	: 1,3-bis(tert-butylperoxy-isoprpyl) benzene
DIPP	: α, α′-di(*tert*-butylperoxy) diisopropyl benzene
DMAEMA	: dimethylaminoethyl methacrylate
DSC	: Differential scanning calorimetry
DTBH	: 2,5-di (*tert*-butyl peroxy)-2,5-dimethyl hexane
DTBPIB	: α, α′-di(tert-butylperoxy) diisopropylbenzene
DVB	: Divinyl Benzene
DYBP	: di(*tert*-butylperoxy)-2,5-dimethyl hexyne
e	: Polarity of monomer or radical in Q-e Scheme
EAA	: Poly-(ethylene-*co*-acrylic acid)
EAAZn2+	: Poly-(ethylene-*co*-acrylic acid) Zn (Ionomer)
E-EA-GMA	: Ethylene-ethylacrylate glycidyl methacrylate terpolymer
E-GMA	: Ethylacrylate glicidyl methacrylate copolymer
EMA	: Poly-(Ethylene methyl acrylate)
E-MA-GMA	: Poly-(methyl acrylate-*co*-glycidyl methacrylate)
ENR	: Epoxidized Natural Rubber
EP or EPR	: Ethylene propylene copolymer
EPDM	: Ethylene propylene-diene rubber
EPDM-*g*-MA	: EPDM grafted with MA
EPR-*g*-GMA	: Glycidyl methacrylate grafted EPR
EPR-*g*-MA	: Maleic anhydride grafted EPR
EPR-*g*-OXA,	: Oxazoline grafted EPR

EVA	: Poly-(ethylene-*co*-vinyl acetate)
EVA-*g*-MA	: Maleic anhydride grafted EVA
EVA-SH	: Mercapto modified copolymer EVA
EVE	: Ethyl vinyl ether
FTIR	: Fourier Transform Infrared
f	: Initiator efficiency
g-MA	: Grafted MA
g-GMA	: Grafted GMA
GMA	: Glycidyl methacrylate
HCl	: Hydrochloric acid
HDPE	: High density Poly(ethylene)
HDPE-*g*-MA	: Grafted MA onto HDPE
HEMA	: 2-hydroxyethyl methacrylate
HIPS	: High impact polystyrene
HNBR-*g*-OXA	: OXA-grafted onto hydrogenated NBR
HPMA	: Hydroxypropyl methacrylate
I	: Initiator, primary free radical
IA	: Itaconic acid
IPO	: 2-isopropenyl-2-oxazoline
KOH	: Pottasium Hydroxide
k_d	: Rate of decomposition
k_p	: Rate of propagation reaction
k_t	: Rate of termination reaction
LDPE	: Low density polyethylene
LLDPE	: Linear low density polyethylene
LLDPE-*g*-MA	: Maleic anhydride grafted LLDPE
L-101	: 2,5-dimethyl-2,5-(di-*tert*-butyl peroxy) hexane
LPO	: 2,5-di(*t*-butylperoxy)-2,5-dimethyl-3-hexyne
Lupersol 130	: 2,5 dimethyl-2,3-di-(tert-butyl peroxy) hexyne-3
Lupersol 231	: 1,1-di(terbutylperoxy)-3,3,5-trimethyl cyclohexane
M	: Monomer
MA	: Maleic anhydride
MAc	: Methyl acrylate
MAA	: Mathacrylic acid
MAN	: Methacrylonitrile
MBTS	: dibenzothiazole-3-yl disulphide
MMA	: Methyl methacrylate
MMA-MA	: methyl methacrylate-*co*-maleic anhydride copolymer
mhr	: Molar hundreds ratio to monomer
mr	: Molar ratio to monomer
MMA	: Methyl methacrylate
MMA-GMA	: Methyl methacrylate-glycidyl methacrylate copolymer
MMA-GMA-EA	: Methyl methacrylate-glycidyl methacrylate-ethyl acrylate terpolymer
MW	: Molecular weight
NBR	: Poly(acrylonitrile-*co*-butadiene-*co*-acrylic acid)
NBR-*g*-Oxa	: Oxazoline grafted NBR
NMR	: Nuclear magnetic resonance
NR	: Natural rubber

NR-*g*-GMA : GMA grafted to Natural Rubber
NRP : Novel reactive processing
OPS : Oxazoline modified Polystyrene
OXA : Ricinoxazoline maleinate
PA-6 : Polyamide 6
PA-6,6 : Polyamide 6,6
PA1010 : Polyamide 10,10
PBT : Poly(butylene terephthalate)
PBT-*g*-PS : Graft copolymer of PBT and PS
PC : Polycarbonate
PE : Polyethylene
p-GMA : Poly (glycidyl methacrylate)
PE-*g*-GMA : Grafted GMA onto PE
PE-*g*-MA : Grafted MA onto PE
PE-*g*-OXA : Grafted OXA onto PE
PEO : Poly (ethylene oxide)
PET : Poly(ethylene terephthalate)
phr : Part per hundred (weight) ratio to polymer
PMMA : Poly(methyl methacrylate)
PP : Polypropylene
PP-*g*-AA : Grafted Acrylic acid onto PP
PP-Elf : Polypropylen from Elf Atochem company
PP-*g*-GMA : Grafted Glycidyl methacrylate onto PP
PP-*g*-HI : Grafted Isocianate onto PP
PP-ICI : Polypropylene from ICI company
PP-*g*-MA : Grafted Maleic anhydride onto PP
PP-*g*-Oxa : Grafted oxazoline onto PP
PP-*g*-PA : Poly (propylene-grafted-nylon)
PP-*g*-VAr : Vinyl aromatic monomer grafted onto PP
PS : Polystyrene
PS-*g*-GMA : Grafted glycidyl methacrylate onto PS
PS-OH : ω-hydroxypolystyrene
PS-*g*-OXA : Grafted oxazoline onto PS
PS-b-PBT : Poly (styrene-*block*-butylene terephthalate)
PS-b-PET : Poly (styrene-*block*-ethylene terephthalate)
PS-b-PCL : Poly (styrene-*block*-caprolactam)
PS-b-PMMA : Poly (styrene-*block*-methyl methacrylate)
PS-*g*-PE : Poly (styene-*graft*-ethylene)
PSU : Poly sulfone
PSU-*g*-MA : MA-grafted onto PSU
PVC : Poly(vinyl chloride)
Q : Intrinsic reactivity of monomer
$R^{\cdot}$: Alkyl macroradical
r : Monomer reactivity ratio
R_d : Rate of decomposition
SAN : Styrene-acrylonitrile
SAN-*g*-GMA : Grafted GMA onto SAN
SAN-*g*-MA : Grafted MA onto SAN
SBS : Styrene-butylene copolymer

SEBS	: Styrene-block-(ethelene-*co*-butene)-block- styrene triblock copolymer
SEBS-*g*-GMA	: Glycidyl methacrylate grafted SEBS
SEBS-*g*-MA	: Maleic anhydride grafted SEBS
SEBS-*g*-OXA	: Oxazoline grafted SEBS
SEP	: Styrene-b-(ethylene-*co*-propylene) copolymer
SGMA	: Styrene-*co*-glycidyl methacrylate copolymer
SMA	: Poly-(styrene-*co*-maleic anhydryde)
SMMA	: Styrene-methyl methacrylate random copolymer
St	: Styrene
SMR-L	: Standard Malaysian Rubber
T-101	: (2,5-dimethyl-2,5-bis-tertiarybutyl peroxy)hexane, Trigonox 101
Trigonox-B	: di*tert*-butyl peroxy
Trigonox-T	: Tert Butyl cumyl peroxy
T-29B90	: 1,1-di(*tert*-butylperoxy)-3,3,5-trimethylcyclohexane, Trigonox-29B90
TBAEMA	: *tert*-butyaminoethyl methacrylate
TPE	: Thermoplastic elastomer
TPR	: Thermoplastic rubber
TR	: Torque rheometer
TRIS	: Trimethylolpropane trimethacrylate
VA	: Vinyl acetate
VTES	: Vinyl tri-ethyl silane
4VP	: 4-Vinyl pyridine
VTMS	: Vinyl tri-methyl silane

CHAPTER 1
INTRODUCTION

1.1 Background

Recently, a significant amount of research has been devoted to modifying the physical and chemical properties of existing polymers in order to obtain functional and/or engineered materials [1-13]. Although synthesis of new polymers from new monomers to develop new engineering materials is possible, functionalisation and blending of existing polymers with complementary properties has become a more attractive approach [1,14,15]. Consequently, the field of polymer reactive processing and reactive blending has been developing rapidly, in terms of both scientific understanding and commercial utility of the products obtained. The modification of polyolefins with functional monomers, carried out by free radical reactions, is the most readily available method among those developed in recent years. Indeed, free radicals are so reactive that homopolymerisation of the functional monomer cannot be excluded *a priori* and the possibility of obtaining functional groups of different length and structure must be taken into account. The functionalisation of polyolefins has become a commercially viable approach for producing materials with improved properties. Polypropylene (PP) is one of the most industrially relevant of the polyolefins, but because of its non polar nature, it finds limited use in emerging technologies. To overcome these limitations, PP is commonly functionalised with various monomers, including glycidyl methacrylate (GMA) and maleic anhydride (MA). For these free-radical reactions, it is anticipated that the monomer can be grafted without the architecture of the polymer backbone being influenced; however, this seldom occurs. The use of functionalised copolymers to strengthen the interface between immiscible polymer components where strong interaction are lacking, has emerged to be the industrially preferred route in generating useful products from what would otherwise be highly incompatible blends. Generally, compatibility and adhesion can be improved either by adding a third component, a suitable block or graft copolymer that can act as an emulsifying agent localized at the interface between the immiscible phases (compatibiliser), or by blending suitable functionalised polymer(s) capable of enhanced specific interaction and/or chemical reaction [16-19].

The key to achieving high performance properties that would lead to their technical, and ultimately commercial, success relies on improving compatibility and adhesion characteristics of the blend's components. Poly (butylene terephthalate) (PBT) is a conventional semicrystalline engineering polymer having high degree and rate of crystallization, good chemical resistance, thermal stability, and excellent flow properties and possesses good tensile strength, flexural modulus, and dimensional stability, especially in water, and has high resistance to hydrocarbons [20-26]. Polypropylene (PP), on the other hand, has been one of the fastest growing polymers in recent decades because of its intrinsic properties, low cost, and versatility. The hydrophobic nature and lack of polar sites on PP restrict its applications in blends with polar polymers and in composites with inorganic fillers [26-32]. Blends of poly (butylene terephthalate) (PBT) with polypropylene (PP) are extremely promising, not only from a scientific point of view, but also in terms of their possible applications, as it would be interesting to match the good mechanical and barrier properties of PBT with the processability and the impact resistance of polypropylene. Unfortunately, Polypropylene (PP) is neither miscible nor compatible with poly (butylene terephthalate) (PBT) due to a great difference in polarity. In addition, PP does not contain the necessary functional groups to react with PBT. Physical blending of these polymers leads to poor mechanical properties due to their incompatibility. These limitations may be overcome by graft copolymerisation of various functional monomers onto the PP backbone via a free radical mechanism [33-35].

1.2 Free Radical Grafting and Graft Reaction Mechanism

The properties of polyolefins may be extended by chemical modification introducing polarity and/or functionality from the polymer backbone. Free radical grafting of vinyl monomers from polyolefins is one of the oldest and cheapest approaches with the additional attraction of being readily applied in many existing industrial processes. The process of free radical grafting has been exploited over the years for chemically modifying polymers by reactive modifiers either 'on the bench', in the presence of solvents [36-41], or *in situ* without solvents, e.g. in polymer melts [42-52]. A typical grafting system comprises, at least three components (reactant): polymer, reactive monomer (containing unsaturation bond such as vinyl groups) and free radical initiator (often a peroxide) [1,52-54]. **Scheme**

1.1 outlines some of the main reactions normally encountered in grafting of reactive monomer on polymers.

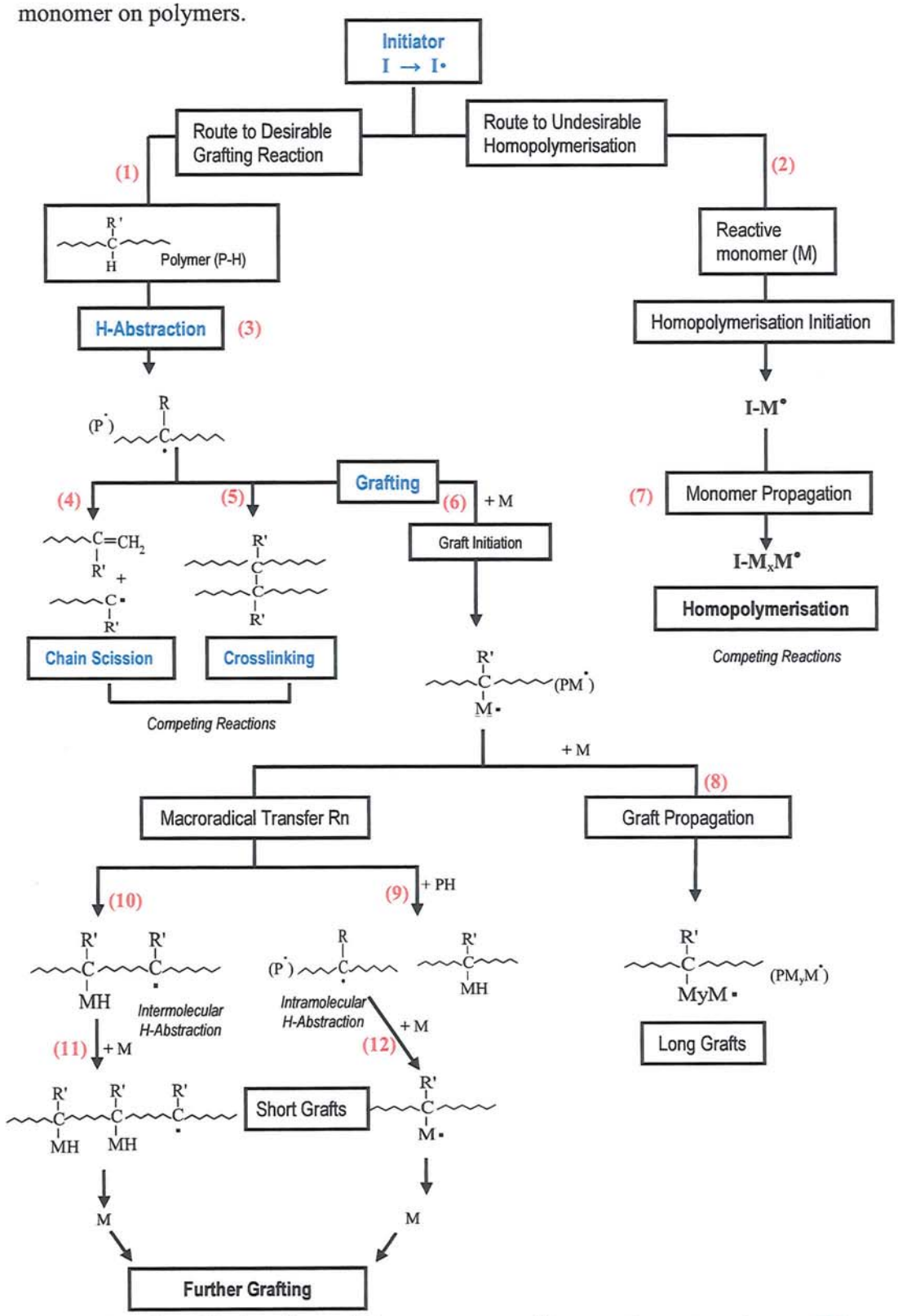

Scheme 1.1 Simplified outlines of the monomer grafting reaction onto polymers [1]

Free radical reaction of a vinyl monomer to a hydrocarbon or polyolefin is typically initiated by alkoxyl radicals (I˙) formed by the decomposition of a peroxide (I) [54-68]. The structures of the radicals formed vary from one peroxide to another but as far as reactivity is concerned, they are well represented by the *tert*-butoxyl radical, $(CH_3)_3CO\cdot$. The *tert*-butoxyl radicals are particularly reactive in abstraction of a hydrogen atom (from C-H bonds in polymer chains) and can undergo additional reactions including β-scission and addition reaction to monomer. The *tert*-butoxyl radical $(CH_3)_3CO\cdot$) thus formed may follow two completely different reaction pathways, with one leading to undesired process of homopolymerisation of the reactive monomers (**Scheme 1.1, Rn-2**) and the other leads to the formation of macroradicals by hydrogen atom abstraction from the polymer which results in the target grafting reaction (**Scheme 1.1, Rn-1**). At low temperature, β-scission of *tert*-butoxyl radicals is slow compared with hydrogen atom abstraction thus very few of the radicals decompose to give methyl radicals. However, at 160°C, 25-50% of *tert*-butoxyl radicals break down to give methyl radicals which are more reactive to addition reactions to the monomer. Reaction of free radicals (I·) with the monomer (M) results in homopolymer initiation forming a monomer radical (I–M·) which propagates to form a homopolymer (**Scheme 1.1, Rn-7**). The grafting of this oligomer or polymer onto the desired polymer backbone rarely occurs because propagating monomer radicals usually have a limited hydrogen atom abstraction capacity unless it is very reactive, such as the vinyl acetate radical. On the other hand, when the primary free radical (I·) undergoes H-abstraction with the polymer (**Rn-1**) a macroradical is then formed which will lead to one of the following three reactions, the probability of which depends on its structure: (1) chain scission (**Scheme 1.1, Rn-4**), (2) crosslinking (**Scheme 1.1, Rn-5**), or/and (3) grafting (**Scheme 1.1, Rn-6** and **Rn-8**). Reaction of the macroradicals with a monomer forms a branched macroradical (PM·) that may continue to react with more monomer molecules forming longer grafts (**Rn-8**). It may, on the other hand, undergo a transfer with a hydrogen atom of the same or another polymer molecule forming a new macroradical (**Scheme 1.1, Rn-10, Rn-11,** and **Rn-12**) resulting in short grafts.

If the **Rn-6** and **Rn-8** determine graft size, the length of the graft depends on the ratio constant, k_6/k_7, and the concentration of monomer in the hydrocarbon or polymer substrate. For large radicals, i.e. in grafting to polyolefins, the grafts are likely to consist of only a few monomers unit. The length of the graft is limited by the alternative intramolecular hydrogen

atom abstraction process (**Rn-9** and **R-10**). The fact that this reaction can be of importance is strongly suggested by spectroscopic analysis results for the grafting of vinyl monomers to model hydrocarbons [1,69]. In the reaction of maleic anhydride (MA) with dodecane, pristane, and squalane (peroxide Lupersol-130, temp. 160°C), it was found [69] that isothermal grafting of maleic anhydride to a hydrocarbon polymer leads to a predominance of single grafts. In homogeneous solution, at the low concentration of maleic anhydride employed, there is a little evidence for oligomeric or polymeric grafts to the model hydrocarbons. Initiator decomposition rates are usually very high at 160-200°C, the kinetic chain length for homopolymerisation is thus much lower and degrees of polymerisation are relatively low. At lower temperatures, however, homopolymer may be the major product. Russel *et al* [70] grafted dimethylaminoethyl methacrylate (DMAEMA) to model hydrocarbons at 130°C and with 0.48 M monomer found that the main product was a homopolymer of molecular weight 10,000. Relatively high molecular weight homopolymer may also be obtained if the monomer is not completely soluble in the hydrocarbon substrate. The homopolymerisation of the monomer, chain scission and cross linking of macro radicals are detrimental to the progress of the target graft reaction. In addition, chain scission and cross linking of the polymer give rise to unacceptable changes in its mechanical properties. It is important, therefore, to reduce or eliminate the entire undesirable and, sometimes, dominant reaction pathways to produce a polymer with highly grafted reactive monomer functions. The final level of grafting of a monomer is therefore, a complex function of the physical nature, chemical structure and reactivity of the individual components in the system and their dependence on reaction and process conditions. The overall outcome will generally depend on the relative reactivities of the initiator towards hydrogen atom abstraction from the polymer and with the monomer, as well as the reactivity of the macroradicals formed toward the monomers.

The success of grafting experiments is usually measured in term of grafting yields, the fraction of the monomer that is grafted onto the polymer *vs.* that which is either unchanged or is consumed in side reaction such as homopolymerisation. A large number of interdependent factors need to be optimised in order to maximise the grafting yield and to minimise side reaction, for example in polyolefins this include:

(a) *Structure of the base polymer* [71-76]

(b) *Structure and concentration of monomer and comonomer* [77-82]

(c) *Structure and concentration of initiator* [83-88]

(d) *Mixing efficiency*; efficient mixing of the monomer and initiator with the polymer. The mixing efficiency will determine the local reactant concentrations and is a function of the screw design, the melt temperature, the pressure, the rheological properties of the polyolefin, and the solubility of the monomer and the initiator in the polyolefin [89,90]

(e) *Temperature*; higher processing temperature would generally favour polyolefin degradation, reduce initiator half-life, modify the rate or specificity of reactions, and influence various solubility and rheological parameters [91]

1.2.1 Polyolefins

Functionalisation of polyolefins has long been a scientific challenge and industrially an important research area, which represents a route to expand polyolefin applications and to produce higher value products. By far, the functionalised polyolefins are the most important class of polymers in commercial applications due to their unique combination of low cost, high activity, and good processability. They are the general choice of material in improving compatibility, adhesion, and paintability of polyolefins. Depending on the nature of the polyolefin used, free radical induced side reactions will widely differ [92-94]. The major side reaction of polyethylene (PE) is branching and crosslinking of the polymer (see **Scheme 1.1, Rn-5**). Unless the grafting reaction is controlled, free-radical induced chain-branching and thermo-mechanical degradation can lead to crosslinking and gel formation, which may, in turn, cause severe problems in the processing of the grafted PE. Branched polyethylenes contain tertiary hydrogen atoms which are three or four times more reactive than secondary hydrogen atom at 160°C [93]. In the case of polypropylene (PP), free radicals generate tertiary radicals that evolve into β-chain scission (**Scheme 1.1, Rn-4**). The molecular weight then decreases, leading to a decrease in the viscosity. Polypropylene shows a surprisingly low reactivity towards *tert*-butoxyl radicals at 45°C [94] though it contains a high proportion of tertiary hydrogen atoms. At high temperatures, the grafting reaction is complicated by the facile breakdown of polypropylene radicals to give products of much lower molecular weight [93,95].

1.2.2 Monomers and macromonomers

A wide range of monomers and macromonomers have been successfully grafted onto polyolefin substrates by free radical chemistry including various monosubstituted (e.g. acrylate esters, vinyl silanes, and styrene) and disubstituted compounds (e.g. glycidyl methacrylates, maleic anhydride, oxazoline, maleate esters, and maleimide derivatives). Macromonomer are poly- or oligomers or other high molecular weight species containing a reactive (susceptible to radical addition) double bond. The inherent reactivity of the macromonomer double bond towards radicals in solution often resembles that of the analogous simple monomers. However, due mainly to steric factors, macromonomer show generally a lesser tendency to undergo homopolymerisation [96-98]. A number of monomer related factors need therefore to be considered in designing experiments. These include: the monomer concentration, the solubility of the monomer, the reactivity of the monomer towards initiator and substrate derived radicals, and the susceptibility of the monomer to homopolymerisation. The inherent susceptibility of a monomer to undergo homopolymerisation under melt processing conditions is an important factor in determining the extent of homopolymer formed as a by-product during polymer modification and the length of the grafted chain. The susceptibility to homopolymerisation depends both on the propagation rate constant (k_p) and the propagation/depropagation equilibrium constant (see **Scheme 1.2**). The ceiling temperature is that temperature at which the rates of depropagation and propagation are equal. The ceiling temperature for MA is reported to be $\leq$ 150°C, that for methacrylate esters is ca. $\leq$ 200°C, while those for acrylate esters and styrene are < 400°C [83,99]. These values suggest that ceiling temperature effects should be important in grafting of MA [56,100] and methacrylate esters [71,101]. With a few common vinyl monomers, there is a further restriction on chain growth. Homopolymerisation may have a low ceiling temperature and depropagation becomes important at temperatures as low as 100°C. The main factor determining the ceiling temperature is the enthalpy of polymerisation [99-102].

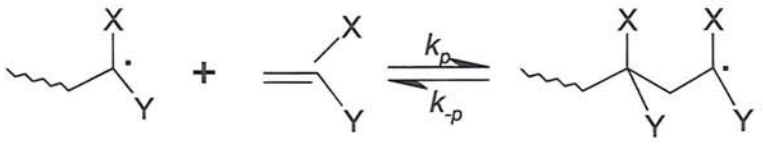

Scheme 1.2

In reactive extrusion, the monomer can be added with the polyolefin (i.e. adsorbed onto the polymer pellets or powder). It can also be added in the molten polyolefin directly, adsorbed on further polymer, or be dissolved in an appropriate solvent. The method of introduction will depend on the solubility of the monomer in the polyolefin melt and stability and volatility of monomer. The monomer acts to trap radicals that would otherwise undergo chain scission or crosslinking. Thus, use of a higher monomer concentration may result in less degradation of the polyolefin substrate. It may also be necessary to select the initiator according to the particular monomer(s). Factors to consider are the partition coefficient of the initiator between the monomer and polyolefin phases and the reactivity of the monomer *vs.* the polyolefin towards the initiator-derived radicals.

1.2.3 Initiator

The initiators most commonly used in grafting (co)polymerisation are alkoxyl or acyl peroxides [83,102] (see **Table 1.1** for the nomenclature of peroxide compounds). Homolysis of the weak peroxide bond leads to the formation of highly reactive alkoxyl radicals **(Scheme 1.3, Rn-1),** which can readily abstract hydrogen atom from the polymer matrix (**Scheme 1.3, Rn-2**), or undergo further decomposition by β-scission giving rise to further 'small' radicals (secondary radicals) and 'small' stable molecules (**Scheme 1.3, Rn-3**) [86,103-105]. It is well established that the reactivity and specificity shown by initiator-derived radicals in abstraction and addition reactions depend strongly on the nature of the radicals and thus on the particular initiator. *Tert*-alkoxyl radicals (e.g. *t*-butoxyl, cumyloxyl radicals) have a propensity for hydrogen atom abstraction and this tendency is enhanced at higher temperatures. Thus, the selection of an initiator which generates alkoxyl radicals might be one way to minimise homopolymerisation as a side reaction. By way of contrast, methyl radicals show a lesser propensity for hydrogen atom abstraction [65,104]. The rate constant for methyl radicals adding (to styrene) is some three orders of magnitude greater than that for abstraction (from 2,2,4-trimethylpentane) [105]. Addition of alkoxyl radicals to the grafting monomer, which would lead to homopolymers as undesired by-products, usually can be neglected, but alkyl radicals formed by decomposition of the primary radicals are known to preferably add to the monomer. The chemical structure, reactivity and concentration of peroxide, as well as its dependence on process variables and reaction conditions, affects the outcome of the grafting reaction. For example, peroxides with weak

polarities are 'soluble' in polymer and will preferentially lead to a recombination of macroradicals rather than grafting. On the contrary, a polar peroxide will preferentially concentrate on the monomer, generating a large number of reactive sites in this monomer, thus leading to homopolymerisation [62,106].

Table 1.1 Nomenclature of peroxide compounds

Generic Names of Compounds	
Alkyl peroxide	RO—OR
Acyl peroxide	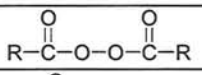
peroxyacid	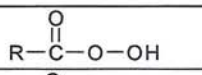
peroxyester	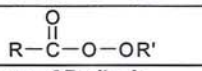
Generic Names of Radicals	
Alkoxyl radical	RO·
Alkyl peroxy radical	ROO·
Acyl radical	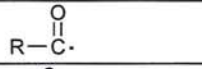
Acyloxyl radical	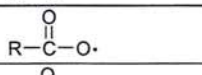
Acyl peroxy radical	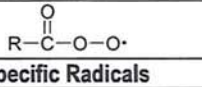
Names of Specific Radicals	
Methyl	CH_3·
Methoxyl	CH_3O·
Acetyl	
Acetoxyl	CH_3-CO_2·
Acetyl peroxy	CH_3-C(O)O_2·
Benzoyloxyl	ϕ-CO_2·
benzoylperoxy	ϕ-C(O)O_2·

So, several factors need to be considered when choosing a peroxide for a grafting reaction [107]:

(1) *The rate of peroxide decomposition*. The initial process of decomposition to generate free radicals is strongly dependent on reaction conditions and process variables.

(2) *The reactivity of generated radicals towards hydrogen atom abstraction from polymer backbones*. The nature and reactivity of radicals formed from further decomposition of the initial alkoxyl radical are also important. *t*-Butoxyl and methyl radicals for example abstract a hydrogen atom efficiently, whereas the more stable ethyl radical

arising from amiloxyl radicals (**Scheme 1.3, Rn-3**, R' = $CH_3\dot{C}H_2$) favours polymerisation over H-abstraction.

(3) *The reactivity of initiating radicals towards the monomer leading to homopolymerisation.* Homopolymerisation of a reactive monomer increases with higher initiator reactivities for polymerisation, resulting in lower levels of free radical grafting.

(4) *Peroxide half-life time ($t_{1/2}$).* This provides a measure of the decomposition rate of the peroxide under specific reaction conditions which include temperature, the physical state of the polymer among other factors.

(5) *The physical state of the peroxide.* The physical state (liquid, solid, absorbed on solid carrier) can be very important for delivery and mixing regimes in addition to its physical characteristics (volatility, solubility), and its odour and toxicity.

Scheme 1.3 Mechanisms for radical generation of peroxide [107]

Rn-1. Homolysis Reaction of a Peroxide

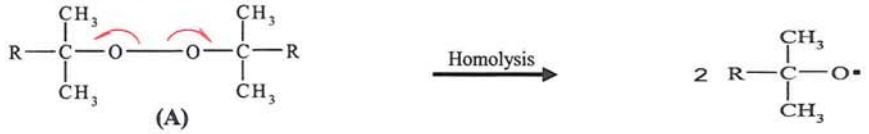

(A)

Rn-2. Hydrogen atom Abstraction of Polymer or Monomer

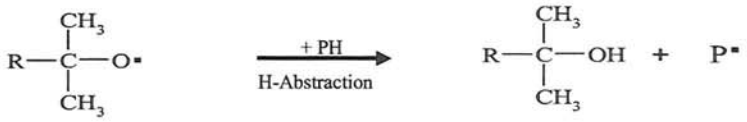

Rn-3. Decomposition by β-Scission of Peroxide Radicals

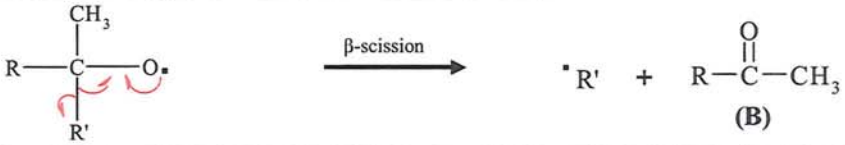

(B)

when R = CH_3	: A = di-t-butyl peroxide	: R' = $\cdot CH_3$	B = acetone
when R = 	: A = dicumyl peroxide	: R' = $\cdot CH_3$	B = acetophenone
when R = CH_3-CH_2	: A = di-t-amyl peroxide	: R' = $\cdot CH_2CH_3$	B = acetone

Other parameters to be considered when selecting an initiator include [83,107]:

(a) *The solubility of the initiator* in the polyolefin melt and its partition coefficient between the various phases in the case of multiphase melts.

(b) *The method of introducing the initiator*. In reactive extrusion, the initiator may be introduced with the polyolefin feedstock through the main hopper, with the monomer, or as a separate feed. It may be added directly, be adsorbed onto the polymer, or be added as a solution in the monomer or a solvent. It may be added all at once or by multipoint addition.

(c) *The extent of cage reaction and the formation of initiator derived by-products*. The cage reaction depends on the nature of the initiator and increases in importance with the viscosity of the medium. The susceptibility of the initiator to induced decomposition and other side reactions.

The initiator half-life should be considered with reference to the concentration of transient radical species generated and with respect to the residence time of reactants in the reaction zone of the reactor. It is desirable that the initiator be converted into radicals wholly within the reaction zone of the extruder. An initiator with a half-life that is too long may not be completely utilised. This is unattractive from an economic vantage point. More important, however, is the negative impact that any residual initiator may have on ultimate product stability. Thus, ideally, the half-life of the initiator should be short compared with the residence time in the extruder. If the residence time corresponds to five half-lives there will be > 97% consumption of the peroxide. A shorter half-life initiator will initially give a higher transient radical concentration for the same concentration of initiator. This may increase the likelihood of crosslinking by radical–radical combination. Another possible consequence is that grafting yields may become limited by the rate of monomer (or macromonomer) diffusion to the site of reaction particularly where the melt is heterogeneous. It follows that, for short half-life initiators, the initiator concentration and the method of introducing the initiator will become more important and there may be difficulties in introducing such species into the polymer melt.

The understanding of free radical chemistry comes mainly from studies carried out in dilute solutions at modest temperatures (<100°C). Few studies [102,108-110] have probed free radical reactions under the conditions likely to be encountered in melt phase polymer reactions. Usually these conditions involve:

(a) *Relatively high temperatures >150°C*. The specificity of radical reactions will usually, though not always, decrease with increasing temperature. Higher ratios of

hydrogen atom abstraction and addition reactions and the transformation of primary radicals into secondary radicals are generally favoured by higher temperatures.

(b) *Relatively high pressures.* High pressures will tend to disfavour processes involving bond scission.

(c) *Media of relatively high viscosity.* Diffusion controlled processes, in particular radical–radical reactions, will proceed at a slower rate in the melt than in solution. As a consequence, rates of initiator decomposition may be slowed (due to cage return) and initiator efficiencies may be lowered [71,110].

1.3 Functionalisation of Polymers via Reactive Processing

Polyolefin chemical reactivity can be modified without substantial loss of physical properties by grafting various functionalised monomers on the polyolefin matrix **[1]**. A wide range of vinyl monomers have been successfully grafted onto a number of polymer substrates by free radical chemistry. The most widely used monomers are glycidyl methacrylate (GMA), maleic anhydride (MA) and Oxazoline due to the high reactivity of their functional groups. Polyolefins such as polypropylene (PP) and polyethylene (PE) have versatile properties and are low cost polymers with growing commercial applications, however they lack chemical functionality. Introduction of these functional groups onto the chains of these polymers can significantly improve their compatibility with other polymers, their paintability, and adhesion to metal or glass [6,7,85,111]. Grafting yields obtained with PP are usually low (< 20%) and are dependent on the particular monomer [1,3,112,113]. Liu *et al.* [112] have carried out a comparative study of the grafting of various functional methacrylate esters to polypropylene and explored the functionalised-PP as reactive compatibiliser for PP-NBR blends. The experiments were performed in a batch mixer at 180°C with 7 wt. % monomer and 0.05 wt. % DHBP (Trigonox-101) as an initiator. Grafting levels (wt. %) obtained under these conditions were as follows: HPMA (1), TBAEMA (1), GMA (0.8), HEMA (0.4), DMAEMA (0.3), IPO (0.2). The effectiveness of these modified PPs was related to the ease of in situ graft formation. The GMA and IPO modified PP were found to be substantially more effective at improving blend performance than any of the other materials. This was attributed to the reactivity of the epoxy (GMA) and oxazoline (IPO) groups towards the carboxylic acid functionality in the NBR [113].

The development of new methods for producing chain end-functionalised polymers should make graft formation by inter-chain polymer reactions a more attractive proposition. Guyot [114] has described the synthesis of a variety of end-functional PP (anhydride, carboxylic acid, alcohol, thiol, silane, and borane) from a terminally unsaturated PP synthesised by use of a metallocene catalyst. An alternate means of synthesising MA terminated PP from terminally unsaturated PP via Borane chemistry has recently been described by Lu and Chung *et al.* [115-117]. The MA terminated PP has been used as an in situ compatibiliser for PP/nylon blends by melt mixing and the formation of block copolymers was proposed [116,117]. However, the use of free radical polymerisation in the synthesis of end-functional polymers has traditionally been spurned because of difficulties in achieving the desired degree of functionality.

1.3.1 Grafting Glycidyl Methacrylate (GMA) onto Polymers

In recent years, glycidyl methacrylate (GMA) gained large attention for functionalisation of polyolefins. GMA is a bifunctional monomer containing an unsaturated group capable of free-radical grafting and a highly electrophilic epoxide moiety (see **Figure 1.1)** which can react with different nucleophilic functions such as carboxylic (—COOH), hydroxide (—OH), and amine groups (—NH_2). The melt phase grafting of GMA onto polyolefins has been investigated by several researchers in polypropylene (PP) [118-125], polyethylene (PE) [125,126], ethylene-propylene copolymer (EPR) [127-129], ethylene propylene diene terpolymer (EPDM) [130], and styrene-butadiene-styrene tri-block copolymer (SBS) [131]. The advantages in the use of GMA functionalisation have been related to the faster grafting reaction onto polyolefins when compared to that of maleic anhydride (MA) or acrylic acid (AA) [1,112] and moreover, the bulky structure of GMA is believed to reduce crosslinking and chain scission in the polymer backbone [132].

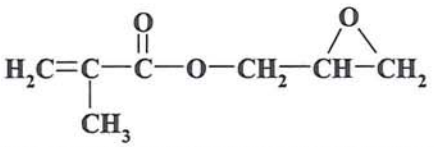

Figure 1.1 Chemical structure of glycidyl methacrylate (GMA)

Galluci *et al.* [125] worked on the radical melt grafting of GMA onto low-density polyethylene (LDPE), high-density polyethylene (HDPE), ethylene-propylene copolymer

(EPR) and polypropylene (PP) using dicumyl peroxide (DCP) and benzoyl peroxide (BPO) as initiator. The grafting was carried out in the batch mixer at 175 °C, 40 rpm, 5 minutes. When GMA and DCP were introduced into the molten PP or LDPE, the GMA did not graft onto PP, whereas the grafting yield of GMA onto LDPE (determined by FTIR) was only 0.2-7.0 wt %. The authors show that the grafting yield of GMA onto high-density polyethylene (HDPE) is inferior to the grafting yield of GMA onto LDPE. Grafting to EPR and EPDM was possible, but undergoes considerable cross-linking during the grafting reaction. However, Baker *et al.* [112,113] successfully grafted GMA onto PP using peroxide initiators and used the grafted PP in the reactive compatibilisation of PP blends with acrylonitrile-butadiene-acrylic acid rubber (NBR). Grafting was carried out at 180 °C in a batch mixer. The monomer, the initiator, and the polymer were introduced simultaneously into the batch mixer. After reaction, the samples were purified and characterized by FTIR and nuclear magnetic resonance (NMR) spectroscopy. Grafting yield of GMA onto PP did not exceed 2 wt %. The differences observed between the results of Galluci *et al.* [125] and Baker *et al.* [112,113] on the grafting of GMA onto PP probability come from the type and the concentration of the peroxides used and the method of introducing these products into the batch mixer. One of the most important challenges of melt free radical grafting is to obtain a sufficient amount of grafting while retaining the mechanical properties and thus molecular weight of the virgin polymer. PP macroradicals are highly reactive species that react with the functional monomer present in the melt system. However, the PP macroradicals can also undergo chain-scission (β-scission) because of the presence of methyl side-groups. Hence, there exists a competition between the grafting of monomer molecules onto PP and β-scission of the polymer. This means that effectively utilizing macroradicals for the sake of grafting is the only way to minimize homopolymerisation and to reduce side reactions responsible for changes in molecular architecture and corresponding physical and mechanical properties of the original polymer substrates. Pesetskii *et al.* [59,62] studied the problem of how the peroxide type influences the kinetics of grafting monomers onto polyethylene [59] and polypropylene [62]. The nature of the peroxide initiator determines the grafting efficiency and the degree of chain degradation, estimated from changes in the MFI of the polymer. The solubility of peroxide in the polymer and its thermal stability are the most important factors that determine the course of the GMA grafting reaction and macromolecular breakdown. To reach a high yield of a grafted product, peroxides are recommended to have thermodynamic affinity to PP and

a temperature range for thermal decomposition that coincides with the thermal regime of reactive extrusion. It is suggested that functionalisation of GMA onto PP that results in the desired grafting degree and with little degradation of PP, could be obtained by the use of mixed initiators. Huang *et. al.* [118], reported that a novel method was developed to obtain a high grafting degree with little degradation of PP using a mixture of benzoyl peroxide (BPO) or 2,5-di(*tert*-butylperoxy)-2,5-dimethyl-3-hexyne (LPO) with acrylamide (AM) as the initiating agent. It was also shown that the grafting degree increased rapidly with increasing AM concentration and reached high level of 4.7 % at an AM concentration of 0.5 wt % when 5 % GMA was added initially. Unfortunately, increasing peroxide concentration is accompanied by an increase in the rate of side-reactions resulting in molecular weight changes. The GMA grafting level can also be enhanced by increasing the initial GMA concentration, although some authors have also reported a plateau value in the dependency of the grafting level of the initial GMA content. A higher initial GMA concentration increases the number of GMA molecules available per free radical. This favours both the grafting and the homopolymerisation reactions, the latter is an undesirable side reaction. When the total number of available radical sites remains about the same for a given initiator concentration, increasing GMA monomer concentration shifts the reaction balance towards more extensive grafting. Although higher GMA monomer concentration does not eliminate the *β-scission* reaction, it does reduce the effect of the degradation of PP molecules [118].

Hu and Lambla *et al.* [119,120] work has shown that the GMA grafting level is affected primarily by the residence time in which free radicals are not depleted. There was no grafting observed after consumption of the initiator (as estimated by its half-life). This means that the use of long mixing zones in conjunction with short half-life initiators has no beneficial effect and, moreover, may lead to shear induced degradation. For short half-life initiators, the initiator concentration and the method of introducing the initiator will become more important and there may be difficulties in introducing such species into the polymer melt. However, recent work [132,134,135] suggests that the use of short half-life initiators may offer both higher grafting yields and a fewer side reactions (e.g. lower extent of GMA homopolymerisation). **Scheme 1.4** shows some reactions involved in the free radical grafting system of PP with GMA. A free radical grafting process starts with the formation of macroradicals along the polymer chains by hydrogen atom abstraction (**Scheme 1.4, Rn-**

1). These macroradicals may subsequently follow two competing reaction pathways. They can either initiate the grafting of the monomer (which is desirable) or undergo branching, crosslinking, chain scission (undesirable) (**Scheme 1.4, Rn-2**).

Scheme1.4 Grafting and polymerisation of GMA onto PP [1,119,120].

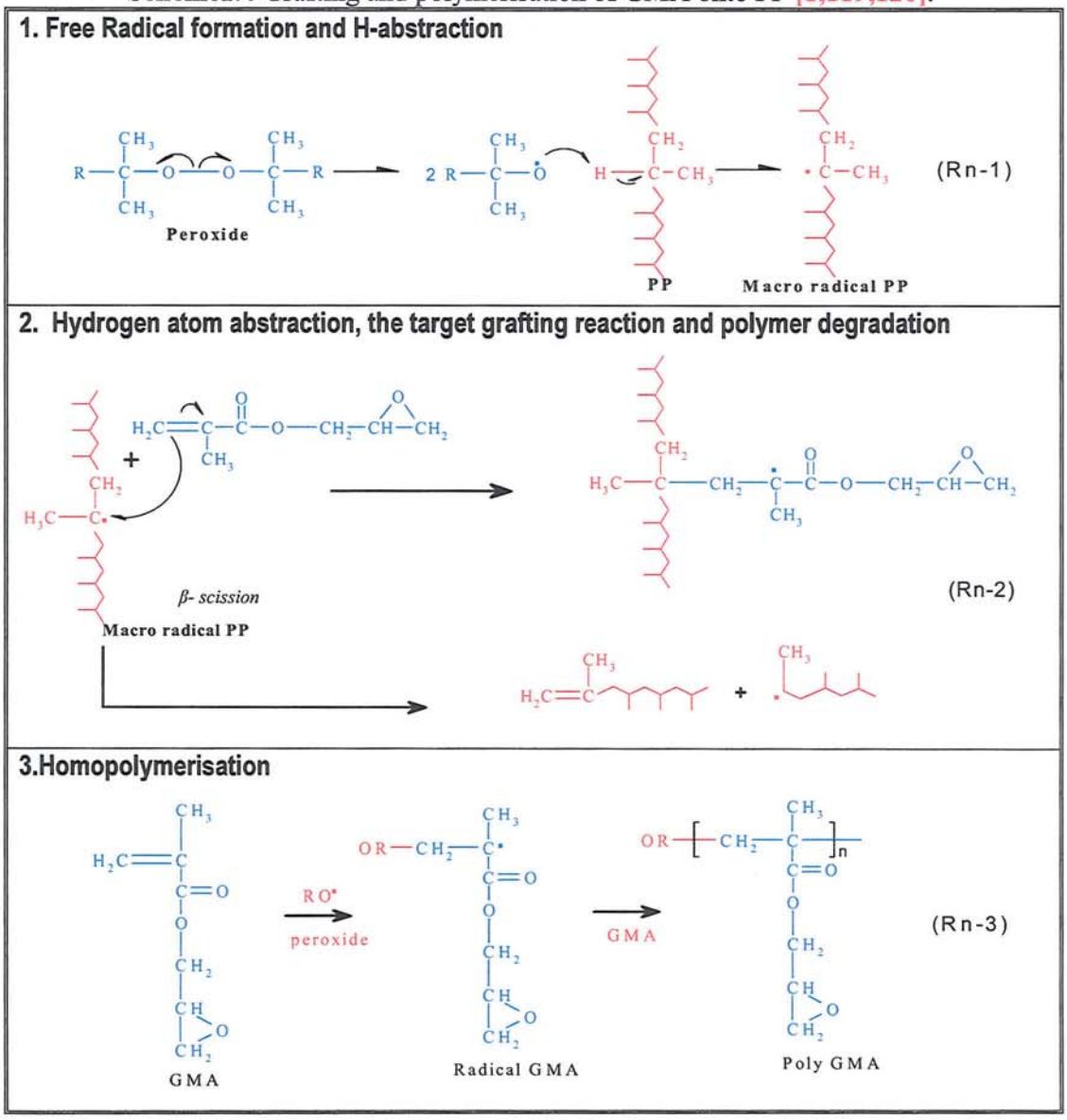

In order to enhance the free-radical grafting efficiency of GMA on the polymer and minimise side reactions, the grafting process was carried out in the presence of comonomers (coagents). This strategy involves choosing a monomer combination such that the comonomer is both effective in trapping the radicals formed on the polyolefin backbone and such that the propagating radical formed is highly reactive towards the desired

monomer. Various electron-rich comonomers, in particular styrene, have been shown to be effective as coagents for improving the grafting yield of functional monomers such as glycidyl methacrylate (which the more electron-deficient) and in their unwanted (e.g. homopolymerisation) side reactions [123,126,128]. Hu and Cartier studied the reaction of grafting GMA onto PP [123], PE [126] and EPR [128] using both a batch mixer and a co-rotating twin screw extruder in the presence of styrene as a comonomer. Five types of peroxides di(*tert*-butylperoxy)-2,5-dimethyl hexyne (DYBP), 2,5-di (*tert*-butyl peroxy)-2,5-dimethyl hexane (DTBH), α,α′-di(*tert*-butylperoxy) di-isopropyl benzene (DIPP), dicumyl peroxide (DCP), and di-benzoyl peroxide (BPO) were used as radical initiators. When GMA alone was grafted onto PP in the mixer, the grafting yield was reported to be a mere 0.4 phr with respect to 8 phr GMA initially introduced in the presence of 0.2 phr DHBP at 180°C. When the peroxide concentration was raised to 0.5 phr, there was not much increase in the GMA grafting yields. However, when the comonomer, styrene, was added to the GMA/PP system, the GMA grafting yield was increased by a factor more than three and the PP molecular weight was not reduced significantly. Similarly, the addition of styrene to an EPR/GMA/peroxide system increases not only GMA grafting level but also its grafting rate [128]. To reach a given GMA grafting level, the time required for the EPR/GMA/peroxide system in the presence of styrene is only one-tenth of what it would take without styrene. The significant reduction in reaction time as a result of adding styrene is crucial for a successful free radical grafting of GMA on EPR in a corotating twin screw extruder. In this way, instead of grafting GMA directly onto PP chains, the comonomer (styrene), serves as a mediator to bridge the gap between the PP macroradicals and GMA monomer. Baker *et al.* [132,135] studied the melt grafting of GMA onto PP with the comonomer styrene in a Banbury-like batch mixer (Haake Rheomix 600, 50ml, temp. 180°C, peroxide Lupersol-130 and Lupersol-231). They suggested that the GMA grafting level and molecular weight of the functionalised PP can be controlled by carefully manipulating various reaction factors such as monomer concentration, initiator concentration, and reaction temperature. The addition of a second monomer styrene in the grafting process helped to increase GMA grafting further and reduced chain scission. The GMA modified PP copolymer was found to be able to reactively compatibilise PP/acrylonitrile-co-butadiene-co-acrylic acid rubber (NBR) blends. Up to an eight-fold increase in the impact energy of the PP/NBR blend was obtained [135]. The higher grafting yields obtained with the comonomer may be associated with:

(a) *Longer chain grafts.* Rates of copolymerisation of electron donor-electron acceptor pairs (styrene/GMA) are substantially greater than that for homopolymerisation GMA.

(b) *More grafting sites.* More efficient trapping of radical sites on the polymer backbone should lead to a greater number of grafts.

However, addition of styrene as the comonomer did not enhance the grafting yield of ricinoloxazoline maleinate (OXA), a maleate ester, but markedly reduced the PP degradation [1]. Also, little homo and/or copolymers of OXA and/or styrene were found in the grafting system. It was found that OXA and styrene did not copolymerise easily [136,137]. **Scheme 1.5** shows the reactions involved in the free radical grafting system of PP with GMA in the presence of styrene.

Scheme 1.5 The mechanism of melt free radical grafting GMA onto PP in the presence of styrene as coagent [123].

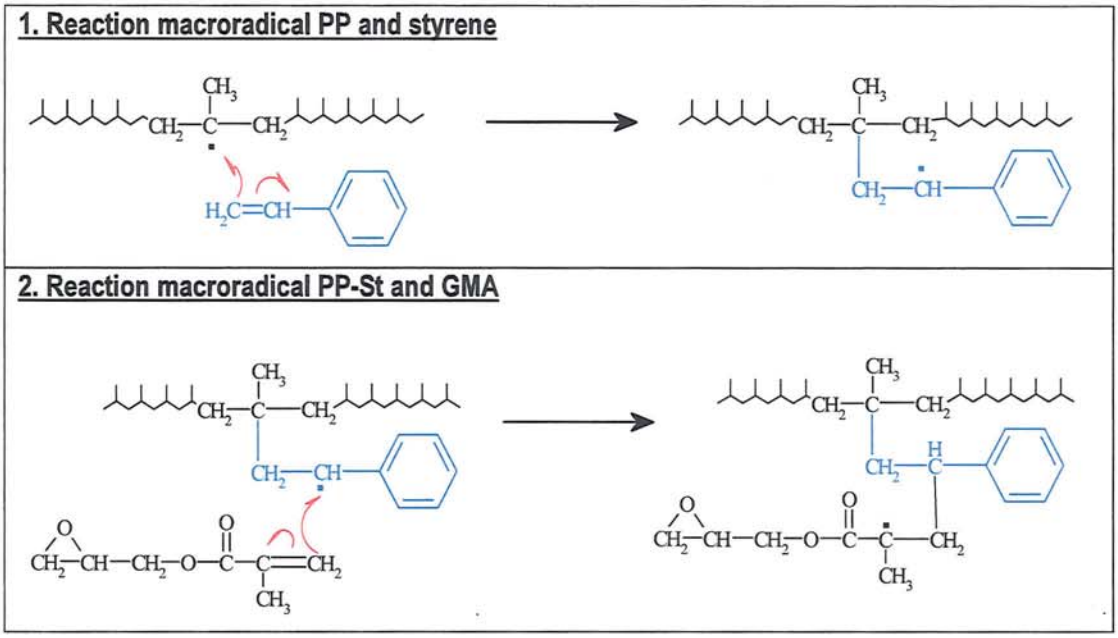

Al-Malaika *et al.* [96-98] have described the use of trifunctional monomers, in particular the triacrylate monomer TRIS **(Figure 1.2),** as a coagent for improving the grafting yields of various monomers on PP (referred to as novel reactive processing, NRP). This polyfunctional monomer (TRIS) in fact acts as a crosslinking agent [138,139]. However, the intermediate crosslinked material undergoes degradation by chain scission under the

processing conditions to ultimately yield a gel-free, xylene-soluble, product. For example, the antioxidant 3,5-di-*tert*-butyl-4-hydroxy benzyl acrylate (DBBA) was shown to react with the trifunctional coagent trimethylol propane triacrylate (TRIS) in the presence of a small concentration of free radical initiator Trigonox-101 in PP melt during processing to give very highly grafted DBBA [97].

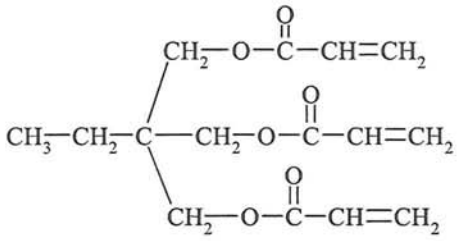

Figure 1.2 Chemical structures of trimethylol propane triacrylate (TRIS)

This method was shown to be generally applicable to the grafting of other monomers onto polymers, were functionalised with GMA during melt processing using TRIS as coagent. The success of this method, in which the coagent acts as a reactive linker between the modifier and the polymer, relies on achieving a delicate balance between the molar ratios of the reagents (agent, coagent, initiator) and the process variables (e.g., temperature, residence time). It was shown, for example, that the use of the trifunctional coagent TRIS with different reactive modifiers, i.e. antioxidants [96,97], glycidyl methacrylate (GMA) [129] and maleic anhydride (MA) [140], gave rise to a dramatic increase in the level of grafting of these modifiers on polymers. It was also demonstrated that, for example, in the case of reactive antioxidants, the antioxidant grafts on the polymer are indeed copolymers of the antioxidant and the coagent which are grafted on the polymer via one, or more, of the reactive sites of the coagent [96-98]. It was further demonstrated [129,134] that the microstructure of the functionalized EPR affects the morphology of the blends. For example, reactive blends containing rubber functionalized with GMA in the presence of the comonomer TRIS, which had higher GMA grafting level and no homopolymerised GMA, gave rise to finer dispersion of the rubber phase indicating higher extent of compatibilisation compared to similar blends but with the rubber functionalized in the absence of TRIS. **Table 1.2** lists some of the studies of functionalisation of polymers with GMA.

Table 1.2 Functionalisation of Polymers with GMA

POLYMER	REACTOR (CONDITION)	[GMA]i (wt %)	Type of Peroxide	[Peroxide]	g-GMA (%)	Ref.
Polypropylene (PP)						
PP	Haake Rheocord 90 (180°C, 100 rpm, 6 min)	5	AM	0.35 mhr	3.4	[118]
			BPO	0.35 mhr	1.5	
			LPO	0.35 mhr	0.9	
			AM +BPO	0.35 mhr	2.8	
PP	Haake Rheocord Mixer 180°C, 64 rpm, 15 min)	6	DHBP	0.2 phr	0.4	[119] [120]
		6 + St 1.5 mr	DHBP	0.2 phr	1.5	[123]
PP	Haake Rheomix 600 (120°C, 60 rpm, 15 min)	10	BPO	1 phr	3.6	[122]
PP	Haake Rheomix 600 (180°C, 90 rpm, 6 min)	11	L 130	1 phr	2	[132]
			L 231	1 phr	3.6	
		13 + 6.5 S	L 130	0.7 phr	3.8	[135]
Polyethylene (PE)						
LDPE	Haake mixer (120-175°C, 40rpm, 5 min)	10	DCP	0.02 mr to GMA	2.38	[125]
		5	BPO	0.05 mr to GMA	1.62	
HDPE	Batch mixer (Rheocord Haake) (180°C)	6	DHBP	0.4 phr	1.2	[126]
		6 + St 1 mr	DHBP	0.4 phr	3.8	
HDPE	Brabender internal mixer (175°C, 50 rpm, 5 min)	10	DCP	0.16 phr	2	[141]
		10 + St 1.2 mr	DCP	0.16 phr	3	
HDPE	Haake Rheocord mixer (190°C, 64 rpm, 10 min)	6	Trigonox T	0.3 %	0.8	[142]
		6 + St 3 mr	Trigonox B	0.3 %	4.2	
LDPE	Internal mixer (175°C, 50 rpm, 5min)	5.6	BTP	0.8 %	1.8	[143]
		5.6 + St 1 mr	BTP	0.8 %	2.2	
LLDPE	Twin screw extruder	3	L 231	0.4 % to GMA	1.5	[144]
Ethylene Propylene Rubber (EPR)						
EPR	Brabender like mixer (190°C, 32 rpm, 6 min)	6	DCP	0.2 %	0.77	[127]
EPR	Internal mixer (190 °C, 65 rpm)	10	T-101	0.05 mr	1.2	[129]
		10 + TRIS	T-101	0.05 mr	3.8	
EPR	Rheocord Haake mixer & Twin screw extruder (165°C, 30 min)	3	DCP	0.3 phr	1	[128]
		3 + St 1 mr	DCP	0.3 phr	2.4	
		3	DTBPIB	0.3 phr	0.8	
EPDM and SBS						
EPDM	Internal mixer (180oC, 65 rpm, 10 min)	10	T-101	1 phr	1.7	[130]
		10 + TRIS 2.5 phr	T-101	0.002 phr	3.6	
SBS	Haake Rheomix 600 (170°C, 40 rpm, 10 min)	5	DCP	0.1 phr	0.87	[131]

NOTES:
[GMA]i = GMA concentration initially added ; **St** = Styrene ; **mr** = molar ratio (mol/mol) to GMA; **phr** = part per hundreds (weight) ratio to polymer; **mhr** = molar hundreds ratio to monomer; **DCP**= Dicumyl peroxide; **BPO** = Benzoyl peroxide; **Trigonox T** = *tert*-Butyl cumyl peroxyde; **Trigonox-B** = di*tert*-butyl peroxy; **L-130** = 2,5 dimethyl-2,3-di-(tert-butyl peroxy) hexyne-3; **L-231** = 1,1-di(terbutylperoxy)-3,3,5-trimethyl cyclohexane; **BTP** = bis[1-(*tert*-butylperoxy)-1-methylethyl]benzene; **DHBP** = 2,5-bis(*tert*-butylperoxy)-2,5-dimethylhexane; **LPO** = 2,5-di(*t*-butylperoxy)-2,5-dimethyl-3-hexyne; **AM** = acrylamide; **T-101** = 2,5-dimethyl-2,5-bis(*t*-butylperoxy) hexane ; **DTBPIB** = α,α'-di(*t*-butyl-peroxy)-1,3-diisopropylbenzene; **TRIS** = trimethylol propane triacrylate

1.3.2 Grafting Maleic Anhydride (MA) onto Polymers

Maleation is one of the most widely used methods for the functionalisation of polymers, especially in reactive processing [145]. The free radical-induced grafting of MA onto polyolefin substrates is one of the most studied reactions of polyolefin modification processes. The process has been carried out in the melt phase in various forms of extruders and batch mixers (PE [146-148], HDPE [149] LDPE [150,151], LLDPE [152], EP [153,154], PP [155-157]) and there are numerous patents covering the process. It has also been carried out successfully in solution [158] and in the solid state [159-161]. Maleic anhydride has also been successfully grafted onto other polymers including ethylene vinyl acetate (EVA) [162,163], ethylene propylene diene terpolymer (EPDM) [164], acrylonitrile–butadiene–styrene terpolymer (ABS) [165], styrene–butadiene–styrene triblock copolymer (SBS) [166]. In addition, MA is also known to add readily to natural rubber (NR) or poly-isoprene at elevated temperature or in the presence of free radical initiator in solution and in the solid state [167-169]. The Maleation takes advantage of the dual-functionality of MA the 'ene' or radically active double bond and the nucleophilically reactive anhydride or ester group (see **Figure 1.3**) [170].

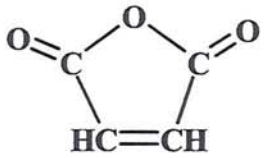

Figure 1.3 Chemical structure of maleic anhydride (MA)

Similar with GMA, the grafting reactions of maleic anhydride onto PP, in the melt, show that these reactions are accompanied by undesirable side reactions (chain scissions in polypropylene). Generally, a limited degree of grafting and severe degradation of PP during the melt grafting of MA onto PP are caused by the low reactivity of MA towards PP macroradicals and its low solubility in the PP melt [1]. The low free-radical reactivity of MA is inherent due to its structural symmetry and deficiency of electron density around the double bond. The materials have a range of applications including their elaboration into graft copolymers either directly or in situ during the preparation of blends [171-173]. Maleic anhydride grafting onto polypropylene (PP), for example, has been carried out with the aim of achieving compatibility between polar and non polar polymers, coupling between polypropylene and inorganic fillers [174-176], and adhesion to metals [6,7].

There are some controversies in the literature surrounding the structure of MA functionalised polyolefins both with respect to the nature of the grafted units and the distribution of the graft sites. In earlier studies using a solution and molten grafting process, Gaylord *et. al.* [150-153,155] proposed that the graft reaction involved mainly the appending of MA to tertiary carbons along the PP backbone suggesting that MA might be appended to the PP backbone as a single ring or as short branches that were attributed to homopolymerisation of MA. Moreover, Roover *et. al.* [95,177,178] showed by detailed FTIR analysis of PP-*g*-MA and poly-MA that short oligomers are grafted. They concluded that β-scission occurred before grafting and led to the grafting of MA at the end of PP chains. Size-exclusion chromatography performed on unbound species also showed the presence of some MA oligomers [177]. However, Heinen *et. al.* [93,179] and Zang *et. al.* [180] have pointed out that according to the ceiling temperature, there is no possibility for the homopolymerisation of MA to occur under the melt grafting process conditions (190°C). They used ^{13}C enriched MA to enable detailed ^{13}C-NMR analysis structure of polyolefins grafted with MA in a melt and a solution process. Under these conditions, they showed that only single-unit grafts were found on PP and homopolymerisation of MA does not take place under the conditions used in solution and in a reactive extrusion process.

Martinez *et. al.* [49,181] carried out functionalisation of MA onto PP both in solution (xylene) and in a melt process (internal mixer) using dicumyl peroxide (DCP) as initiator. It was found that the grafting yield of MA in solution process was very low. Nevertheless, the grafting on atactic polypropylene (a-PP) was found to be three times higher than that on isotactic polypropylene (i-PP) [181]. Many studies revealed that a major problem for melt free-radical grafting MA onto PP is the more serious competition between the desired grafting reaction and the undesired degradation of the polymer by β-chain scission. Finding the optimum conditions of the grafting process is a very complicated investigation, due to the great number of variables involved, among which are: type and concentration of peroxide, maleic anhydride concentration, reaction time, reaction temperature, rotor speed, addition sequence of the reagents, and presence or not of stabilizers. Bettini *et al.* [89,182,183] studied the grafting of MA onto PP in a batch mixer (Haake Torque Rheometer) in the presence of 2,5-dimethyl-2,5-di(*tert*-butylperoxy) hexane (Trigonox-101). The modified polypropylene was characterized by FTIR spectroscopy, melt-flow index measurements, size-exclusion chromatography, differential scanning calorimetry, and

nuclear magnetic resonance. They concluded that grafting of MA is always associated with molecular weight decrease. When 2 phr MA and 0.1 phr Trigonox-101 were added, only 0.5 phr (i.e. 25 %) of the total MA was grafted, and the PP thus modified was highly degraded with MFI greater than 140 g per 10 min (230°C, 2.16 kg), i.e 70 times higher than the virgin PP [182]. They also concluded that the grafted-PP with maleic anhydride presented higher crystallinity percentages and lower melt temperatures than the unmodified PP. The rise in the percentage of crystallinity was attributed to the reduction in molecular weight and to increased polarity of the grafted samples. The reduction of melt temperature was ascribed to the reduced perfection of the crystals, deriving from the anhydride groups, and the presence of possible branching. Many studies have been undertaken on optimising the reaction conditions and extruder parameters to promote the desired reactions while suppressing the undesired ones. However, because of the inherent complexity of free radical reactions, it is very difficult to incorporate the desired MA content without extensive side reactions [183].

In order to minimise side reactions it is important that the radicals formed on the polyolefin backbone are trapped as rapidly as possible. Gaylord *et al.* [150-153,155,184], have reported that various 'electron donor additives' are effective both in limiting the amount of crosslinking (various PE, [150,151,152,184], EP [153]) or chain scission (PP [155,184]) that occurs during melt phase maleation (typical conditions: 180°C batch mixer, MA 10 % w/w, additive 1–2 wt.%, DCP or BPO initiator 0.5–2 wt.%). The additives used in this context include various amides, sulphoxide, and phosphites. A mechanism of action for these coagents based on the propensity of MA to form charge transfer complexes (CTC) was proposed [1]. It was found that these coagents act as inhibitors of MA homopolymerisation, but not of methyl methacrylate (MMA) homopolymerisation. Baker *et al.* [70,88,185] also examined the influence of many of these reagents on the grafting of *tert*-butyl amino ethyl methacrylate (TBAEMA) onto LLDPE but observed no substantial effects. The addition of a known transfer agent (carbon tetrabromide) decreased both the grafting yield and the side reactions (homopolymerisation, crosslinking of LLDPE).

The effect of various comonomers on grafting yield of MA onto LLDPE (e.g. styrene, MMA, maleate esters) [146] and PP (e.g. styrene, vinyl acetate, methyl methacrylate, *N*-vinylpyrrolidone) [1,186] has been studied. The use of styrene, in particular, appears to substantially increase grafting yields [148]. Hu *et al.* [1,186] found that grafting yields to

PP decreases in the series where the comonomer is styrene >> α-methyl styrene > MMA > vinyl acetate > (no comonomer) > *N*-vinylpyrolidone. Several explanations for the comonomer effect have been proposed [1]. Higher grafting yields have been attributed to formation of a charge transfer complex (CTC) between the comonomer and MA. This complex may have a higher reactivity than MA itself. It is also likely that more efficient grafting may, in part, simply be due to attachment of a longer chain length graft rather than a greater number of graft sites. Hu *et al.* [1] have provided NMR data for styrene–MA grafts to PP which suggests that the graft is a copolymer chain and not a single styrene–MA pair. It would appear from the copolymer composition that styrene and MA do not show the same tendency to alternate in the chain in graft copolymer formation as is seen in conventional free radical copolymerisation in solution (at lower temperatures). It was found that the styrene–MA ratio in the graft exceeds the initial styrene–MA ratio irrespective of that ratio. The styrene:MA ratio in the graft copolymer varies from ca. 0.7:1 to 4.5:1 when the monomer ratio is varied in the range 0.25:1–3:1 (batch mixer 215°C, MA 4 % w/w , 0.5 wt.% DTBH initiator) [1]. Li *et. al.* [187] also studied the melt grafting of MA onto PP with styrene in single-screw extruder (temp. 170-210°C, 30 rpm) with dicumyl peroxide as initiator. The addition of styrene as comonomer could greatly improve the graft degree of MA and the maximum MA graft degree is obtained when the molar ratio of MA to St is approximately 1:1 for the same concentration of MA. They reported that the addition of styrene not only allowed an increase in the grafting yield of MA but also led to a reduction of PP degradation. When styrene (St) was added, the two monomers, St and MA, interacted with each other (one to one) to form a Charge Transfer Complex (CTC), the existence of which has been known [1] was used to explain the formation of alternating copolymers of MA and St in bulk or solution copolymerisation (see **Scheme 1.6**). The formation of CTC increases electric asymmetry on the double bond of MA, thus enhancing the monomer's reactivity. The two monomers can also copolymerise with each other under initiation of peroxide to form a chain of MA-St copolymer (SMA), which may then react with PP macroradicals producing branches by termination between the radicals. Therefore, the graft degree of MA can be significantly improved in the presence of styrene. For the grafting system into which equimolar amounts of MA and St were added, the two monomers can easily interact and copolymerise with each other. **Table 1.3** lists some studies of functionalisation of polymers with MA.

Scheme 1.6 The mechanism of the melt free radical grafting MA onto PP in the absence and presence of styrene [1,187].

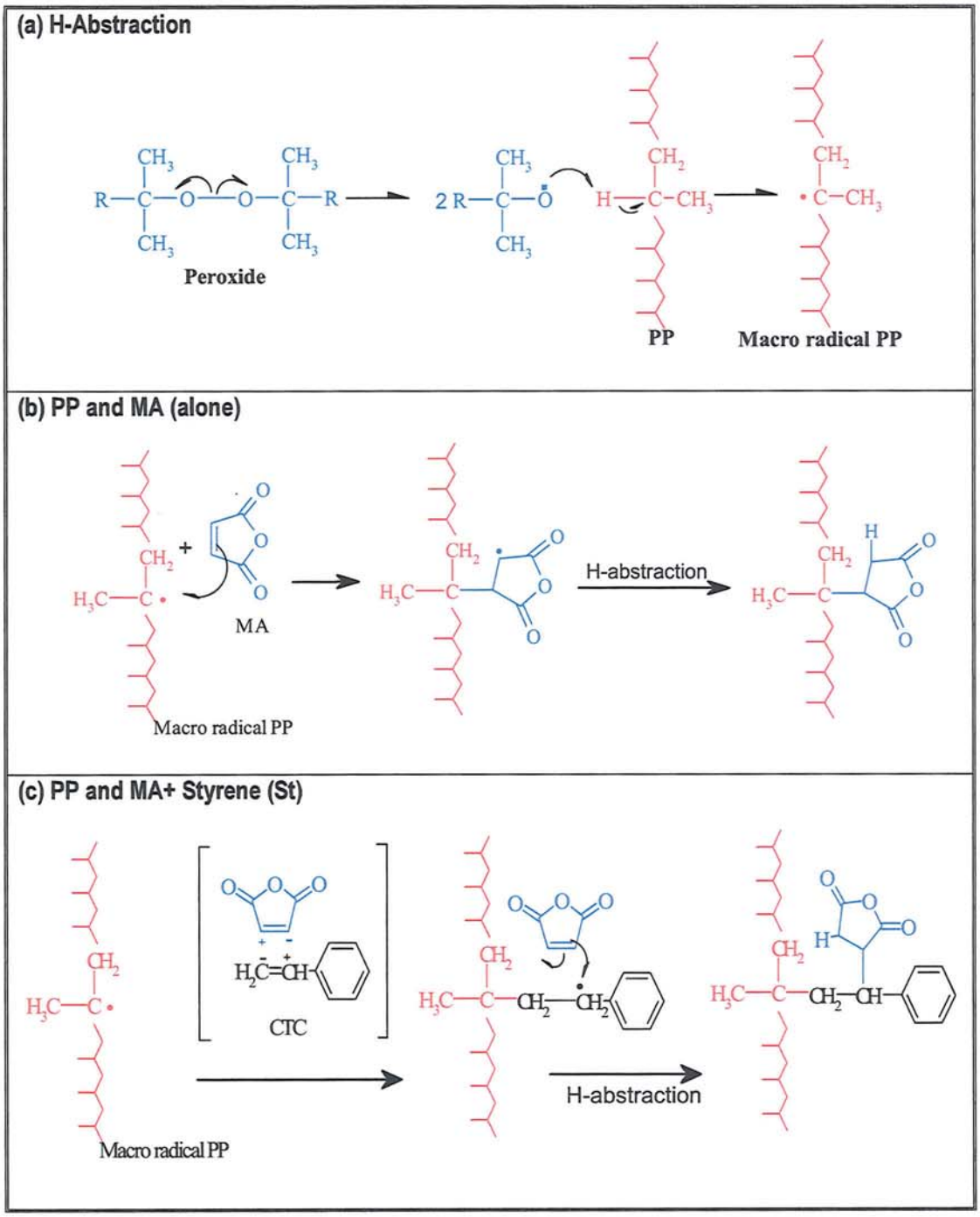

Table 1.3 Functionalisation of polymers with maleic anhydride (MA)

POLYMER	REACTOR (CONDITION)	[MA]i (phr)	Type of Perox	[perox] (wt %)	g-MA (%)	Refs.
Polyethelene						
PE	Twin screw extruder (200°C, 75 rpm, 5kg/h)	4.7	DHBP	0.94	1.96	[73-75]
HDPE,LDPE, LLDPE	Haake Rheomix 600 (180°C, 70 rpm, 8 min)	5 + St 9%	L-101	0.25	1.9-2.1	[147]
HDPE	Twin screw extruder (200°C, 75 rpm)	5	DHBP	1	1.7	[148]
LDPE	Haake Rheocord extruder (140-200 °C, 60 rpm)	3	DCP	0.1 wt %	0.90	[149]
Polypropylene						
PP	Twin screw extruder (130-175°C, 14 rpm)	2.5	DCP	1	0.5	[50]
PP	Home-made twin screw extruder (175-190°C, 120 rpm)	7	DCP	5	1.3	[51]
PP	Twin screw extruder (200°C, 75 rpm, 5kg/h)	4.7	DHBP	0.94	0.64	[73]
PP	Brabender Plasti-Corder (180°C, 80 rpm, 8min)	5	DHBP	0.8	0.45	[90]
PP	Haake Rheomix (180°C,60 rpm, 10 min)	3	DCP	2	1.6	[158]
PP	Planetary Ball Milling (85°C, 300rpm, 8 h)	2	BPO	1	1.5	[159,160]
PP	CJF supercritical CO2 Reactor (90°C, 4 h)	10 + 1 mr St	AIBN	0.8	1.2	[161]
PP	Internal mixer Rheomix 600 (140°C,9min)	9	DCP	2.1	4	[181]
	Glass reactor 140°C(in Xylene)	9	DCP	2.1	1.2	
PP	Twin screw extruder (200°C, 150 rpm)	4	L-101	0.1	0.7	[182,183]
PP	Single screw extruder (180°C, 30 rpm)	3 + 1 mr St	DCP	0.3	2	[187]
Ethylene vinyl acetate copolymer and other polymers						
EPR	Twin screw extruder (200°C, 75 rpm, 5kg/h)	4.7	DHBP	0.94	1.57	[73]
EVA	Haake Internal Mixer (140°C, 60 rpm, 8min)	5	DCP	0.5	2.4	[162]
EVA	Haake Rheocord 9000 175°C, 50rpm, 10 min	2	DCP	0.4	1.1	[163]
EPDM	Brabender Plasticorder 180°C, 75rpm, 10 min	5	T-101	1 wt %	4	[164]
ABS	Haake Extruder (190°C, 20rpm)	3	DCP+BPO (3:2)	1.2	1.8	[165]
SBS	Haake Rheomix 600 150°C, 55rpm, 20 min	8	BPO	0.2	3.3	[166]
NR	Toluene Solution (80°C, 2hrs)	10	BPO	3	3.3	[167]
NR	Toluene Solution	10	BPO	1	2.1	[168]
		10 + 0.1 % St	BPO	1	4	

NOTES: **[MA]i** = MA concentration initially added ; St = Styrene ; **phr** = part per hundreds (weight) ratio to polymer; **mr** = molar ratio (mol/mol); **DHBP** = **T-101** = 2,5-bis(*tert*-butylperoxy)-2,5-dimethylhexane; **L-101**=2,5-dimethyl-2,5-(di-*tert*-butyl peroxy) hexane; **AIBN**= 2,2'azobisisobutyronitrile; **DCP** = Dicumyl peroxide; **BPO** = Benzoyl peroxide

1.3.3 Functionalisation of Polymers with Oxazoline (OXA) and Other Reactive Monomers

Oxazoline moiety has also been used as a reactive functional group in polymer modification by reactive extrusion [136,137,188-195]. Long-chain oxazolines have been reported to be less toxic than maleic anhydride and glycidyl methacrylate, and their boiling points are well above those of MA and GMA [191]. Oxazolines react fast with carboxyl and amino groups, which makes them suitable for use in blends containing these end groups and also react with other functional groups such as phenol and mercaptan [190]. Polymers containing oxazoline functionality are described to be produced by the following methods:

1. Free-radical polymerisation or copolymerisation of monomers bearing oxazoline ring, like 2-isopropenyl-2- oxazoline (IPO) or 5-oxazolinyl-pentylmethacrylate, (**Figure 1.4**) [188,189].
2. Free-radical grafting of oxazoline monomers onto polymers. For examples, 2-isopropenyl-2- oxazoline, IPO (**Figure 1.4**) and Ricinoloxazoline maleinate (**Figure 1.5**) was grafted onto PP, EPR and SEBS [136,137,188,190].
3. Conversion of functional groups existing in polymer into oxazoline functionality, for example, catalyzed reaction of nitrile groups with 2-aminoalcohols or epoxide [191,192].
4. Reaction between polymer functional groups (acidic, amine) with oxazoline derivatives or bis-oxazoline compounds [193].

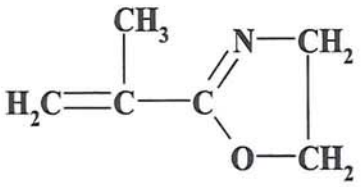

Figure 1.4 Chemical structure of 2-isopropenyl-2-oxazoline (IPO) **[188]**

Vaino *et. al.* [136,137] have investigate grafting of ricinoxazoline maleinate (OXA) **(Figure 1.5)**, to produce an oxazoline functional PP (in the presence of comonomer styrene) by melt processing either in a batch mixer (200°C, 64 rpm, 15 min residence time) [136] or a twin screw extruder (200°C, ca. 150s residence time) [137]. The initiator was

1,3-bis(*tert*-butylperoxy-isoprpyl) benzene (DIPB) in both sets of experiments. Ricinoxazoline maleinate which is in a liquid form exhibited very low volatility (bp>25°C at 0.1 mbar). The grafting reaction was very fast and the conversion of the OXA monomer to grafted OXA ranged from about 15 to 50%, depending on the initial concentrations of the monomer and peroxide [136]. The addition of comonomer styrene as coagent was found to reduce the extent of PP degradation that accompanied grafting but, the grafting yield was not enhanced because the two monomers can not copolymerise easily [137].

Vocke *et al.* [191,192] also attempted the grafting reaction of ricinoloxazoline maleinate onto polypropylene (PP), polyethylene (PE), ethylene propylene copolymer (EP) and styrene ethylene/butylene styrene (SEBS) in a twin extruder. They reported that the maximum conversions of ricinoxazoline maleinate were about 30 % for EP and SEBS and 23 % for PE. Increasing concentrations of peroxide and ricinoxazoline maleinate increased grafting, but MFI decreased significantly, especially for PE even with a low initial monomer and peroxide concentrations, indicating crosslinking. With a suitable choice of peroxide (1,1-bis(*tert*-butylperoxy)-3,3,5-trimethylcyclohexane, Trigonox 29-C90) grafted polymers could be produced with good yield and without gel formation [191].

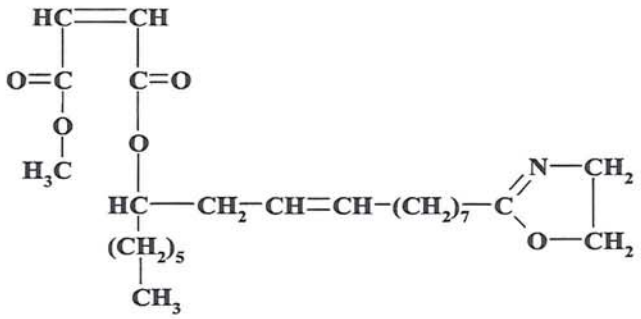

Figure 1.5 Chemical structure of ricinoxazoline maleinate (OXA) [119].

Apart from maleic anhydride (MA), glycidyl methacrylate (GMA) and Oxazoline (OXA) which have been intensively studied, a wide range of other monomers have been successfully grafted onto polyolefin and rubbers to obtain good toughening or compatibilising effects such as isocyanate (-NCO) or carbamate [196-199], acrylate and unsaturated carboxylic acid monomers [200-203], alkyl maleate and maleimide [204,205] and vinyl silane [206-208], see **Figure 1.6** for their molecular structures. Isocyanate or

carbamate monomer (-NCO), for example, have been successfully grafted onto polymer to enhance the compatibility of immiscible PBT/polyolefins blend. Park *et al.* [196-199,209,210] suggested that isocyanate group has a good reactivity towards amine, hydroxyl, and carboxyl groups.

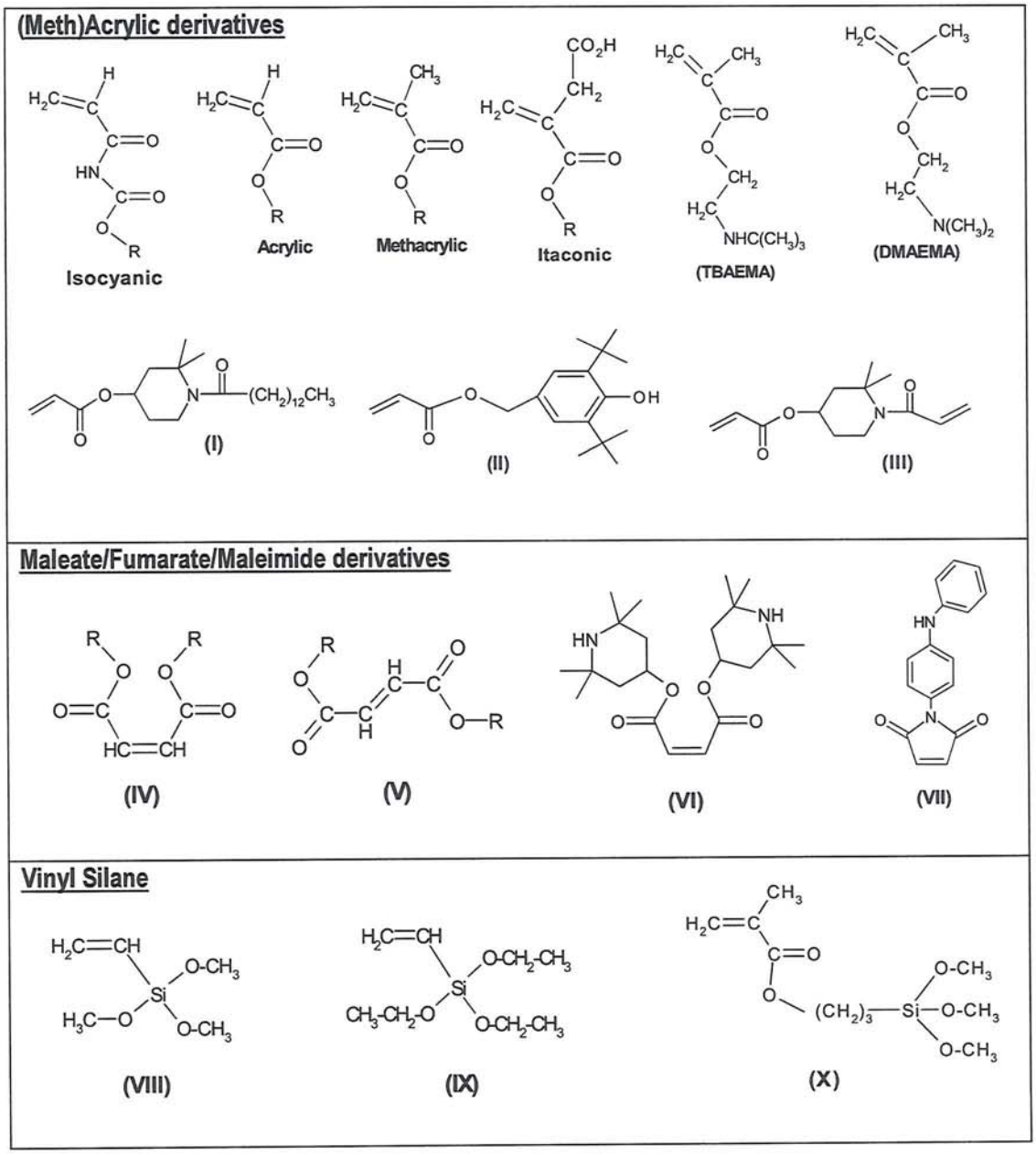

Figure 1.6 Chemical structures of vinyl monomers of (meth)acrylate, maleate, and vinyl silane derivatives used for grafting on polymers melts.

In the case of acrylic/methacrylate monomer onto polyolefins, grafting to polyolefins is often accompanied by homopolymerisation of the monomer and high degradation of the polymer (crosslinking of PE or chain scission of PP), especially processing with high concentration of peroxide [43,156,201,211]. Several methods used to minimise this side reaction are described in patent literature [3]. Al-Malaika *et al.* [96-98] have reported on the grafting of methacrylate derivates of antioxidant moieties onto PP as mono **(I** and **II)** or bis- **(III)** acrylic derivatives. Grafting 3,5-di-*tert*-butyl-4-hydroxyl-benzyl acrylate (DBBA) **(II)**, for example, very high extent of antioxidant homopolymerisation (≈ 60%) was observed in the case of reactive processing carried out in the absence of coagent TRIS and led to low grafting levels to PP. In the presence of TRIS, however, has drastically reduced the level of competing reaction (mainly homopolymerisation) to less than 10% and giving rise to over 90 % grafting efficiency of the antioxidant **(II)** on the polymer (batch mixer, 180°C, 10 min reaction time, DBBA 10 wt %, T-101 initiator 0.02 molar ratio to DBBA). The remarkable finding was that the final products in the processes involving polyfunctional monomers were not crosslinked and, indeed, were completely soluble in xylene. It was proposed that crosslinking did in fact occur. However, the initially formed product undergoes *in-situ* degradation by chain scission when subjected to further processing to ultimately yield a soluble, gel-free material [96-98].

The melt phase grafting of various dialkyl maleates **(IV)** and fumarates **(V)** onto polyethylene, polypropylene and SEBS [42,157,204,205], has been studied and used as compatibilisers. Similar to maleic anhydride (MA), the maleate esters shows little tendency to homopolymerise. The use of maleate esters has been advocated over MA (all may be used as a precursor to nylon graft) due to their lower volatility and lower toxicity. However, the maleate esters are significantly less reactive towards free radical addition than MA and grafting yields are generally lower. Even though maleate esters are less reactive than MA, the side reactions associated with peroxide induced grafting (crosslinking, chain scission) appear to be negligible. This may reflect the greater solubility of the maleate esters in the polyolefin melt.

The modification of polyolefins (HDPE, LDPE, PP) with vinylsilanes (e.g. vinyl tetra methyl silane **(VTMS)**, vinyl tetra ethyl silane **(VTES)** or, less commonly, 3-(trimethoxysilyl) propyl methacrylate **(VIII)**) (see **Figure 1.6**) has been widely studied

[206-208]. The principal application of these materials is the preparation of a moisture curable crosslinked polyolefin and they are widely used in the cable industry. Silane treatment has also been used for surface modification of polyolefins. The vinyl silanes monomers do not readily homopolymerise. Grafting reaction of VTMS onto dodecane has been studied as a model system for the melt grafting of the monomer onto polyethylene. NMR studies strongly indicate that the multiple grafts consist predominantly of multiple single grafts rather than homopolymer grafts [213]. Their work suggests that grafting occurs as shown in **Scheme 1.7** (R = -OCH_3) and involves an inter- and intra-molecular hydrogen atom transfer step.

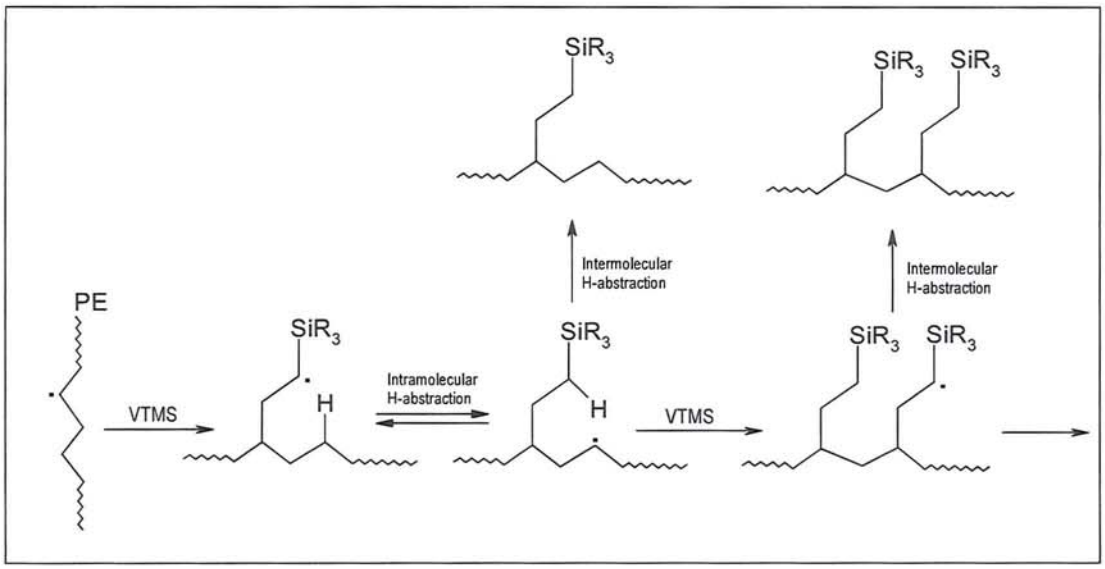

Scheme 1.7 Grafting Reaction of vinyl silane onto PE [213].

1.3.4 Challenges of Melt Free Radical Grafting

The chemistry of melt free radical grafting is complicated by the high temperature, high viscosity and heterogeneity of the reacting medium. First of all, the desired grafting reaction is always accompanied by undesirable polymer degradation reaction and homopolymerisation of monomers which can alter significantly their valuable mechanical properties and processing characteristics. Good understanding of these effects of processing parameters, the grafting mechanism and the microstructure of grafts help achieve successful grafting reactions [1]. Higher processing temperatures generally will favour polyolefin degradation, reduce initiator half-life, modify the rate or specificity of reactions, and

influence various solubility and rheological parameters. Increasing the temperature favoured hydrogen atom abstraction and also increases the amount of macroradicals formed via thermo mechanical degradation. Therefore, an increase in temperature should lead to an increase in the grafting degree. On the other hand, increasing the temperature decreases the initiator efficiency and accelerates the evaporation of monomer and initiator. Thus, it has been hard to clarify the precise role of temperature on the grafting degree and the extent of chain scission/crosslinking [1,3]. The extent and type of any side reaction not only depend on the particular polyolefin used but also on type and concentration of peroxide and monomers. As for the initiators, important factors affecting the grafting reaction include the initiator's half-life time and concentration, the solubility and partition coefficient in the polymers and monomer, the reactivity and specificity of the derived radicals, side reactions and the nature of any initiator-derived by products, its volatility and toxicity. Numerous works have attempted to maximise grafting yield by simply increasing the initiator concentration but this approach is counterproductive because of the consequent increase in the extent of undesirable side reactions. Overall, although the main steps in the free radical mechanism of grafting are well known, there is much less information in the open literature on the microstructure of the graft (e.g. grafts sites, graft length and graft sequence distribution). Thus the mechanism of free radical grafting or microstructures of the resulting grafts have to be speculated. For example, the grafting of GMA onto PP could be enhanced by addition of styrene as a comonomer, resulting in high grafting yield [119,120,133]. However, it was found that the GMA grafted PP in the presence of styrene was less effective in compatibilising PP/NBR blends than GMA grafted on PP without using styrene [135]. This means that the microstructure of GMA grafts in the presence or absence of styrene are different, which determines the efficiency of the grafted GMA groups towards other functional groups during reactive blending, and this difference may result from the different grafting mechanisms. However, little information is available on the microstructure of GMA grafts. With more studies made on the grafting mechanism and microstructure of grafts by using model compounds and ^{13}C or ^{1}H NMR, the fundamental understanding of melt radical grafting will become more clear.

1.4 Polymer Blends

Polymer blending is a convenient route for the development of new polymeric materials, able to yield materials with property profiles superior to those of the individual components. This method is usually cheaper and less time-consuming for the creation of polymeric materials with new properties than the development of new monomers and/or new polymerisation routes [214-223]. An additional advantage of polymer blends is that the properties of the materials can be tailored by combining component polymers and changing the blend composition. To improve the interfacial adhesion and to stabilise phase morphology in polymer blends different methods have been developed in the past. Generally, there are two routes for improving compatibility of immiscible blends [18]:

(a) By reactive blending suitable functionalised polymers capable of enhanced specific interaction and/or chemical reactions. Functionalisation can be carried out in solution or in a compounding extruder and may involve the formation of block or graft copolymers, halogenation, sulfonation, hydroperoxide formation, end capping, etc.

(b) By adding a third component (compatibiliser) capable of specific interaction and/or chemical reaction with the blend constituents. Block and graft copolymers and a variety of low molecular weight (MW) reactive chemicals fall under this category. The choice of a block or graft copolymer as compatibiliser is based on the miscibility or reactivity of its segments.

i. Reactive Blending

A later development for the production of compatible thermoplastics blends was based on reactive blending, which relies on the *in situ* formation of copolymers or interacting polymers. Usually reactive polymers can be generated by free radical copolymerisation or by melt grafting of reactive groups onto chemically inert polymer chains. In order to successfully apply reactive polymers as block or grafted copolymer precursors, the functionalities must have a suitable reactivity in order to react across the melt phase boundary during the short blending time. Functional groups, such as anhydride, epoxy, oxazoline, are highly reactive and polymers containing those groups are often chosen for reactive blending. **Table 1.4** lists of the compatibilised systems that have been studied recently.

Scheme 1.8 Examples of common compatibilisation reactions between functionalised blend constituent **[15,205-266]**. (cont.)

Compatibilisation Reaction	Refs.
1. Anhydride + amine 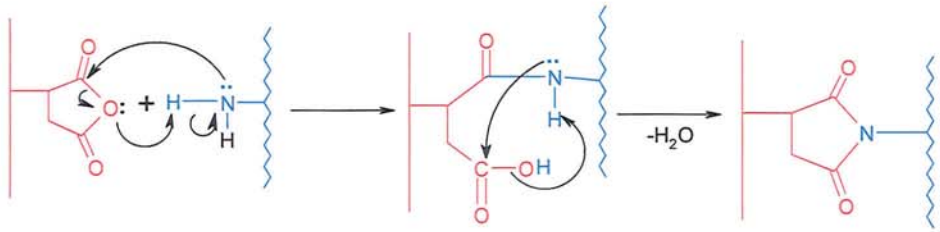	[224-243]
2.Anhydride + Carboxylic acid 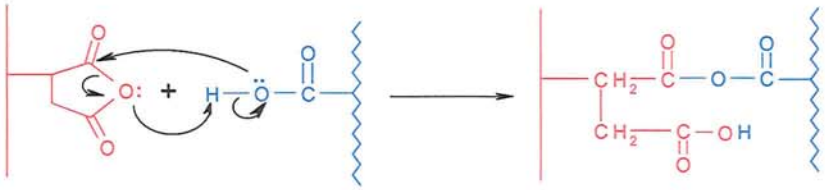	[244-252]
3.Epoxide and amin 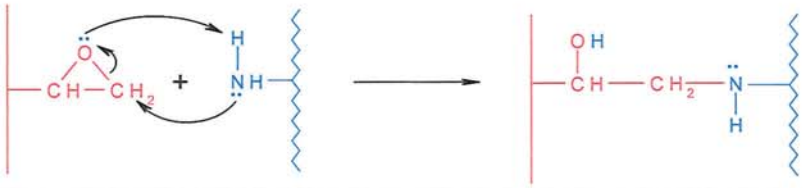	[236,237, 253-261]
4.Epoxide and carboxylic acid 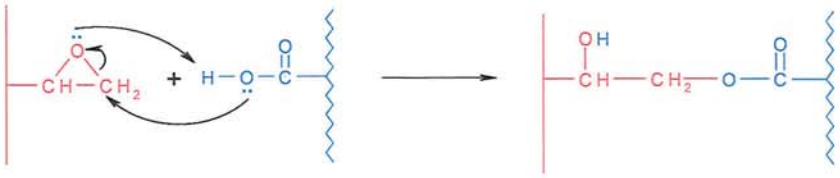	[262-270]
5.Oxazoline and carboxylic acid 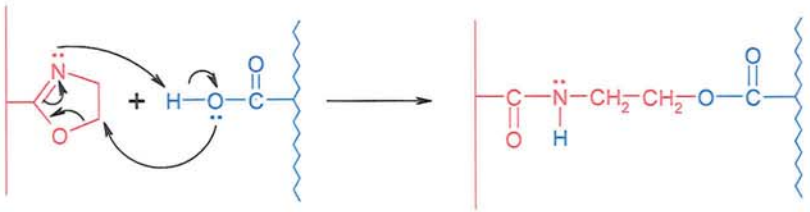	[136,137, 194, 271,272]

Scheme 1.8 (cont.) Example of common compatibilisation reactions between functionalised blend constituent **[15,205-266]**.

6. Oxazoline and Hydroxyl or Mercapto 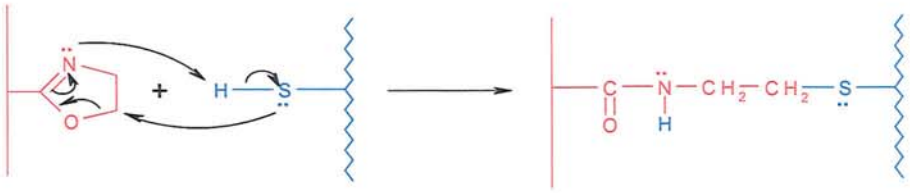	[190]
7.Oxazoline and amin 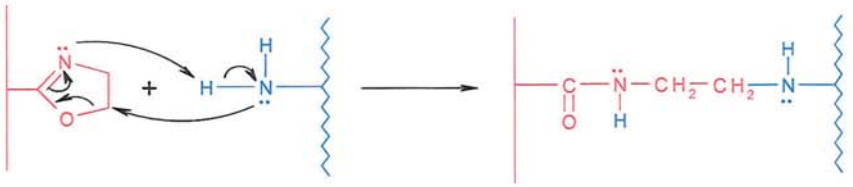	[194]
8. Isocyanate and amin 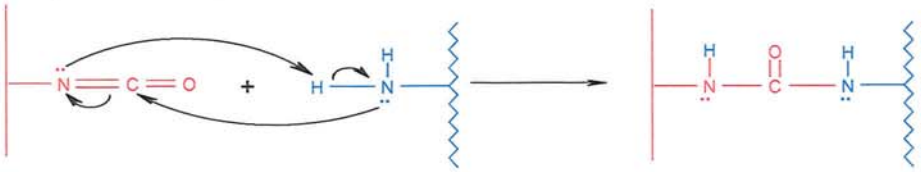	[199]
9. Isocyanate and carboxylic acid 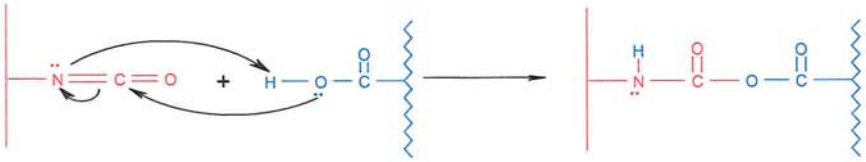	[196-199, 209,210]
10. Hydroxyl/Carboxylic (Transesterification) 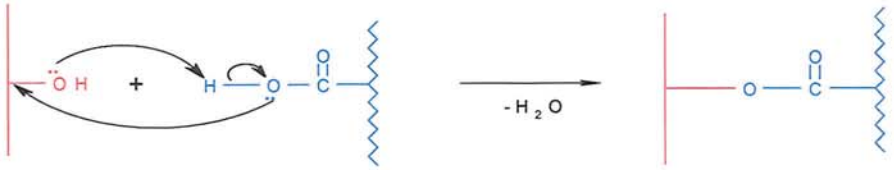	[273-280]
11. Ionomer 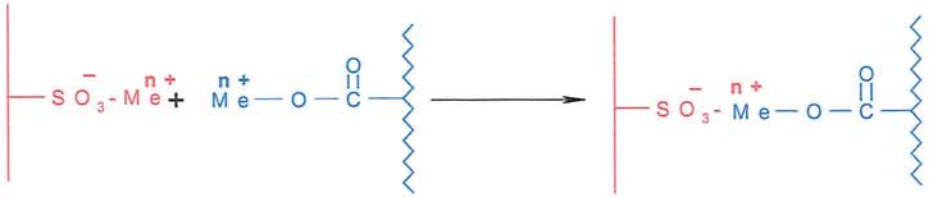	[281-286]

Table 1.4 Compatibilisation of polymer blends through the reaction of functionalised polymers

Compatibilising Reaction	Polymer Blend	References
Anhydride/ Amine	PSU-g-MA/PA6	[224]
	PP-g-MA/PA-6 and PA-12	[117,225-232]
	PE-g-MA/PA-6	[233-240]
	EP-g-MA/PA-6	[237,240]
	EVA-g-MA/PA-6	[241]
	PA-1010/HIPS-co-MA	[242]
	NR-g-MA/PA	[243]
Anhydride/Carboxyl	PP-g-MA/PBT	[22,244]
	HDPE-g-MA/PET	[245]
	EVA-g-MA/PBT or PET	[163,246,247]
	SEBS-g-MA/PET	[248]
	SAN-g-MA/PBT	[249]
	ABS-g-MA/PC	[250]
Epoxy and Amine	PP-g-GMA/PA-6 and PA-1010	[253-257]
	PE-g-GMA/PA6 or PA11	[258,259]
	ABS-g-GMA/PA-6 and PA-1010	[260,261]
Epoxy and Carboxyl	PP-g-GMA/PET or PBT or CNBR	[23,262-266]
	HDPE-g-GMA/PET	[251]
	EP-g-GMA/PET	[267]
	PS-g-GMA/PBT	[21,268,269]
	ABS-g-GMA/PBT	[270]
Oxazoline/ carboxyl acid, hydroxyl (OH) or Mercapto (-SH)	NBR-g-OXA/EVA-SH or EPDM-SH	[190]
	PP-g-Oxa/PBT	[136,137]
	PP-g-Oxa/PA	[192]
	NBR-g-OXA/EVALVA	[193]
	HNBR-g-OXA/PBT	[194,195]
	PS-g-Oxa/PBT	[271,272]
Isocianate/Carboxyl or amine	EPR-g-Isocianate/PBT	[208]
	LDPE-g-Isocianate/PA or PBT	[199]
	PP-g-HI/PBT and PET	[208,209]
Hydroxyl/Carboxylate	PS-OH/PBT	[273,274]
	PET/PEEA	[275]
	PET/PP-Maleate	[252]
Transesterification	PET/PC and bisphenol-A	[276-280]
Ionomers	PA or PET/PS- SO_3^-	[281-283]
	ABS/SAN-SO_3^{2-}	[284]
	Polyoxymethylene/EMA Na^+ or Zn^{2+}	[285]
	P(S-b-vinylpiridine)/PS-SO_3^-	[286]

ii. Addition of Reactive Block/Grafted Copolymers and Low Molecular Weigh (MW)

Usually a polymer chemically identical to one of blend components is modified to contain functional (or reactive) units, which have some affinity for the second blend components; this affinity is usually the ability to chemically react with the second blend component (**see Table 1.5**).

Table 1.5 Compatibilisation of polymer blend by addition of functionalised polymer

Compatibilisation Reaction	Polymer Blend	Compatibiliser	Ref.
Anhydride/Amine	LDPE/PA-6	SEBS-g-MA	[287]
	PP/PA-6	SEBS-g-MA	[288-290]
	PMMA/PA-6	SMA	[291, 292]
	PP/PA6	EVA-g-MA	[293]
	PP/PA-6	TPE-g-MA	[294]
Anhydride/Carboxylate	PP/PET	SEBS-g-MA, LLDPE-g-MA	[172,295,396]
	LLDPE/PBT	EVA-g-MA	[20]
	PET/HDPE	EPR-g-MA,SEBS-g-MA,E-GMA	[297]
	ABS/PA	MMA-MA	[298,299]
Epoxide/Amine	LDPE/PA-6	SEBS-g-GMA	[287]
		E-GMA	[300]
	ABS/PA	MMA-GMA	[298,299]
Epoxide/Carboxylate	PBT/ABS	S-GMA and MMA-GMA	[301]
	PBT/AES	MMA-GMA-EA	[302]
	PET/HDPE	E-GMA , E-EA-GMA,	[303]
		SEBS-g-GMA,E-MA-GMA	[304]
	PBT/PC	E-GMA	[305]
	PBT/E-EA	E-MA-GMA	[306,307]
	PBT/ABS	MMA-GMA-EA	[308]
	PET/PP	E-GMA	[309,310]
		SEBS-g-GMA, SEP-g-GMA	[311,312]
	PET/EPR	E-GMA	[313,314]
Acrylic acid/Polyester or amide	PBT/EVA	E-AA	[315,316]
	PA-6/LDPE	E-AA	[317]
Oxazoline/Carboxyl	PP/PBT	SEBS-g-Oxa , E/P-g-Oxa	[192]
Oxazoline/amine	PP/PA-6	SEBS-g-Oxa, EPR-g-Oxa	[192]

Table 1.6 Compatibilisation of polymer blends through addition of low molecular MW.

Polymer Blends	Compatibiliser(Low MW Compounds)	Ref
	Peroxide:	
PP/unsaturated Polyester	2-*tert*-butylperoxy-2-methyl-5-hexene-3-yn + octyl methacrylate	[318]
PE/PVC/PS/PP/EPDM or SBS	Dicumyl peroxide (DCP)	[319]
PP/unsaturated polyester	2,5-dimethyl-2,5-bis(*tert*-butylperoxy) hexane	[320]
	Bi, Multifunctional Chemicals & Peroxides:	
PS/EPDM	DVB or TRIS	[138]
PVC/NBR	Maleic anhydride (MA)	[321]
PP/PS	MA and styrene	[171]
PBT/PPE	Diglycidyl ether (bisphenol-A)	[322]
PBT/LDPE or EPDM	Bismaleimide	[323]
	Dynamic Vulcanisation:	
PP/NBR or PP/EPDM	Dimethylol phenolic compound	[324]
PP/NR/LDPE	Dimaleimide (HVA-2)	[325]
	Catalyst:	
PBT/EVA	di-butyl tin oxide	[326]
PBT/Acrylate rubber	di-butyl tin dilaurate	[327]
PE/PS	$AlCl_3$/Styrene (Friedel Craft Rctn)	[328-330]
	Filler:	
PP/PS, PMMA/PP or PE	Silica or clay	[174,175,331]

In some cases, in order to improve the compatibility of polymer blends addition of low molecular weight (MW) compounds has been described for the early stages of polymer blends development. Various procedures may be distinguished, depending on the added chemical(s): peroxide, bifunctional/multifunctional compound that forms block copolymers, selective cross linking agent (dynamic vulcanisation), catalyst system, and addition of reactive fillers as compatibilisers (see **Table 1.6).** Hu *et al.* [186,332,333] have examined the kinetics of reactions of various ethylene copolymers with low molecular weight model compounds in the melt phase in a batch mixer and also examined the effects of various catalysts on these reactions.

1.5 Process Consideration

Both reactive functionalisation and blending of polymers can be carried out in batch mixer or extruder (reactive processing). The mixer or the extruder would act as a reactor where the specific chemical reactions take place. A particular advantage of reactive processing is the absence of solvent as the reaction medium so no solvent stripping or recovery process is required, and product contamination by solvent or solvent impurities is avoided [1]. The fundamental basis behind the successful use of these types of machines in melt free radical grafting or reactive blending is primarily related to their ability and efficiency to handle and mix highly viscous polymer fluids.

1.5.1 Reactive Extrusion

Reactive extrusion refers to the performance of chemical reactions during extrusion processing of polymers and is carried out either in single or twin-screw extruders, capable of transporting and mixing highly viscous fluids in an environment where temperature and pressure are controlled. An advantage of an extrusion device as a reactor is the combination of several process operations into one piece of equipment with accompanying high space-time yields of product. The grafting process is usually performed in the melt in an extruder, that is, via reactive extrusion is carried out at elevated temperatures with highly viscous and probability heterogeneous systems. The extruders used should, therefore, contain intensive mixing zones because efficient mixing of the monomer with the polymer is essential for minimizing the formation of free homopolymer. Their use has advantages over alternative processes, including the absence of solvents, which avoids product isolation; short

residence times; and a continuous operation. However, important functional characteristics, such as the temperature profile, the screw speed, the degree and type of mixing, and the residence time distribution should be taken into account. Combining processing and chemical reactions makes reactive extruder very complex and, for free-radical grafting in the melt, gives rise to a tremendous challenge in terms of reactivity, selectivity, processing, and product optimization and control. Some authors [1,3,23,46,90] developed a general kinetic model and combined it with generally accepted models for melting in a single-screw extruder. The required input consists of data on the extrudate, such as the molecular weight, grafting content, residence time, and temperature.

1.5.2 Torque Rheometer (Batch Mixer)

The torque rheometer, such as a Haake Rheocord, Brabender type batch mixer, is a kind of multi-functional and modularised reactor, and is widely used in most laboratories working on polymer processing. With the recording of torque varying with time, it can provide quantitative information on the flow behaviour of polymer melts and gives a view of the structural changes during processing and the influence of various additives on new formulations, as well as being valuable for quality control and product development. Due to its particular structure, the mixing chamber of the rheometer is not perfectly sealed. This may bring about complication when adding liquid monomer and/or other types of additives whose boiling points are low compared to temperature in the mixing chamber. In such a case, loss of liquid and/or easy-to-sublime reactant can become important. In fact, so far a batch mixer is considered a unique device that best suits the need to understand the chemistry of reactive processing in a screw extruder. Due to the irregular geometry of rotors and the three-dimensional nature of the flow field in the mixing chamber, there are some difficulties in evaluating rheological properties of polymers melt by the torque rheometer. Despite its limitation, a batch mixer is often preferred over a screw extruder as a chemical reactor for achieving a fundamental understanding of melt free radical grafting or reactive blending [334-340]. Unlike reactive extrusion, mixing time or reaction time can be changed with ease. A batch mixer also bears other useful features:

- Its ability to mix highly viscous polymers;
- The relatively small capacity of the mixing chamber (e.g. 50 cm^3), which permits trial with expensive or exotic chemicals and facilitates temperature control;
- The possibility of varying the following processing parameter which resembles more or less those encountered in a screw extruder: temperature, mixing time, mixing intensity, via the rotating speed of rotors, and the mode with which reactants are charged to the mixing chamber.

1.6 Characterisation of Functionalised Polymers

The characterisation of the grafted functionality in modified polyolefins is rendered difficult by the small number of modified units with respect to the normal polyolefin repeat units. The extent of modification can be down to 0.1 mol% and is typically in the range 0.5–2 mol%. This corresponds to only about one to five modified units per molecule in a polymer of typical molecular weight (*M*n 20000 – 40000). A further problem is the low solubility of most polyolefins, in particular, conventional PP and PE in any solvent at room temperature and in a limited range of solvents at elevated temperatures. Various methods have been described in the literature like titration and infrared (IR) spectroscopy [341], elemental analysis [163] and nuclear magnetic resonance (NMR) [342]. The most widely used method for qualitative analysis of the functionalisation is IR spectroscopy [118-134,343].

i. Chemical methods

Chemical methods have been developed to determine reactive functionality grafted to polyolefins. Acid–base titrations of maleic anhydride grafted polyolefins are commonly performed in aromatic solvents such as xylene or toluene. Other studies also mention the use of a butanol–xylene mixture [344], or even a titration method on a polyethylene suspension in xylene [108]. The solvent used is pure or saturated with water leading to quantification of the anhydride groups or their hydrolysed form, respectively. Work in dry conditions requires a previous vacuum–thermal treatment of the polyolefins to ensure the total conversion of the grafted maleic anhydride in its anhydride form. The results of 1–3 days at 75–120°C are generally reported [150]. Conversely, in wet organic solvents, all the cyclic anhydride functions have to be opened into carboxylic acid groups. The solvent is

saturated with water [150,155], or added with 2 mL of water after matrix dissolution [95,177]. The hydrolysis is carried out by refluxing in solvent for 1–1.5h [95,155,177]. Finally, when alcohol in non-aqueous solvents is used, it opens the anhydride ring, into an ester function and an acid function [36,95,109,150,155,170,177,344]. The titration goes on until the visual end point of a coloured indicator, corresponding to the neutralisation of the grafted functions. Thymol blue is often chosen as the coloured indicator to determine this equivalence point [36,150,155,341,345,346]. In some cases, phenolphthalein in an alcoholic solution is used [95,109]. The titration agent is an alcoholic base solution, most often KOH in ethanolic solution [36,95,109] or solution of tetra-butyl ammonium hydroxide (TBAOH) free of water is noted [344-346]. Other authors use a back-titration method adding an excess of base to the solution and titrating it back with HCl [109,150,155]. It is important that the solution remains hot during the titration procedure to prevent precipitation of the polymer [155]. Procedures for determining grafted GMA based on titration or chemical analysis have been reported [125,127]. For example a film sample is first extracted with refluxing benzene, to remove any residual monomer, then a hot xylene solution is treated with dilute hydrochloric acid, to open the epoxide, and the solution back titrated with sodium hydroxide [127].

ii. FTIR Spectroscopy Method

Infrared spectroscopy is currently the most widely used method for identifying and quantifying grafted functionality in modified polyolefins [347]. For quantitative work, FTIR spectra are generally measured on melt pressed films. The procedure involves determining the intensity of a band due to the particular functionality relative to a band that can be attributed to the polyolefin backbone. A calibration curve based on standards containing known concentrations of groups is then necessary to convert the intensity data into concentrations. The intensity of the polyolefin bands used as a reference will depend not only on the particular polyolefin substrate and also on the particular grade of polyolefin [347]. Infrared band positions for grafted functionality derived from common monomers are listed in **Table 1.7**.

Table 1.7 Principal infrared absorptions peaks of modified polyolefins

Graft Monomer	Functional Group	IR peak(s) (cm^{-1}) (a)	Ref.
MA	C=O (Single Unit)	1792, 1715 (b)	[95,112,177 345,346]
	C=O (attributed to oligo-MA, α, β-unsaturated anhydride	1784,1860 (b)	
	C=O	1713,1790,1867(b)	[177,181-183]
Diethyl maleate	C=O	1740	[157]
GMA	C=O	1730	[122]
		1735	[131]
Isocianate	N=C=O	1680, 1730, 3300	[199]
Oxazoline (OXA)	-C(O-)(=N-), C=O	1671, 1734	[136,137]
Acrylic acid	C=O	1710	[43]
		1720	[200]
VTMS	C-O-$SiMe_3$	789, 1092, 1192	[207]
		1000, 1085	[208]
		799, 1088, 1192	[213]

(a) IR band used for quantifying and or identifying grafts, may vary ± 4 cm^{-1} from this value and are for film samples.
(b)The anhydride functional group gives rise to two bands at ca. 1790 and 1860 cm^{-1} due to symmetrical and unsymmetrical stretching modes. The lower frequency band is usually more intense and is generally used for quantification.

The following example (analysis of MA–polyolefins) serves to illustrate the complexity of FTIR analysis. It is one of the worse case examples because the grafted MA units (in whatever form) are inherently unstable and on standing are rapidly (extent and rate depend on available moisture) converted to maleic acid grafts. It is possible to overcome this latter complication by drying the samples prior to analysis. MA can be grafted in a number of different environments (e.g. as unsaturated anhydride units, succinic anhydride units, and oligo-MA blocks. De Roover *et al.* [95,177,178] who have conducted a most comprehensive study of MA-PP, have indicated that a band in the region 1780–1800 cm^{-1} associated with the C=O of MA–PP can be resolved into two bands centred at 1792 and 1784 cm^{-1}. They attribute these bands to isolated succinic anhydride units and blocks of oligo-MA, respectively on the basis of the infrared spectra of simple model compounds. However, a concern is that the aforementioned groups may not be the only ones that give rise to bands in the quoted positions. Infrared absorption bands are unfortunately not sufficiently sensitive to their immediate chemical environment for the assignments to be completely unambiguous [8]. The interpretation appears at odds with NMR characterisation of MA–PP [93]. A similar analysis to that carried out by De Roover *et al.* [95] on MA–LLDPE would suggest that polymer possesses an even higher concentration of oligomeric grafts [345,346]. In view of these complications, it is perhaps surprising that the relatively simple method reported for determining MA or GMA graft levels can be successful.

1.7 Aims and Objectives of This Study

From the literature review on the technology of grafting of monomers onto polymers, it is revealed that the low grafting level of GMA and MA along with severe polymer degradation is attributed to the weak free radical reactivity of the monomer towards polyolefins macroradicals. One of the major objectives of this research work was to investigate the functionalisation process of two polymers, i.e. natural rubber (NR) and polypropylene (PP) in absence and presence of comonomers as enhancing agents. This involved the *in-situ* melt free radical grafting of two functional monomers, GMA and MA, onto the polymers using an internal mixer (torque rheometer) as a chemical reactor. However, due to the low reactivity of GMA and MA towards the polymers, which would result in low grafting yield, a novel approach (developed at Aston University PPP research group) where a highly reactive comonomers (coagents) was used in combination with the functional modifiers (i.e. GMA and MA).

The main aim of this work was therefore to examine the effect of two comonomers, i.e. trimethylolpropane trimethacrylate (TRIS) and divinyl benzene (DVB) in the grafting system by using various peroxides, i.e. benzoyl peroxide (BPO), dicumyl peroxide (DCP), 1,1-di(*tert*-butylperoxy)-3,3,5-trimethylcyclohexane (T-29B90), and 2,5-dimethyl-2,5-bis-*tert*-butyl peroxy)hexane (T-101) as initiators. To achieve this aim, appropriate methodology, chemical composition and reactive processing parameters were examined and optimised. The functionalised polymers products were characterised using various techniques and accurate methods (i.e. titration and FTIR) were developed to evaluate the grafting levels of the functional monomers (i.e. GMA and MA). The research work also evaluated the efficiency of various methods of purification the grafting reaction products. The reaction mechanisms were also investigated. Preliminary examination of the compatibilisation of PP/PBT was conducted by reactive blending of the polymers with the GMA- or MA-functionalised polypropylene (*f*-PP) (developed in this work) in an internal mixer with the purpose of identifying the *in-situ* reaction that results in the formation of PBT-GMA-PP and PBT-MA-PP graft copolymers. The morphology of PBT/PP-g-GMA/PP and PBT/PP-g-MA/PP were compared with the uncompatibilised PP/PBT (physical) blends to examine the compatibilising effect of the *f*-PP polymers.

CHAPTER 2
EXPERIMENTAL AND ANALYTICAL TECHNIQUES

2.1 Materials

2.1.1 Polymers

Natural rubber was a commercial grade (SMR-L) supplied by the Malaysian Rubber Producer's Research Association (MRPRA), UK. Two commercial grades of polypropylene were used (HF-26 ex. ICI in powder form and APPRYL 3020/BNI ex. Elf Atochem Ltd in granular form). Poly (butylene terephthalate) (PBT) (Arnite T08200 ex. Eastman Chemical Ltd. had a terminal hydroxyl and carboxyl groups concentrations of 0.032 and 0.040 meq/kg as specified by the manufacturer). **Table 2.1** gives the characteristics of the different polymers. **Figures A2.1-A2.3** and **Table A2.1** (in appendix A) show their FTIR spectra and list of their infrared assignment [310,345-349].

Table 2.1 Chemical Structure of Polymers

No	Name	Structure (repeat unit)	Grade, Form & Properties	Supplier	FTIR
I	Natural rubber (NR)	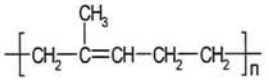	SMR-L (Bale)	MRPRA	Fig. A2.1
II	Polypropylene (PP)	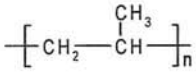	APPRYL-3020/BNI (granular) MFI = 2.0 kg/10min*)	Elf-Atochem	Fig. A2.2
			HF-26 (powder) MFI: 1.7 g/10 min*)	ICI	
III	Poly (butylene terephthalate) (PBT)	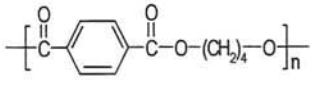	Arnite T08200 (granular) m.p. = 223°C Mw = 654 g/mol Mn = 141 g/mol Hydroxyl :0.032 meq/kg Carboxyl : 0.040 meq/kg	Eastman Chem. Ltd	Fig. A2.3
*) measured according to ASTM D1238 (2.16 kg, 230°C, 1 mm diameter die)					

2.1.2 Monomers and Coagents

Glycidyl methacrylate (GMA), maleic anhydride (MA), trimethylolpropane triacrylate (TRIS) and divinyl benzene (DVB) were all obtained from Aldrich Chemicals Co. and used without further purification. **Table 2.2** gives the characteristics of the different reagents and additives. **Figures A2.4-A2.7** (in appendix A) show their FTIR spectra, see also **Table A2.2** (in appendix A) for their IR assignment.

Table 2.2 Monomers and comonomers used in the functionalisation.

NO	Name	Structure	Colour, form & Purity	Supplier	FTIR
IV	Glycidyl methacrylate **(GMA)**	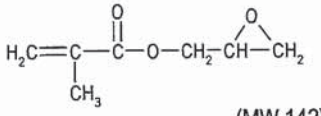 (MW 142)	Colourless liquid Purity: 95 %	Aldrich Chemical Co	Fig. A2.4
V	Maleic anhydride **(MA)**	 (MW 98)	White pellets Purity: 99 %	Aldrich chemical Co.Ltd	Fig. A2.5
VI	Trimethylol propane triacrylate **(TRIS)**	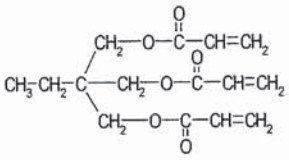 (MW 296)	Viscous colourless liquid Technical grade	Aldrich chemical Co.Ltd	Fig. A2.6
VII	Divinyl benzene **(DVB)**	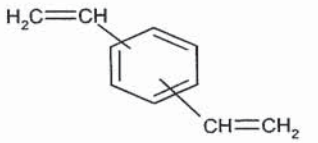 (MW 130)	Colourless liquid Purity: 95 %	Aldrich chemical Co.Ltd	Fig. A2.7

2.1.3 Peroxides

Four different peroxides were used for free radical grafting reactions: 2,5-di(*tert*-butylperoxy)-1,5-dimethyl hexane (TRIGONOX-101®) (T-101), 1,1-di(*tert*-butyl peroxy)-3,3,5-trimethyl cyclohexane (TRIGONOX 29-B90®) (T-29B90) were kindly donated by AKZO Chem. Netherlands, dicumyl peroxide (DCP) ex. Aldrich Chemical Co., and benzoyl peroxide (BPO) ex. Fluka Chemika. Azo-iso-butyronitrile (AIBN) was used for homopolymerisation of monomers, was purchased from Aldrich Chemical Co. **Table 2.3** gives the characteristics of the different peroxides. **Figures A2.8-A2.12** (in appendix A) show their FTIR spectra, see also **Table A2.3** (in appendix A) for their IR assignment.

Table 2.3 The structure, radicals formed, and the half-life time of peroxides [3,53,350].

No.	Structure & Molecular Weight	Form & Purity	Supplier	Radicals formed		Half time (*), $t_{1/2}$ (min) at temp. (°C)						IR
				Primary	Secondary	100°	120°	140°	160°	180°	200°	
IX	2,5-di(*tert*-butylperoxy)-1,5-dimethyl hexane TRIGONOX 101 (T-101) 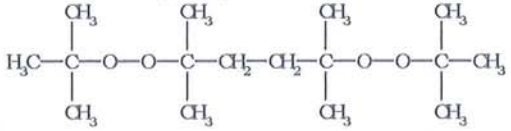 (MW 290)	Colorless (liquid) Purity: 97 %	AKZO	*tert*-butoxy alkoxy 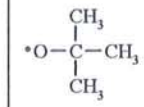	Methyl 	1700	180	23	2.1	1.42	0.30	Fig. A2.8
X	1,1-di(*tert*-butylperoxy)-3,3,5-trimethyl cyclohexane, TRIGONOX 29-B90 (T-29B90) 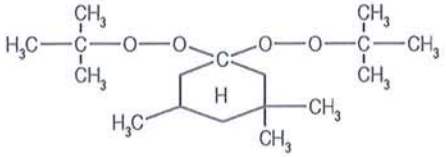 (MW 301)	Colorless (liquid) Purity: 90 % (in dibutyl phthalate)	AKZO	*tert*-butoxy 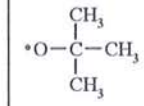	Methyl 	97	14	1.7	0.83	0.1	0.032	Fig. A2.9
XI	Dicumyl peroxide (DCP) 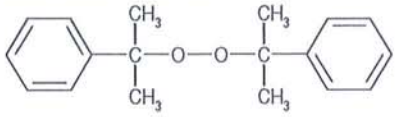 (MW 270)	Colorless (liquid) Purity: 97 %	Aldrich	Cumyl-oxy 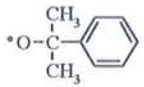	Methyl, phenyl 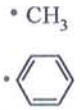	890	120	20	3	1.2	0.25	Fig. A2.10
XII	Benzoyl peroxide (BPO) 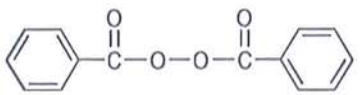 (MW 242)	White (powder) purity 98 %	Fluka	Benzoyl- oxy 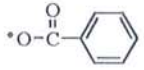	Phenyl 	29	2.5	1	0.32	0.02	0.013	Fig. A2.11
XIII	Azoisobutyronitrile (AIBN) 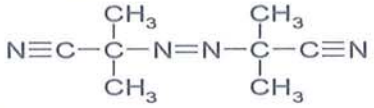 (MW 164)	White (powder) Purity: 99 %	Aldrich	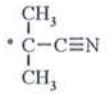		7.2	0.5	-	-	-	-	Fig. A2.12

*) Data estimated from activation parameters provided in commercial product literature from AKZO; MW =Molecular weight

2.1.4 Additives and Solvents

All other chemicals were of reagent grade and were used without further purification. Solvents employed for normal purpose were laboratory reagent grade, for titration were HPLC grade, used as supplied from Fisons, see **Table 2.4** and **Figure A2.13-A2.16** (in appendix A) for their characteristic and FTIR spectra.

Table 2.4 Chemical additives and major solvents used in this work

No	Name	Structure & MW/BP	Supplier	Colour, Form &Purity	FTIR
1	Maleic acid	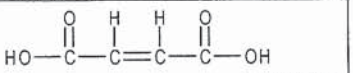 (MW 116)	BDH	White powder Purity: 99%	Figure A2.13
2	Succinic acid	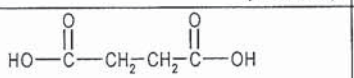 (MW 118)	FISONS	White powder Purity: 99% (AR Grade)	Figure A2.14
3	Succinic anhydride	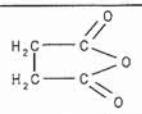 (MW 100)	SIGMA	White pellet Purity: 99% (Analytical Grade)	Figure A2.15
4	Trichloroacetic acid **(TCA)**	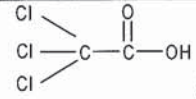 (MW 163)	SIGMA-Aldrich	White powder Purity: 99.5% ACS Reagent	Figure A2.16
5	Stearic acid	$CH_3 (CH_2)_{16} COOH$ (MW 284)	BDH	White pellets Purity: 90%	-
6	Sulfur	S_8 (MW 256)	Robinson Brother	Yellow powder 80%	-
7	Zinc oxide	ZnO (MW 81)	BDH	white powder Purity: 99.7%	-
8	N-Cyclohexyl- 2-benzotiazole Sulphamide **(CBS)**	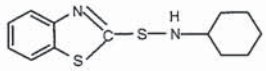 (MW 264)	Robinson Brother	green pellets Purity: 75%	-
9	Xylene	$CH_3(C_6H_4)CH_3$ B.P. 138-139°C	Fisons	HPLC grade	-
10	Toluene	$(C_6H_5)CH_3$ B.P. 110-111°C	Fisons	HPLC grade	-
11	Hexane	C_6H_{14} B.P. 68-69 °C	Fisons	HPLC grade	-
12	di-Chloromethane (DCM)	CH_2Cl_2 B.P. 39-40°C	Fisons	HPLC grade	-
13	Ethyl acetate	$CH_3COOCH_2CH_3$ B.P. 76-77°C	Fisons	HPLC grade	-
14	Methanol	CH_3OH B.P. 64-65°C	Fisons	HPLC grade	-
15	Ethanol	CH_3CH_2OH B.P. 78-79°C	Fisons	HPLC grade	-
16	Acetone	CH_3COCH_3 B.P. 55-56°C	Fisons	HPLC grade	-
17	Chloroform	CH_3Cl B.P. 60-62°C	Fisons	HPLC grade	-

2.2. Polymer Processing

An internal mixer, (HAMPDEN-RAPRA torque rheometer), consisting of a pair of counter rotating rotors in a mixing chamber run by a Brabender motor drive, having a digital torque displaying unit was used to carry out the functionalisation of polymers with GMA and MA and for blending of the polymers. The mixing chamber was heated by circulating oil and controlled by a Churchill heater with a temperature of up to 300°C. The rotor speed was also adjustable (0-250 rpm). Two thermocouples were fitted at the head (head temperature) and the bottom (melt temperature) of the chamber to measure and control the material's temperature.

2.2.1 Preparation of Functionalised PP with GMA and MA

Functionalisation of Polypropylene with Glycidyl methacrylate (GMA) and Maleic anhydride (MA), was conducted in the torque rheometer in the presence or absence of either one of two coagents; trimethylol propane triacrylate (TRIS) or divinyl benzene (DVB). Unless otherwise stated, compounds for reactive processing were prepared by pre-weighing exact amount of the polymer, monomers and coagents (total weight 35 g). In the absence of coagent, the polymer was charged in the preheated mixing chamber, which was initially flushed with oxygen-free nitrogen for more than 15 seconds. After melting and torque stabilisation at the selected processing temperature (about 2-4 minutes after charging of the polymer), the ram was raised for the addition of any other chemicals (GMA and peroxide) by using a long metal-needle syringe to avoid losses (in the case of MA functionalisation, the amount of MA and peroxides was wrapped in a thin film of PP). The ram was lowered down quickly to minimise the loss of GMA or MA due to their high vapour pressure and volatility and this was taken as the zero time of reaction, see **Scheme 4.1** (p.198) and **Scheme 5.1** (p.295) for the processing GMA and MA, respectively. The reaction product was discharged and cooled under a stream of nitrogen or dry ice to avoid further oxidation and stored in a dry and cool place for further analysis. During mixing, the torque reading and mixing temperature were recorded throughout each run using PICOLOG Software. A different method of addition was adopted when a comonomer (coagent) was included in the formulation while maintaining the same processing conditions (i.e. temperature, rotor speed and time). **Table 2.5** summarises typical the processing conditions used in the work.

Table 2.5 The condition for grafting reaction

Processing Conditions Used in The Brabender Torque Rheometer	
Total weight (polymer+monomer+ comonomer+peroxide) (g)	35
Temperature (°C)	120-220
Rotation speed (rpm)	40-100
N_2 flushing time (min)	0.25-0.5
Melting time (pre-mixing) (min)	0 - 4
Mixing time (min)	2.5-15
Mixing atmosphere	Nitrogen, closed system
Cooling	N_2 or dry ice

2.2.2 Preparation of Functionalised Natural Rubber with GMA

Melt free radical grafting of Glycidyl methacrylate (GMA) onto Natural rubber (NR) (SMR-L) was carried out in a similar way to that described above. SMR-L supplied as a large rubbery slab were cut into wafers then strips and dumped out onto a two-roll mill for two minutes, sheeted out, cut into small pieces. The required amount of SMR-L was charged in the preheated torque rheometer mixing chamber. Two minutes premixing was performed followed by the addition of the required amount of GMA and peroxide. At the end of the processing, the reacted NR was discharged and placed into a cup which was purged with nitrogen until it cooled down to below 90°C to avoid further oxidation, see **Scheme 3.1** (p.121)

2.2.3 Blending of PP/PBT

Physical and reactive blending of PP with PBT was also carried out in the Hampden-RAPRA torque rheometer. The PP and PBT were pre-dried at 90°C and 130°C, respectively, in vacuum oven for 24 hours before blending. Due to the density difference between PP and PBT, the weight to fill the mixing chamber depended on the blending weight ratio of PP to PBT. It was found that at a ratio of 80/20 PP/PBT, the actual weights of the blend components were 28g and 7g, respectively. Pre-weighed PP and PBT and functionalised PP (when used) were tumble mixed in a paper cup. The polymer mixture was introduced into the preheated mixing chamber after flushing with nitrogen and then the ram was lowered down quickly to keep a closed system. The mixing temperature, rotor

speed and mixing time were fixed at 265°C, 65 rpm, and 10 minutes. At the end of the processing, the polymer blends were removed from the chamber and cooled down in dry ice to prevent further oxidation of the polymers. The processed polymer blends were granulated, placed into air-tight plastic bags, and used for the preparation of films or plaques for further analysis.

2.3 Preparation of Polymer Films, Plaques and Sheets

2.3.1 Preparation of Polymer Films for FTIR Analysis

Thin films (100-200 μm thickness) of processed PP, NR, and their blends with PBT were prepared for FTIR analysis by compression moulding using Daniel Press equipped with electrically heated plates which can be cooled down using circulating cooling water. About 0.2 g of functionalised polymers (purified or unpurified), or polymer blends samples were placed between two PTFE (Teflon) coated fabric sheets placed between polished flat stainless steel plates. After one minute preheating at 150° and 180°C for NR and PP, respectively, the sheets were pressed into thin films for 1-2 minute under pressure of 60 kg/cm^2 followed by cooling the press platens (with the mould plates inside) down to 50°C before taking the plates out and removing the film samples.

In the case of natural rubber, it was difficult to press the processed polymer samples into thin films directly for FTIR measurement due to the tackiness of the rubber. The grafted or raw natural rubber samples were therefore cured first to produce films. The rubber (weights based on part per hundred rubber, phr) ingredients used for curing (conventional vulcanizing system) were: zinc oxide (3 phr), stearic acid (2.5 phr), accelerator CBS (0.75 phr), and sulfur (3 phr). The Rubber and the curing ingredients were mixed on a two-roll mill for less than 1 minute at room temperature. In the mixing procedure, sulfur was added at the final stage to avoid pre-vulcanization (scorching). **Table 2.6** gives the composition of chemicals used in curing the natural rubber. The compounded rubber was sheeted out as thin as possible. To produce a film of natural rubber with a thickness of ~100-200 nm, about 0.2 g of the compounded rubber sheets were cut out and placed in the middle area between two polished stainless steel plates which were laminated across both surfaces with a folded sheet of special heat resistant grade cellophane and the plates assembly pressed

using a Daniel Press at 150°C for 2 minutes under pressure of 60 kg/cm^2. **Figure 2.1** (p.85) shows a typical FTIR of a cured thin NR-*g*-GMA film.

Table 2.6 Compounding for Making Cured NR Films

Composition	Concentration		Vulcanisation Conditions
	phr	g	
SMR-L	100	5	
Zinc oxide	3	0.15	Temp.: 150°C
Stearic acid	2.5	0.125	Time : 2 minutes
Accelerator	0.75	0.0375	Pressure: 60 kg/cm^2
Sulfur	3	0.15	(Daniel Compression Moulding Press)

2.3.2 Preparation of Polymer Plaques and Sheets

Plaques of polymer blend samples of ~3 mm thickness were prepared by compression moulding scanning electron microscopy (SEM) analysis. About 8 g granulated polymer samples which were dried in a vacuum oven at 85°C for 24 hours were placed inside a stainless steel spacer with the appropriate thickness laminated across both surfaces with a folded sheet of PTFE (Teflon). This assembly which was covered with two polished stainless steel plates, was placed between the electrically heated platens of Daniel press, set at 265°C and held for 2 minutes under minimum pressure. The lower platen was raised up slowly under pressure of 60 kgf/cm^2 applied for 1 minute, heating was then switched off and cold water circulated through the platens, whilst maintaining full pressure until temperature dropped down to 50°C. Sheet samples with thickness of ~1 mm were also prepared for tensile properties measurements using similar procedure as above. About 1 g of the blend samples (dried) were placed inside 1 mm thickness spacers place in between stainless steel plates and pressed under similar condition as above.

2.4 Purification of Reaction Products

In order to ensure accurate evaluation of the grafting degree, the reaction products were purified to eliminate any unreacted monomers (e.g. free-GMA), homopolymer of the monomer and all side reaction products. Two methods were used, i.e. precipitation and Soxhlet extraction.

2.4.1 Precipitation

In the case of GMA grafted PP products in the absence of coagent (conventional), purification was carried out as follows: 4 g processed sample was dissolved in 100 ml hot xylene (temperature was kept at 110-120°C, 30 minutes). The reaction product (completely soluble in the hot xylene) was precipitated by drop-wise addition in either 7 times excess of methanol or acetone (the precipitation was conducted in a beaker 1000 ml using magnetic stirrer). When coagents TRIS or DVB was used, the homopolymer of the coagents (poly-TRIS or poly-DVB), the copolymer of coagents and GMA (GMA-*co*-TRIS or GMA-*co*-DVB), and crosslinked polymer, were separated out first by Soxhlet extraction as xylene insoluble, before precipitated by methanol or acetone. The precipitated product was filtered out, washed by methanol or acetone, and then dried in vacuum oven for 24 hours at temperature of 80°C. By using different solvents for the precipitation, the concentration of grafted-GMA (PP-*g*-GMA), homopolymerised GMA (poly-GMA) and unreacted GMA (free-GMA) can be determined by titration and FTIR analysis methods (see **Section 2.5.2** and **2.5.4**).

2.4.2 Soxhlet Extraction

Soxhlet extraction was used to purify the GMA functionalised NR (NR-*f*-GMA) and the MA functionalised PP (PP-*f*-MA) samples. In the case of NR-*f*-GMA, thin sheets or films of the reaction products (produced by vulcanization as describe in **Section 2.3.1**) were exhaustively Soxhlet extracted with acetone for 24 hours to remove free-GMA, poly-GMA and other low molecular mass materials. The concentration of grafted-GMA in the sample films before and after extraction was determined by titration and FTIR (**Section 2.5.2** and **2.5.4**).

In the case of PP-*f*-MA, thin film of the functionalised PP was exhaustively Soxhlet extracted by dichloromethane (DCM) to remove unreacted MA (free-MA or poly-MA). It was found that 24 hours extraction was sufficient to remove the free-MA and poly-MA from the reaction product. The extracted samples were dried overnight in a vacuum oven at room temperature. The concentrations of MA in the sample films before and after extraction was determined by titration and FTIR (see **Section 2.5.3** and **2.5.4**)

2.5 Determination of GMA and MA Grafting Degree

2.5.1 Definition of Grafting Degree and Grafting Efficiency

The grafting parameters were calculated from the mass of a sample before and after grafting. The percentage of grafting yield or grafting degree and the grafting efficiency were calculated according to the following definitions.

1. **Grafting Degree (%)** is defined as the weight percentage of grafted-monomer onto a polymer backbone (purified reaction products) (**Eq.2.1**).

$$\text{Grafting Degree (\%)} = \frac{\text{Mass of grafted monomer (after purification)}}{\text{Mass of polymer sample}} \cdot 100 \qquad \textbf{(Eq. 2.1)}$$

   For example, if the amount of GMA in 2 g of purified (acetone purification) reaction products (PP-*g*-GMA) was determined by titration (**Section 2.5.2**) and contained 0.01 g grafted-GMA, then the GMA grafting degree in the reaction product is,

$$\text{Grafting degree of GMA} = x \frac{0.01\ g}{2\ g} 100 = 0.5\ \%$$

2. **Grafting Efficiency (%)** is the percentage ratio of the amount of a functional monomer that becomes grafted onto a polymer to the amount of the same functional monomer initially added to the polymer (**Eq. 2.2**).

$$\text{Grafting Efficiency (\%)} = \frac{\text{Mass of grafted monomer (g)}}{\text{Mass of GMA initially added (g)}} \cdot 100 \qquad \textbf{(Eq. 2.2)}$$

For example, if 4g monomer GMA added initially in processing with 40g of polymer Polypropylene (≅ 10 phr GMA) and after processing the GMA grafting degree was 0.5 %. The actually amount of GMA converted to grafted-GMA will be 0.5/100 x 40 = 0.2 g), then the grafting efficiency of the GMA would be 5 %.

$$\text{Grafting Efficiency, \%} = \frac{0.2\ g}{4\ g} \times 100 = 5\ \%$$

The purified reaction products were determined by a titration method and/or FTIR analysis. In reaction products of PP/GMA/TRIS/T-101 system (GMA functionalised-PP in the presence of coagent TRIS), for example, the reaction products may contain: unreacted GMA (free-GMA), grafted-GMA (PP-*g*-GMA), GMA homopolymer (poly-GMA), unreacted TRIS (free-TRIS), homopolymerised TRIS (poly-TRIS), copolymer of GMA and TRIS (GMA-*co*-TRIS), crosslinked PP, and TRIS-assisted crosslinking of PP. **Table 2.7** gives the solubility of the different products and reactants in different solvents.

Table 2.7 Solubility of monomers reactants and products typically found in the grafting system.

COMPOUND	Solubility at room temperature (RT) and at the solvent boiling temperature (BT)							
	Methanol		Acetone		DCM		Xylene	
	RT	BT	RT	BT	RT	BT	RT	BT
GMA	Y	Y	Y	Y	Y	Y	Y	Y
MA	Y	Y	Y	Y	Y	Y	Y	Y
DVB	Y	Y	Y	Y	Y	Y	Y	Y
TRIS	Y	Y	Y	Y	Y	Y	Y	Y
PP	N	N	N	N	N	N	N	Y
NR	N	N	N	N	partly	Y	N	N
Poly-GMA	N	N	Y	Y	N	Y	N	Y
Poly-DVB	N	N	N	N	N	N	N	N
Poly-TRIS	N	N	N	N	N	N	N	N
GMA-*co*-DVB	N	N	N	N	N	N	N	N
GMA-*co*-TRIS	N	N	N	N	N	N	N	N
PP-*g*-GMA	N	N	N	N	N	N	N	Y
PP-*g*-MA	N	N	N	N	N	N	N	Y
NR-*g*-GMA	N	N	N	N	N	partly	N	N
Y = soluble, N= Not soluble, RT = room temperature, BT = solvent boiling temperature								

In the case of GMA, after the Soxhlet extraction therefore, the xylene extract (soluble) contains mainly:

1. Grafted GMA (PP-*g*-GMA)
2. Homopolymer GMA (poly-GMA]
3. Unreacted GMA (free-GMA)

The total GMA was determined by a titration method and/or FTIR analysis from unpurified reaction products whereas PP-*g*-GMA, poly-GMA and free-GMA were calculated by subtraction of the total-GMA from the GMA obtained from the different precipitation methods (methanol and acetone) (see **Eq. 2.3–2.6**)

Total GMA was determined by titration and/or FTIR method from unpurified samples,

$$\textbf{Total GMA} = \textbf{Grafted GMA + Poly-GMA + Free GMA} \qquad \textbf{Eq. 2.3}$$

Grafted GMA was determined by titration and/or FTIR method from purified (acetone precipitation) samples,

$$\textbf{Grafted GMA} = \textbf{Total GMA} - \textbf{(Poly-GMA + Free GMA)} \qquad \textbf{Eq. 2.4}$$

Free-GMA was determined by titration and/or FTIR method from unpurified and purified (methanol precipitation) samples:

$$\textbf{Free GMA} = \textbf{Total GMA} - \textbf{(Grafted GMA + Poly-GMA)} \qquad \textbf{Eq. 2.5}$$

Poly-GMA was determined by titration and/or FTIR method from purified (acetone and methanol precipitation) samples,

$$\textbf{Poly-GMA} = \textbf{Total GMA} - \textbf{(Grafted GMA + Free GMA)} \qquad \textbf{Eq. 2.6}$$

2.5.2 Determination of GMA Grafting Degree by Titration

An acid-base, non-aqueous back titration method was established to determine the grafting degree of GMA **[119,125,127]**. A modified procedure of the literature employing trichloro acetic acid (TCA)-xylene method was used in this work to determine the epoxy content in PP-*g*-GMA and NR-*g*-GMA as follows: 1 g of the purified reaction product (PP-*g*-GMA) was dissolved in 100 ml of hot xylene (120-130°C) in a two-neck flask, connected to a condenser and maintained under nitrogen atmosphere. After the PP-*g*-GMA had completely dissolved (15-30 min) the condenser was removed. The flask was stoppered and placed in an oil bath maintained at lower (stable) temperature of 105-110°C. It was very important to keep the system at this temperature (thermometer was placed in the oil bath) before addition of 5 ml (excess) of 0.3 N trichloro acetic acid (TCA) and the reaction was allowed

to continue for 90 min in order to achieve complete ring opening of the epoxy group by its reaction with the acid (**Scheme 2.1, Rn-1** and **Rn-2**). The hot solution was then titrated with 0.1 N KOH (standard solution) in methanol. In the presence of indicator (five drops of 1 % w/v phenolphthalein in ethanol), endpoint was reached when the colour (pink) had formed and remains for at least 30 seconds (see **Scheme 2.1, Rn-2.3**).

Scheme 2.1 Acid-Base Reaction of titration in determination of grafting degree GMA on NR and PP

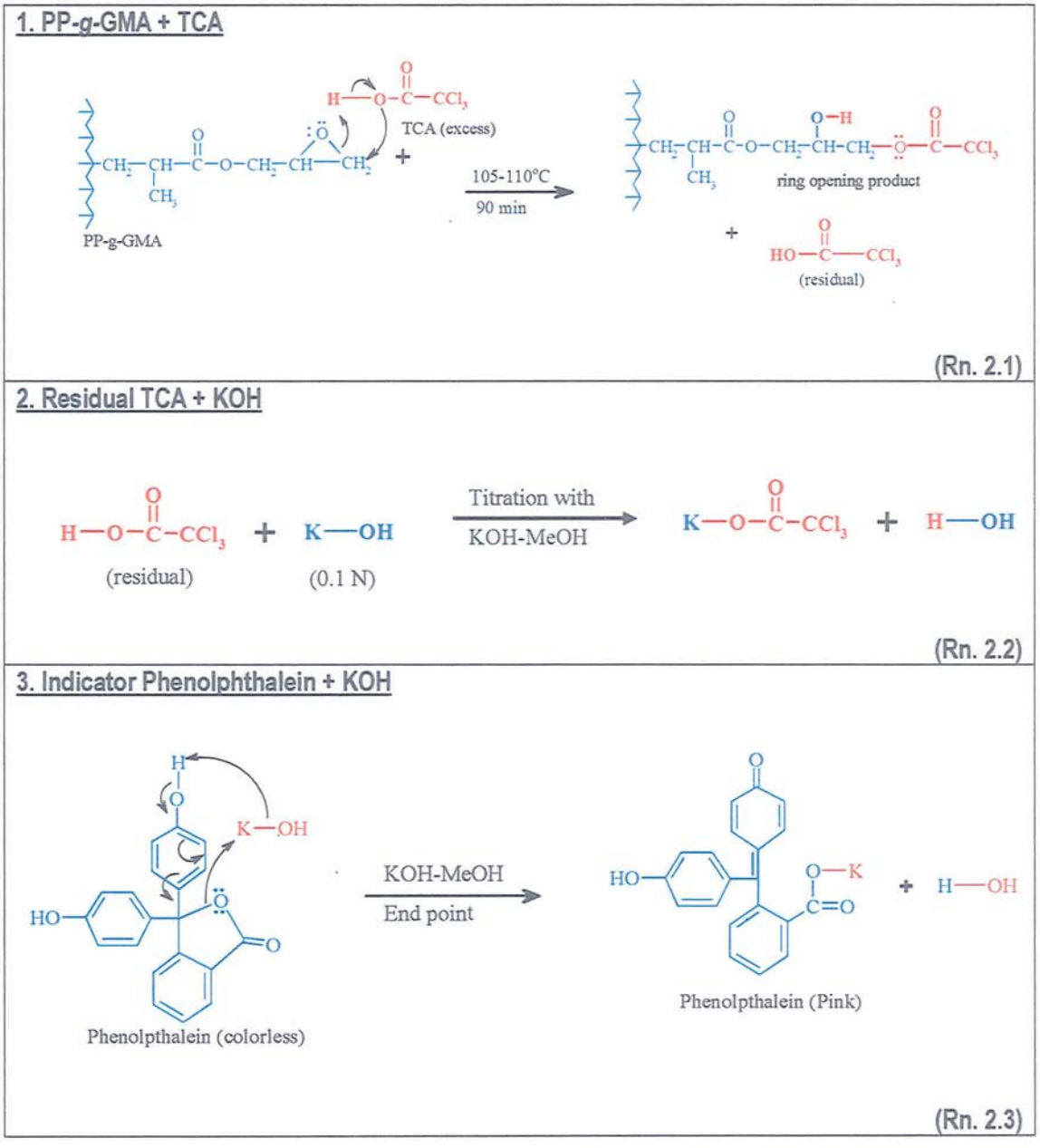

Similarly a 1g unmodified processed PP which was used as a blank sample was dissolved in xylene, reacted with excess TCA, precipitated and filtered out, then titrated with KOH solution in the same way as that described above for the modified sample. Theoretically, the amount of KOH (0.1 N) consumed to neutralise 5 ml TCA (0.3 N) was 5 x 0.3/0.1 = 15 ml (in a blank sample). Less KOH would be consumed by the modified polymer (NR-*g*-GMA or PP-*g*-GMA) than in the case of the blank sample due to the reaction of TCA with GMA in the former case.

Titration for every purified sample was carried out in duplicates or triplicates to establish the experimental error, (see **Eq. 2.7**). The percent error of the grafting degree determined by titration was found to be in the range of ± 7 %.

$$\text{Grafting Degree GMA (\%)} = \frac{\text{N (eq/L)}\ [(V_o\text{-}V)\ \text{ml}]\ MW_{GMA}\ \text{g/eq}}{1000\ \text{mg/1g}} \times 100 \quad \textbf{(Eq. 2.7)}$$

Where,

N = concentration of KOH (0.1 N)

V = ml KOH used in titration of the modified polymer sample

V_o = ml KOH used in titration of unmodified (blank) sample

MW_{GMA} = the molecular weight of GMA, 142 g/mol

1000 = weight of 1000 mg, conversion from 1g)

For example, if 1 g purified reaction product from PP-*g*-GMA which was dissolved in xylene, reacted with 5 ml TCA, titrated with KOH (0.1 N) had consumed 13.1 ml, whereas a 1 g PP (a blank sample) consumed 14.5 ml KOH, then the degree of grafting of GMA on PP-*g*-GMA will be:

$$\text{Grafting degree (\%)} = \frac{0.1\ (14.5\text{-}13.1) \times 142}{1000} \times 100 = 2.0\ \%$$

For measurement of experimental error, some samples were processed in a torque rheometer in triplicate; for example, sample G9-2 (GMA 9 %, T-101 0.002 mr). After purification, each sample was then titrated in triplicates. The experimental error of grafting yield by titration method was found to be 5 - 12 %, see **Table 2.8**. Standard deviation in the measurement of grafting degree by titration is shown in **Eq. 2.8**

$$SD = \sqrt{\frac{\sum (G_i - G)^2}{n}} \qquad \textbf{(Eq. 2.8)}$$

Where,

SD = standard deviation of measurements

G_i = Grafting yield measurement i (%)

G = Average of grafting yield

n = numbers of samples titrated

The GMA-grafted PP films were also characterised by using Fourier Transform Infrared (FTIR) to determine the relative amount of grafted GMA onto PP and NR (**Section 2.5.4**).

Table 2.8 Standard deviation in the grafting degree measurement by titration for sample G4-3 processed in triplicates in the torque rheometer; GMA 9%, T-101 0.3 phr (0.016 mr).

Number of Processing	Volume 0.1M KOH used (ml) [a]	Grafting yield (%) [b]	Average grafting yield	Standard deviation [c]
I	V_1 = 13.6	1.8	1.97	0.12
	V_2 = 13.5	2.0		
	V_3 = 13.4	2.1		
II	V_1 = 13.5	2.0	1.87	0.09
	V_2 = 13.6	1.8		
	V_3 = 13.6	1.8		
III	V_1 = 13.7	1.7	1.73	0.05
	V_2 = 13.6	1.8		
	V_3 = 13.7	1.7		

a) Volume KOH used for blank sample = 14.9 ml
b) Using equation 2.7
c) Using equation 2.8

2.5.3 Determination of the Grafting Degree of MA by Titration

The quantity of grafted MA onto the PP backbone molecules was determined by a back titration method of the acid groups derived from the anhydride function **[177,181,344-346]**. 1 g sample of the MA grafted polypropylene was dissolved in 100 ml of xylene in a two-neck round-bottom flask (at boiling temperature, 135°C for 15-30 min). In order to

hydrolyse the maleic anhydride function, 1 ml of water was introduced into the solution of PP-*g*-MA/xylene system and the reaction was controlled at lower temperatures, 105-110 °C for 90 min in order to achieve complete hydrolysis (**see Scheme 2.2, Rn.2.4**). Bromothymol blue indicator, BTB (5 drops) was added before titration with KOH in methanol 0.1 N (titration was established in the hot solution). The addition of KOH was stopped after the change of colour, visual end point, from pale yellow to blue, and excess KOH (0.5 ml) was added, dark blue solution obtained). Back titration was then carried out with HCl solution (0.1 N standard solution in methanol) until the endpoint (when the blue colour solution changed to a stable pale yellow). The volume (ml) of KOH and HCl consumed in the titration was used to calculated the amount of MA in the MA functionalised-PP (see **Scheme 2.2, Rn. 2.4** to **Rn. 2.7).** The carboxylic acid concentration from the hydrolysed MA was converted to grafting degree of MA onto polypropylene and calculated as follows:

$$\text{Grafted degree MA (\%)} = x \quad \frac{(V_B.N_B) - (V_A \,.\, N_A)}{2 \times 1000 \times W_s} \; MW_{MA} \times 100 \qquad \textbf{(Eq. 2.9)}$$

Where,

V_B : volume of KOH used, ml

V_A : volume of HCl used, ml

N_B : concentration of KOH (Normality) meq/ml

N_A : concentration of HCl, (Normality) meq/ml

MW_{MA}: Molecular weight of Maleic anhydride, 98 g/mol

W_s : weight of the samples of PP-*g*-MA, g.

2 : conversion factor of two carboxylic acid formed from 1 molecule MA

1000 : conversion factor from 1g to 1000 mg.

For example, 1 g of the purified PP-MA (solution in hot xylene) titrated and consumed 4.5 ml KOH (0.1 N) and 0.6 ml HCl (0.1 N).

$$\text{MA Grafting degree (\%)} = x \quad \frac{(4.5 \times 0.1\text{meq/ml}) - (0.6\text{ml}.0.1\text{meq/ml})}{2\text{eq/mol} \times 1000 \times} \; 98 \text{ g/mol} \times 100$$

$$= 1.9\ \%.$$

In similar way, the maleated-PP films were also characterised by using Fourier Transform Infrared (FTIR) to determine the relative amount of grafted MA onto PP.

Scheme 2.2 Acid-Base Reaction of titration in determination of grafting degree MA on PP (using indicator: Brom thymol blue, BTB)

1. Hydrolysis Grafted MA

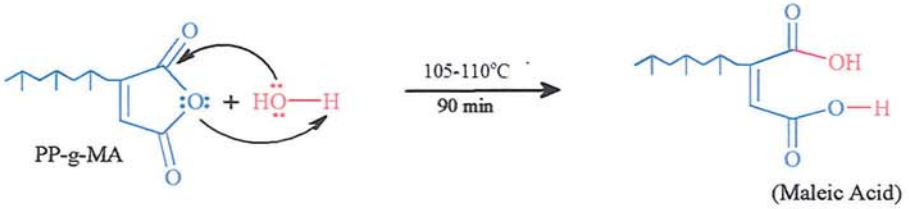

(Rn. 2.4)

2. Hydrolysed Grafted-MA + KOH

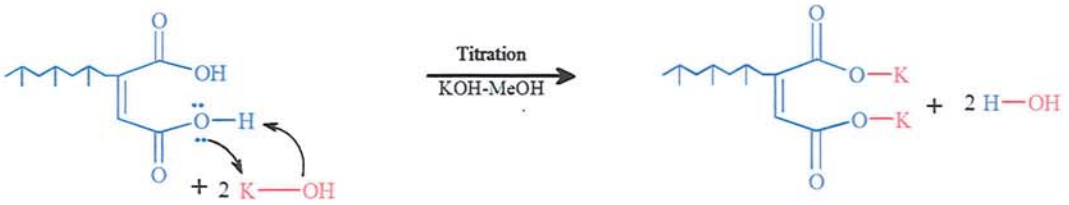

(Rn. 2.5)

3. KOH (excess) + HCl

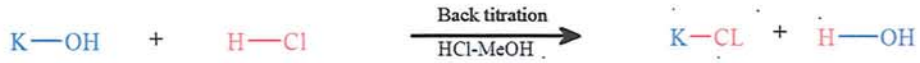

(Rn. 2.6)

4. Indicator BTB + KOH and HCl

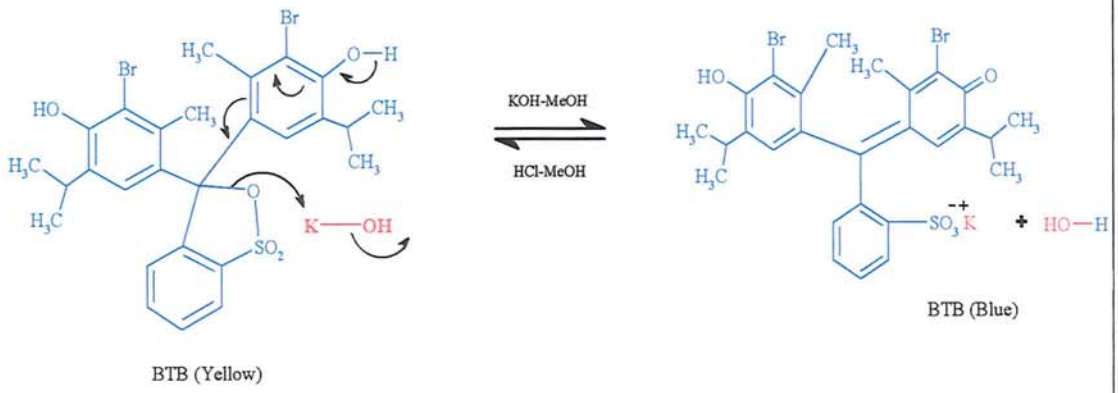

(Rn. 2.7)

2.5.4 Determination of the Grafting Degree of GMA and MA by FTIR Method

The entire modified polymer samples (purified and unpurified) were also characterised by Fourier Transform Infrared (FTIR) analysis. The modified polymers were made into thin films as described in **Section 2.3.1**. A Perkin Elmer Spectrum-1 and NICOLET 5DXC-FTIR spectrometers were used to analyse the polymer films with spectra obtained over the range 4000 cm^{-1} to 400 cm^{-1} for 64 scans with a resolution of 4 cm^{-1}. Semi quantitative analysis of the extent of grafting was also obtained from IR absorption area ratio of a characteristic group peak (e.g. carbonyl peak of MA and GMA) relative to a polymer reference peak (used as internal standard) in order to eliminate experimental error due to variation in film thickness. In the FTIR instrument systems, it has been equipped with a menu called 'normalised scale' in data processing whose function was to normalise the absorbance measurement or absorbance subtraction in order to eliminate the problem of differences in thickness.

The grafting degree of GMA onto NR (NR-*g*-GMA) was calculated from the peak area absorbance of peak at 1731 cm^{-1} ($A_{1731\ cm\text{-}1}$) with the range of 1680 cm^{-1} to 1770 cm^{-1} ($A_{1680\text{-}1770\ cm^{-1}}$) and an internal reference peak at 2725 cm^{-1} with range 2705 cm^{-1} to 2745 cm^{-1}($A_{2705\text{--}2745\ cm^{-1}}$), see **Fig. 2.1**. The peak 1731 cm^{-1} is characterised as vibration of carbonyl group, υ (>C=O), of grafted GMA (>C=O) on NR. The peak 2725 cm^{-1} is assigned to a stretching-mode vibration of methyl group, υ(C-CH_3), of NR, served as an internal standard. The value of the normalised absorbance (the absorbance was normalised for the film thickness) at 2725 cm^{-1} do not change practically with increasing the normalised absorbance at 1731 cm^{-1} ($A_{1731\ cm\text{-}1}$), see **Fig. 2.2.** It shows that the peak area absorbance at 2725 cm^{-1} as internal reference is independent of the peak area absorbance of carbonyl peak of grafted GMA. This finding demonstrates that the internal standard peak at 2725 cm^{-1} was selected correctly as it did not change as a function of the grafting degree of GMA onto NR.

A calibration curve was then set up between the peak area absorbance from the carbonyl peak at 1731 cm^{-1} and peak area absorbance from internal reference peak at 2725 cm^{-1} (referred as peak area index) from IR and amount of grafting degree calculated from the

titration, see **Fig. 2.3**. The grafting degrees of GMA on NR (NR-*g*-GMA) were then determined from the **Eq. 2.10** as follows:

$$Y = 2.35\,X \qquad \textbf{(Eq. 2.10)}$$

Where, Y is the peak area index from FTIR measurement ($A_{1680\text{-}1770\ cm\text{-}1}/(A_{2705\text{-}2745\ cm\text{-}1}$) and X is resulting grafting degree of GMA to PP from titration. Similar to the above procedure, the grafting degrees of GMA onto PP (PP-*g*-GMA) was calculated from **Eq. 2.11** (see **Fig. 2.4** to **2.6**)

$$Y = 0.9\,X \qquad \textbf{(Eq. 2.11)}$$

and grafting degree of MA on PP (PP-*g*-MA) from Eq. 2.12 (see **Fig. 2.7** to **2.9**).

$$Y = 1.95\,X \qquad \textbf{(Eq. 2.12)}$$

In the case of grafting MA on PP, grafted-MA has three peak of carbonyl at 1724 cm^{-1}, 1781 cm^{-1} and 1856 cm^{-1}, peak area index was calculated as total area of the peaks ($A_{1672\text{-}1752\ cm\text{-}1} + A_{1752\text{-}1820\ cm\text{-}1} + A_{1820\text{-}1890\ cm\text{-}1}$).

2.6 Determination of Insoluble Gel

The insoluble gel, or gel content, is a measure of the insoluble fraction caused by crosslinking of a modified polymer after being exhaustively extracted with a solvent that dissolves the virgin polymer. 1 gram of processed polymer sample was placed in a known weight paper thimble and was Soxhlet extracted using xylene as a solvent for 24 hours. The extractor was covered with aluminium foil to maintain hot xylene temperature at 135°C. Nitrogen was introduced into the system to avoid oxidation during extraction. The thimble was dried in vacuum oven at room temperature for 24 hours and reweighed. The net weight of the residue was obtained and gel content was calculated as shown in **Eq. 2.13**.

$$\text{Gel Content (\%)} = \frac{W_1}{W_2} \times 100 \qquad \textbf{(Eq. 2.13)}$$

Where,

W_1 = weight of the extracted polymer which remains insoluble in the thimble

W_2 = weight of the polymer before extraction.

2.7 Measurement of Melt Flow Index (MFI)

The melt flow index, MFI, is a measure of melt viscosity, critically influenced by the physical properties and molecular structure, giving an indication of changes in the molecular weight and molecular weight distribution of the polymer (polydispersity) at the condition of measurement. The MFI test method measures the rate of extrusion of molten polymer through a die of a specified length and diameter under prescribed conditions of temperature, load, and piston position in the barrel. MFI of polypropylene was measured on a Devonport Melt Flow Indexer at a constant extrusion temperature of 230°C and 2.16 kg load in accordance with ASTM D-1238. A standard die of 1 mm diameter was used for all samples. Three gram of granulated samples was inserted into the barrel within one minute to ensure minimum degradation. Any air was trapped in the polymer must be excluded from the barrel by tapping down the polymer with the charging tool. The piston with the pre-extrusion weight, 2.16 kg, was then placed into the barrel and lowered until it reached the metal block. After 3 min preheating, the metal block was removed and the polymer was left to extrude through the die until the lower mark of the piston coincided with the top of the barrel. The extrudate was then cut off to start the measurement, cutting strands at time interval at 0.25, 0.50, 1.00, 3.00, or 6.00 min depending on the flow rate of the polymer. The melt flow index (MFI) sample and the change of the MFI (relative to the virgin polymer) were calculated as shown in **Eq. 2.14** and **2.15**.

$$\text{MFIs (g/10min)} = \frac{10 \cdot m}{t} \qquad \textbf{(Eq. 2.14)}$$

$$\%\ \text{MFI change} = \frac{MFI_s - MFI_v}{MFI_v} \times 100 \qquad \textbf{(Eq. 2.15)}$$

Where,

m : the average weight of extrudates, g
t : time of extrusion, min
10 : 10 minutes
MFI_s : the Melt Flow index of the processed polymer.
MFI_v : the Melt Flow index of unprocessed polymer (virgin)

2.8 Fourier Transform Infrared Spectroscopy (FTIR)

FTIR measurements were performed on a Nicolet spectrophotometer 5DXC over the range of 4000-400 cm^{-1} at 4 cm^{-1} resolution and spectral collection over 64 scans. A dedicated computer was used to control the spectrophotometer with OMNIC software. Polymer film specimen was clamped by magnetic ring onto a metal plate having a 25 x 14 mm aperture. The FTIR spectra of liquid samples were recorded as thin film of the chemical used held in the infrared beam between two KBR discs. For the solid samples, FTIR spectra were obtained using potassium bromide disc. The obtained spectra were saved on the computer for subsequent analysis and manipulation.

2.9 Scanning Electron Microscopy (SEM)

Morphology of the blends was characterised from a cross-section of cryogenically fractured surfaces of the compression moulded plaques using Cambridge Instruments Stereoscan 90 Scanning Electron Microscope. Strips cut out from the compression moulded plaques (3 mm thickness) were immersed in liquid nitrogen for more than 15 minutes to cool down and then taken out to fracture manually. The middle of the cooled sample strips was clamped with an adjustable spanner and the free part of the strips were bended quickly by hand to fracture the samples. For better observation, the fractured surfaces were subjected to etching with the mixture solvent (chloroform: phenol, 2:3 weight ratio) to remove poly (butadiene terephthalate), PBT phase. After the extraction for 3-4 hours, the samples were dried overnight in a vacuum oven at temperature 80°C. The ends having fractured surfaces were sliced with a sharp razor blade and attached to a metal stub using a double sided sticky carbon pad with the fractured surface facing up. The samples were sputter coated with gold using an Emscope SM300 Coater prior to SEM examination. The viewed SEM micrographs at appropriate magnification were saved as individual files for subsequent analysis.

2.10 Homopolymerisation of Monomers and Coagents

During the grafting process of GMA onto PP in the presence of the co-agent TRIS or DVB, homopolymerisation of GMA, TRIS, and DVB and copolymerisation of GMA and TRIS or DVB (GMA-*co*-TRIS or GMA-*co*-DVB) could also take place. To analyse the reaction

products poly-GMA, poly-TRIS or Poly-DVB, and GMA-*co*-TRIS or GMA-*co*-DVB were synthesised on the bench.

2.10.1 Homopolymerisation of GMA in Hexane

Homopolymerisation of glycidyl methacrylate (GMA) was carried out using α, α', Azo-iso-butyronitrile (AIBN) as an initiator in hexane. 9g GMA and 1 g AIBN (0.1 molar ratio AIBN/GMA) were mixed in 100 ml hexane using a 250 ml two-neck round bottom flask. After assembling the two-neck round bottom flask with a thermometer, a condenser and purging with oxygen-free nitrogen, the solution was maintained at a temperature of 68°C for 5 hours. After cooling to room temperature, the solution was precipitated into 500 ml methanol, filtered off and washed thoroughly with methanol. The precipitation in methanol was to remove any free GMA. And after drying in vacuum oven for 24 hours at room temperature, the white solid obtained was characterised by FTIR. The FTIR spectrum of the white particle (poly-GMA) is shown in **Figure A2.17** (in appendix A) and FTIR characterisation is given later in **Chapter 4**.

2.10.2 Homopolymerisation of TRIS in hexane

Homopolymerisation of Trimethylolpropane triacrylate (TRIS) was carried out using α, α', Azo-iso-butyronitrile (AIBN) as an initiator in hexane. An amount of 9g TRIS were mixed with 1 g AIBN (0.2 molar ratio AIBN/TRIS) mixed in 100 ml hexane in a 250 ml two-neck round bottom flask. After assembling with a thermometer and a condenser and purging with oxygen-free nitrogen, the solution was maintained at a temperature of 68°C for 5 hours. The hot solution was precipitated in 500 ml of acetone, filtered off and washed thoroughly with acetone before drying in vacuum oven for 24 hours at room temperature. The precipitation in acetone was to remove any free TRIS and the reaction product obtained was characterised by FTIR. The FTIR spectrum of the white solid (poly-TRIS) is shown in **Figure A2.18** (in appendix A) and FTIR characterisation is given later in **Chapter 4**.

2.10.3 Homopolymerisation of DVB in Hexane

Homopolymerisation of divinyl benzene (DVB) was carried out using α, α', Azo-iso-butyronitrile (AIBN) as an initiator in hexane. 9g DVB was mixed with 2.3 g AIBN (0.2 molar ratio AIBN/DVB) in 100 ml hexane in a 250 ml three-neck round bottom flask. After

assembling with a thermometer and a condenser and purging with Oxygen-free Nitrogen gas, the solution was maintained at a temperature 68°C for 5 hours. The hot solution was then precipitated in 700 ml of acetone, filtered off and the precipitate was dried in vacuum oven for 24 hours at room temperature. Precipitation in acetone was to remove any free DVB and the product obtained was characterised by FTIR. The FTIR spectrum of the white solid (poly-DVB) is shown in **Figure A2.19** (in appendix A) and FTIR characterisation is given later in **Chapter 4**.

2.10.4 Copolymerisation of TRIS and GMA in Hexane

Copolymerisation of Trimethylolpropane triacrylate (TRIS) and glycidyl methacrylate (GMA) was carried out using α, α', Azo-iso-butyronitrile (AIBN) as an initiator. 6 g GMA, 2.6 g TRIS (3/7 weight ratio of TRIS/GMA) and 1.7 g AIBN (0.2 molar ratio AIBN/TRIS+GMA) were mixed in 100 ml hexane using a 250 ml two-necked round bottomed flask. After assembling with a thermometer and a condenser and purging with oxygen-free nitrogen gas, the solution was maintained at a constant temperature of 68°C for 5 hours. The hot solution was then precipitated in 700 ml of acetone, filtered off, washed thoroughly with acetone before drying in a vacuum oven for 24 hours at 80°C. The precipitation in acetone was to remove any free-GMA, free-TRIS and poly-GMA and the reaction product obtained was characterised by FTIR. The FTIR spectrum of the white solid (GMA-*co*-TRIS) is shown in **Figure A2.20** (in appendix A) and FTIR characterisation is given later in **Chapter 4**.

2.10.5 Copolymerisation of DVB and GMA in Hexane

Copolymerisation of divinyl benzene (DVB) and glycidyl methacrylate (GMA) was carried out using α, α', Azo-iso-butyronitrile (AIBN) as an initiator in hexane. 6 g GMA, 2.6 g DVB (3/7 weight ratio DVB/GMA) and 2.1 g AIBN (0.2 molar ratio AIBN/DVB+GMA) were mixed in 100 ml hexane using a 250 ml two- necked round bottomed flask. After assembling with a thermometer and a condenser and purging with oxygen-free nitrogen gas, the solution was maintained at a constant temperature of 70°C for 5 hours. The hot solution was then precipitated in 700 ml of acetone, filtered off and washed thoroughly with acetone before dried in vacuum oven for 24 hours at 60°C. The precipitation in the acetone was to remove any free-GMA, free-DVB and poly-GMA. After drying in vacuum

oven for 24 hours, the white solid obtained was characterised by FTIR. The FTIR spectrum of the white particle (GMA-*co*-DVB) is shown in **Figure A2.21** (in appendix A) and FTIR characterisation is given later in **Chapter 4**.

2.10.6 Copolymerisation of TRIS and MA in Hexane

Copolymerisation of Trimethylolpropane triacrylate (TRIS) and maleic anhydride (MA) was carried out using α, α', Azo-iso-butyronitrile (AIBN) as an initiator. 6 g MA, 2.6 g TRIS (3/7 weight ratio of TRIS/MA) and 1.7 g AIBN (0.2 molar ratio AIBN/TRIS+GMA) were mixed in 100 ml hexane using a 250 ml two-necked round bottomed flask. After assembling with a thermometer and a condenser and purging with oxygen-free nitrogen gas, the solution was maintained at a constant temperature of 68°C for 5 hours. The hot solution was then precipitated in 700 ml of acetone, filtered off, washed thoroughly with acetone before drying in a vacuum oven for 24 hours at 80°C. The precipitation in acetone was to remove any free MA, free TRIS and the reaction product obtained was characterised by FTIR. The FTIR spectrum of the white solid (MA-*co*-TRIS) is shown in **Figure A2.22** (in appendix A) and FTIR characterisation is given later in **Chapter 5**.

2.10.7 Copolymerisation of DVB and MA in Hexane

Copolymerisation of divinyl benzene (DVB) and maleic anhydride (MA) was carried out using α, α', azo-iso-butyronitrile (AIBN) as an initiator in hexane. 6 g MA, 2.6 g DVB (3/7 weight ratio DVB/MA) and 2.1 g AIBN (0.2 molar ratio AIBN/DVB+MA) were mixed in 100 ml hexane using a 250 ml two- necked round bottomed flask. After assembling with a thermometer and a condenser and purging with oxygen-free nitrogen gas, the solution was maintained at a constant temperature of 70°C for 5 hours. The hot solution was then precipitated in 700 ml of acetone, filtered off and washed thoroughly with acetone before dried in vacuum oven for 24 hours at 60°C. The precipitation in acetone was to remove any free MA, free DVB. After drying in vacuum oven for 24 hours, the white solid obtained was characterised by FTIR. The FTIR spectrum of the white particle (MA-*co*-DVB) is shown in **Figure A2.23** (in appendix A) and FTIR characterisation is given later in **Chapter-5**.

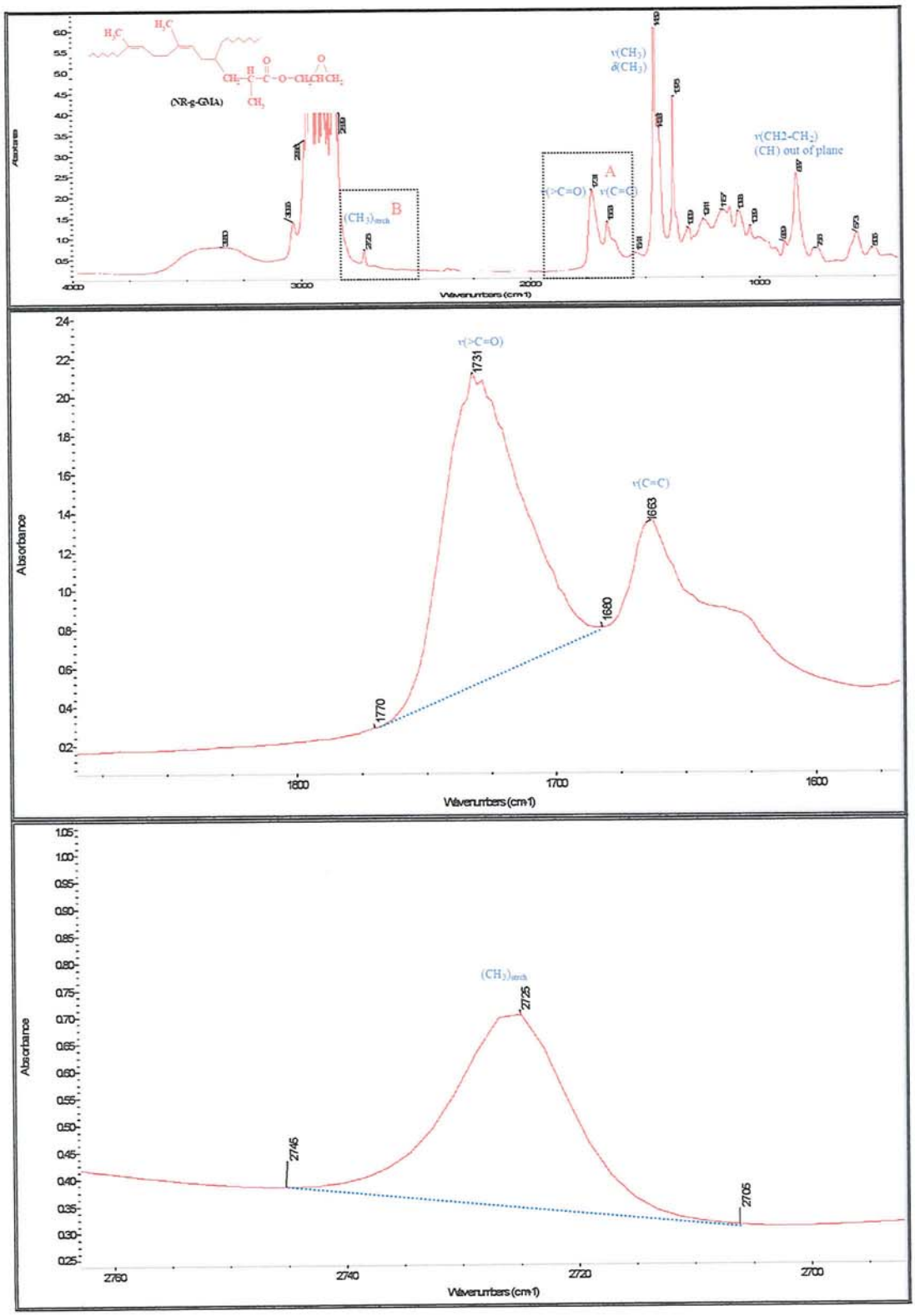

Figure 2.1 Comparison carbonyl peak (A) and reference peak (B) in calculation of peak area index in the FTIR spectrum of NR-*grafted*-GMA

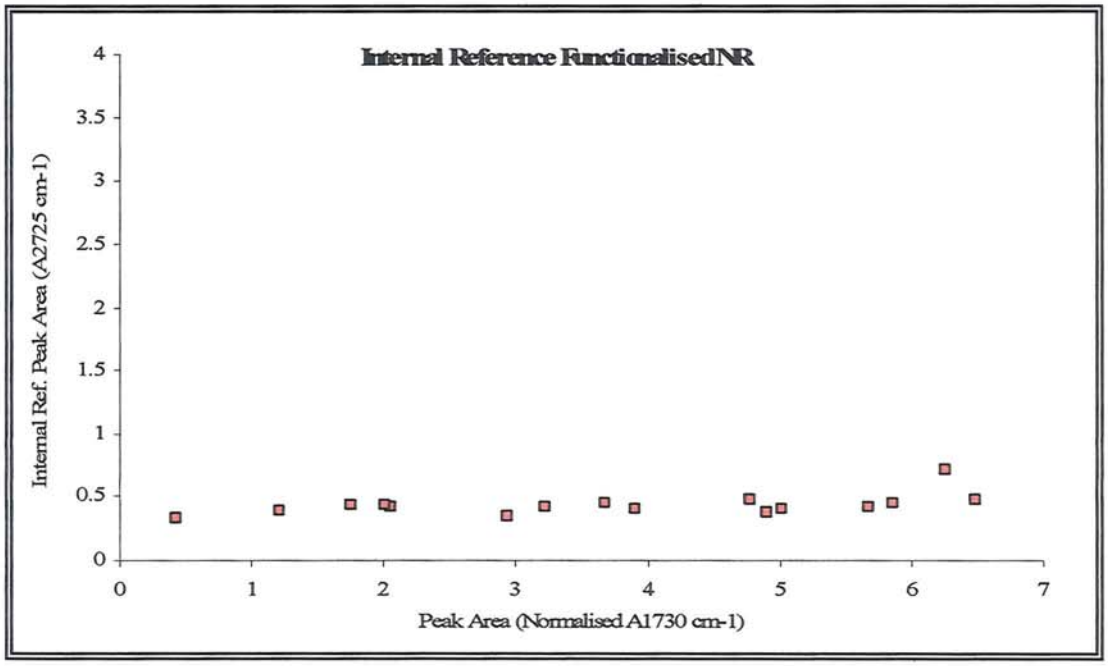

Figure 2.2 Dependences of the sample normalised absorbance of the 2725 cm-1 band of internal standard (of thickness) as a function of normalised absorbance of the 1730 cm-1 band (of GMA content) for the NR-*grafted*-GMA.

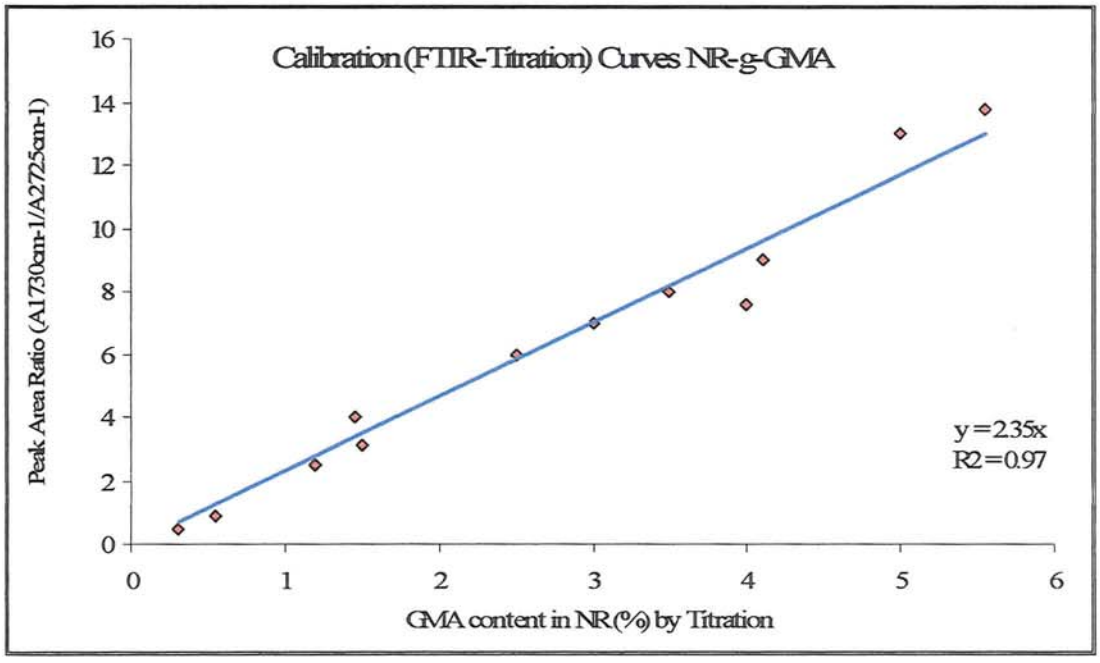

Figure 2.3 Calibration curve obtained from correlation between GMA content in NR measured by titration and area ratio ($A_{1730\ cm\text{-}1}/A_{2725cm\text{-}1}$) from FTIR.

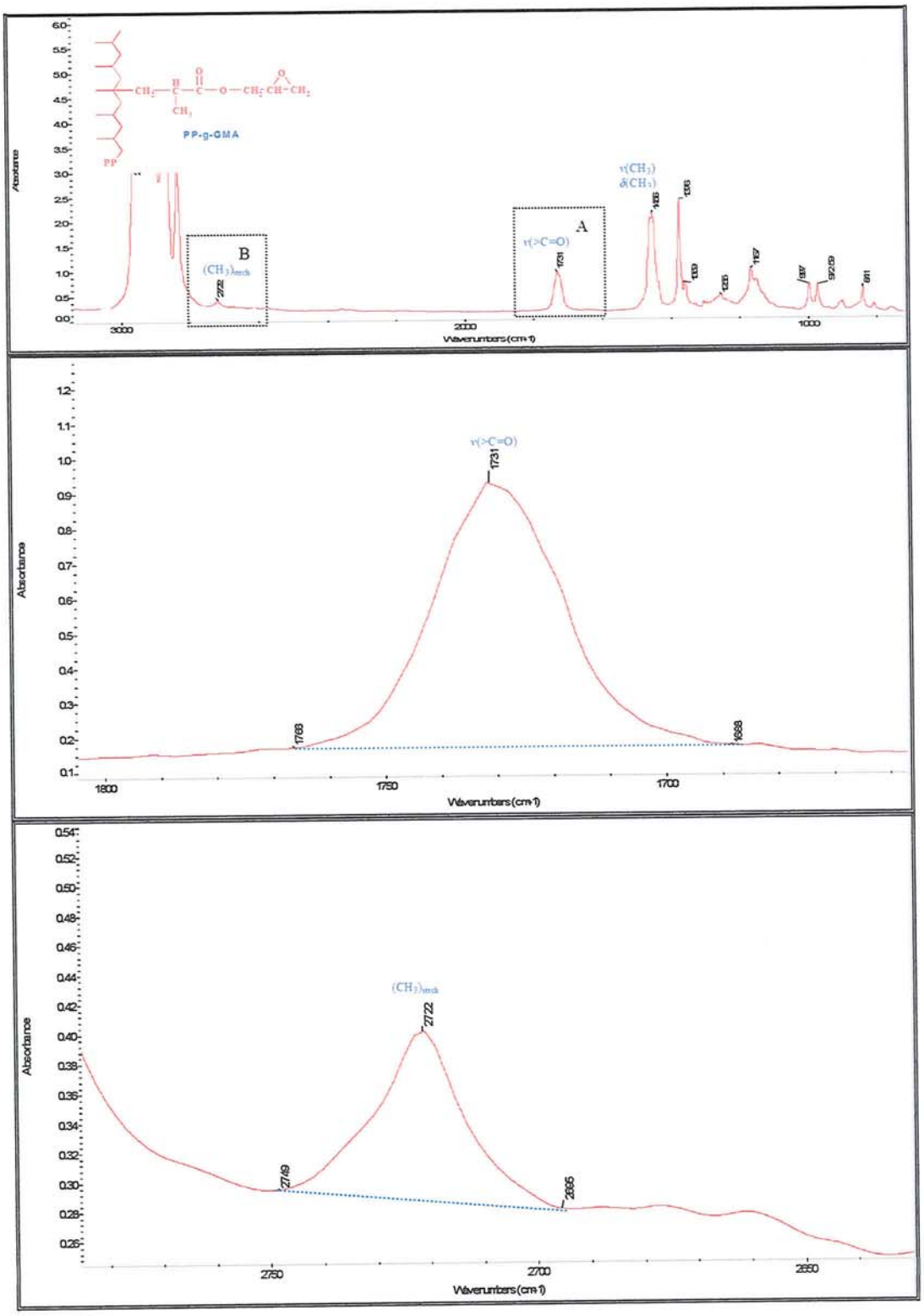

Figure 2.4 Area boundaries for absorption peak area index calculation of PP-*grafted*-GMA (A) Carbonyl peak at 1730 cm^{-1} and (B) Reference peak at 2720 cm^{-1}.

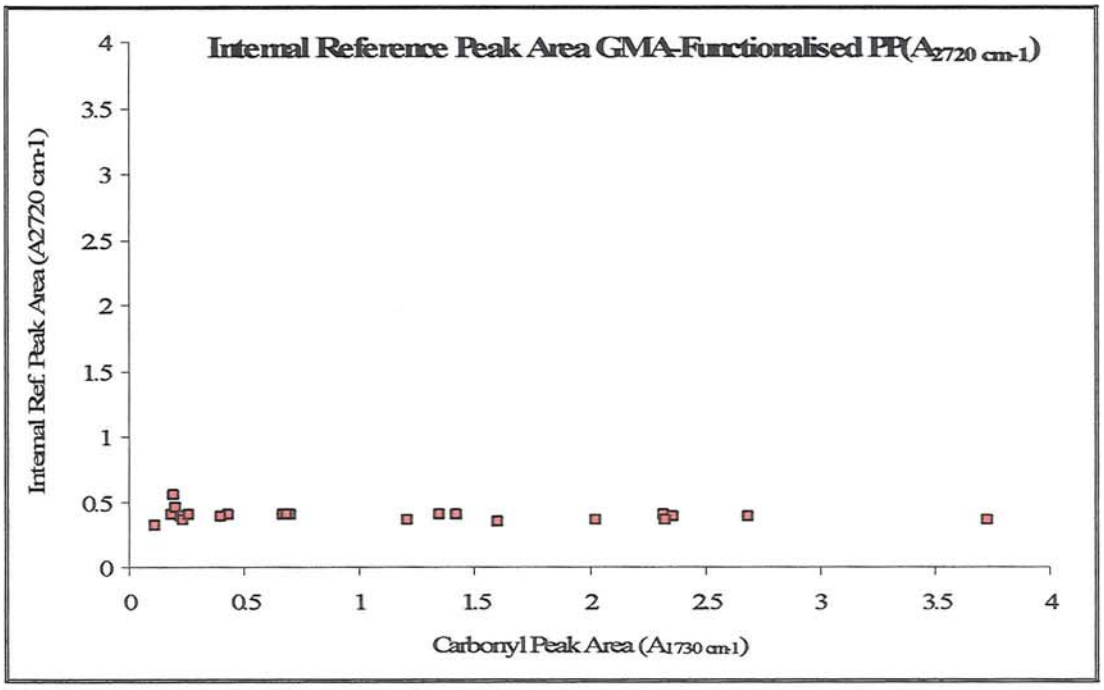

Figure 2.5 Dependences of the sample normalised absorbance of the internal standard (a) 2720 cm^{-1} as a function of normalised absorbance of the 1730 cm^{-1} band for the PP-*grafted*-GMA.

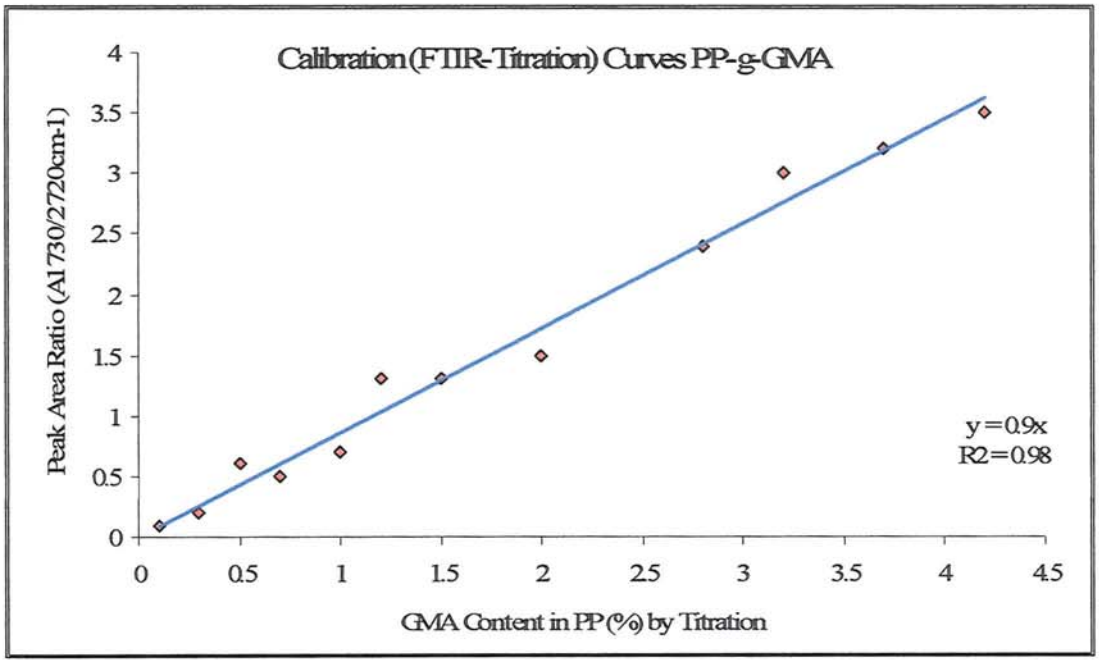

Figure 2.6 Calibration curve obtained from correlation between GMA content in PP measured by titration and area ratio ($A_{1730\ cm-1}/A_{2720cm-1}$) from FTIR.

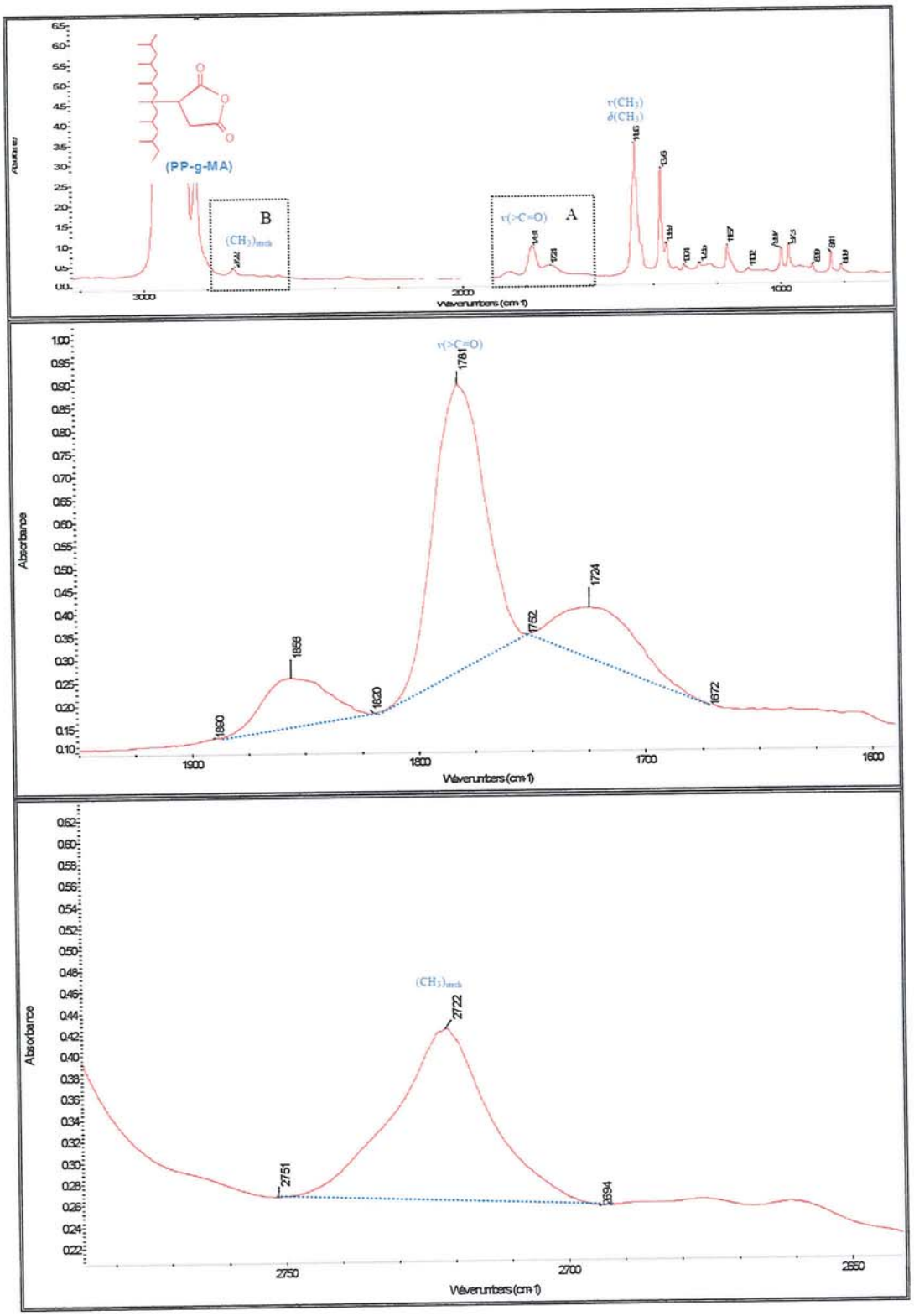

Figure 2.7 Area boundaries for absorption peak area calculation of PP-*grafted*-MA (A) Carbonyl peak (B) Reference peak.

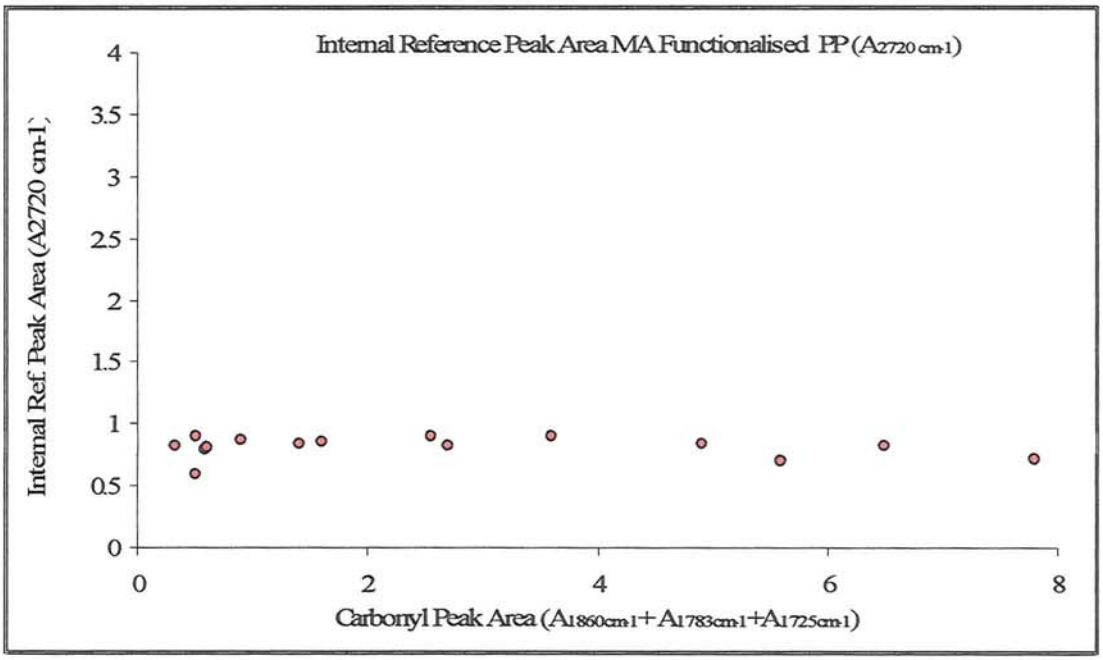

Figure 2.8 Dependences of the sample normalised absorbance of the internal standard 2720 cm^{-1} as a function of normalised absorbance of the 1730 cm^{-1} band for the PP-*grafted*-MA.

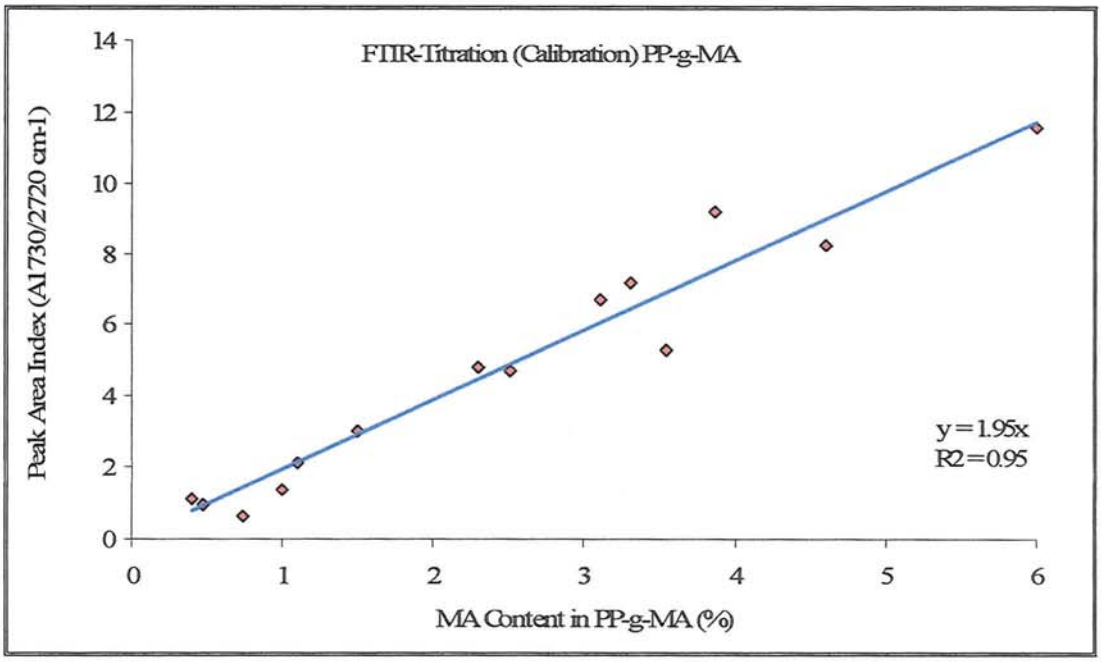

Figure 2.9 Calibration curve obtained from correlation between MA content in PP measured by titration and area ratio ($A_{total\ 1723,\ 1785,\ 1861\ cm\text{-}1}/A_{2720cm\text{-}1}$) from FTIR.

CHAPTER 3
FUNCTIONALISATION OF NATURAL RUBBER WITH GMA

3.1 Objective and Methodology

Natural rubber (NR) which is an unsaturated elastomer containing 93–95% *cis*-1,4-polyisoprene [352] has many desirable properties such as high elongation, and outstanding resilience but also with some shortcomings such as its high sensitivity to heat and oxidation due to the presence of double bonds in its chains [352,353]. Most of its industrial applications (automotive tyres, load bearing, pads, and silent blocks) require the use of particulate fillers to obtain the desired reinforcement (increase of the modulus, wear resistance, and ultimate properties) [354]. NR has also low tensile strength, tensile modulus, and poor creep characteristics unless it is highly vulcanised [354,355]. One of the major problems encountered during tyre manufacture, for example, is the poor adhesion between the tyre cord (mostly nylon, rayon, polyester, and aramid fibres) and the rubber materials as a result of poor bonding affinity between the polar cord material and the hydrophobic rubber molecules. To overcome this drawback, adhesion-promoting systems, such as recorcinol-formaldehyd latex and polyisocyanates, have been utilised to provide a coating on the cord surface during tyre manufacture to improve adhesion at the interface between the cord or metal and rubber [356-359]. Graft copolymerisation of glycidyl methacrylate onto natural rubber could be an attractive technique to enhance adhesion without drastically altering the original properties of the rubber [356]. Different chemical modifications have been performed in NR in order to increase its useful properties; this includes preparation of graft copolymers of NR with various types of vinyl monomers such as styrene (St) [360], maleic anhydride (MA) [167-169,361-364], glycidyl methacrylate (GMA) [359], methyl and alkyl methacrylate [365-377]. The copolymer products have been used extensively in the area of polymer reactive blending as compatibilisers for

certain incompatible polymer pairs [378-387]. However, there is a limited amount of work in the literature on the grafting of GMA **(I)** onto natural rubber.

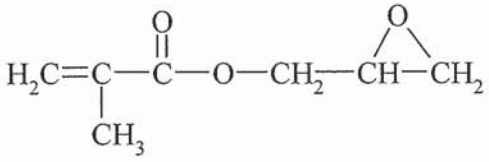

(I) Glycidyl methacrylate (GMA)

In this study, natural rubber was functionalised with GMA onto commercial grade of natural rubber (SMR-L). The grafting of GMA onto the rubber was carried out in an internal mixer (a torque rheometer, TR) either by thermal or by free radical initiation. In the case of thermal initiation, GMA was mixed with the masticated natural rubber in a close chamber of the TR in the absence of peroxide, whereas in the free radical initiation system, organic peroxides such as benzoyl peroxide, BPO **(II)**, dicumyl peroxide, DCP **(III)**, 2,4-dimethyl-2,5-bis-(*tert*-butyl peroxy)hexane, Trigonox-101, T-101 **(IV)**, and 1,1-di(*tert*-butylperoxy)-3,3,5-trimethyl cyclo- hexane (Trigonox-29B90, T-29B90) **(V)** were used to initiate the reactions; These were added with the GMA into the masticated natural rubber, see **Scheme 3.1** (p.121).

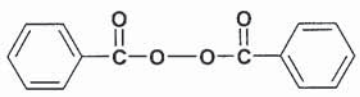

(II) Benzoyl peroxide (BPO)

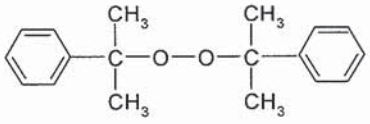

(III) Dicumyl peroxide (DCP)

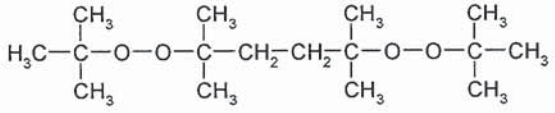

(IV) Trigonox-101 (T-101)

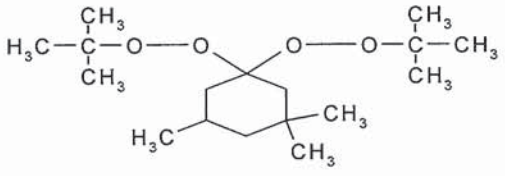

(V) Trigonox-29B90 (T-29B90)

Before processing, the bale of natural rubber was cut down into small pieces ready for masticating on a two-roll mill at room temperature for 2 minutes in order to form sheet natural rubber and reduce its molecular weight. The sheeted (masticated) rubber was then cut into small pieces so that it is available for further processing in the torque rheometer. The effect of processing conditions and chemicals composition on the grafting efficiency of

GMA onto NR was examined. The set of experiments representing the various parameters can be seen in **Tables B3.1-B3.7** (in appendix B). The key process parameters and chemical variables examined were:

1. Processing temperature (120-220°C)
2. Processing time (2.5 – 15 min)
3. Rotor speed (40-100 rpm)
4. Atmosphere (N2, air)
5. Concentration of GMA (2-18 phr)
6. Type and concentration of peroxide (T101, T-29B90, DCP, and BPO/0.01-0.1 phr)
7. Addition sequence of GMA and peroxides

To ensure the best methodology in terms of the addition sequence, different addition methodologies were used, keeping the concentration of the monomer and peroxide constant. Four different mixing methods were examined to investigate the effect of sequence of addition of the reactive components to the rubber on the degree of grafting of GMA onto natural rubber, see **Scheme 3.2** (p.122).

Method-1: Both monomer (GMA) and peroxide (T-101) were premixed by using ultrasonic bath for 5 minutes before introducing (through long needle syringe) into the masticated NR (NR was masticated for 2 minutes before mixing). After the mixing (NR+GMA+T-101) (time needed for introducing the reactant less than 15 seconds), processing was then continued for a total time 15 minutes, see **Scheme 3.2 (M-1)**.

Method-2: The monomer GMA and part of the peroxide T-101 were premixed and introduced into the masticated NR through long needle syringe after 2 minutes initial processing. Processing was continued for 1 minute before the remaining peroxide (wrapped in 1g of NR) was introduced (at the 3rd minutes) and processing was continued for total time15 minutes, see **Scheme 3.2 (M-2)**.

Method-3: The masticated natural rubber was processed for 2 minutes before GMA was introduced and processing continued for one more minute before addition of the peroxide (after 3 minutes) and processing was continued for total time of 15 minutes, see **Scheme 3.2 (M-3)**.

Method-4: A part of the peroxide (wrapped in 1g NR) was introduced to the masticated natural rubber after an initial 2 minutes processing followed by addition a

mixture of GMA and the remaining peroxide after 3 minutes, then processing was continued for a total time of 15 minutes, see **Scheme 3.2 (M-4)**.

To ensure that only grafted-GMA was measured, the GMA-modified NR samples were purified by Soxhlet extraction with different solvents including acetone, chloroform, methanol, and dichloromethane. It was found that acetone was the most suitable solvent for extraction of ungrafted GMA due to the high solubility of the GMA-homopolymer (poly-GMA) and free-GMA in this solvent.

It was difficult to prepare thin films for FTIR measurement directly due to the tackiness and high viscosity of GMA-functionalised natural rubber (NR-*f*-GMA) samples, hence thin cured films had to be prepared. The rubber ingredients, zinc oxide, stearic acid, accelerator CBS (N-cyclohexyl-2-benzothiazole sulphamide), and sulfur were compounded on a two roll mill, see **Table 2.6** (p.68). Since curing of natural rubber was necessary in order to prepare films for FTIR analysis, three purification procedures became possible; either before or after compounding and curing. In order to determine which the most suitable purification procedure is, three different films were prepared and subjected to different extraction methodologies and compounding procedures before examination by FTIR, see **Scheme 3.3** (p.123).

***Procedure 1*, Films A**, the unpurified reaction products of NR-*g*-GMA samples were compounded with ingredients on a two-roll mill and cured to films by compression moulding at a temperature of 150°C for 2 minutes. These films were expected to contain all the side reaction products, i.e. homopolymerised-GMA (poly GMA) and free-GMA as well as grafted-GMA formed during melt grafting, compounding and curing stages.

***Procedure 2*, Films B** were produced from route of films A (unpurified, compounded and cured) but were Soxhlet extracted (in acetone for 24 hours) after the curing stage. The acetone extraction after curing was carried out in order to remove all side reaction products, poly GMA and remaining free GMA after reactive processing and compounding and curing stages. It is assumed that any remaining free GMA after the reactive processing stage could react to grafted GMA or homopolymerised GMA (poly GMA) during compounding and the curing stages. Thus these films can be expected to contain GMA-grafted during the

reactive processing as well as in compounding and curing and thus would contain higher amount of GMA-grafted NR. By comparing the FTIR spectra obtained from films A and B, it was found that the areas of the absorption band at 1730 cm^{-1} after extraction (film B) were slightly different from those before extraction (film A). This is due to the fact that a small amount of free GMA may have remained in the films after reactive processing and converted to GMA-grafted NR during the compounding and/or curing process.

***Procedure 3*, Films C**. Another extraction procedure was adopted to confirm the existence of grafted-GMA, $[GMA]_g$. The unpurified reaction products of NR/GMA/T-101 samples were milled into thin sheets and Soxhlet extracted with acetone for 24 hours. After the reactive processing stage and before compounding and curing in order to remove any remaining free GMA that otherwise could further react and result in additional conversion to GMA-grafted NR during the compounding and curing stages. After being dried in vacuum oven at room temperature for 24 hours, curing agents were compounded on a two roll mill, vulcanised in press moulding giving films C. These films were expected to contain the grafted GMA produced only during the reactive processing stage.

3.2 Results

3.2.1 Characterisation of GMA-Grafted Natural Rubber

When natural rubber is processed with GMA in the presence or absence of peroxides, the processed rubber samples may contain grafted-GMA (NR-*g*-GMA), homopolymerised GMA (poly-GMA) and unreacted GMA (free-GMA), as well as branched or cross linked natural rubber, see **Scheme 3.4** (p.124). In order to eliminate any unreacted GMA and poly GMA from the reaction products and to ensure the correct measurement of grafting degree of GMA-grafted NR, the processed rubber were purified by extraction method with acetone (**Section 2.4.2,** p.69). The content of GMA-grafted NR of purified sample were then determined and characterised by titration and/or FTIR methods, see **Scheme 3.5** (p.125)

It is well known that natural rubber contains some natural substances, mainly protein and lipids (phospholipids, ester of higher fatty acids, and sterols) **[352,388-390]** and when it was Soxhlet extracted with acetone those substances were extracted and removed. The acetone extracted natural rubber (for 24 hours extraction) became light and more

transparent. The FTIR spectrum of acetone extracted natural rubber shows similar absorption peaks to those of raw natural rubber with the exception of the absorption peak at 3285 cm^{-1} (due to υO-H of protein) and 1742 cm^{-1} (shift to1718 cm^{-1}) most likely due to stretching of >C=O group of natural protein which becomes much smaller (**Fig. 3.1**).

Processing natural rubber with GMA in the presence or absence of a peroxide gives rise to significantly different physical appearance from that of raw natural rubber. The products obtained at processing temperatures above 180°C and in the absence of peroxide showed a brown colour and became tacky, whereas no obvious colour change was observed when the reaction was carried out below 160°C in the presence or absence of peroxide. The higher the processing temperature and the higher the GMA concentration, the deeper was the brown colour of the reaction product.

Natural rubber is normally soluble in ordinary hydrocarbon solvents, such as benzene, toluene, xylene, and becomes swelled in polar solvents, such as acetone, chloroform, and dichloromethane. The solubility of the reaction products (NR-*g*-GMA) was lower than that of the unmodified rubber in hydrocarbon solvents. Rubber samples containing only small amount of grafted GMA became like 'jelly' or partially soluble in such hydrocarbon solvents even at temperature of 100°C. Generally, the reaction products obtained using raw (unpurified) natural rubber under the conditions studied in this work resulted in a normal rubbery material. However, when purified (acetone extracted) natural rubber was used, with or without peroxide, and the processing temperature was kept below 160°C, the mixture became crumbled. The samples were rough, dry and tattered when sheeted on a two-roll mill. However, when the processing temperature was raised to above 160°C, the products showed a normal rubbery state.

Since the unreacted GMA (free GMA) and poly GMA gave rise to infrared absorption bands in the same region where the GMA-grafted NR bands appears, it is of great importance to eliminate all unreacted GMA and poly-GMA from the reactively processed NR. The elimination of free-GMA and poly-GMA after purification can be verified by the disappearance and decreases of the characteristic carbonyl absorption band (1730cm^{-1}). The FTIR spectra of NR-*g*-GMA films produced from the processing of natural rubber with GMA at a lower temperature (100°C) in the absence of peroxide before and after acetone

Soxhlet extraction are shown in **Fig. 3.2**. The acetone Soxhlet extraction is shown to remove the carbonyl absorption of GMA (free- and poly-GMA) at 1730 cm^{-1}. This extraction was used throughout to purify the natural rubber and the products of functionalised NR-*g*-GMA. The same Soxhlet extraction procedure was therefore adopted for natural rubber processed with GMA (processing temperature 180°C) in the presence of the peroxide T-101 (free radical initiation for grafting). **Figure 3.3** shows that the carbonyl band at 1730 cm^{-1} corresponding to grafted GMA remains even after exhaustive Soxhlet extraction with acetone as evidence of grafting of GMA onto NR. The adoption of the preparation of cured films for FTIR analysis gives rise to two possible purification procedures, e.g. either before or after compounding and curing. To determine an accurate purification procedure, three different films using different extraction methodologies and compounding procedures were examined by FTIR, see **Scheme 3.3** (p.123)

Comparison of the FTIR spectra of films A, B, and C (see **Fig. 3.4**) shows that the absorption area of carbonyl group of film A is higher than that of films B and C. This demonstrates that free-GMA in the reaction products may have reacted further with the rubber during the milling of the compounding stage (film A), thus it is important to extract all the unreacted GMA (free-GMA) before the compounding stage (i.e. Film C) for calculating the grafting degree of reaction products during the processing stage. Films C therefore was used throughout for calculating grafted GMA during the melt grafting in an internal mixer.

The spectra of the purified GMA grafted NR (Films C, see **Scheme 3.3**, p.123) via both thermal initiation (see **Fig. 3.5**) and peroxide initiation (**Fig. 3.6**) show new bands at 1723 cm^{-1} (in thermal initiation) and at 1730 cm^{-1} (for peroxides initiation). The grafting degree of GMA onto NR for each sample was determined by examining the FTIR spectrum of the film C. The absorption peak area ratio of the carbonyl peak at 1723 cm^{-1} (thermal initiation) or 1730 cm^{-1} (peroxide initiation) to the internal reference peak at 2725 cm^{-1} ($A_{1730cm-1}/A_{2725cm-1}$) was calculated and the actual grafting degree was obtained by comparing the absorbance area ratio to a calibration curve (see **Section 2.5.4,** p.78). The epoxide peaks of GMA at 909 and 805cm^{-1} could not be used as they were masked by rubber backbone absorption peaks at 836 cm^{-1} (assigned to C=CH deformation, C-H out of plane), see **Fig. 3.1** and **3.2**.

3.2.2. Processing of Raw Natural Rubber

Figure 3.7 shows the torque-time curves of masticated and processed raw natural rubber (in the absence of GMA and peroxide) at various processing temperatures (65 rpm, 15 min). When purified raw natural rubber was processed (in absence of GMA) at temperatures of 100-200°C, the difference in the change of torque values at the different temperatures was very small as shown in torque-time curves of the processed NR alone (**Fig. 3.7**). This shows that the main changes in torque values were at the first minute (torque maximum; loading torque max) with this value being lower at higher processing temperatures. The loading torque maximum gives an indication of the tendency of the rubber towards cross linking or chain scission reactions. On further processing, the mechanical force and oxidation under high temperature resulted in a reduction in a molecular weight and the rubber became more plastic and the torque decreased gradually. However, after 2 minutes processing (the ram was closed), the torque values remained constant up to 15 minutes processing and the change in final torque and torque maximum at various temperatures were not significant. Natural rubber is known to contain small amounts of abnormal functional groups such as aldehyde, epoxide, and lactone which have been postulated to be responsible as natural stabilisation of the rubber [352,388-390]. The processed natural rubber in the absence of monomer and peroxide at high temperature (above 200°C) became tacky and had a brown colour. For comparison purpose, the processed raw natural rubber at 180°C was used as a control sample (blank) for titration and FTIR analysis.

3.2.3 Grafting of Glycidyl Methacrylate onto Natural Rubber

Glycidyl methacrylate (GMA) was grafted onto natural rubber (NR) at elevated temperatures in the presence or absence of free radical initiators in a torque rheometer (**Section 2.2.2**) and see **Scheme 3.1** for experimental detail. To establish the optimum processing conditions and composition, the effect of processing temperature, mixing sequence (method), rotor speed, processing time, and the concentration of GMA and peroxide, on the grafting degree were examined, see **Table B.3.1** to **B.3.5** (in appendix B).

A. Grafting of GMA onto NR by Thermal Initiation

In the case of thermal initiation, natural rubber was processed with GMA in the absence of peroxide at temperature of 100-200°C, sample T1-n (GMA 6 %) and T2-n (GMA 15 %),

see **Table B.3.1** (in appendix B). It was shown in **Fig. 3.8** that there was a little difference in the changes of torque values at the different processing temperatures used for thermal initiation. Initially, as expected, the torque values increased to a maximum value (loading torque maximum) with this value being lower at higher processing temperatures. On further processing, after addition of GMA into the molten NR and lowering the ram (closed ram), the torque values increased to obtain a torque maximum (highest value at 160°C) and there was a more clear change in the final torque values which decreased at higher processing temperatures. The natural rubber at higher temperatures (above 200°C) also became brown and tackier.

In the case of thermal initiation, the grafting reaction of GMA was shown to require a temperature higher than 160°C and preferably about 160-200°C. When purified raw natural rubber was processed with GMA (in absence of peroxide) at temperatures of 100-200°C, there was a larger difference in the change of torque values at the different temperatures (compared to processed NR alone without GMA at the same temperatures). **Figure 3.8** shows that after 2 minutes processing when GMA was added the torque max and final torque values were higher than that of NR alone and they decreased at higher processing temperatures. The reaction products became brown in colour and the rubber was more tacky.

Increasing the processing temperature could significantly improve the dispersion of GMA in the rubber and also affect the balance between the various competing reactions (conversion of GMA to homopolymerisation (poly-GMA), crosslinking and chain scission of NR chains) with that of the target GMA grafting reaction. The degree of grafting of GMA onto natural rubber depends on processing temperatures and initial concentration of GMA. **Figure 3.9** shows that grafting is highest at processing temperatures of 160°C for GMA of 6 % and at 190°C for GMA of 15 %. The torque max – torque min ($Tq_{max-min}$) was highest at 140-160°C, c.f. **Fig. 3.8** and **3.9,** though the overall extent of grafting remained low (grafting efficiency was about 10 %). It appears that there is a correlation between the degree of grafting of GMA and the torque maximum (or torque maximum – torque minimum value) in terms of optimum grafting and highest torque value at the same processing temperature. **Figure 3.8** shows that the time to torque maximum became shorter with increasing processing temperature. It is likely that the change in the degree of grafting

is paralleled by a shorter time to torque maximum. At higher processing temperatures the degree of grafting of GMA decreased, most probability due to dominance of NR degradation reactions (by chain scission), see **Scheme 3.4** (p.124) for grafting mechanism.

To investigate the effect of GMA concentration on the grafting degree in the thermal initiation system, a set of experiment with a fixed set of processing conditions (temp 160°C, 65 rpm, 10 min) (see **Table B.3.1**, samples G0-n, in appendix B) was prepared. **Figure 3.10** shows that increasing concentration of GMA initially added has led to higher grafting degree of GMA onto NR.

B. Grafting GMA onto NR by Free Radical Initiation

In the case of free radical initiation, processing NR with GMA in the presence of peroxide, it was demonstrated that the addition sequence of GMA and peroxide T-101 could affect the extent of GMA grafting reaction and the level of cross-linking or chain scission of the poly isoprene as reflected from changes in the torque characteristics and degree of grafting (see **Fig. 3.11**). It was found that the highest degree of grafting of GMA onto NR was achieved by method-2, method-1, and method-4 (the difference in extent of grafting degree was small), see **Scheme 3.2** (p.122) for difference in the sequence of addition methods.

A further set of experiments was prepared to compare method-2 and method-4 (**Scheme 3.2**, **M-2** and **M-4**); in which part of the peroxide T-101 was introduced in the molten NR separately. In Method-4 (M-4), introduction of (part of) T-101 was done in the first stage before addition of GMA (and the remains of T-101) and this resulted in higher cross linking (as shown with higher torque max and final torque, see **Fig. 3.12**). The higher the peroxide concentration (at the 1st stage) introduced into the molten NR resulted in higher crosslinking, reflected from higher final torque, and the lower GMA grafting onto NR. In contrast, Method-2, in which (part of) the peroxide was introduced together with GMA in the first stage; it was found that the higher initial peroxide concentration that was mixed with GMA (1st stage), the lower was the cross linking and the higher the level of grafted GMA onto NR. **Figure 3.12** shows that the higher the T-101 concentration initially mixed with GMA (total T-101 concentration was kept constant) the higher the grafting degree, both in addition method-2 (M-2) and method-4 (M-4). Moreover, in method-1, **Scheme 3.2**

M-1 all the peroxide T-101 was introduced together with GMA (mixing T-101 + GMA) in one stage and this had resulted in higher grafting degree than was the case with method-4 (lower than method-2 but not a significant difference). Therefore, method-1 (**M-1**) was used for all subsequent investigations (method-1 was adopted for processing of all natural rubber with GMA samples processed in the presence of peroxides).

Rotor speed is one of the variables that can improve the mixing efficiency of the monomer to react with the molten polymer. In this case, the rotor speed favours the mastication of NR and formation of more natural rubber macroradicals that can react with the GMA. A set of experiments was carried out in the torque rheometer (TR) with the same initial composition (concentration of GMA 12 % and T-101 0.03 mr) and same processing conditions (temperature 170°C, mixing time 15 min, using either nitrogen or 'air') except for varying the rotor speeds (see **Table B.3.2,** sample S3-n and S4-n, in appendix B) . **Figure 3.13** shows the effect of shear (rotor speed) on the torque characteristic of the processed NR with GMA (initiated by T-101) samples using different atmospheres. A decrease in viscosity (reflected by declining final torque values) with an increase in shear rate (increased rotor speed) indicates a pseudoplastic behaviour. According to the impulse theory of *pseudo plasticity* **[363,364,389-391]**, the behaviour is due to two independent effects, *Newtonian effect* where the shearing force is proportional to the rate of shear, and the other is a *thixotropic* effect where the shearing force is constant irrespective of the rate of shear. However, it was found that the change in the shear level (different rotor speeds) had a negligible effect on the level of GMA grafting (see **Fig. 3.14**). The rotor speed is an independent variable that cannot be analysed individually. Its influence on the grafting efficiency depends on the level of the remaining independent variables. For all further experiments, the rotor speed was set at 65 or 75 rpm.

In the study of grafting reaction by free radical initiation (in the presence of peroxide), four different peroxides were used to initiate the grafting reaction of GMA onto natural rubber; benzoyl peroxide (BPO), dicumyl peroxide (DCP), 2,5-dimethyl-2,5-bis (*tert*-butyl peroxy) hexane (T-101), and 1,1-di(*tert*-butylperoxy)-1,5-dimethyl hexane (T-29B90), see **Table 2.3** (p.63) for half-lives time ($t_{½}$) of these peroxides. The effect of peroxides different peroxides (BPO, DCP, T-101, and T-29B90) as initiators in terms of their concentration, the GMA concentration, processing temperature, and time, on GMA grafting degree on NR

was investigated in detail. The experimental conditions-compositions are presented in **Tables B.3.2** to **B.3.5** (in appendix B).

(i) Effect of Benzoyl Peroxide (BPO)

The melt reaction was initially carried out with a fixed amount of GMA at 12 % and concentration of BPO at 0.02 molar ratio to the GMA under different processing temperatures (120-160°C) (samples B1-2, B2-2 and B3-2 **Table B3.3**, in Appendix B). **Figure 3.15** shows the torque behaviour of natural rubber processed with GMA in the presence of benzoyl peroxide (BPO). The torque max and final torque values were highest for the lowest processing temperature of 120°C. The torque max – torque min ($Tq_{max-min}$) values did not change and overall there was a low GMA grafting level, see **Fig. 3.16**; not much improvement compared to GMA-grafting by thermal initiation. The correlation between grafting degree and time to torque max and the half-life time of the peroxide BPO at different temperatures are shown in **Fig. 3.16B** and **C**.

The effect of BPO concentration in NR/GMA/BPO system was also examined at a fixed temperature of 140°C (see **Table B.3.3**, samples B2-n) and 160°C (**Table B.3.3**, samples B3-n, in Appendix B). **Figure 3.17** shows the torque characteristic and the GMA grafting degree of GMA on NR which is clearly very low and even lower than that obtained from thermal initiation (at temp >140°C). Increasing BPO concentration has no effect on the grafting degree. The GMA concentration has a different effect on the grafting level. **Figure 3.18** shows the torque-time curves and torque characteristic of processed NR/GMA/BPO. The reaction was carried out at a preferable temperature of 140°C at a fixed peroxide concentration (BPO 0.03 molar ratio to GMA) (see **Table B.3.3**, samples B4-n, in Appendix B). Similar to the thermal initiation, the grafting level of GMA on NR in the NR/GMA/BPO system increased with increasing GMA concentration (see **Fig 3.18E**).

ii. Effect of Dicumyl Peroxide (DCP)

The changes in torque-time curves and grafted-GMA of processed natural rubber with GMA (12 %) in the presence of dicumyl peroxide (0.04 mr) at different processing temperatures (**Fig. 3.19** and **3.20**), with a range of DCP concentrations (**Fig. 3.21**), and various GMA concentrations (**Fig. 3.22**) were examined. It is clear that the use of dicumyl

peroxide (DCP) resulted in the formation of a significantly different final torque and torque maximum compared to BPO (though both torque curves decrease at higher temperatures). When the torque characteristics were compared with the torque values of melted raw natural rubber at the same temperature, the torque maximum and the final torque of NR/GMA/DCP system had much higher values indicating that there is more competition between the grafting reaction (conversion GMA to GMA-grafted NR) and the side reactions (GMA conversion to homopolymerisation, poly-GMA, crosslinking/chain scission) (**Fig. 3.19**). Furthermore, the maximum value of torque-max and torque-min (**Fig. 3.19**) occurred at processing temperature of 160°C which also corresponds to the temperature resulting in the highest grafting yield, **Fig. 3.20**).

Figure 3.21 shows torque-time curves of NR/GMA/DCP samples processed at various DCP concentrations (0.001 – 0.3 molar ratio to GMA) under the same processing conditions (temperature 160°C, 65 rpm, 15 min) and the same concentration of initial GMA (12 %). It shows that torque maximum and final torque increased with increasing the DCP concentration. The extent of grafting, which is higher than in the case of BPO, is further increased at higher concentrations of DCP. However the rubber tended to undergo extensive cross-linking at concentrations of DCP higher than 0.03 mr (reflected by the high final torque and observed crumbling of the rubber). A set of experiments of processed NR/GMA/DCP system using various GMA concentrations was carried out at fixed processing conditions (temp 160°C, 65 rpm, 15 min) and the same DCP concentration (0.03 mr) (samples D3-n Table B 2.4, in Appendix B). **Figure 3.22** shows the GMA grafting level increased with increasing GMA initial concentration.

iii. Effect of Trigonox (T-101)

Natural rubber was functionalised with GMA in the presence of the peroxide T-101 at different composition and processing conditions. The effect of processing temperature, peroxide concentration, GMA concentration, addition sequence, and processing time on the torque characteristic and grafting degree of GMA onto NR were investigated in more detail. The experimental conditions and results are presented in **Table B.3.2** (in appendix B). The changes in torque-time curves, torque characteristics and grafting degree of GMA

on NR at different processing temperatures, with a range of T-101 concentrations, and various GMA concentrations are shown in **Figures 3.23** to **3.28.**

The peroxide Trigonox-101 (T-101), as compared to BPO and DCP, has an even longer half times at higher temperatures ($t_{1/2}$ = 11.4 min at 160°C, $t_{1/2}$ = 1.2 min at 180°C, and $t_{1/2}$ = 0.3 min at 200°C) (see **Table 2.3,** p.63). It was found that this peroxide could initiate the reaction of GMA and natural rubber at temperatures above 140°C quite efficiently leading to much higher overall grafting degree compared to BPO and DCP. When the temperature was raised to 160°C, the grafting reaction was initiated quite efficiently by T-101 and the grafting degree of GMA increased at higher T-101 concentration, see **Fig. 3.26A**. However, at higher T-101 concentration or processing temperature, the degree of NR cross linking became obvious and unacceptable. Through a series of experiments, the optimum temperature was found to be between 140-170°C (**Fig. 3.24**) and peroxide concentration less than 0.05 molar ratio to GMA (**Fig. 3.25**).

As shown in **Fig. 3.23** the final torque and the torque max of the NR/GMA/T-101 system, processed with different processing temperatures (Table **B.3.2**, samples T5-n, in Appendix B), show a large difference compared to that of the thermal initiation (at the same temperatures) due to the competition between grafting reaction (GMA conversion to GMA-grafted NR) and the side reaction including homopolymerisation, cross linking and chain scission of the rubber. The peroxide T-101 could initiate the grafting reaction of GMA onto natural rubber more effectively. By increasing the processing temperature, the grafting degree of GMA increased at a range temperature of 140-180°C and then decreased with further increase in temperature (**Fig. 3.24**). On the other hand, when the peroxide concentration was raised up to 0.05 mr (molar ratio to GMA), the grafting degree increased (**Fig. 3.26**). However, increasing the concentration of T-101 has resulted in a much higher final torque (**Fig. 3.25**) indicating an increase in the degree of cross linking of the rubber. Increasing the initial concentration of GMA resulted in a similar persistently increase in level of grafting GMA (see **Fig. 3.27** and **3.28**). Through a series of experiments, the optimum temperature was found to be between 140°-180°C and concentration of T-101 less than 0.05 molar ratio to GMA.

iv. Effect of Trigonox-29B90 (T-29B90)

It was reported that the peroxide 1,1-di(*tert*-butylperoxy)-3,3,5-trimethyl cyclo- hexane (T-29B90 or L-231) was a very effective initiator for grafting of GMA onto PP [132] or EPR [134] at low temperatures. To investigate the effect of temperatures, a set samples were prepared with fixed composition (GMA 6%, T-29B90 0.002 mr) and similar processing conditions (65 rpm, 15 min) except for a different processing temperatures. After a required amount of NR was charged into the preheated mixing chamber (under nitrogen and selected set at selected temperatures of 150-200°C), a mixture of GMA and T-29B90 was injected into the chamber (at t = 0 min). After 15 min processing, a similar purification procedure to that used for other peroxides was adopted and the grafting degree was determined by the FTIR method (using films C, see **Scheme 3.3**). **Figures 3.29** and **3.30** show torques-times curves and torque characteristics grafting degree of GMA onto NR of processed NR/GMA/T-29B90 system at various temperatures. It seems that the grafting reaction of GMA onto NR is much more effective at lower temperature (< 150°C) when using a very low concentration (0.002 mr) of this peroxide.

v. Effect of Initial GMA Concentration

The effect of the initial GMA concentration on the torque-time curve and hence the level of grafted GMA in the presence of different peroxides (T101, DCP, BPO) is shown in **Fig. 3.31**. These series of grafting processing experiments of GMA onto NR were prepared using different initial GMA concentrations of 3-18 % with a fixed peroxides concentration 0.02 mr (processing temperature 120°C for BPO, 160°C for DCP and 180°C for T-101). In the reactive processing step, GMA acts by trapping the macro alkyl radicals that would otherwise undergo chain scission or cross linking. Thus, use of a higher GMA concentration should give rise to higher grafting degree and less NR degradation. When the reaction was carried out at the optimum processing temperature for each of the three peroxides (BPO at 120 °C, DCP and T-101 at 160 °C), see **Fig. 3.31**, the grafting level was shown to increase continuously with increasing GMA concentration and the degree of GMA-grafted NR in the NR/GMA/BPO system (BPO as initiator) was very low compared to the other peroxides. In the presence of BPO, the higher values of the final torque indicates a higher level of cross linking reactions, whereas the lower torque max - torque min ($Tq_{max-min}$) suggests a lower extent of the reaction between GMA and NR (see **Fig.**

3.31). The efficiency of the grafting reaction is most likely to be dependent on the rate of GMA diffusion into the natural rubber phase, especially at high peroxide concentrations and GMA content with the rate likely to increase with increasing both the GMA content and the temperature. This suggests that the GMA content is one of the major parameters, which affects the grafting reaction at a given constant temperature and mixing speed.

vi. Effect of Processing Time

In order to investigate the kinetics of the grafting reaction of GMA onto NR a set of experiments was prepared at a fixed composition, in the presence or absence of peroxide, with GMA concentration of 6 % and 12 %, T-101 0.02 molar ratio to GMA and temperature of 170°C and 200°C. It was found that the grafting reaction took place rapidly in both thermal and peroxide initiation conditions. However, the reaction in the presence of peroxide (T-101) proceeded faster than that of the thermal initiated reaction and had nearly finished within 10 minutes (see **Fig. 3.32**). The percentage of conversion of GMA monomers increased rapidly in the first 2.5 minutes, after which the extent of increase slowed down. The grafting efficiency increased first gradually up to 80% conversion and then increased slowly.

vii. Processing of NR-GMA in the Presence of a Coagent

Natural rubber was also processed with glycidyl methacrylate (GMA) in the presence of peroxide Trigonox-101 (T-101) and the coagent trimethylol propane triacrylate (TRIS). In the presence of TRIS, however, the torque values went up to a high torque maximum indicating a high extent of cross linking between natural rubber macroradicals and the coagent (**Fig. 3.33**). The reaction product was found to be hard and crumbly indicating that it contained high amount of gel.

3.4 Discussion

3.4.1 Grafting Mechanism

In the preparation of the GMA grafted-NR, initiation of grafting reaction is due to free radicals produced by the interaction of peroxide, GMA and NR. In the NR/GMA/T-101 system, for example, the peroxide T-101 decomposes to yield alkoxyl, butoxyl, and alkyl radicals (RO•) formed in the 'molten' NR system, which might interact with the monomer GMA or the rubber molecule producing a macroradical that initiates grafting. **Scheme 3.6** gives a proposed mechanism for the graft copolymerization of GMA onto NR via the free-radical initiation.

Scheme 3.6 Reaction mechanism of GMA grafting onto NR (cont.)

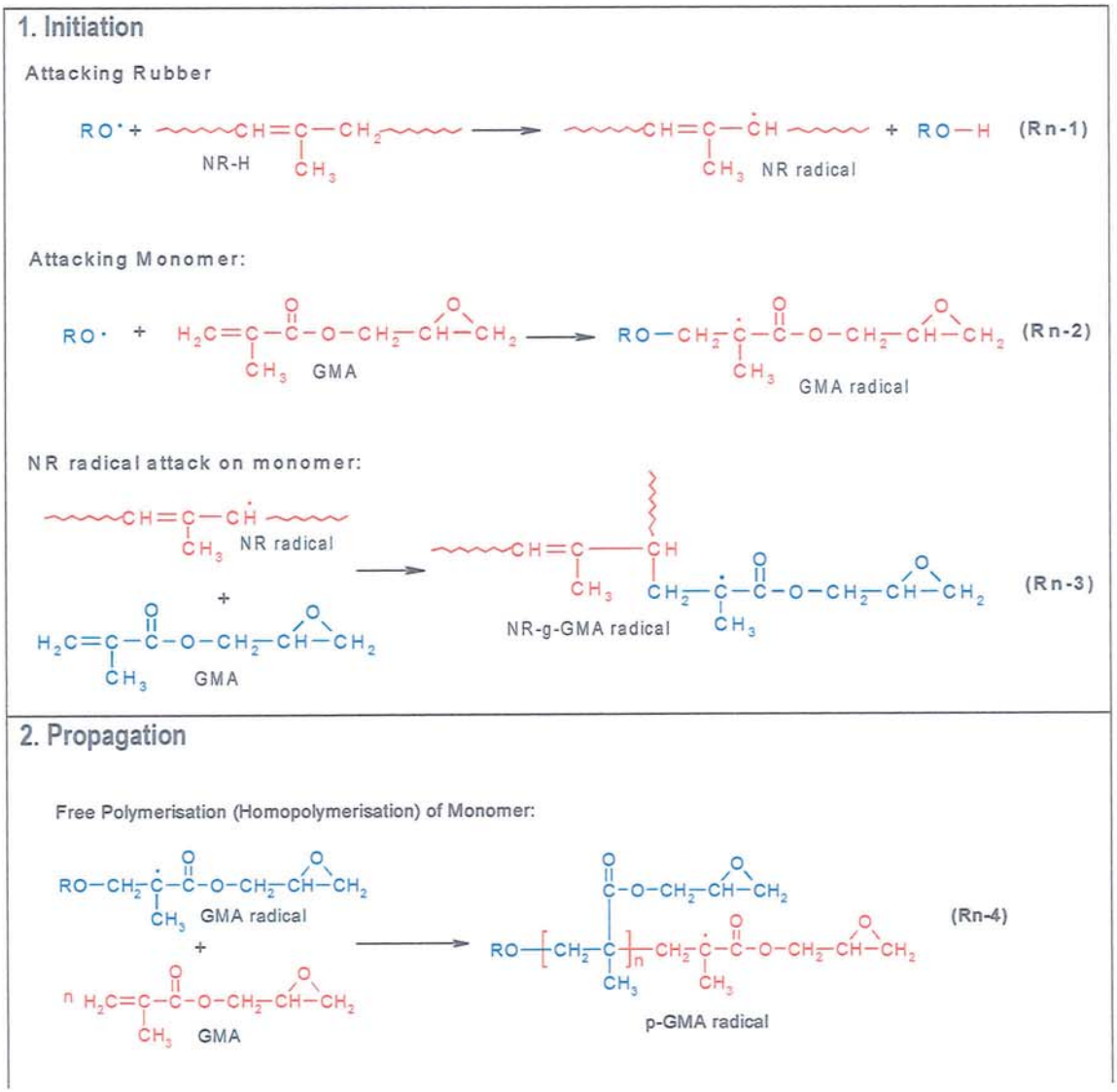

Scheme 3.6 (cont.) Mechanism of GMA grafting onto NR

Graft copolymerisation:

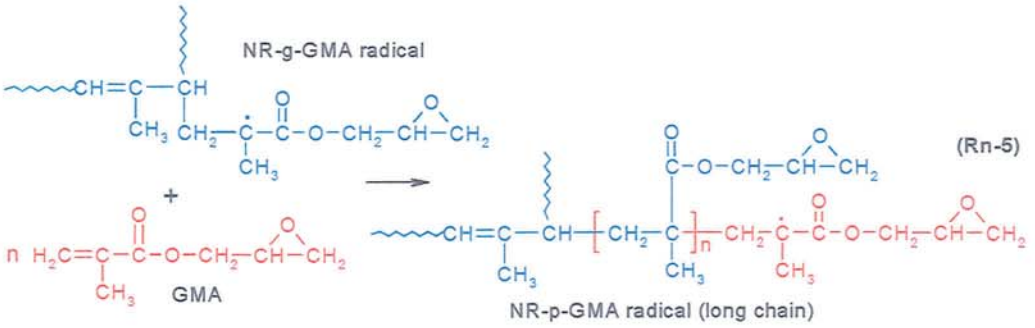

3. Chain Transfer to Macroradical

Transfer to rubber (NR-H)

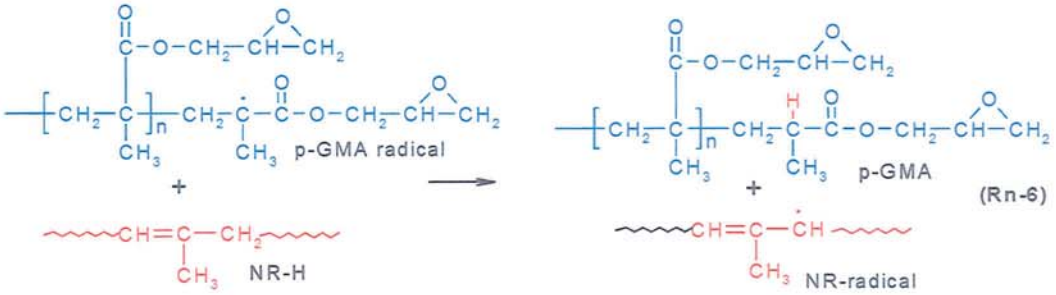

Transfer to rubber:

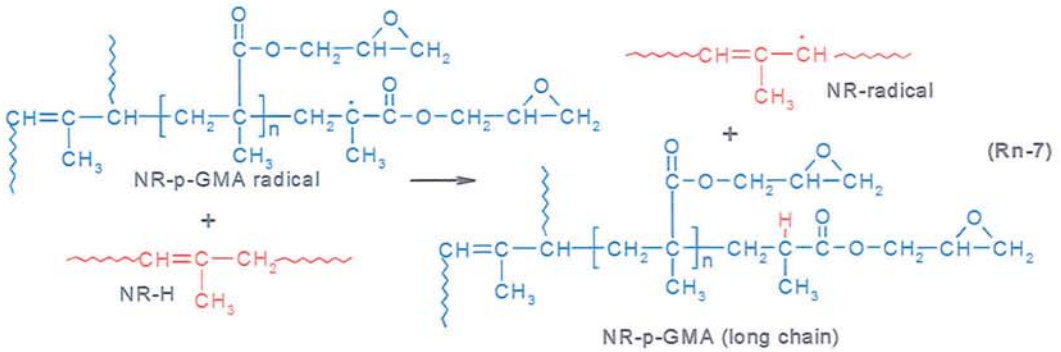

Scheme 3.6 (cont.) Mechanism of GMA grafting onto NR

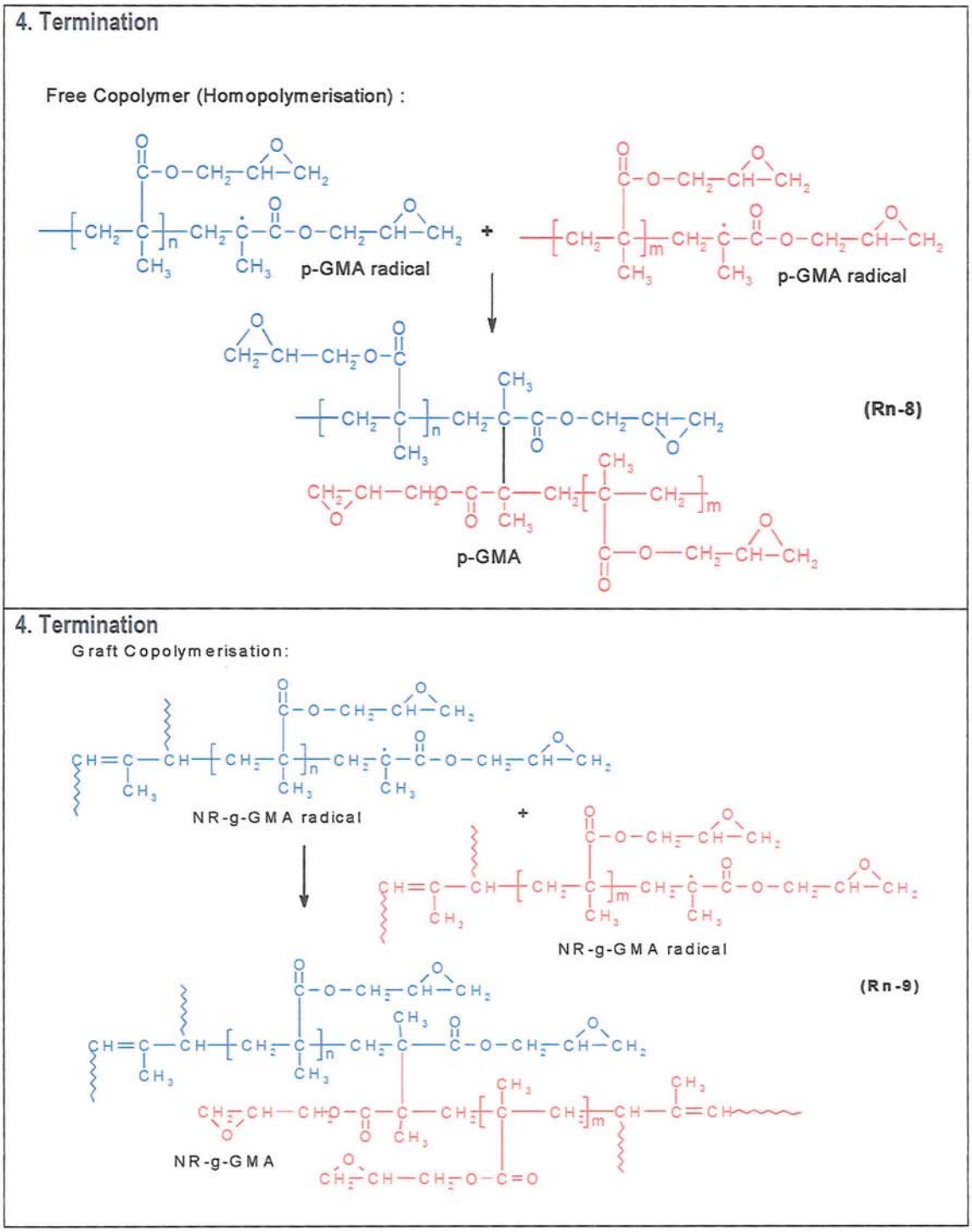

The alkoxyl, butoxyl, and alkyl radicals not only can add to double bonds or abstract hydrogen atoms to produce polyisoprenyl radicals (**Scheme 3.6, Rn-1**), which initiate monomers to form the graft copolymers (**Rn-3**), but also to initiate monomers (**Rn-2**) to

form polymeric radicals (**Rn-4**), which also can combine with polyisoprenyl radicals to terminate (**Rn-9**) or transfer to NR to form graft copolymers (**Rn-5, Rn-6,** and **Rn-7**). Moreover, some of the free homopolymer-GMA radicals can still terminate to form free copolymers (**Rn-8**). It is reasonable that grafting occurs by initiator radical attack on natural rubber; however, the chain-transfer processes can not be neglected. Lehrle *et al.* [368] studied the mechanism of the graft copolymerization of methyl methacrylate (MMA) on natural rubber in the presence of vinyl acetate (VA) and suggested that the formation of graft copolymers involved the chain transfer reaction when peroxide azo-isobutyronitrile (AIBN) was used as initiator. A similar observation was made by Merkel *et al.* [392] in the case of grafting of methyl methacrylate onto polybutadiene. In the case of grafting methyl methacrylate onto natural rubber, the excessive free PMMA radicals react with each other to form free copolymers more than to graft on the natural rubber and decrease the chain length of the grafts. Therefore, the production of PMMA is promoted more at high initiator content. On the other hand, the probability for the rate of chain transfer for the free polymer radicals to the natural rubber backbone is less than the rate of termination of free polymer radicals, favouring the termination process of copolymers over the chain-transfer process.

The success of a typical melt grafting experiment is usually measured in terms of the grafting yield dictated by the fraction of the monomer that becomes grafted onto the polymer backbone versus that which either remains unchanged or is consumed in side reactions such as homopolymerisation. In the experiments examined here, the results clearly showed that grafting glycidyl methacrylate (GMA) on natural rubber (NR) can be achieved by both thermal and peroxide initiation in the melt, though to varying degrees, the grafting efficiency of GMA by thermal initiation was quite low compared to that achieved by free radical initiation, see **Fig. 3.31** and **3.32**. However, if one compares this with a typical reaction of grafted GMA on polyolefins (e.g. PP [124,125], EPR [127]), then the observed grafting degree of GMA on NR by thermal initiation becomes quite meaningful. Similar results reported in grafting of maleic anhydride onto NR [134,394]. This is almost certainly due to the reactivity of the double bond on the NR backbone, which would give rise to sufficient amount of macro radicals via mechano-scission that would react with the GMA monomer. The grafting reaction of GMA onto NR in the solid state however, is complicated due to the extremely high viscosity of the natural rubber. Even at high temperatures, the natural rubber does not behave like a normal plastic melt and hence high

shearing forces would be exerted onto the rubber during the mixing (pseudo plasticity) [363,364,372,389-391].

3.4.2 Comparison of Effectiveness of Different Peroxides on GMA Grafting onto Natural Rubber

Figure 3.34 shows a comparison of the torque characteristic for the four different peroxides examined in this study and also under thermal initiation. Comparison of the efficiency of the different peroxides used in this work on the grafting of GMA onto natural rubber, see **Figure 3.35**, shows clearly that Trigonox 101 (T-101) is much more effective than benzoyl peroxide (BPO), dicumyl peroxide (DCP) and Trigonox-29B90 (T-29B90) at all processing temperatures except at temperature of 150°C where the latter peroxide (T-29B90) gave higher GMA grafting yield. The different results from the four peroxides may be caused by differences in their half-life times (**Table 2.3,** p.63), the reactivity of the initiator-derived radicals towards the natural rubber substrate, their solubility and partition coefficient, and the extent of cage reactions. The effect of the three peroxides (BPO, DCP, T-101) on the grafting yield and the torque characteristic of NR/GMA/peroxides was examined (**Fig.3.36**) as a function of peroxide concentration, while the GMA concentration was kept constant at 6 % w/w (processing temperature for BPO was 140°C, DCP and T-101 at 160°C). The GMA grafting degrees for the three peroxides used were seen to increase with an increase in the molar ratio of initiators from 0.01 to 0.05 (**Fig. 3.36E**). This trend can be explained by the fact that the radicals transfer to either rubber or monomer, producing macroradicals, which is enhanced on increasing the initiator, thus resulting in an increase in grafting. Observations of the torque behaviour during the grafting process gave an indication that the competition between the grafting reaction on the one hand and side reaction including poly-GMA and NR cross linking/chain scission on the other hand in the three peroxide systems differ significantly. It can be seen that the torque values were influenced by the amount of peroxides used. Increasing the peroxides concentration resulted in the production of more free radicals, depending on the nature of the peroxide and its ability for hydrogen atom abstraction from the natural rubber substrate. The grafting degree and the extent of crosslinking/chain scission are also found to be dependent on the type of peroxide used. The torque maximum in the case of DCP gave the highest values indicating the possibility of larger extent of side reactions, thus lower grafting degree compared to that of T-101. The

type of peroxide used as initiator for the GMA-NR modification reaction plays an important role, not only in terms of the level of the grafting degree, but also the nature of side reactions, disproportionation of NR and homopolymerisation of GMA. In the presence of a peroxide BPO, for example, there seems to be a correlation between the clear shorter time needed to reach the torque peak maximum and the rate of decomposition of the peroxide (see **Fig. 3.16 B** and **C**). With the curves in the two figures being almost identical, the higher the processing temperature, the shorter the half-life time of the peroxide, and the shorter time was required for a torque peak to appear indicating a faster rate of GMA modification. The grafting reaction in the presence of BPO resulted in a lower grafting degree (g-GMA_{BPO} = 0.5, 0.3, and 0.5 % at temp. 120, 140, and 160°C, respectively) compared to other peroxides (see **Figures 3.20, 3.24,** and **3.30 B** and **C**). The low GMA grafting degree of BPO is probability due to the fact that rate of decomposition of the peroxide is too fast, which is characterised by its short half-lifetime ($t_{1/2}$), compared to the overall rate of grafting (the half-life of BPO, $t_{1/2}$ = 2.5 min at 120°C, $t_{1/2}$ = 1 min at 140°C, $t_{1/2}$ = 0.32 min at 160°C, see **Table 2.3,** p.63). When BPO is replaced by DCP, T-101, and T-29B90, the location of second peak maximum, which is characterised by time to torque max, are not the same for these four peroxides (see **Fig. 3.19A** and **3.23A**). If there is indeed a correlation between peak location (time to Tq-max) and the half-lifetime of the peroxides, it would be expected that a shift of the torque maximum to a longer time when decreasing the grafting temperature. It is clearly observed in the presence peroxide DCP (see **Fig. 3.20B** and **C**), for example, the peak maximum (time to Tq-max) is located at t = 0.25, 0.75, 1.25, 2, and 4 min when temperature of 200,180,160, 140, and 120°C, respectively.

There are two points that remain difficult to understand. The first one is that the time to torque max is shorter than the half-life time of the peroxide. At the processing temperature of 140, 160,180, and 200°C, the time to Tq-max of T-101 are 2, 1.25, 0.75, and 0.25 min, respectively, whereas, at these temperatures, the half-life time of peroxide are 23, 2.1, 1.4, and 0.25 min, respectively. This mismatch may be explained by the fact that the values of the half-life time of the peroxides, as reported in **Table 2.3**, are a measure of the rate of formation of primary radicals. As discussed above, the peroxides DCP and T-101 resulted GMA grafting degree, higher than that of BPO, because of the two former has a longer

half-life times. However, at lower temperatures in which their half-life time is longer, resulted in a low GMA grafting level (see **Fig. 3.20** and **3.24**).

Since the peak maximum is believed to be related to the reaction competition between GMA grafting and other side reactions (poly-GMA and chain scission or crosslinking), it is understandable that there is a correlation between half-life time of a peroxide and location of the peak (time to Tq-max). However, there is no a perfect match between the half-lifetime of the peroxide and GMA grafting degree (**Fig. 3.35**). It is important to note that the success of a free radical grafting depends very much on the competition between the grafting and side reaction, which in turn is associated not only with the rate of formation of primary radicals, which is characterised by the half-life time ($t_{1/2}$) of the free radical generator used, but also the ability the primary radicals to abstract hydrogen atoms from NR to form NR macroradicals. Hu *et al.* **[1,45,123]** suggested that a good peroxide should have a half-life time which is about one-fifth of the reaction time so that once the reaction is over, the free radical generator is also exhausted. The type of peroxide and the reactivity of its primary radicals also play an important role **[395-399]**. The decomposition processes of BPO results in the formation of acyloxyl radicals of benzoyloxyl ($C_6H_5COO\cdot$) which undergo a subsequent β-scission reaction to give the corresponding phenyl radicals ($C_6H_5\cdot$) and carbon dioxide (CO_2), see **Scheme 3.7** (p.126). Benzoyloxy radicals have insufficient lifetime to react directly with the substrate during the grafting process of GMA on the natural rubber backbone, and it is known **[397,398]** that diacyl peroxides such as BPO, are more prone to induced decomposition than most other dialkyl peroxides. From studies on PP cross-linking efficiency of various types of peroxides it was concluded that the peroxides which released benzoyloxy or phenyl radicals are the most efficient in the cross linking reaction **[52,400,401]**. On the contrary, initiators giving alkyl radicals are inefficient **[395,398]**. It is understandable from the torque curves in **Fig. 3.34B**, that the final torque in the BPO system are higher than the others.

When NR and GMA were processed with the peroxides DCP and T-101, a higher grafting degree resulted. Dicumyl peroxide (DCP) is a dialkyl peroxide that (compared to BPO) has longer half-life times at higher temperatures ($t_{1/2}$ = 3 min at 160°C, $t_{1/2}$ = 1.2 min at 180°C, and $t_{1/2}$ = 0.25 min at 200°C), see **Table 2.3** (p.63). The decomposition pathway of DCP is well established **[3]** and involves the initial O-O bond homolysis to generate cumyloxyl

radicals ($C_6H_5C(CH_3)_2O\cdot$) which undergo β-scission to methyl radicals and benzophenone and phenyl radicals (see **Scheme 3.8,** p.126). According to Borsig *et al.* **[395-398]**, the fragmentation of the cumyloxyl radical is still greater, more than 80% of primary radicals are fragmented into phenyl radicals (temp. 170°C), which are prone to a cross linking reaction. This is probability why the cross linking efficient of DCP is still higher in the NR/GMA/DCP system as shown by its higher final torque when compared to T-101 (**Fig. 3.34B**). The methyl radicals obtained are also more reactive towards hydrogen atom abstraction, thus producing more macroradicals of natural rubber available to react with GMA which would account for the increased level of GMA grafted NR compared to BPO (see **Fig. 3.35A**).

The greater influence of the reactivity of primary peroxide radicals of various types of peroxides on the grafting reaction efficiency is rather complex, not only the rate of decomposition ($t_{1/2}$) and reactivity of primary radicals of peroxides but also kinetic parameters and physical factors like solubility play an important role. The great difference between the efficiencies of T-101 and DCP is probability connected with the fragmentation of primary cumyloxyl radicals to reactive phenyl radicals and with a diffusion rate of cumyloxyl radicals lower than that of *tert*-butyloxyl radicals of T-101. Decomposition of T-101 leads to a larger formation of primary and secondary alkyl radicals and so increases the portion of recombination and disproportion reactions towards fragmentation instead of NR branching/crosslinking. As a quantitative illustration of the difference between various radical primers and the reactivity of individual radicals of initiator, **Table 3.1** lists the value of transfer constants (k_{tr}) and the corresponding relative distance (d) of various initiator radicals to the methyl group of toluene **[52,395]**.

Table 3.1 Transfer constant (k_{tr}) of free radical typical for some commercial peroxide decomposition onto toluene and relative distance (d) of a pair of polymer radicals after transfer reaction of primary radicals in peroxide **[52]**.

Type of Free radical	$\cdot CH_3$	$(CH_3)_3CO\cdot$	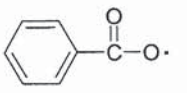	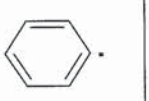
k_{tr} ($dm^3/mol/s$)	5×10^3	9×10^4	1×10^6	1×10^7
d	45	10	3	1

From the chain transfer constants (k_{tr}) of primary radicals of initiators on the polypropylene unit, Borsig *et al.* **[395-398]** calculated the corresponding relative distance (*d*). The lower the value of the transfer constant (k_{tr}), the greater is the probability to diffuse further from each other and both the primary radicals from the side of formation: the *d* value will increase. The distance *d* is, furthermore, indirectly in proportional to the mutual recombination or disproportionation reaction of NR. The relative distance, *d*, between NR and radicals arising at the transfer from methyl radicals in comparison with phenyl ones are much greater. The greater the distance between NR macroradicals, the greater is the probability of a fragmentation reaction. This is why the final torque in the T-101 system is lower than the others (**Fig. 3.34B**). The decomposition processes of T-101 and T-29B90 are more complex because of the presence of *tert*-butoxyl and the large alkoxyl radical intermediates which cleave to give a series of other radicals (see **Scheme 3.9** and **3.10**). As mentioned above, the efficiency of a peroxide to initiate the grafting reaction is dictated not only by the rate of peroxide decomposition ($t_{1/2}$) and reactivity of primary radicals of peroxides but also kinetical parameters and physical factors like its solubility and volatility play an important role. As shown in **Scheme 3.9** the breakdown of a T-29B90 molecule gives a low-reactive *biradical*, (3,3,5-trimethyl-cyclohexana)-1,1-di-oxyl radical, and two *tert*-butoxy ($\cdot OC(CH_3)_3$) radicals, which, during fragmentation, produce methyl reactive radicals $\cdot CH_3$. In a more complicated way, the broken down T-101 molecule leads to producing more $\cdot OC(CH_3)_3$ radicals (**Scheme 3.10**), the latter is highly capable of H-abstraction giving rise to a high extent of the grafting reaction. Despite the increased concentration of reactive radicals (methyl, alkyl, and *tert*-butoxyl) during its thermal decomposition of T-101 (**Scheme 3.10**), as compared with T-29B90 (**Scheme 3.9**), the latter ensures a higher grafting efficiency, especially at a lower temperature (150°C), see **Fig. 3.35**. This is indicative of the fact that chemical activity of peroxides and the half-life times may not be the only decisive factors for the yield of grafting and side reaction products. To explain the differences in the initiating capacity of the peroxide T-101 and T-29B90 could be explained as follows. In the same processing temperature (<150°C), T-29B90 which has a shorter half-life time decomposes to give a higher transient methyl ($\cdot CH_3$) radical concentration compared with the same initial concentration of T-101. In a different way, the decomposition of T-101 is rendered more complex because the alkoxy radical intermediate cleaves to give a higher alkyl radical preferentially rather than a methyl radical (**Scheme 3.10**). The differences in the types of radicals resulted from the two

peroxides and the different transfer constants (k_{tr}) between methyl and *tert*-butyl radicals (as shown in **Table 3.1**) would explain why at a lower temperature the GMA grafting in T-29B90 system higher than when using a longer half-life peroxide such as T-101 (see **Figure 3.35B**). It is connected with the above-mentioned idea concerning the nearness when pairs of radicals are formed, which is important at the formation of transition structures before the grafting reaction or other side reaction. It follows the rate of peroxide decomposition (momentary radical concentration) also plays an important role.

The influence of T-101 content (0.01–0.05 molar ratio to GMA) on the GMA grafting degree on the rubber was investigated in the presence of various GMA concentrations (3-18 % phr) at 160°C. It was found that by increasing the amount of initiator from 0.01 to 0.05 (molar ratio to GMA), the grafting content doubled (see **Fig. 3.25** and **3.26**). This may be explained by the fact that, by increasing the amount of T-101, the concentration of the radical sites on the rubber chain increased, leading to an increase in the possibility of the reaction between GMA and the rubber chain. The decomposition of peroxides generates free radicals which react with the NR macroradicals via initiation by H-abstraction via the double bonds of the rubber chains. These macroradicals would not only initiate the grafting reaction of GMA onto the rubber chains, but would also lead to cross linking or chain scission due to the high radical reactivity of double bond of the rubber chains which makes the crosslinking much more prevalent in at higher peroxide concentrations ($\geq$ 0.05 mr), see final torque value at higher peroxide concentration **(Fig. 3.36)**. The cross linking should be avoided or minimised and this could be achieved by carefully balancing the concentration of peroxide and processing temperature. The GMA grafting reaction on NR is suggested to follow the mechanism shown in **Scheme 3.11**. The overall mechanism consists of reactions in the elastomer matrix, in the GMA domains, and between the elastomer and the GMA. In the elastomer matrix, the allylic hydrogens (**Scheme 3.11-A,** position (a),(b), and (c)) are easily abstracted by peroxide radicals resulting in resonance stabilised macroradical of *cis*-1,4-polyisoprene. Resonance structures of the polyisoprene radicals result in different structures as shown in **Scheme 3.11(A)** and numerous other structures are possible in the NR/GMA/peroxide system that result in the final grafting and crosslinking reactions and some probable structures are shown in **Scheme 3.11(B)**.

Scheme 3.11 Chemical structure and grafting reaction of GMA on NR [402] (Cont.)

A. H-Abstraction NR + Peroxide

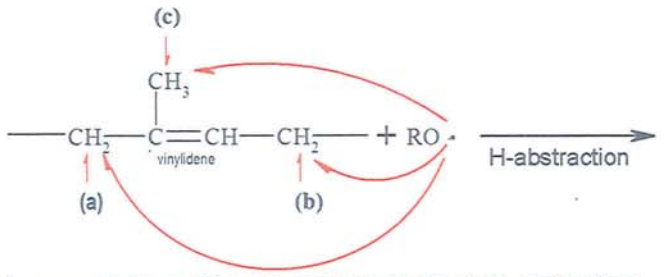

(a, b, c are allylic position, the most vulnerable to H-abstraction)

Resonance:

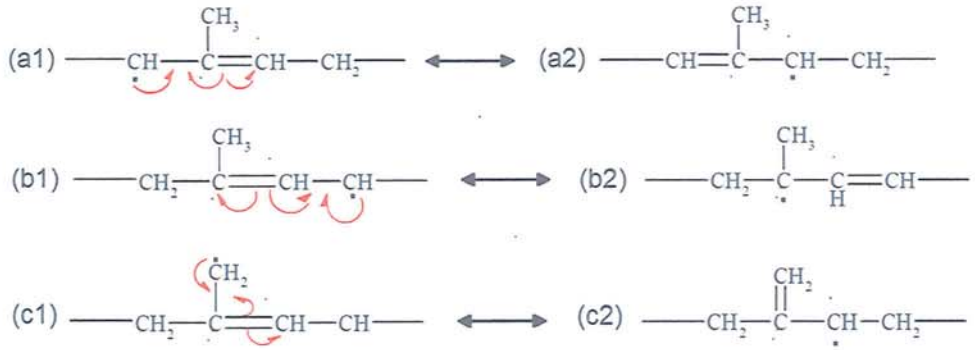

B. NR + GMA reaction Products

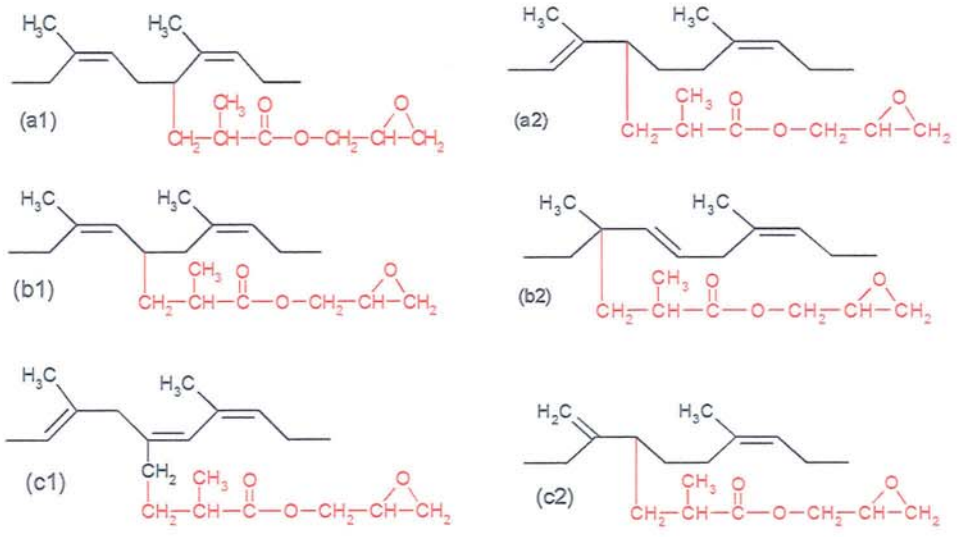

Scheme 3.11 (Cont.) Chemical structure and grafting reaction of GMA on NR.

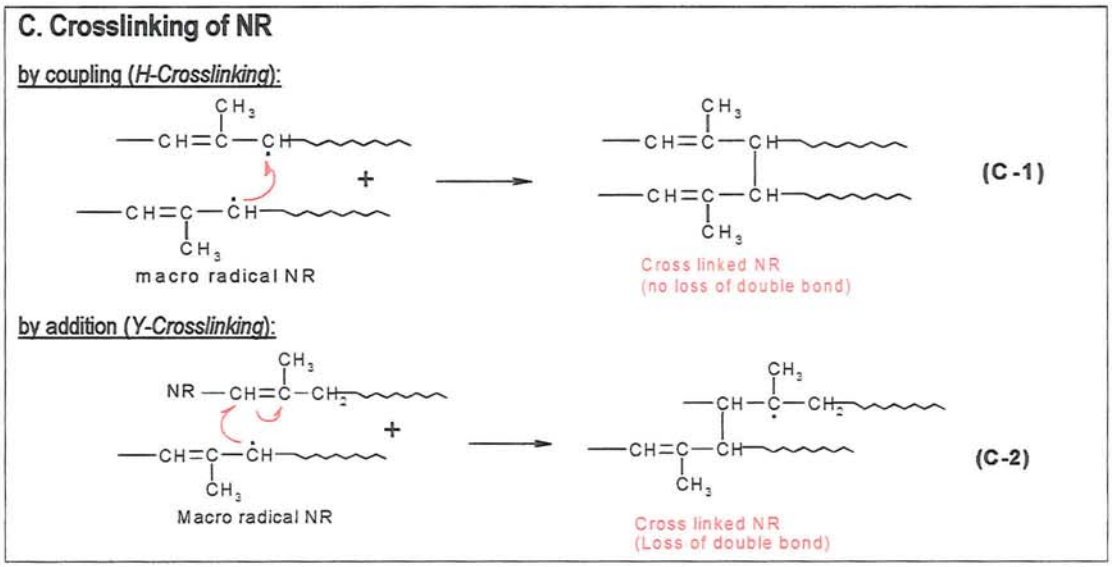

The polyisoprenic macroradicals not only initiate the grafting reaction of GMA onto the polymer chains, but also lead to branching and crosslinking of the polymer. The processing temperature influences the overall free radical grafting process as both the kinetic and thermodynamic aspects of all the elementary reactions are involved. Allyl radicals will recombine or combine with other (primary formed) radicals 100 times faster than their disproportionation reactions [396,398] and so would increase the molecular weight of NR. The vinylidene bonds in natural rubber are probability also effective in the reaction with NR macroradicals giving rise to a new covalent bond between two NR chains compared to mutual recombination reaction of two primary NR macroradical formed (see step **C-2** in **Scheme 3.11**). Therefore, *H-crosslinking* reactions by coupling reactions (see step **C-1**) and *Y-crosslinking* by addition reactions (step **C-2**) are both possible [402]. The reaction of grafting GMA onto natural rubber in the presence of peroxide results in highly crosslinked clusters and the structure of crosslinked natural rubber are complicated by resonance of the macroradicals. Crosslinking reactions in natural rubber (*cis*-1,4-isoprene) would result from a *'coupling reaction'* of two radicals via H-abstraction (referred as *H-crosslinking*), without involving the diene bond, as well as by *'addition reaction'* through the double bonds (referred to as *Y-crosslinking*) by thermal initiation and/or peroxide initiated-NR (see **Scheme 3.11C**). Furthermore, it was also shown that the 1662 cm^{-1} peak area index of the processed rubber at every temperature above 140°C in the presence of peroxides was higher than that in their absence, see **Figure 3.37C**. It can be concluded that the crosslinking

reaction which involves the diene double bond (addition reaction, step **C-2** in **Scheme 3.11**) occurs more intensively at temperatures above 140°C (see **Fig. 3.38A**). An interesting finding is that for the grafting process below 140°C, the cross linking reaction which involves the diene bond does not seem to be important as shown by the absence of any change in the peak area index (1662 cm^{-1}) for the temperature range below 140°C (**Fig. 3.38A**). At the same time however, the grafting reaction increased substantially with increasing temperatures from 100°C-160°C. It is worth noting that for temperatures above 170°C, the extent of the cross linking reaction seems to increase (as shown by sloping down of the double bond peak area index) and simultaneously GMA grafting reaction decreases (**Fig. 3.38A**). This happens due to the fact that the cross linking reaction is more dominant compared to the GMA grafting reaction onto NR at temperatures above 170°C, thus, the optimum temperatures for the GMA grafting under these condition are in the range of 140°C-160°C. A decrease in elastomeric double bond, υ(C=C) at 1662 cm^{-1}, was observed with increasing processing temperature under both thermal and peroxide initiation and this can be clearly observed from FTIR analysis (see **Figure 3.37**) and therefore it is suggested that the crosslinking reaction formed by addition cross-linking (*Y-crosslinking*) increases at higher temperatures. At a constant processing temperature of 160°C, a higher T-101 concentration gave rise to higher grafting degree and interestingly the double bond peak area index was found to remain constant (see **Fig. 3.38B**). The increasing peroxide concentration does not affect the peak area index (amount of the diene bond) but it does drive up the grafting degree. It should be noted that the grafting product at higher T-101 concentration (above 0.04 mr) showed visually a higher degree of cross linking (i.e. rubber was crumbled). This suggests that the cross linking reaction, in the presence of peroxide is affected mainly by temperature and to a lesser extent by the concentration of the peroxide and takes place predominantly by a coupling mechanism, without involving the diene bond. Meanwhile, the cross linking reaction in the absence of peroxide (thermal initiation) seems to occur more predominantly by an addition reaction mechanism, involving the diene bond (**Scheme 3.11** step **C-2**). Therefore, an effort to maximise grafting degree of monomers by simply increasing the initiator concentration is likely to be counterproductive because of the consequent increase in the extent of side reactions. In another strategy by adding appropriate coagent can act to improve both the grafting yield and minimise the extent of degradation. The addition of styrene **[168,376]** as a comonomer to the grafting system of MA onto NR significantly improved the grafting percentage of MA (NR in toluene

solution, MA 5-25 %, BPO 0.5-1.25 molar ratio, St 0.01-0.1 molar ratio, 60-80°C, 2h) [168]. It is proposed that the styrene plays a role as a charge transfer complex with MA. The styrene can react first with the rubber macroradical generated from the reaction of BPO initiator, followed by the reaction with MA molecules, leading to improvement of the grafting efficiency of MA. However, in this work, an attempt to add a reactive coagent, e.g. TRIS resulted in excessive crosslinking because of the very high reactivity of the coagent and C=C from the natural rubber. Therefore, the use of any multifunctional and highly reactive coagent such as TRIS or DVB could not be applied successfully in the grafting of GMA onto natural rubber. When graft copolymerization of mixtures of acrylonitrile (AN) and methyl methacrylate (MMA) on crumb natural rubber was carried out in toluene at 60°C, it was found that the presence of comonomer AN reduced the extent of homopolymerised MMA (PMMA) and grafted MMA [403]. In this copolymerization system, the electronic charge (*e*-value in *Q-e Scheme*) or monomer reactivity ratio (*r*) is an important factor that may affect monomer reactivity in radical polymerization: monomer with relatively high *e*-value will produce radicals that are relatively less reactive toward propagation. The reactivity ratio of acrylonitrile (AN) is threefold lower than value for MMA (r_{AN} = 0.56 and r_{MMA} = 1.5) [404]. It may therefore be expected that acrylonitrile radicals will react relatively less readily than radicals derived from MMA in graft polymer formation, see **Section 5.3.5** (p.279) for further discussion.

It was found that the purity of natural rubber had also affected the grafting efficiency. Compared to raw natural rubber, acetone purified natural rubber samples gave rise to higher grafting degree. The modified natural rubber obtained from unpurified natural rubber at low temperature (below 160°C) was crumbly, indicating high degree of crosslinking. This may be attributed to the fact that the natural rubber contains 5-8 non-rubber constituents that have been shown [353,388,389] to give ^{13}C NMR signals of hydroperoxide, aldehyde, epoxy and tertiary hydroxyl groups typical for oxidized rubber. The fraction of non-rubber in the natural rubber can compete or interfere with many reactions. This is an indication that virgin rubber contains polyisoprene molecules capable of acting as scavengers of free radicals to form crosslinked rubber and contribute also to oxidative degradation of the rubber. The purification by Soxhlet extraction with acetone can reduce the amount of non-rubber substances giving rise to higher grafting (all results in this work were obtained after an initial acetone extraction of the raw rubber).

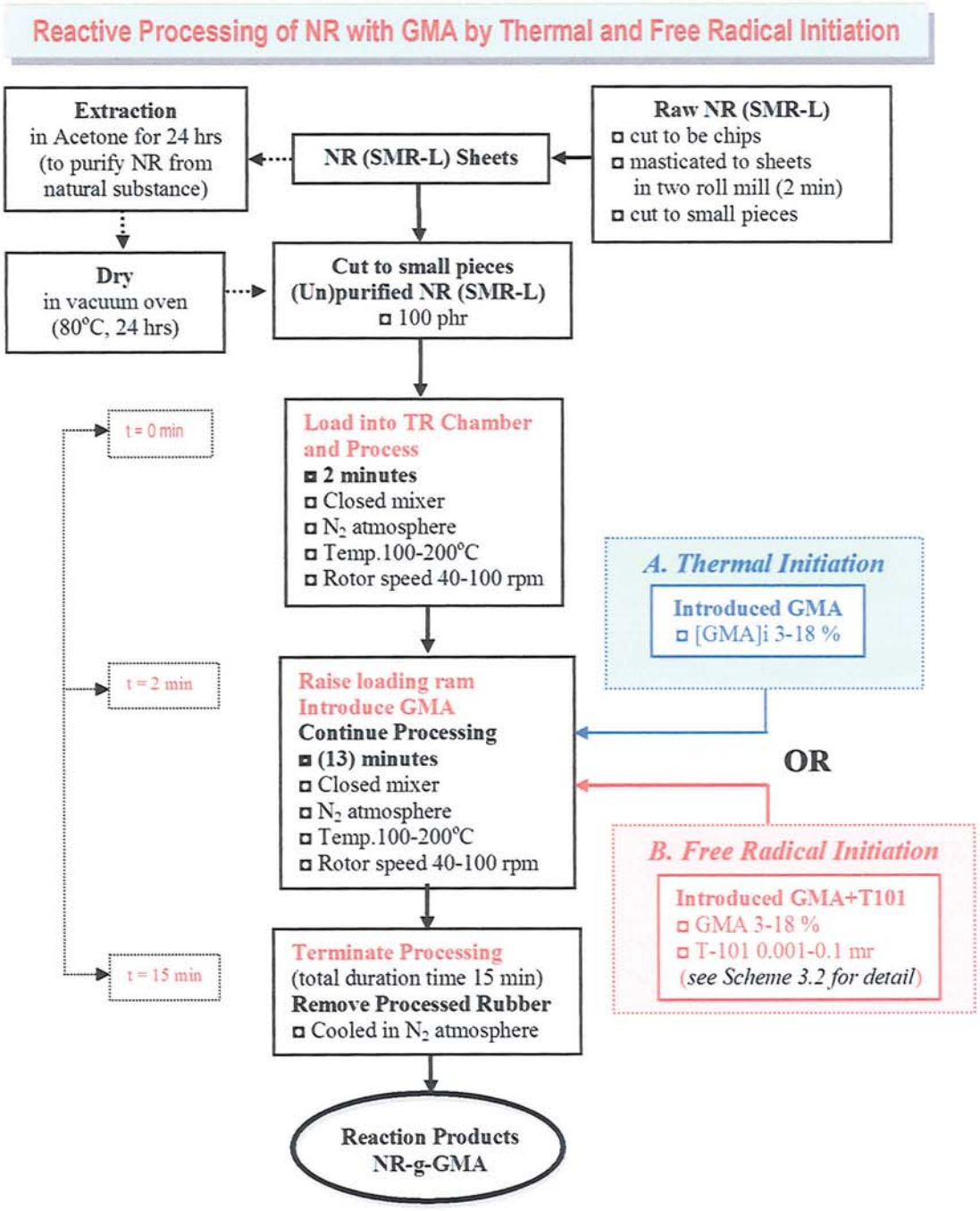

Scheme 3.1 Flow chart for reactive processing of NR (SMR-L) with GMA by (A) Thermal and (B) Free radical (peroxide) initiation

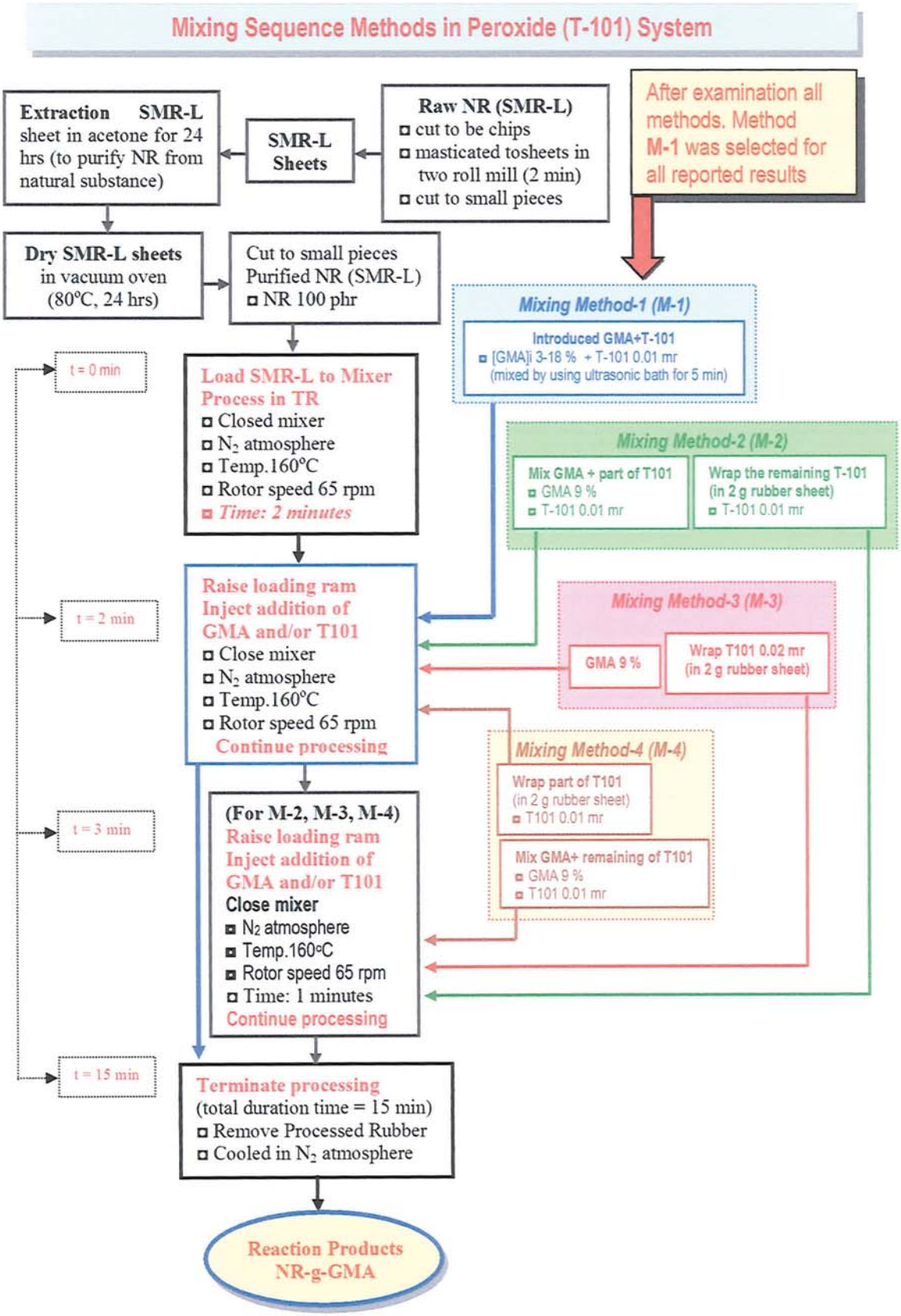

Scheme 3.2 Flow chart for mixing sequence method (M-1, M-2, M-3, and M-4)

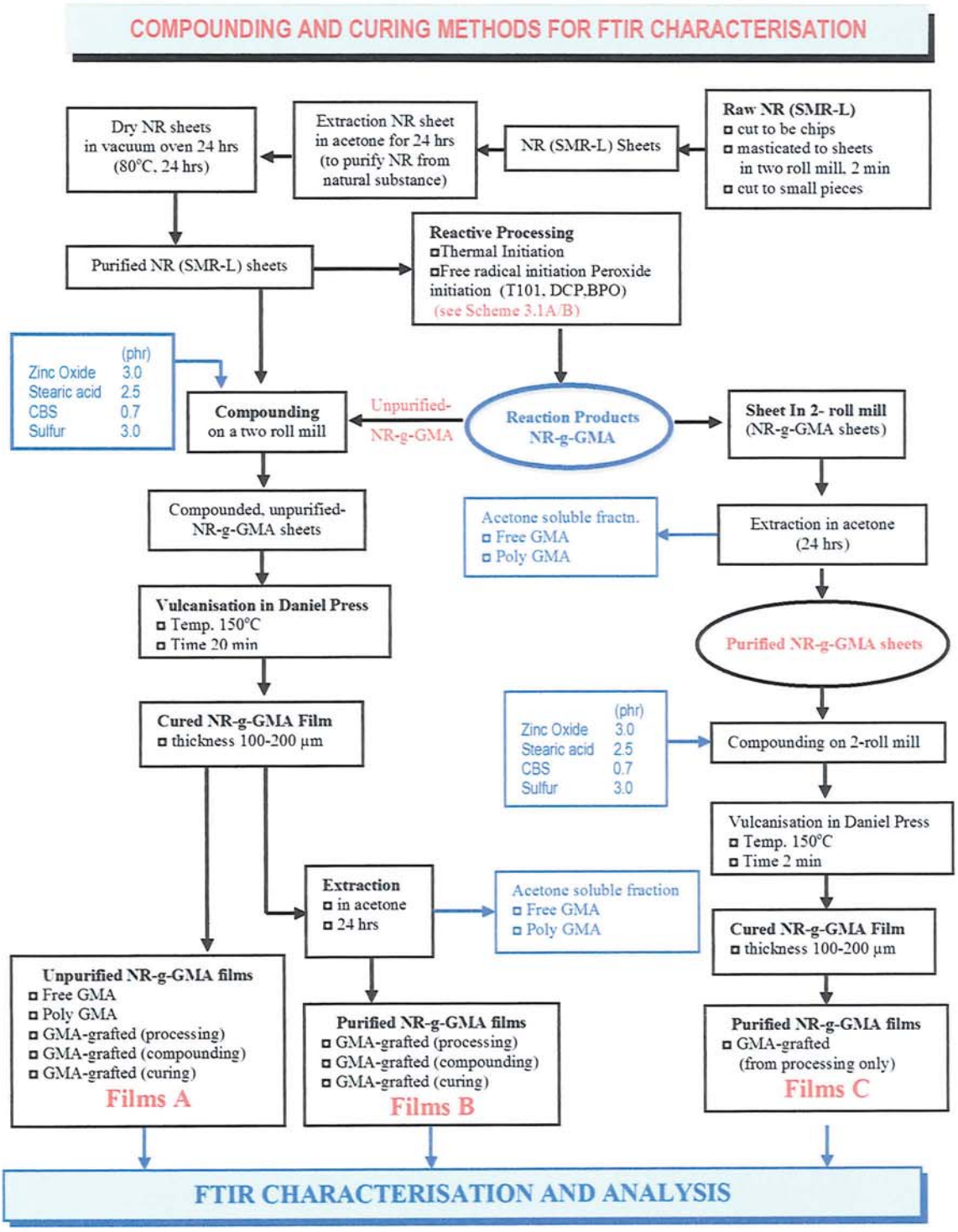

Scheme 3.3 Flow chart for compounding and curing methods (before characterisation in FTIR spectroscopy)

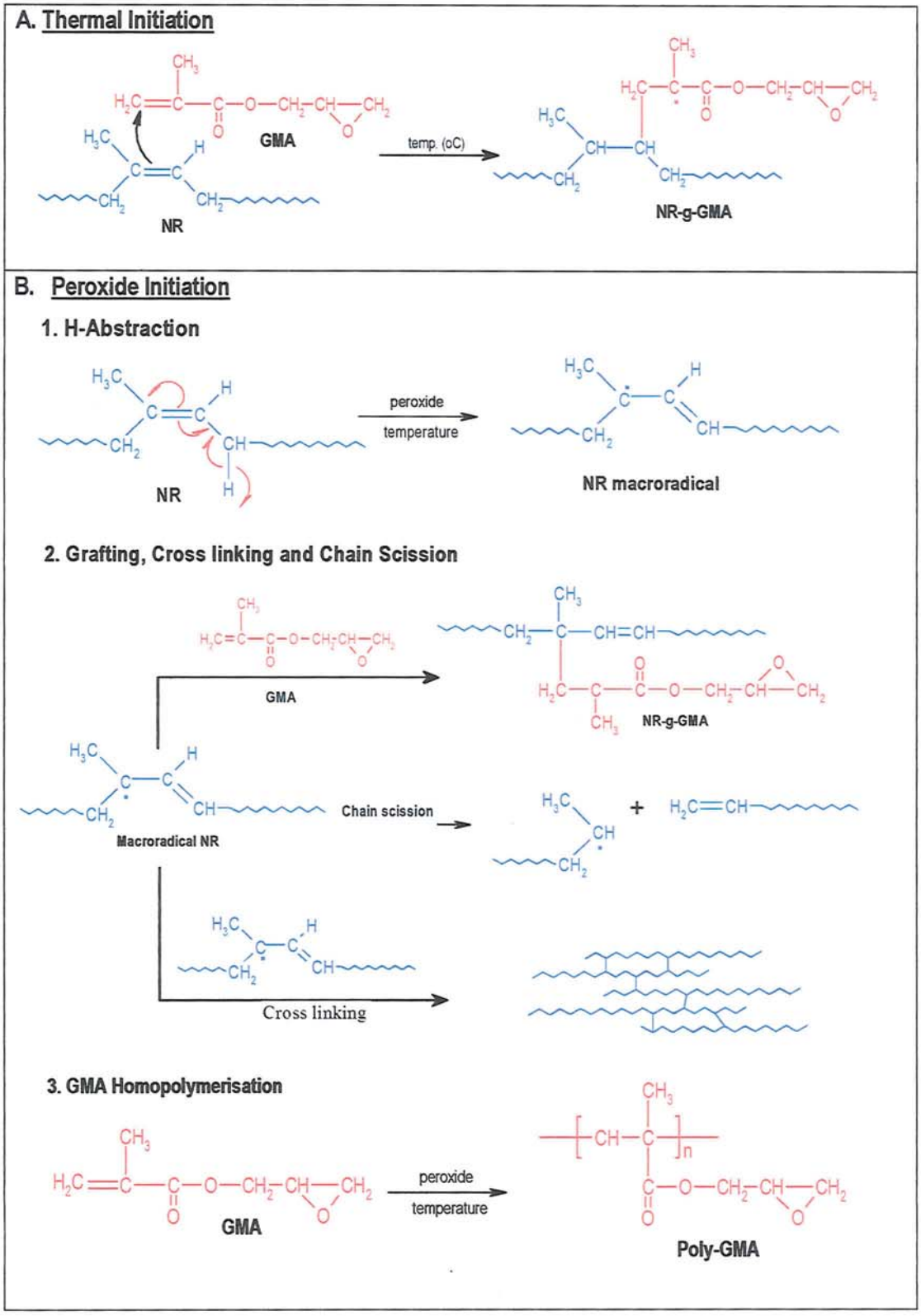

Scheme 3.4 The grafting reaction product of GMA onto natural rubber

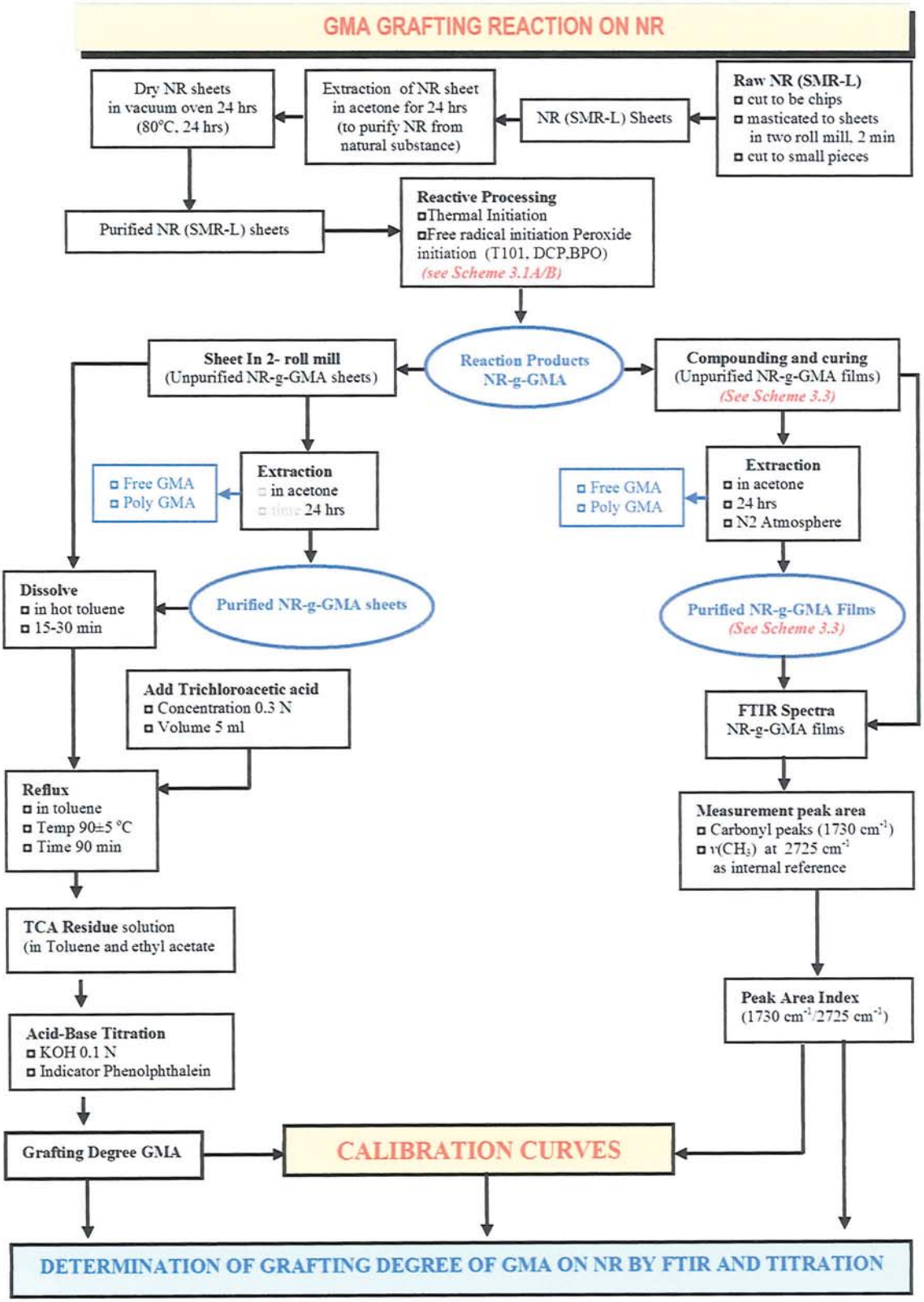

Scheme 3.5 Flow chart for determination of grafting degree of GMA on the processed natural rubber by FTIR and titration

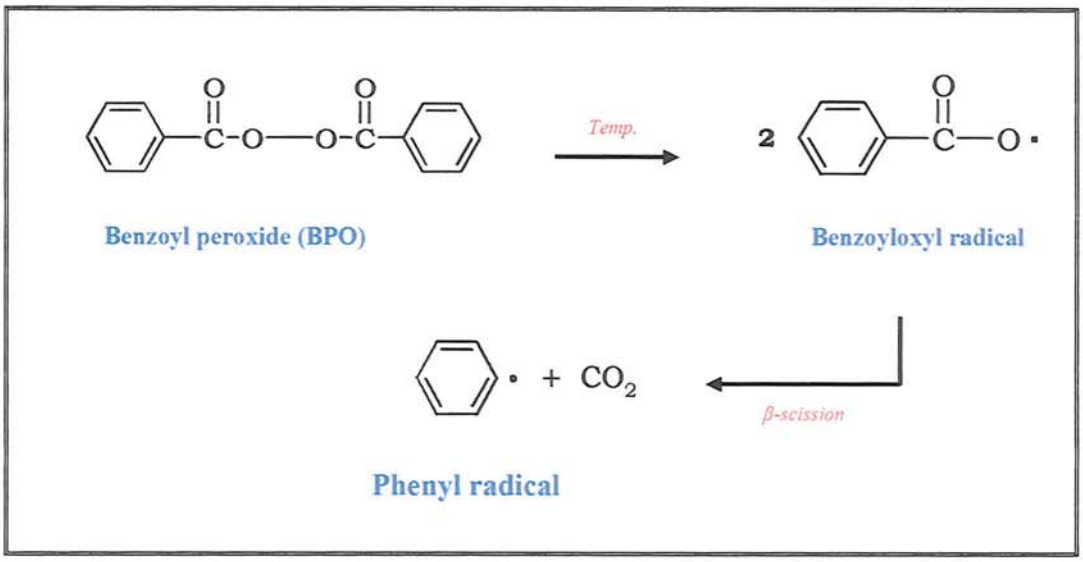

Scheme 3.7 The mechanisms for radical generation from **benzoyl peroxide (BPO)**

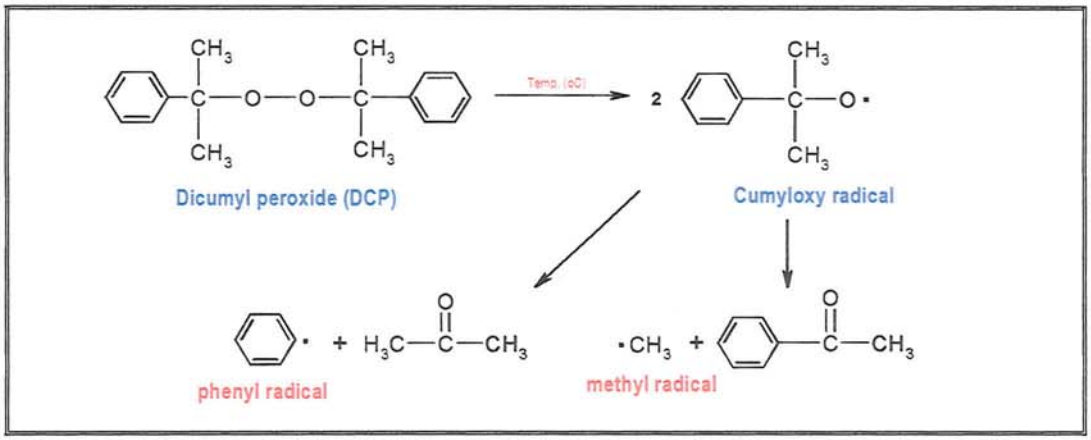

Scheme 3.8 The mechanisms for radical generation from **dicumyl peroxide (DCP)**

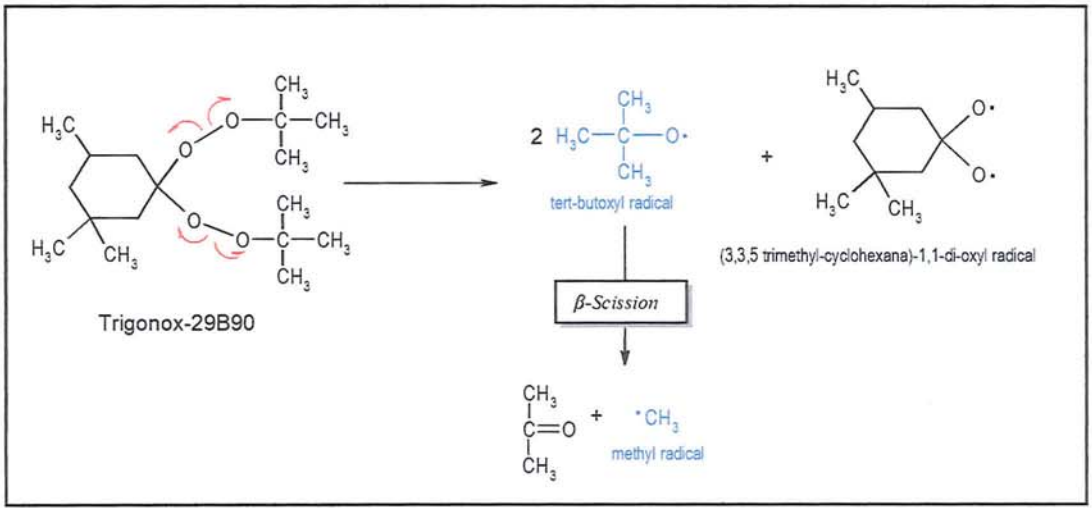

Scheme 3.9 The mechanisms for radical generation from **Trigonox-29B90**

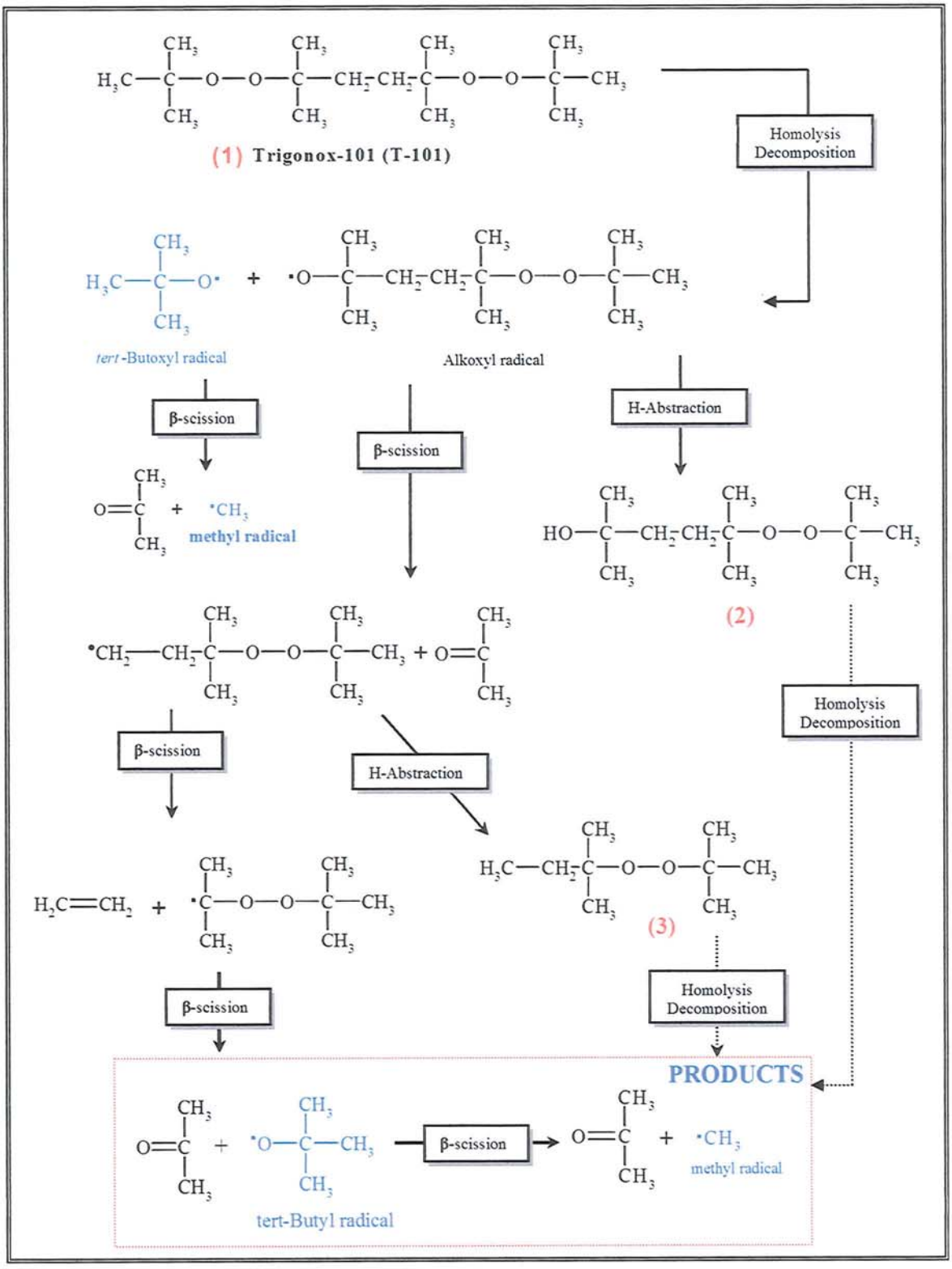

Scheme 3.10 The mechanisms for radical generation from **Trigonox-101**

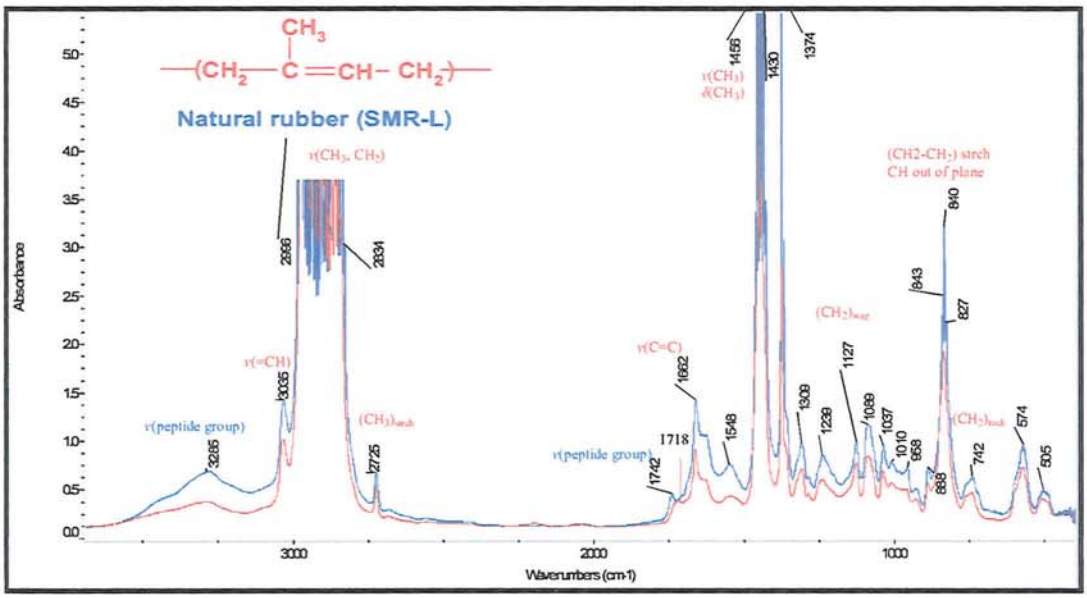

Figure 3.1 FTIR spectra of cured pressed raw NR before (blue) and after (red) extraction with acetone for 24h, pressed at 150°C for 2 min. (Sample C1-0 Table B.3.1 in Appendix B)

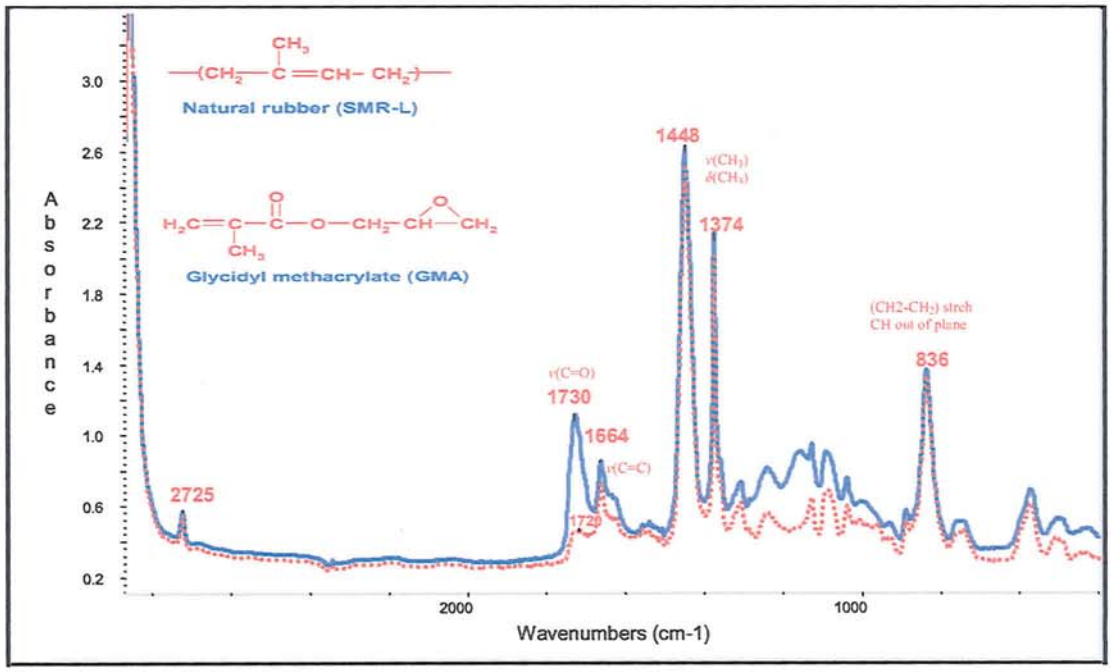

Figure 3.2 FTIR spectra before (blue) and after (red) acetone Soxhlet extraction cured pressed films (pressed at 150°C, 2 min) of processed NR-GMA, thermal initiation at low temperature. Sample T1-1 Table B.3.1 in Appendix B ([GMA]i = 6%, no peroxide, 100°C, 65 rpm, 15 min).

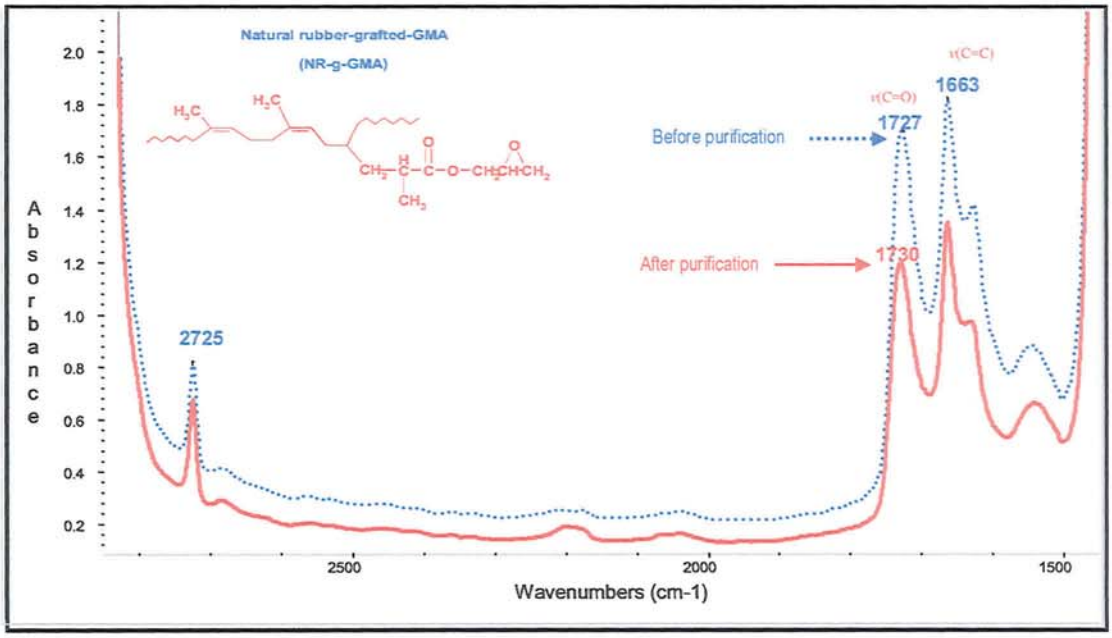

Figure 3.3 FTIR spectra of cured pressed films of processed NR/GMA/T-101 before (blue) and after (red) purification by extraction in acetone for 24 hours (Sample G4-3 Table B3.2 in Appendix B; [GMA]i = 12 %. [T-101] = 0.03 molar ratio to GMA, 160°C, 65 rpm, 10 min, mixing method M-1).

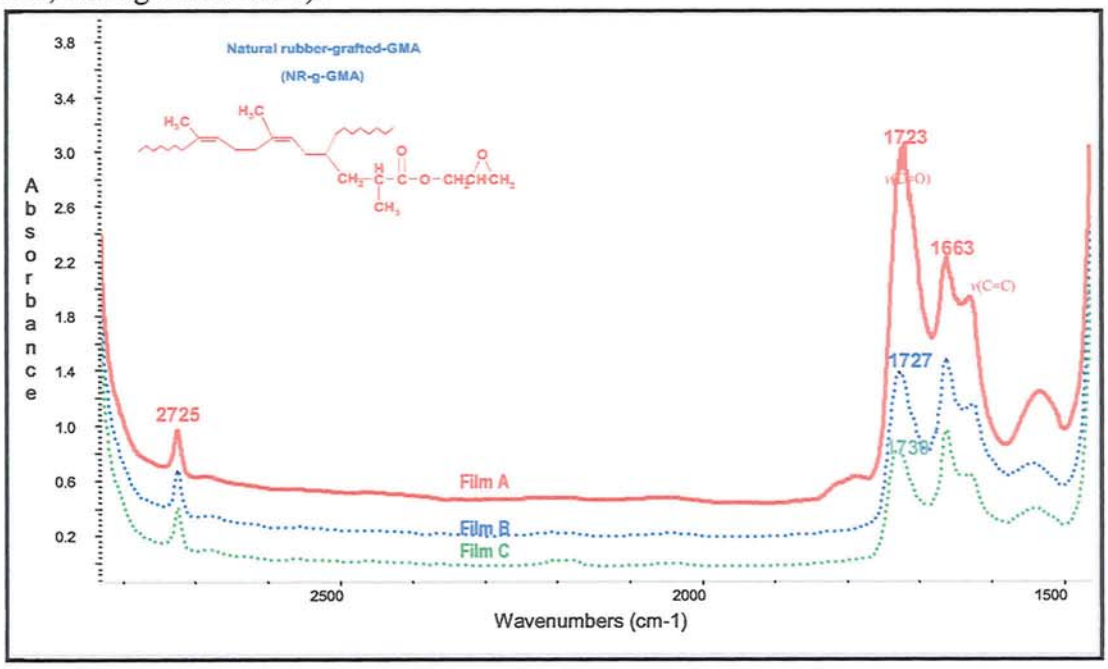

Figure 3.4 Comparison of FTIR spectra from cured films of NR-g-GMA using different extraction and compounding procedures, see **Scheme 3.3** (p.123) (Sample G4-3 Table B3.2 in Appendix B; [GMA]i = 12 %. [T-101] = 0.03 molar ratio to GMA, 160°C, 65 rpm, 10 min, mixing method M-1).

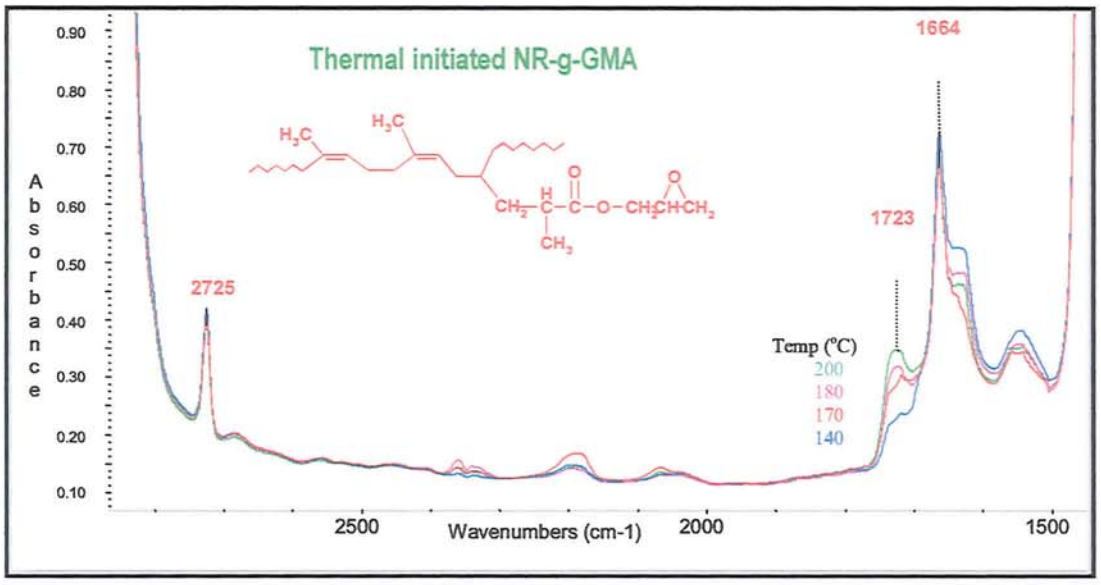

Figure 3.5 FTIR spectra of processed NR-g-GMA by thermal initiation (Films C), samples T1-n Table B.3.1 in Appendix B (extracted NR 100 phr, [GMA]i = 6%, no-peroxide,160-220°C, 65 rpm, 15 min, mixing method M-1).

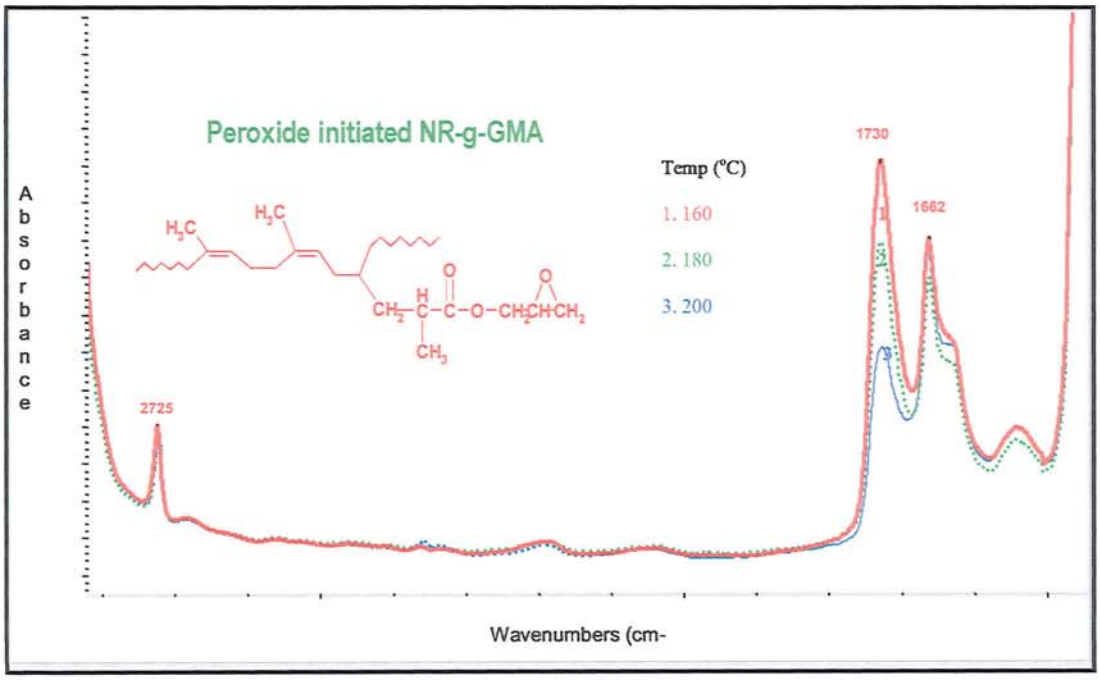

Figure 3.6 FTIR spectra of (Films C) processed NR/GMA/T-101 (free radical initiation with peroxide T-101). Sample T3-1 in Table B.3.1 in Appendix B (extracted NR 100 phr, [GMA]i =12 %, [T-101] 0.02 mr,160-200 °C, 65 rpm, 15 min, mixing method M-1).

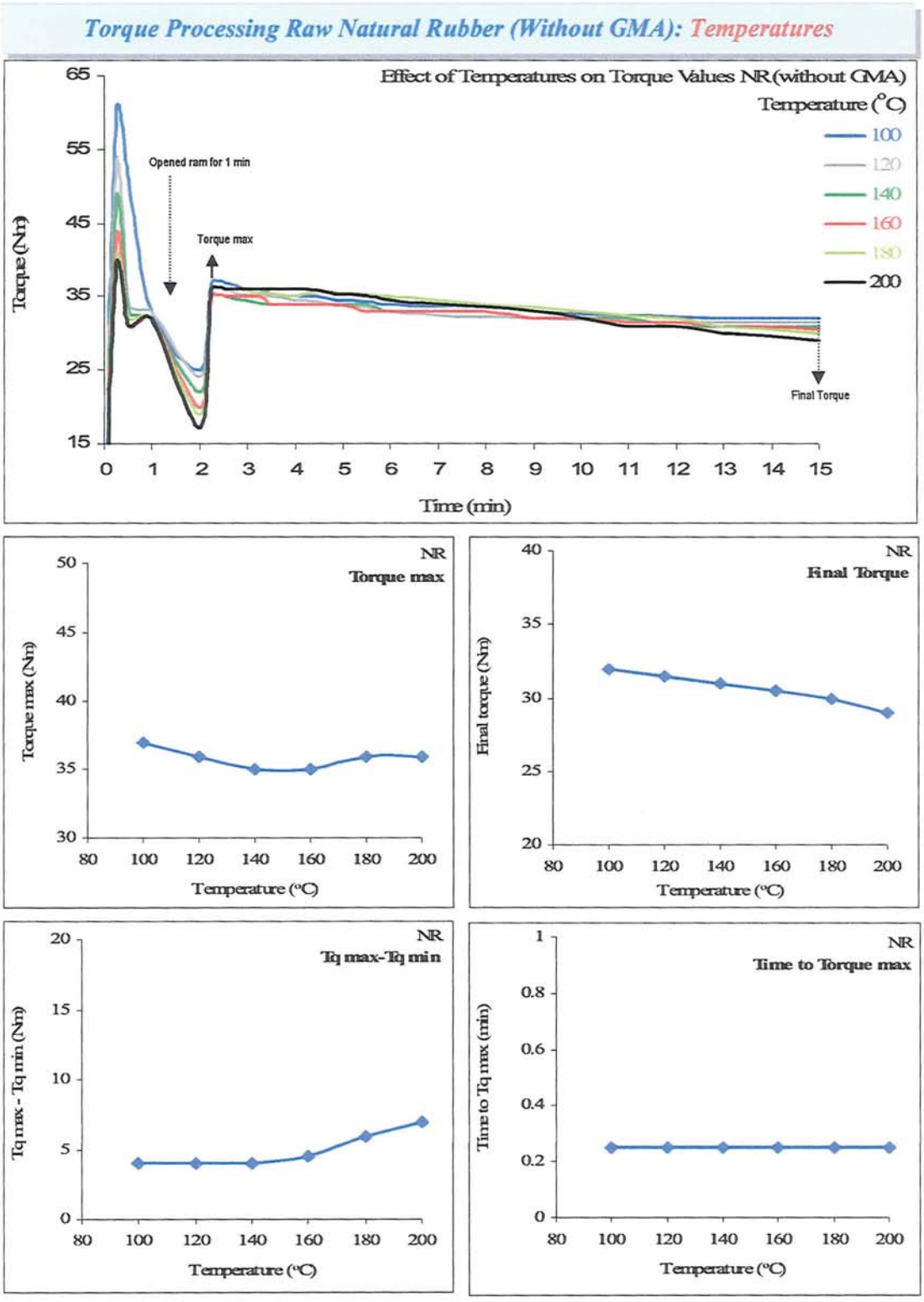

Figure 3.7 Effect of temperature on torque-time curves and torque characteristics of processed raw NR (without GMA, Samples C1-n in Table B.3.1 in Appendix B, mixing method M-1).

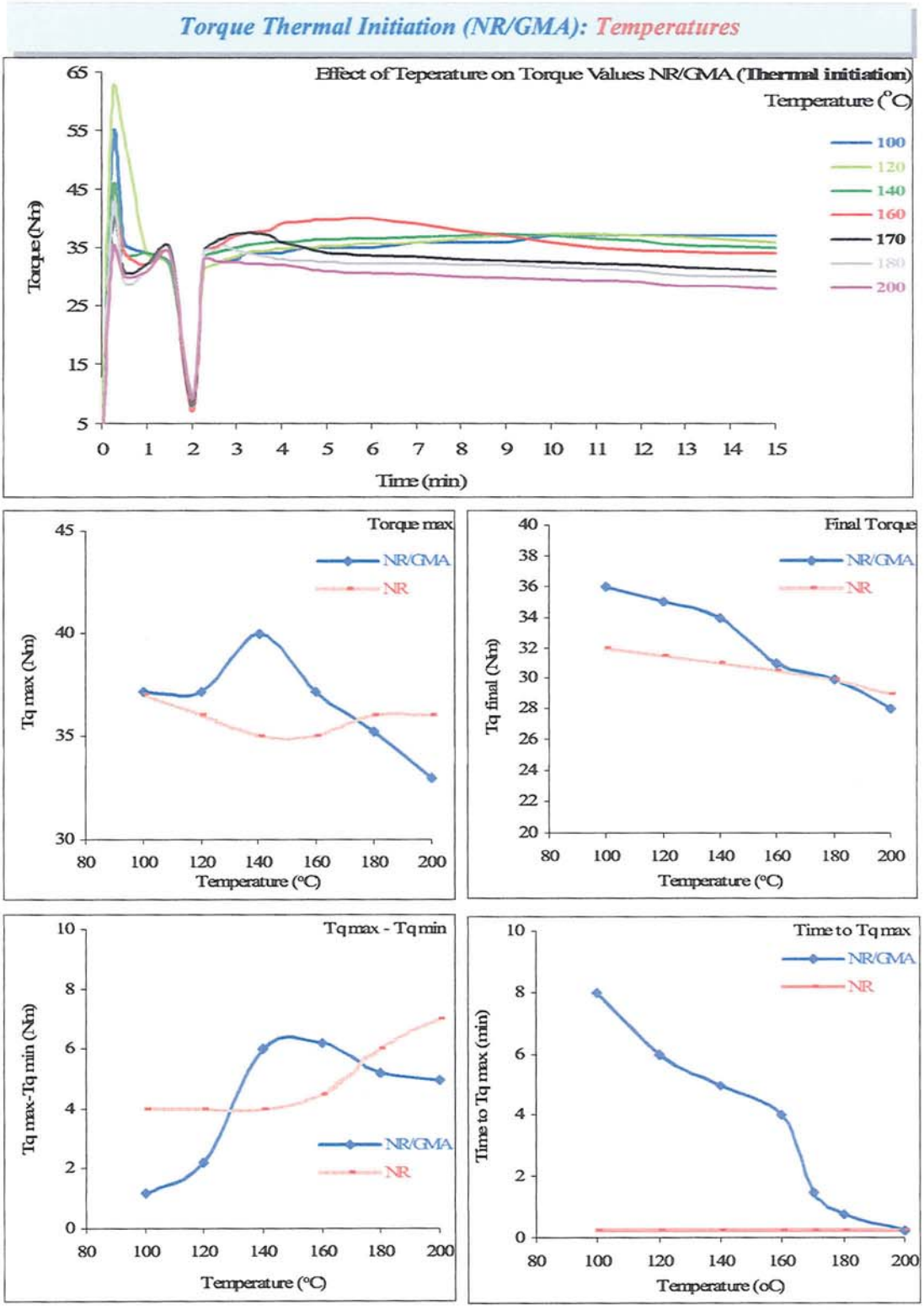

Figure 3.8 Effect of temperature on torque-time curves and torque characteristics of processed NR/GMA (thermal initiation) system and compared with processed NR (without GMA) at same temperature. (Samples T1-n in Table B.3.1 in Appendix B; [GMA]i = 6%, 65 rpm,15 min, mixing method M-1).

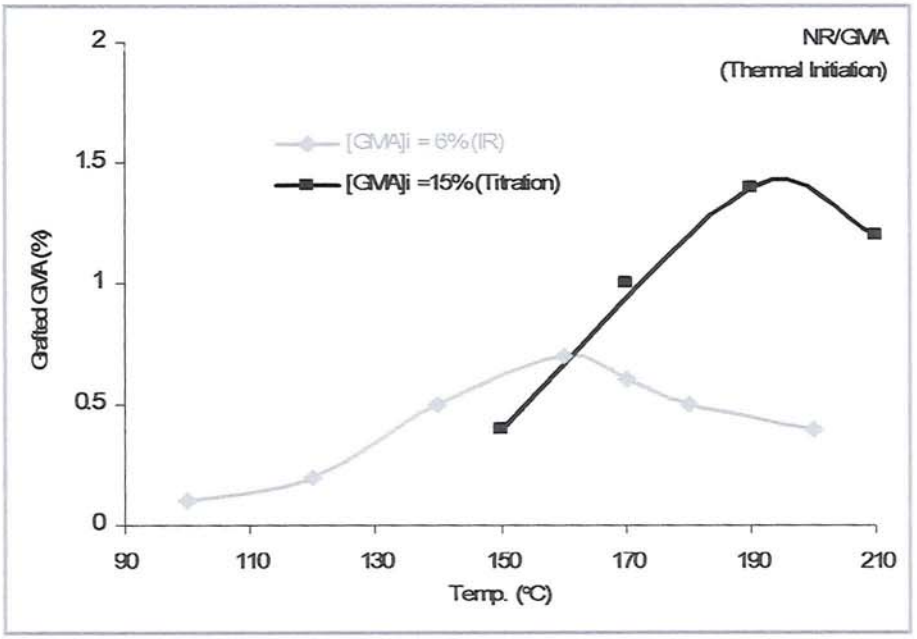

Figure 3.9 Effect of temperatures on grafting degree of processed NR/GMA (thermal initiation). (Samples T1-n in Table B3.1 Appendix B; [GMA]i = 6% and samples T2-n in Table B3.1 Appendix B; [GMA]i = 15%, no-peroxide, 100-210°C, 65 rpm, 15 min, mixing method M-1).

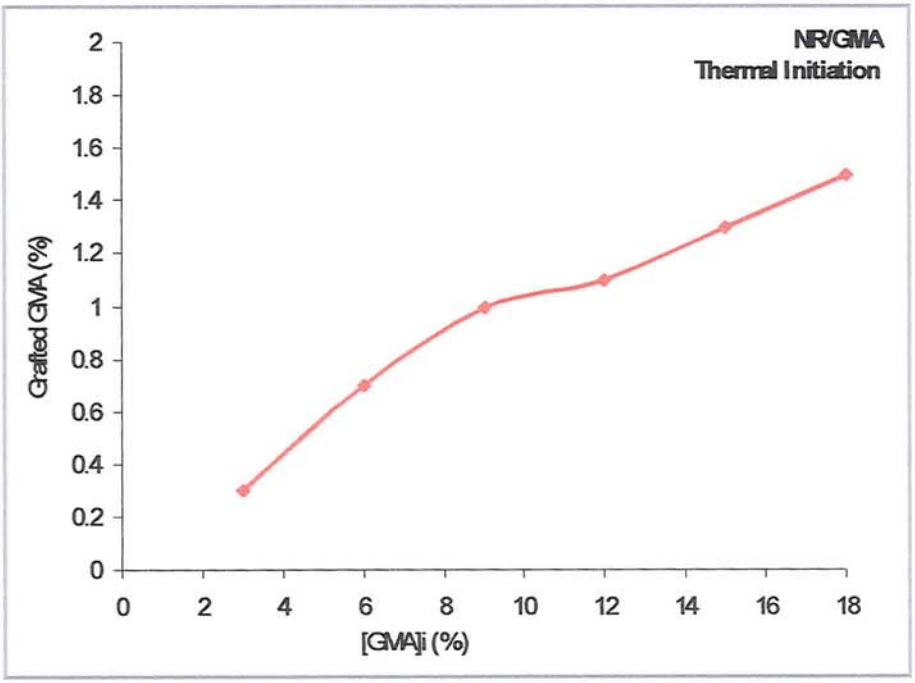

Figure 3.10 Effect of GMA concentrations on grafting degree by of processed NR/GMA by thermal initiation. (Samples G0-n Table B3.1 in Appendix B; [GMA]i = 3-18 %, 160°C, 65 rpm, 15 min, mixing method M-1).

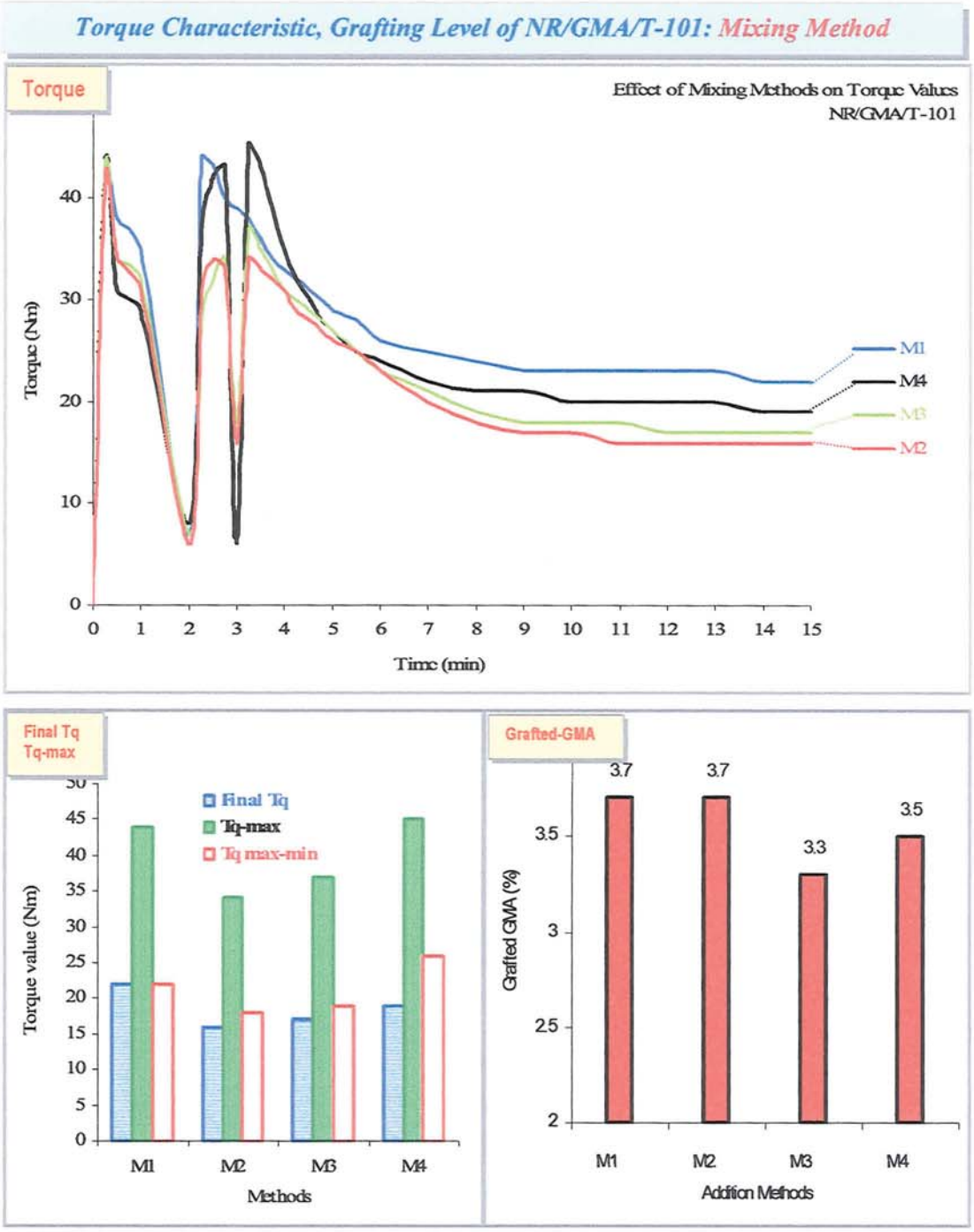

Figure 3.11 Effect of mixing sequence methods (see **Scheme 3.2**, p.122) on torque-time curves, torque characteristics and grafting degrees of GMA onto NR of processed NR/GMA/T-101, Samples M-1, M2-2, M-3, and M4-12 in Table B3.2 Appendix B; [GMA]i = 12%, T-101 0.02 molar ratio to GMA, 160°C, 75 rpm, 15 min).

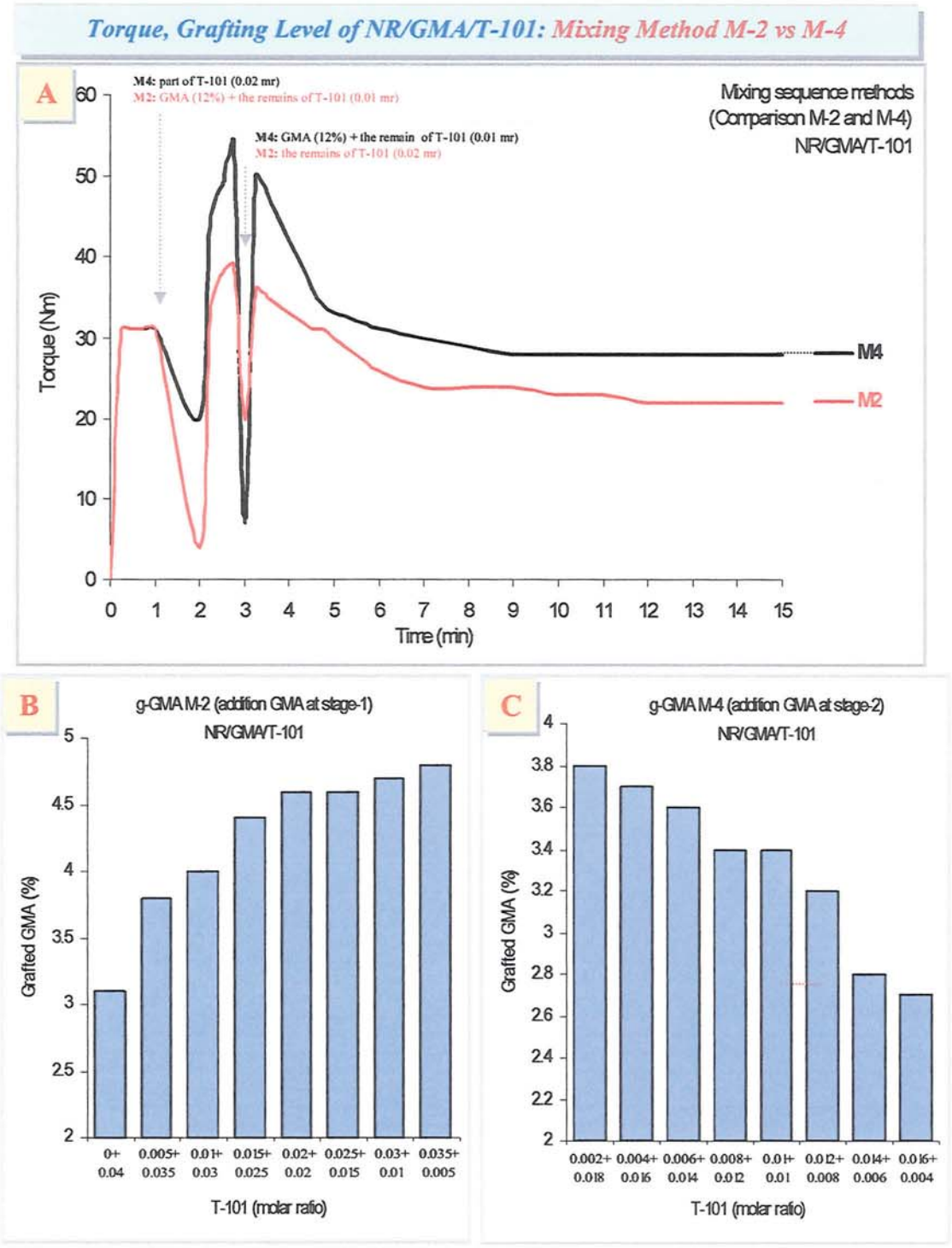

Figure 3.12 Changes of torque values and grafting degrees of GMA on NR of processed NR/GMA/T-101 in mixing method M-2 and M-4 (see **Scheme 3.2**, p.122); samples M2-41 to M2-48 for method M-2 (T-101 0.04 mr) and M4-31 to M4-39 for method M-4 (T-101 0.02 mr) in Table B3.2 Appendix B; [GMA]i = 12%, 160°C, rotor speed 65 rpm for method M-2 and 75 rpm for M-4, 15 min).

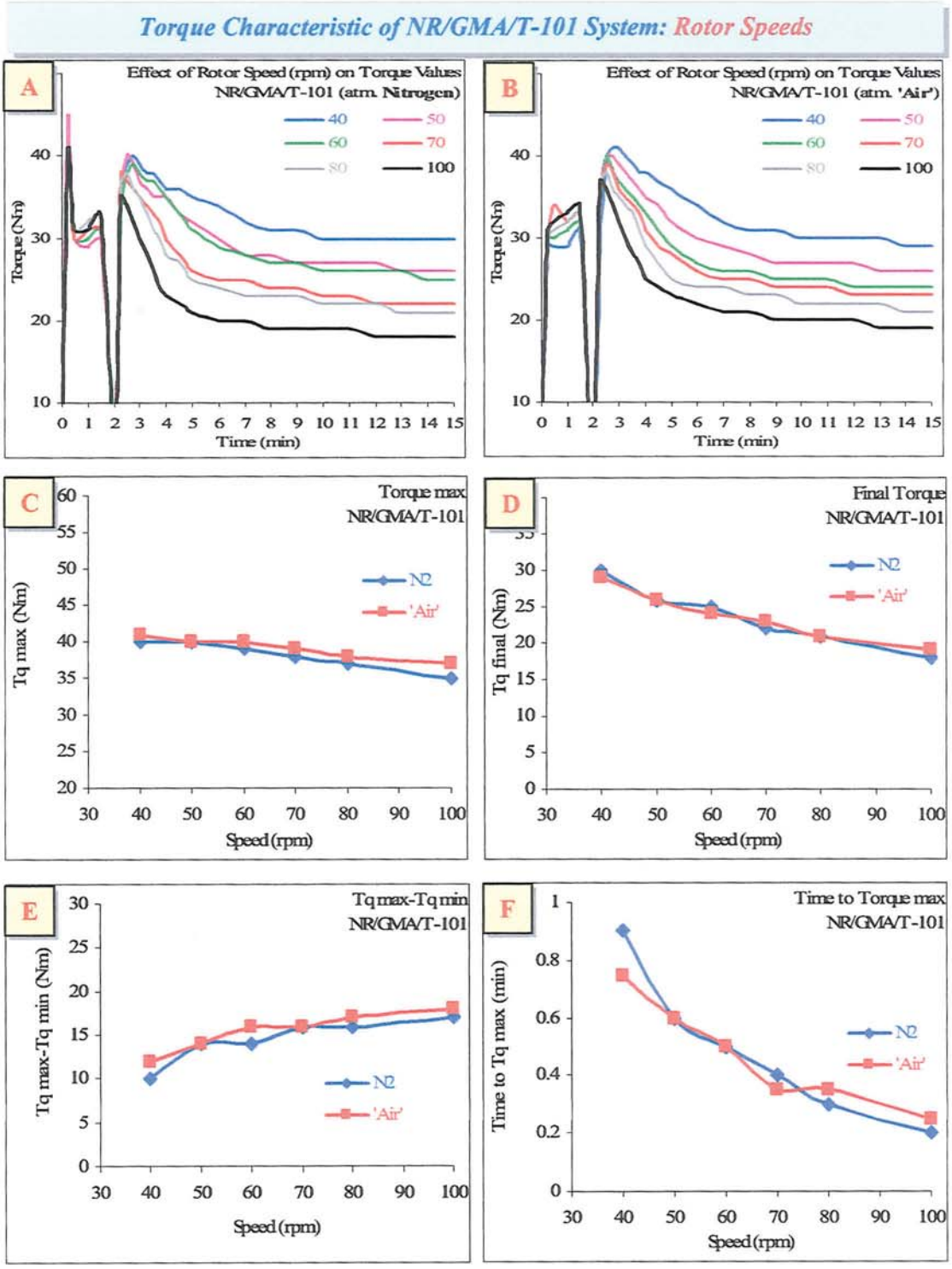

Figure 3.13 Effect of rotor speeds on torque-time curves and torque characteristics of processed NR/GMA/T-101. (Samples S3-n and S4-n Table B.3.2 Appendix B; [GMA]i = 12 %, T-101 0.03 molar ratio to GMA, 170°C, 65 rpm, 15 min, mixing method M-1).

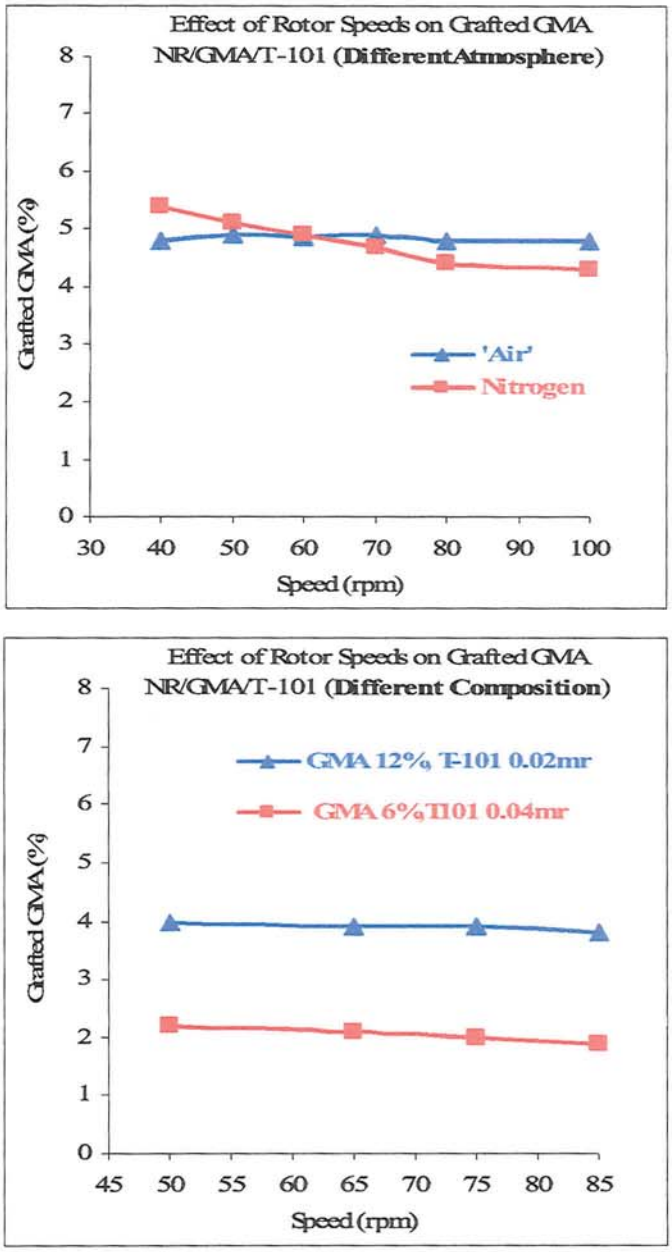

Figure 3.14 Effect of rotor speeds on grafting degrees of processed NR/GMA/T-101. (Samples S3-n and S4-n in Table B.3.2 Appendix B; [GMA]i = 12 %, [T-101] = 0.03 molar ratio to GMA, 170°C, 40-100 rpm,15 min, mixing method M-1).

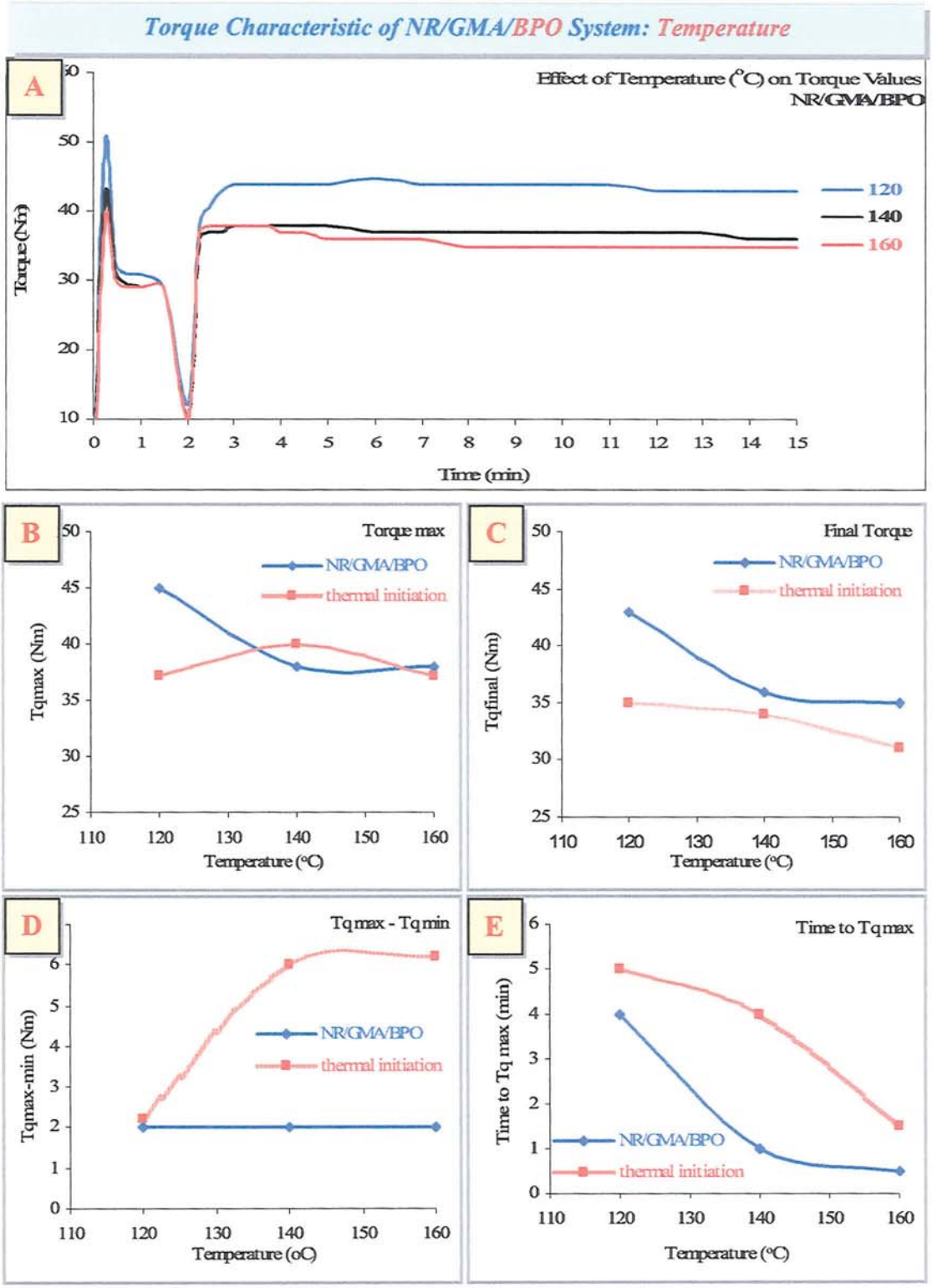

Figure 3.15 Effect of temperature on torque-time curves and torque characteristics of processed NR/GMA/**BPO** (compared to thermal initiation) system. (Samples B1-2, B2-2, B3-2 in Table B.3.3 Appendix B; ([GMA]i = 6%, [BPO] = 0.02 molar ratio to GMA, 120-160°C, 65 rpm,15 min, mixing method M-1).

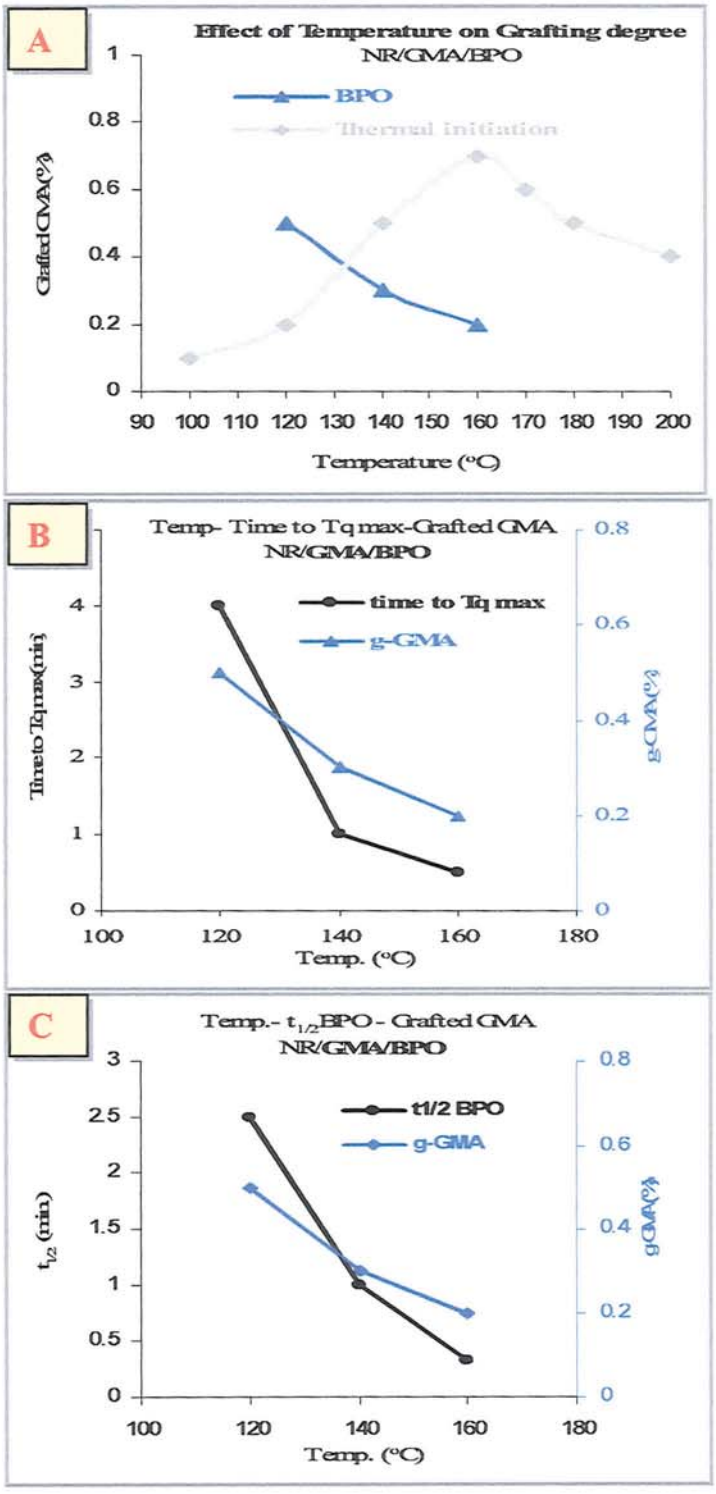

Figure 3.16 (A) Effect of temperature on GMA grafting level of processed NR/GMA/BPO (compared to thermal initiation), (B) correlation the GMA grafting level with time to torque max and (C) with half life times ($t_{1/2}$) of BPO. (Samples B1-2, B2-2, B3-2 in Table B.3.3 appendix B; [GMA]j = 6%, [BPO] 0.02 molar ratio to GMA, temp. 120-160°C, 65 rpm,15 min, mixing method M-1).

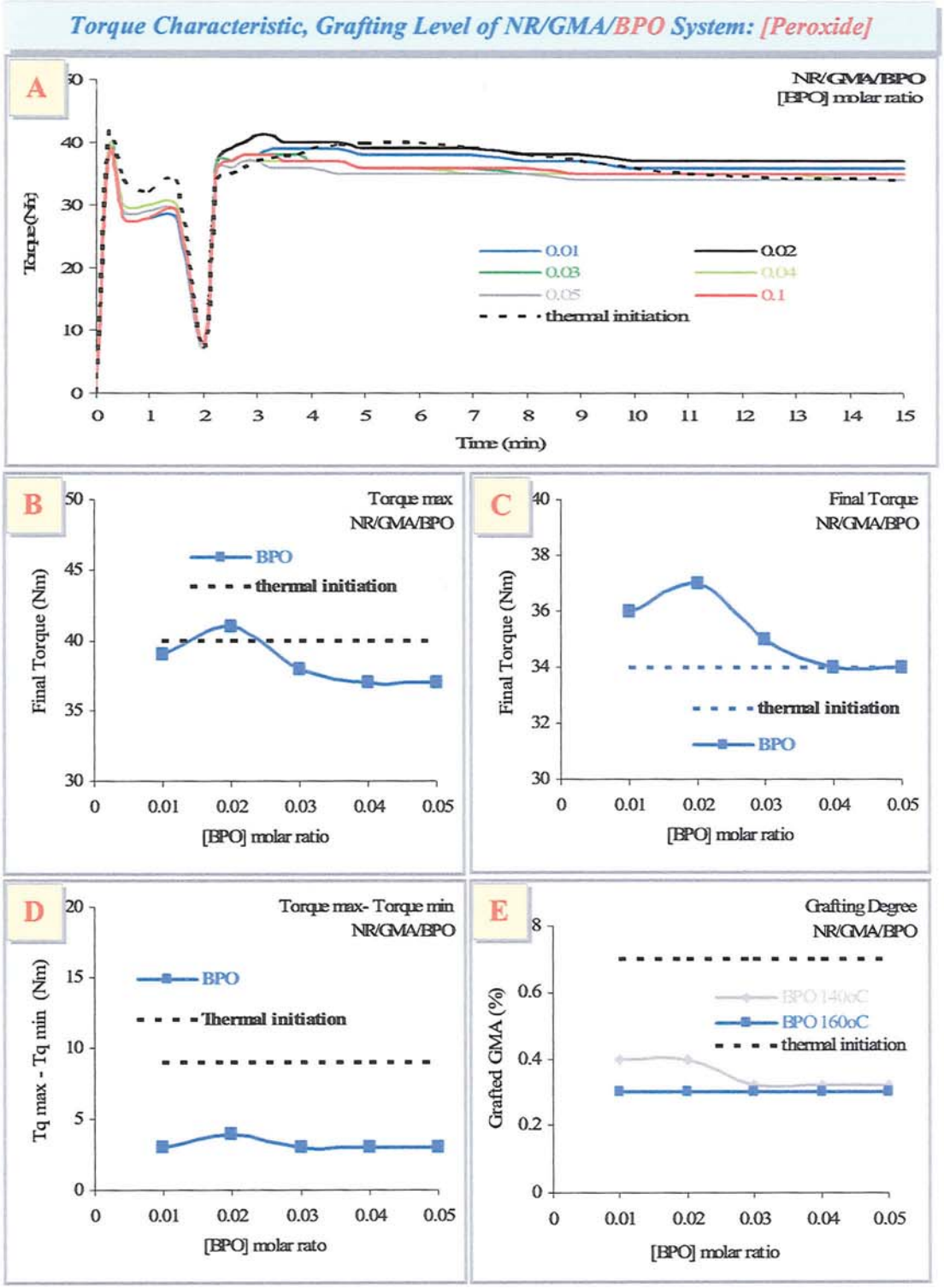

Figure 3.17 Effect of BPO concentration on torque-time curves and torque characteristics and GMA grafting level of processed NR/GMA/BPO (compared to thermal initiation) system. (Samples B2-n and B3-n in Table B.3.3 Appendix B; [GMA]i = 6%, [BPO] = 0.01-0.05 molar ratio to GMA, temp.140° C and 160°C, 65 rpm, 15 min, mixing method M-1).

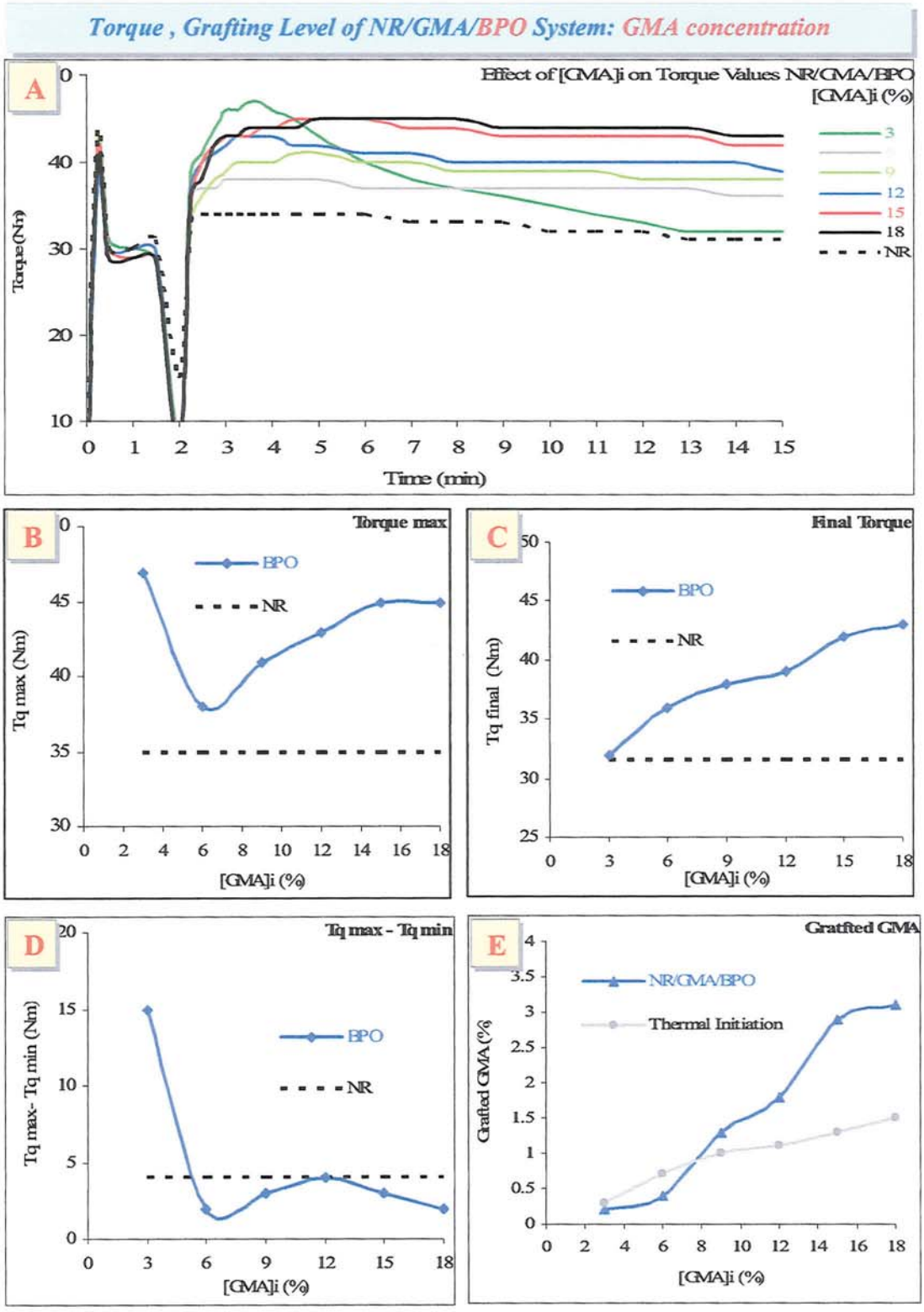

Figure 3.18 Effect of GMA concentration on torque-time curves, torque characteristics (in comparison with NR control) and grafted GMA on NR in the presence of BPO (in comparison with thermal initiation). (Samples B4-n in Table B.3.3 Appendix B; [GMA]i = 3-18 %, [BPO] = 0.03 molar ratio to GMA, 140°C, 65 rpm, 15 min, mixing method M-1).

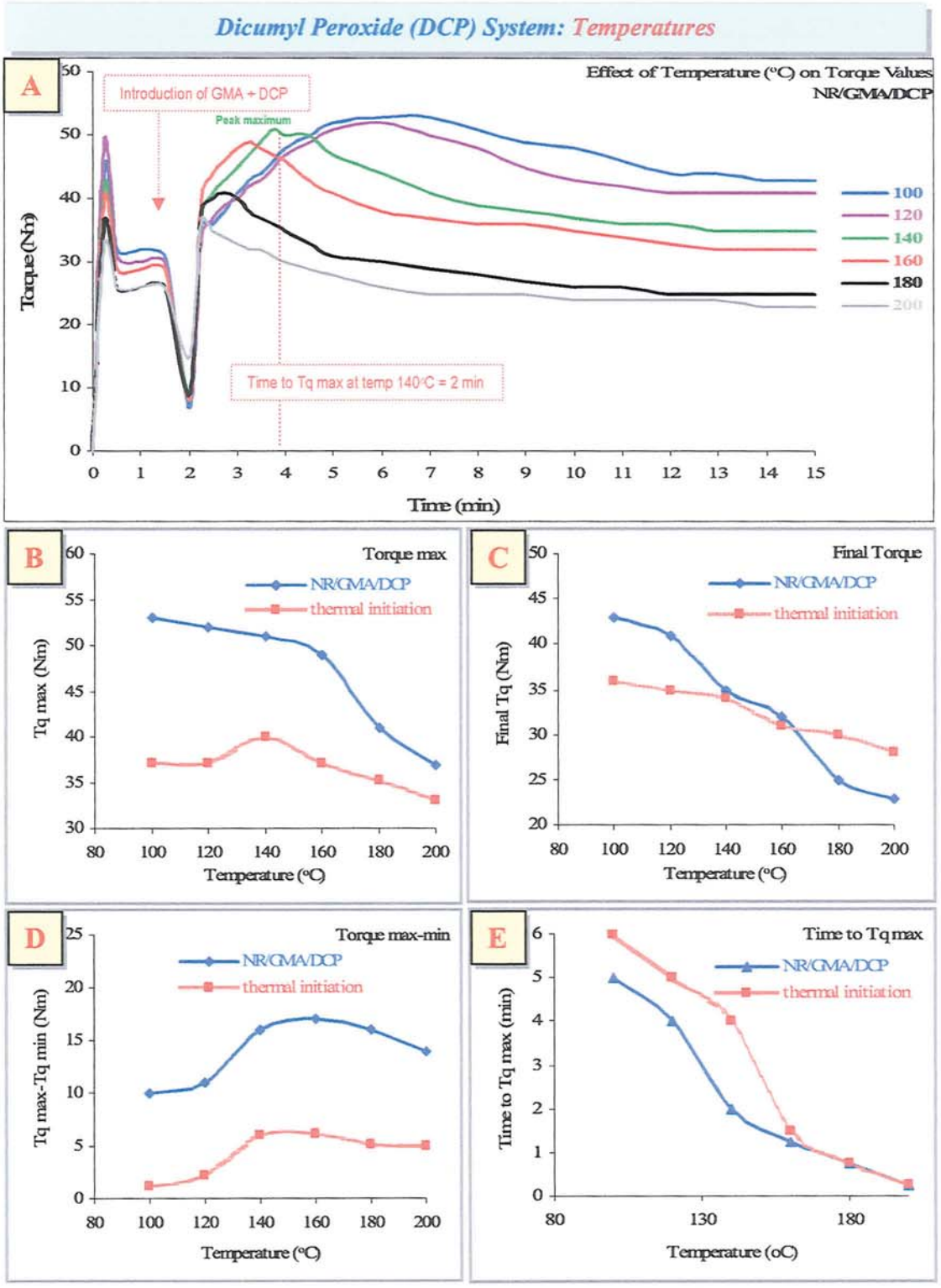

Figure 3.19 Effect of temperature on torque-time curves and torque characteristics of processed NR/GMA/DCP (compared to thermal initiation) system. (Samples D1-n in Table B.3.4 Appendix B; [GMA]i = 6%, [DCP] 0.04 molar ratio to GMA, 65 rpm,15 min, mixing method M-1).

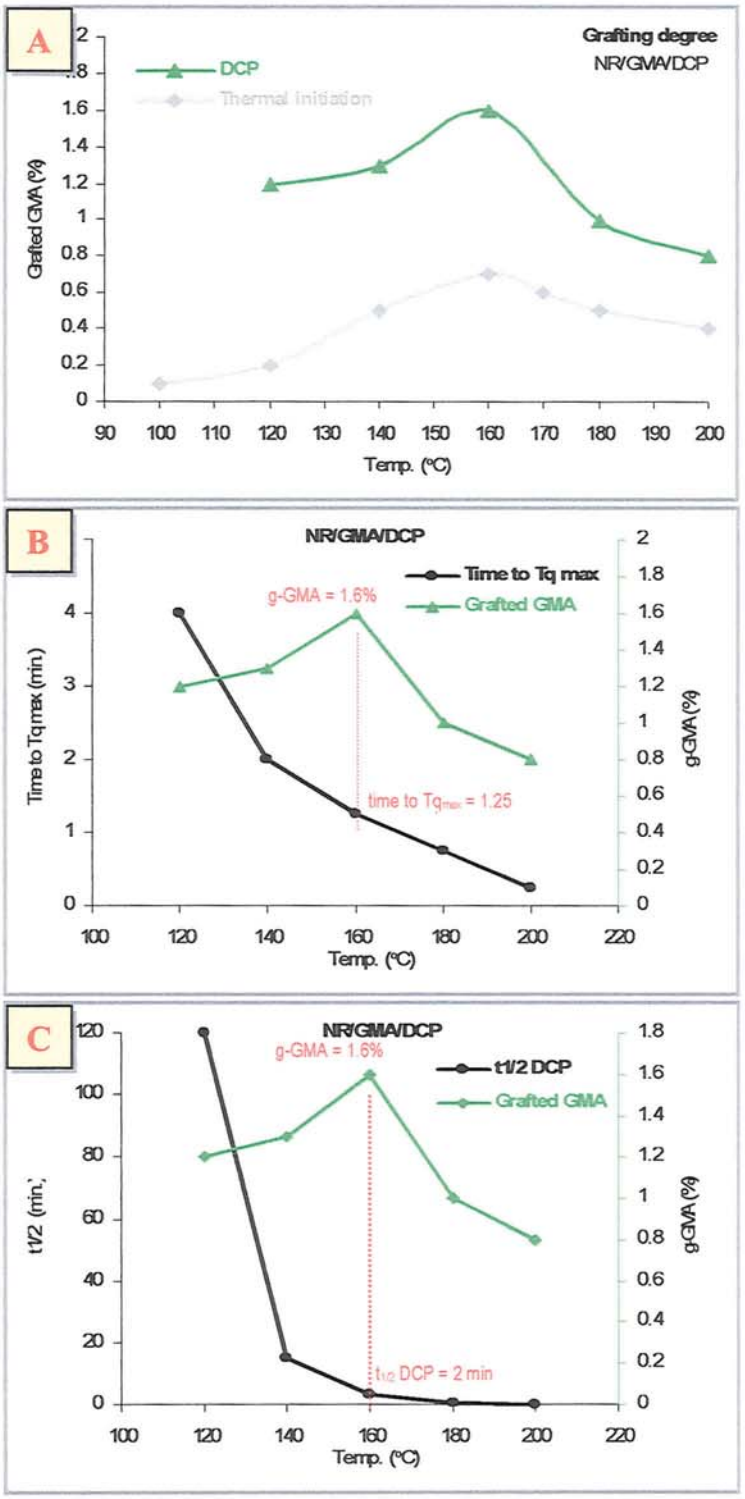

Figure 3.20 (A) Effect of temperature on GMA grafting level of processed NR/GMA/DCP (compared to thermal initiation), (B) correlation the GMA grafting level with time to torque max and (C) with half life times ($t_{1/2}$) of DCP (Samples D1-n Table B.3.4 Appendix B; [GMA]i = 6%, [DCP] 0.04 molar ratio to GMA, 65 rpm,15 min, mixing method M-1).

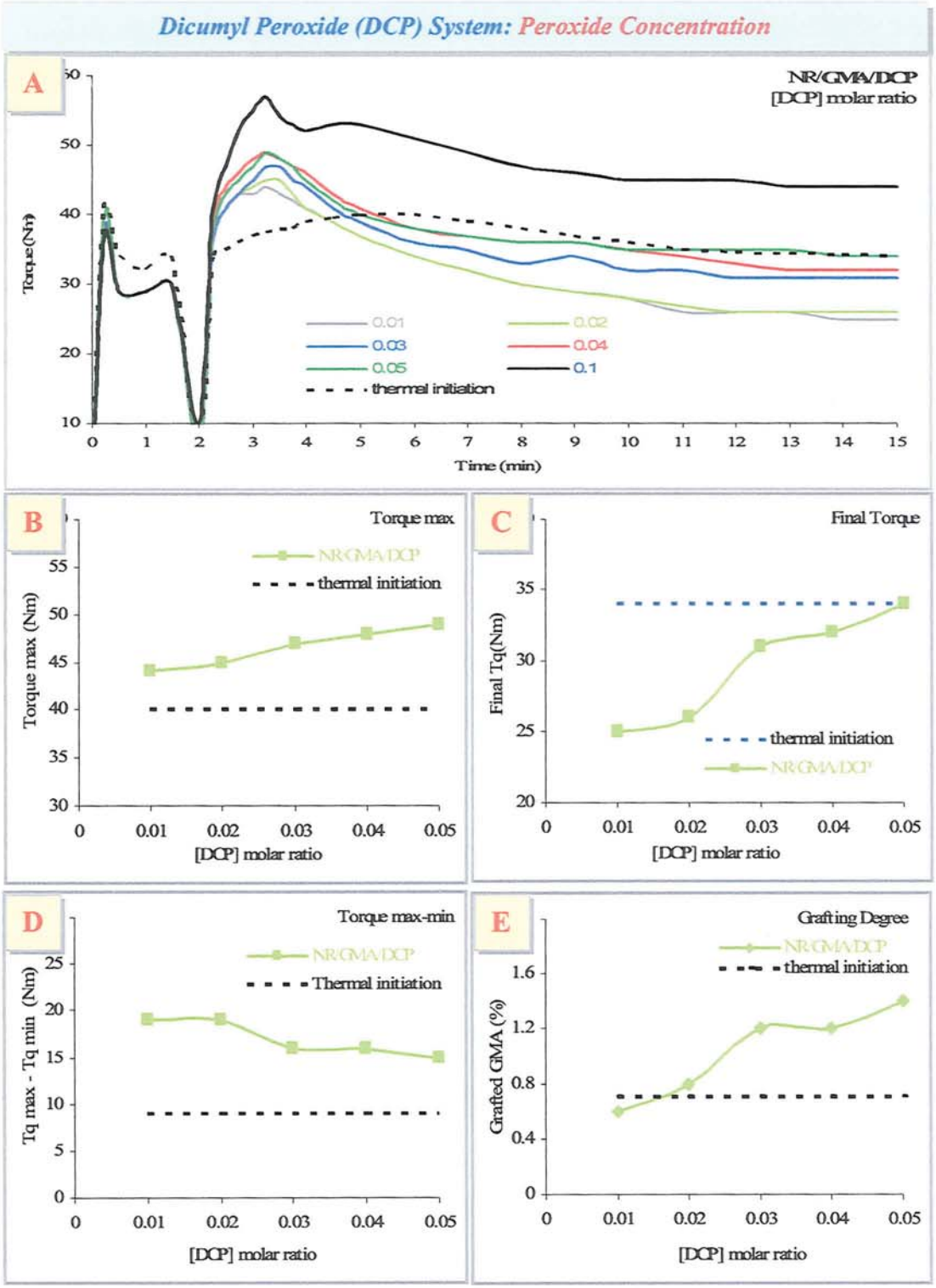

Figure 3.21 Effect of DCP concentration on torque-time curves, torque characteristics, and GMA grafting level of processed NR/GMA/DCP (compared to thermal initiation) system. (Samples D2-n in Table B.3.4 Appendix B; [GMA]i = 6%, [DCP] = 0.01-0.05 molar ratio to GMA, temp. 160°C, 65 rpm, 15 min, mixing method M-1).

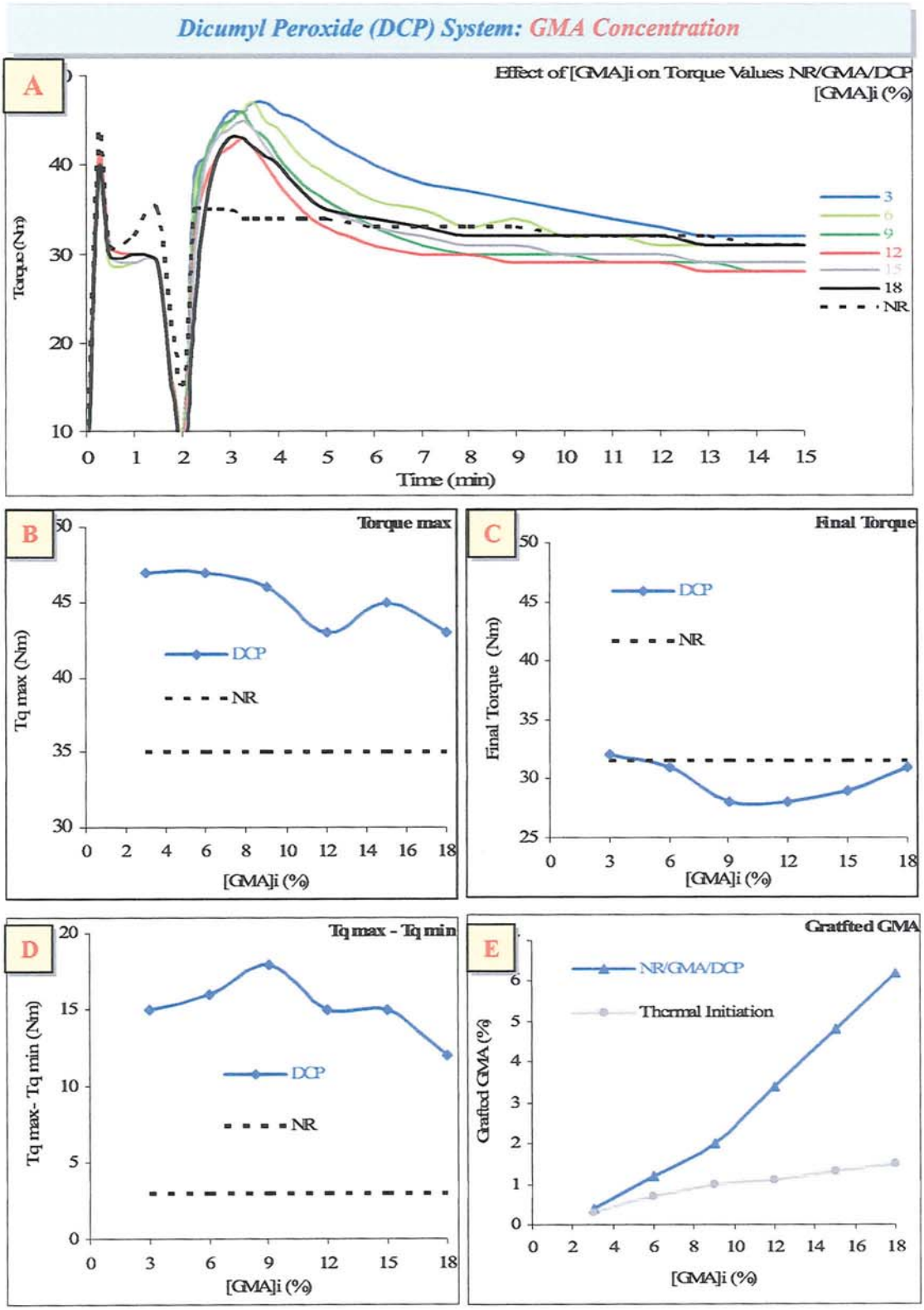

Figure 3.22 Effect of [GMA]i on torque characteristics and GMA grafting level of processed NR/GMA/DCP system. (Samples D3-n in Table B.3.4 Appendix B; [GMA] = 3-18 %, [DCP] = 0.03 molar ratio to GMA, 160°C, 65 rpm, 15 min, mixing method M-1).

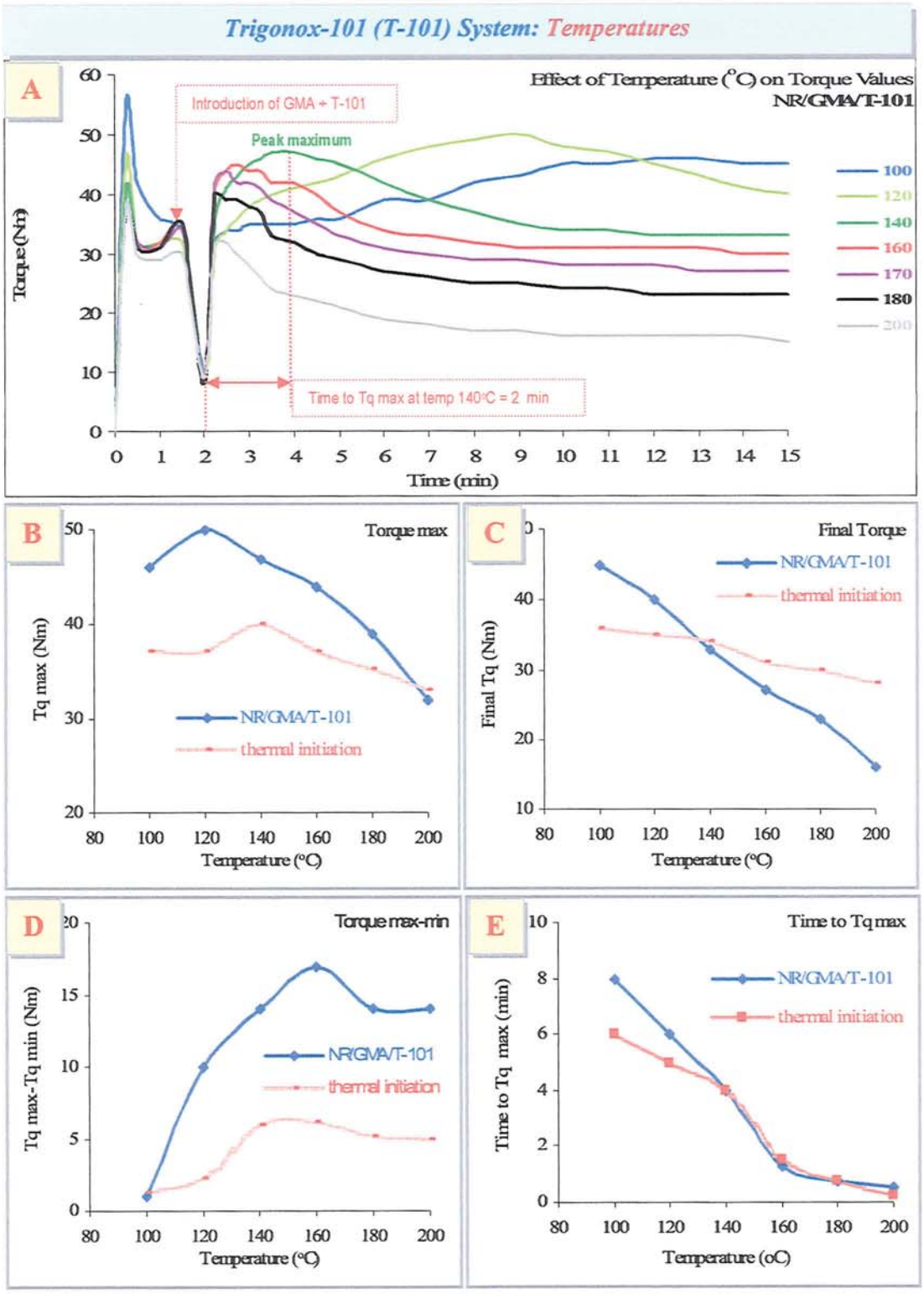

Figure 3.23 Effect of temperature on torque-time curves and torque characteristics of processed NR/GMA/T-101 (compared to thermal initiation) system. (Samples T5-n in Table B.3.2 Appendix B, [GMA]i = 6%, [T-101] = 0.04 mr, 160°C, 65 rpm, 15 min, mixing method M-1).

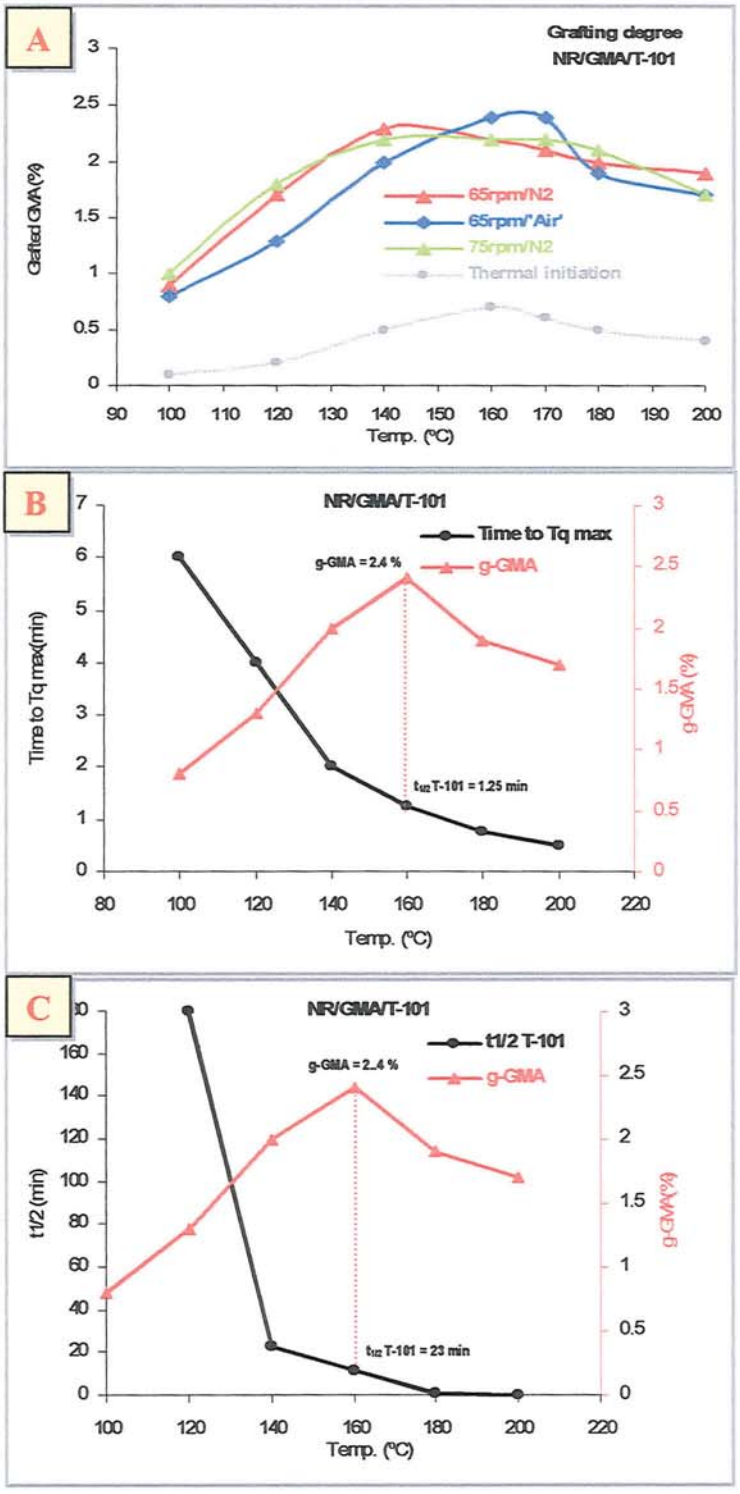

Figure 3.24 (A) Effect of temperature on GMA grafting level of processed NR/GMA/T-101 (different rotor speeds, compared to that of thermal initiation) (B) correlation the GMA grafting level with time to torque max and (C) with half life times ($t_{1/2}$) of T-101. (Samples T5-n, T6-n, T7-n in Table B.3.2 Appendix B; ([GMA]i = 6%, [T-101] = 0.04 molar ratio to GMA, temp 160-200°C, 65 rpm, 15 min, mixing method M-1).

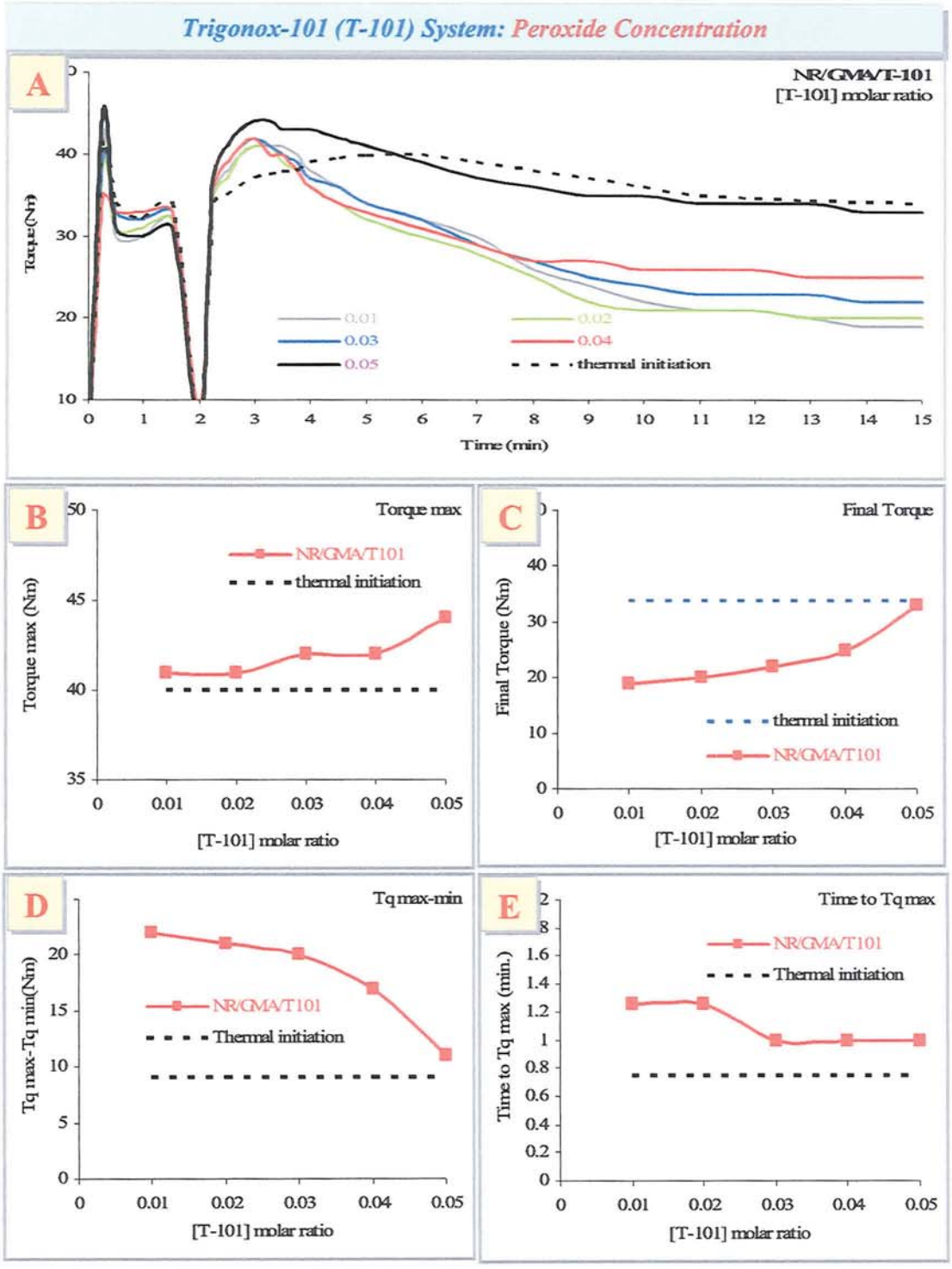

Figure 3.25 Effect of T-101 concentration on torque-time curves and torque characteristics of processed NR/GMA/T-101 (compared to thermal initiation) system. (Samples G2-n in Table B.3.2 Appendix B; [GMA]i = 6%, [T-101] = 0.01-0.05 molar ratio to GMA, temp 160°C, 65 rpm, 15 min, mixing method M-1).

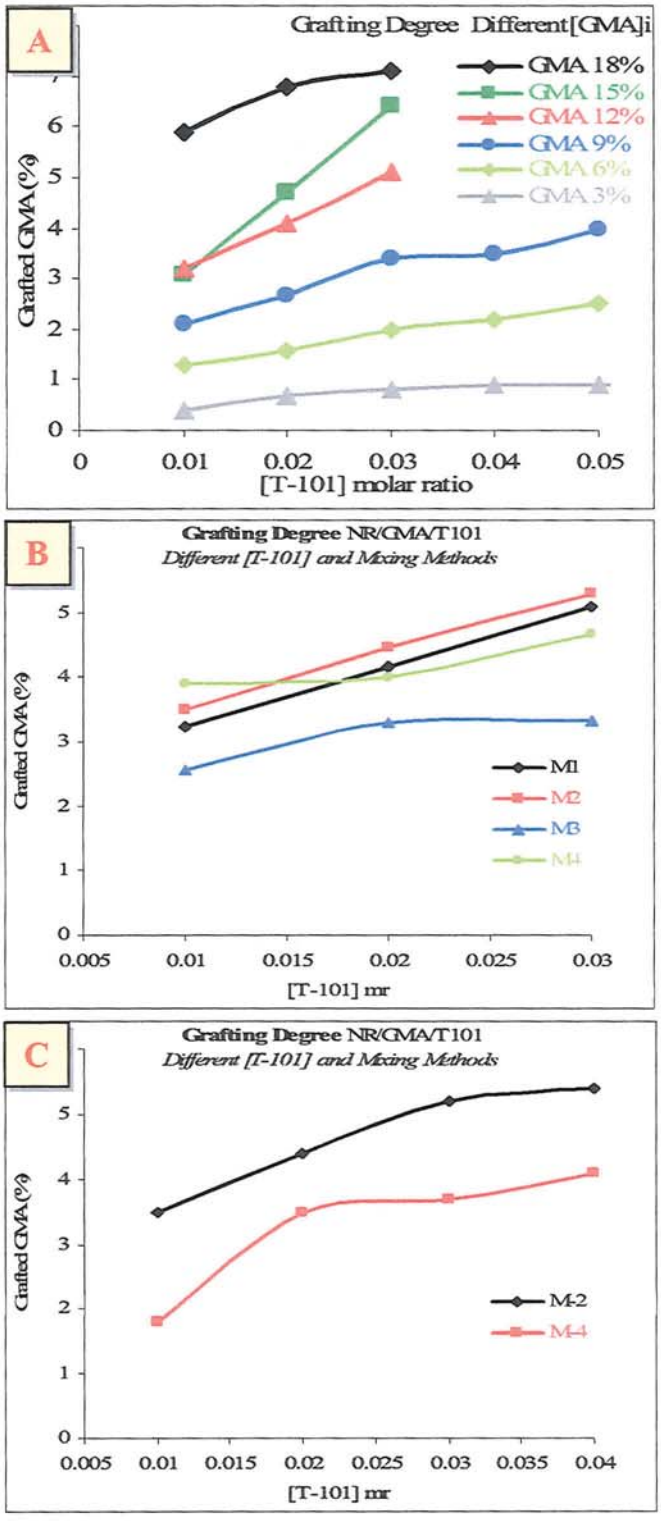

Figure 3.26 Effect of T-101 concentration on GMA grafting degrees of processed NR/GMA/T-101. (A) at various GMA initial concentration (mixing method M-1), (B) and (C) in different mixing method (see **Scheme 3.2**, p.122) ([GMA]i = 12%, Temp 160°C, 65 rpm, 15 min).

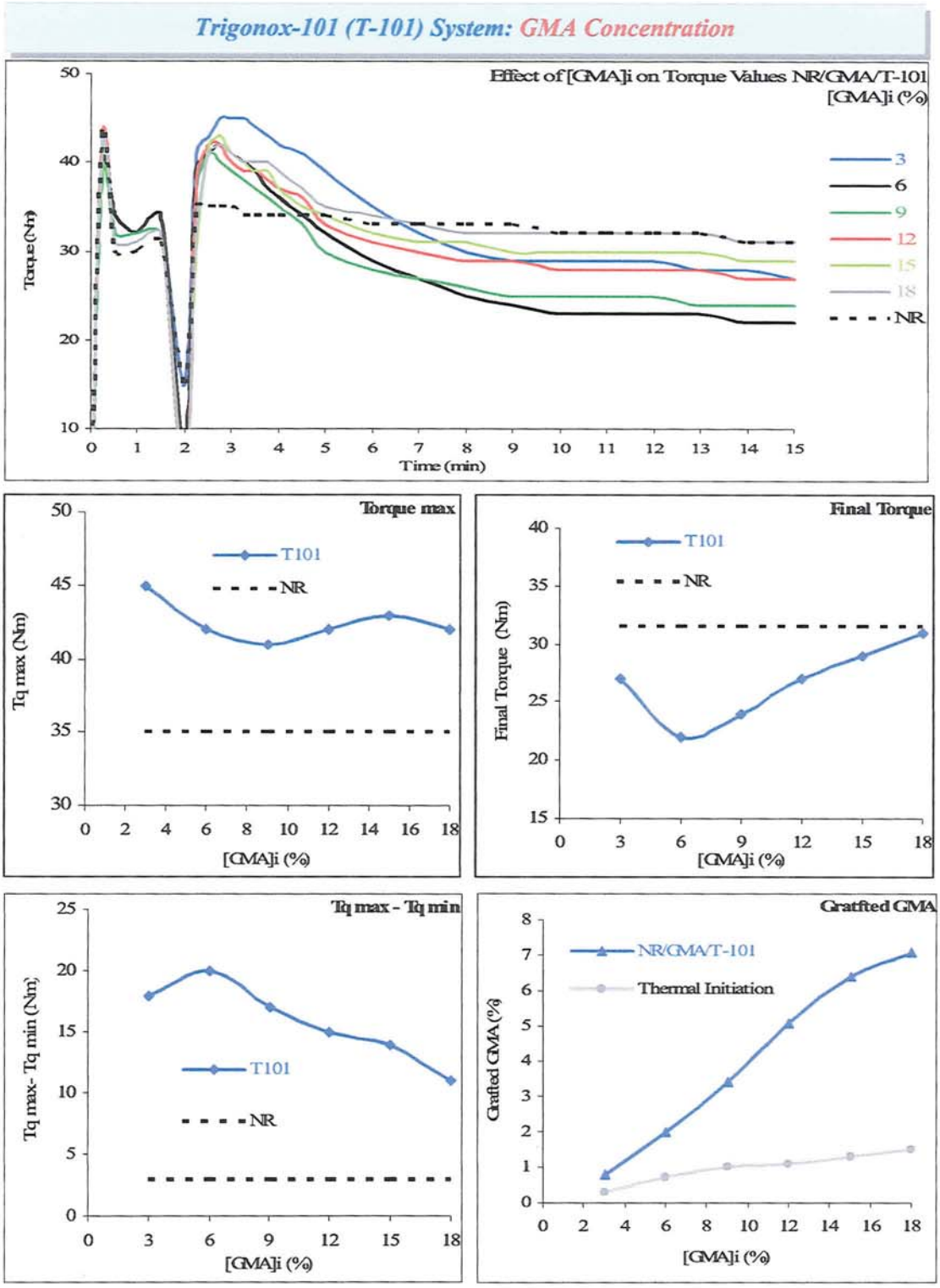

Figure 3.27 Effect of GMA concentrations on torque-time curves, torque characteristics and GMA grafting degrees of processed NR/GMA/T-101. (Samples G1-3, G2-3, G3-3, G4-3, G5-3 and G6-3 in Table B.3.2 Appendix B; [GMA]i = 3-18%, [T-101] = 0.03 molar ratio to GMA, 160°C, 65 rpm, 15 min, mixing method M-1).

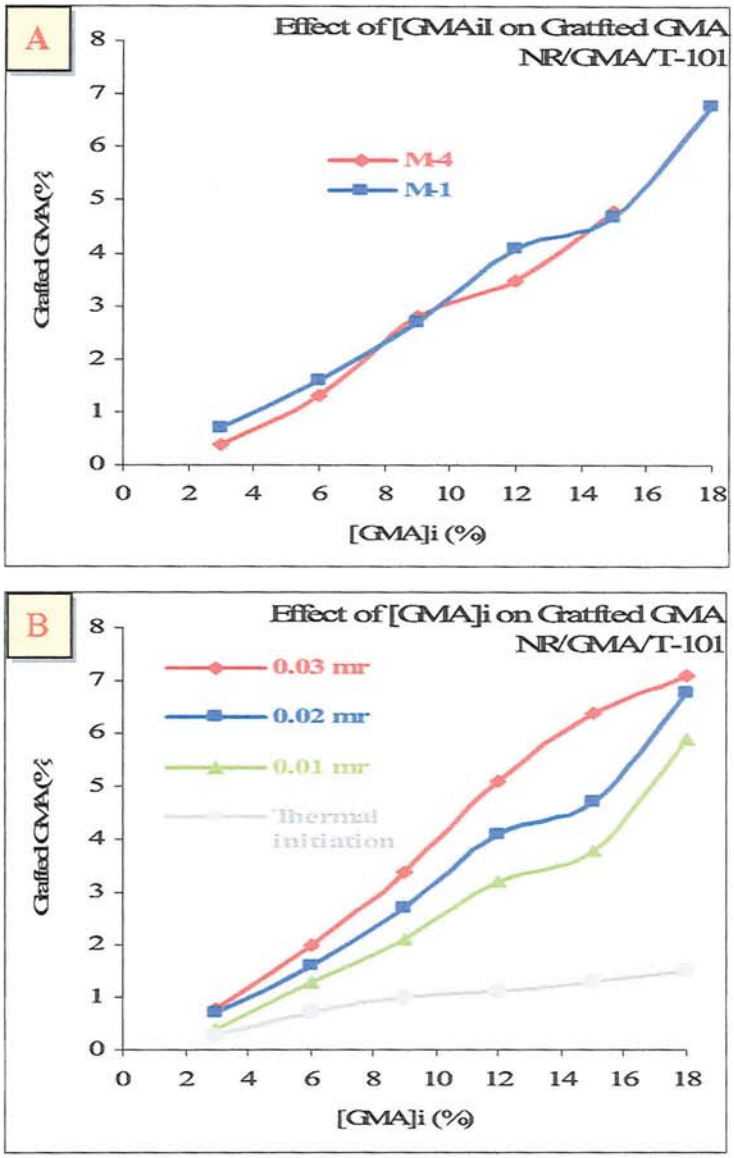

Figure 3.28 Effect of GMA concentrations (comparisons in different mixing methods) on grafting degrees of GMA on NR of processed NR/GMA/T-101. Samples G1-n to G6-n in Table B.3.2 Appendix B; [GMA]i = 3-18%, T-101 0.01 to 0.03 mr, 160°C, 65 rpm, 15 min, otherwise stated mixing method M-1).

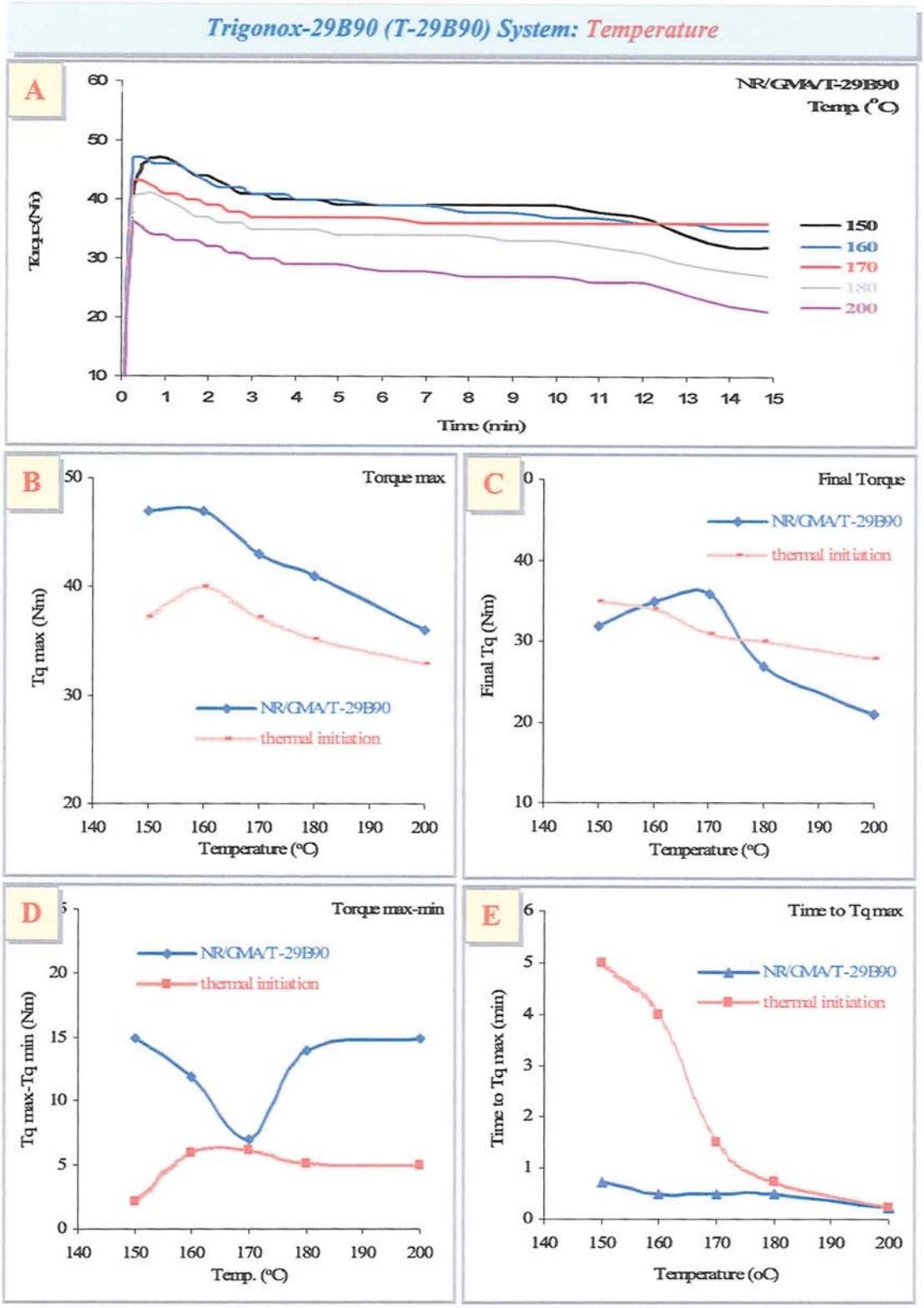

Figure 3.29 Effect of temperature on torque-time curves and torque characteristics of processed NR/GMA/T-29B90 (compared to thermal initiation) system. (Samples G29-n in Table B.3.5 Appendix B; [GMA]i = 6%, [T-29B90] = 0.002 molar ratio to GMA, 65 rpm, 15 min, mixing method M-1).

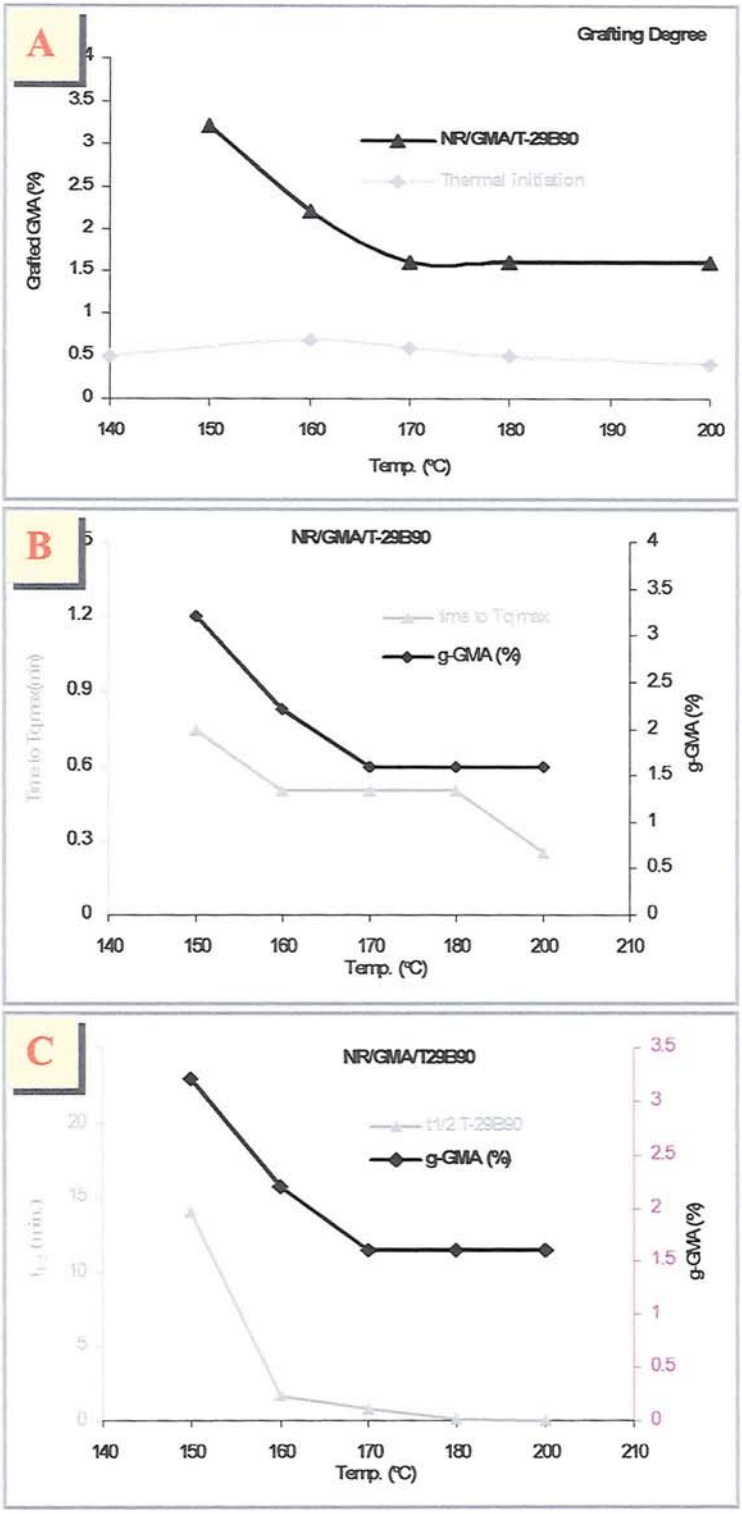

Figure 3.30 (A) Effect of temperature on GMA grafting level of processed NR/GMA/T-29B90 (compared to thermal initiation), (B) correlation the GMA grafting level with time to torque max and (C) with half life times ($t_{1/2}$) of T-29B90. Samples G29-n in Table B.3.5 Appendix B;[GMA]i = 6%, T-29B90 0.002 molar ratio to GMA, 65 rpm, 15 min, mixing method M-1).

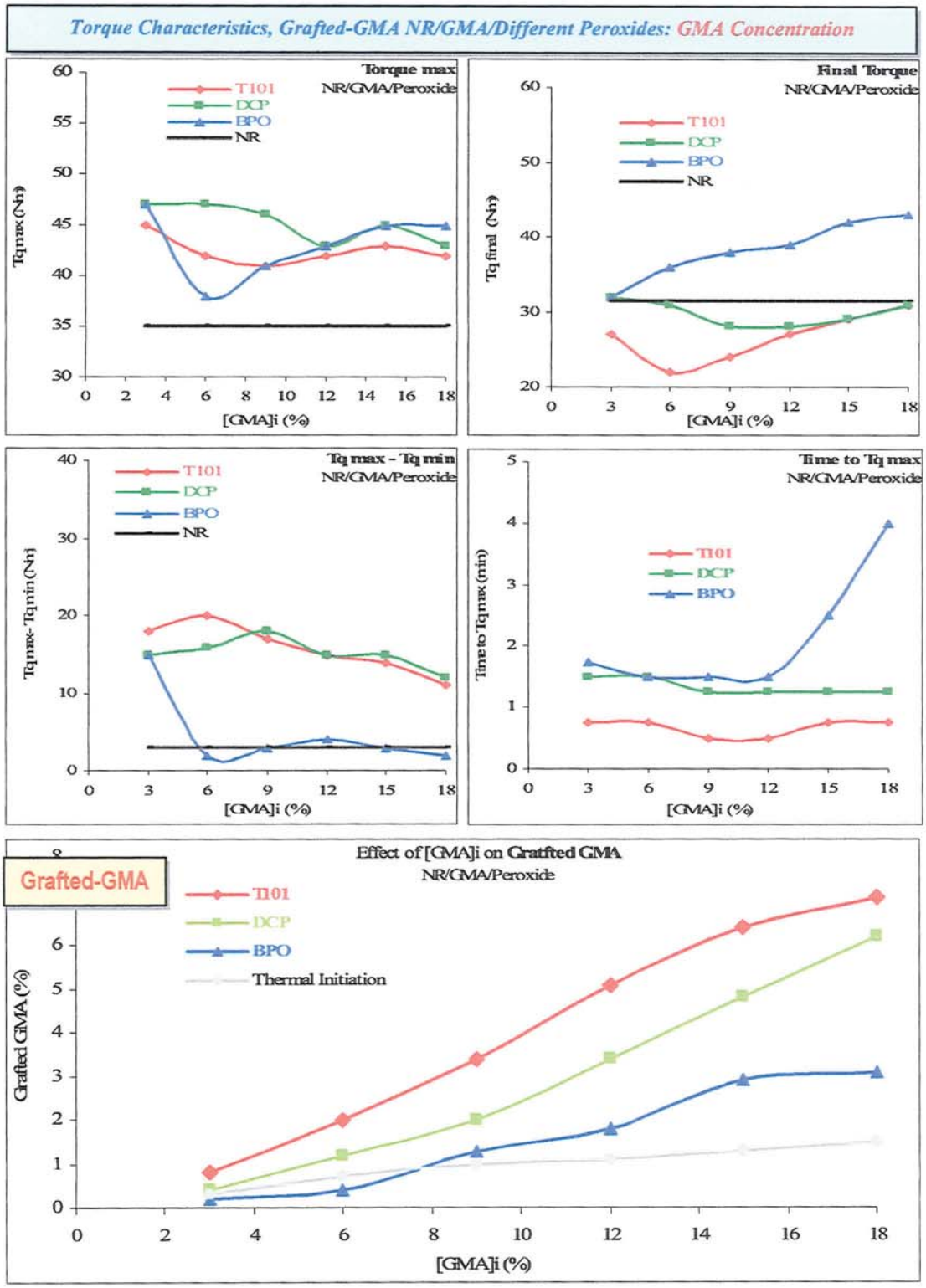

Figure 3.31 Effect of [GMA]i on torque characteristic and GMA grafted on NR of processed NR/GMA/Peroxides ([GMA]i = 3-18%, [perox] 0.03 mr, temp. 160°C for thermal initiation, T-101 and DCP and 140°C for BPO, 65 rpm, 15 min, mixing method M-1).

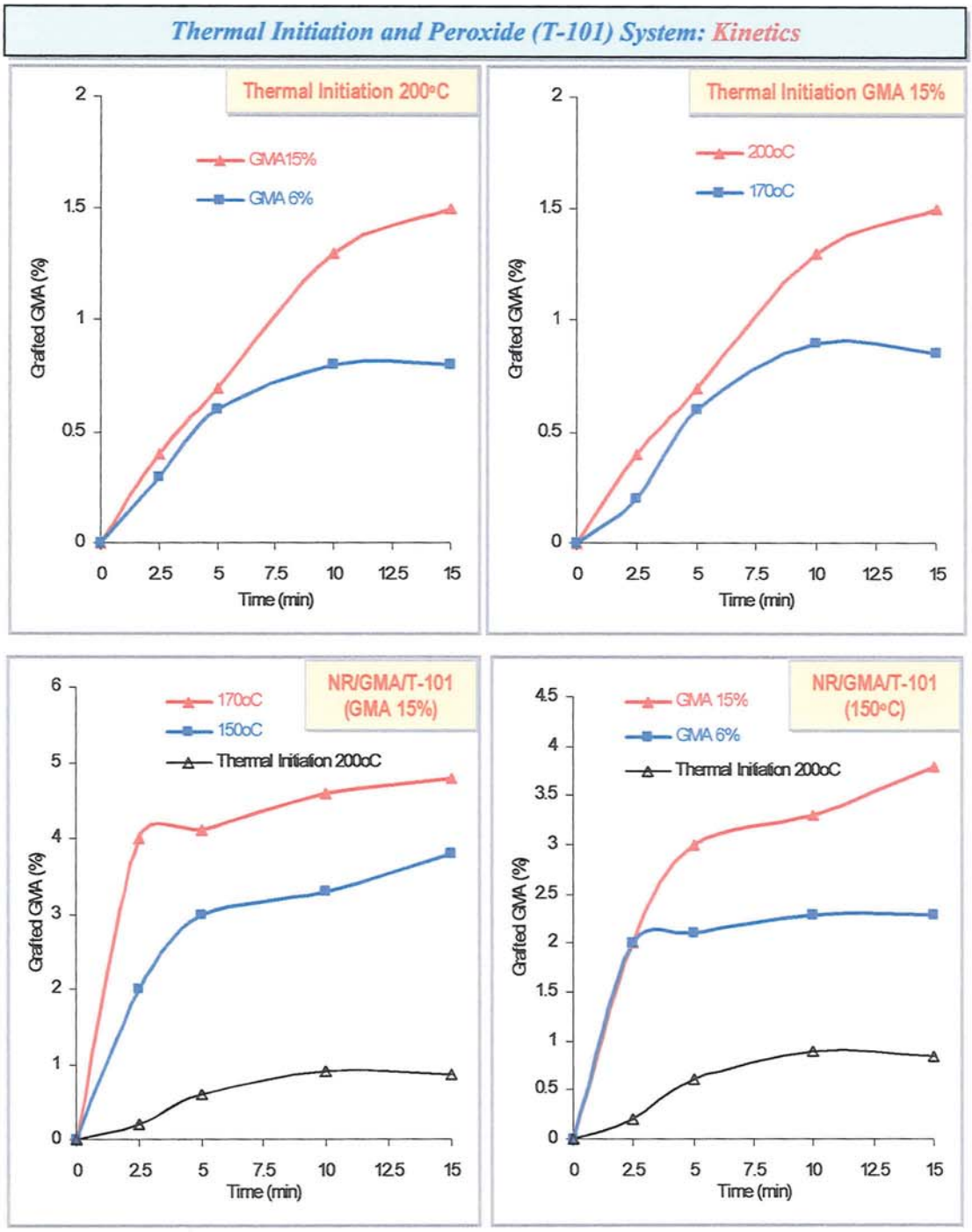

Figure 3.32 Effect of processing time on GMA grafting degrees of processed NR with GMA in the absence (thermal initiation) and presence of peroxide T-101 in different GMA initial concentration and different temperatures (65 rpm, mixing method M-1)

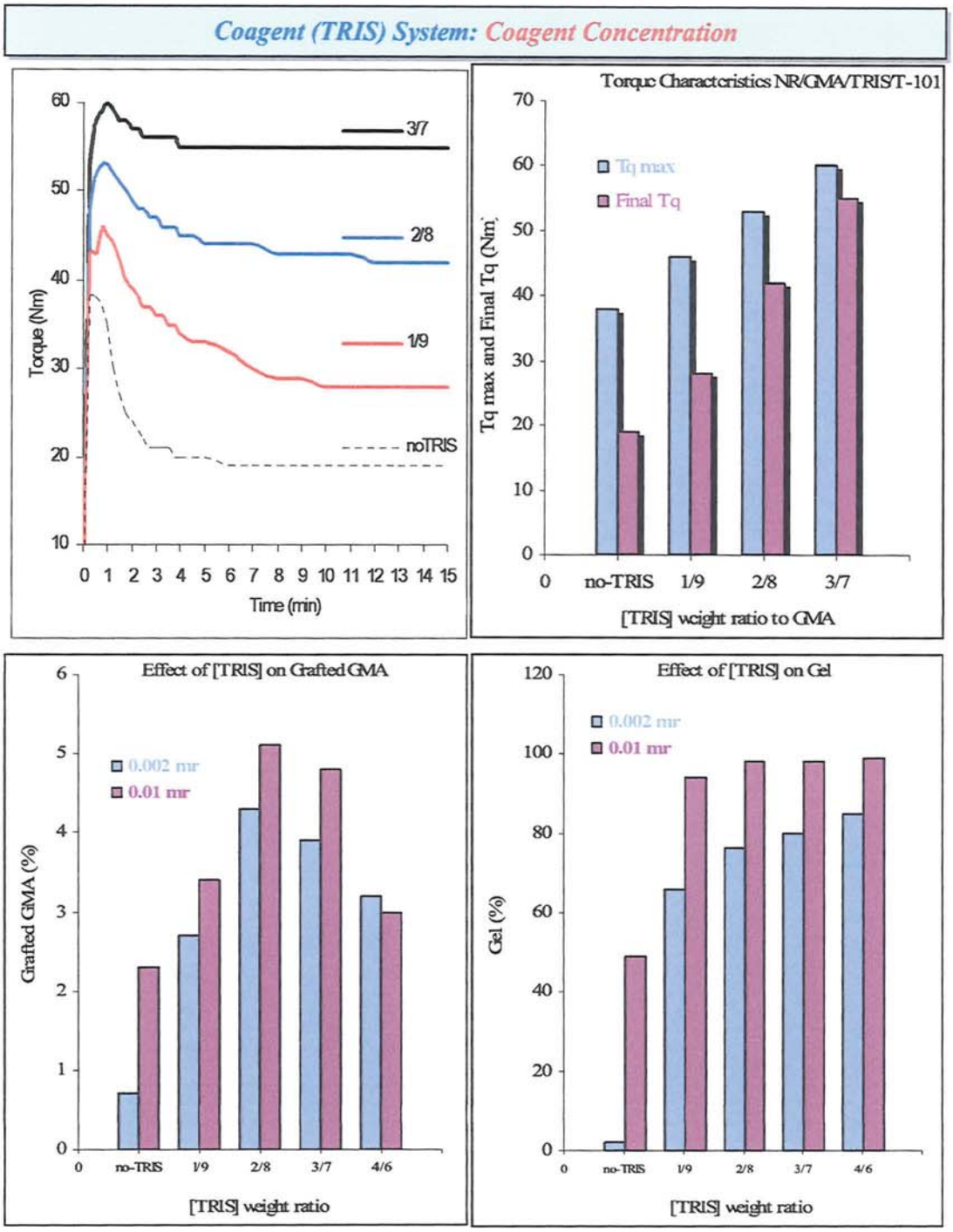

Figure 3.33 Effect of coagent (TRIS) concentrations on torque, grafting degrees and gel content (%) of processed NR/GMA/TRIS/T-101 system. (Samples GT1-n and GT2-n in Table B.3.6 Appendix B; [GMA]i = 6-9%, [TRIS] = 1/9 to 3/7 weight ratio to GMA, [T-101] 0.002 and 0.01 molar ratio to GMA+TRIS, rotor speeds 60 and 65 rpm, 15 min, mixing method M-1)

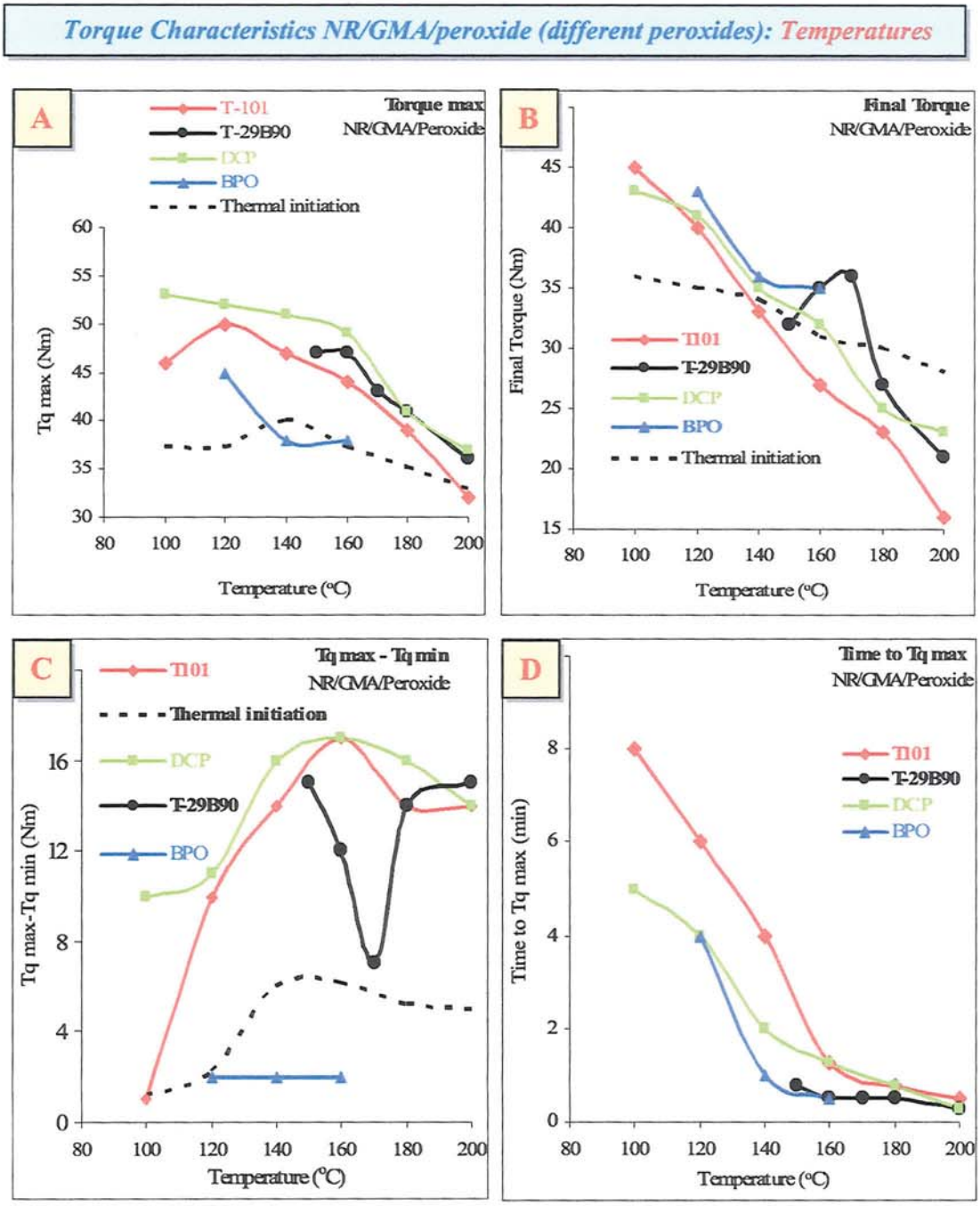

Figure 3.34 Comparison the effect of processing temperature (100-200°C) on torque characteristics of processed NR/GMA/Peroxides (different peroxide). Samples [GMA]i = 6 %, [T-101], [BPO] = 0.02 mr, [DCP] = 0.03 mr, [T-29B90] = 0.002 mr, 65 rpm, 15 min, mixing method M-1)

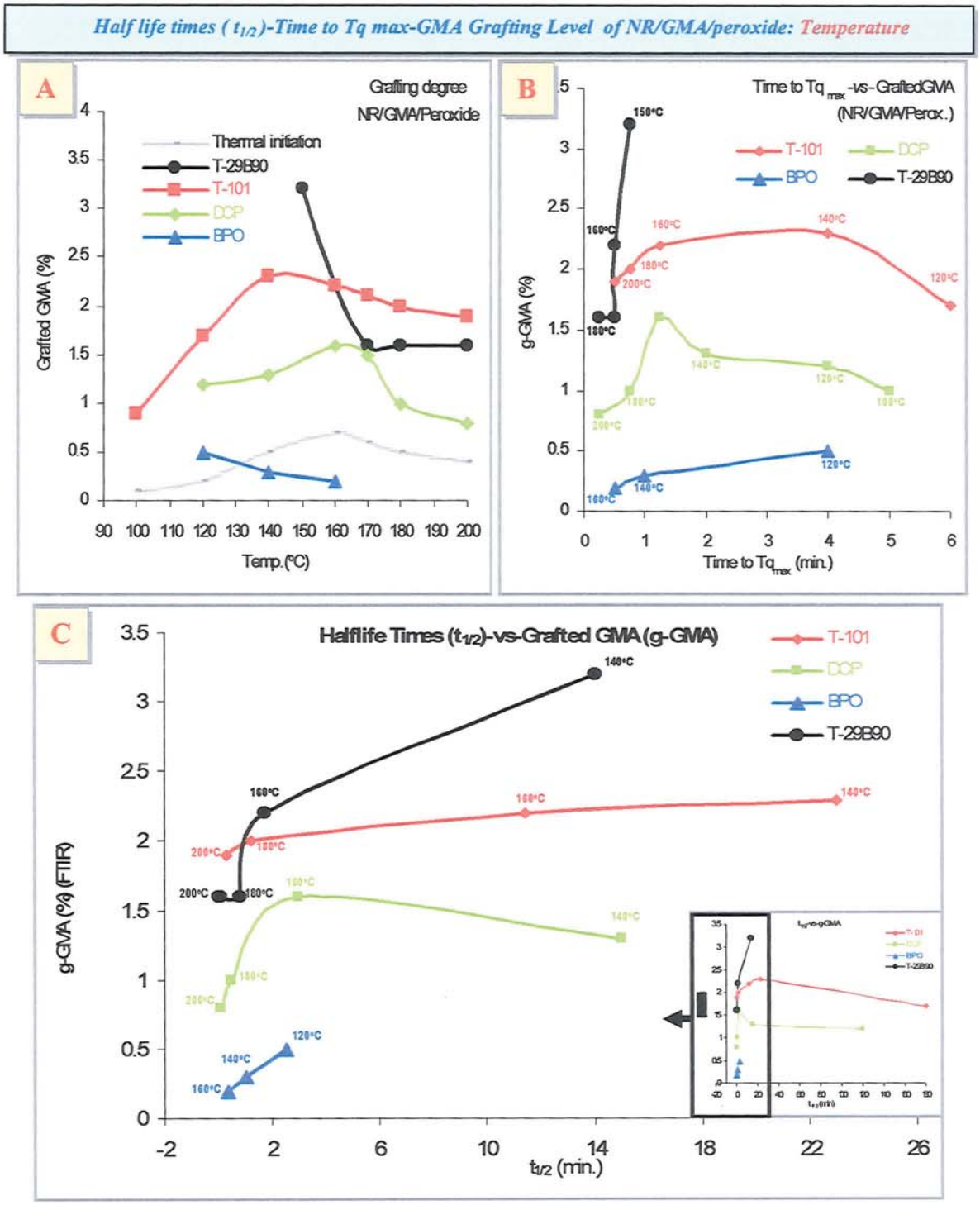

Figure 3.35 (A) Comparison effect of temperature on GMA grafting level of processed NR/GMA/peroxide (different peroxide), (B) correlation the grafted-GMA with time to Tq max and (C) with half life times ($t_{1/2}$) of peroxides; ([GMA]i = 6%, [T-101] and [BPO] = 0.02 mr, [DCP] = 0.04 mr and for [T-29B90] = 0.002 mr, 65 rpm, 15 min, mixing method M-1)

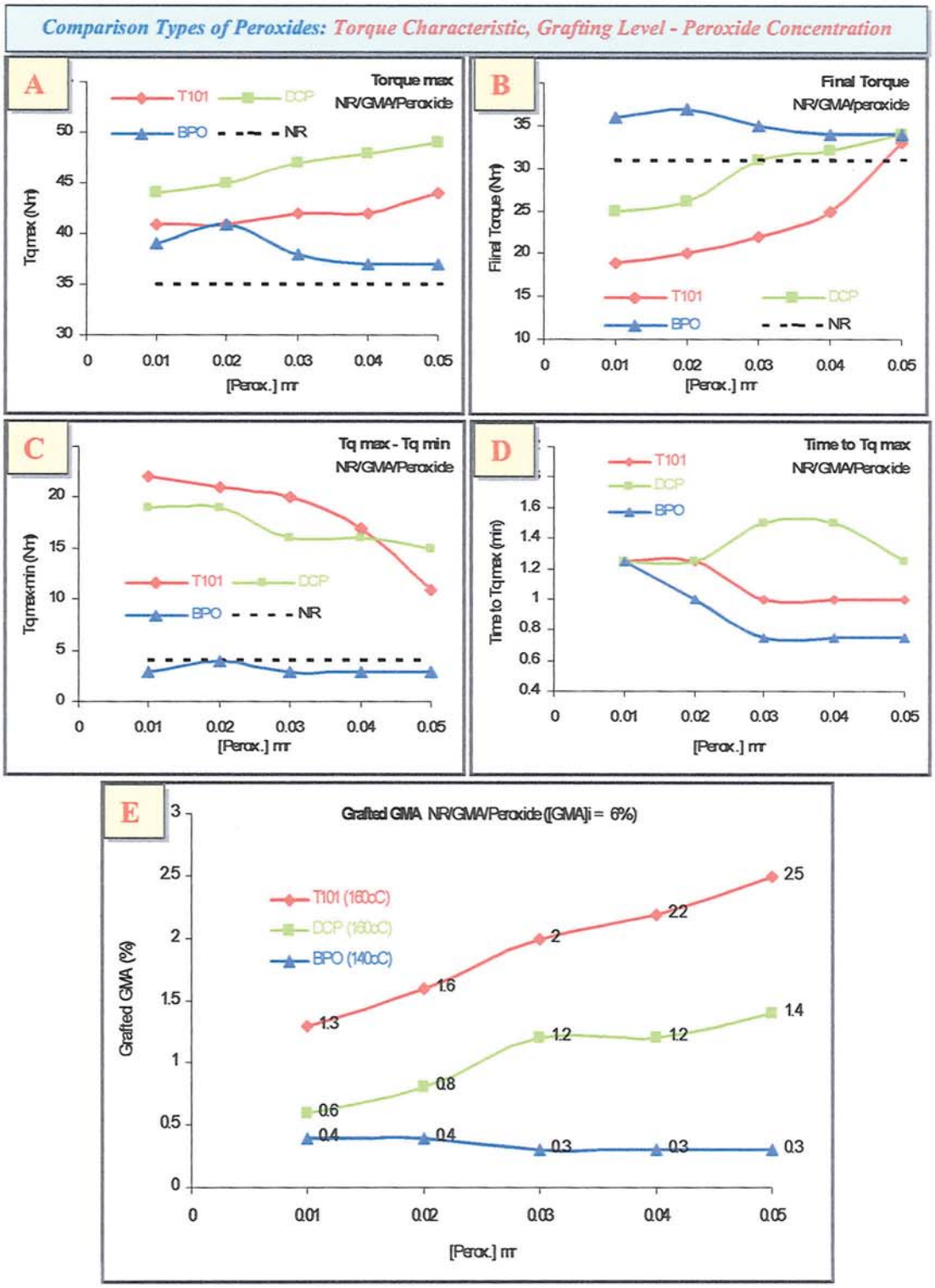

Figure 3.36 Comparison effect of peroxide concentration on torque characteristics and GMA grafting level of processed NR/GMA/peroxide (different peroxide). ([GMA]i = 6%, temp. 160°C for T-101 and DCP, 140°C for BPO, 65 rpm, 15 min, mixing method M-1). Numbers on curves in curves are GMA grafting level on NR.

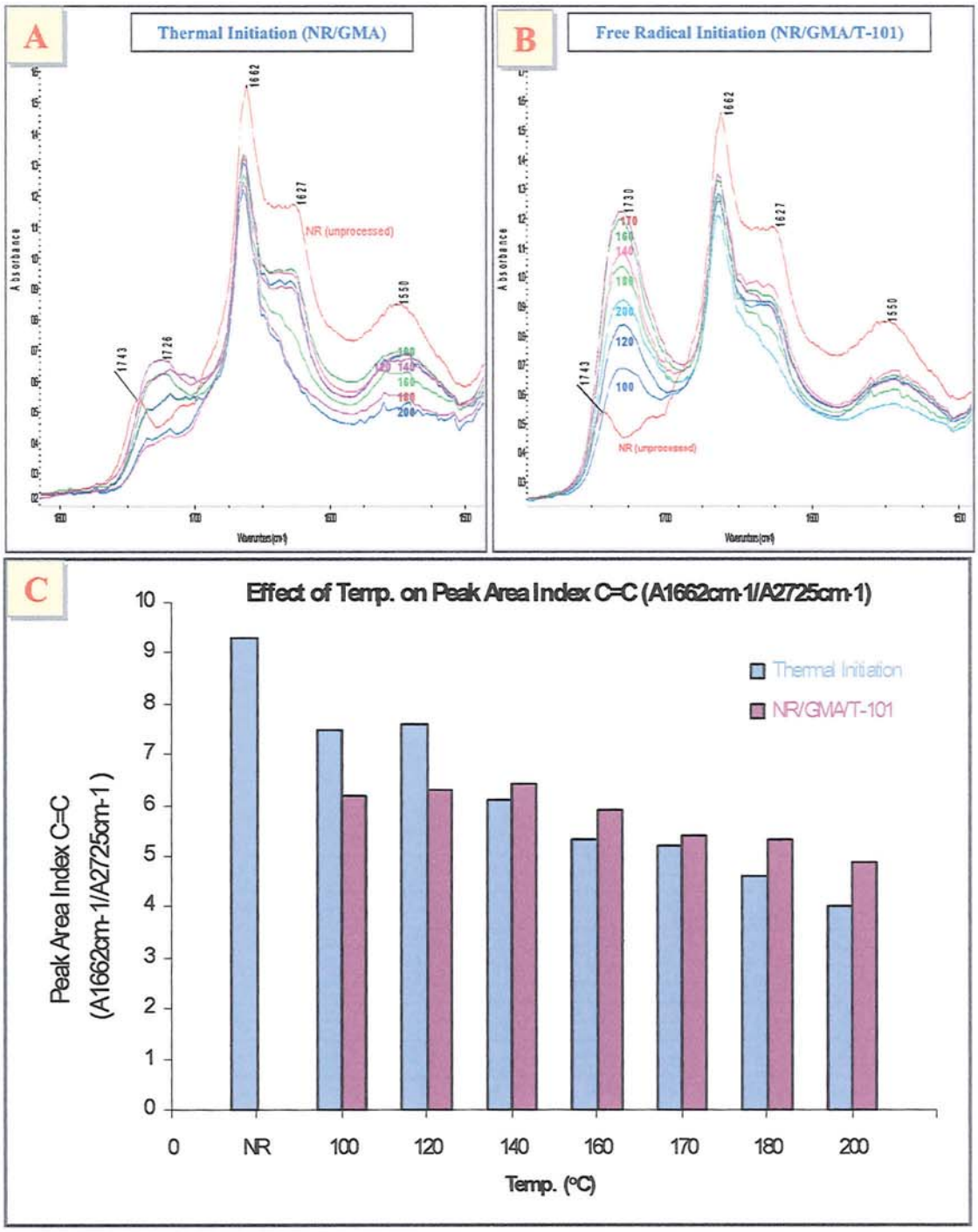

Figure 3.37 Effect of temperatures on C=C peak area index ($A_{1662\ cm\text{-}1}/A_{2725\ cm\text{-}1}$) and spectra of pressed thin films of processed NR-GMA by thermal initiation and free radical initiation (in the presence of peroxide T-101). (Sample T1-n in Table B3.1 in Appendix B; [GMA]I = 6 %, 65 rpm, 15 min and T6-n in Table B3.2 in Appendix B; ([GMA]i = 6%, [T-101] = 0.04 mr, 65 rpm, 15 min, mixing method M-1)

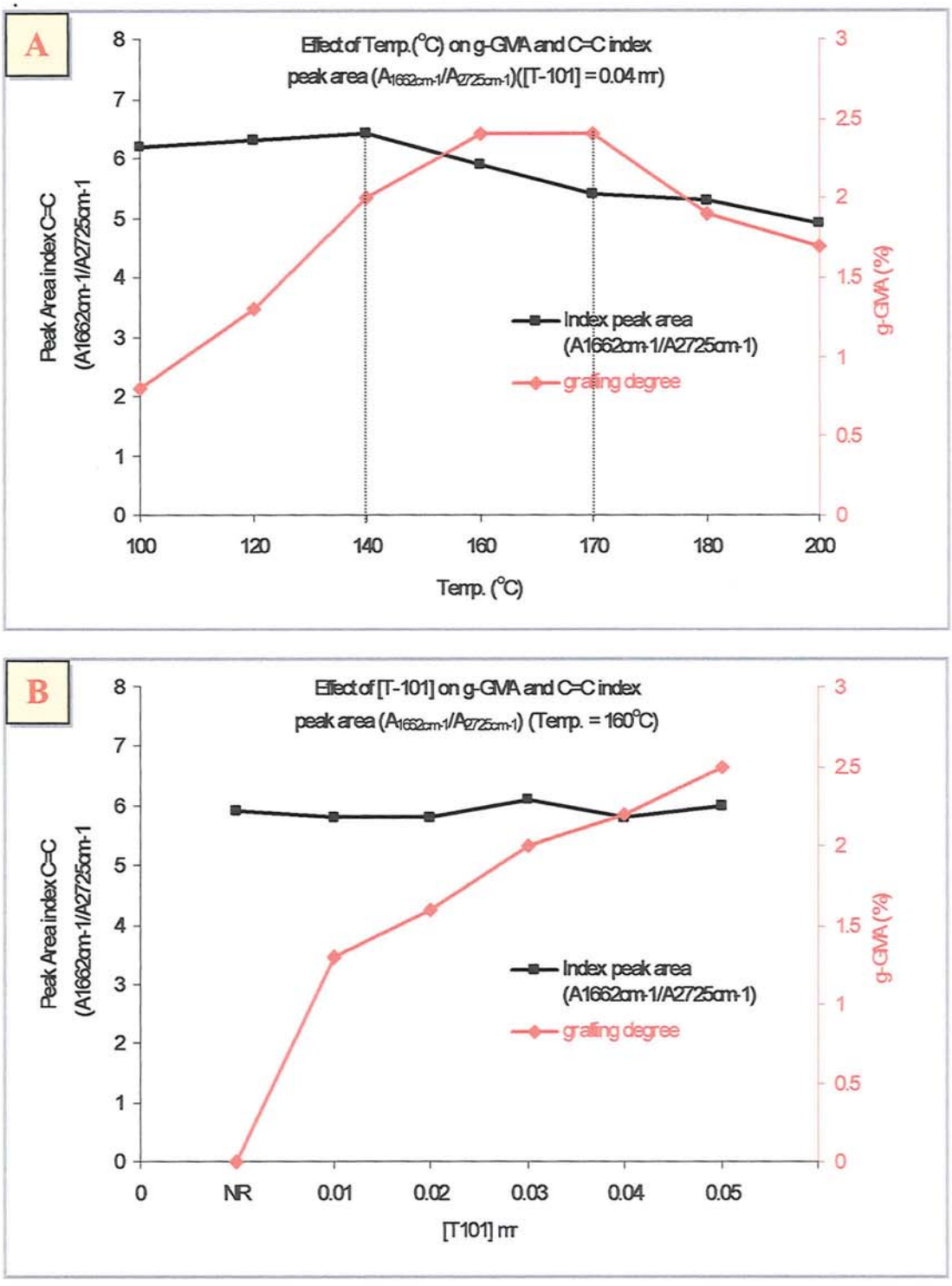

Figure 3.38 Effect of temperature (A) and T-101 concentration (B) on grafted GMA (red) and the extent (peak area index) of C=C double bond. Sample T5-n and G2-n in Table B.3.2 in Appendix B ([GMA]i = 6 %, 65 rpm, 10 min, mixing method M-1).

CHAPTER 4
FUNCTIONALISATION OF POLYPROPYLENE WITH GMA

4.1 Objectives and Methodology

Functionalisation of polyolefin by introduction of polar groups has been the subject of intensive investigation [1-7]. Glycidyl methacrylate, GMA (**I**) has been used increasingly as a grafting monomer because of its epoxide function which is highly electrophilic and capable of reacting with variety of functional groups such as carboxylic acid (—COOH), amide (—NH_2), hydroxyl (—OH), and sulfide (—SH) **[1]**. GMA has played an important role in the chemical modification of different commercial polymer melts including PP [118-124], PE [125,126,141-144], EPR [127-129], and EPDM [130] and has been used intensively to promote compatibility of immiscible blends [253-270]. As was described in **Section 1.3.4** (Chapter-1), the melt free radical grafting reactivity of GMA on polymers is generally low due to competing side-reactions e.g. chain scission, cross-linking of the polymer substrate and homopolymerisation of the monomer always. One approach that has been used to reduce the extent of these side reactions, thus enhancing the grafting efficiency is to add a second reactive monomer (used as a coagent) during the melt grafting process.

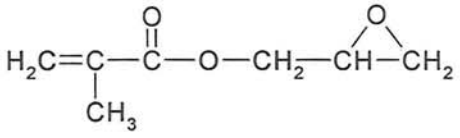

(I) Glycidyl Methacrylate (GMA)

The objective in this part of the study was to enhance the extent of the functionalisation reaction of GMA on PP via melt grafting in an internal mixer. A novel approach which has been developed at Aston University [96-98,129,130,134,138] is explored here with the aim

of enhancing the grafting efficiency and reducing the side reactions during the melt grafting. This involves the use of two highly reactive coagents having multi-functionality namely TRIS **(II)** and DVB **(III)** during the reactive processing.

The grafting of GMA onto PP was carried out in a closed system of an internal mixer (torque rheometer) using different processing conditions and chemical composition. A detailed study of GMA grafting onto PP under thermal and free radical initiated reactions in the absence (see **Scheme 4.1**, p.198) or presence of a coagent, TRIS or DVB (see **Scheme 4.2**, p.199) using different peroxides as free radical initiators was first conducted to establish the appropriate methodology and to investigate the grafting mechanism.

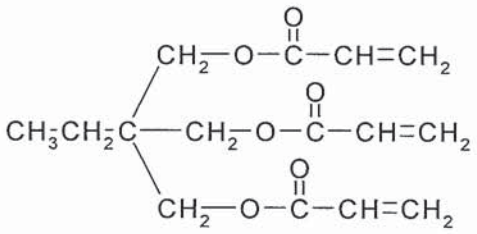

(II) Trimethylol Propane Triacrylate (TRIS)

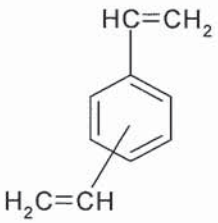

(III) di-Vinyl Benzene (DVB)

The methodology and optimum conditions were established by examining the following variables:

1. Processing temperature (120-200°C)
2. Processing time (0-10 min)
3. Concentration of GMA (2-18 w/w %)
4. Concentration of coagent TRIS or DVB (1/9 to 4/6 weight ratio to GMA)
5. Type of peroxides and their concentrations; of BPO **(IV)**, DCP **(V)**, T-101 **(VI)**, T29B90 **(VII)** (0.001-0.01 molar ratio to GMA or GMA+coagent).
6. The addition sequence of various reactants (see **Scheme 4.2**)

The reaction products were purified by means of Soxhlet extraction and precipitation using different solvents (see **Scheme 4.3**, p.200) and characterised by FTIR (see **Scheme 4.4**, p.201). The level of GMA content in unpurified (referred to as total-GMA), methanol-purified (as reacted-GMA) and acetone-purified reaction products (grafted-GMA) were evaluated by FTIR method and by titration (see **Scheme 4.4**).

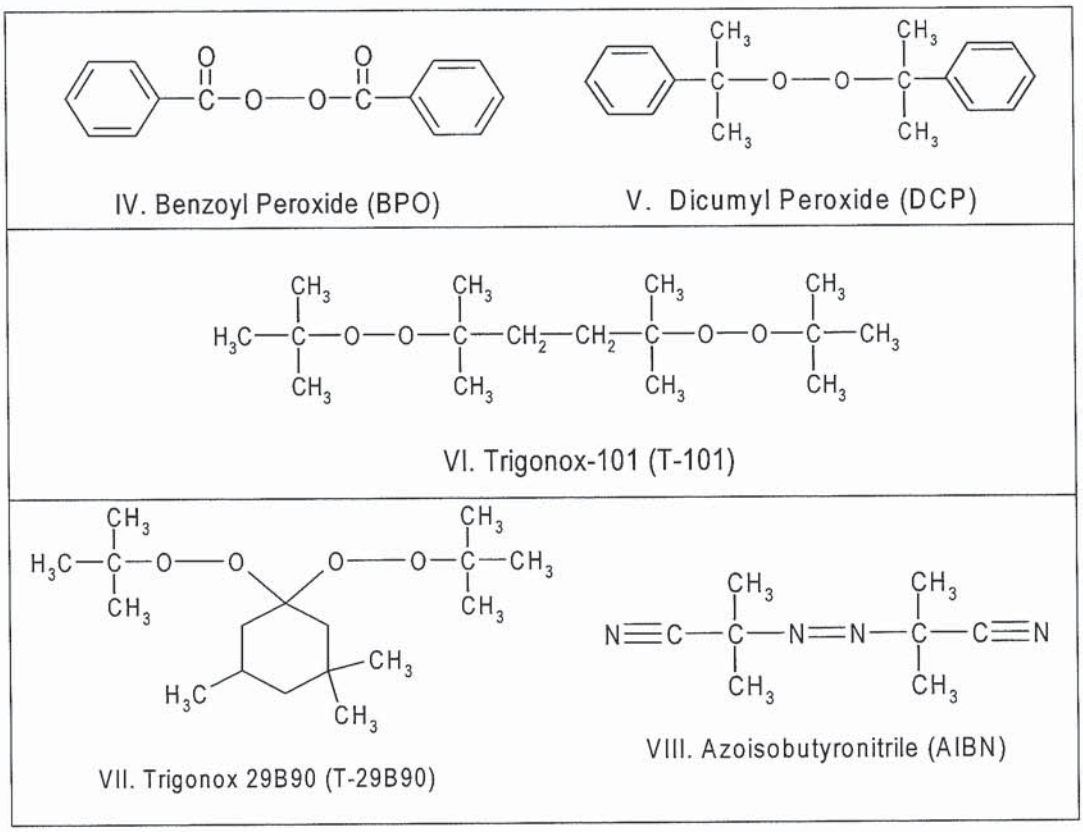

To achieve a better understanding of GMA grafting onto polypropylene and analysis of the grafting products, poly-GMA, poly-TRIS, poly-DVB, GMA-co-TRIS, and GMA-co-DVB were polymerized on the bench (see **Section 2.10** in **Chapter 2**, p.81) and characterised by FTIR. **Tables C.4.1** to **C.4.8** (in appendix C) list the experimental composition and results for the grafting of GMA onto PP by thermal and free radical initiation in the absence or presence of the coagents.

4.2 Results

4.2.1 Characterization of Side Reaction Products

Homopolymerisation of the monomer GMA (poly-GMA) and the coagents TRIS (poly-TRIS) or DVB (poly-DVB) and copolymerisation of the monomer and the coagents (GMA-co-TRIS or GMA-co-DVB) could take place during melt grafting of GMA onto PP. To analyse the reaction products, the above homopolymers and copolymers were polymerised on the bench using a free radical initiator (Azo-iso-butyronitrile, AIBN **(VIII)**) and were then characterised by FTIR.

4.2.1.1 Characterization of Poly-GMA

The synthesised homopolymer of GMA (poly-GMA) (see **Section 2.10.1** in **Chapter 2**, p.82) was soluble in chloroform, dichloromethane (DCM), acetone, toluene and xylene but insoluble in n-hexane, methanol and ethanol (see **Table 2.7** in Chapter 2, p.71). The FTIR spectrum of poly GMA is compared with that of the monomer GMA (see **Fig. 4.1** and **Table C.4.9** in appendix C for its infrared assignment). The ester carbonyl stretching absorption (υC=O) of GMA observed at 1720 cm^{-1} (unsaturated ester group) has shifted to 1732 cm^{-1} in poly GMA due to formation of saturated ester groups. The unsaturated acrylic double bond (υC=C) in GMA which appear at 1638 cm^{-1} (stretching), C-H bending (δC=CH_2) at 1317 cm^{-1} and 1296 cm^{-1}, C-H twisting (τC=CH_2) at 944 cm^{-1} and C-H wagging (ϖC=CH_2) at 815 cm^{-1} have reduced or disappeared in the poly GMA spectrum. The peaks at 908 cm^{-1}, 843 cm^{-1}, and 762 cm^{-1} which are characterised as the stretching absorption of the epoxy group remain unchanged in the poly GMA (**Rn-4.1**).

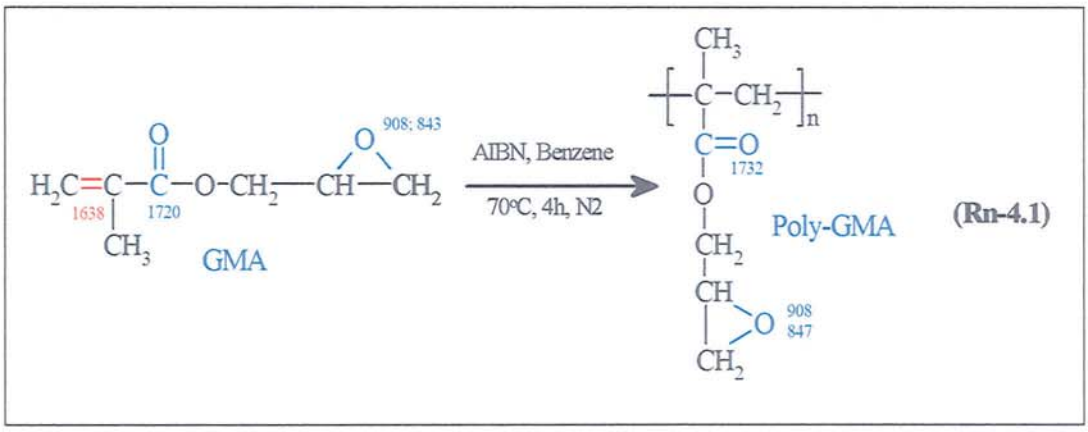

(Rn-4.1)

4.2.1.2 Characterisation Poly-TRIS

The homopolymerised TRIS (poly-TRIS) (see **Section 2.10.2** in **Chapter 2**, p.82) was found to be insoluble in almost all (normal) organic solvents whereas TRIS monomer is fully soluble (see **Table 2.7** in **Chapter 2**, p.71). The FTIR spectrum of virgin TRIS and the FTIR-ATR of synthesised poly TRIS are compared in **Fig. 4.2** and **Table C.4.9** (in Appendix C) gives the infrared assignments. The unsaturated absorption at 1728 cm^{-1} in TRIS has shifted to 1735 cm^{-1} due to the formation of saturated ester groups in poly TRIS . The stretching of acrylic double bonds (υC=C) are observed at 1635 cm^{-1}, 1618 cm^{-1} and

C-H symmetrical and asymmetrical stretching absorption ($\upsilon CH=CH_2$) at 1466 cm^{-1} and 1408 cm^{-1}, C-H bending out of plane and in plane ($\delta CH=CH_2$) at 1295 cm^{-1} and 1270 cm^{-1}, C-H twisting ($\tau CH=CH_2$) at 986 cm^{-1} and C-H wagging ($\varpi CH=CH_2$) at 809 cm^{-1}, see **Rn-4.2.**

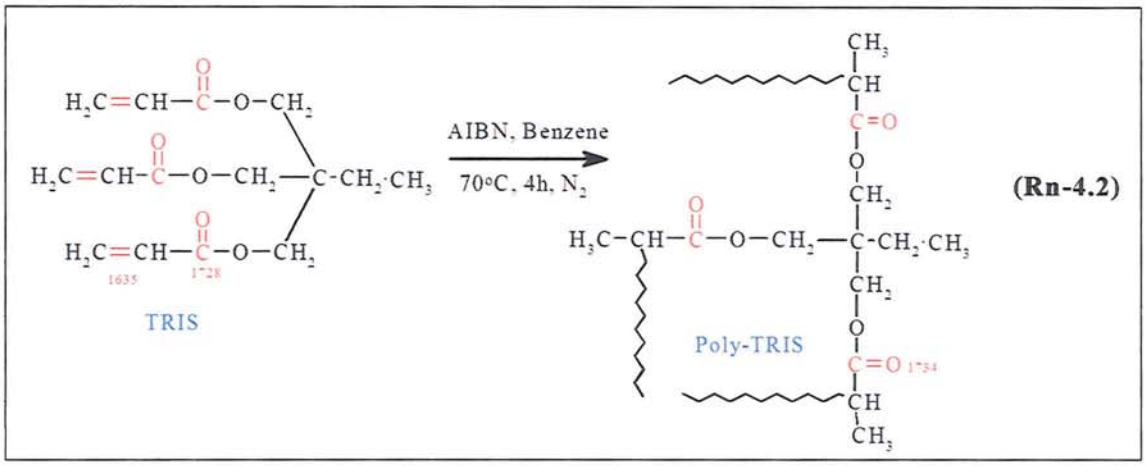

(Rn-4.2)

4.2.1.3 Characterization of Poly-DVB

The homopolymerised DVB (poly-DVB) (see **Section 2.10.3** in Chapter 2, p.82) was insoluble in methanol, ethanol, acetone, DCM, toluene and xylene whereas DVB is fully soluble in these solvents (see **Table 2.7** in Chapter 2, p.71). The FTIR-ATR spectrum of poly DVB is compared with the FTIR spectrum of neat DVB in **Figure 4.3** and **Table C4.9** (in Appendix C) gives the infrared assignments. Although it is difficult to compare FTIR-ATR spectrum of synthesised poly DVB with FTIR spectrum of neat DVB in terms of intensity correlation as intensity varies non-linearly with the frequency range in ATR measurement, the insoluble nature of the synthesised poly DVB indicates that it is a polymer, see **Rn-4.3.**

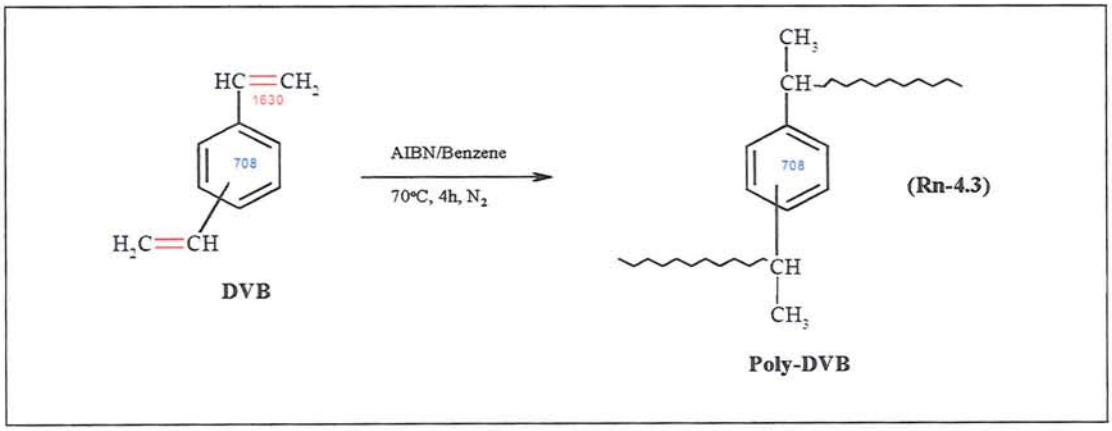

(Rn-4.3)

4.2.1.4 Characterization of GMA-co-TRIS

The FTIR-ATR spectrum of the synthesised GMA-co-TRIS (see **Section 2.10.4** in **Chapter 2**, p.83) was compared with that of poly GMA and poly TRIS (see **Fig. 4.4**). As in the case of homopolymerisation of GMA or homopolymerisation of TRIS, the copolymerisation of GMA-co-TRIS was characterised by the disappearances of the peaks at 1638 cm^{-1} and 1635 cm^{-1} corresponding to the double bond stretching absorption ($\upsilon C=C$) of GMA and TRIS (see **Rn-4.4**).The strong peak due to the carbonyl stretching absorption ($\upsilon C=O$) are shifted to 1734 cm^{-1} (poly GMA at 1732 cm^{-1}, TRIS at 1735 cm^{-1}). The bending absorptions of C-O-C is observed at 1157 cm^{-1} and this is similar to that of poly GMA (1172 cm^{-1}) and poly TRIS (1150 cm^{-1}). The peaks corresponding to the epoxy group absorption at 907 cm^{-1} and 847 cm^{-1} are similar to those of poly GMA at 908 cm^{-1} and 847 cm^{-1}.

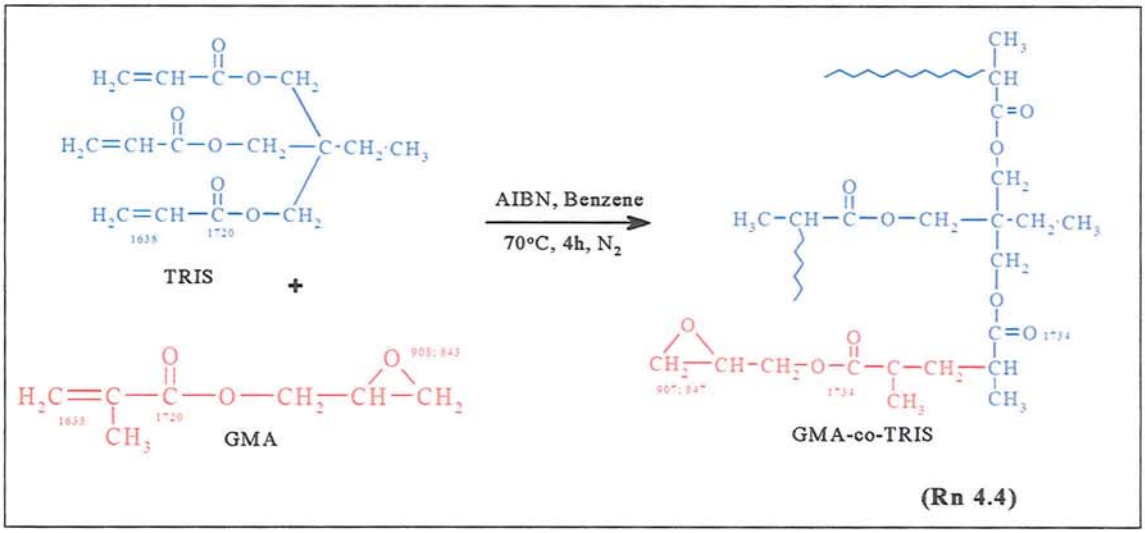

(Rn 4.4)

The area ratio of the carbonyl absorption peak at 1734 cm^{-1} to that of the epoxy group absorption peak at 907 cm^{-1} ($A_{1734\ cm^{-1}}/A_{907\ cm^{-1}}$) was found to be 18.8 for GMA-co-TRIS copolymer which is much larger than the corresponding ratio in the case of poly-GMA ($A_{1732\ cm^{-1}}/A_{907\ cm^{-1}} = 11.2$) and this is almost certainly due to the additional contribution to the copolymer of the ester group (in this region) from TRIS. Furthermore, this copolymer was found not to be soluble in acetone and chloroform in which both TRIS and GMA monomers are soluble.

4.2.1.5 Characterization of GMA-co-DVB

The synthesised copolymer of DVB and GMA (GMA-co-DVB) (see **Section 2.10.5** in **Chapter 2**, p.83) was characterised by comparing its FTIR-ATR spectrum with that of poly DVB and poly GMA. The GMA-co-DVB was found not to be soluble in acetone and chloroform (the corresponding monomers were soluble). Similar to poly DVB, the FTIR-ATR spectrum of GMA-co-DVB was characterised by the disappearance of the peaks corresponding to the stretching double bond absorption (υC=C) aliphatic at 1630-1576 cm^{-1} ($\upsilon C=C_{phenyl}$ remains) and bending absorption ($\delta CH=CH_2$) at 987-800 cm^{-1}. The carbonyl stretching absorption (υC=O) at 1727 cm^{-1} and the υC-O-C at 1124 cm^{-1} and epoxide at 908 cm^{-1} are similar to that of poly GMA (1732 cm^{-1}, 1150 cm^{-1}, 907 cm^{-1}, respectively) The appearance of peaks at 712 cm^{-1} and 799 cm^{-1} are similar to that of poly DVB at 708 cm^{-1} and 798 cm^{-1} corresponding to phenylene stretching absorptions (see **Figure 4.5** and **Rn-4.5).**

(Rn-4.5)

4.2.2 Separation of Reaction Products and Characterisation of GMA Functionalised PP

Since the ungrafted GMA (free GMA) and poly GMA gave rise to carbonyl stretching (υC=O) absorption peaks in the region of the grafted GMA (saturated and unsaturated aliphatic ester at 1700-1750 cm^{-1}) (see **Fig. 4.6** and **Rn-4.6**), it is of great importance to eliminate all ungrafted GMA and poly-GMA before determining the grafting yield. Five different purification methods were examined to purify the reaction products. **Figure 4.7** shows a comparison of FTIR spectra (carbonyl peak at 1727-1733 cm^{-1}) for the different

purifications: heating in vacuum oven (80°C, 12 hrs), extraction with methanol and acetone (24h) and precipitation with different solvents (methanol and acetone). **Figure 4.8** shows the area index of carbonyl peaks ($A_{1730s\ cm\text{-}1}/A_{2722\ cm\text{-}1}$) (see **Section 2.5.4** in **Chapter 2**, p.78) calculated for grafted-GMA from the different purification methods. It was found that purification by precipitation with different solvents is a more effective and suitable method for determining the GMA grafting degree and the amount of homopolymerised GMA (poly GMA). In conventional (PP/GMA/T101) system (referred to as melt grafting in the absence of coagent), the reaction may contain unreacted GMA (free-GMA) and poly-GMA, hence a precipitation method with methanol and acetone was adopted to eliminate the free-GMA and poly-GMA (see **Scheme 4.3,** p.200). The procedure was established based on the difference in solubility of poly-GMA in methanol (insoluble) and acetone (soluble). When the reaction products were precipitated in methanol, the free-GMA (soluble in methanol) was removed hence the remaining product was expected to contain only poly-GMA and grafted GMA. On the other hand, precipitation in acetone removed poly-GMA and free-GMA (soluble in acetone) hence the products in this case contained only grafted GMA. Thus this can be used to establish the extent of competition between GMA grafting reaction and GMA homopolymerisation in PP melt. Processing of PP with GMA in the presence of the comonomers TRIS or DVB resulted in more complicated grafting reactions. The reaction product is not only expected to contain free-GMA and poly-GMA, but also unreacted comonomers, homopolymerised TRIS (poly-TRIS), copolymer GMA-co-TRIS (in the presence of coagent TRIS) or homopolymerised DVB (poly-DVB) and GMA-co-DVB (in the presence of DVB). The reaction product was placed in a Soxhlet extraction with xylene where the PP and PP-g-GMA are completely soluble and poly-TRIS, GMA-co-TRIS or poly DVB and GMA-co-DVB were removed as they were insoluble. The amount of free-GMA, poly-GMA, and grafted GMA could be obtained by calculating the difference between these three samples, as described in **Section 2.5**, Chapter 2 (p.70). It is important to note that in the case of PP-*g*-GMA_{TRIS}, the carbonyl peak is quite strong due to the higher level of GMA grafting in addition to a contribution of carbonyl absorption from grafted-TRIS (its carbonyl absorption overlaps with that of the grafted GMA, see **Fig. 4.9** and **Rn-4.7**). Therefore, the amount of grafted GMA onto PP in the PP-*g*-GMA_{TRIS} can only be calculated by titration. In the case of PP/GMA/DVB/T101 system, the amount of grafted GMA (PP-g-GMA_{DVB}) can be determined by titration and FTIR methods (see **Fig. 4.9** and **Rn-4.8**).

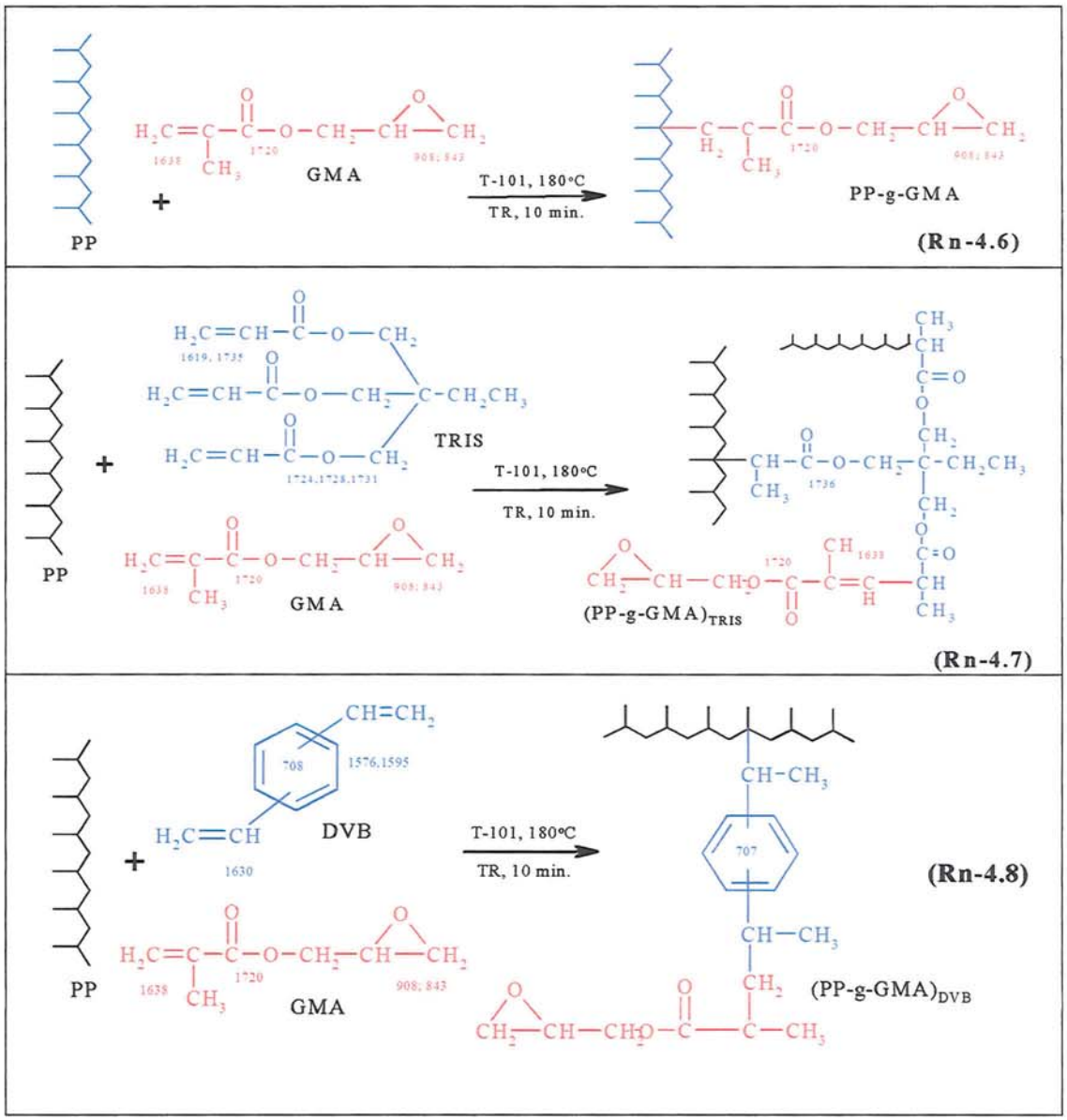

4.2.3 Determination of Grafted-, Poly-, Free-GMA in the Reaction Products

Due to the high volatility of GMA, it is very difficult to establish a calibration curve by preparing a series of PP films which contain known amounts of GMA accurately. A non-aqueous back titration procedure was adopted to determine the grafting degree as described in **Section 2.5.2** (p.72). This method was based for the reaction of epoxy group of GMA with an acid (trichloro acetic acid). In order to confirm the ring-open reaction with trichloro acetic acid, the ring open product was pressed into a thin film, referred to as film-X (see **Scheme 4.4**, p.201) and its IR showed the elimination of characteristic absorption peaks of the epoxy group at 908 cm^{-1} and the formation of a new peaks at 3500 cm^{-1} due to

stretching υ(O-H) (–OH groups formed during the ring open reaction (see **Rn. 2.1** in **Chapter 2**, p.73) and a peak at 1799 cm^{-1} υC=O (trichloro ester group), see **Fig. 4.11.** Because this titration method is very time consuming, a calibration curve was also established based on a correlation of the grafting degree measured by titration and the absorption area ratio ($A_{1720\text{-}1740cm}^{-1}/A_{2722cm}^{-1}$) measurement by FTIR from a set of purified samples as described in **Section 2.5.4** (**Chapter 2**, p.78).

4.2.4 Grafting GMA onto PP by Thermal Initiation

In order to investigate the effect of temperature in the GMA grafting reaction on PP by thermal initiation, a set of samples (GMA 12%) was prepared and melt processed with PP in a torque rheometer (temperature 180°C, 65 rpm, 10 min), see **Table C.4.1** (Appendix C). It was found that the thermally initiated grafting reactions of GMA onto PP resulted in very low grafting efficiency.

4.2.5 Grafting GMA onto PP in the Absence of a Coagent

The peroxide-initiated grafting of GMA on PP in the absence of a coagent (conventional system) was carried out in a closed system of the torque rheometer. Unless otherwise stated, the processing was carried out under a standard condition, i.e. rotor speed 65 rpm, and processing time 10 minutes. In this study, two different peroxides were used to initiate the grafting reaction of GMA on PP; 2,5-di(tert-butylperoxy)-1,5-dimethyl hexane (Trigonox-101, T-101) and 1,1-di-(tert-butylperoxy)-3,3,5-trimethyl cyclohexane (Trigonox-29B90, T-29B90), see **Table 2.3** in **Chapter 2** (p.63), for half-life time, $t_{1/2}$, of these peroxides). The effect of processing temperature, the peroxides concentration and GMA concentration were investigated. During the free radical process, polypropylene chains may undergo degradation and result in a decrease in viscosity of the polypropylene and, thus, a torque change can be expected to be seen during the batch mixing. The experimental condition-compositions are presented in **Table C4.2** (in Appendix C).

(i) Effect of Trigonox-101

Figure 4.12 demonstrates the changes in torque time curves of PP/GMA/T101 system under different processing temperatures and peroxide concentrations. The observed decrease in the final torque at all peroxide concentrations with increasing processing

temperature is likely to be due to peroxide-initiated β-scission of PP. **Figure 4.12** also shows the influence of the peroxide concentration on torque values under different processing temperatures. Increasing peroxide concentration would increase the formation of PP radicals, leading to a higher level of grafting reaction. However, at a higher temperature (above 180°C) the final torque and torque maximum leveled off (see **Fig. 4.13**). This would suggest that the grafting reaction level is very low due to the very short life time of the radical at higher temperatures, as well as the dominance of chain scission at higher peroxide concentrations reflected by lower final torque at higher processing temperatures (**Fig. 4.13**). It can be seen from **Fig. 4.14** that the grafting degree decreases at higher processing temperatures at all peroxide concentrations examined and the grafting degree reaches a maximum value at a peroxide concentration of 0.005 mr (molar ratio to GMA) at level temperature of 160°C. Similarly, the degree of homopolymerised GMA (poly-GMA) is also higher at lower processing temperatures (except for T-101 0.001 mr). It is interesting to compare the degree of GMA conversion into grafted-GMA, poly-GMA and unreacted-GMA (free-GMA) at different temperatures and different peroxide concentrations with the torque characteristics of these samples (**Fig. 4.14** and **4.15**). The higher level of grafting reaction of GMA onto PP at the lower processing temperature of 160°C at all peroxide concentrations examined can be predicted from the corresponding torque behaviour, e.g. highest torque maximum and longest time to the maximum torque at 160°C (see **Fig. 4.13**). However, the grafting yield of GMA on PP in the PP/GMA/T-101 system was overall quite low. For example, when 12% GMA was processed with PP at optimum temperature (160°C) and peroxide T-101 concentration 0.001 mr (≈ 0.03 phr), the grafting degree was just 0.8 % (i.e. only 6 % of the total amount of initial GMA amount used). When T-101 was increased five times to 0.005 mr (≈ 0.15 phr) T-101, the grafting degree reached to 2.2 % (18 % from total initial amount of GMA). It is important to point out that a further increase in the peroxide concentration (up to 0.01 mr, ≈ 0.3 phr) resulted in leveling off the grafting degree with a clear increase in the extent of the main side reaction, i.e. homopolymerisation of GMA (**Fig. 4.14** and **4.15**) as well as increasing in degradation of PP by chain scission (as shown by an increase in the MFI at **Fig. 4.18**). It is clear therefore that both processing temperature and peroxide concentration have an important role in controlling the level of GMA grafting degree and amount of poly-GMA formation along with the extent of PP degradation (via chain scission in the grafting system). However, the effect of processing temperature on the grafting degree of GMA is more severe than on the

degradation of PP (shown by the change of its MFI). For example, when processing temperature was raised from 160°C to 200°C, the grafting degree of GMA dropped from 2.3 % to 0.2 % (more than ten times less), but the MFI changed from only 7 to 6 g/10min (**Fig. 4.18**). On the contrary, the effect of peroxide concentration is more obvious on changes in MFI (degree of the degradation by chain scission reaction of PP). When the peroxide concentration was increased from 0.001 to 0.01 mr (160°C), the grafting degree of GMA improved by doubling from 0.7 to 1.8 %, but the MFI enhanced to almost 400 % change from the PP origin (**Fig. 4.18**).

(ii) Effect of Trigonox-29B90

It was reported that peroxide T-29B90 was a very effective initiator for the grafting of GMA onto ethylene propylene copolymer at extremely low temperature **[134]**. To verify this, the effect of the peroxide on the grafting reaction of GMA on PP was examined (the processing composition and condition and its results are listed in **Table C4.3** (in Appendix C). **Figure 4.16** shows torque-time curves and GMA content in the PP/GMA/T-29B90 system processed under different temperatures and different peroxide (T-29B90) concentrations. The torque characteristic in the PP/GMA/T-29B90 system is similar to that when the peroxide T-101 was used. For example, the final torque decreased with increasing temperature (see **Fig.4.17**). It is clear that the melt reaction resulted in the highest grafting level at lowest processing temperature of 160°C and lower peroxide concentration (**Fig.4.16**) which is paralleled by highest torque maximum formation (see **Fig. 4.17**). However, very high concentration of poly-GMA was also formed under these conditions (**Fig.4.16**). **Figure 4.17** compares the effect of the two peroxides T-29B90 and T-101 on the torque behaviour. The high torque maximum must be due to the extent of grafted GMA and poly GMA formation and the high final torque indicates the degree of degradation by chain scission of the PP backbone. It is interesting to note that the difference between the two peroxides in terms of the grafting level under all conditions is not too significant but the difference in the degree of chain scission reaction is very obvious as reflected from the large difference in the polymer's MFI values (**Fig. 4.18**).

(iii) Effect of GMA Concentration on Grafting Degree

Effect of GMA concentration on the torque characteristics and grafting level is shown in **Fig. 4.19**. Increasing the concentration of GMA up to 18 % initially added has led to higher

grafting both in the PP/GMA/T101 and PP/GMA/T-29B90 systems but the increase in GMA initial concentration had also given rise to a drastic increase in the level of the homopolymerisation reaction. It is very interesting that processing PP with high concentration (e.g. 18 %) of GMA in the presence of T-29B90 results in higher grafting levels and lower extent of degradation and lower level of poly GMA compared to T-101.

4.2.5 Grafting GMA onto PP in the Presence of a Coagent

It was demonstrated in the previous section that GMA could be melt grafted onto PP by free radical initiation, in the presence of a peroxide (T-101 and T-29B90). However, the overall level of grafting of GMA was shown to be relatively low. Though an increase of peroxide concentrations led to a higher level of grafted-GMA; high extent of homopolymerised GMA (poly-GMA) as well as increased chain scission of PP also occurred during the melt grafting, especially when the peroxide Trigonox-101 was used. The torque behaviour of PP processed with the coagents TRIS and DVB in the presence and absence of added peroxide (no GMA used here) is shown in **Fig. 4.20**. It is clear that there is a very high increase in the maximum torque (peak) in the presence of a small concentration of peroxide (T-101) when compared to the torque of GMA modified PP ([GMA]i = 4%) in presence of the same peroxide. The use of a very small amount of a free radical initiator (T-101) in the DVB-system causes an even more noticeable increase in the torque maximum (peak) but with further processing the torque level then decreases (**Fig.4.20**). **Figure 4.21** shows a comparison in the torque behaviour of the processed PP with GMA (with peroxide T-101 or T-29B90) in the presence and absence of TRIS or DVB. The high torque peak maxima suggests that the grafting reaction of GMA in the presence of the comonomers occurs intensely and at even faster rate than in their absence indicating the occurrence of both grafting and branching/crosslinking reactions which predominate at earlier stages of processing. However, the subsequent reduction in torque values on further processing (except in PP/GMA/DVB/T-29B90 system), suggests that some chain scission occurs at the later stages giving rise to a reduction in the polymer viscosity and lowering of the extent of the DVB- or TRIS-initiated crosslinking/branching. The presence of these highly reactive comonomers can be expected to result in a more complicated grafting process. Whereby in addition to the formation of poly GMA, a number of other side reactions may have an even more important contribution to

controlling the overall grafting yield of the modifier. These reactions include the formation of ungrafted copolymer of GMA with the comonomers (GMA-co-TRIS or GMA-co-DVB) as well as the homopolymers of the comonomers (poly TRIS or poly DVB), together with possible polymer crosslinking reactions that may occur via reaction of the reactive function of the comonomers with the polymer macroradicals.

i. Optimisation of the Addition Sequence in the Presence of DVB

To optimise the effect of DVB on GMA grafting, six different addition sequences (see **Scheme 4.2**) were investigated at a fixed composition and processing conditions ([GMA]i = 12 wt%, [T-101] = 0.005 molar ratio to GMA+DVB, weight ratio of DVB to GMA 2/8, temperature 160°C, rotor speed 65 rpm, and residence time 10 minutes, samples GV-M1 to GV-M6 see **Table C4.5** in Appendix C).

Addition Sequence	Procedure	g-GMA (%)	Aryl Peak Area Index of DVB ($707cm^{-1}/2720cm^{-1}$)
Method 1 **(M-1)**	All ingredient (PP+GMA+DVB+T-101) mixed in paper cup before introducing to the mixing chamber and then processed for 10 minutes	7.6	0.37
Method 2 (M-2)	After charging PP in the mixing chamber (for 2-4 min), injected the mixture of GMA+DVB+T-101, then processed for further 6- 8 minutes	8.5	0.45
Method 3 **(M-3)**	After charging PP in the mixing chamber (for 2 min), injected the coagent DVB (processed in 1 min), injected mixture of GMA+T-101 and then processed for further 7 minutes	5.7	0.27
Method 4 **(M-4)**	After charging PP in the mixing chamber (for 2 min), injected the mixture of DVB+T-101 (processed in 1 min), injected mixture of GMA+T-101 and then processed for further 7 minutes	5.9	0.31
Method 5 **(M-5)**	After charging PP in the mixing chamber (for 2 min), injected the mixture of GMA+T-101 (processed in 1 min), injected mixture of DVB+T-101 and then processed for further 7 minutes	7	0.34
Method 6 **(M-6)**	After charging PP in the mixing chamber (for 2 min), injected the mixture of DVB+GMA (processed in 1 min), introduced T-101 (wrapped in PP thin film) and then processed for further 7 minutes	7.6	0.41

Figure 4.22 shows that the addition sequence has a significant effect on the torque characteristic indicating the competition between the grafting, branching/crosslinking, and copolymerisation reactions. When a mixture of PP, GMA, DVB, and T-101 was processed by method-1 (**M-1**), the primary radicals formed from the decomposition of T-101 would initiate the copolymerisation and homopolymerisation reactions, especially at the first minute before the melting of PP, thus reducing the grafting efficiency. When method 2 (**M-2**) was adopted, the grafting degree was shown to be highest. This may be due to the high reactivity of DVB which reacts with PP macro radicals resulting in rapid formation of PP-

g-DVB or GMA-co-DVB. In the case of method-3 (**M-3**) and method 5 (**M-5**) the chance of copolymerisation (GMA-co-DVB formation) were minimised in the reaction product but the grafting degree was low. In the following investigation on the effect of DVB on the grafting degree, method-2 (**M-2**) or method-3 (**M-3**) was adopted for further preparation of samples.

ii. Effect of Temperature on Grafting Degree in Presence of DVB

The effect of temperature using different peroxides on the GMA grafting reaction in presence of the coagents was also examined. In PP/GMA/DVB/peroxide system (peroxides: T-101, T-29B90, DCP, BPO), the effect of temperature and peroxide concentration on torque characteristics and GMA grafting reaction was obviously different from that in the single monomer system without the coagent (see **Fig. 4.23** to **4.26)**. A set of samples was prepared using a fixed composition ([GMA]i = 12 %, DVB/GMA = 2/8 w/w ≅ 3.4 phr, [T-101] 0.001-0.01 molar ratio to GMA+DVB and processing conditions (65 rpm, 10 minutes) except for different temperatures (160°C-200°C). It is interesting that the change in torque characteristics (e.g. time to torque maximum) with increasing temperatures (**Fig. 4.25**) is paralleled by the half-life time ($t_{1/2}$) of the peroxides at the various temperatures, see **Table 2.3** in **Chapter 2** (p.63) for $t_{1/2}$ of the peroxides. At temperature of 160°C, for example, time to torque maximum of T-101, DCP, T-29B90, and BPO are 2.18, 1.63, 0.77, and 0.4 minutes and this corresponds to the order of peroxides half-live times of 2.1, 3, 0.83, and 0.32 minutes, respectively, and the lower the half-life time of the peroxides, the higher was the final torque (indicating high branching/crosslinking reaction) and the lower their GMA grafting degree. The melt temperatures (actual temperature measured in the polymer melt) at the same processing temperature was obviously different and probability correlates with the extent of branching/crosslinking reaction (exothermic) of PP-DVB in presence of the different peroxides (**Fig.4.24**). Similarly (to the conventional, in the absence of coagent), the grafting degree in presence of DVB reaches the highest value at 160°C and decreased noticeably with increasing temperature, see **Fig. 4.26**. The peroxides T-101 and DCP gave rise to the highest grafting levels at all temperatures, but the latter resulted in a slightly higher poly-GMA and more branching/crosslinking (lower MFI), **Fig. 4.27A**. A very small amount of poly GMA was measured over the whole range of temperatures (160°C – 200°C) (**Fig. 4.27A**). This is due to the high reactivity of DVB towards PP macroradicals and GMA, thus

enhancing the extent of the grafting reaction and increasing the grafting degree. Similarly (to the DVB system, in the presence of coagent DVB), the torque values and grafting level in the presence of TRIS are higher than that of the conventional (in the absence of coagent) system but is slightly lower than the DVB system (see **Fig. 4.27B** and **4.28**). The coagents DVB or TRIS can therefore enhance the grafting whereby initially DVB or TRIS grafts onto the PP chains, then GMA co-grafts rapidly via the multi-functionality of DVB or TRIS. As a result, the chance of homopolymerisation of GMA would be reduced drastically (**Fig.4.27B**)

iii. Effect of Peroxide Concentration on Grafting Level in Presence of DVB

Figures 4.29 - 4.31 show the effect of peroxide concentration on the torque characteristics and grafting reaction of PP/GMA/DVB/peroxide (different types of peroxides) system. When the DVB concentration was fixed at a 2/8 weight ratio (≅ 3.4 phr) with GMA at 12 %, the torque curves (torque max and final torque) of the PP/GMA/DVB/T-101 system increased with increasing peroxide concentrations (**Fig.4.30**), indicating high competition between chain scission, branching/crosslinking, and grafting reactions. Nevertheless, the grafting degree decreased with increasing peroxide concentration and a similar trend was observed for all the different peroxides used, **Fig. 4.31**. This feature supports that the reactivity of DVB is very high in its reaction with GMA and PP macroradicals but the PP-DVB branching and crosslinking reactions are more dominant at higher peroxide concentrations resulting in a lower MFI (**Fig. 4.29**) and lower GMA grafting degree (**Fig. 4.31**). Comparing the GMA grafting degree DVB systems with the conventional system, see **Fig. 4.31**, it is clear that DVB has an enhancing effect on the GMA grafting reaction onto PP. It is very interesting to note that the GMA grafting degree for the different peroxides used is high and the difference between them is relatively small. Even with the peroxide BPO which has a short half-life time, it gives rise to a meaningful GMA grafting degree and this is due to the high rate of reaction in the DVB system (**Fig 4.31**). With 12 % GMA initially added, a maximum value of 1.2 % grafting degree was achieved by adding of 0.005 mr T-101 in the absence of DVB, whereas with a much lower T-101 concentration of only 0.001 mr in the presence of DVB, as high as 6.3 % grafting degree was measured; that is nearly a four times improvement. It is very clear that in the GMA/DVB system a

very low concentration of T-101 was needed to achieve high grafting degree and lower extent of side reactions.

iv. Effect of GMA Concentration on Grafting Level in Presence of Coagent

The effect of GMA concentration on torque behaviour and grafting reaction of PP/**DVB**/GMA/T-101 and PP/**TRIS**/GMA/T-101 system is shown in **Fig. 4.32** and **4.33**. The GMA grafting level increased significantly at higher initial GMA concentrations but without any adverse effect on the formation of poly-GMA (poly-GMA level stayed very low at all initial GMA concentrations used), see **Fig. 4.33**. As expected (a higher torque behaviour at DVB system, **Fig.4.32**) DVB resulted in a higher grafting level compared to TRIS.

v. Effect of Coagent Concentration on Grafting Degree

Figures 4.34 to **4.36** show the effect of coagent concentration (coagent/GMA weight ratio) on torque and GMA grafting behaviour. PP was processed with a fixed composition ([GMA]i = 12 wt %, [T-101] or [T-29B90] = 0.005 molar ratio to GMA+coagent) and conditions (temperature 180°C for T-101 and 160°C for T-29B90; 65 rpm, 10 min). It is interesting to compare the torque and melt temperature characteristics in the PP/GMA/coagent/T-101 systems which have a similar trend (**Fig. 4.34). Figure 3.35** shows that the higher the coagent concentration, the higher was the torque peak maximum and the higher the final melt temperature, indicating probability the extent of the GMA grafting reaction and the branching/crosslinking reactions. **Figure 4.35** also clearly shows that the grafting degree in the comonomer/T-101 systems increased monotonously with increasing coagent concentration. Whereas, in the DVB/T-29B90 system, the grafting degree increased initially with increasing DVB concentration but then leveled off with further increase in the coagent concentration (**Fig. 4.35**). This is probability because in presence of the peroxide T-29B90 the branching/cross linking reaction is more severe as shown by its higher torque max and final torque (see **Fig. 3.35**) and lower MFI values compared to the comonomers/T-101 system (see **Fig. 4.36**). **Figure 4.36** also shows that the aryl peak area index (711 cm^{-1}/2720 cm^{-1}) of the PP/DVB/GMA/T-101 system increased continuously by increasing the DVB concentration.

vi. Effect of Reaction Time on the Grafting Reactions

In order to investigate the kinetics of the GMA grafting reactions by thermal and peroxide (in presence or absence coagents system) initiation, a set of samples was prepared having a fixed composition ([GMA] 12 %, [coagent] = 2/8 weight ratio to GMA, [T-101] = 0.005 molar ratio to GMA or GMA+coagent) and similar processing conditions (temp 160°C, rotor speed 65 rpm). **Figure 4.37** shows that for the thermal initiation, the extent of both GMA grafting reaction and poly GMA formation is very low. In the conventional (absence of a coagent) system, the grafting reaction proceeds rapidly. However, in the presence of comonomers TRIS and DVB, the grafting reaction becomes faster. In the conventional system grafting initially increases gradually and the rate of homopolymerisation is much faster and increases rapidly during the first 2 minutes of processing but then decreases gradually with further processing time though overall remains higher than the amount of grafted-GMA level at end of the reaction (10 minutes). On the other hand, much less poly-GMA was formed compared with that of conventional system. In the presence either of the coagents the initial rate of grafting reaction is seen to be much faster and occurred with almost no homopolymer formation throughout the total processing time of 10 min. It is interesting to note that the grafting reaction in the TRIS system was faster compared with that with DVB system. **Figure 4.38** shows a further comparison of the GMA grafting kinetics illustrating that the grafting reaction, poly-GMA formation and chain scission reaction (as shown by as change in MFI) compete effectively during the first couple minutes of processing and the presence of comonomers TRIS or DVB completely change the GMA grafting kinetics. In the presence of comonomers, it seems that the grafting reaction dominated.

4.3. Discussion

4.3.1 Grafting vs. Side Reactions in the Absence of Coagents

In the melt grafting of GMA onto PP in the presence of peroxide, alongside the target free radical-initiated grafting reaction of GMA on PP, there are a number of other undesirable competing side reactions: homopolymerisation of GMA (poly-GMA) and radical-induced degradation reaction (chain scission) of PP (see **Rn-4.9**). The relative contribution of these reactions depends on both the chemical composition and the processing conditions; the main aim of the work described in this chapter was to optimise these conditions to increase

the level of target reaction at the expense of those unwanted side reactions. A major challenge in conducting monomer grafting experiments is to devise process conditions so as to minimize or control the aforementioned undesirable side reactions while at the same time maximising the grafting yield to achieve optimal product properties. GMA was melt processed with PP in the presence and absence of peroxides and the GMA-grafted polymer was characterised by FTIR before and after purification of the reaction products. It was demonstrated that GMA was successfully grafted on the polymer (examined after all unreacted GMA and poly-GMA removed first) confirmed by appearance of new absorption peak at 1732 cm^{-1} ascribed to the formation of saturated carbonyl ester, compared to the GMA unsaturated carbonyl appeared at 1720 cm^{-1} (the epoxide ring absorptions at 908 cm^{-1} and 843 cm^{-1} extend beyond the rocking absorption of the methyl group in the PP backbone, ρCH_3) (see **Fig. 4.7**) with the homopolymer of GMA (poly-GMA) forming alongside the grafting products.

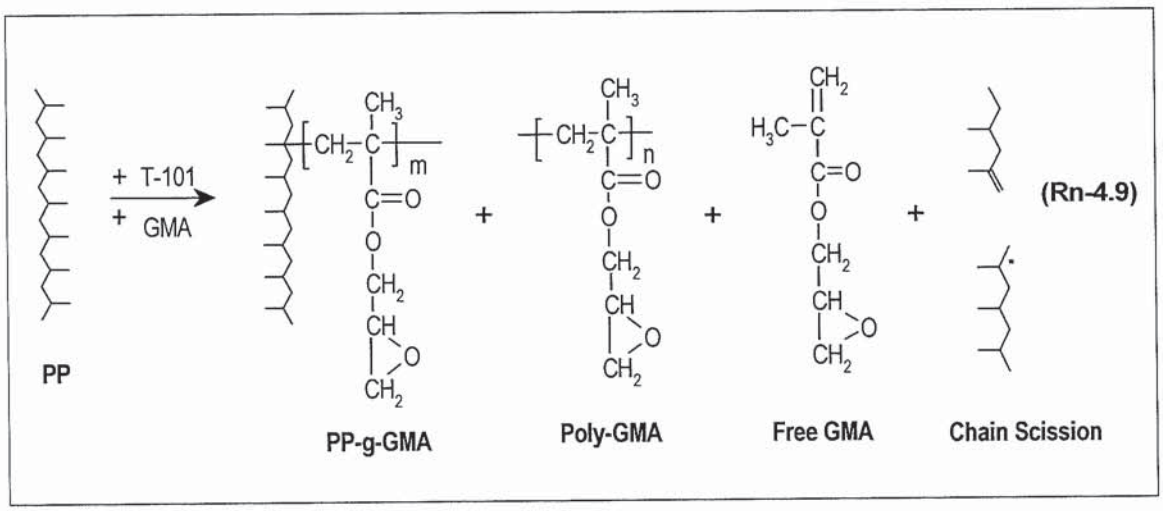

The results for the conventional grafting system of GMA on PP (free radical initiation but no-coagent) shows that homopolymerisation of GMA competes strongly with the desired grafting reaction resulting in higher concentration of the homopolymers compared to grafted-GMA and only at a lower processing temperature (<160°C) and lower peroxide concentration (<0.001 molar ratio to GMA ≅ 0.03 phr) could grafting degree exceeds the poly-GMA level (**Fig.4.14** and **4.15**). However, under such processing conditions, the grafting degree is very low (grafting efficiency only about 6 %), see **Fig. 4.15**. A further increase in temperature led to a sharp increase in the level of poly GMA with a decrease in the extent of grafting degree (see **Fig. 4.14**). At a high temperature of 200°C, for example,

poly GMA became 10 times higher whereas the grafting degree dropped by a factor of 4 than that achieved at lower temperature of 160°C . This observation is probability related to both the fact that homopolymerisation would be more favoured at higher temperatures and to the rate of decomposition of the peroxide at the different temperatures and a small amount of peroxide concentration used is not enough to generate initiating free radicals to produce enough PP macroradicals available for propagating the grafting reaction. When the peroxide concentration was increased five times to 0.005 mr (molar ratio to GMA, ≅ 0.15 phr), an increase in the extent of grafted-GMA resulted but was paralleled by an increase in the extent of poly GMA concentration **(Fig. 4.15)**. The overall GMA grafting degree remained low and poly GMA level stayed higher than the grafting degree particularly at higher GMA concentrations (**Fig. 4.19**). The results clearly show that high concentrations of GMA coupled with high processing temperatures makes the GMA homopolymerisation more favorable. This also reflects a lower GMA reactivity towards PP macroradicals giving rise to the observed low grafting levels. Furthermore, in the kinetic study for the grafting reaction of GMA (at 12%) onto PP, it was shown that the rate of homopolymerisation at the initial stage was faster than that of the grafting reaction **(Fig. 4.37)**. Besides the desired grafting reaction and undesired formation of poly GMA during the melt grafting, branching/crosslinking or chain scission reactions always accompany the grafting reaction and the extent of each would depend on the chemical structure of the polymer substrate. Literature studies on the melt grafting of GMA on PP revealed that the main polymer side reaction was that of chain scission, whereas in the case of PE, EPR, or EPDM, cross linking predominated resulting in low monomer grafting **[1,3,118-130]**. In this work, a high extent of chain scission in PP is clearly illustrated from the observed rapid increase in MFI at higher peroxide concentration used in the PP-GMA grafting system, see **Fig. 4.18**. Further examination of the behavior of the conventional peroxide-initiated GMA grafting system during the PP reactive processing step shows that, even at lower peroxide concentrations (0.001 molar ratio to GMA) much lower torque levels were observed compared to a control processed in the absence of a peroxide (see **Fig. 4.12**) and this is associated with lower polymer viscosity, indicating a higher extent of chain scission which supports the observed higher MFI values obtained (see **Fig. 4.18)** thus increased β-chain scission (MFI changes >300% in the first couple minutes of the melt grafting reaction, see **Fig.4.37**) (see **Rn-4.9**). **Scheme 4.5** illustrates the proposed mechanism of GMA grafting in the absence of coagent (conventional) system. In the GMA grafting reaction in the melt of

PP, two peroxides, T-101 and T-29B90, were used at range temperatures of 160-200°C. Both peroxides, Trigonox-101 and Trigonox-29B90, form *tert*-butoxyl radicals in the thermal decomposition **(Scheme 4.5, Rn-1)** (see also **Scheme 3.9** (p.126) and **3.10** (p.127)).

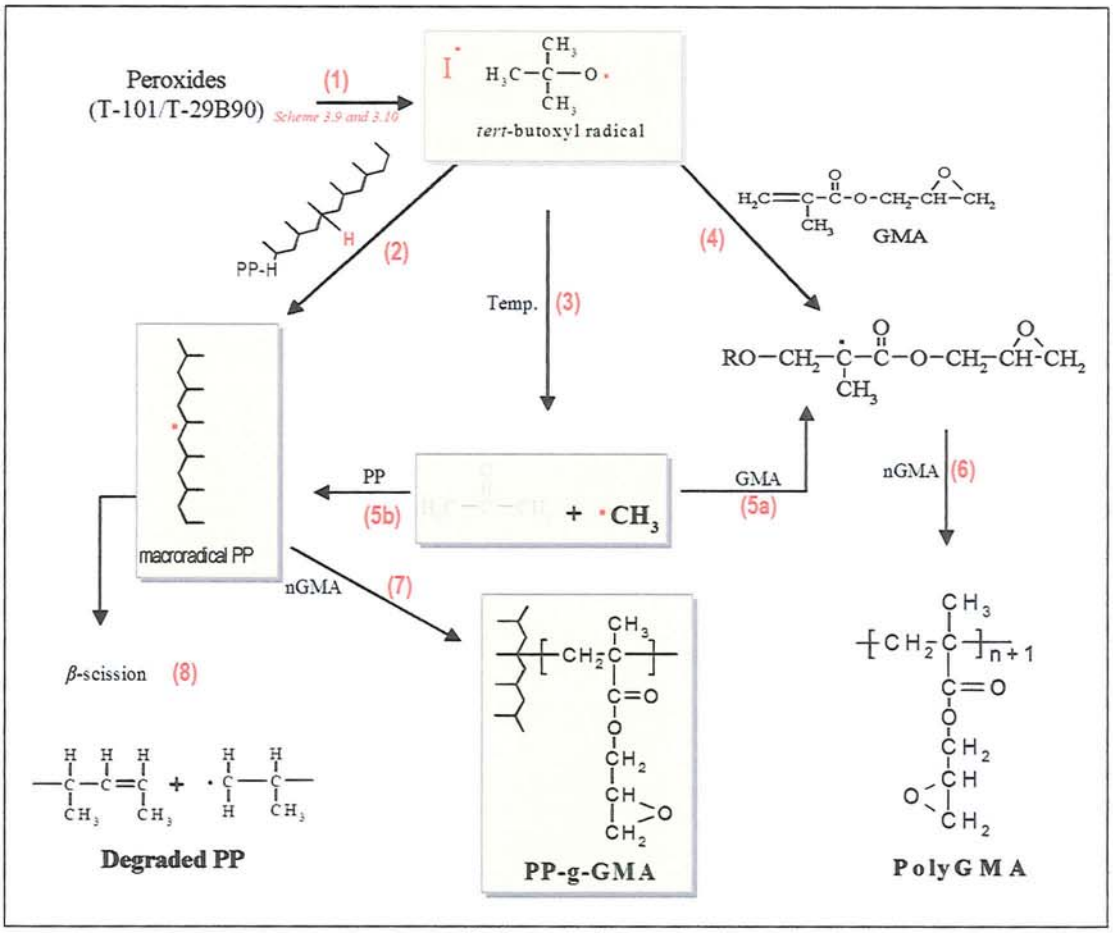

Scheme 4.5

Decomposition mechanisms of *tert*-butoxyl (includingT-101 and T-29B90) appear to be the preferred initiators for reactive processing experiments because they exhibit enhanced propensities for hydrogen atom abstraction compared to other primary radicals over the addition to monomer, which suggests that grafting could be competitive with unwanted homopolymerisation [55,64,69,71]. *β*-scission of the *tert*-butoxyl radicals which are produced from the peroxide initial decomposition gives rise to methyl radicals and acetone **(Scheme 4.5, Rn-3)**. Because the reactivity of the methyl radicals is such that they prefer addition to GMA (vinyl monomer) **(Scheme 4.5, Rn-5a)** rather than abstraction of a

hydrogen atom from the PP substrate (**Scheme 4.5, Rn-5b**), the grafting yield of GMA onto PP when using the peroxide Trigonox-101 is quite low and the degree of poly GMA was very high as shown in **Fig. 4.37**. It is worth noting that the β-scission reaction of *tert*-butoxyl radicals is strongly temperature dependent. Thus, higher reaction temperatures favour *tert*- butoxyl radicals undergoing β-scission (**Scheme 4.5, Rn-3**) over either H-abstraction of PP (**Scheme 4.5, Rn-2**) or addition to double bond of the monomer GMA (**Scheme 4.5, Rn-4**), and H-abstraction (**Scheme 4.5, Rn-2**) over addition (**Scheme 4.5, Rn-4**). Thus increasing the temperature from 160°C to 200°C had a profound effect on the GMA grafting kinetic resulting in both lower GMA grafting degree and poly GMA formation (**Fig. 4.14** and **4.18**).The initiator 1,1-di(*tert*-butylperoxy)-3,3,5-trimethyl cyclohexane (T-29B90) which has a shorter half-life time gave comparable grafting efficiencies and, more astonishingly, lower melt-flow indices than values observed when T-101 was used (**Fig. 4.18**). Abstraction of hydrogen atoms from C-H bonds of polypropylene (PP-H) produce PP macroradicals as initial centers for the grafting process (**Scheme 4.5, Rn-2**). The specificity of hydrogen atom abstraction has been shown to depend on a complex array of polar, steric and stereo electronic factors **[83]**. It is generally accepted that the degradation of PP proceeds only through β-scission according to reaction **(8)** in **Scheme 4.5**, see reaction below **[396]**.

The fragmentation reaction of PP chains by β-scission in the free radical (peroxide) initiation is only one of the complex reactions, which more or less prevails, depending on the reaction conditions. The decrease in the average molecular mass of PP, the increase MFI, will depend on the amount of PP macroradicals formed on the tertiary carbon, which are able to fragment into smaller polymer chains **[397]**. It is well established that the reactivity and specificity shown by initiator-derived radicals in abstraction and addition reactions depend strongly on the nature of the radicals and thus on the particular initiator **[398,399]**. The differences in the rates of decomposition of the various initiators are related to difference in the structures of the initiators and of the radicals produced. Both peroxides T-101 and T-29B90 breakdown independently to yield a variety of alkoxy and alkyl radicals as shown in **Scheme 3.9** and **3.10** in **Chapter 3**. *Tert*-butoxyl radicals have a propensity for hydrogen atom abstraction and this tendency is enhanced at higher

temperatures. As shown in **Scheme 3.9** (p.126) the breakdown of a T-29B90 molecule gives a lower-reactive (3,3,5-trimethyl-cyclohexana)-1,1-di-oxyl) radical, and two *tert*-butoxyl ($\cdot OC(CH_3)_3$) radicals, which, during fragmentation, produce methyl reactive radicals ($\cdot CH_3$) The decomposition of Trigonox-101, 2,5-di(*tert*-butylperoxy)-1,5-dimethyl hexane **(1)**, however, is more complex because the alkoxyl radical intermediate cleaves further to give preferentially the higher alkyl radicals preferentially (rather than a methyl radical) **[65,83]**. If not trapped by reaction with the substrate, the initially formed alkoxyl radicals would undergo β-scission with preferential cleavage of the weakest C–C bond. The formed intermediate peroxides, 2,5-dimethyl-2-hydroxy-5-(*tert*-butylperoxy)hexane **(2)** and *tert*-amyl-*tert*-butyl peroxide **(3)** in **Scheme 3.10** (p.127), are labile and undergo further decomposition with half-life time of the same order of magnitude to that of Trigonox-101 (**1**) and give rise to methyl radical products **[103]**. It has been noted by several authors **[1]** that, based purely on a consideration of bond dissociation energies, methyl and alkoxy radicals should be equally proficient at hydrogen atom abstraction (the reactions are similarly exothermic). However, it should also be pointed out that C–CH_3 bonds are significantly stronger than C–OR bonds. Thus, whereas alkoxyl radicals have a propensity for hydrogen atom abstraction, methyl radicals prefer to add to double bonds. This tendency is greater for higher alkyl radicals. The alkyl radical formed in the decomposition of T-101 has a low reactivity for transfer reaction with PP is effective in a termination reaction with polymeric radicals. This reaction decreases the probability of the fragmentation of polymer radicals. The lower reactivity of alkyl radicals in the transfer reaction with PP will be reflected in the possibility of greater diffusion of alkyl radicals from the original cage which finally leads to a greater distance between the PP macroradical and the second alkyl radical. This fact suppresses the termination of the new radical pair and thus supports the fragmentation of the PP macroradical. The degradation efficiency was markedly influenced by the reaction temperature which controlled the macroradical fragmentation and intermolecular radical transfer reactions. As a result, poly GMA formation (**Scheme 4.5, Rn-6**) when using Trigonox-101 is higher, and GMA grafted level (**Scheme 4.5, Rn-7**) is slightly lower than that of Trigonox-29B90. This is probability because of different competing reactions of the alkyl, methyl and alkoxyl radical in H-abstraction PP-chain (**Scheme 4.5, Rn-2**) and β- scission of the alkoxyl radicals (**Scheme 4.5, Rn-3**), and addition alkyl radical to the monomer double bond (**Scheme 4.5, Rn-4**).

The comparison of the local concentration of free radicals after the chain transfer reaction from methyl and *tert*-butoxyl radicals gives a difference of about two orders of magnitude, which is significant for the competition, between bimolecular-termination and monomolecular-fragmentations. The ratio between spontaneous and induced decomposition reactions depends on the concentration of peroxide. These differences between the properties of primary radicals will be reflected in the formation of a pair vicinity in the case of T-29B90; this will support the production of cross links between macromolecules. The differences grafting reaction efficiency between T-101 and T-29B90 follows not only the reactivity of primary radicals of peroxide but also kinetical parameters and physical factors like solubility and diffusion rate play an important role. The influence of the greater reactivity of primary peroxide radicals on the grafting efficiency and PP fragmentation can be also accounted for as a result of smaller selectivity of the attack on a PP chain. This can lead to a larger formation of primary and secondary alkyl radical and so increase the proportion of recombination and disproportion towards a fragmentation reaction.

4.3.2 Effect of Coagents TRIS and DVB on Grafting Reaction

The above discussion highlighted the problems of low overall grafting efficiency; hence the low conversion of GMA to grafted-GMA in PP, and the fact that a much higher peroxide concentration is needed to achieve higher conversion rates but this would only occur at the expense of severe degradation of the polymer, and the formation of high levels of GMA homopolymer. The idea of grafting the monomer GMA on PP in the presence of a coagent such as TRIS and DVB is based on two assumptions: (a) the coagent has to be more reactive towards the PP macroradical than the monomer GMA, and (b) the coagent should have a high efficiency towards copolymerisation with GMA. However, the presence of a reactive comonomer (coagent) in the GMA grafting system results in a number of additional side reactions involving the coagents in addition to the formation of poly-GMA. These reactions include the formation of ungrafted copolymer of DVB or TRIS and GMA (GMA-co-DVB) or (GMA-co-TRIS) as well as the formation of homopolymer of the coagent (poly-DVB or poly-TRIS), together with possible polymer coagent-assisted crosslinking reaction that may occur via reaction of the reactive functions of the coagents with the PP macroradicals (see **Rn-4.10** and **Rn-4.11**). The results however, show clearly that the use of a coagent (e.g. DVB) leads to a significant improvement in the grafting

efficiency of GMA on PP and that higher level of grafting can be achieved at much lower peroxide concentrations (see **Fig. 4.31**).

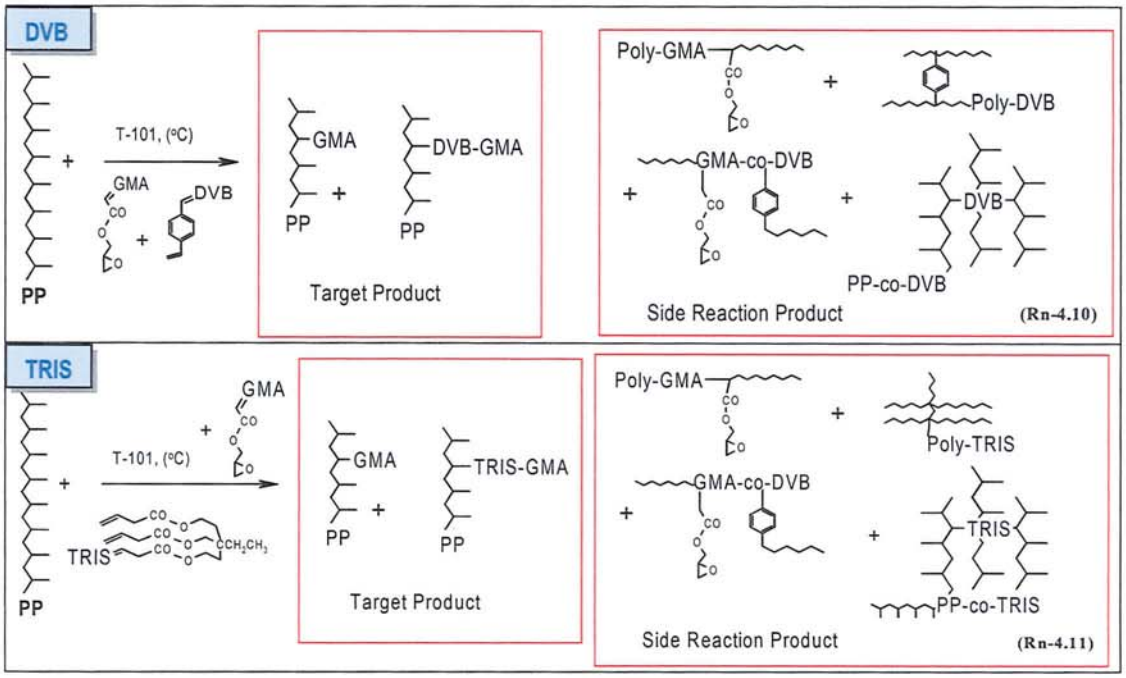

One of the important features of grafting GMA onto PP in the presence of coagent is that a very small amount of peroxides is required at a fixed concentration of the coagent. For example, when GMA concentration was fixed at 12 % w/w and the coagent concentration, e.g. DVB:GMA was 2:8 w/w % (≅ 3.4 phr), it was shown that the use of only 0.001 mr (molar ratio to GMA+DVB or ≅ 0.04 phr) of peroxide was enough to achieve 5-7 % grafting degree (40-60 % grafting efficiency), see **Fig. 4.31**. This clearly contrasts the case of GMA grafting degree in the conventional (in absence of coagent) system, which result in only 0.3-0.7 % grafting degree (grafting efficiency of 3-6 %). A further increase in peroxide concentration did not give rise to an increase in the GMA grafting degree (see **Fig. 4.31**) but the MFI of the processed PP decreased continuously indicating a more branching/crosslinking reaction of PP with this coagent (DVB) (see **Fig.4.29**). This phenomenon can be understood since the high reactivity of poly functional coagents give rise to their action as linkers, i.e. to facilitate the linking (grafting) of the monomer onto the polymer, but at the same time, if the peroxide concentration is high enough they could result in branching/cross linking of the polymer chains (PP-DVB-PP or PP-TRIS-PP), see **Rn-4.10** and **Rn-4.11 [97]**. The optimal grafting in the presence of DVB can therefore be achieved with a delicate balance between the molar ratio of the reagents (monomer,

coagent, and initiator) and the processing conditions (e.g. temperature and mixing time) [1,3,129].

4.3.3 The Mechanism of GMA-Grafting on PP in the Absence of Coagents

In a melt free radical grafting process, the monomer of interest undergoes not only grafting but also polymerisation. The thermodynamic characteristics (ΔG, ΔH, ΔS) of polymerisation are important for an understanding of the effect of monomer structure on its polymerisation [407,408]. Grafting GMA onto PP is an exothermic (negative ΔH) process and exoentropic (negative ΔS). The exothermic nature of the graft copolymerisation arises because the process involves the exothermic conversion of a π-bond in the monomer (GMA) and comonomer (TRIS or DVB) molecules into σ-bonds in the polymer. The negative ΔS for grafting copolymerisation arises from the decreased degree of freedom (randomness) for the polymer relative to the monomer. Thus, homopolymerisation and copolymerisation of the monomer and comonomers are favourable from an enthalpy viewpoint but unfavourable from the entropy viewpoint [407].

$$\Delta G^\circ = \Delta H^\circ - T\Delta S^\circ = -RT\,ln\,K \qquad \textbf{(Eq. 4.1)}$$

For most grafting copolymerisations there is some *ceiling temperature* (*Tc*) at which the reaction becomes a reversible that is there is a propagation-depropagation equilibrium, which is given by

$$M_n\cdot + M \underset{k_{dp}}{\overset{k_p}{\rightleftharpoons}} M_{n+1}\cdot \qquad \textbf{(Eq. 4.2)}$$

The equilibrium constant is defined by k_p/k_{dp}, or

$$K = \frac{[M_{n+1}\cdot]}{[M_n\cdot]\,[M]} = \frac{1}{[M]} \qquad \textbf{(Eq. 4.3)}$$

For an equilibrium situation ΔG = 0, the equilibrium constant is defined by $k_p/k_{dp} = 1/[M]$, so,

$$T_c = \frac{\Delta H^\circ}{\Delta S^\circ} = \frac{\Delta H^\circ}{\Delta S^\circ_p + R\ln[M]_c} \qquad \textbf{(Eq. 4.4)}$$

or

$$ln\,[M]_c = \frac{\Delta H^\circ}{RT_c} - \frac{\Delta S^\circ}{R} \qquad \textbf{(Eq. 4.5)}$$

Equation 4.5 shows the equilibrium monomer concentration $[M]_c$ as a function of the reaction or ceiling temperature T_c. Since $\Delta H°$ is a negative quantity, the monomer concentration in equilibrium with the polymer increases with increasing temperature, that is, a plot of $[M]_c$ versus 1/T is linear with a negative slope of $\Delta H°/R$ and intercept of $-\Delta S°/R$. This means that there is a series of ceiling temperatures corresponding to different equilibrium monomer concentrations **[99,407]**. A quantitative discussion of grafting of methacrylates is best approach by considering the grafting of methyl methacrylates for which relevant rate constants at low temperatures are generally available **[63-65,68]**. Homopolymerisation occurs at the same time as grafting and the grafts were thought to be polymer chains. Grafting is initiated in the usual way by hydrogen atom abstraction from hydrogen atom substrate using *tert*-butoxyl radicals from the initiator. For the grafting of 0.1 M methyl methacrylate to eicosane or PE at 160°C in the presence of 0.05 M di-*tert*-butyl peroxide, few of the alkoxyl radicals add to the monomer and the competition is again between hydrogen atom abstraction from substrate and β-scission of the radical **[65]**. A considerable proportion of the methyl radicals formed by β-scission add to the monomer to initiate homopolymerisation. The rest largely react with the substrate and thus contribute to initiation of the grafting process. At lower temperatures, the radicals resulting from methyl addition to monomer would propagate to form homopolymer. The kinetic chain length for the homopolymerisation is relatively high at low initiation rates and high proportion of the reacting monomer is converted to homopolymer. As the temperature is raised and initiation rate increases, the kinetic chain length decreases but considerable fractions of poly(methyl methacrylate) would still be formed. Russel *et al.* **[70]** attempted to study the detailed reaction kinetics of the grafting and the homopolymerisation reaction. It was found that both grafting and homopolymerisation showed a half order dependence on initiator concentration at 130-160°C, a result typical of a chain reaction in which radicals disappear in pairs.

4.3.4 The Mechanisms of GMA-Grafting on PP in the Presence of Coagents

In order to maximise the monomer grafting reaction and minimise the side reactions, it is important that the radicals formed during initiation (polymer macroradicals, monomer radicals, and alkoxyl and methyl radicals) are trapped as rapidly as possible. Some monomers are more effective than others in trapping such radicals **[41,58]**. This may arise

because of the relative solubility of the monomers in the polymer melt or it may be due to the inherent reactivity of the monomers. One strategy involves choosing a monomer combination whereby the comonomer is both effective in trapping the radicals formed on the polymer backbone and that the propagating radical formed is highly reactive towards the desired monomer **[1]**. The incorporation of a small concentration of the highly reactive comonomers (coagents) TRIS or DVB in the GMA-grafting system has been shown here to bring about important changes dominated by: a clear improvement in the grafting yield, which is achieved at a faster rate, a substantial reduction in the main competing side reactions, namely the GMA homopolymerisation and polymer chain scission or cross linking. First of all, the high reactivity of TRIS and DVB towards PP macroradicals (in the absence of GMA) was clearly illustrated from the distinct torque behaviour during the reactive processing (see **Fig. 4.20** and **4.39**). The presence of the coagents resulted in a torque peak under both shear-initiation (without peroxide) and free radical-initiation (in the presence of a peroxide) indicating the occurrence of reaction which leads to an increase in polymer melt viscosity due to a higher crosslinking as indicated by a lower MFI (see **Fig. 4.27A**). The much faster rate of formation of the torque peak (i.e. faster rate of reaction) under the free radical initiated condition (see **Fig. 4.38**) indicates that both TRIS and DVB give rise to both grafting and branching reactions, with the polymer which are kinetically favourable compared to their absence. It is important to point out that TRIS and DVB are more highly reactive towards macroradicals when compared to GMA. Another fact is that the high reactivity of the coagents towards GMA was demonstrated **[129,130]** by the formation of copolymer of the coagent with GMA in the grafting process on other polymers. As a result of the high coagent reactivity, DVB or TRIS would be expected to first graft onto the polymer chains and then the GMA would react with the grafted DVB. This process may be similar to the enhancing effect described for styrene on the grafting of GMA onto PP **[123]**, PE **[126]** and EPR **[128]**. The kinetics of the GMA grafting reactions in PP/GMA/coagent/peroxide system was examined by taking out samples at different time intervals during the reactive processing followed by purification and analysis to determine the extent of the target and side reactions. The results (see **Fig. 4.37** and **4.38**) reveal that the rate of GMA grafting is much higher in the presence of the coagents TRIS or DVB when compared to their absence. It is also clear that the presence of both coagents results in almost a complete disappearance of the poly-GMA and also gives rise to a low extent of PP chain scission (in the case of TRIS) as shown by a lower MFI (compared to the absence of

coagent) or even promotes coagent-assisted branching/cross linking reaction (in the case of DVB) resulting in a slightly lower MFI compared to virgin PP. It is interesting to evaluate the difference in GMA grafting kinetic between GMA/TRIS and GMA/DVB systems as shown in **Fig. 4.38**. Almost 100 % of the GMA grafting onto PP in the TRIS system was achieved during the first two minutes of processing whereas, for the same time in the GMA/DVB system, the grafted-GMA onto PP was less than 40 %. It is also worth noting that their MFI characteristic differ in opposite ways. The MFI of the processed PP in the GMA/DVB system decreased with processing time up to 70 % less than that of the virgin PP indicating a severe branching/crosslinking reaction (see **Fig. 4.38**). This fact supports the suggestion that DVB is more reactive towards PP macroradicals and this occurs before the copolymerisation with GMA. In contrast, in the GMA/TRIS system, TRIS is more reactive towards GMA and copolymerises with GMA before causing TRIS assisted PP cross linking. As shown in **Fig. 4.20, 4.21, 4.28, 4.32, 4.35,** and **4.39** the torque maximum and final torque in the DVB/T-101 system are higher than that in the TRIS/T-101 system indicating a more intense branching/cross-linking reaction in the initial stages of processing (see **Section 5.3.6** (p.284) for further discussion about the reactivity of DVB and TRIS). In the absence of a coagent, the poly-GMA concentration builds up to a maximum at the early stages of the melt reaction but, subsequently, decreased to a lower concentration on further processing. In contrast, in the presence of coagents, although the concentration of poly-GMA is very small, its formation actually increases with processing time to maximum value of only 0.1 %. This may suggest that the very small concentration of poly-GMA formed in the presence of a coagent has a higher molar mass and is more stable for the duration of the grafting reaction whereas the poly GMA formed in the absence of a coagent at the initial stages of the reaction is of a lower molar mass and is relatively unstable thus, undergoes depropagation leading to a reduction in its final concentration in the polymer at the end of the processing (**Fig. 4.37**). **Schemes 4.6** and **4.7** illustrate the proposed mechanism of GMA grafting in the presence of DVB and TRIS, respectively. At the initiation stage, the alkoxyl radicals formed by decomposition of the initiator (**Scheme 4.6** and **4.7, Rn-1**) are particularly very reactive in abstraction of a hydrogen atom from PP (**Scheme 4.6** and **4.7, Rn-3**). There are, however, competing reactions which involving β-scission of the alkoxyl radical decomposition to give methyl radicals (**Scheme 4.6** and **4.7, Rn-2**). The second competing reaction is the addition of *tert*-butoxyl radicals to GMA (**Scheme 4.6** and **4.7, Rn-4**) and coagent (**Scheme 4.6** and **4.7, Rn-5**). Rate constants for

this process are relatively low and at the low monomer concentrations typically used in grafting and the addition reaction of *tert*-butoxyl radicals to to vinyl monomer GMA (**Scheme 4.6** and **4.7, Rn-4**) and coagent (**Scheme 4.6** and **4.7, Rn-5**) can be neglected [3]. So, the main primary products from the reaction mixture in the initiation stage are PP$^{\bullet}$ macroradicals, adducts of a methyl radical, the vinyl monomers (GMA and coagent).

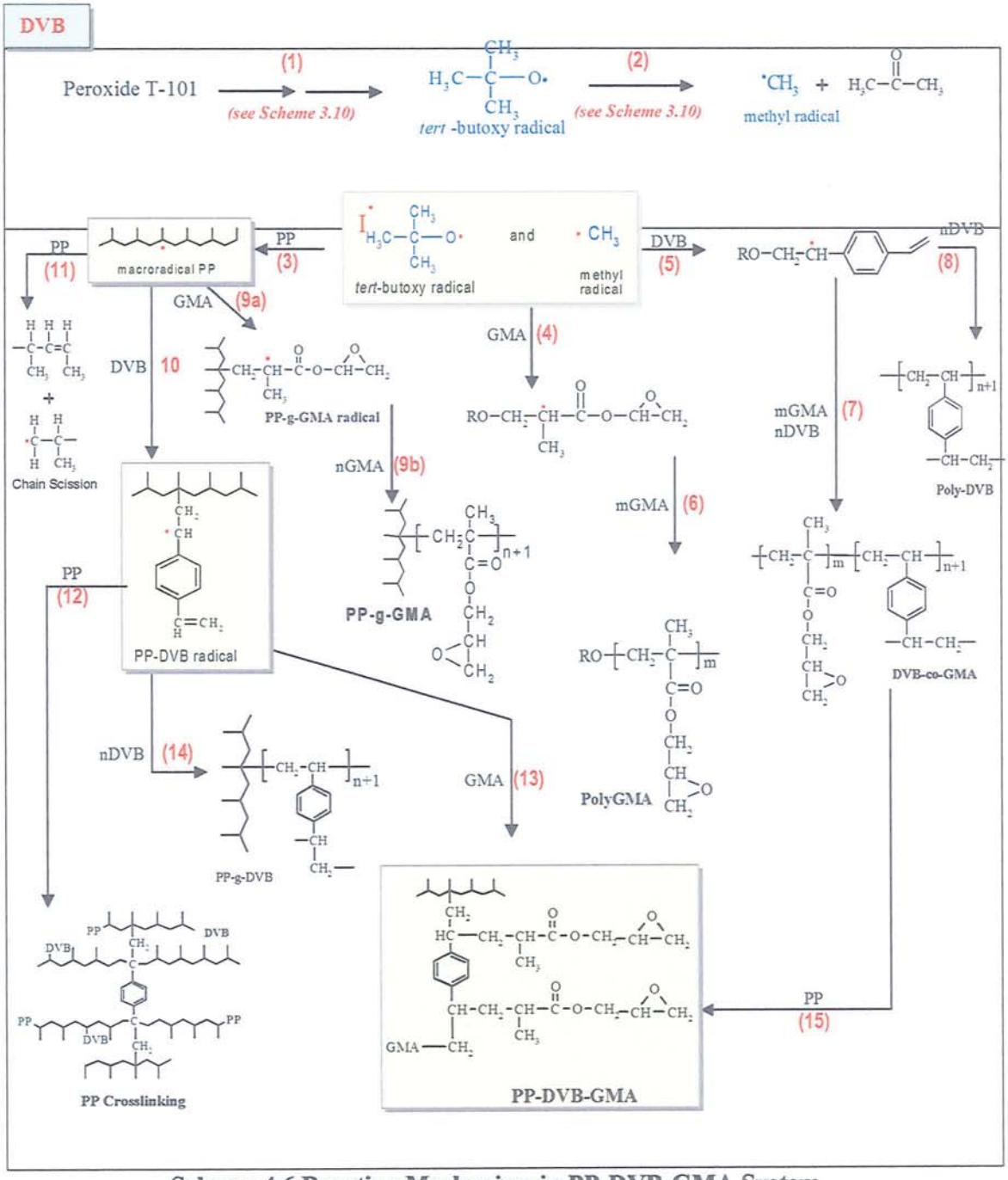

Scheme 4.6 Reaction Mechanism in PP-DVB-GMA System

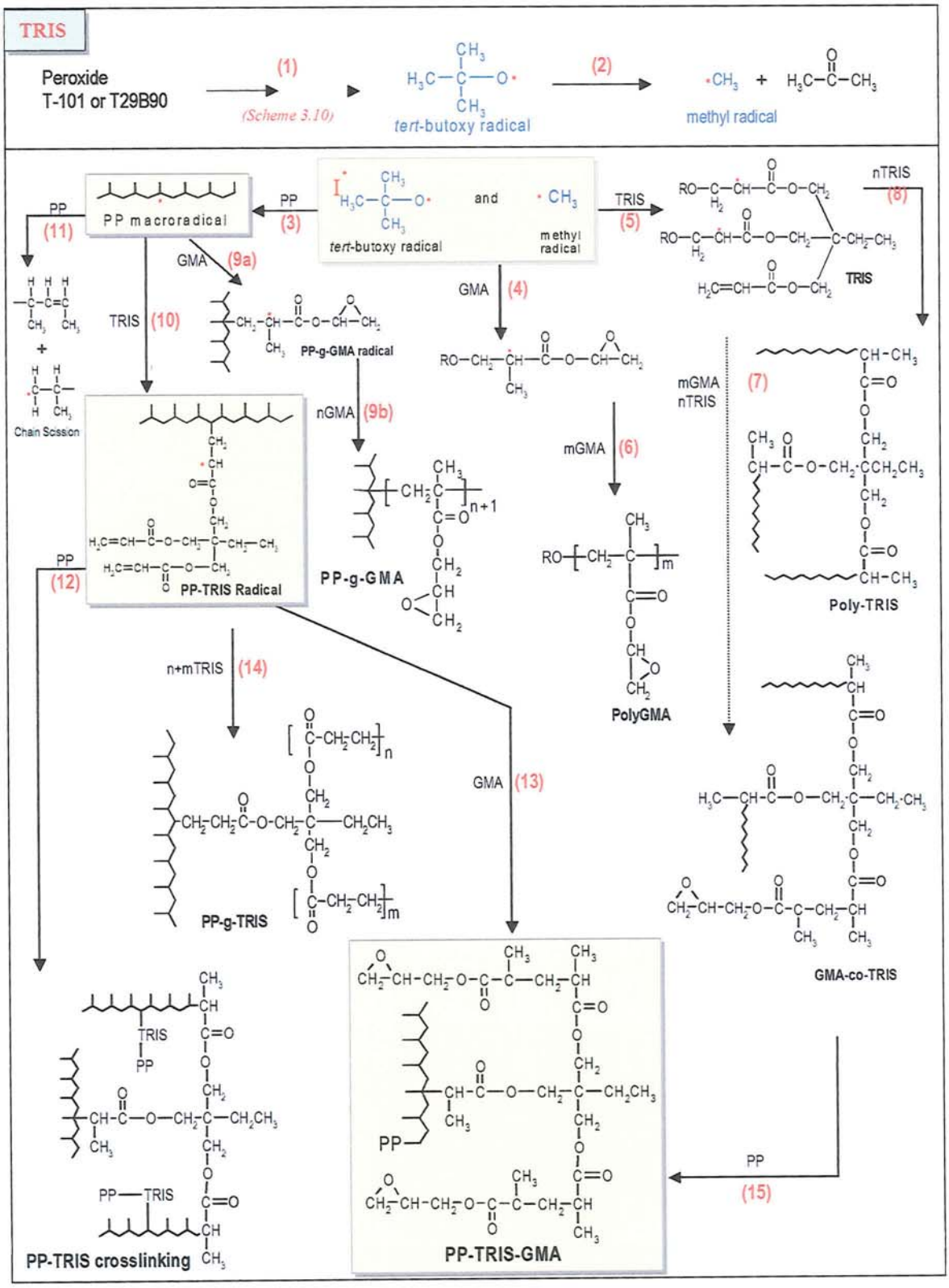

Scheme 4.7 Reaction Mechanism in PP-TRIS-GMA

Under the grafting conditions used in the presence of the coagent, kinetic data of the reaction indicated that GMA grafting on PP occurred at a high rate, see **Fig. 4.37**. The grafting reactions begun with the addition reaction of vinyl monomers, GMA (see **Scheme 4.6** and **4.7, Rn-9a)** and DVB (see **Scheme 4.6, Rn-10)** or TRIS (see **Scheme 4.7, Rn-10**) onto PP• macroradicals or methyl radicals. Rate constant for the addition reaction involving PP• macroradicals and methyl radicals are not directly available but can be roughly estimated from the reactivity ratio (r_1) of the monomers in free radical polymerisation. Addition of GMA or DVB on PP• yields the radical PP-GMA• or PP-DVB• that can add to the monomer and thus increase the graft size or it may react with PP-H giving a graft consisting of a single monomer unit. The radicals CH_3-GMA• and CH_3-DVB• or CH_3-TRIS• formed by methyl radical attack on GMA (see **Scheme 4.6** and **4.7, Rn-4**) and coagents DVB or TRIS (see **Scheme 4.6** and **4.7, Rn-5**) can continue addition to the monomer (see **Scheme 4.6** and **4.7, Rn-6**) and the coagents (see **Scheme 4.6** and **4.7, Rn-8**) and in principle can go on to form poly-GMA or poly-DVB or poly TRIS. Because of the lower reactivity of GMA (compared to DVB), the main products in the first propagation stage would be PP-DVB• or PP-TRIS• and CH_3-DVB• or CH_3-TRIS• (various factor determine the reactivity of the monomer and comonomer will be discussed in **Section 5.3.5** (p.279) and **5.3.6** (p.284) in **Chapter 5**). Due to the high reactivity of DVB and TRIS towards the PP• macroradical (**Scheme 4.6** and **4.7, Rn-10**) and towards GMA (**Scheme 4.6** and **4.7, Rn-7**), the DVB- or TRIS-containing branched macroradical PP (**Scheme 4.6** and **4.7, Rn-12**) and the PP-DVB- or PP-TRIS-containing branched GMA (**Scheme 4.6** and **4.7, Rn-13**) are rapidly formed at the onset of the melt processing operation. As expected, the 'free' GMA-co-DVB or GMA-co-TRIS copolymer could also bond to the PP (**Scheme 4.6** and **4.7, Rn-15**). However, the experimental evidence presented shows that there was no 'free' copolymer (after purification of the grafted polymer product) at the end of grafting reaction. This reaction occurred during the initial stages of the grafting process, probability to a small extent, but the propagating GMA-co-DVB or GMA-co-TRIS copolymer radicals (**Scheme 4.6** and **4.7, Rn-7**) would further react, on further processing (**Scheme 4.6** and **4.7, Rn-15**), with PP macroradicals, a DVB containing branched radical giving rise to further PP-DVB-GMA or PP-TRIS-GMA grafting. The initiation and propagation reactions described above give rise to a wide variety of radicals and the number of possible

termination reactions is very large. The idea of functionalisation of PP with GMA in the presence of a comonomer TRIS or DVB is based on two assumptions: (i) The double bonds of the comonomer will react with tertiary PP macroradical and so suppress the fragmentation reaction. (ii) The double bond of the comonomers will hinder chain scission of PP macroradical. As found experimentally, the fragmentation reaction was completely eliminated because of the radical formed in the bonded comonomers to the PP chain can also recombine with another macroradical and so create, step by step, a crosslinked structure by connecting neighbour macromolecules. For example, at the cross linking of PP with TRIS, the coagent can contribute to the formation of cross links as shown in the **Rn-12** in **Scheme 4.6** and **4.7**.

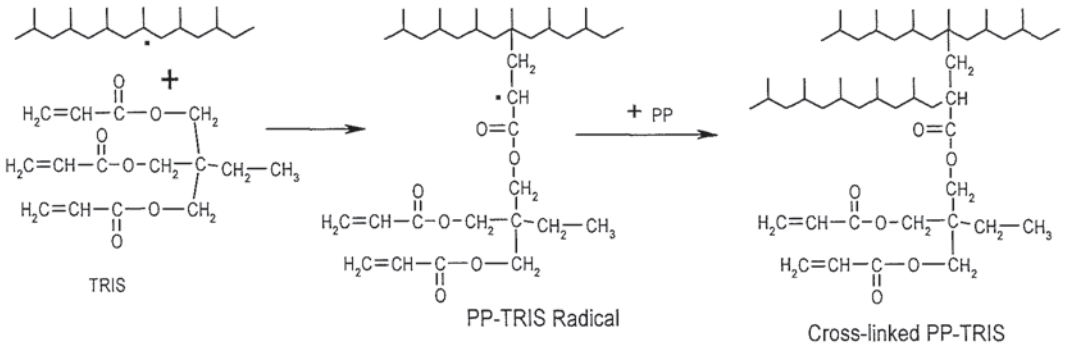

In this case of TRIS and DVB, chain transfer reaction radicals can be formed on the polyfunctional monomers bonded to the PP chain. They are a very effective means for the trapping of another PP radical and the creation of new crosslinked PP-TRIS-PP or PP-DVB-PP. Residual double bonds from alkyl radical can still be used for the grafting formation of another crosslink between PP-chains or for grafting with GMA in the PP/comonomer/ GMA/T-101 system. **Figure 4.20** shows that in PP/TRIS/T-101 or PP/DVB/T-101 ([coagent] 3 phr, in the absence of GMA) system yield mainly crosslinked products as shown by higher final torque and torque maximum compared that of PP/GMA/T-101 (in the absence of coagent) and PP/T-101 (as control). Thus a combination of macroradicals PP-TRIS• or PP-DVB• is an important termination process. Addition of GMA and the coagent results in the formation of coagent-monomer radicals and the combination with PP• macroradical also terminates the reaction process (**Scheme 4.6** and **4.7,** Route **Rn-7** and **Rn-15**, Route **Rn-10** and **Rn-12**). The melt index of the grafted product in the DVB system (PP+DVB+GMA+T101) decreased rapidly as the reaction proceeded (**Fig. 4.38**) indicating that these steps are important. Kinetic analysis of the

grafting reactions in the coagent system is complicated by the presence of a second phase, i.e. the homopolymerisation of GMA (**Scheme 4.6** and **4.7, Rn-6**) and of the coagents TRIS or DVB (**Scheme 4.6** and **4.7, Rn-8**) and the copolymerisation of the coagent with GMA which may not become completely bonded to the polymer. This problem can be minimised by using low concentrations of peroxide and coagent with high concentrations of monomer GMA. It is very clear in the PP/GMA/DVB/T-101 system, for example, that an increasing concentration of coagent DVB:GMA to 3/7 wr (weight ratio to GMA) results an intolerable extent of branching/crosslinking of PP-DVB **(Scheme 4.6** and **4.7, Rn-12**) as shown by a very low MFI (**Fig. 4.36**).

4.3.5 Initiator Efficiency *(f)*

In this work, the use of a short half-life initiator, T-29B90, resulted in higher grafting yield and less side reactions (poly-GMA formation and PP degradation) compared to that of T-101 (see **Fig. 4.19**). It is concomitance with the previous work when T-29B90 was used in grafting EPR with GMA [**134**] as well as results of this work of GMA grafting on NR at low temperature (<160°C) (see **Fig 3.35** in **Chapter 3**, p.158). As described in **Section 1.2.3** (p.25) there are several factors that affect the *initiator effectiveness* (*f*) for grafting of a monomer to a polymer substrate, i.e. (1) the initiator half-life, (2) the reactivity and specificity of initiator-derived radicals towards polyolefin and monomer, (3) structure of the initiator, (4) the initiator concentration, (4) the initiator solubility and its diffusion coefficient, and (5) the extent of cage reaction. In this work, the type of peroxides (T-101, T-29B90, DCP, BPO) on the PP modification with GMA has an important role, not only the level of the grafting but also of the fragmentation of PP chain. It was found that the grafting degree in the peroxide T-101 (conventional) system decreased steeply by raising the temperatures but the change in molecular weight (MFI) was not significant (see **Fig. 4.18**). Dissimilar result was observed when the peroxide concentration was increased from 0.001- 0.005 (molar ratio to GMA), a much higher MFI was observed but the grafting degree levelled off (**Fig. 4.18**). Despite what has been discussed in terms of the competition between the grafting and side reaction in the case of two peroxides, one more point remains difficult to understand as to why would high peroxide concentration result in a negative effect on the grafting level, especially with the peroxide that has shorter half-life time (T-29B90). The influence of peroxide concentration on the grafting reaction of PP at the

constant temperature is generally positive. Hence, the higher the peroxide concentration, the larger the quantity of primary radicals formed and, consequently, the higher the concentration of macroradicals available for the reaction with the GMA. Thus, as a result there will be a higher level of grafting. However, when the molar ratio of T-29B90 (to GMA) was increased from 0.001 to 0.01 (ten times higher) the GMA grafting degree levelled off. It is probability because the efficiency of the peroxide (*f*) becomes lower at high initiator concentrations. The *initiator efficiency* (*f*) is defined as the fraction of radicals formed in the primary step of initiator decomposition, which are successful in initiating the grafting reaction. Some of the radicals formed in the primary decomposition step undergo reactions to form neutral molecules instead of initiating grafting reaction. The rate of producing primary radical by thermal homolysis (R_d) is given by **[83,408]**

$$R_d = 2.f.k_d.[I] \qquad \textbf{(Eq.4.6)}$$

where [I] is the concentration of initiator and k_d is the rate of decomposition of the peroxide. In most polymerisation and copolymerisations the rate of (co)polymerisation is given by **[408,409]**

$$R_p = k_p [M] \left(\frac{f k_d [I]}{k_t} \right)^{1/2} \qquad \textbf{(Eq.4.7)}$$

Similarly with the polymerisation and copolymerisation, **Eq. 4.7** shows the grafting rate by free radical initiation to be dependent on the square root of the initiator concentration. Doubling the peroxide concentration does not double the grafting level. This dependence has been abundantly confirmed for many different monomer-initiator combinations over wide range of monomer and initiator concentration **[181-187,410]**. The decreasing of GMA grafting degree with a higher peroxide concentration in the absence (see **Fig. 4.18)** and the presence of coagent DVB (**Fig. 4.31**) may be due to a decrease in *initiator efficiency* (*f*) with increasing initiator concentration. Under typical grafting conditions, i.e. high temperature and low monomer concentration, the kinetic chain length for homopolymerisation is much lower and there is a further restriction of chain growth of poly-GMA due to low ceiling temperatures. It was shown **[119,132]** that chain scission in PP may occur simultaneously with the graft reaction. The wastage of initiator is more likely due to induced decomposition or chain transfer to initiator (see **Scheme 4.8, Rn-3** to **Rn-5**)

and involvement of the radical formed in the primary step of initiator decomposition in other side reaction. Alternately, the termination mode may change from the normal bimolecular termination between propagating radicals to *primary termination*, which involves propagating radicals reacting with primary radicals [63]. The lower efficiency of initiators would also occur because the high concentration of primary radicals to be completely and rapidly scavenged by monomer (**Scheme 4.8, Rn-6** and **Rn-7**) which would lead further to homopolymerisation reaction. This is probability due to the inefficiency initiator T-29B90 at high peroxide concentration which results in high concentration of unreacted GMA (free-GMA) > poly-GMA>grafted-GMA (see **Fig. 4.16**).

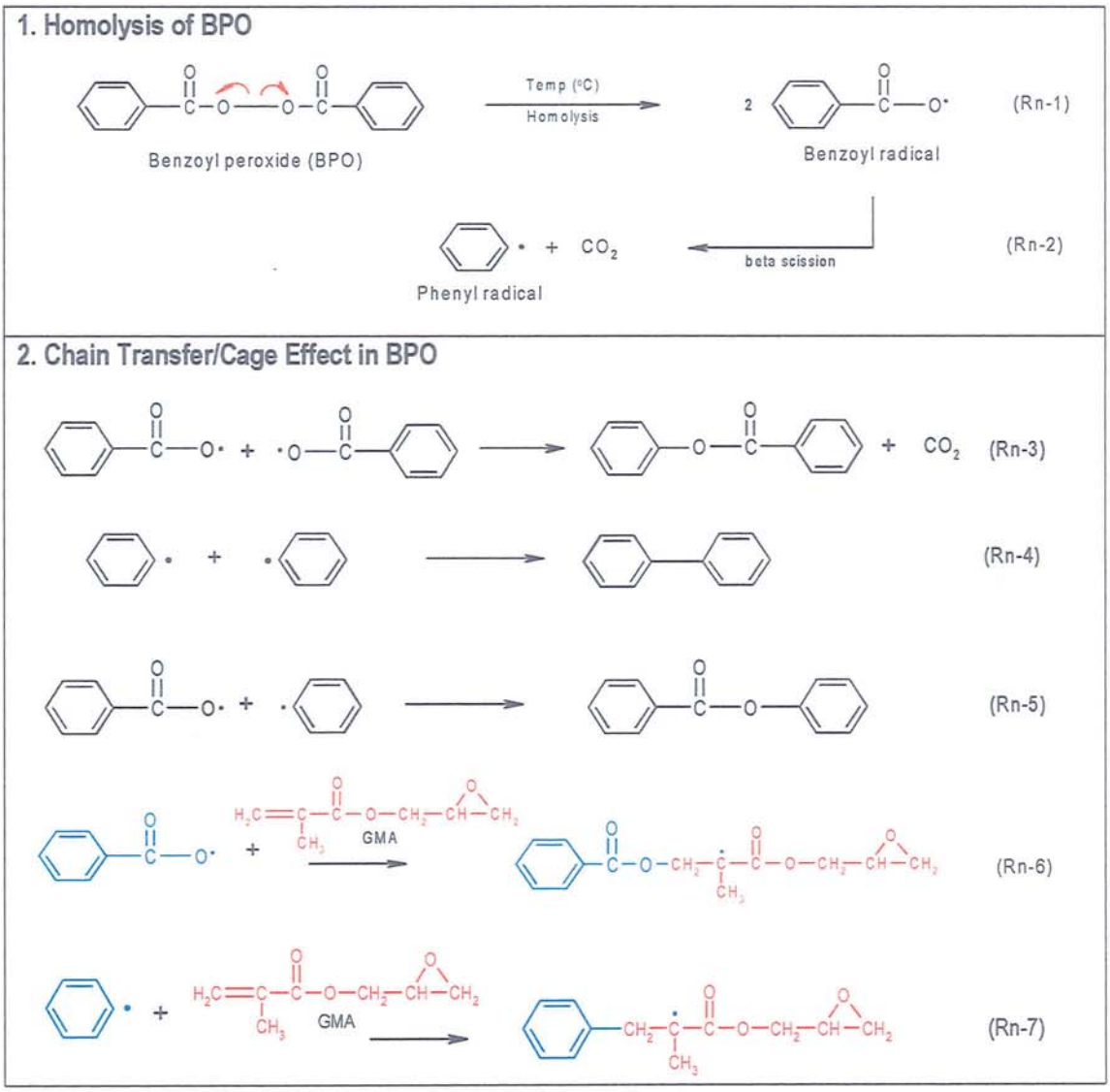

Scheme 4.8 Cage Effect (initiator efficiency)

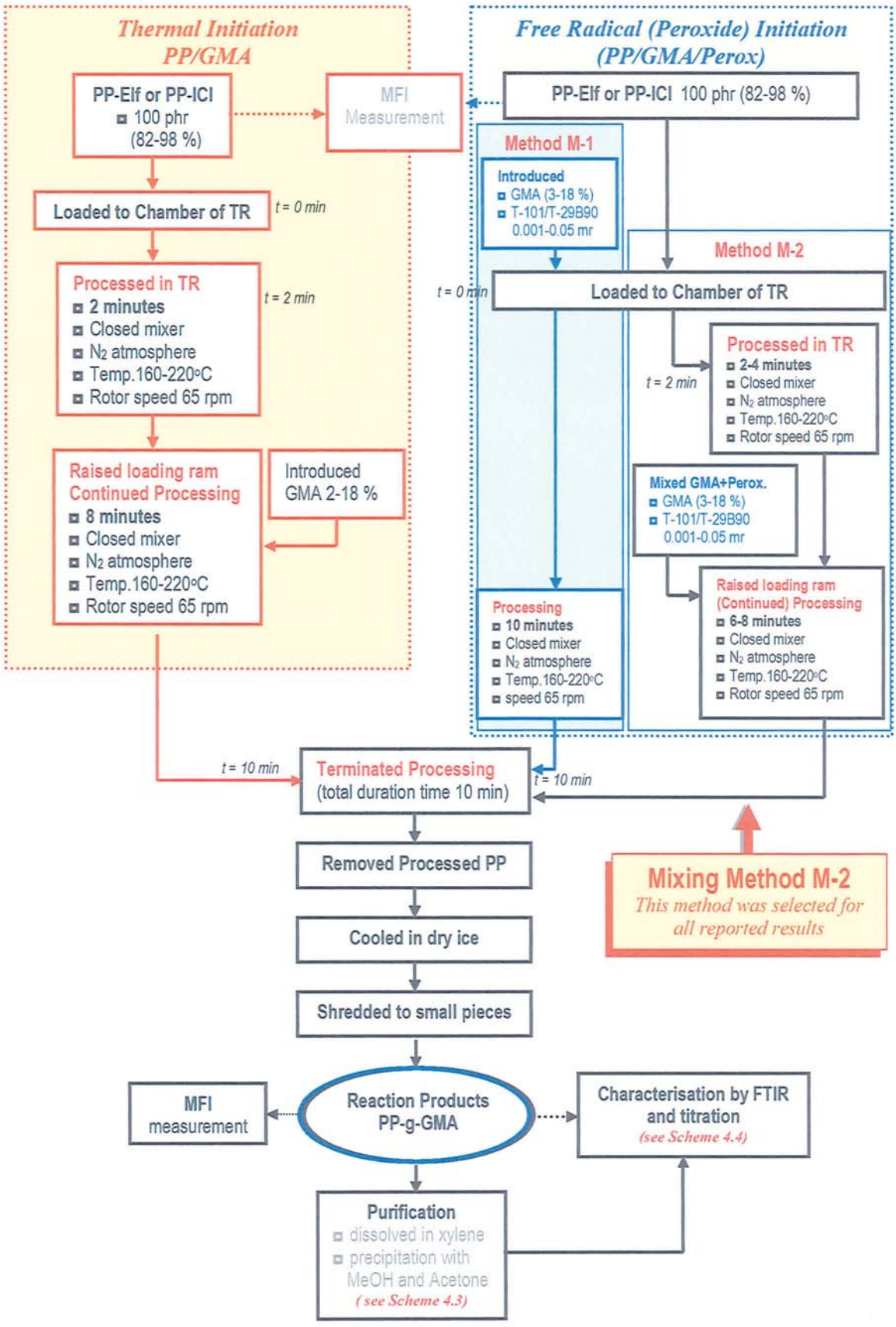

Scheme 4.1 Flow chart for reactive processing of PP with GMA by Thermal and Free Radical Initiation (FRI) system , peroxides T-101 and T-29B90

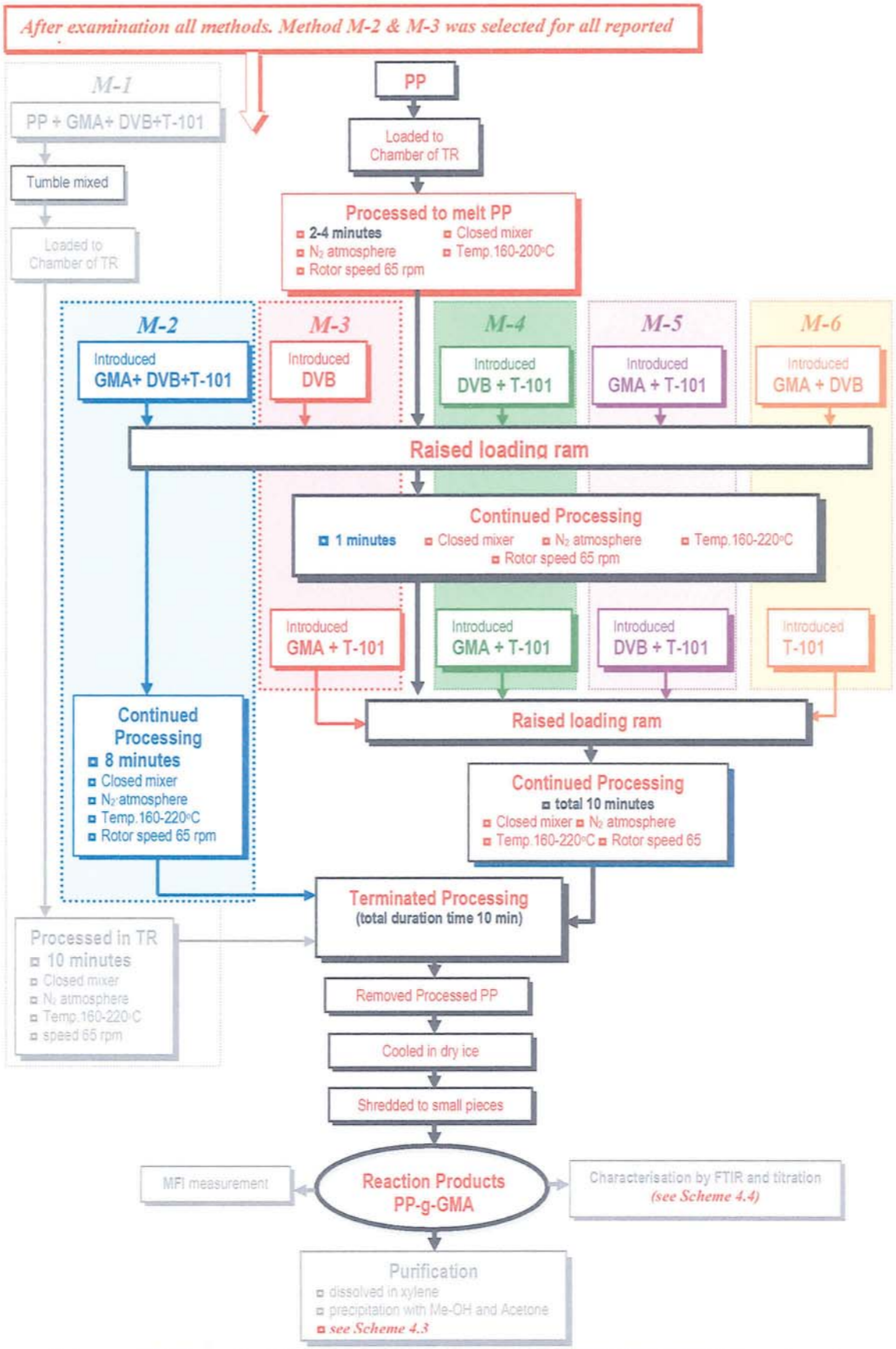

Scheme 4.2 Flow chart for reactive processing of PP/GMA/DVB/T-101 system in different **Addition sequence mixing method.**

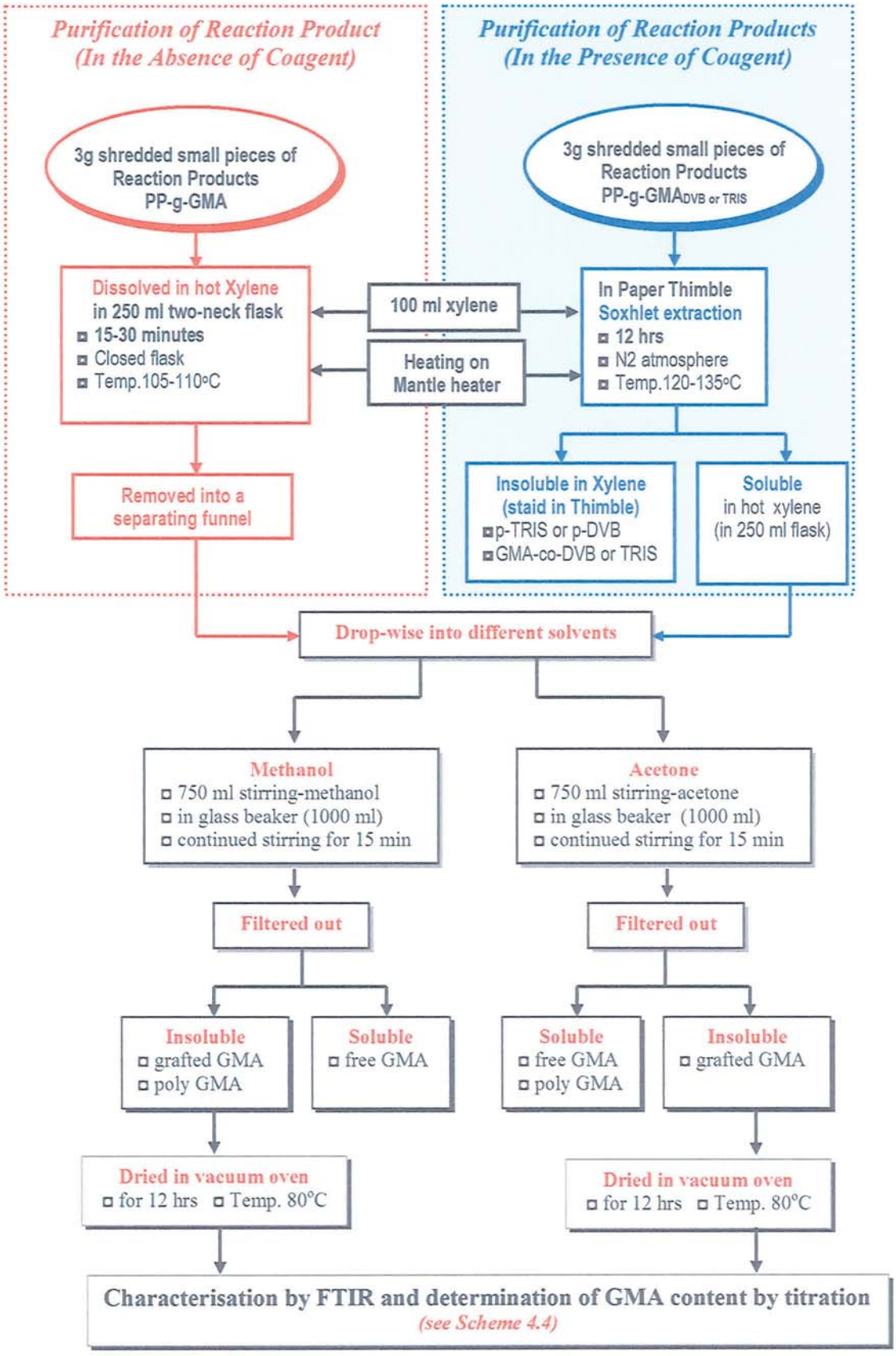

Scheme 4.3 Flow-chart for purification of reaction products, PP-g-GMA, in the presence of coagent using Soxhlet extraction and precipitation.

CHARACTERISATION OF REACTION PRODUCTS (TITRATION & FTIR)

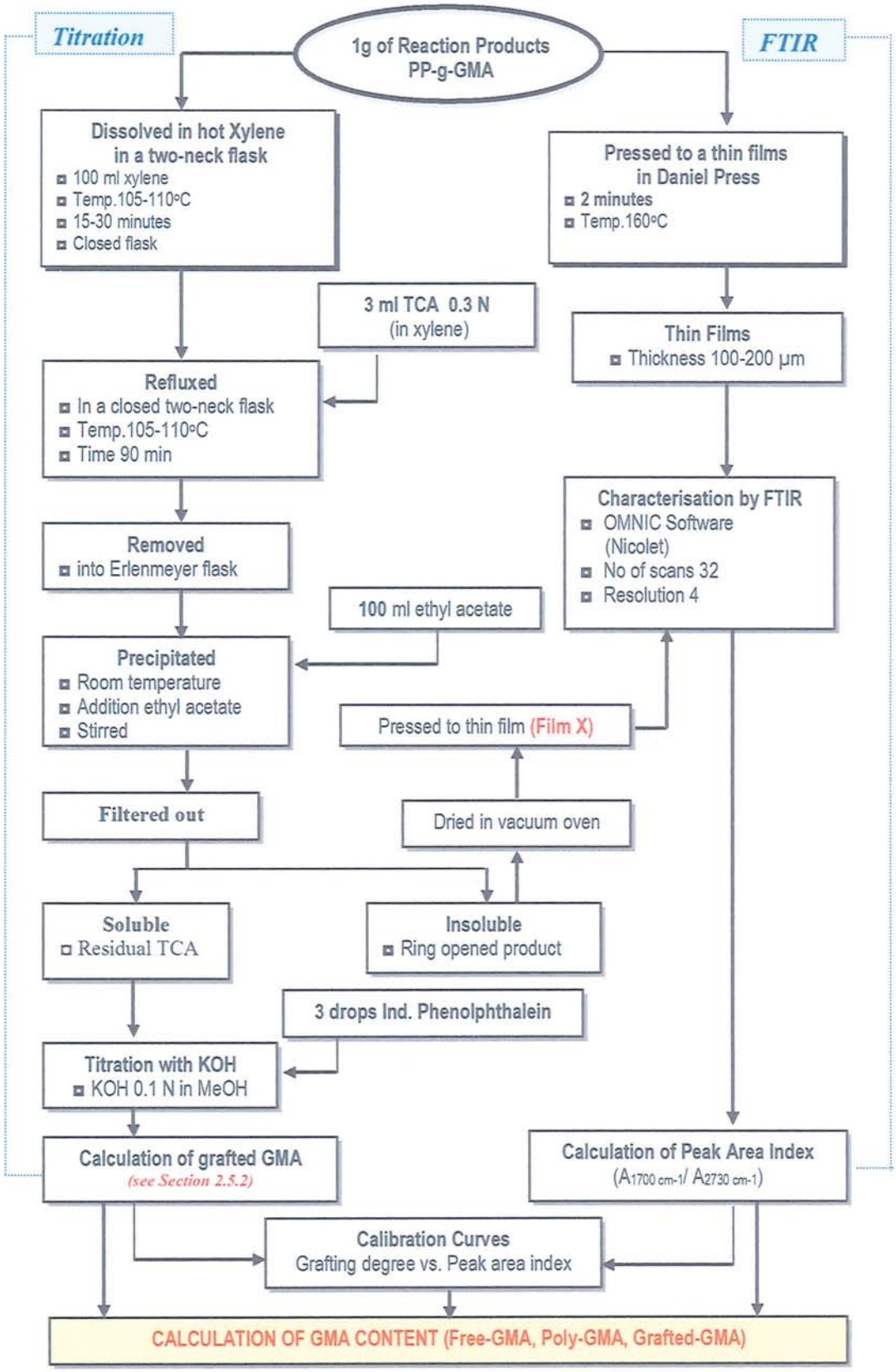

Scheme 4.4. Flow-chart for the characterisation of reaction products (PP-g-GMA) by titration and FTIR methods.

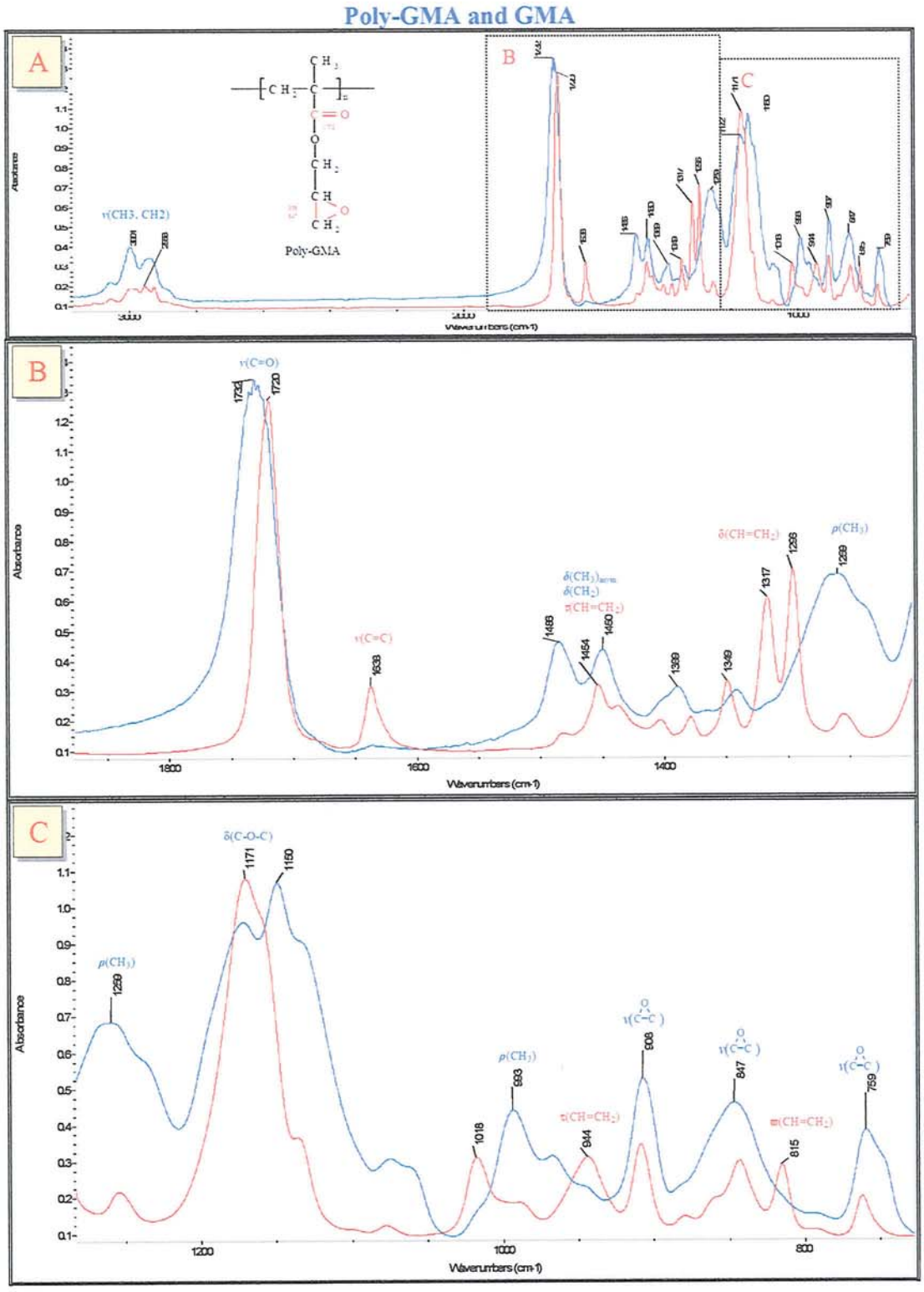

Figure 4.1 Comparison of FTIR spectra of poly-GMA (blue) (placed on diamond FTIR-ATR attachment) with GMA (red) (as thin liquid film placed between KBr windows).

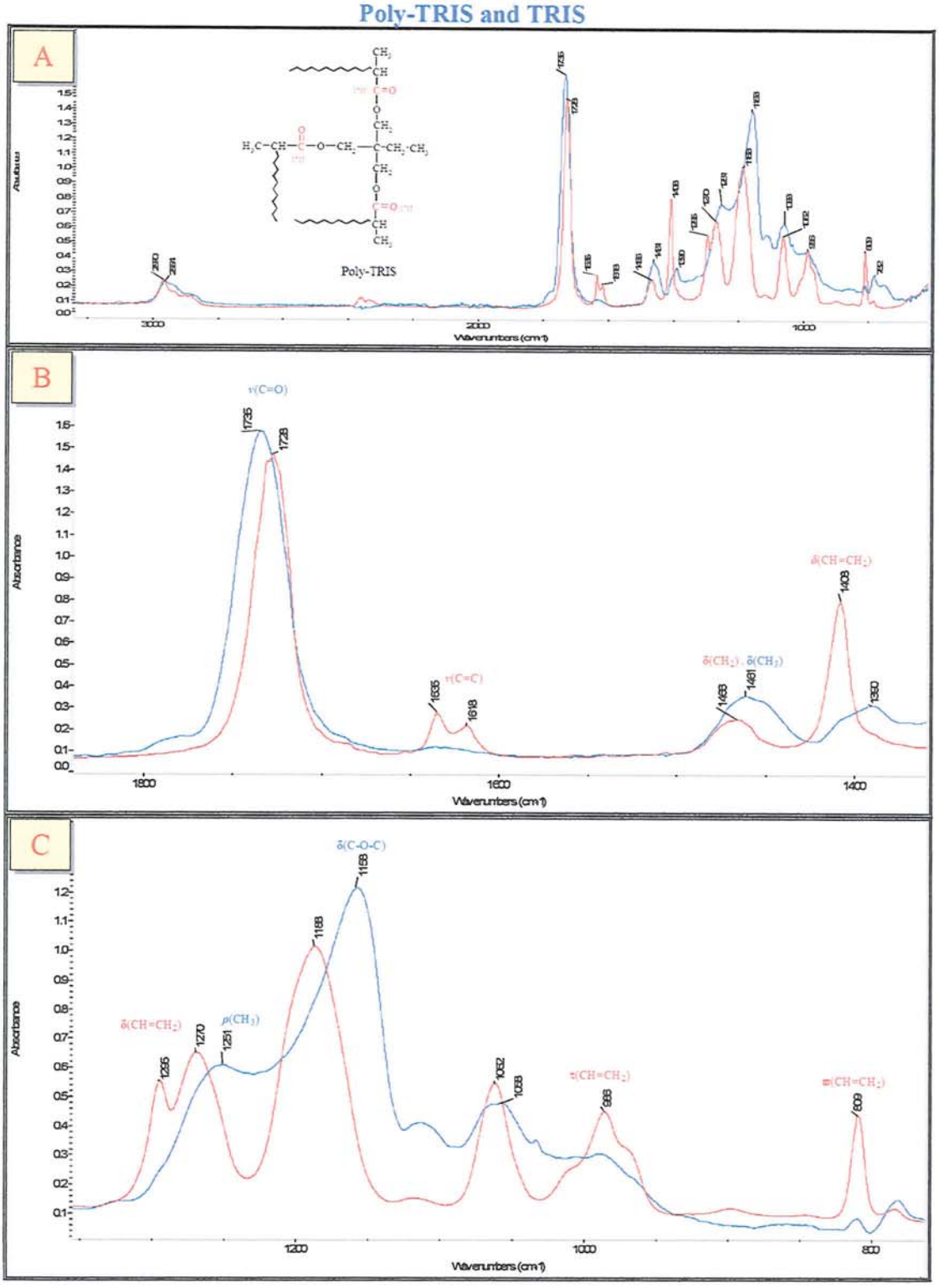

Figure 4.2 Comparison of FTIR spectra of Poly-TRIS (red) (placed on diamond FTIR-ATR attachment) and TRIS (red) (as thin liquid film placed between KBr windows).

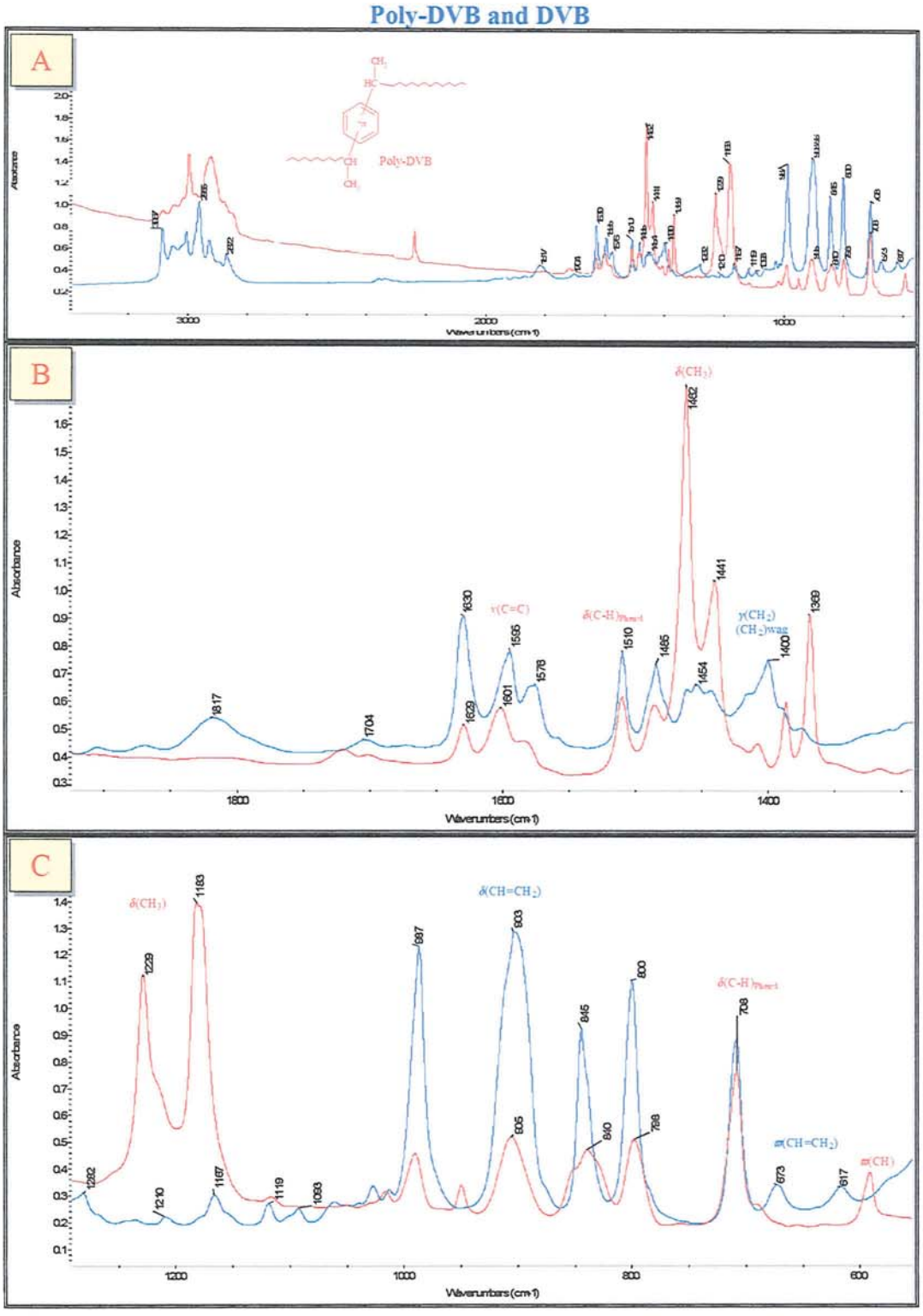

Figure 4.3 Comparison of FTIR spectra of Poly-DVB (red) (placed on diamond FTIR-ATR attachment) and DVB (blue) (as thin liquid film placed between KBr windows).

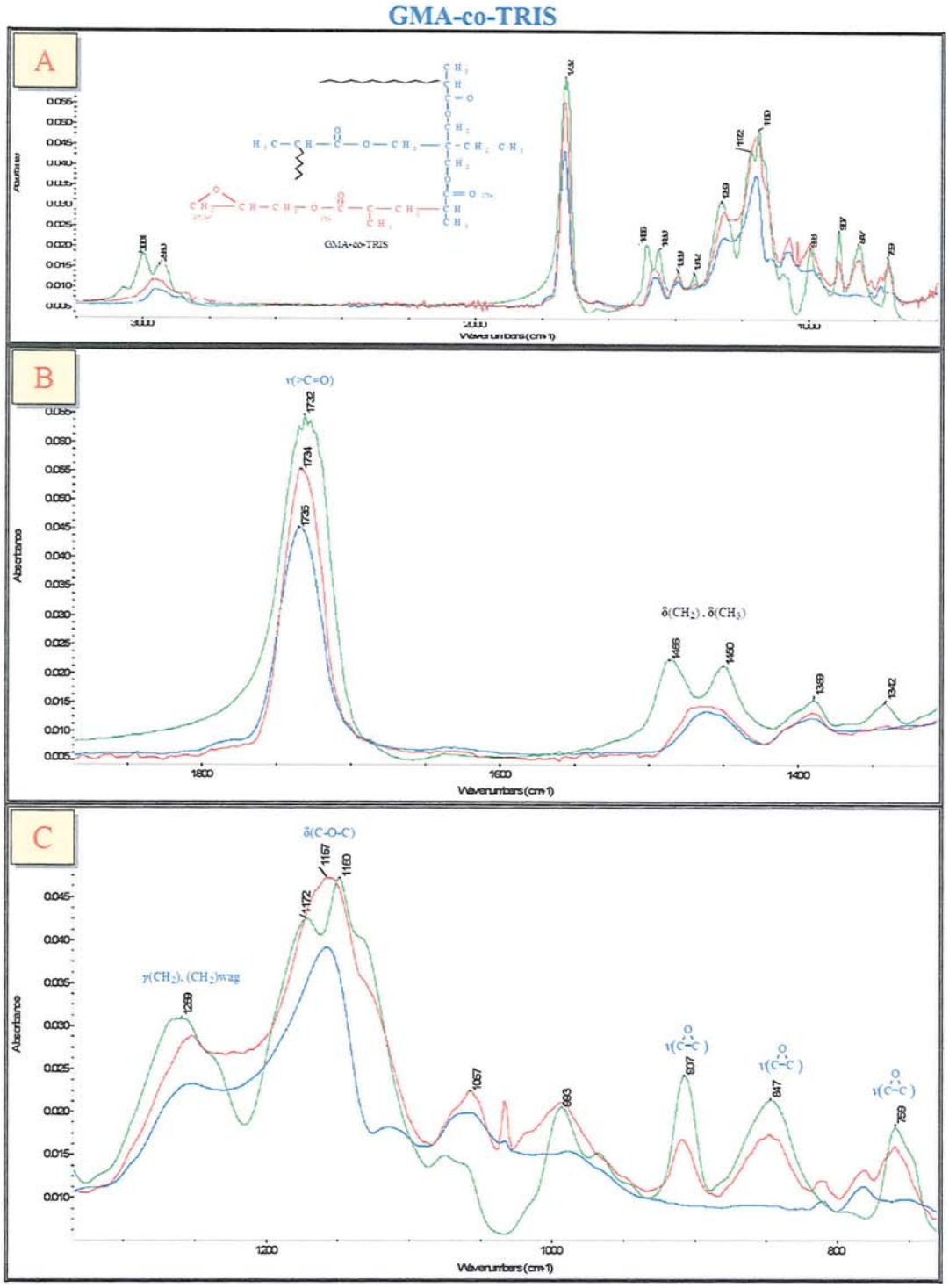

Figure 4.4 Comparison FTIR spectra of copolymer GMA-co-TRIS (red), poly-GMA (green) and poly-TRIS (blue) (placed on diamond FTIR-ATR attachment).

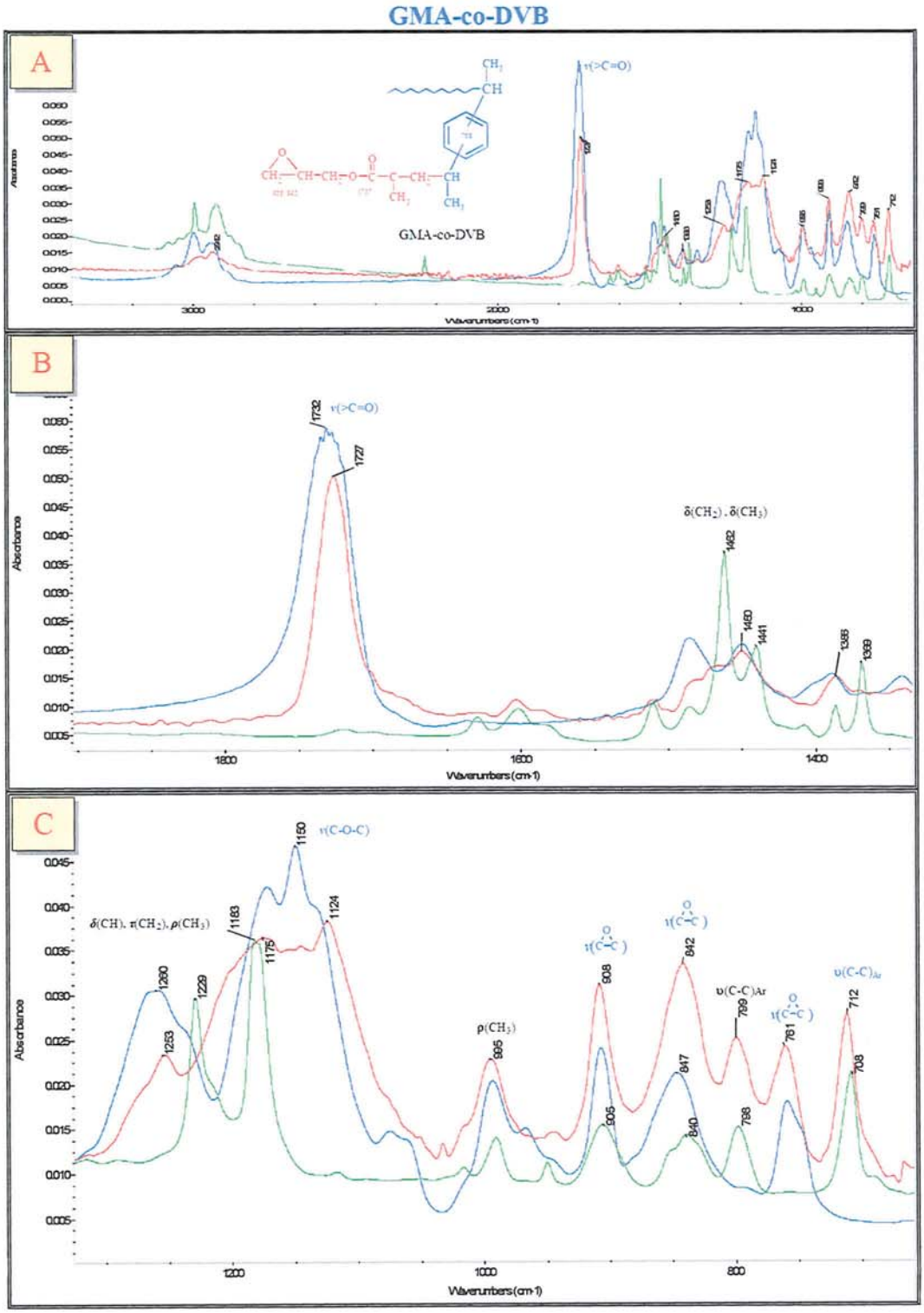

Figure 4.5 Comparison FTIR spectra of copolymer GMA-co-DVB (red), poly-DVB (green), and poly-GMA (blue) (placed on diamond FTIR-ATR attachment).

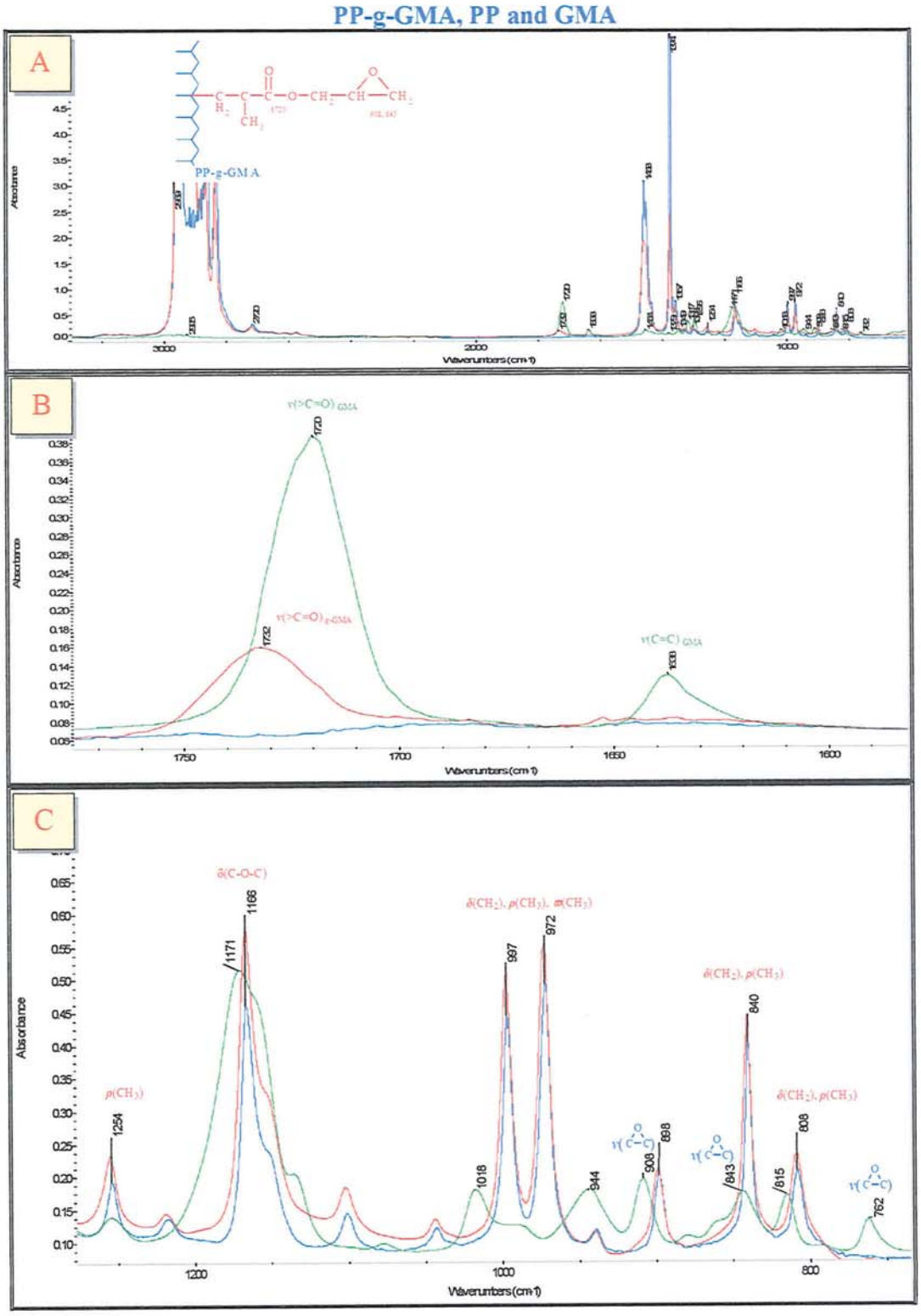

Figure 4.6 Comparison of FTIR spectra of PP-g-GMA (red) and PP alone (blue) (thin films, thickness ~ 0.1 mm) (red), and neat GMA (thin liquid film between KBr windows) (green).

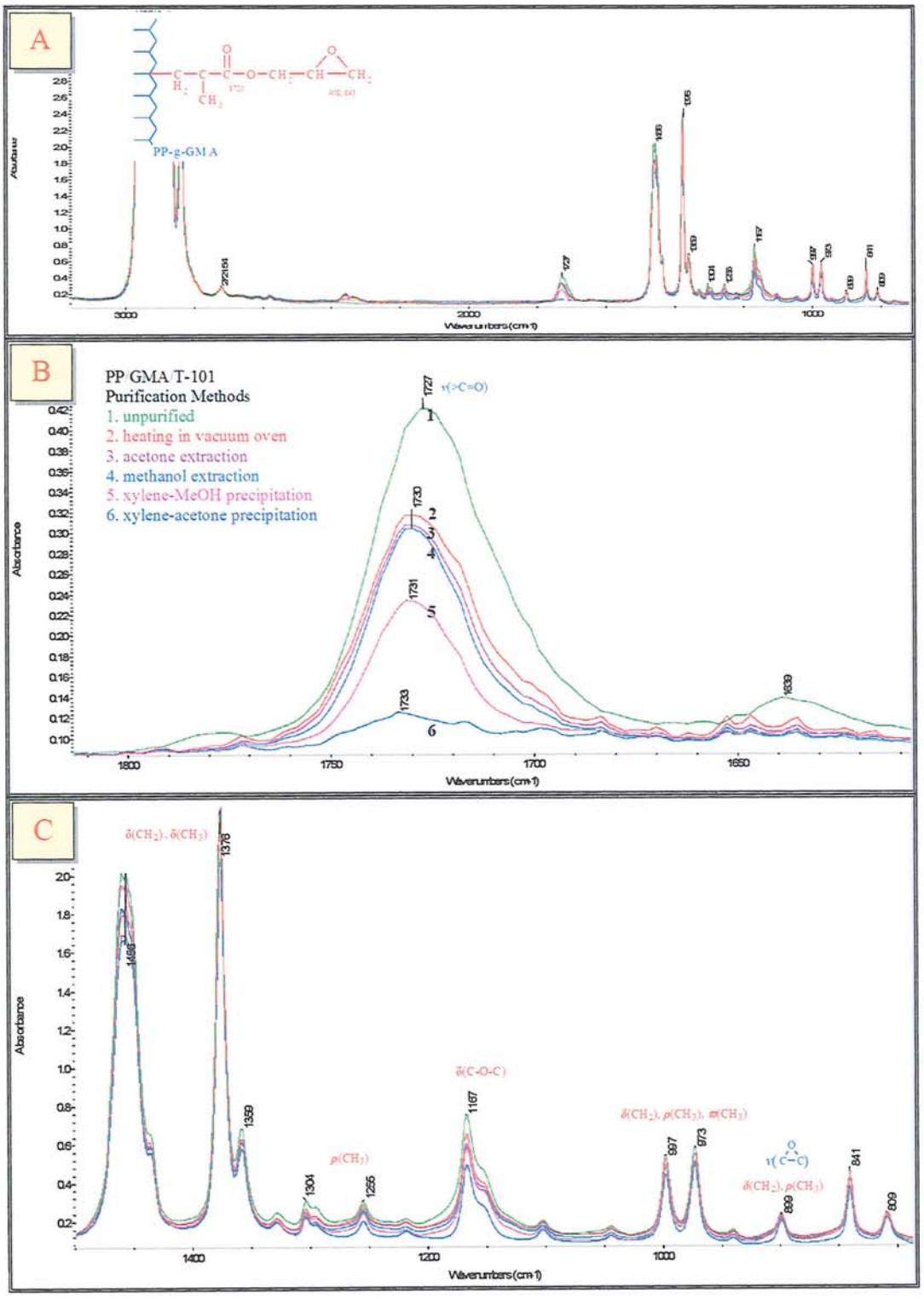

Figure 4.7 FTIR spectra (at carbonyl peak) of thin films of PP-g-GMA (thickness ~ 0.1 mm) before and after purification (different purification methods).

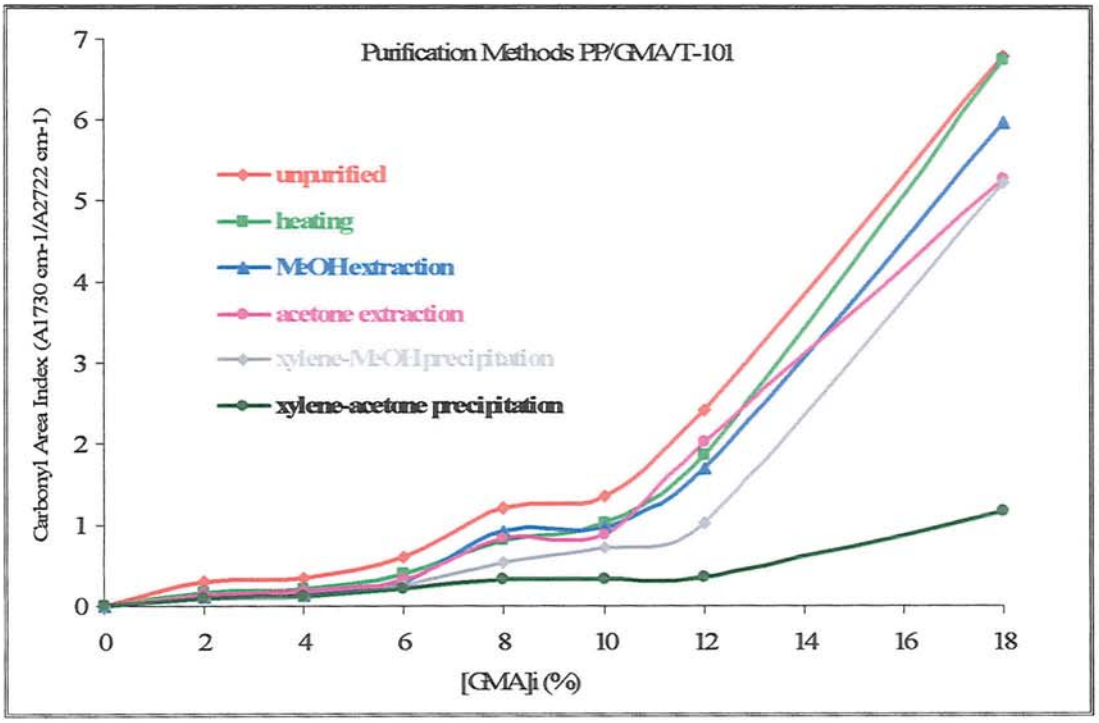

Figure 4.8 Carbonyl area index ($A_{1730s\ cm\text{-}1}/A_{2722\ cm\text{-}1}$) for different purification methods. (Samples [GMA]i = 0-18 %, [T-101] = 0.005 mr, 160°C, 65 rpm, 10 min).

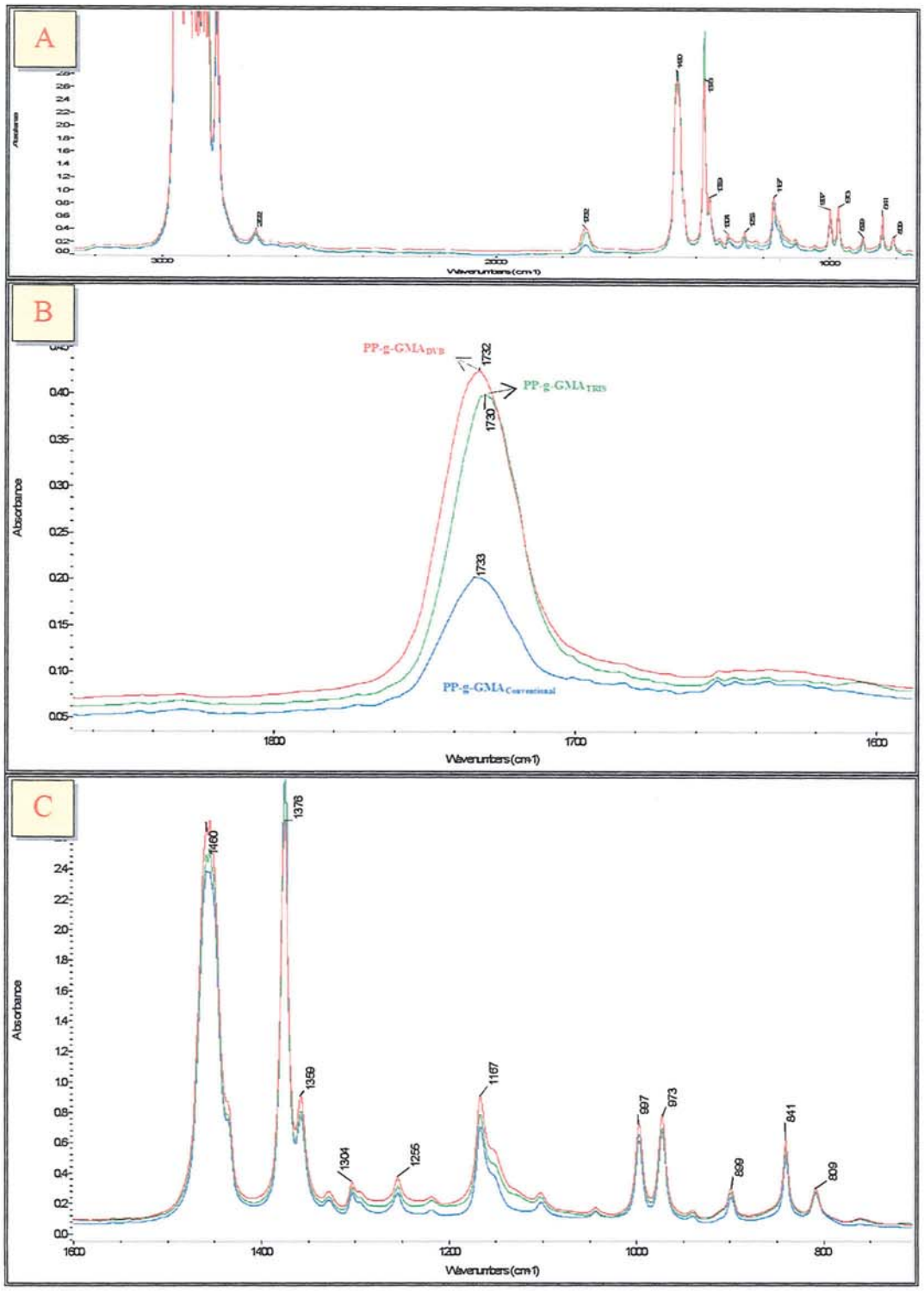

Figure 4.9 FTIR spectra of thin films (thickness ~ 0.1 mm) of PP-*g*-GMA, melt grafting in the absence of coagent (blue) and in the presence of TRIS, PP-*g*-GMA$_{TRIS}$ (red) and DVB, PP-*g*-GMA$_{DVB}$ (green).

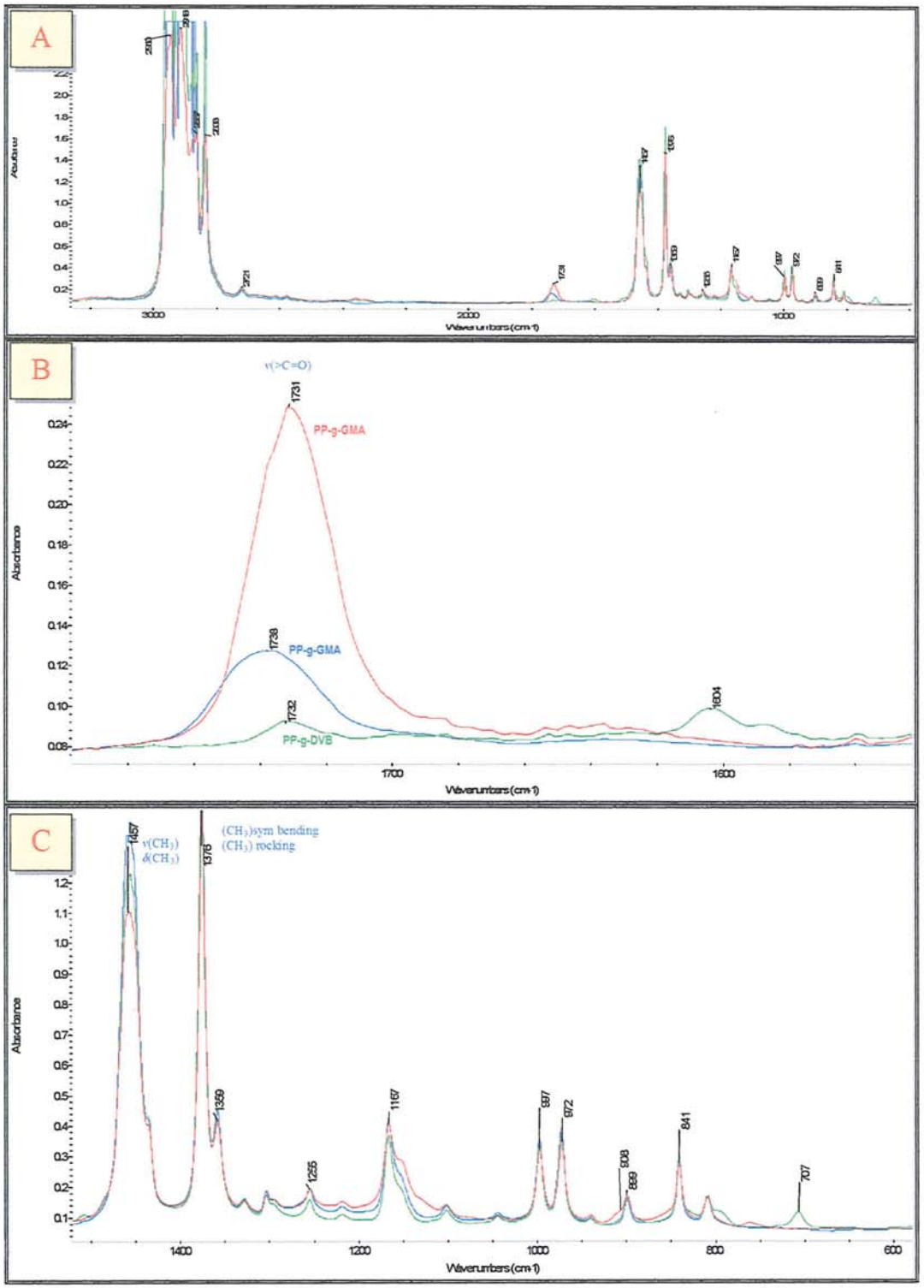

Figure 4.10 Comparison of spectra of thin films (thickness ~ 0.1 mm) PP-*g*-GMA (red), PP-*g*-TRIS (blue), and PP-*g*-DVB (green).

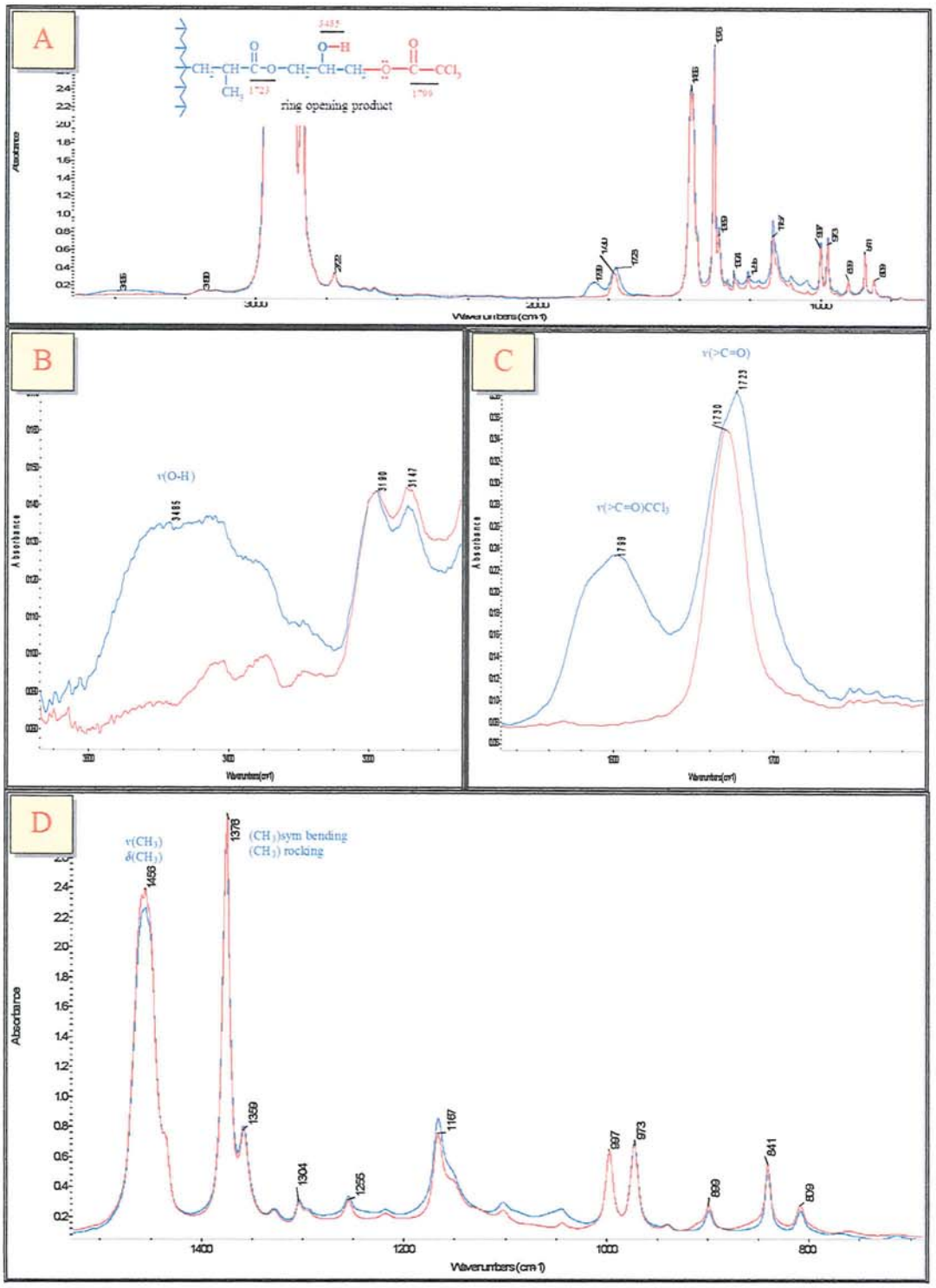

Figure 4.11 FTIR spectra of grafted GMA onto PP (in the presence of coagent DVB) before (red) and after (blue) titration.

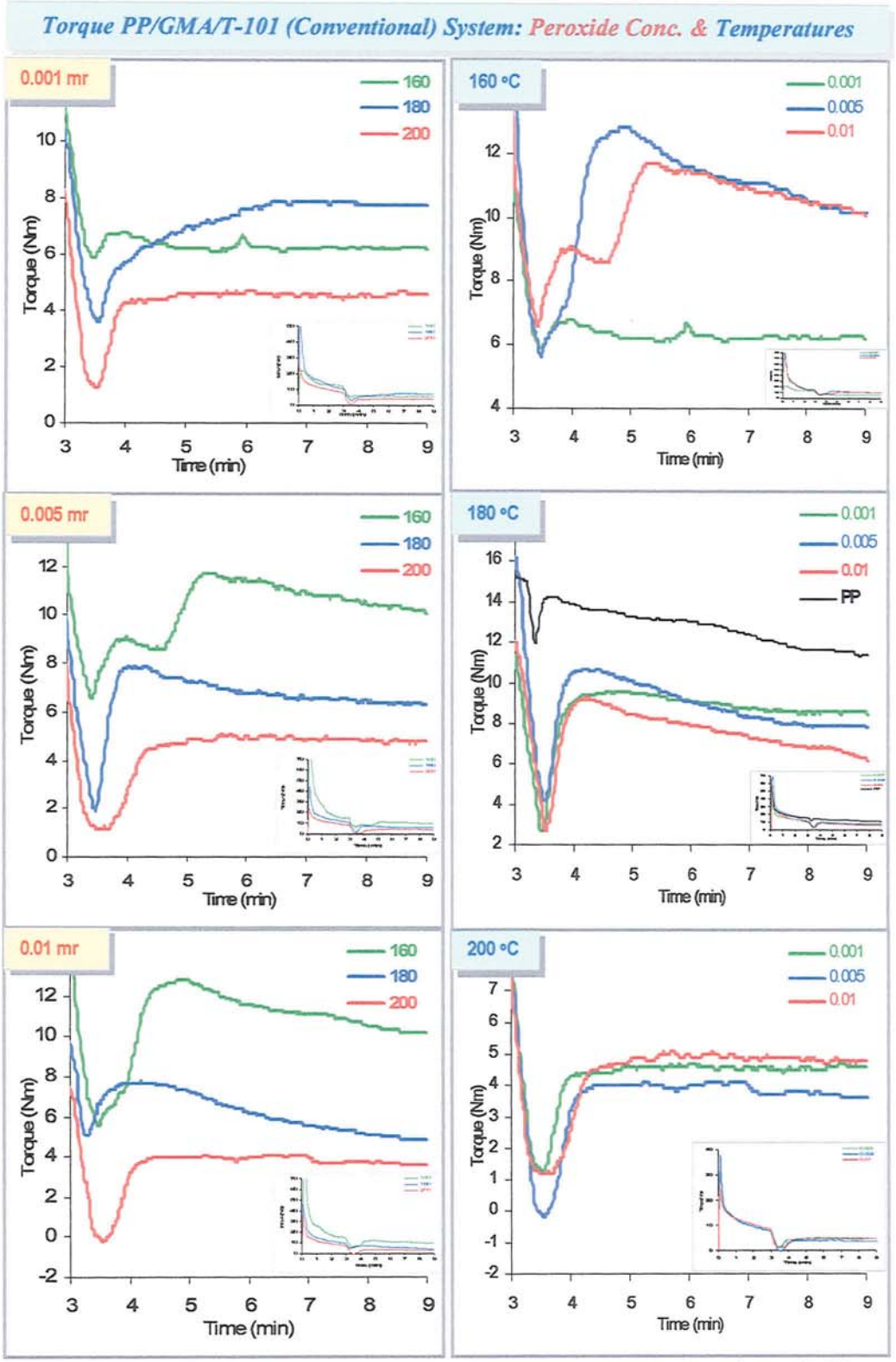

Figure 4.12 Effect of temperature and peroxide concentration (molar ratio to GMA) on torque of the PP/GMA/T-101 (conventional) system (*inset: full scale curves*). (Samples G1-n, G2-n, G3-n, G5-n in Table C.4.2 Appendix C; [GMA]i = 12%, [T-101] = 0.001-0.01 molar ratio to GMA, temp. 160-200°C, 65 rpm, 10 min, mixing method M-2).

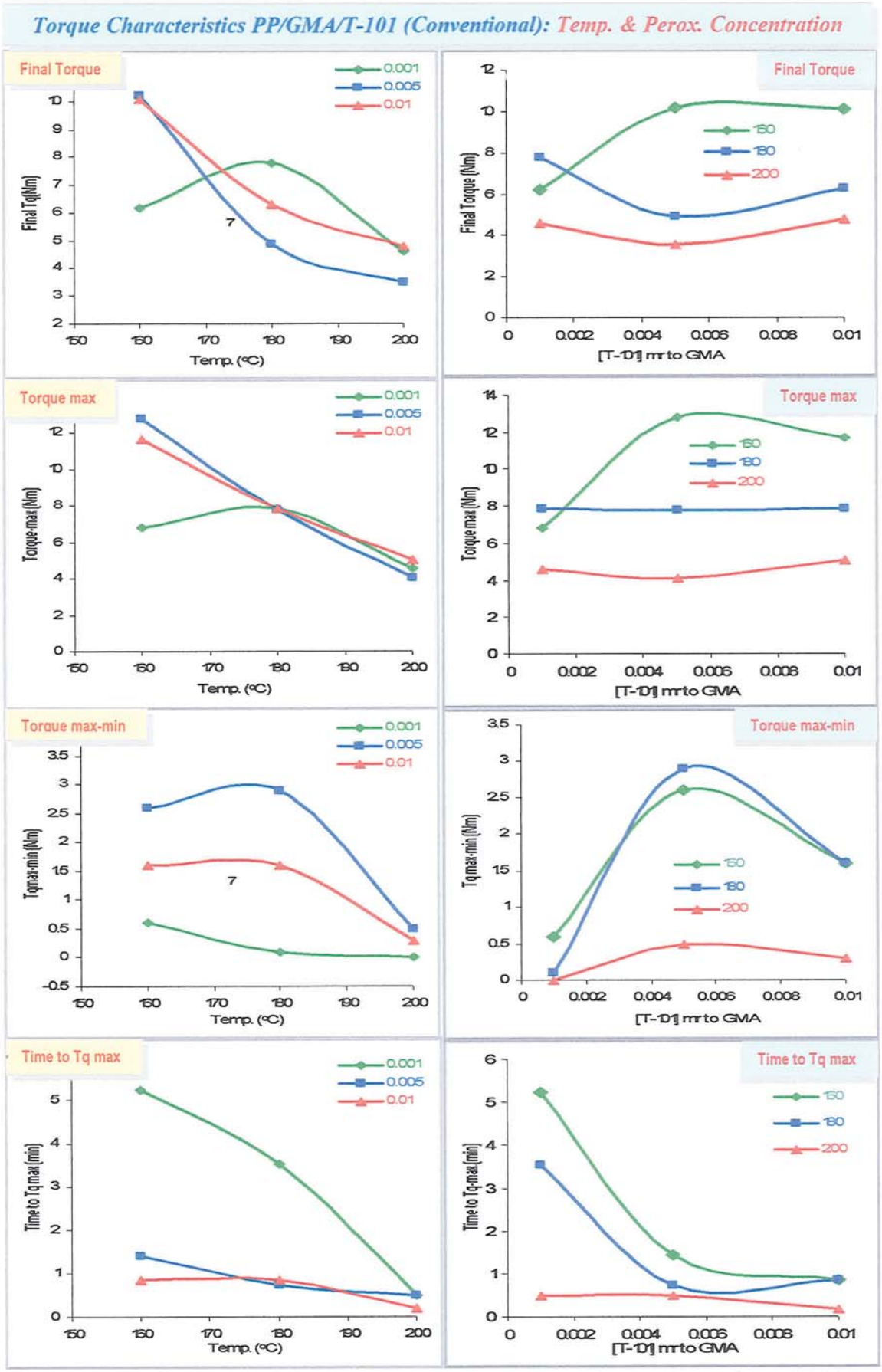

Figure 4.13 Effect of temperature and peroxide concentration (molar ratio to GMA) on torque characteristic of the PP/GMA/T-101 (conventional) system. (Samples G1-n, G2-n, G3-n in Table C.4.2 Appendix C; [GMA]i = 12%, [T-101] = 0.001-0.01 molar ratio to GMA, temp. 160-200°C, 65 rpm, 10 min, mixing method M-2).

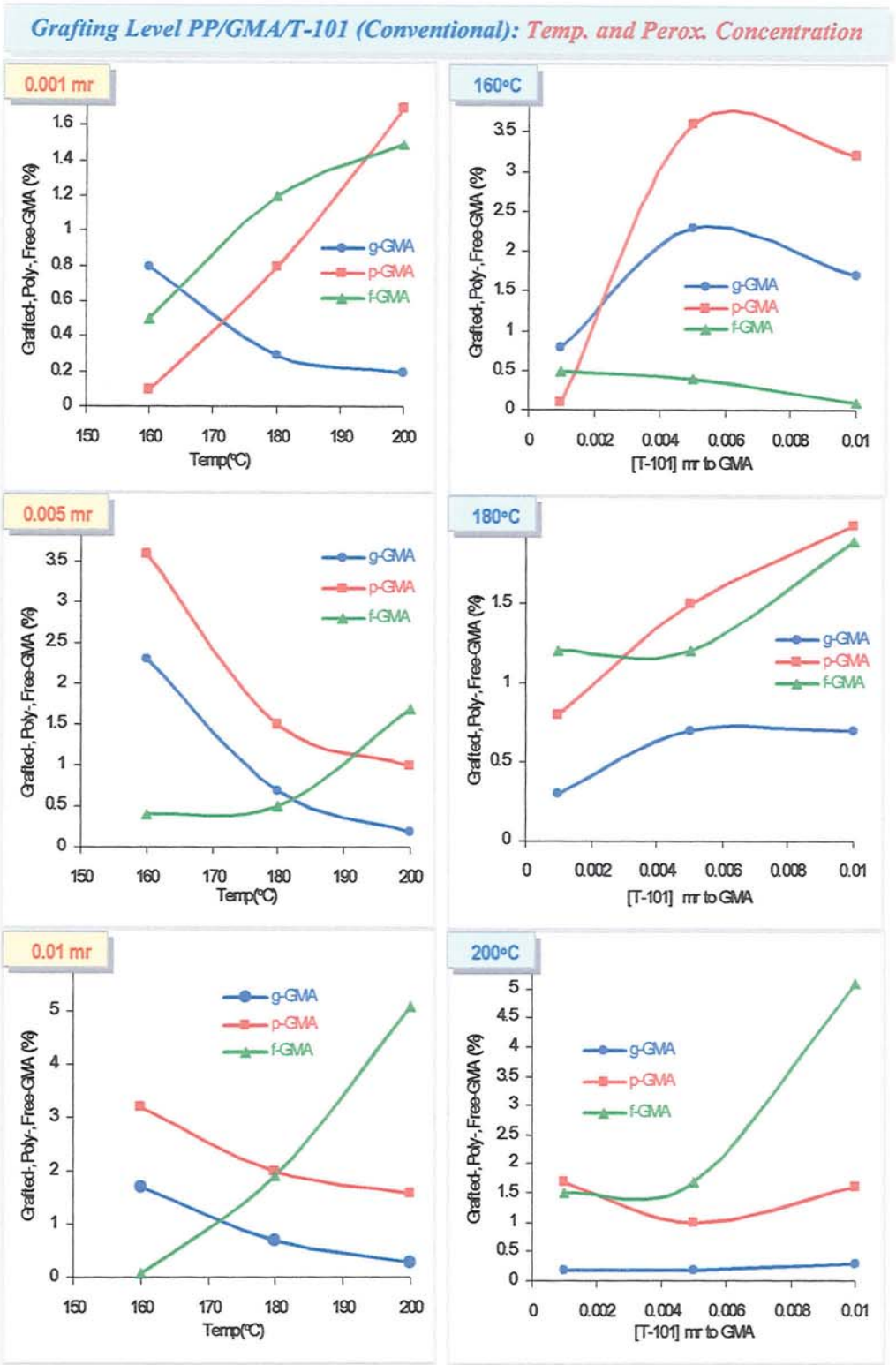

Figure 4.14 Effect of temperature and peroxide concentration (molar ratio to GMA) on grafting level, GMA polymerisation, and unreacted (free) GMA of the PP/GMA/T-101 (conventional) system. (Samples G1-n, G2-n, G3-n in Table C.4.2 Appendix C) ([GMA]i = 12%, [T-101] = 0.001-0.01 molar ratio to GMA, temp. 160-200°C, 65 rpm, 10 min, mixing method M-2) (*g-* = grafted, *p-*= poly, and *f-* = free or unreacted GMA).

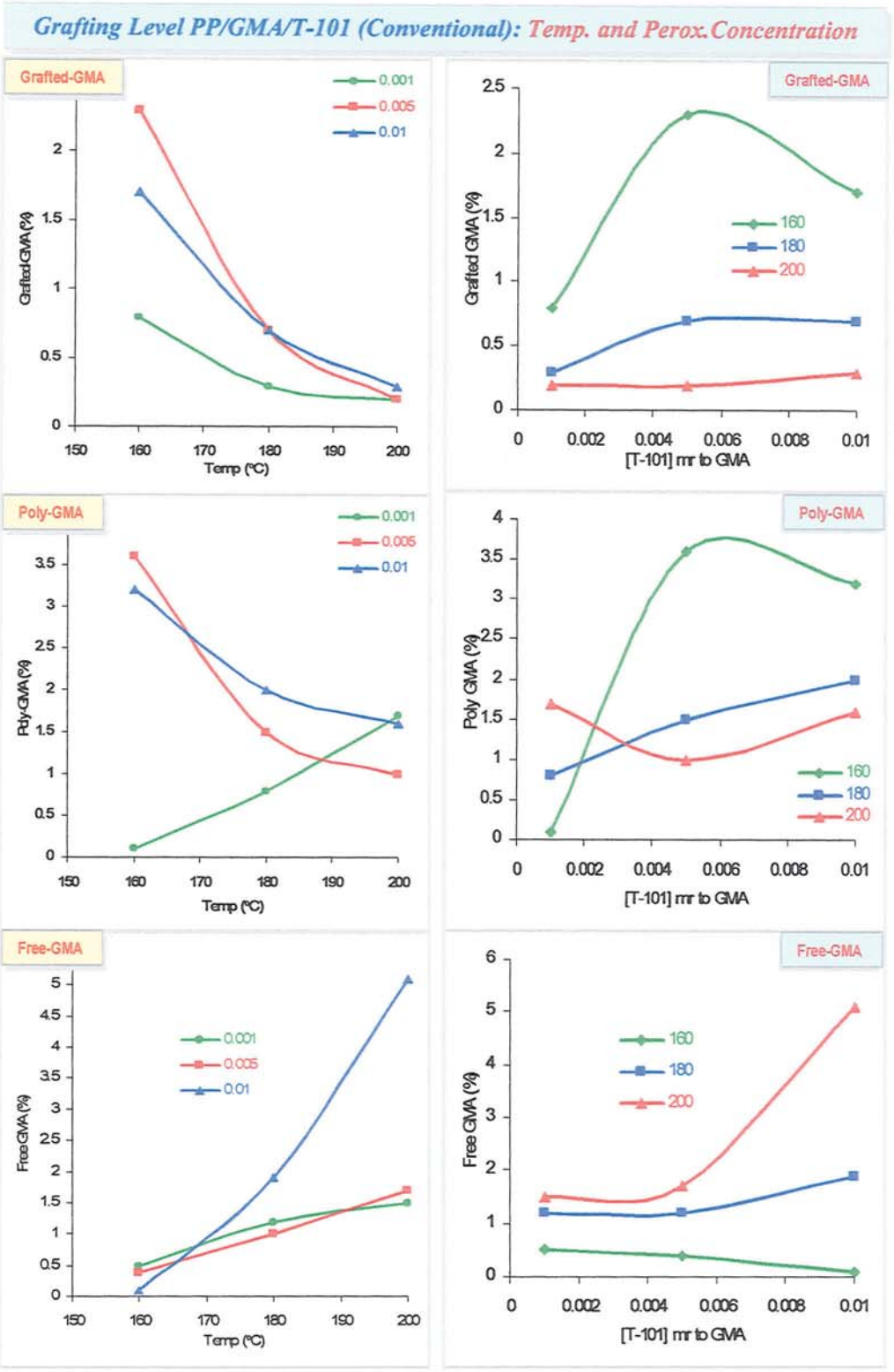

Figure 4.15 Effect of temperature and peroxide concentration on grafting level, poly-GMA and unreacted (free) GMA of the PP/GMA/T-101 (conventional) system. (Samples G1-n, G2-n, G3-n in Table C.4.2 Appendix C; [GMA] = 12%, [T-101] = 0.001-0.01 molar ratio to GMA, 65 rpm, 10 min, mixing method M-2).

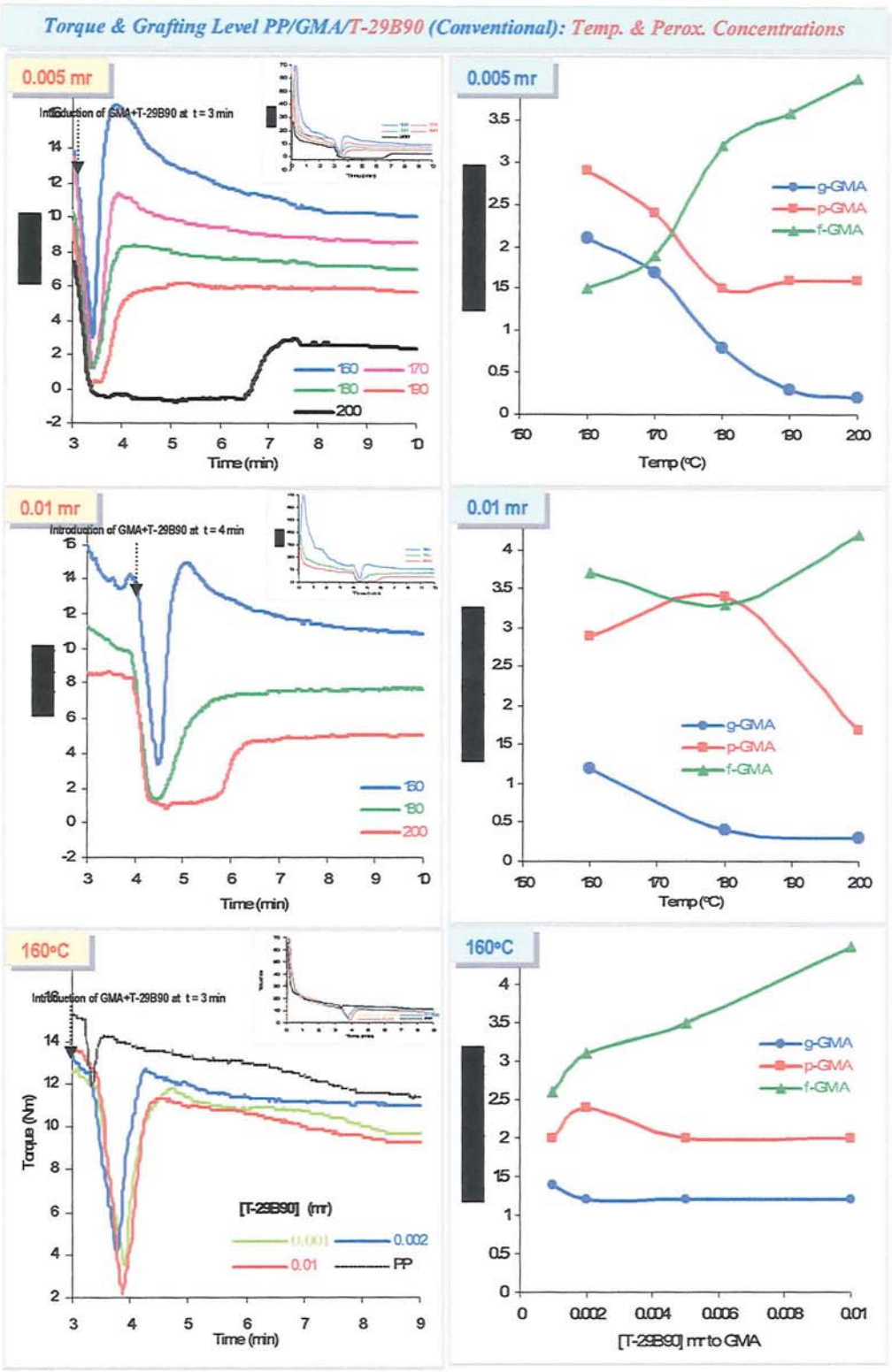

Figure 4.16 Effect of T-29B90 concentration and temperature on torque, GMA grafting level, and the extent of poly-GMA (Samples G13-n, G14-n, G16-n, in Table C.4.3, Appendix C) ([GMA]i = 12%, [T-29B90] = 0.001-0.1 molar ratio to GMA, temp.160-200°C, 65 rpm, 10 min, mixing method M-2). (Inset: full scale curves, ***g***- = grafted, ***p***-= poly, and ***f***- = free or unreacted GMA).

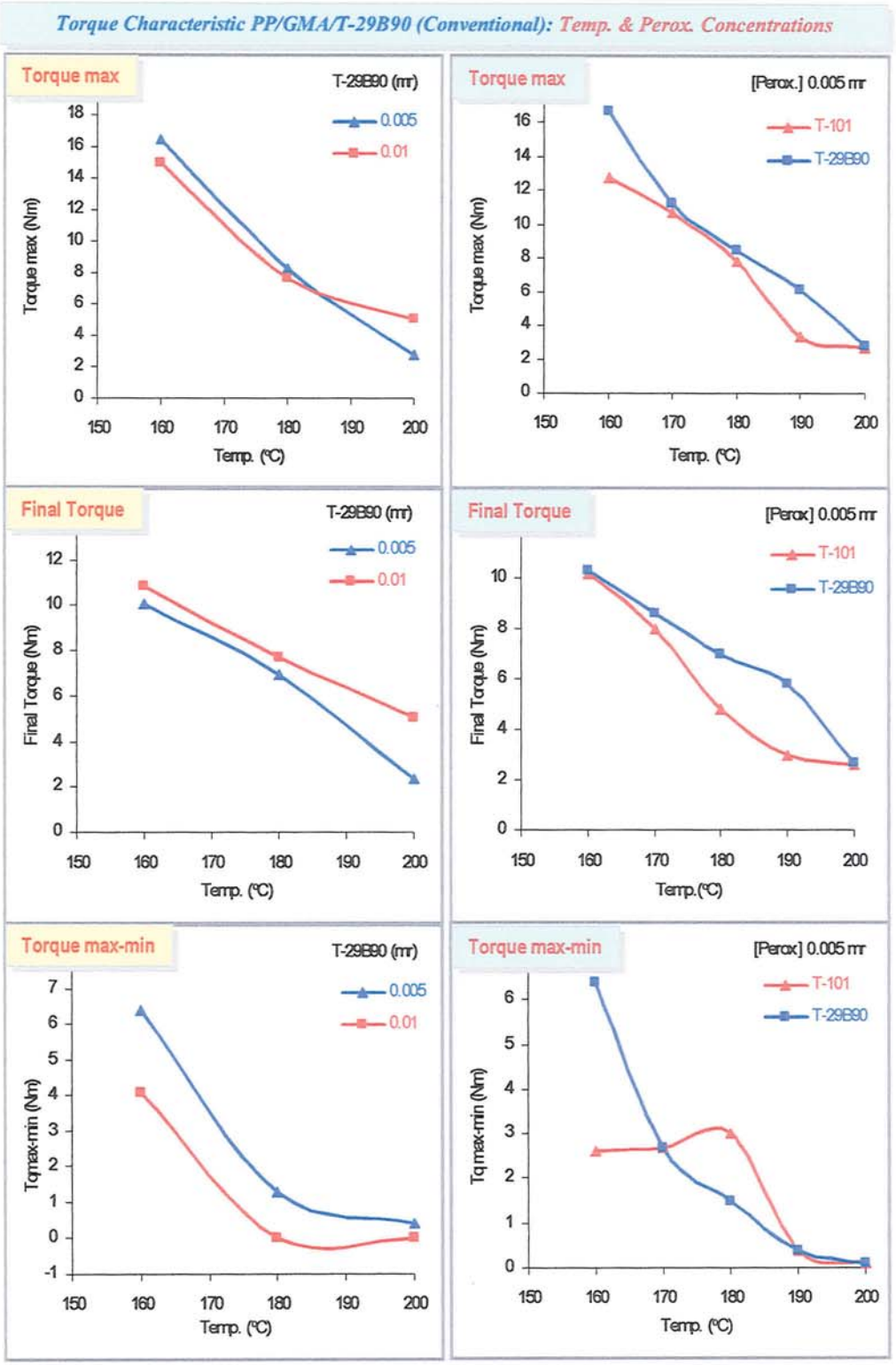

Figure 4.17 Effect of temperature on torque characteristic of the PP/GMA/T-29B90 (conventional) system with different peroxide concentration and compared to T-101 system. ([GMA]i = 12%, [T-29B90] = 0.005 and 0.1 mr, [T-101] 0.005 mr, 65 rpm, 10 min, mixing method M-2).

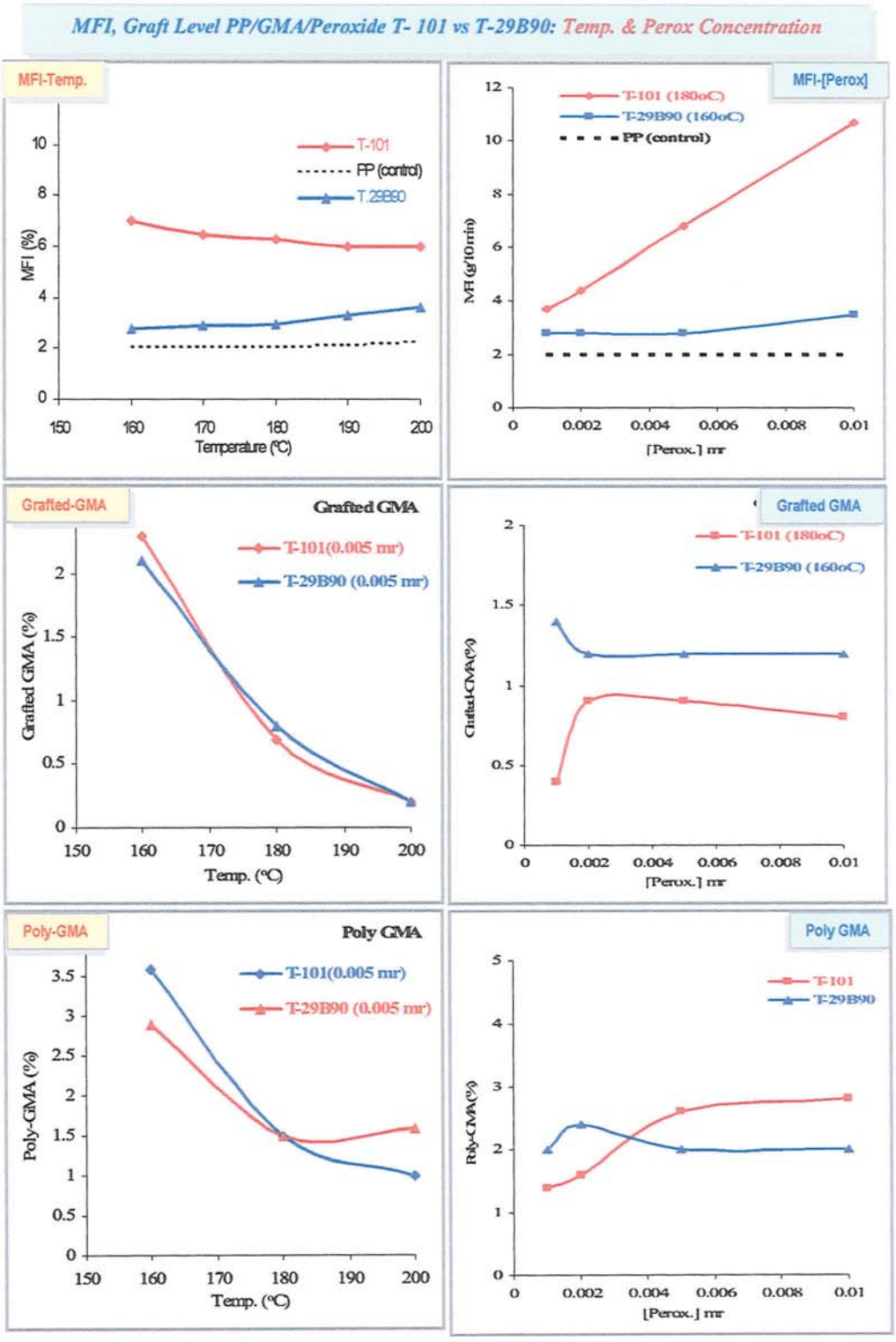

Figure 4.18 Comparison Effect of peroxide concentration and temperature on torque, grafting level and MFI in the processed PP/GMA/**T-101** (samples G2-n in Table C.4.2) and PP/GMA/**T-29B90** (samples G13-n in Table C.4.3 Appendix C) ([GMA]i = 12%, 65 rpm, 10 min, mixing method M-2) (PP control is a processed PP-Elf virgin).

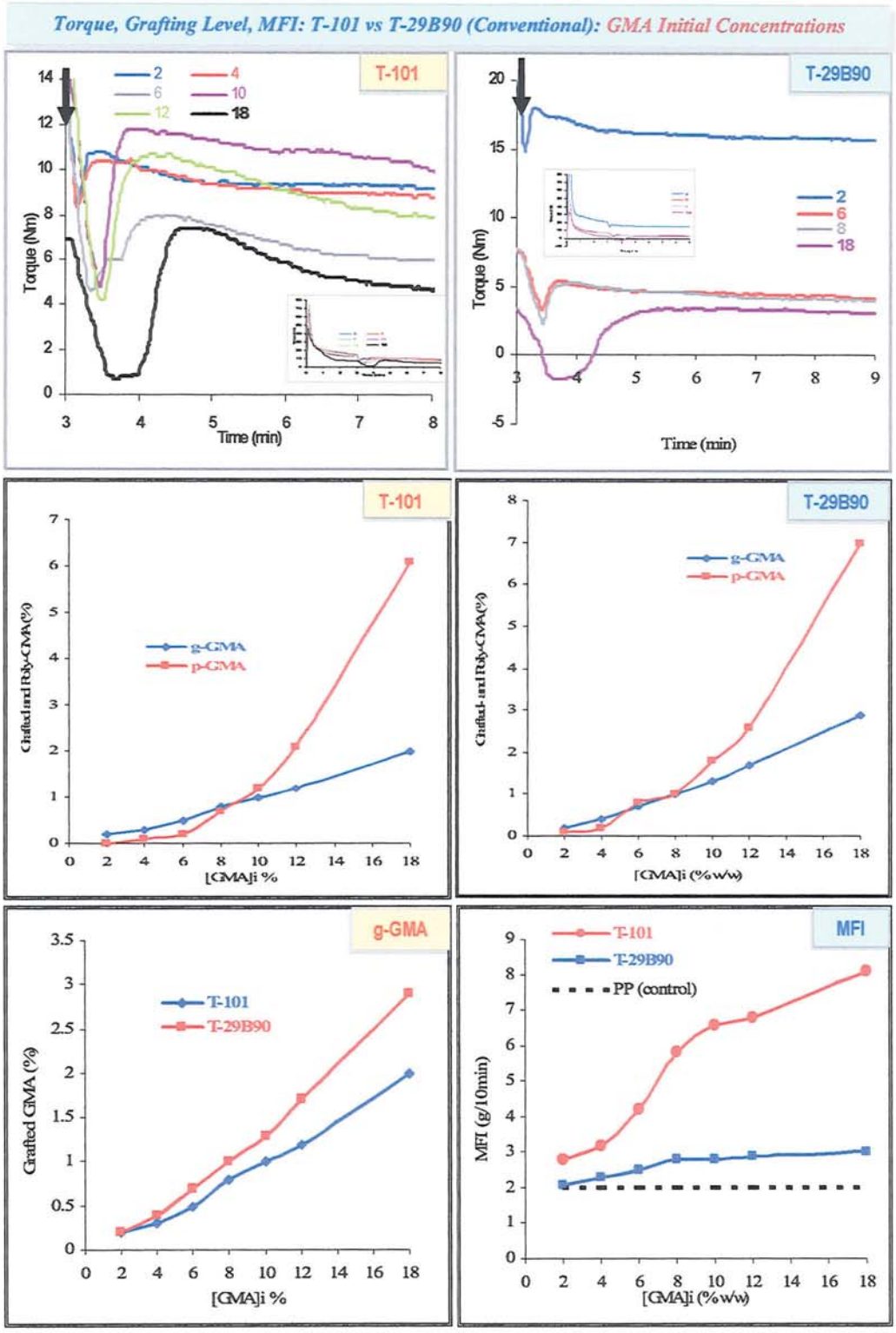

Figure 4.19 Comparison effect of GMA initial concentration on torque, GMA grafting level and MFI in the PP/GMA/perox (conventional, different peroxide) system (Samples for T-101: G8-n in Table C.4.2 and for T-29B90 G17-n in Table C.4.3 Appendix C); [GMA]i = 2-18%, [perox] = 0.005 molar ratio to GMA, temp. for T-101 = 180°C and for T-29B90 = 160°C, 65 rpm, 10 min, mixing method M-2).

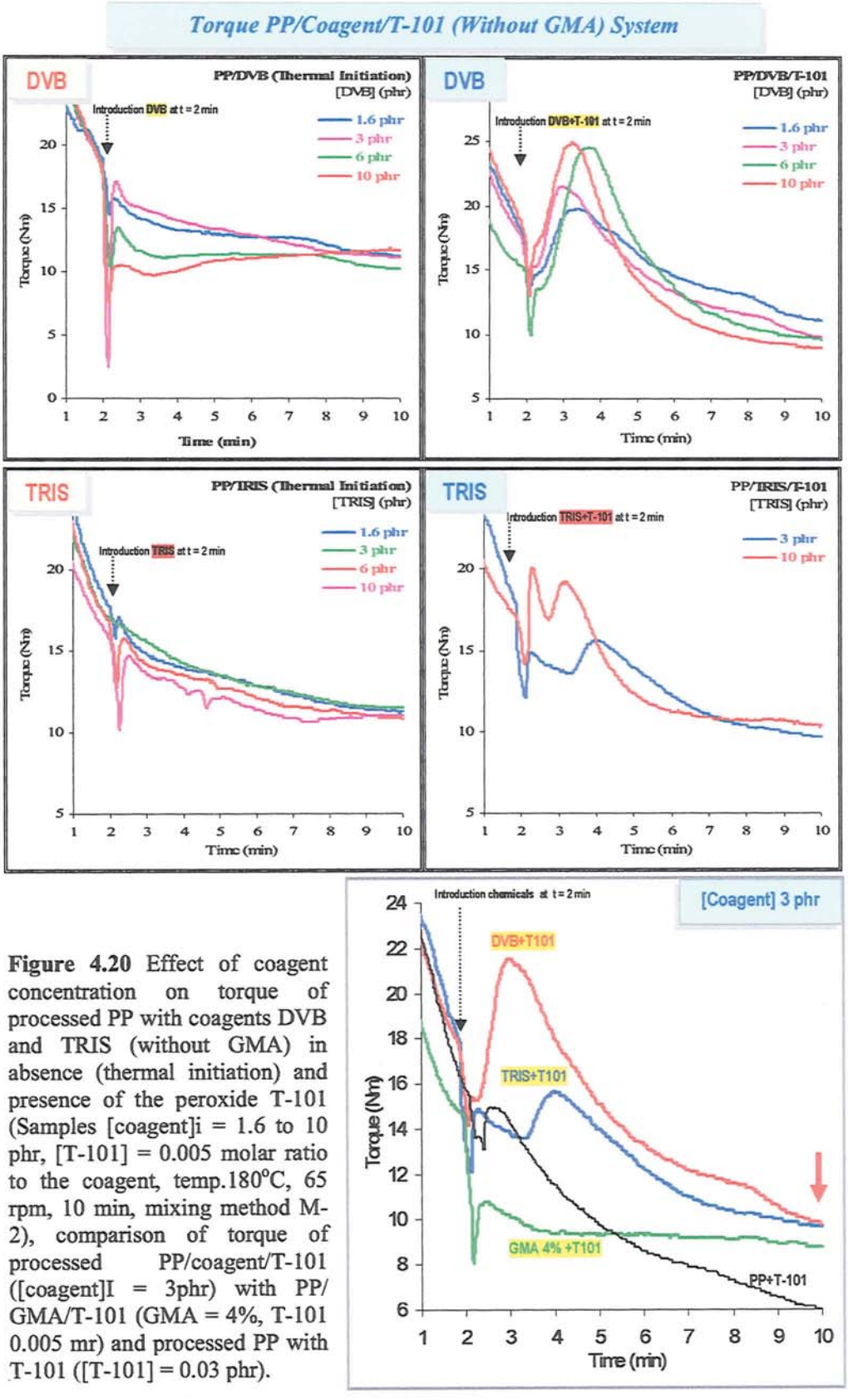

Figure 4.20 Effect of coagent concentration on torque of processed PP with coagents DVB and TRIS (without GMA) in absence (thermal initiation) and presence of the peroxide T-101 (Samples [coagent]i = 1.6 to 10 phr, [T-101] = 0.005 molar ratio to the coagent, temp.180°C, 65 rpm, 10 min, mixing method M-2), comparison of torque of processed PP/coagent/T-101 ([coagent]I = 3phr) with PP/GMA/T-101 (GMA = 4%, T-101 0.005 mr) and processed PP with T-101 ([T-101] = 0.03 phr).

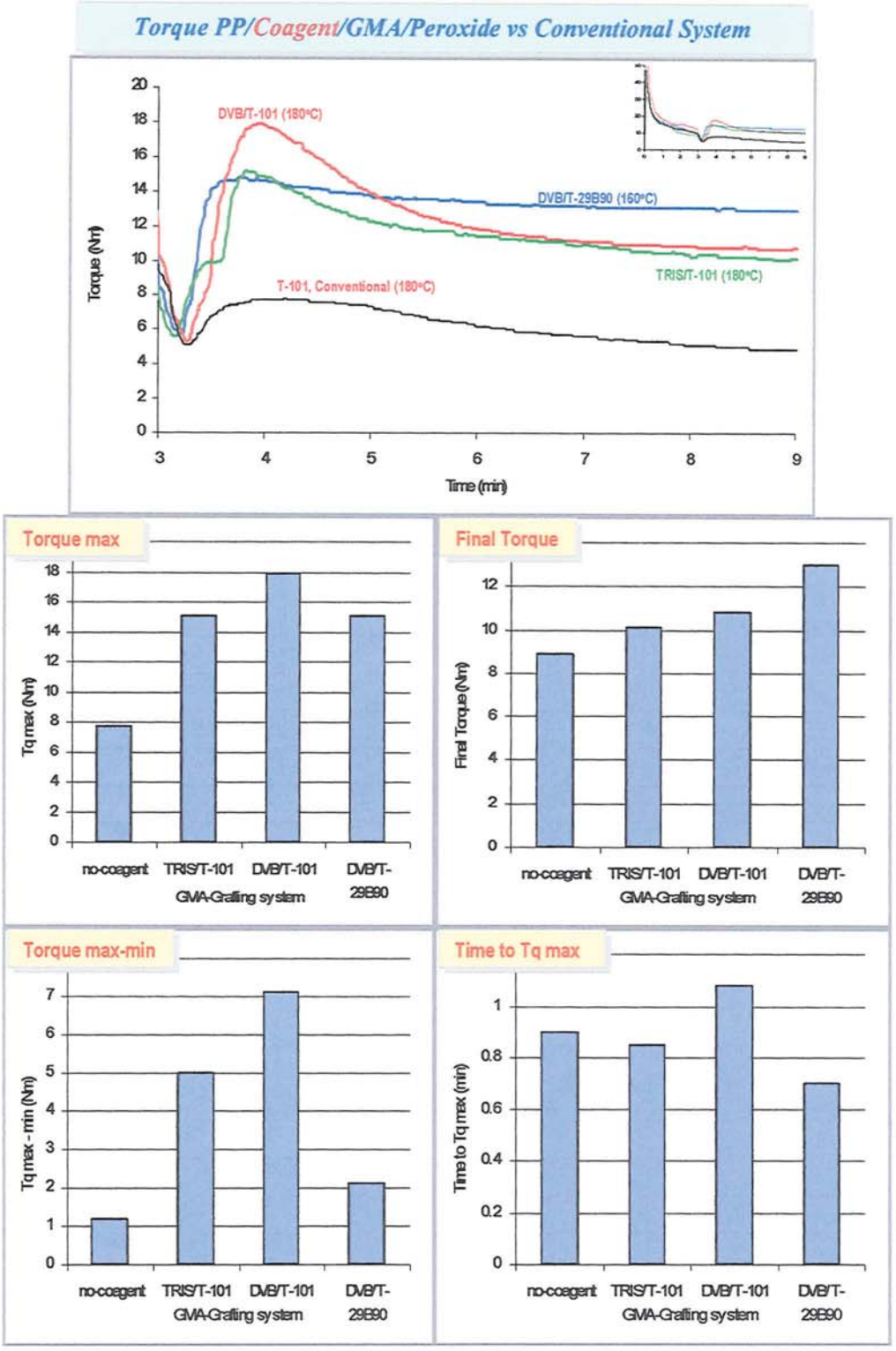

Figure 4.21 Comparison of torque and torque characteristic of processed PP with GMA in the absence (conventional) or presence of coagents (TRIS or DVB). (Samples: [GMA]i = 12%, [coagent] = 2/8 weight ratio to GMA, [peroxide] 0.005 molar ratio to GMA or GMA+coagent), temp.180°C for T-101 and 160°C for T-29B90, 65 rpm, 10 min, mixing method M-2) (inset = full scale curves).

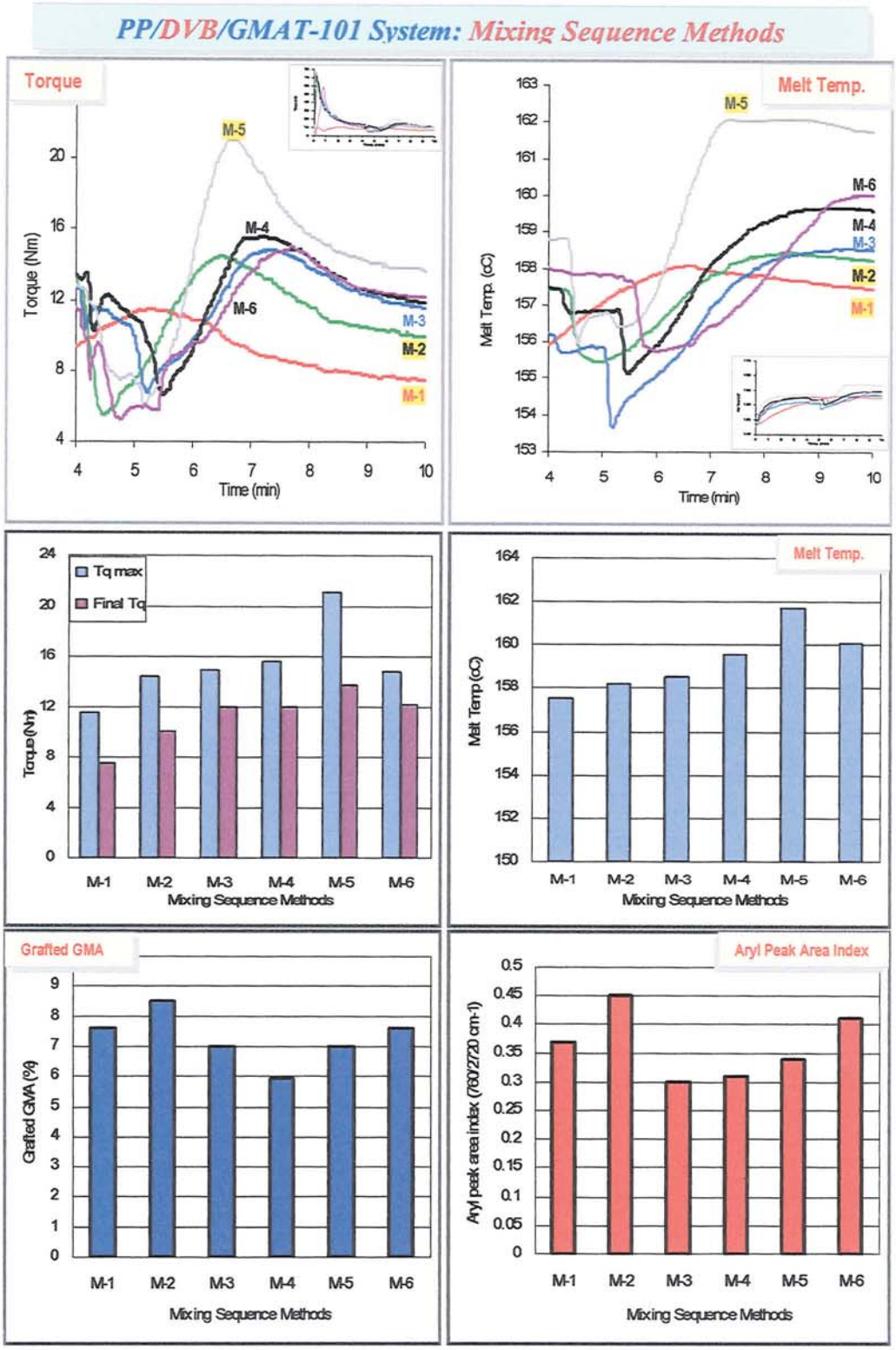

Figure 4.22 Effect of mixing sequence methods (see **Scheme 4.2**, p.199) on torque, melt temp., grafted-GMA, and aryl peak area index of processed PP/DVB/GMA/T-101 system. (Samples; GV-M1 to GV-M6 in Table C.4.5 Appendix C; [GMA]i = 12%, [DVB] = 2/8 weight ratio to GMA, [T-101] = 0.005 molar ratio to GMA+DVB, temp. 160°C, 65 rpm, 10 min) (inset = full scale curves).

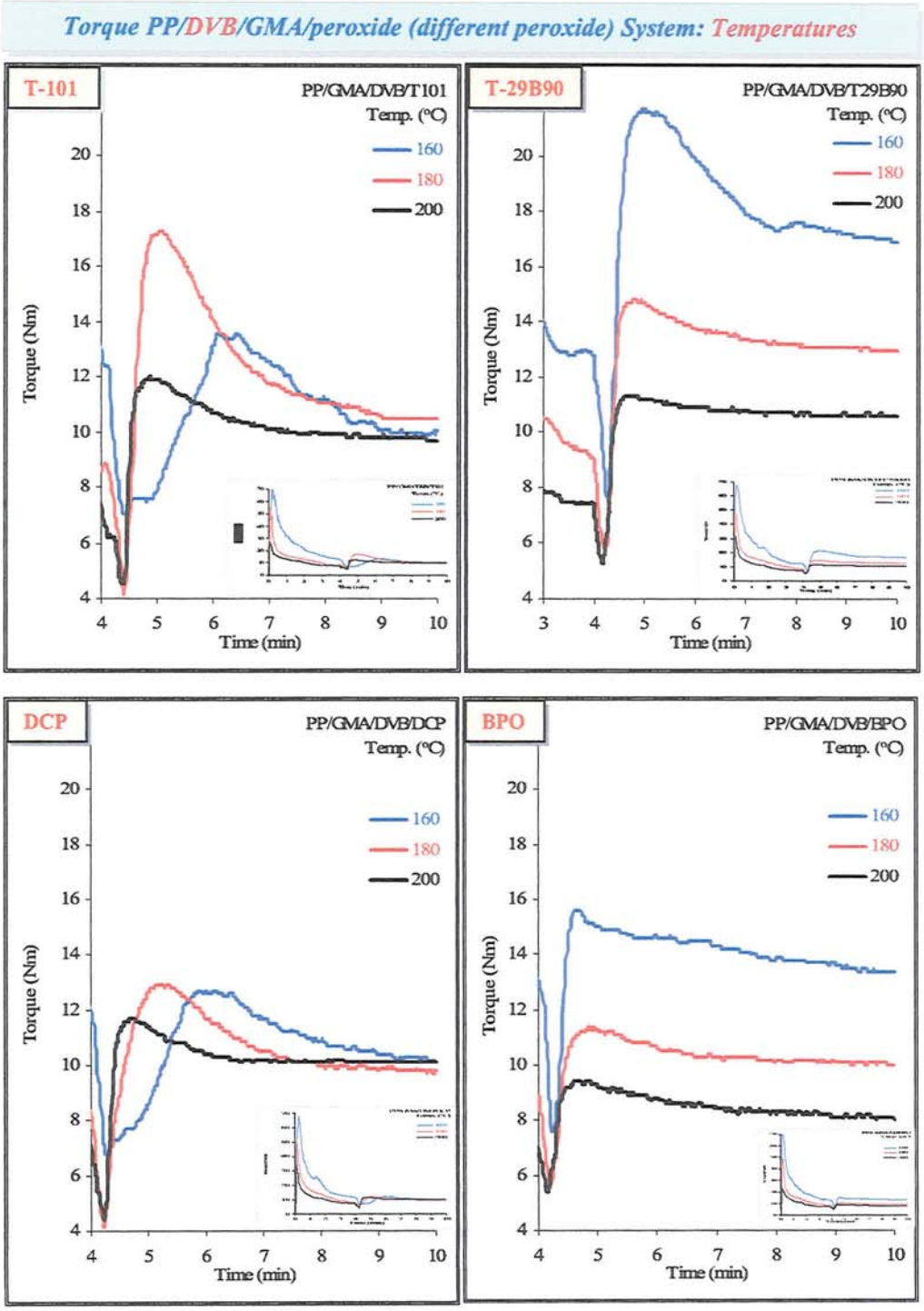

Figure 4.23 Effect of temperatures on torque-time curves of processed PP/DVB/GMA/peroxide (different peroxides). (for T-101 samples GV1-n in Table C.4.5), for T-29B90 samples GV9-n in Table C.4.6, for DCP samples GV15-n in Table C.4.7, and for BPO samples GV17-n in Table C.4.8 Appendix C; PP-Elf, [GMA]i = 12 %, [DVB] = 2/8 weight ratio to GMA, [perox] = 0.005 molar ratio to GMA+DVB, 65 rpm, 10 min, mixing method M-2) (Inset: full scale curves).

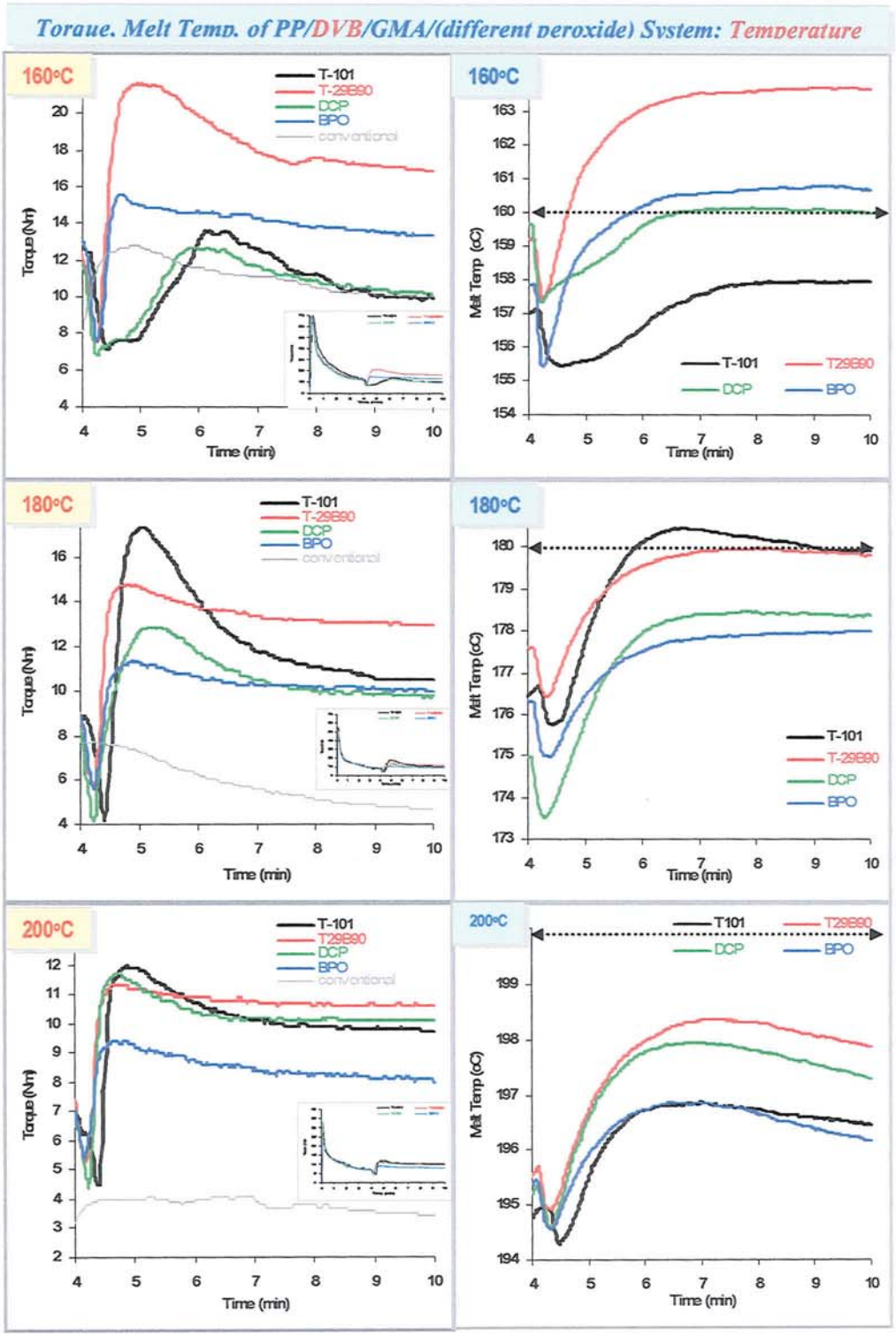

Figure 4.24 Comparison effect of type peroxide on torque and melt temperature of the processed PP/GMA/DVB/peroxide in various temperatures. (Samples: T-101 (GV1-n in Table C.4.5), T-29B90 (GV9-n in Table C.4.6), DCP (GV15-n in Table C.4.7), and BPO (GV17-n in Table C.4.8 Appendix C); PP-Elf, [GMA]i = 12%, [DVB] = 2/8 weight ratio to GMA, [perox.] = 0.005 molar ratio to GMA+DVB, 65 rpm, 10 min, mixing method M-2) (inset = full scale curves).

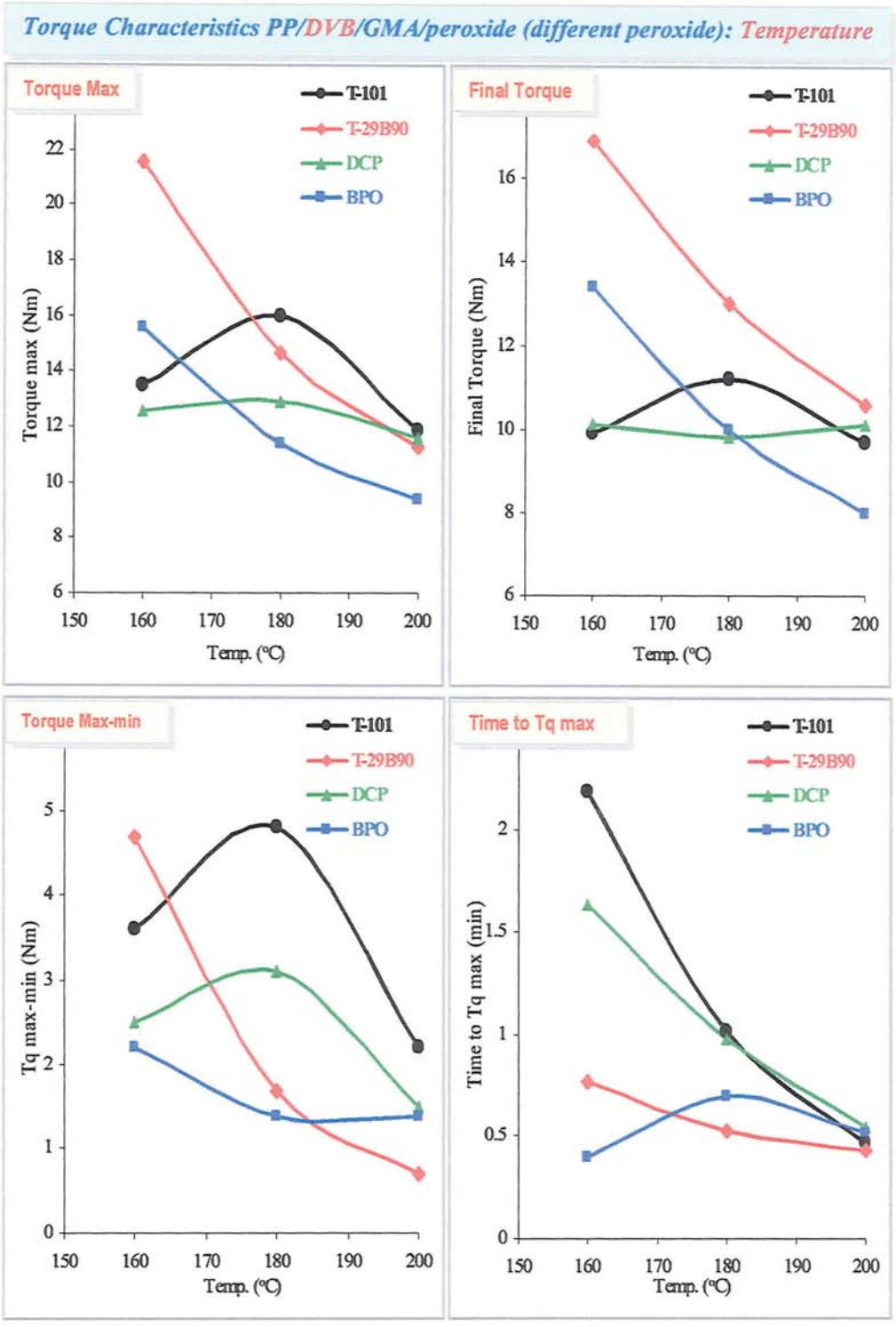

Figure 4.25 Comparison effect of temperature on torque characteristic of processed PP/GMA/DVB/peroxide (different peroxide) system. (Samples: T-101 (GV1-n in Table C.4.5), T-29B90 (GV9-n in Table C.4.6), DCP (GV15-n in Table C.4.7), and BPO (GV17-n in Table C.4.8 Appendix C); PP-Elf, [GMA]i = 12%, [DVB] = 2/8 weight ratio to GMA, [perox.] = 0.005 molar ratio to GMA+DVB, 65 rpm, 10 min, mixing method M-2).

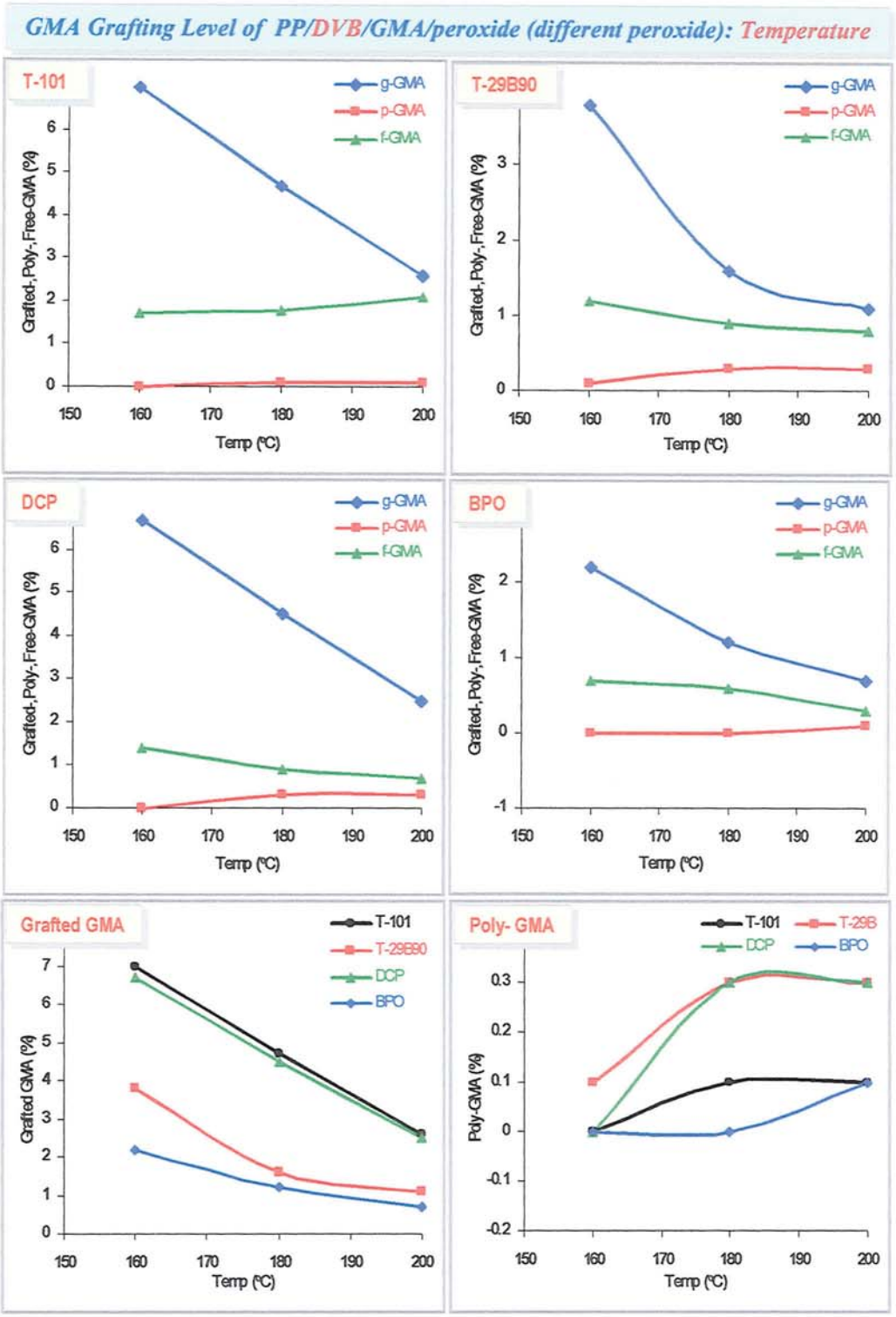

Figure 4.26 Effect of temperature on grafting level and poly-GMA of the PP/GMA/DVB/peroxides (different peroxide) system. Samples: T-101 (GV1-n in Table C.4.5), T-29B90 (GV9-n in Table C.4.6), DCP (GV15-n in Table C.4.7), and BPO (GV17-n in Table C.4.8 Appendix C); PP-Elf, [GMA]i = 12%, [DVB] = 2/8 weight ratio to GMA, [perox.] = 0.005 molar ratio to GMA+DVB, 65 rpm, 10 min, mixing method M-2).

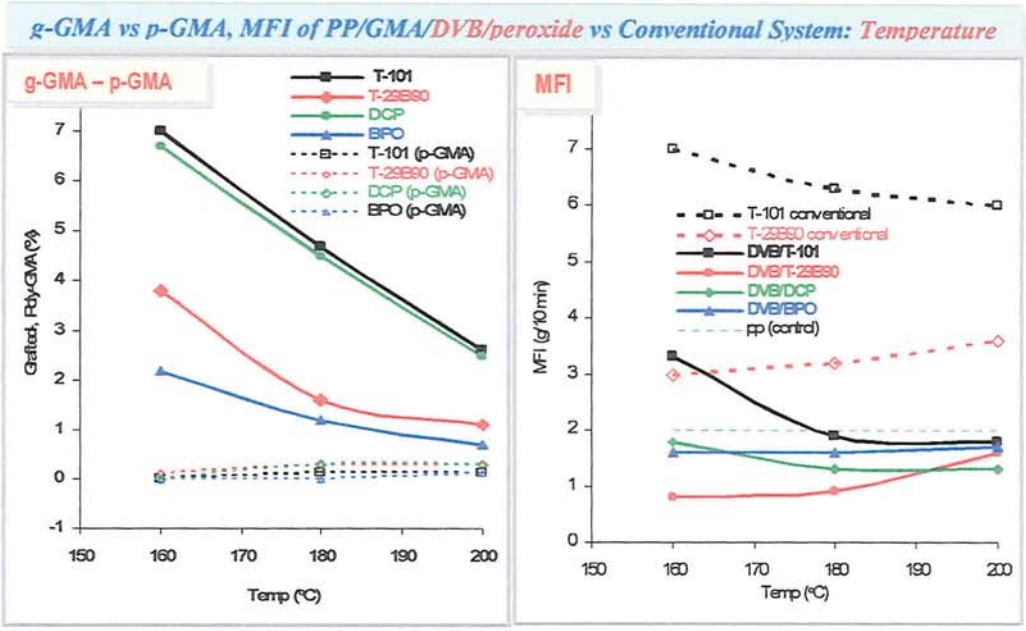

Figure 4.27A Comparison effect of temperature on grafted-GMA, poly-GMA and MFI of the processed PP/GMA/**DVB**/peroxides (different peroxides) compared with the conventional system. (Samples: T-101 (GV1-n in Table C.4.5), T-29B90 (GV9-n in Table C.4.6), DCP (GV15-n in Table C.4.7), and BPO (GV17-n in Table C.4.8 Appendix C); (PP-Elf, [GMA]i = 12%, [DVB] = 2/8 weight ratio to GMA, [perox.] = 0.005 mr, 65 rpm, 10 min, mixing method M-2).

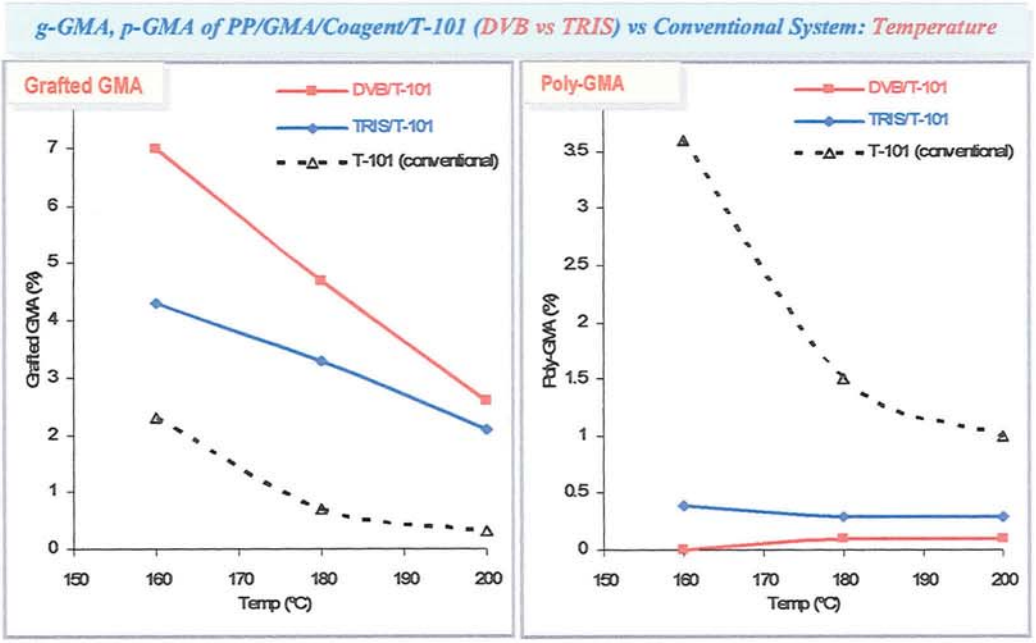

Figure 4.27B Comparison effect of temperature on grafted-GMA and poly-GMA of processed PP/GMA/***coagent***/T-101 (different coagents, DVB or TRIS) and compared to the conventional system. (Samples: DVB (GV1-n in Table C.4.5) and TRIS (GT17-n in Table C.4.8 Appendix C); PP-Elf, [GMA]i = 12%, [coagent] = 2/8 weight ratio to GMA, [T-101] = 0.005 molar ratio to GMA or GMA+coagent, 65 rpm, 10 min, mixing method M-2).

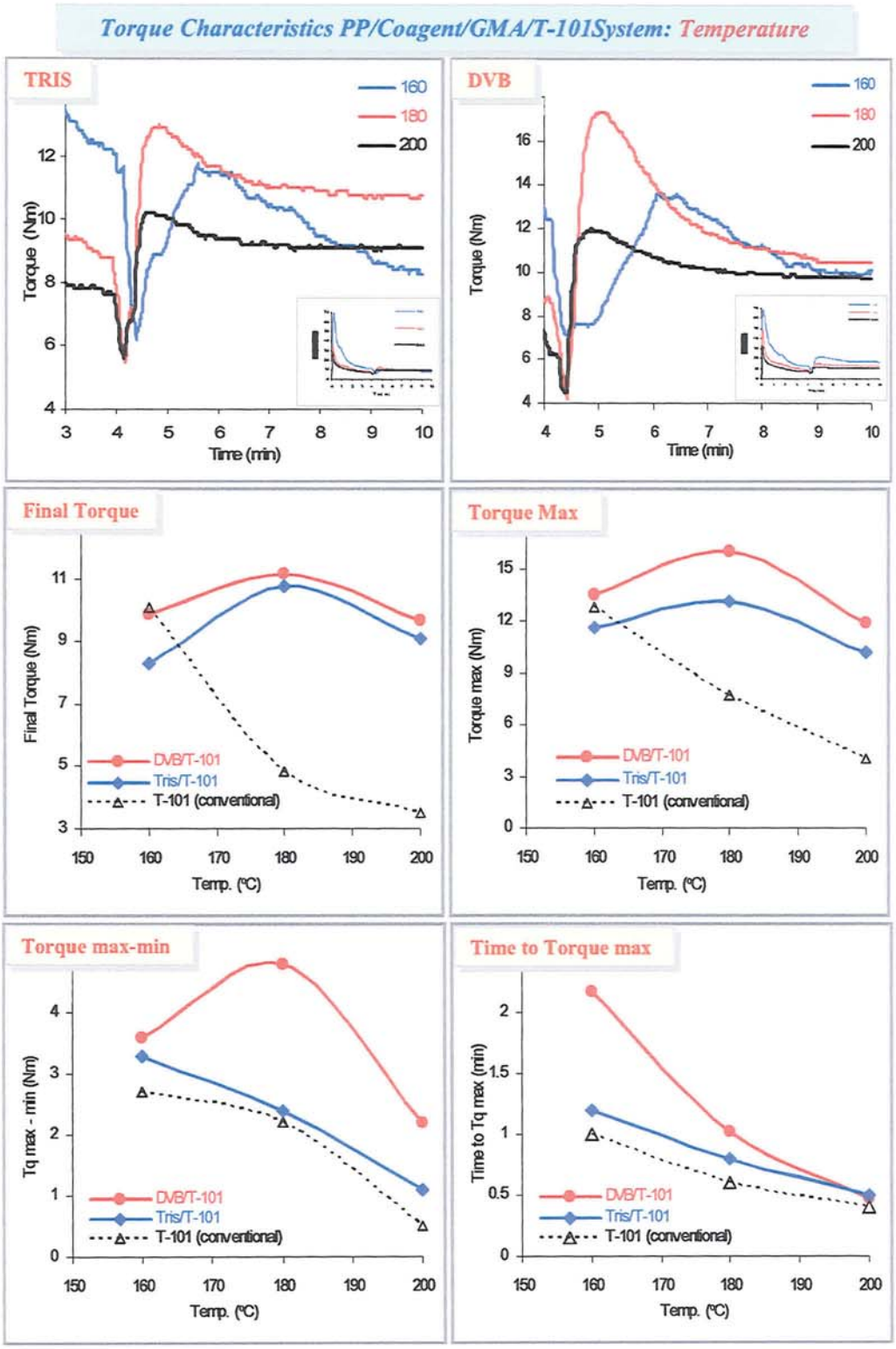

Figure 4.28 Comparison effect of temperature on torque characteristics of the processed PP/GMA/*coagent*/T-101 (different coagent) and compared to the conventional system. Samples DVB (GV1-n in Table C.4.5) and TRIS (GT17-n in Table C.4.8 Appendix C); PP-Elf, [GMA]i = 12%, [coagent] = 2/8 weight ratio to GMA, [T-101 = 0.005 molar ratio to GMA+DVB, 65 rpm, 10 min, mixing method M-2) (inset = full scale curves).

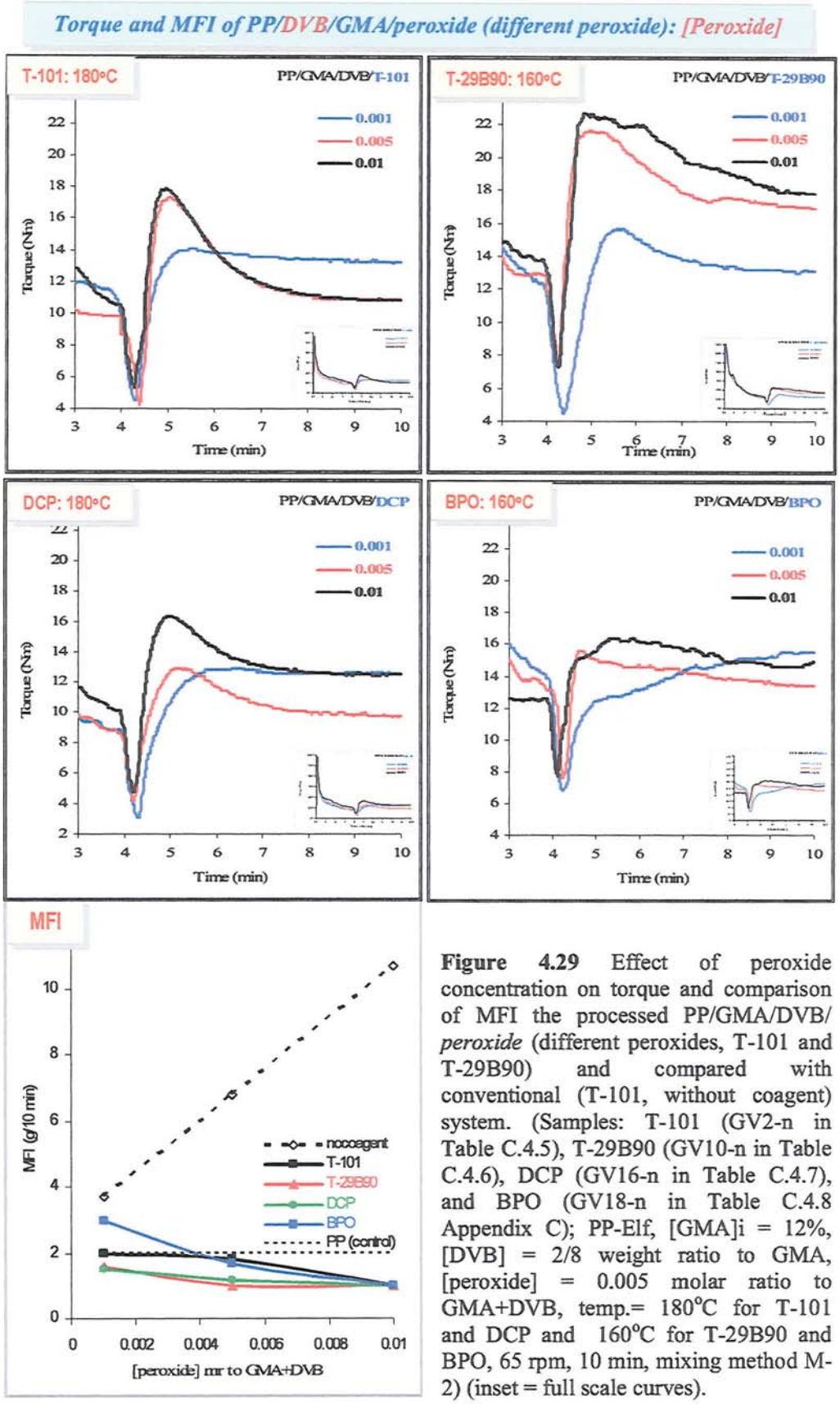

Figure 4.29 Effect of peroxide concentration on torque and comparison of MFI the processed PP/GMA/DVB/ *peroxide* (different peroxides, T-101 and T-29B90) and compared with conventional (T-101, without coagent) system. (Samples: T-101 (GV2-n in Table C.4.5), T-29B90 (GV10-n in Table C.4.6), DCP (GV16-n in Table C.4.7), and BPO (GV18-n in Table C.4.8 Appendix C); PP-Elf, [GMA]i = 12%, [DVB] = 2/8 weight ratio to GMA, [peroxide] = 0.005 molar ratio to GMA+DVB, temp.= 180°C for T-101 and DCP and 160°C for T-29B90 and BPO, 65 rpm, 10 min, mixing method M-2) (inset = full scale curves).

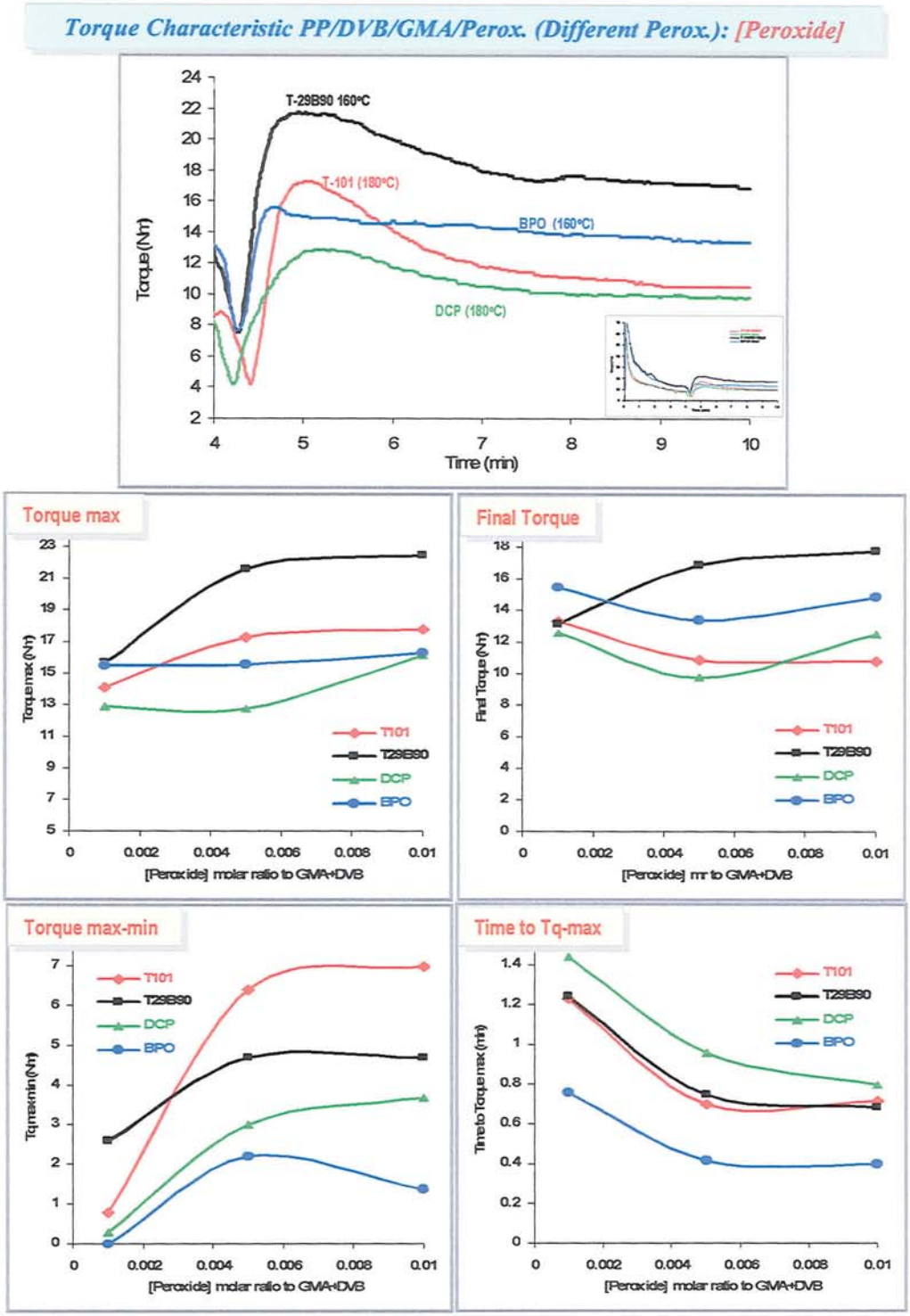

Figure 4.30 Comparison effect of peroxide concentration on torque characteristics of processed PP/GMA/DVB/peroxide (different peroxide) system. (Samples T-101 (GV2-n in Table C.4.5), T-29B90 (GV10-n in Table C.4.6), DCP (GV16-n in Table C.4.7), and BPO (GV18-n in Table C.4.8 Appendix C); PP-Elf, [GMA]i=12%, [DVB]=2/8 weight ratio to GMA, [peroxide] = 0.001-0.005 molar ratio to GMA+DVB, temp.= 180°C for T-101 and DCP and 160°C for T-29B90 and BPO, 65 rpm, 10 min, mixing methods M-2) (inset = full scale curves).

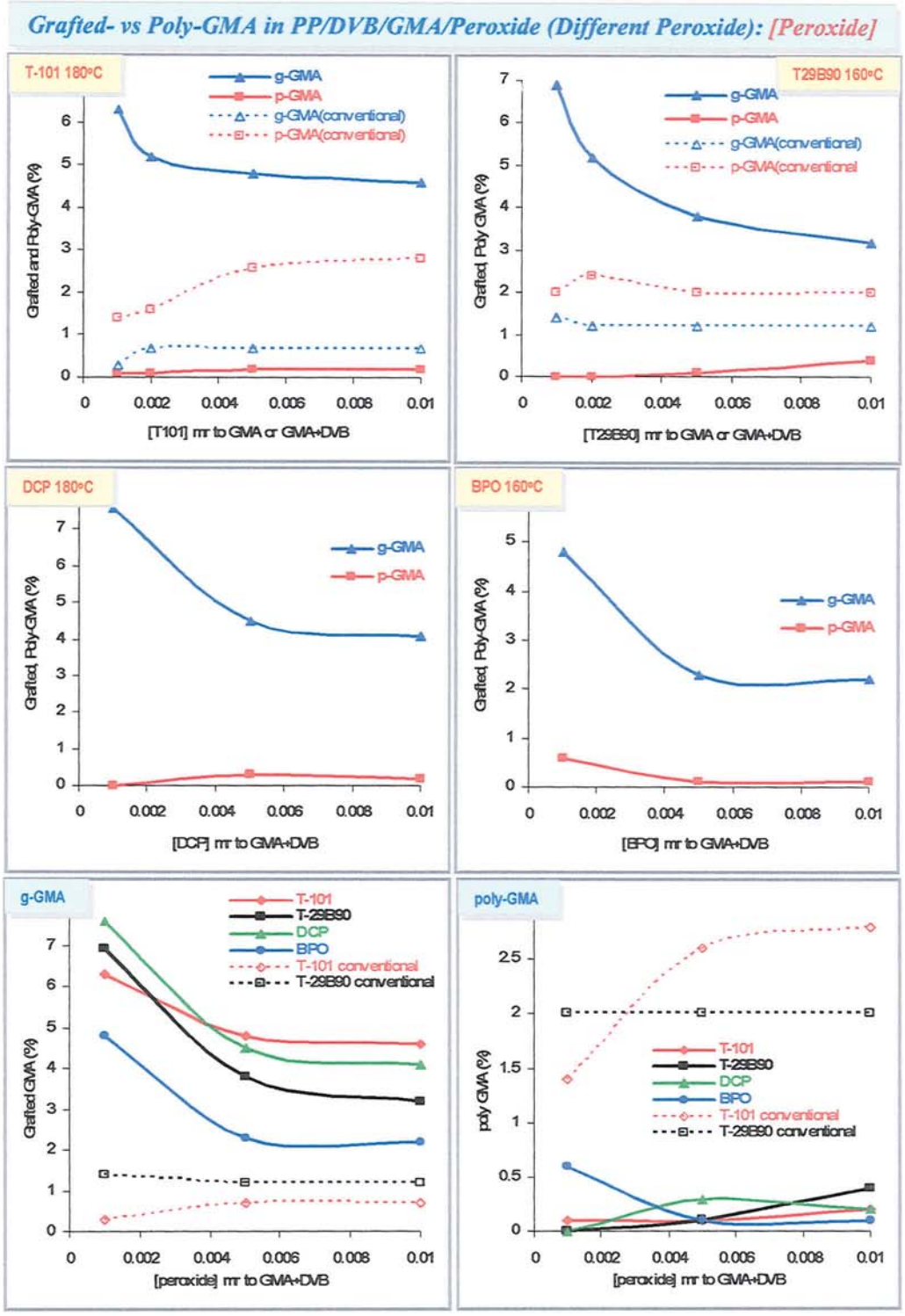

Figure 4.31 Comparison effect of peroxide concentration on GMA grafting level and poly-GMA of processed PP/GMA/DVB/*peroxides* (different peroxides) system. (Samples T-101 (GV2-n in Table C.4.5), T-29B90 (GV10-n in Table C.4.6), DCP (GV16-n in Table C.4.7), and BPO (GV18-n in Table C.4.8 Appendix C); PP-Elf, [GMA]i = 12 %, DVB/GMA = 2:8 w/w %, temp.160°C for T-29B90 and 180°C for T-101, 65 rpm, 10 min, mixing method M-2).

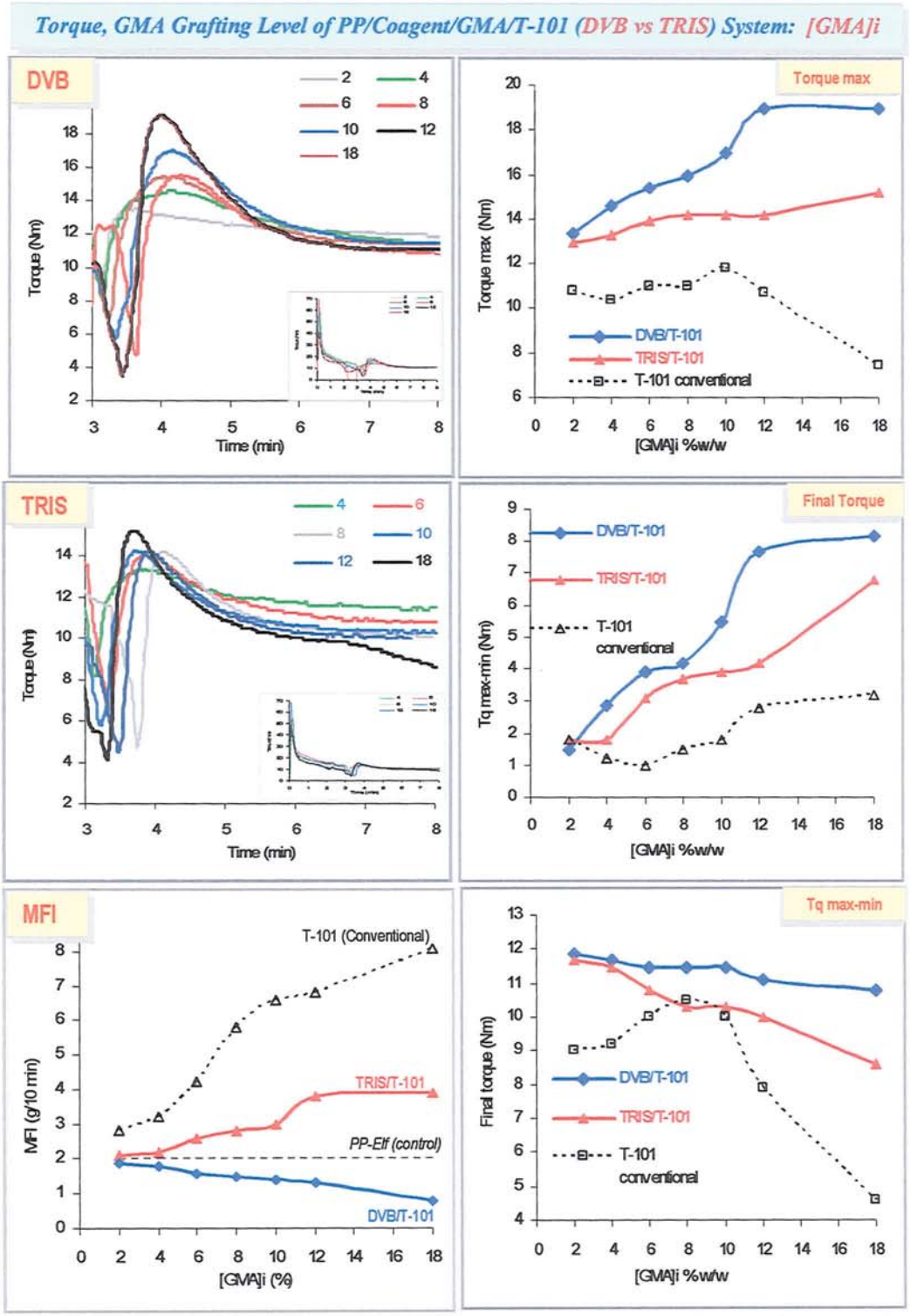

Figure 4.32 Comparison effect of GMA concentration on torque and MFI of processed PP/GMA/*coagent*/T-101 (different coagents, DVB or TRIS) system (Samples TRIS (GT5-n in Table C.4.4) and DVB (GV4-n in Table C.4.5 Appendix C); PP-Elf, [GMA] = 2-18%, [coagent] = 2/8 weight ratio to GMA, [T-101] = 0.005 mr, temp.180°C, 65 rpm, 10 min, mixing method M-3) compared with conventional system (in the absence of coagent, samples G8-n in Table C.4.2 Appendix C) (inset = full scale curves).

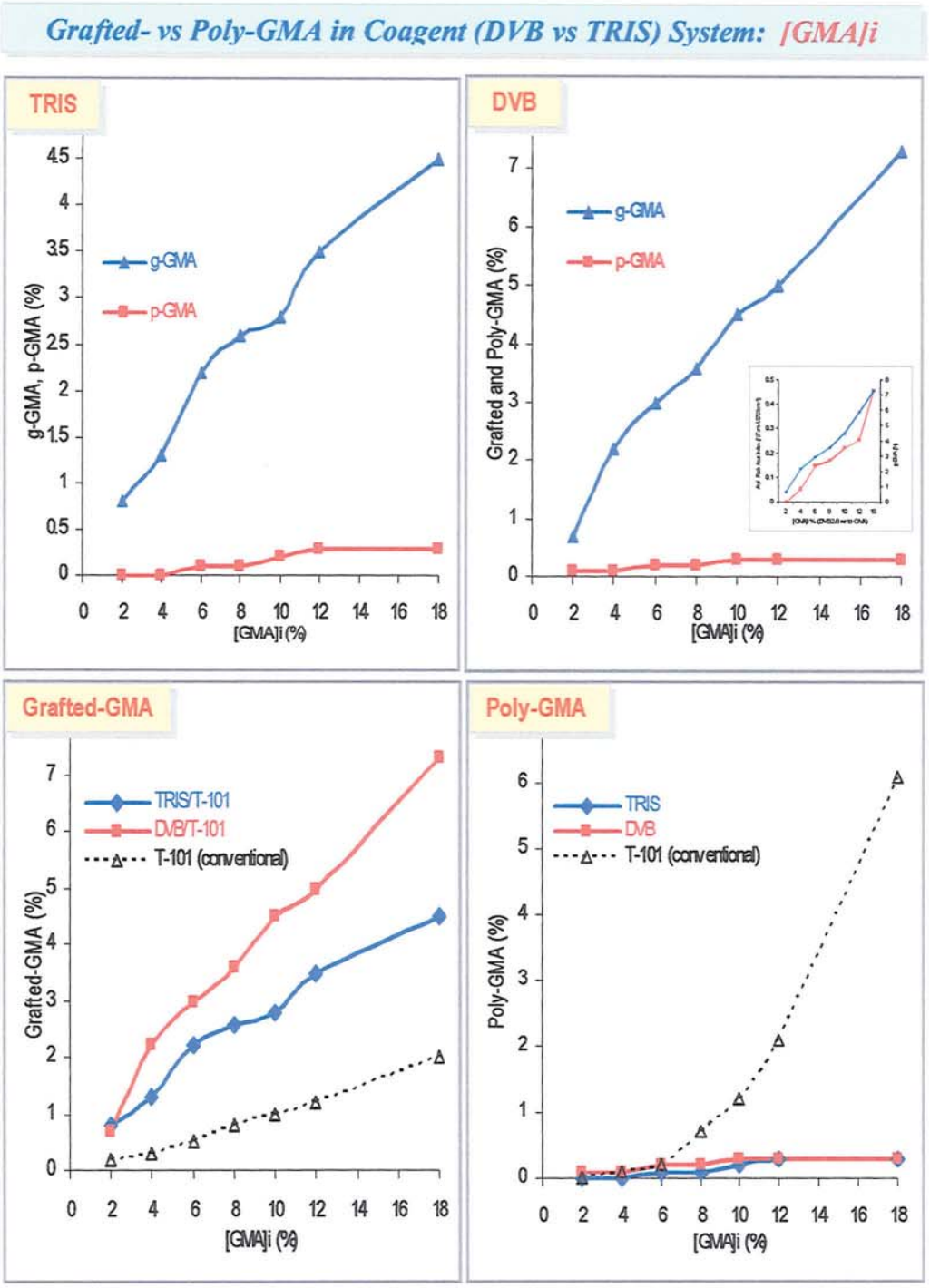

Figure 4.33 Effect of GMA initial concentration on GMA grafting level and the extent of poly-GMA formation of processed PP/GMA/*coagent*/T-101 system and comparison between TRIS (samples GT5-n Table C.4.4) and DVB (samples GV4-n Table C.4.5) and the conventional system (samples G8-n Table 4.2 Appendix C); PP-Elf, [GMA]i = 2-18%, [coagent] = 2/8 weight ratio to GMA, [T-101] = 0.005 molar ratio to GMA+coagent, temp. **180°C**, 65 rpm, 10 min, mixing method M-3) (Inset: Aryl peak area index (red) compared to g-GMA (blue) in DVB/T-101 system).

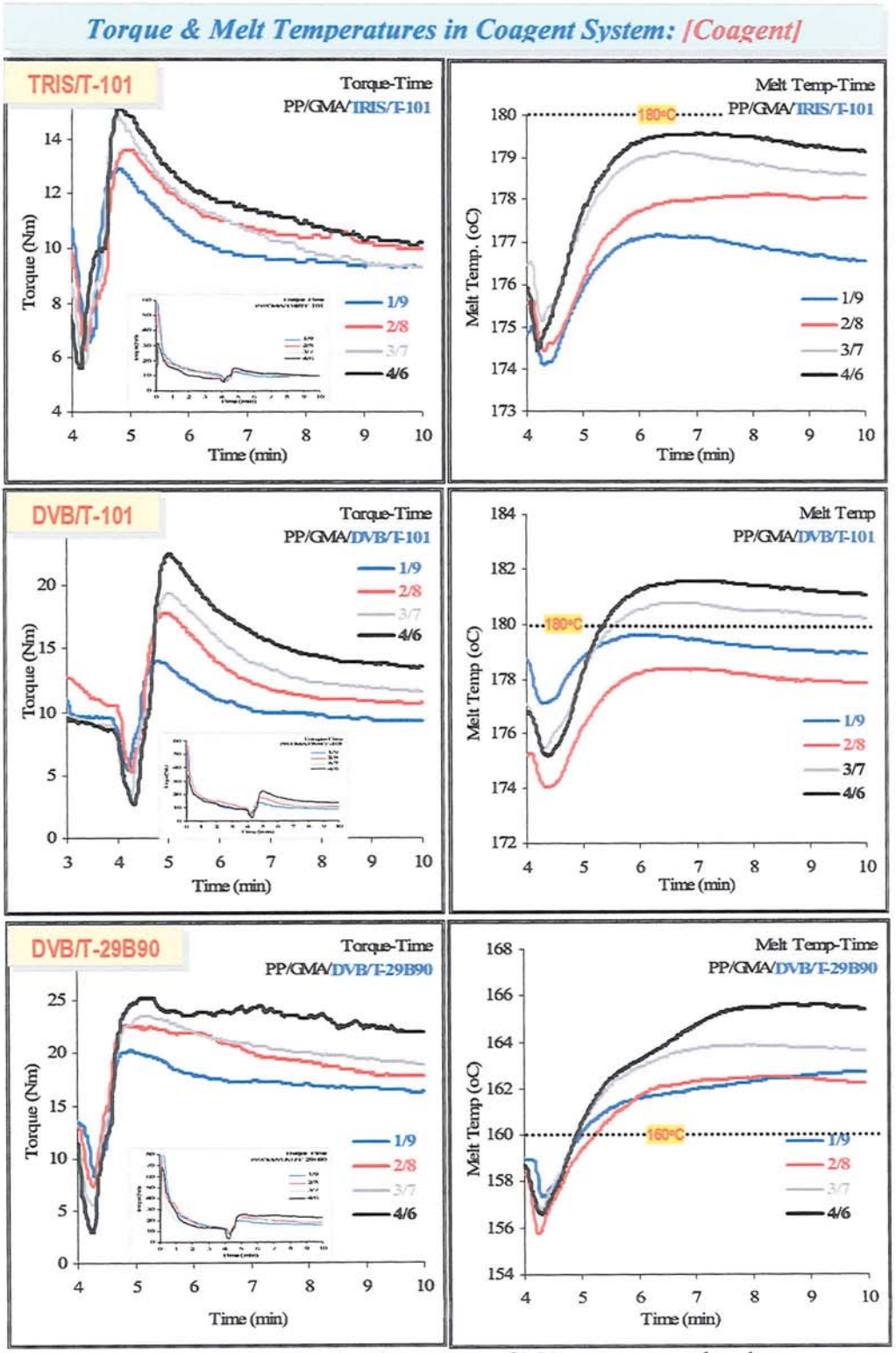

Figure 4.34 Effect of weight ratio of coagent to GMA on torque and melt temperature in processed PP/GMA/coagent/peroxide (different coagent, TRIS or DVB and different of peroxide, T-101 or T-29B90) system. (Samples: PP-Elf, [GMA]i = 12 %, [perox.] = 0.005 molar ratio to [GMA]+[coagent], temp 160°C for T-29B90 and 180°C for T-101, 65 rpm, 10 min, mixing method M-2) (inset = full scale curves).

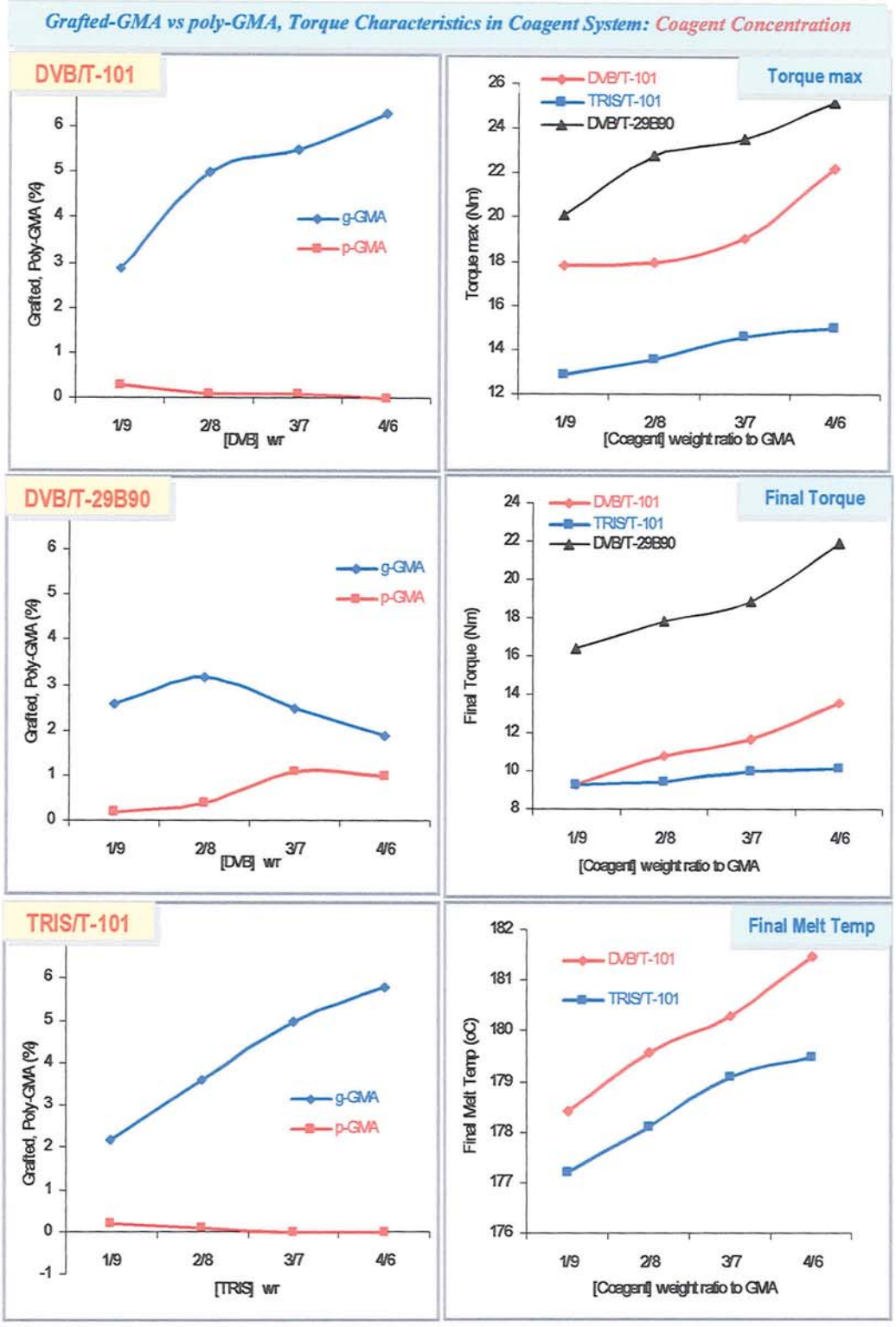

Figure 4.35 Effect of weight ratio coagent to GMA on grafting level and poly-GMA formation and torque characteristics (different coagents, DVB or TRIS, different peroxides T-101 or T-29B90) system. (Samples: PP-Elf, [GMA]i = 12 %, [perox.] = 0.005 mr to GMA+coagent, 160°C for T-29B90, 180°C for T-101, 65 rpm, 10 min, mixing method M-2).

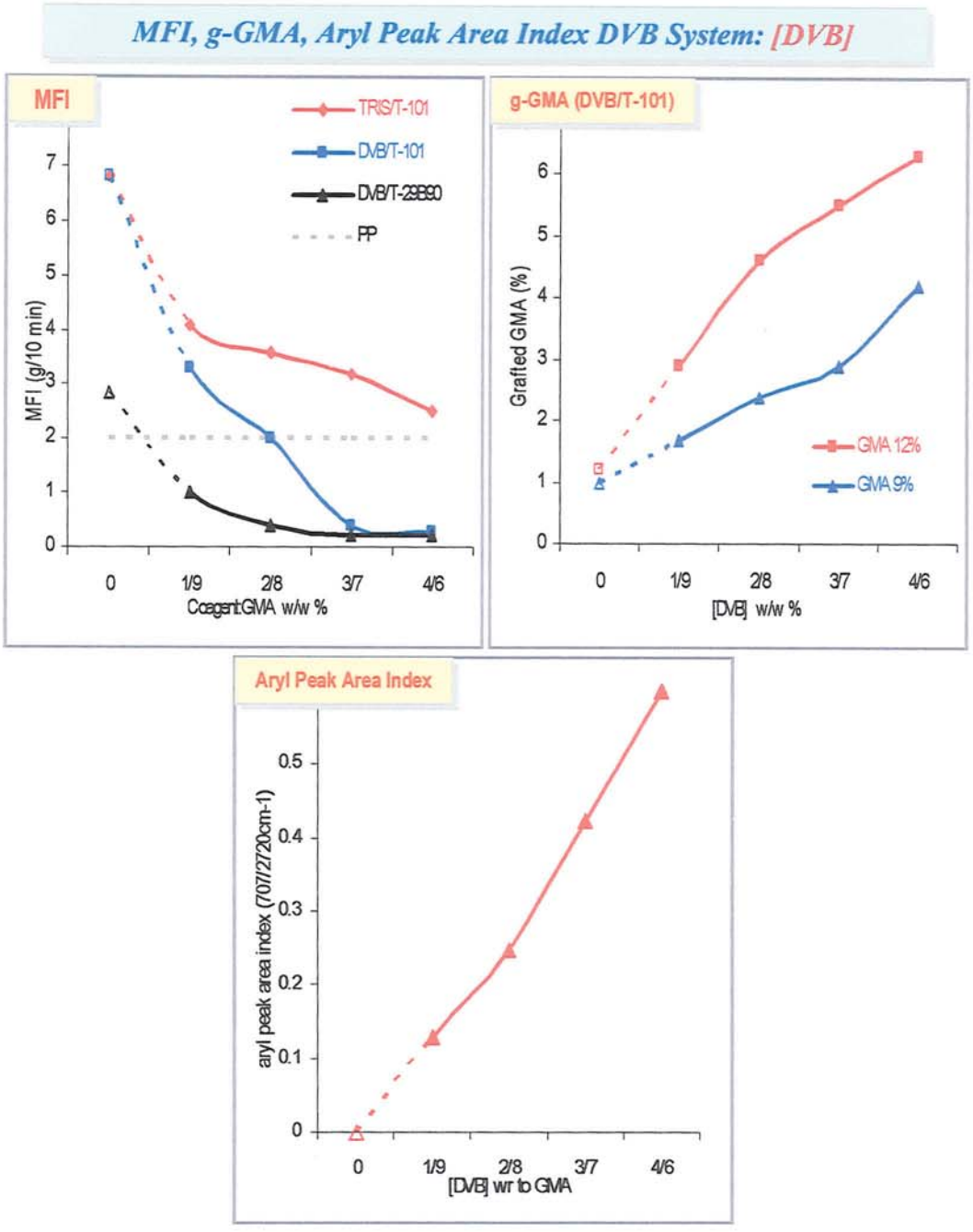

Figure 4.36 Effect of weight ratio of coagent/GMA on MFI and grafted-GMA of processed PP/coagent/GMA/peroxide (different coagents, TRIS or DVB and different peroxides, T-101 or T-29B90) system. (Samples: PP-Elf, [GMA]i = 9 and 12 %, [perox.] = 0.005 molar ratio to [GMA]+[coagent], temp 160°C for T-29B90 and 180°C for T-101, 65 rpm, 10 min, mixing method M-2)

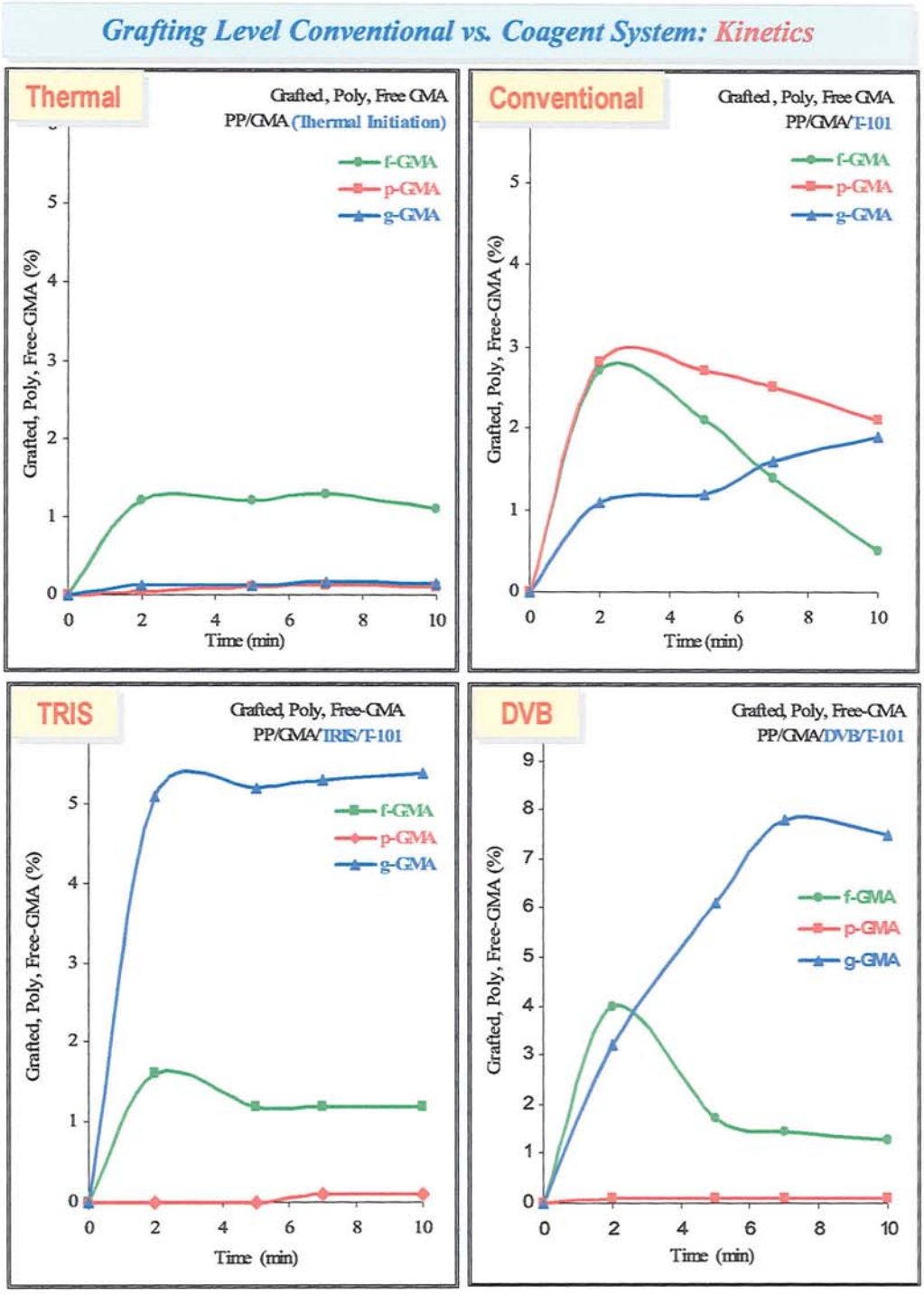

Figure 4.37 Effect of processing time on GMA content in processed PP with GMA by thermal (samples T2-n in Table C.4.1) and peroxide T-101 initiation in absence (G10-n in Table C.4.2) and presence of coagent TRIS (GT15-n in Table C.4.4) or DVB (GV8-n in Table C.4.5 Appendix C); PP-Elf, [GMA]i = 12 %, [coagent] = 2/8 weight ratio to GMA, [T-101] = 0.005 molar ratio to GMA+coagent, temp. **160°C**, 65 rpm, mixing method M-2) (***f-*** = free-, ***p-*** = poly-, and ***g-*** = grafted-GMA).

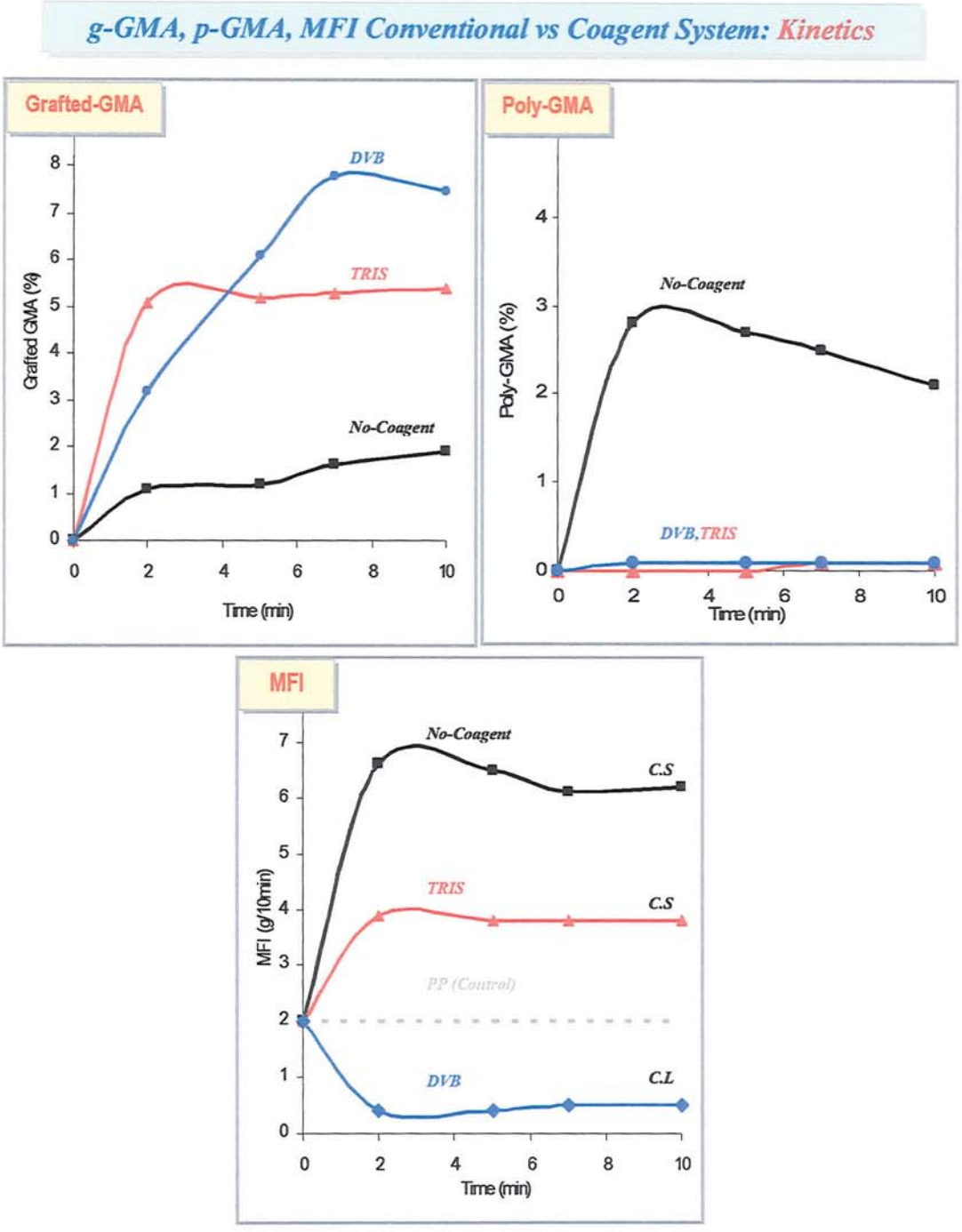

Figure 4.38 Comparison effect of processing time on GMA grafting level, poly-GMA and MFI of processed PP with GMA in the absence (sample G10-n in Table C.4.2) and the presence of coagent, TRIS (sample GT15-n in Table C.4.4) or DVB (sample GV8-n in Table C.4.5 Appendix C); PP-Elf, [GMA]i = 12 %, [coagent] = 2/8 weight ratio to GMA, [T-101] = 0.005 molar ratio to GMA+coagent, temp. 160°C, 65 rpm, method M-2) (PP control at MFI curve is a processed PP-Elf at temp 160°C, 65 rpm).

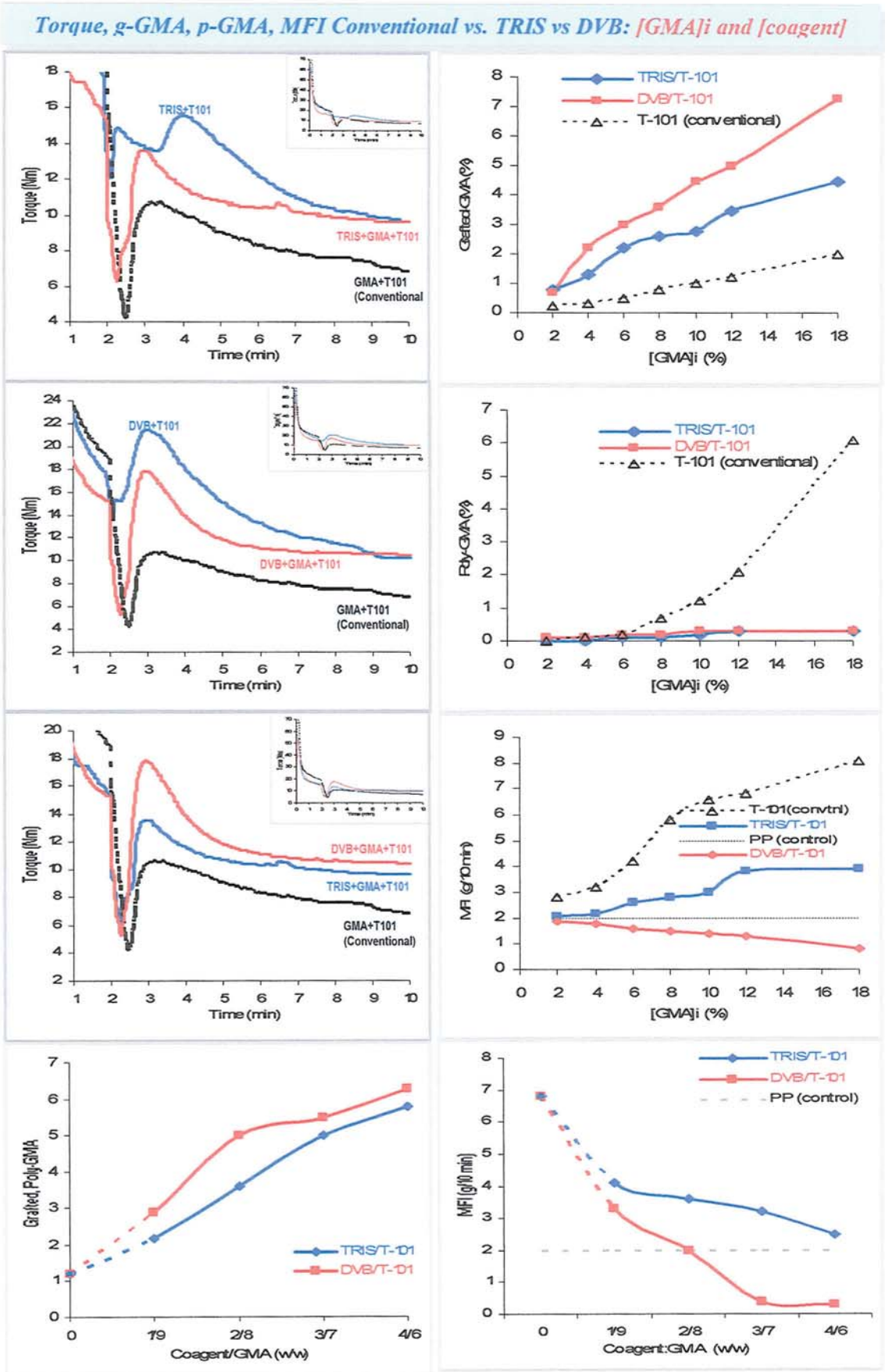

Figure 4.39 Comparison of torque, GMA grafting level, the extent of poly-GMA, MFI in different PP-GMA grafting system, in the absence (conventional) and presence of coagent, TRIS or DVB. (Samples: PP-Elf, [GMA]i = 12 %, [T-101] = 0.005 molar ratio to GMA+coagent, temp 180°C, 65 rpm, 10 min, mixing method M-2) (inset = full scale curves).

CHAPTER 5
FUNCTIONALISATION OF POLYPROPYLENE WITH MA

5.1. OBJECTIVES AND METHODOLOGY

Maleic anhydride (MA) **(I)** has been one of the most important modifiers for polyolefin, because of its low cost, low extent of homopolymerisation (due to deficiency of electrons in the double bond) [79,411] and high reactivity of the anhydride group in successive reactions [1]. As a result, MA-modified polyolefins are used in many commercial applications, such as glass fiber reinforced polyolefins [412], anticorrosive coatings for metal pipes and containers [413], multilayer sheets of paper for chemical and food packaging [414], and in polymer blends e.g. with polyamides [224-243] and polyesters [244-250]. Generally, MA-grafted onto PP is prepared by free radical grafting reaction in the presence of an organic peroxide initiator either in the melt [171-187], in the solid state [52,415], or in solution [158,181]. In most cases however, the grafting yield of MA is low and the grafting reaction is generally accompanied by various side reactions.

(I) Maleic Anhydride (MA)

In order to increase the grafting yield, a high peroxide concentration is generally used, but unfortunately, this approach leads to degradation of the polymer backbone and consequently to reduction of its desired physical properties. It has been shown that the addition of styrene (St) as a second monomer (comonomer) in the melt grafting system results in an increase in the grafting degree of MA on PP [161,168,187]. Styrene reacts with polypropylene much faster than does MA, and the resulting PP-St• macroradical copolymerise readily with MA [161,187]. A different approach developed previously at Aston University-PPP Group [96-98,108,129], utilises a highly reactive comonomers with two or more reactive functions, an approach used in this work with both GMA (in Chapter 4) and with MA (this chapter). In this study, the grafting reaction of MA on PP was carried out in a closed chamber of an internal mixer by free radical initiation using four different peroxides; 2,5-di(*tert*-butylperoxy)-2,5-dimethylhexane (Trigonox-101, T-101) **(II)**, 1,1-di(*tert*-butylperoxy)-3,3,5-trimethyl cyclohexane (Trigonox-29B90, T-29B90) **(III)**, dicumyl peroxide (DCP) **(IV)**, and benzoyl peroxide (BPO) **(V)** in the absence or presence of one of two reactive coagents; trimethylolpropane trimethacrylate, TRIS **(VI)** and divinyl benzene, DVB **(VII)**.

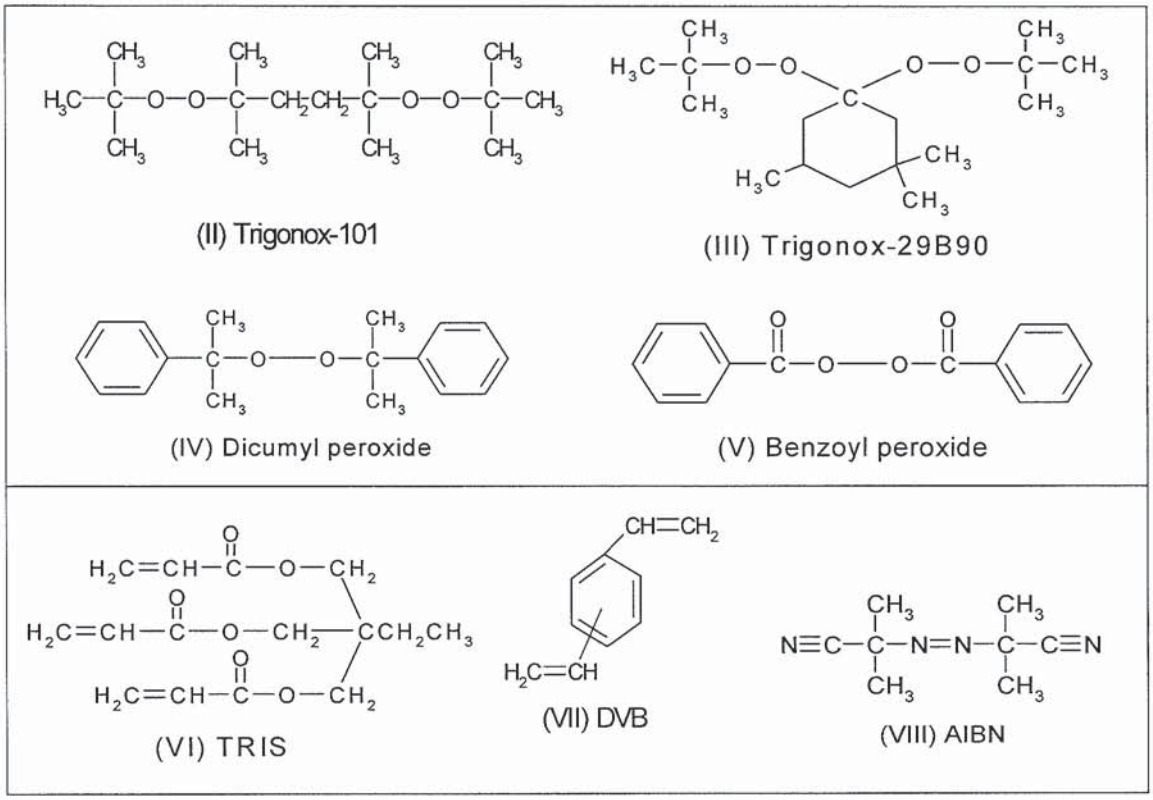

A summary of the processing methods used is shown in **Scheme 5.1** (p.295). The methodology and processing conditions were varied in order to optimise the grafting reaction as follows:

(a) Processing temperature, 140 - 200°C.
(b) Processing time, 2-10 min.
(c) Concentration of MA (2 - 18 wt %)
(d) Concentration of TRIS or DVB (1/9 - 4/6 weight ratio to MA)
(e) Concentration of peroxides (0.001 – 0.3 molar ratio to MA)
(f) Addition mixing sequence (see **Scheme 5.1** and **5.2**)

The reaction products were purified by means of Soxhlet extraction, precipitation and hot drying in vacuum oven (**Scheme 5.3**, p.297). The extent of MA grafting was evaluated by titration (**Scheme 5.4**, p.298) and/or FTIR methods (**Scheme 5.3**). The side reaction products, MA-co-TRIS or MA-co-DVB were polymerised on the bench using an initiator Azo-iso-butyronitrile, AIBN **(VIII)** and were characterised by FTIR (for poly TRIS and poly DVB see **Section 4.2.1.2** and **4.2.1.3** in **Chapter 4**, pp. 165,166). The melt grafting of PP with the coagents (in absence of MA) was also conducted to investigate the reactivity of the coagents. **Tables D.5.1** to **D.5.10** (in Appendix D) list the experimental composition and results for the grafting of MA on PP by thermal and free radical initiation (using different types of peroxides) in the presence or absence of the coagents TRIS and DVB.

5.2 RESULTS

5.2.1. Characterisation of side Reaction Products

Similar to the grafting of GMA on PP in the presence of the coagents TRIS and DVB (**Section 4.2.1** in **Chapter 4**, p.164), homopolymerisation and copolymerisation reactions of the above coagents with the reactive modifier MA can take place during melt processing. To analyse the side reaction products, copolymerisation of MA with TRIS and with DVB was carried out on the bench in the presence of Azo-iso-butyronitrile (AIBN) as initiator and the reaction products (MA-co-TRIS and MA-co-DVB) were characterised by FTIR. The characterisation of the other possible side reaction products poly-TRIS and poly-DVB was described in **Section 4.2.1.2** and **4.2.1.3** in **Chapter 4**.

i. Characterisation of MA-co-TRIS

The copolymer was found not to be soluble in acetone and dichloromethane (DCM). **Figure 5.1** and **Table D5.11** (in Appendix D) show the infrared and assignment for the MA-co-TRIS copolymer. The IR shows the disappearance of all peaks due to double bond absorptions, present in the original monomers TRIS and MA at 1632 cm^{-1}, 1588 cm^{-1}, and 1566 cm^{-1} (υC=C, vinylidene double bond stretching), and the peaks at 1433 cm^{-1}, 1288 cm^{-1}, 1266 cm^{-1}, 1056 cm^{-1}, 894 cm^{-1}, and 870 cm^{-1} (C-H deformation, δCH=CH, C-H twisting, τCH=CH, C-H wagging, ωCH=CH, respectively). Furthermore, the presence of carbonyl absorptions (υC=O) due to succinyl anhydride at 1860 cm^{-1} and 1782 cm^{-1} attributed to symmetric and asymmetric stretching together with an ester peak at 1733 cm^{-1} characterised as carbonyl stretching of ester groups (c.f. υC=O ester of poly TRIS are shown at 1734 cm^{-1}) and that of the C-O-C stretching at 1167 cm^{-1} (c.f. of neat MA and poly TRIS at 1240 cm^{-1} and 1158 cm^{-1}, respectively) confirm the formation of the copolymer (see **Rn 5.1**).

Reaction 5.1

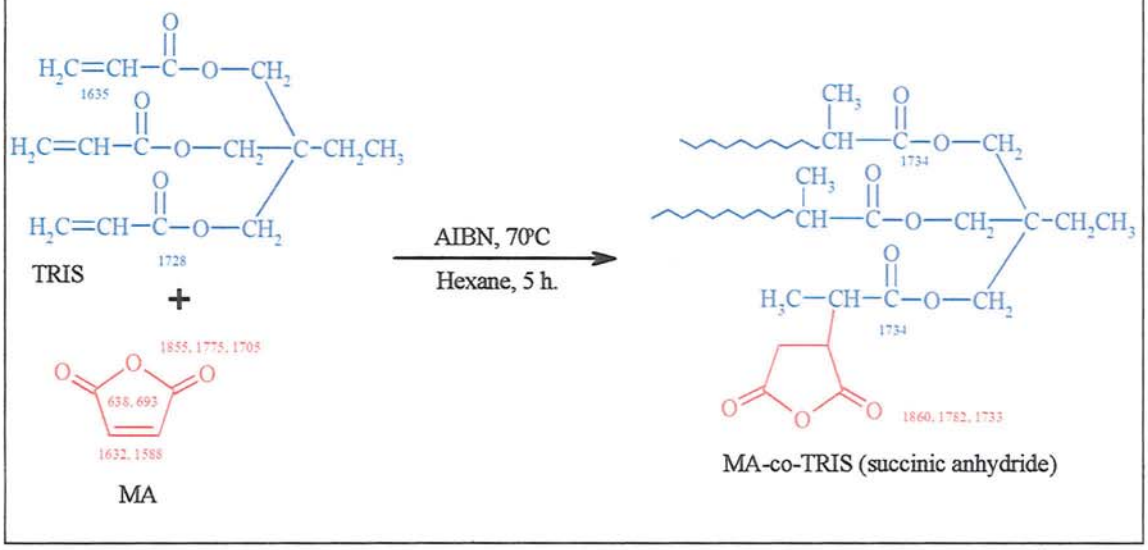

ii. Characterization of MA-co-DVB

The copolymer was found not to be soluble in acetone and dichloromethane (DCM) in which the monomers are soluble. **Figure 5.2** which gives the IR of MA-co-DVB (see **Table D5.11** in Appendix D for its infrared and assignment), shows the disappearance of

all frequencies due to the double bond absorptions, present in the original monomers DVB and MA, at 1632 cm^{-1} , 1588 cm^{-1}, and 1566 cm^{-1} (for MA υC=C, vinylidene double bond stretching), at 1288 cm^{-1}, 1266 cm^{-1}, and 1240 cm^{-1} (MA C-H bending vinylidene, δCH=CH out of plane and in plane), at 894 cm^{-1}, 870 cm^{-1}, 833 cm^{-1} and 693 cm^{-1} (the first two due to C-H twisting, τCH=CH, and the latter due to C-H wagging, ϖCH=CH). The spectrum also shows the presence of carbonyl absorptions (υC=O) due to succinyl anhydride at 1860 cm^{-1} and 1777 cm^{-1} (υC=O asymmetric and symmetric) and that of the υC-O-C and methyl group stretching absorptions at 1223 cm^{-1}, 1082 cm^{-1}, 926 cm^{-1}. Furthermore, absorptions due to DVB at 714 cm^{-1} corresponding to aryl absorption (similar to that of poly DVB at 708 cm^{-1}), and these IR characteristics confirm the MA-co-DVB copolymer formation (see **Rn-5.2**).

Reaction 5.2

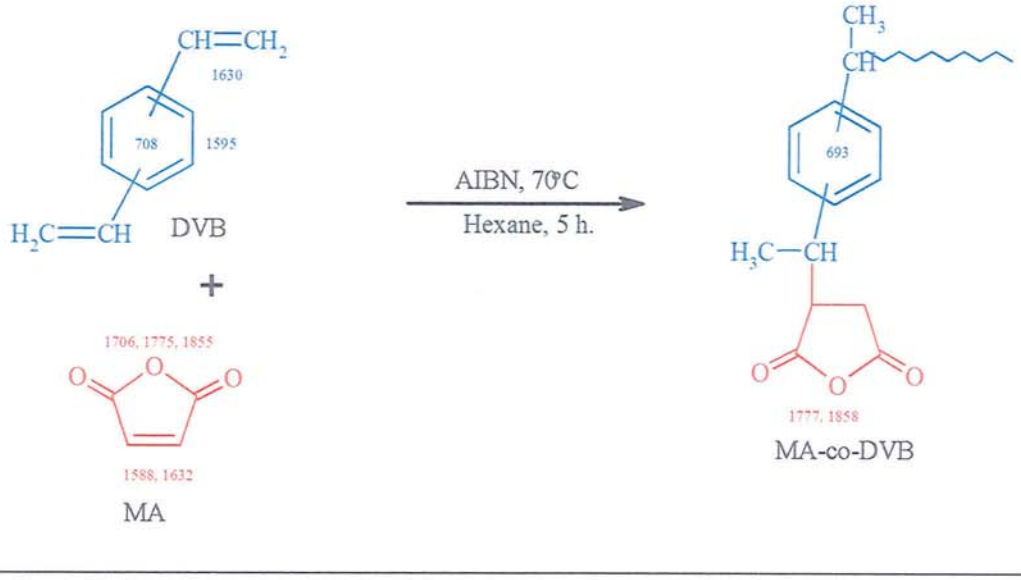

iii. Characterization of Grafted TRIS on PP

The melt grafting reaction of TRIS on PP (PP-g-TRIS) was also carried out in the torque rheometer as described in **Scheme 5.1** (p.295) using a fixed peroxide concentration but with exclusion of MA ([TRIS] = 5 %, [T-101] = 0.005 molar ratio to TRIS, 180°C, 65 rpm, 10 min). The reaction product (PP-g-TRIS) was purified by acetone precipitation (**Scheme 5.3**, p.297) and the purified film was characterised by FTIR. **Figure 5.3** shows a comparison of FTIR spectra of PP-g-TRIS film with that of PP-alone (as film) and TRIS (in

KBr disk). The grafted TRIS spectrum showed the appearance of saturated carbonyl stretching absorption (υC=O) at 1736 cm^{-1} (originally unsaturated ester group in neat TRIS at 1731 cm^{-1}, 1727 cm^{-1} and 1724 cm^{-1}) and the disappearance of the symmetric and asymmetric stretching absorption of acrylate double bond (υC=C) at 1635cm^{-1} and 1617 cm^{-1}, C-H bending (δCH=CH_2) at 1408 cm^{-1}, C-H twisting (τCH=CH_2) at 1295 cm^{-1} and 1269 cm^{-1}, and C-H wagging (ϖCH=CH_2) at 1062 cm^{-1} and 809 cm^{-1} (see **Rn-5.3**).

Reaction 5.3

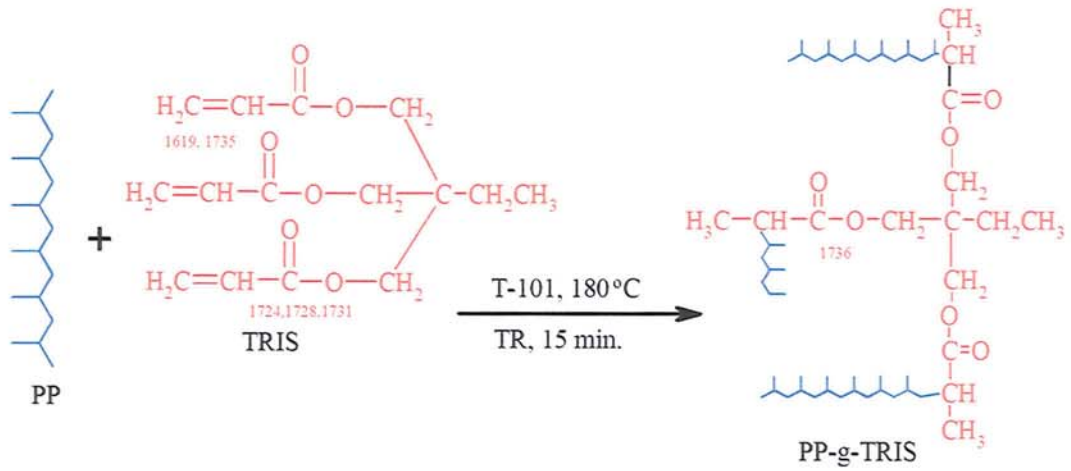

iv. Characterization of Grafted DVB on PP

Similarly, the grafting reaction of DVB on PP (PP-g-DVB) was also done in the torque rheometer using the same methodology described in **Scheme 5.1** (p.295) with a fixed peroxide concentration but with no MA ([DVB] = 5 %, [T-101] = 0.005 molar ratio to DVB, 180°C, 65 rpm, 10 min). The purified reaction product (PP-g-DVB) was pressed into a thin film and characterised by FTIR (see **Scheme 5.3**, p.297). The infrared spectrum of the monomer DVB (in KBr disc) shows important peaks (conjugated vinyl group and aryl double bond) at 1630 cm^{-1}, 1595 cm^{-1}, and 1576 cm^{-1}. The grafted DVB onto PP was characterised by the disappearance of the stretching double bond (υC=C) at 1630 cm^{-1}, 1595 cm^{-1}, and 1576 cm^{-1} (υC=C phenyl ring remains and shifted to 1603 cm^{-1}), C-H bending absorption (δCH=CH_2) at 1510 cm^{-1} and 1485 cm^{-1}, twisting and wagging (τ,ϖCH=CH_2) at 1400 cm^{-1} and 987 cm^{-1}. The absorption peak at 708 cm^{-1} corresponding

to benzene ring absorption appeared in the purified reaction product (for DVB at 707 cm^{-1}). The absorption peaks corresponding to methyl group at 1457 cm^{-1}, 1376 cm^{-1}, 1167 cm^{-1}, 997 cm^{-1}, and 973 cm^{-1} are observed at higher intensity than for PP alone (see **Fig. 5.4** and **Rn-5.4**).

Reaction 5.4

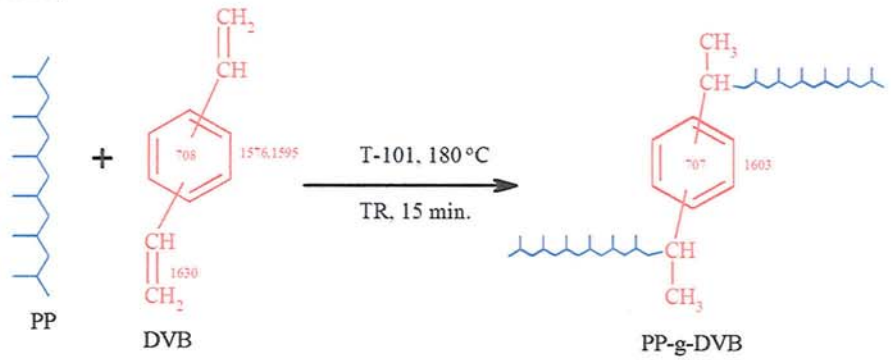

5.2.2 Separation of Reaction Products and Characterisation of Grafted MA on PP

To ensure a correct analysis of the reaction products and accurate determination of the grafting yield of MA on PP, it is important to remove all impurities of reaction products that could directly interfere with the measurement of the grafted MA. The impurities are primarily based on the unreacted MA (free-MA), homopolymerised MA and hydrolysed MA (present as maleic or succinic acid) [345-348]. Several purification methods have been widely utilised in the literatures including extraction in a selected solvent such as dichloromethane (DCM) [140], methanol [177], acetone [181], and toluene [162], dissolution of the modified polypropylene in hot xylene or toluene followed by precipitation in acetone **[90]** or in methanol **[180]**, by hot drying in vacuum oven at high temperature (100-180°C) in order to sublime the free MA [345], and by supercritical carbon dioxide extraction [161,416]. In this work, the first three methods mentioned above were conducted and adapted in two methods, (1) Soxhlet extraction in DCM followed by heating in vacuum oven (applied for grafting reaction product prepared in the absence of coagent and, (2) dissolution in xylene and precipitation in acetone and drying in vacuum oven for reaction product prepared in the presence of a coagent (see **Scheme 5.3,** p.297). The

presence of the MA groups grafted onto PP was confirmed by infrared spectra. The most significant difference in the spectral characteristics, in comparison with virgin PP spectra, is in the peaks at 1700 cm^{-1} to 1900 cm^{-1} corresponding to carbonyl stretching absorption. **Figure 5.5** shows a comparison of the FTIR spectra of virgin PP and MA-functionalised PP (PP-g-MA) films before and after purification with DCM extraction (followed by hot drying). The presence in the unpurified product spectrum of strong absorption peaks at 1638 cm^{-1}, 1603 cm^{-1}, 1573 cm^{-1} corresponding to the double bond and at 1270 cm^{-1} and 872 cm^{-1} (corresponding to C-H bending, δCH=CH and C-H wagging, ϖCH=CH) in the unpurified product spectra suggest that unreacted MA (free MA) remains in the reaction products. After extraction with DCM (followed by hot drying), the main peaks corresponding to the double bond disappeared. The presence of peaks at 1862 cm^{-1}, 1782 cm^{-1}, and 1715 cm^{-1} corresponding to symmetric and asymmetric carbonyl absorption (υC=O) is a further evidence for the grafting of MA onto PP (see **Rn-5.5**) **[95,177,345,346,417-420]**. It is worth noting that the grafted MA onto PP was present partially in the form of a cyclic anhydride (succinic/maleic anhydride) and partially as dicarboxylic acid (succinic/maleic acid). The absorptions at 2722 cm^{-1} can be assigned to the characteristic absorption of the PP skeleton and was chosen as an internal reference. The absorbance ratio of the areas of the carbonyl stretching absorption and the internal reference peak at 2722 cm^{-1} indicates the relative amount of grafted MA **[140]**.

Straightforward measurement of MA grafting degree, therefore, is complicated because of the presence of unreacted maleic anhydride (free MA), homopolymer-MA (oligomer) and the fact that the grafted succinic moiety, may be in the acid or anhydride forms. In order to characterise and determine how many hours of DCM extraction was effectively needed and which purification method is most suitable, a set of samples of PP/MA/T-101 system was prepared and processed in torque rheometer (PP 88 %, MA 12 %, T-101 0.001-0.02 molar ratio to MA, temp180°C, 65 rpm, 10 min). The reaction products were pressed into thin films, extracted with DCM for different times (24, 48, and 72 hours) before drying in vacuum oven (100°C) for 24 hrs. **Figure 5.6** shows clearly the reduction of the anhydride and acid peaks by the different purification methods. 48 h extraction is shown to be enough for the removal of free MA from the reaction product, see **Fig. 5.7**. Hot drying of the

maleated PP films (after DCM extraction) can not only remove unreacted MA (free MA) but help also to revert the maleic/succinic acid to maleic/succinic anhydride form.

Reaction 5.5

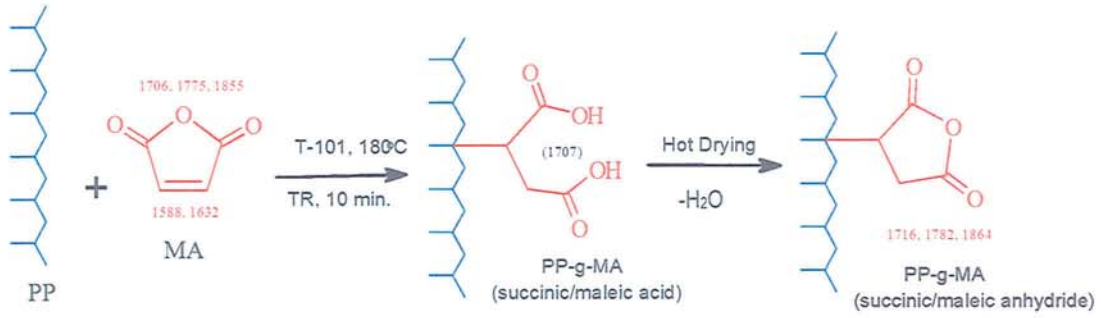

In the PP/MA/TRIS/T-101 system (in the presence of coagent TRIS) (see **Rn-5.6** and **Fig. 5.8A**), the FTIR spectrum of the purified PP-g-MA_{TRIS} film shows the carbonyl characteristic absorption peaks at 1860 cm^{-1} (υC=O asymmetric), 1782 cm^{-1} (υC=O symmetric) and 1736 cm^{-1} (υC=O carboxylate). The intensity absorption of the carbonyl stretching (υC=O) in this system was much stronger than the PP/MA/T-101 system indicating a higher level of grafted MA on PP. However, the stronger absorption peaks at 1732 cm^{-1} would also probability correspond to carbonyl stretching of the ester group of TRIS. This peak overlaps with the carbonyl stretching absorption (υC=O) of the carboxylate group corresponding to MA (in the form of maleic or succinic acid) at 1710 cm^{-1}. Therefore, the amount of grafted MA in the presence of TRIS can not be determined by FTIR method.

Similarly, FTIR spectrum of PP-g-MA_{DVB} (PP/MA/DVB/T-101 system) (see **Fig. 5.8B** and **Rn-5.7**), also shows a stronger characteristic absorption of carbonyl at 1859 cm^{-1} and 1782 cm^{-1} indicating that a higher extent of maleic anhydride become grafted onto PP. The remains of a small absorption peak at 1603 cm^{-1} and 712 cm^{-1} are characteristic of the double bond stretching (υC=C) of phenyl group of grafted DVB (in the neat of DVB are observed at 1595 cm^{-1} and 708 cm^{-1}). **Figure 5.9** shows a comparison of infrared spectra of purified samples with different MA grafting systems (in the presence and absence of coagent TRIS or DVB).

Reaction 5.6

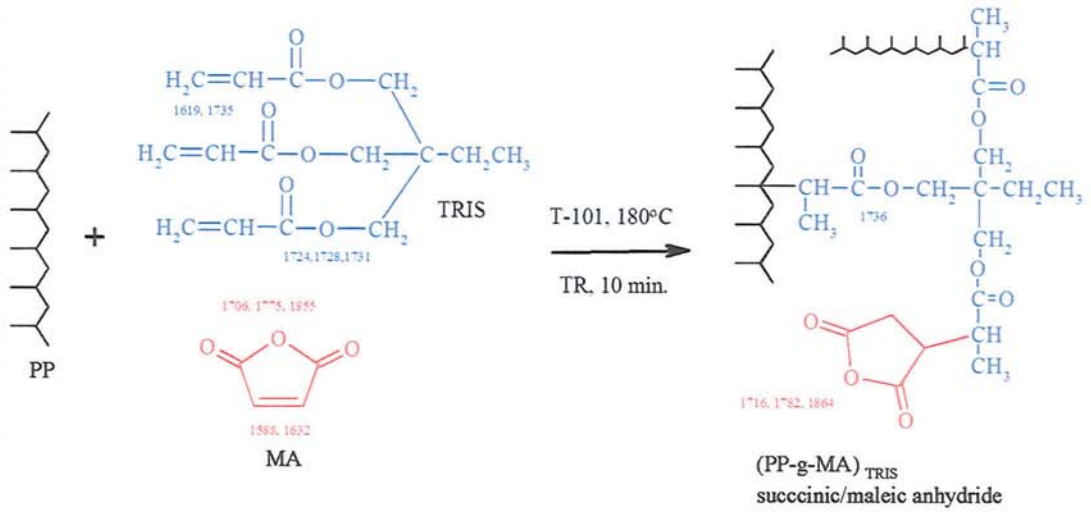

Reaction 5.7

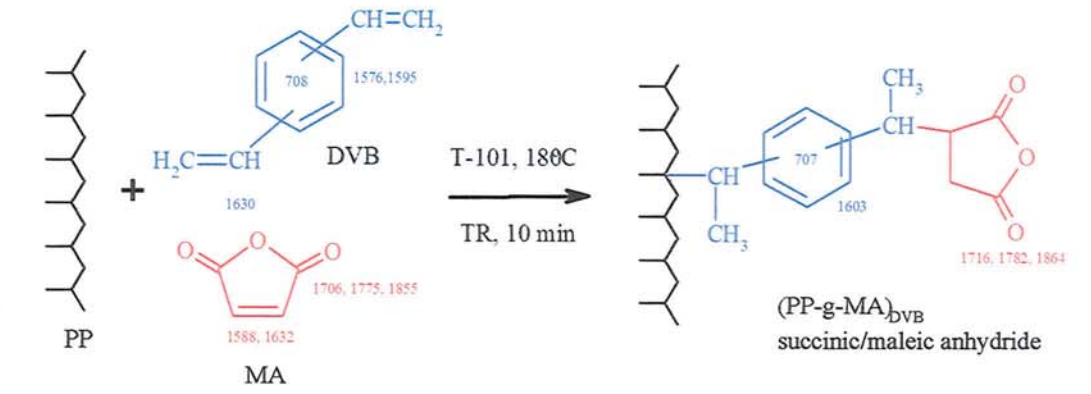

Due to the fact that the homopolymer of the coagents (poly TRIS or poly DVB) and their copolymers with maleic anhydride (MA-co-TRIS or MA-co-DVB) are not soluble in normal solvents, a xylene Soxhlet extraction procedure was adopted whereby the xylene-insoluble poly TRIS or poly DVB and MA-co-TRIS or MA-co-DVB remained in the thimble, but the MA-grafted PP, poly MA, and unreacted MA (free MA) were soluble in xylene. The separation of MA-grafted PP from poly MA and free MA was then obtained by subsequent precipitation methods with acetone (poly-MA and free-MA dissolved in acetone but not grafted-MA). It is interesting to observe that the intensity of carbonyl absorption peaks at 1707 cm^{-1} of the PP-g-MA (see **Fig. 5.5**), 1735 cm^{-1} of the PP-g-MA_{TRIS} (see **Fig. 5.8A**), 1716 cm^{-1} of the PP-g-MA_{DVB} spectra (**Fig. 5.8B**) decreased markedly after purification whereas the peak at 1782 cm^{-1} had either increased or undergone only little

change which indicates a change in the molecular structure of the grafted-MA from carboxylate form (probability as succinic/maleic acid) (see **Rn-5.5**) to succinic/maleic anhydride form (c.f. **Fig.A.2.5** and **A2.13** to **A2.15** in Appendix A). Hot drying of the maleated PP films (after DCM extraction) not only can remove unreacted MA (free MA) but also reverts the products from maleic/succinic acid to the maleic/succinic anhydride form.

5.2.3 Determination of Grafted MA in the Reaction Products

Two procedures were used to measure the amounts of grafted succinic anhydride in the maleated polypropylene products, by non aqueous acid-base titration and by infrared spectroscopy method **[177,181]**. The quantitative measurement of the MA grafting degree was performed according to Gaylord's **[150-155]** and Sclavons' methods **[346]** with a slight modification in the procedure using bromothymol blue (BTB) as end point indicator **[345,346]**. The purified functionalised polymer was refluxed with water in hot xylene to hydrolyse succinic or maleic anhydride to the corresponding dicarboxylic acid (succinic acid) which was then titrated with KOH (see **Section 2.5.3** in Chapter 2, p.75). The polymer was completely soluble at the reflux temperature and did not precipitate during titration. In order to confirm the hydrolysis reaction and the acid-base titration reaction, the reaction products after titration (a solution in xylene) was precipitated with acetone, filtered off to remove the solvents, dried in vacuum oven and pressed into a thin film for infrared characterisation (**Film-X**, see **Scheme 5.4**, p.298). The FTIR spectrum of Film-X (see **Fig. 5.10** and **Rn-5.8**) shows that the characteristic absorption bands at 1716 cm^{-1}, 1782 cm^{-1} and 1860 cm^{-1} for carbonyl absorption were completely eliminated and had shifted to 1779 cm^{-1}, 1700 cm^{-1} and 1576 cm^{-1}. This confirms that the reaction of acid-base titration can be assessed accurately by this method in the MA grafted determination. However, the titration procedure is complicated and is time consuming. Hence a calibration curve was established between the grafting degree measured by titration and the carbonyl absorption area ratio determined from infrared spectra as discussed in **Section 2.5.4**, in **Chapter 2** (p.78). The carbonyl absorption area ratio was defined as the intensity of the carbonyl absorption peak at 1716 cm^{-1}, 1782 cm^{-1}, and 1860 cm^{-1} divided by that of PP CH_3 absorption peak at 2722 cm^{-1}, this was used as a measure of the amount of grafted maleic anhydride. Three films for each sample were used and an average value was reported throughout.

Reaction 5.8

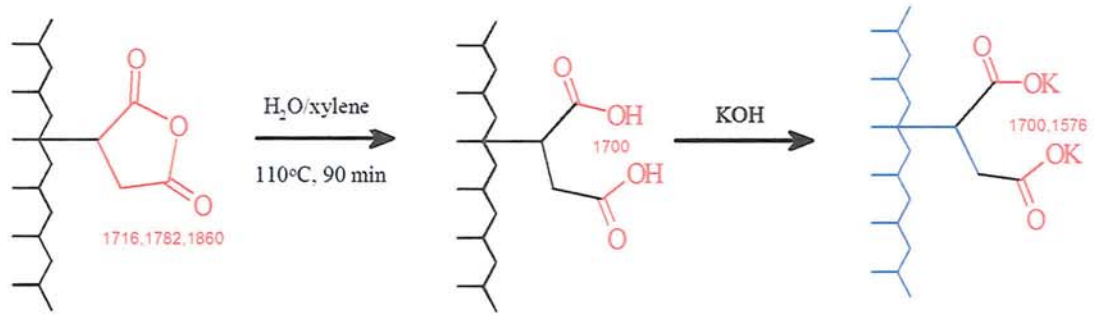

5.2.4 Grafting MA onto PP in the Absence of Coagent

In this study, two different peroxides were used to initiate the grafting reaction of MA on PP; 2,5-di(*tert*-butylperoxy)-1,5-dimethyl hexane, Trigonox-101 (T-101) and 1,1-di-(*tert*-butylperoxy)-3,3,5-trimethyl cyclohexane, Trigonox-29B90 (T-29B90), see **Table 2.3** in **Chapter 2** (p.63), for half-lifetime ($t_{1/2}$) of these peroxides. The effect of processing temperature, the peroxides concentration and MA concentration were investigated. During the free radical process, polypropylene chains may undergo degradation and results in a decrease in viscosity of the polypropylene and, thus, a torque change can be expected to be seen during the batch mixing. The experimental condition-compositions are presented in **Table D4.3** (in Appendix D). Grafting during processing in the absence of any peroxide (referred to as thermal initiation) was also investigated. A set of samples was prepared with a fixed MA concentration of 8% and melt grafted onto PP at various temperatures 140-200°C. **Figure 5.11** shows the effect of processing temperatures on yield of grafted-MA and the MFI of the polymer. It was found that the grafting reaction of MA in this system was extremely low and the melt flow index (MFI) of the processed PP did not change significantly.

i. Peroxide Trigonox-101

In the conventional system, when polypropylene (PP) was processed with MA in the presence of a free radical initiator, peroxide T-101 with a fixed composition ([MA] = 8%, [T-101] = 0.005 molar ratio to MA) and processing conditions (65 rpm, 10 min) except a

difference in the processing temperatures (in the range of 140-200°C), the final torque and torque maximum decreased with increasing of temperature, and this may reflect the occurrence of a shear-assisted disruption of the PP chains which increased at higher processing temperatures (see **Fig.5.12**). It is interesting to note that when the temperature was raised up to 200°C, the grafting degree increased significantly both in polypropylene PP-Elf and PP-ICI (see **Fig. 5.13**). The effect of the type of polypropylene on the extent of grafting of MA was not very different (see **Fig. 5.13**). Further, the grafting degree of MA onto PP processed in the presence of T-101 is clearly shown to be much higher than that of thermal initiation (see **Fig. 5.13**). On the other hand increasing the temperature resulted in a drastic increase in the MFI indicating a severe degree of polymer degradation by chain scission. However, the level of grafting of MA onto PP was still very low, less than 1 % (grafting efficiency less than 8 %), in both PP-Elf and PP-ICI polymers.

ii. Peroxide Trigonox-29B90

When T-101 was replaced by T-29B90, the torque characteristic of the two systems was shown not to be the same (see **Fig. 5.12**). There seems to be a correlation between the torque maximum and the final torque with the reaction competition in the case of these two peroxides, i.e. the extent of grafting reaction and the PP fragmentation by a β-scission reaction. In the case of T-101, grafting level increased with increasing temperature (in the range of 140-180°C) and oppositely in T-29B90 system, the grafting degree decreased constantly with increasing temperature in both PP-Elf and PP-ICI polymers (see **Fig. 5.13**). It was also found that the extent of β-scission in the T-101 system is much higher (the MFI increased) compared to the T-29B90 system with increasing temperature (see **Fig. 5.13).**

The type and amount of the initiator in the feed for MA grafting onto PP are among the most important parameters in grafting **[1,3,53]**. In order to investigate the effect of peroxide concentration, a set of samples was prepared with fixed MA concentration (8%) processed at the optimum temperature for Trigonox-101 of 180°C and for Trigonox-29B90 at 160°C (even though optimum temperature was 140°C, but PP at 140°C did not melt fully). As shown in **Fig. 5.14**, the MA grafting level is also significantly affected by the type and concentration of the peroxides. It is clear that the MA grafting level in T-101 system was higher for all peroxide concentrations at the examined temperatures, i.e. increased with

increasing T-101 concentration (0.001 to 0.01 molar ratio to MA). This is probably due to the larger amount of primary radicals formed at higher T-101 concentration, consequently, a higher concentration of PP· macroradicals would be available for the reaction with maleic anhydride, thus, higher level of grafting. However, higher peroxide concentrations result in an increase in MFI values indicating chain scission. It is quite interesting to note that when the peroxide T-101 was replaced with T-29B90, the MA grafting degree decreased with increasing peroxide concentration. Moreover, the MFI in this system was lower compared to the T-101 system. This is probability due to shorter half-life time of T-29B90, see **Table 2.3** in Chapter 2 (p.63).

iii. Effect of MA Concentration

The effect of the initial maleic anhydride (MA) concentration on the conversion to MA-grafted on PP and on the degradation of polypropylene is an issue that has most divided authors who have been investigating this reaction **[89-115]**. In this work, various initial MA concentrations (2-18%) were reactively processed with PP using the same processing conditions (temp.180°C for T-101 and 160°C for T-29B90, 65 rpm, 10 min) but they were different in terms of the following:

(1) Type of peroxide, T-101 and T-29B90 (PP-Elf, [peroxide] 0.005 molar ratio to MA)
(2) Types of polypropylene, PP-ICI and PP-Elf ([T-101] 0.005 molar ratio to MA)
(3) Peroxide concentration, ([T-101] = 0.002 and 0.005 molar ratio to MA)
(4) Mixing methods (see **Scheme 5.1)** (PP-ICI, [T-101] 0.005 molar ratio to MA)

Figure 5.15 shows the influence of the initial MA concentration on the torque characteristics, grafting level and MFI for samples processed in the presence of the peroxides, T-101 and T-29B90. The final torque in both systems decreased with the increasing MA concentration. It is also seen in **Fig. 5.15** that both the level of grafting and the extent of PP chain scission (increase in MFI) in the PP/MA/T-101 system increased continuously with increasing MA concentration. This implies that at higher initial MA concentration and higher peroxide concentration (as molar ratio), more PP· macroradicals would be produced by H-abstraction, and more MA monomer could react with the macroradicals resulting in an increase in degree of MA grafting. At the same time however,

a higher concentration of more PP• macroradicals in the system (at high initial MA concentration) results also in a higher degree of chain scission (higher MFI). It is interesting to note that when T-101 was replaced by T-29B90, the MA grafting level was very low and increasing MA initial concentration had a negative effect on the grafting level which levelled off at MA concentration of > 2 % (**Fig. 5.16**). This is probability not only because of the short half-life time of the peroxide T-29B90 but also due to the low reactivity of the monomer MA for grafting on PP [**1,187**].

In a number of literature articles [**1,51,90,158,180-182,186**] it was reported that the increase in initial maleic anhydride concentration leads to an increase in the MA grafting level but only up to a certain amount, passing through a maximum value with posterior decline. For example, Hu and Lambla *et al.* [**1,186**] reported that the grafting level of MA on PP in the presence of 0.5 phr peroxide (= 0.014 to 0.170 molar ratio of peroxide to MA) had increased with increasing initial MA concentration up to 6 %, but decreased with further increase in MA concentration. Similarly, the same results were reported by Martinez *et al.* [**181**] but the maximum MA grafted on PP was reported to have been reached at MA concentration of 9-12 % and this depended on the peroxide (DCP) concentration used (at temp.190°C, DCP 2-4 %). These results were interpreted based on solubility of MA in PP so that at higher initial MA concentration all molecules could not totally solved in the polymer and only a certain amount of MA concentration becomes soluble [**181,186**]. These literature results contradict results shown in **Fig. 5.16** where a constant molar ratio of peroxide to MA of 0.005 or 0.002 was used, in that there is a clear continuous increase in the grafting level with increasing initial MA concentration. For the effect of peroxide concentration studied above (see **Fig. 5.17**), the MA grafting degree presents a distinct behaviour, depending on the peroxide concentration employed. In this work, the peroxide concentration was fixed at 0.005 mr (molar ratio of peroxide to MA), thus proportionally the peroxide weight (phr) increased with increasing MA concentration (see **Table 5.1**). By contrast, in the literature by Hu and Lambla *et al.* [**1,186**], the peroxide concentration was fixed at a constant weight of 0.5 phr (part per hundreds resin), which means that the peroxide concentration in molar ratio decreased with increasing maleic anhydride concentration as shown in **Table 5.1**. To confirm this, another experiment was prepared using similar composition and conditions to those used by Hu and Lambla *et al.* [**1,186**]

where 0.5 phr (0.014 – 0.170 mr to MA) was used with varying initial MA concentration and all processing was conducted under fixed conditions (220°C, 100 rpm, 15 min). The results from these experiments (see **Fig. 5.17**) are shown to be very similar to those reported in the literature [1,51,90,158,164,180-182,186].

Table 5.1 Peroxide weight and molar ratio calculation in MA grafting system

[T-101] Base on:	PP (g)	[MA]i (%)	[T-101]	
			(phr)	(mr)
This Work, (in molar ratio, mr)	34.3	2	0.031	0.005
	33.6	4	0.062	0.005
	32.9	6	0.095	0.005
	32.2	8	0.130	0.005
	31.5	10	0.166	0.005
	30.8	12	0.204	0.005
Hu *et al.* [1,186] in part of hundreds resin, phr)	33	1	0.5	0.170
	33	2	0.5	0.084
	33	4	0.5	0.042
	33	6	0.5	0.028
	33	8	0.5	0.021
	33	10	0.5	0.017
	33	12	0.5	0.014
phr = part (weight) of peroxide per hundreds resin, weight PP constant of 33 g mr = molar ratio of peroxide to MA, weight total of samples (PP+MA+T-101) = 35 g				

5.2.5 Grafting Reaction of MA in the Presence of a Coagent

It was demonstrated that MA could be melt grafted onto PP in the presence of the peroxides T-101 and T-29B90. However, the overall grafting of MA on PP was very low. Though an increase in processing temperature (see **Fig.5.13**), peroxide concentration (see **Fig 5.14**) , and MA concentration (see **Fig 5.15**) has led to higher grafted MA, the excessive chain scission reactions during the melt grafting (as indicated by the high value of melt flow index) makes this approach unsuccessful. Similar results have been reported in PP [158,164,180,186], PE [149,148] and ethylene propylene copolymer (EPR) [153,154], where high MA grafting onto these polymers was only achieved by an increase in the peroxide concentration but this was always accompanied by severe degradation of the polymers. In this work, the effect of the comonomers (DVB or TRIS) and different type of peroxides (T-101, T-29B90, DCP, BPO) on the grafting reaction of the much less reactive modifier MA in PP was examined.

i. Effect of Processing Temperature on the Degree of Grafting

Four types of peroxides which have different half-life times ($t_{1/2}$) were used; Trigonox-101 (T-101), Trigonox-29B90 (T-29B90), dicumyl peroxide (DCP) and benzoyl peroxide (BPO), see **Table 2.3** in **Chapter 2** (p.63) for their half-life times. A set of grafting experiments was conducted having fixed composition of reactants ([MA] = 8 wt %, [DVB] = 2/8 weight ratio to MA, and [peroxide] = 0.005 molar ratio to MA+DVB) and processing conditions (time 10 min, rotor speed 65 rpm), except for different temperatures (160 - 200°C) (see **Scheme 5.1**, p.295). During the free radical grafting process in the DVB (PP/MA/DVB/peroxide) system, PP chains may become branched and eventually crosslinked with DVB. When the branching reaction occurs, there would be an increase in the viscosity of the PP, thus a torque increased in torque rheometer. **Figure 5.18** shows the evolution of the torque as a function of time for the DVB (PP/MA/DVB/peroxide) system for the four types of peroxide). First of all it should be noted that the torque characteristic of the DVB system is higher compared to the conventional (T-101 and T-29B90) system (see **Fig. 5.19**) at all temperatures examined. This is mainly from branching/crosslinking reaction along with the grafting and copolymerisation (coagent-co-monomer) reaction. The grafting degree in the DVB/T-101 and DVB/DCP system is much higher than DVB/T-29B90 and DVB/BPO system. It is interesting to note that both peroxides T-29B90 and BPO are also not effective in the DVB system as shown by much lower grafting degree (even lower than the conventional system). **Figure 5.19** shows that the peroxide T-101 was superior compared to the other peroxides at all processing temperatures and the highest grafting degree was achieved at a temperature of 180°C. It is also interesting to note that at higher temperatures (>180°C) the presence of DVB in the coagent system did not suppress the β-scission reaction as shown by the high increase in its MFI of the DVB/T-101 system (see **Fig. 5.19**).

ii. Effect of Peroxides Concentration on Grafting Degree

In order to investigate the effect of peroxide concentration on the coagent system, a set of experiments was conducted in both coagent, TRIS and DVB, using a fixed composition ([MA]i = 8 %, [DVB] or [TRIS] = 2/8 weigh ration to MA) except for varying the peroxide concentration in the range 0.001 – 0.01 mr (molar ratio to MA+coagent) and processing was done under fixed conditions (temperature 180°C for T-101 and 160°C for T-29B90,

rotor speed 65 rpm, time 10 min). **Figure 5.20** shows the effect of T-101 and T-29B90 concentration on torque-time curves and torque characteristics of the MA/coagent PP system. It is interesting to note that the torque max of the DVB/T-101 system is higher than that of TRIS/T-101 system. This is probability due to the different reactivity of two coagents towards the PP macroradical and the monomer (DVB more reactive than TRIS). It was found that the level of MA-grafted on PP in the presence DVB was higher than in the presence of TRIS and was much higher than that of the single monomer without comonomer (conventional) system in both peroxides examined (**Fig. 5.21**). For example, with 8 % MA initially added, a maximum value of 0.4 % grafting degree (grafting efficiency 5 %) was achieved by addition of 0.002 molar ratio (0.05 phr) of T-101 in the absence of a coagent, whereas as high as 1.7 % (more than four times higher) and 3.5 % (more than eight times) grafting degree was measured in the presence of TRIS and DVB, respectively. In the concentration range of peroxides used (0.001 – 0.01 molar ratio to MA+coagent), it was obvious that T-101 was more effective than T-29B90 with both coagents TRIS and DVB. With 0.005 molar ratio (0.1 phr) peroxide, a maximum value of 1.5 % grafting degree was achieved in presence of the peroxide T-29B90, whereas as high as 3.5 (more than twice higher) when using T-101. Similar with the GMA grafting system in the presence of the coagents TRIS or DVB, it is shown here that DVB is also superior compared to TRIS in enhancing MA grafting in the coagent system. However, in the DVB system the crosslinking reaction becomes dominant as shown by a much lower of its MFI (see **Fig.5.21**).

iii. Effect of MA Concentration on the Grafting Degree

In order to observe the effect of MA initial concentration in the MA grafting reaction on PP in the presence of the coagents TRIS and DVB, a set of experiments was conducted using a fixed peroxide concentration of 0.005 mr (molar ratio to MA+coagent) and coagent concentration of 2/8 wr (weight ratio of coagent to MA) and a fixed processing conditions (temp. 180°C for T-101 and 160°C for T-29B90, 65 rpm, 10 min). **Figure 5.22** shows the effect of the MA initial concentration on the torque-time curve. It is interesting to compare the torque characteristic both in different peroxide (T-101 and T-29B90) (see **Fig. 5.23A**) and in different comonomer (DVB and TRIS) (see **Fig. 23B**). It is observed that the torque characteristic (torque max, final torque, and torque max-min) in the coagent/T-101 is higher

than that in the coagent/T-29B90 in both coagents TRIS and DVB (see **Fig.5.23A**). This is probability due to more PP macroradical formed when using T-101 compared to with T-29B90 and the former has a longer half-life time. It is clear that the higher amount of formed PP macroradical, the higher will be the extent of branch/crosslink reaction and/or graft reaction. It is also observed that the torque characteristic in the DVB/peroxide is higher than that of the TRIS/peroxide in the case of both peroxides. This is probability because of the different reactivity between these two comonomers where it is likely that DVB is more reactive than TRIS (see **Fig. 5.23B**). It was found that similar to the MA grafting reaction in the absence of a coagent, the grafting of MA on PP in the presence of TRIS and DVB also increases with increasing the initial MA concentration added (see **Fig. 5.24**). It is interesting to note that the MA grafting degree in the coagent/T-101 system is higher compared to the coagent/T-29B90 (see **Fig. 5.24**). Further, the MA grafting degree in the DVB/peroxide system is higher than that of the TRIS/peroxide. However, the extent of coagent-assisted cross linking in the DVB system is very high and increased with increasing MA concentration. It is difficult however to understand why the MFI in the TRIS system continues to be high at all initial MA concentrations.

iv. Effect of Coagent Concentration on the Grafting Degree

Figure 5.25 shows the effect of concentration of TRIS and DVB on the torque and its characterisation and MA grafting degree using different peroxides (T101 and T-29B90) at a fixed molar ratio of the peroxides (0.005), MA concentration of 8 wt %, and a temperature of 180°C for T-101 and 160°C for T-29B90. The higher torque characteristic of DVB system compared to that of TRIS (with peroxide T-101) coincides with the higher MA grafting degree in the case of the former. It is also found that the grafting degree had initially increased with increasing the coagent concentration and then levelled off with a further increase (see **Fig. 5.26**). This is due to the high concentration of TRIS or DVB giving rise to a higher extent of crosslinking reaction and the formation of copolymers between MA and the coagents (MA-co-DVB or MA-co-TRIS) which could interfere with the grafting reaction. Further, FTIR analysis of the samples of PP/MA/DVB/T-101 showed that the carbonyl absorption peak at 1856 cm^{-1}, 1782 cm^{-1} and 1719 cm^{-1} (carbonyl absorption) and aryl peaks at 711 cm^{-1} became stronger with increasing DVB concentration (see **Fig. 5.26**).

v. Kinetics of Grafting Reaction

In order to study the time-dependent behaviour of the MA grafting onto PP, plots between maleic anhydride grafting (wt %) versus MA grafting reaction time are shown in **Fig. 5.27**. The amount of reactants were fixed ([MA]i = 8 %, coagents [TRIS] or [DVB] = 2/8 weight ratio to MA, and [T-101] = 0.005 molar ratio to MA+coagent) and processed at constant temperature of 180°C and rotor speeds 65 rpm. **Figure 5.27** shows that the grafting level of MA/T-101 (in absence of coagent), reached 0.4 % in the first two minutes of processing and was completed after 7 minutes with a final grafting degree of 0.7% (that is more than 50 % of grafting reaction was achieved by 2 minutes processing). In the presence of TRIS the grafting reaction proceeded more rapidly; At the first two minutes processing, a grafting degree of 1.8% was achieved and by 10 minute it reached 1.86 (that is more than 95% of MA conversion to grafted-MA was achieved at 2 minutes processing). Similarly, in the presence of DVB, the grafting reaction at 2 minutes achieved 86% conversion. From **Fig. 5.27**, grafting rate (*d[grafting]/dt*) can be calculated by statistical analysis. The rate of grafting reaches a maximum at two minutes processing and then drops to lower values when reaction time is increased. This is due to the high reactivity of the coagents with the monomer MA and decrease of free monomer available after 2 minutes grafting process progress.

vi. Comparison of the Effectiveness of DVB and TRIS in the GMA Grafting System

Figure 5.28 shows a comparison of torque time curves and grafting level in the presence of different coagents (TRIS and DVB) and using different MA concentration. It is observed that the torque maximum when PP was processed with DVB or TRIS (without MA) is much higher than that of PP/MA/coagent/T-101 (in the presence of MA) suggest that DVB and TRIS is more reactive toward PP macroradical compared to its reaction with the monomer MA.

5.2.6 Compatibilisation of PBT/PP with Functionalised PP

As discussed in **Section 1.4, Chapter 1** (p.50) the compatibilisation of polymer blends is the key to achieving the required properties and performance and reactive blending has attracted great attention and has been used widely for this purpose. When two polymers are

to be compatibilised and only one contains functional groups and the other one is chemically inert, the inert polymer must be functionalised so that it can be compatibilised with the functional polymer that bears reactive groups capable of chemical reaction. PBT contains two terminal groups: carboxylic acid (-COOH) and hydroxyl (-OH) which can readily react with many functional groups such as epoxide and anhydride attached available onto a second polymer leading to graft copolymer formation during melt blending [21-24].

Table 5.2 Composition and condition for preparation of PP/PBT blends.

Code	Component/ Composition	Condition (°C/rpm/min)	Preparation of *f*-PP Components			
			Component/Composition	Cond.(°C/rpm)/min)	GD (%)	MFI (g/10min)
PB	PP/PBT(80/20)	240/65/10	-	-	-	-
PGB	PP/PP-g-GMA$_{conv.}$/PBT 77.5/2.5/20	240/65/10	PP/GMA/T-101 88%/12%/0.005 mr	180/65/10	0.7	6.1
PMB	PP/PP-g-MA$_{conv.}$/PBT 77.5/2.5/20	240/65/10	PP/MA/T-101 92%/8%/0.005 mr	180/65/10	0.65	5.5
PGVB	PP/PP-g-GMA$_{DVB}$/PBT 77.5/2.5/20	240/65/10	PP/DVB/GMA/T-101 88%/2:8wr/12%/0.005 mr		4.7	1.3
PGTB	PP/PP-g-GMA$_{TRIS}$/PBT 77.5/2.5/20	240/65/10	PP/TRIS/GMA/T-101 88%/2:8wr/12%/0.005 mr	180/65/10	3.3	3.8
PGB-11	PP/PP-g-GMA$_{conv.}$/PBT 75/5/20	240/65/10	PP/GMA/T-101 88%/12%/0.005 mr	200/65/10	**0.2**	6.3
PGB-12	PP/PP-g-GMA$_{conv.}$/PBT 75/5/20	240/65/10	PP/GMA/T-101 88%/12%/0.005 mr	180/65/10	**0.7**	6.1
PGB-13	PP/PP-g-GMA$_{conv.}$/PBT 75/5/20	240/65/10	PP/GMA/T-101 88%/12%/0.005 mr	160/65/10	**2.3**	6
PGB-12	PP/PP-g-GMA$_{conv.}$/PBT 75/5/20	240/65/10	PP/GMA/T-101 88%/12%/0.005 mr	180/65/10	0.7	**6.1**
PGB-22	PP/PP-g-GMA$_{conv.}$/PBT 75/5/20	240/65/10	PP/GMA/T-101 88%/12%/0.01 mr	180/65/10	0.7	**10.7**
PGB-32	PP/PP-g-GMA$_{conv.}$/PBT 75/5/20	240/65/10	PP/GMA/T-101 88%/12%/0.001 mr	160/65/10	0.7	**3.7**

mr = molar ratio of peroxide to monomer or monomer+comonomer, wr = weight ratio of coagent to monomer

In preliminary work, the compatibilising effect of the functionalised-PP (*f*-PP) prepared in this work in blends of PP/*f*-PP/PBT was examined (only morphology via SEM was measured due to time limitation) in the absence (PP-g-GMA$_{conventional}$) and presence of two comonomers in the f-PP (PP-g-GMA$_{TRIS}$ and PP-g-GMA$_{DVB}$). Samples with the same composition of PP/f-PP/PBT (weight ratio 77.5/2.5/20) were processed under the same conditions (temp.240°C, 65 rpm, 10 min) using different functionalised PP (f-PP). In

another experiment, PP/f-PP/PBT (75/5/20 w/w %) blends were prepared where the f-PP component was based on conventional (i.e. no-coagent) samples and had different extent of GMA grafting level and different MFI values (i.e. different viscosity). **Table 5.2** lists the blends composition and conditions used. **Fig. 5.29** and **5.30** compares the SEM morphology of these samples.

5.3 DISCUSSION

5.3.1 Effect of Reaction and Processing Variables on Conventional MA Grafting System

The experimental results of this work have clearly shown that melt grafting of maleic anhydride (MA) onto polypropylene (PP) can be achieved by both thermal and peroxide initiation, see **Fig. 5.13.** However, thermal initiation has resulted in very low grafting efficiency (less than 0.06 %) for any meaningful application. Further, the grafting yield under these conditions could not be increased to any significant extent of neither by raising the processing temperature in order to create more polymer radicals, nor by increasing MA concentration in order to seize the macro-radicals. This is due to the fact that the number of macroradicals formed via mechano-scission is limited and is insufficient to give rise to an increase in the grafting reaction.

In the presence of peroxide initiators, the level of grafting was much higher than that observed in the thermal initiation. The effect of peroxide on the grafting efficiency and PP degradation starts with the transfer reaction of primary peroxide radicals to the PP chain, followed by the main PP reaction mechanism of β-scission. In the polymer (PP), each repetitive unit provides three possible H-abstraction sites (1) methine, (2) methylene, and (3) methyl produce three kinds of macroradical PP (1) tertiary, (2) secondary, and (3) primary (see **Scheme 5.5**). The specificity of hydrogen atom abstraction has been shown to depend on a complex array of polar, steric and stereo electronic factors **[69,106]**. The major product from the reaction between a radical and PP is anticipated to be that derived from abstraction of a methine hydrogen (i.e. **1**). In the presence of the peroxides, T-101 or T-29B90, the relative contribution of grafting reaction and chain scission would depend on both the chemical composition of the grafting system and the melt processing conditions;

the main aim of this work was to optimise these conditions in order to increase the level of target grafting reaction at the expense of these side reactions.

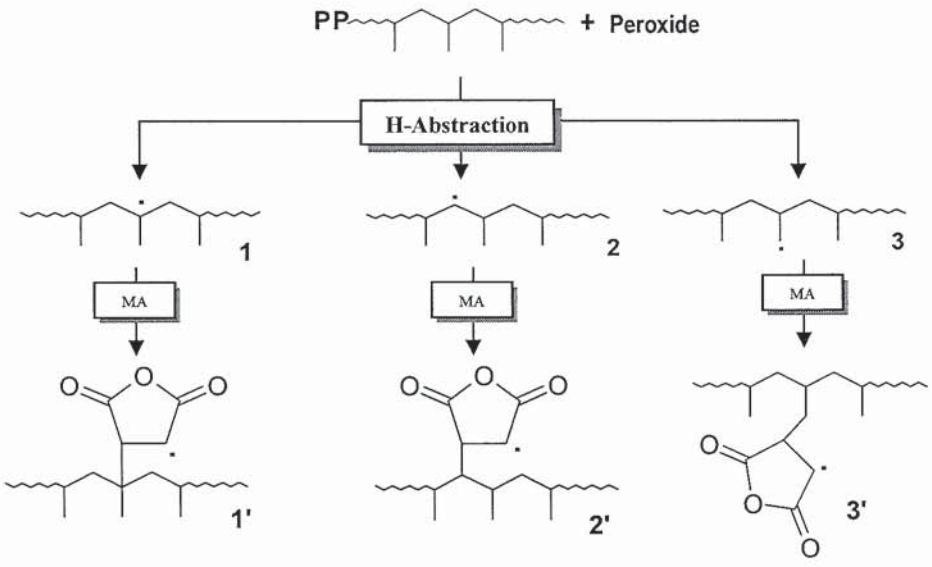

Scheme 5.5 Three types of H-abstraction on PP (1) methine (2) methylene, and (3) methyl and reacted with MA

The competition between the grafting reaction and the fragmentation (chain scission) of PP was quite different in the presence of the peroxides T-101 and T-29B90 (see **Fig. 5.13, 5.14, 5.16,** and **5.21**). This observation is closely related to the difference in the rate of decomposition of the two peroxides at the different processing temperatures. At temperatures of 160-200°C, the half-life time ($t_{1/2}$) of T-101 was 3-15 times higher than that of T-29B90 (**Table 2.3** in Chapter 2, p.63). The results showed that the type of peroxide used played an important role, not only on the level of grafting yield, but also on the degree of PP fragmentation by chain scission (as shown by the change of MFI of the reaction products), see **Fig. 5.13**. In the case of the peroxide T-101, an increase in the reaction temperature resulted in an increase in the degree of MA grafting (see **Fig. 5.13**), with the best results obtained at the reaction temperature of 180°C. This suggests that, at the higher temperatures, the rate of dissociation of T-101 to free radicals (**Rn-1** in **Scheme 5.6**) is more effective leading to an acceleration of the rate of radical formation on the polymer backbone (**Rn-2**) and subsequently the collision between the macro radical species formed and the monomer MA (**Rn-5**), resulting in the observed increase in the rate of grafting. However, the maximum percentage of MA grafting on the polymer was low (about 0.9%

with grafting efficiency only 11%). This is most likely to be due to an increase in the extent of β-chain scission (**Rn-4** in **Scheme 5.6**) at higher temperatures resulting in a rapid decrease in molecular weight of the polymer as indicated by the sharp increase in MFI at temperatures above 180°C. The use of the peroxide T-29B90, on the other hand, resulted in much lower extent of grafting yield at all temperature studied of 140-200°C (maximum grafting was obtained at 140°C with a grafting efficiency of only 2%), see **Fig.5.13**. This may be due to both the shorter half-life time ($t_{1/2}$) and the nature and amount of primary and secondary peroxide radicals formed (see **Scheme 3.9**, p.126) from this peroxide, with lower overall extent of initiator radical formation at higher temperatures, thus less macro radicals available to react with MA.

It is clear therefore that the level of degradation of PP chains was markedly influenced by the reaction temperature and also by peroxide concentration, which controlled the macroradical fragmentation and intermolecular radical transfer reaction. The higher the peroxide concentration, the higher MA conversion to grafted MA on PP (see **Fig.5.14**) but also the higher the β-scission efficiency as shown by the higher MFI of the modified polymer. This suggests that the grafting reaction does not occur simply by a 'chain transfer' mechanism or by a direct addition of the macro-radical PP backbone onto the double bond of MA (see **Rn-14** and **Rn-15** in **Scheme 5.6**). At higher peroxide concentration, the grafting reaction takes place after PP chain scission (see **Rn-4** followed by **Rn-6** and **Rn-7** in **Scheme 5.6**), when the PP free end radical is added onto the double bond of MA (see **Rn-6** in **Scheme 5.6**), or when the end double bond of the other PP fragment enters an 'ene reaction with MA (see **Rn-14** and **Rn-15** in **Scheme 5.6**).

There is currently some controversy surrounding the structure of the MA-grafted onto PP both with respect to the nature of the grafted units and the distribution of the graft sites. Consequently, the mechanism of grafting is still a matter of debate, and it continues to be very difficult to optimise the structure of MA-grafted polymers for certain applications. The types of anhydride functionality proposed to be present in MA modified PP include structures **1-8** [33,49,52,92,93,95,156,177] and it can be rasionalised as the products of conventional free radical-induced grafting as shown in **Scheme 5.5** and **5.6.**

Scheme 5.6 The mechanism of MA-grafting reaction on PP in the free radical (peroxide) initiation system [92,93,156] (Cont.)

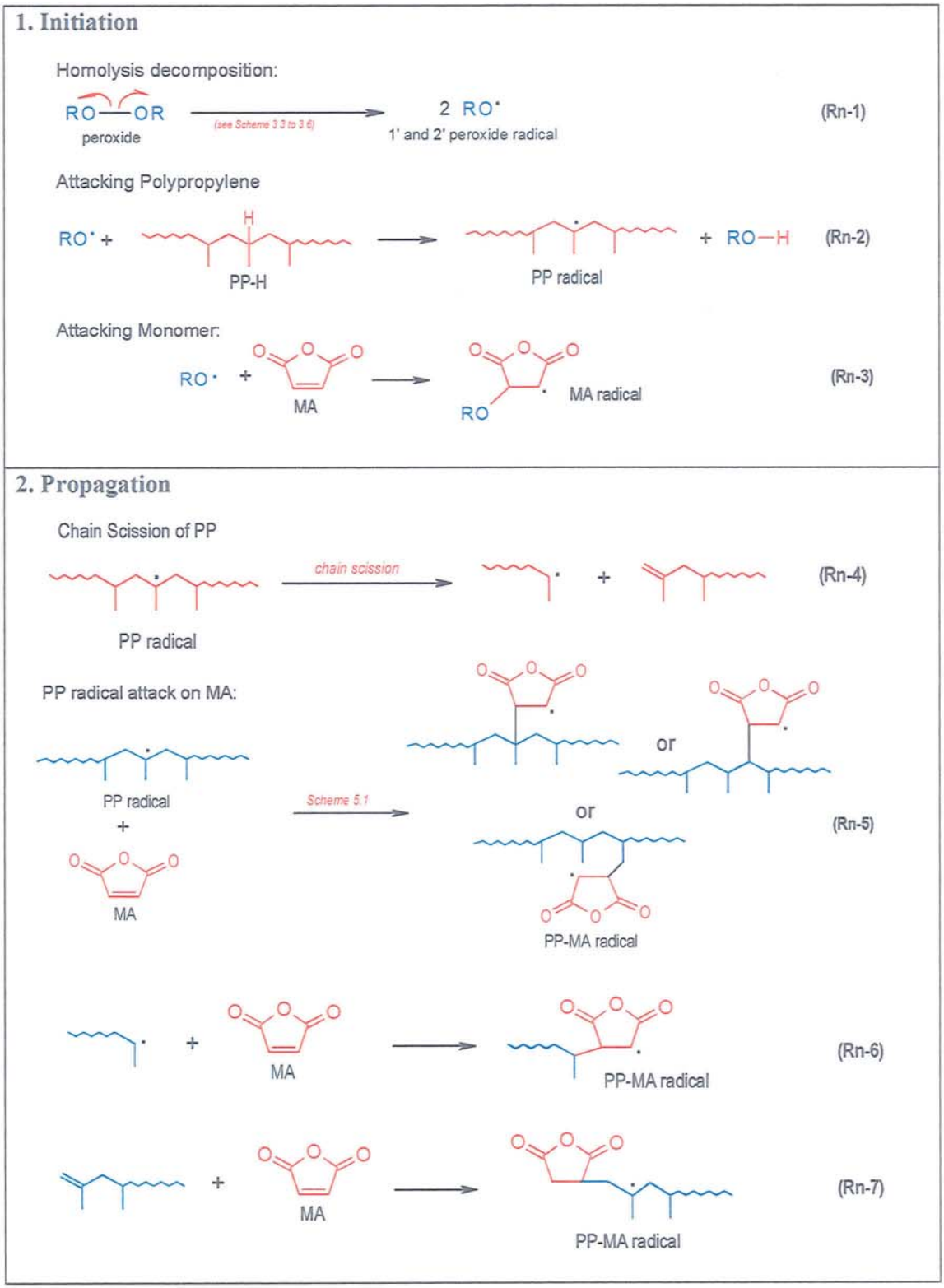

Scheme 5.6 (cont.) The mechanism of MA-grafting reaction on PP in the free radical (peroxide) initiation system

3. Chains Transfer

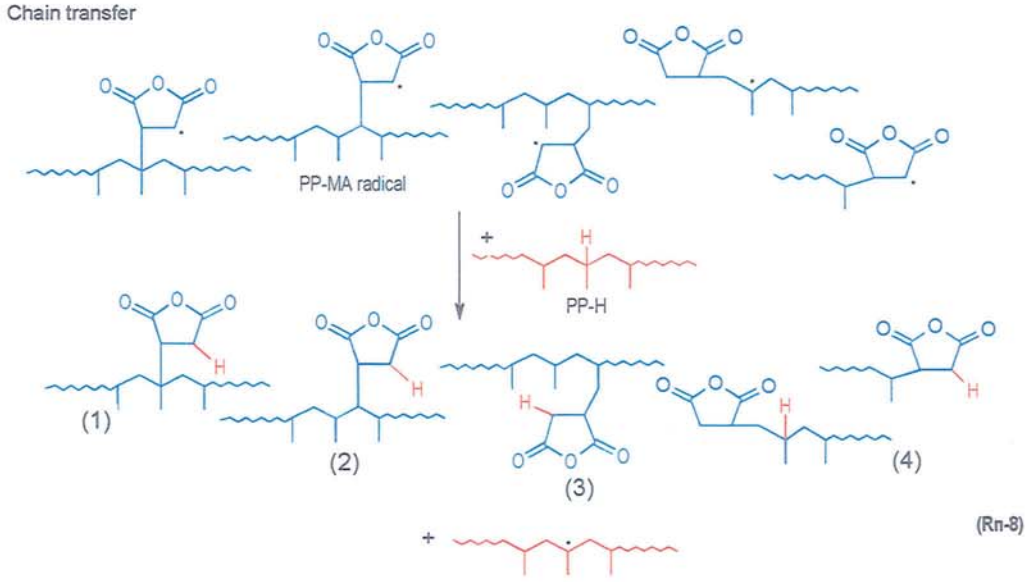

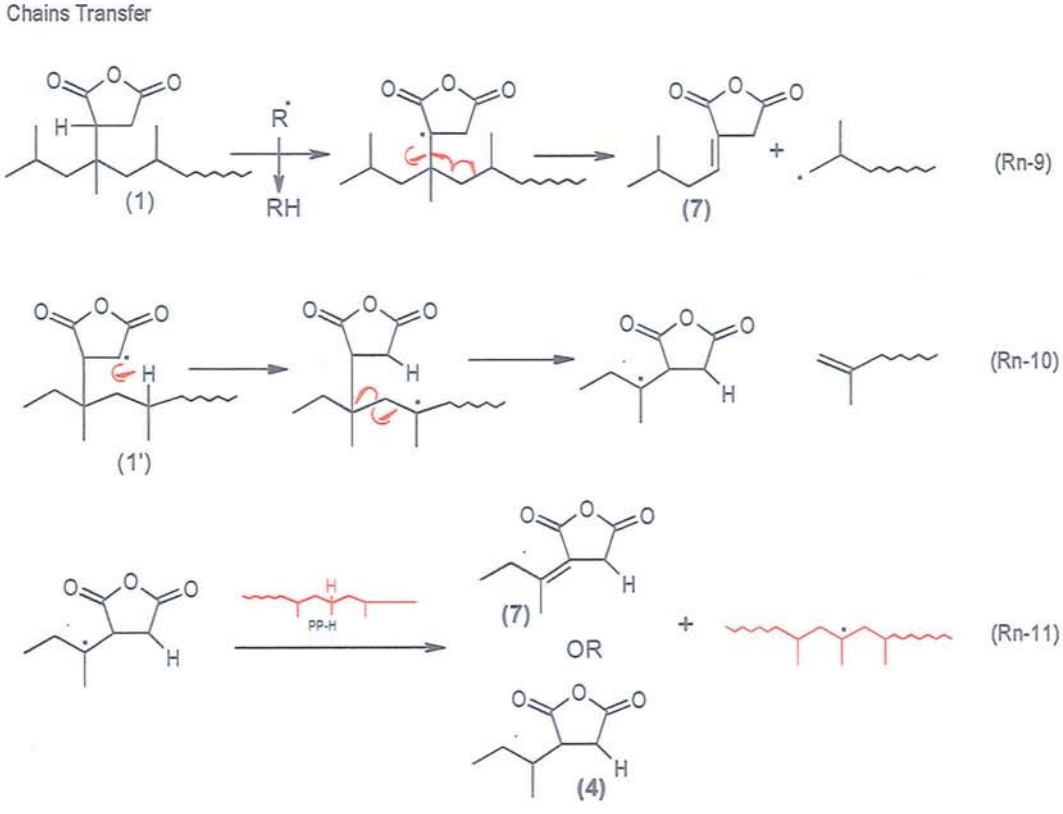

Scheme 5.6 (cont.) The mechanism of MA-grafting reaction on PP in the free radical (peroxide) initiation system

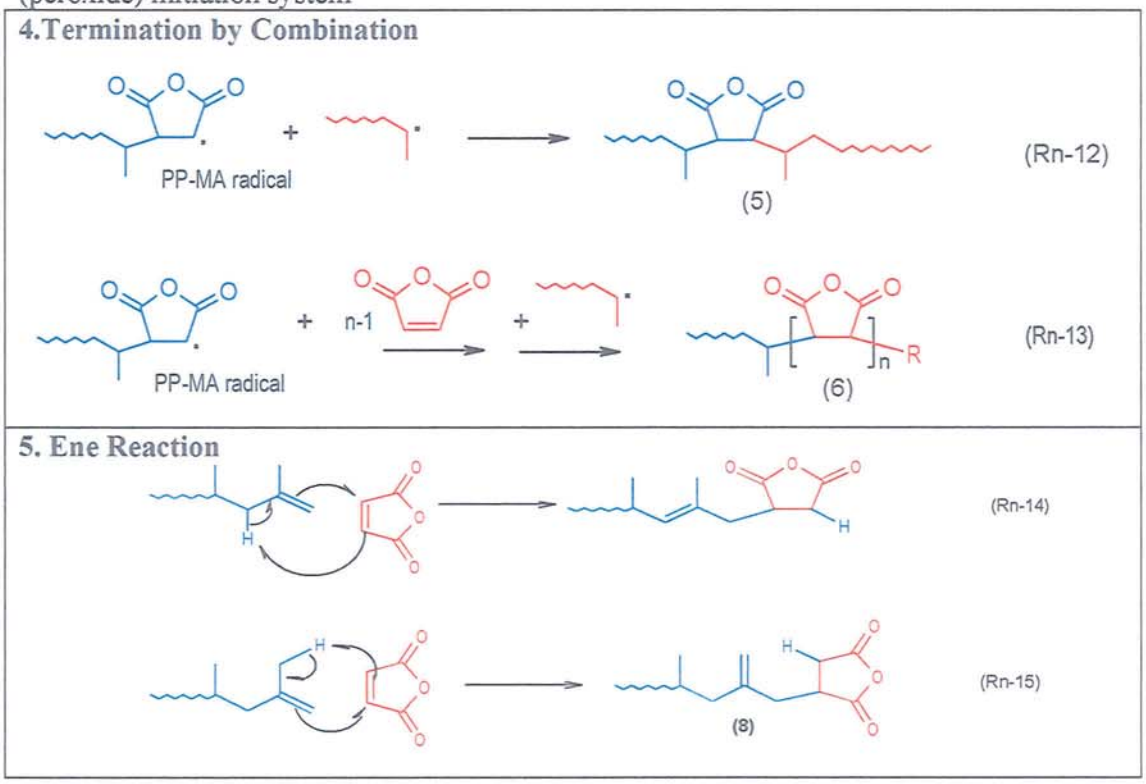

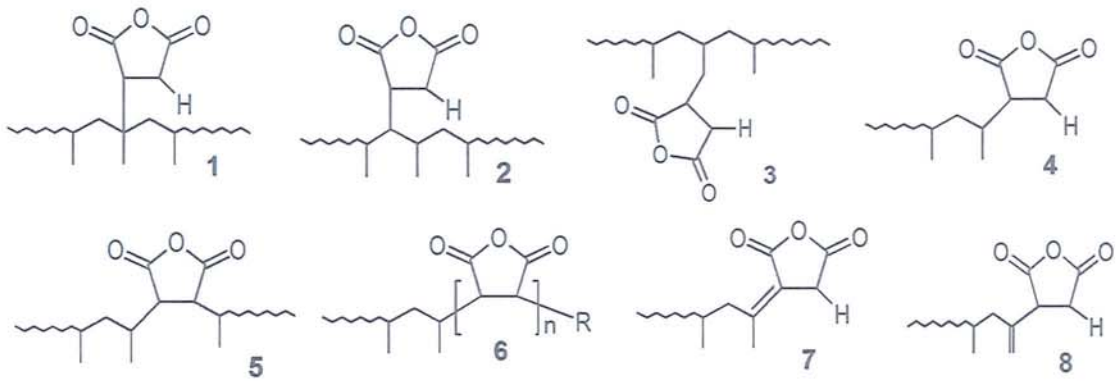

Borsig *et al.* **[33,52,395]** indicated that at 130°C the relative reactivity of the $CH:CH_2:CH_3$ groups in PP under conditions of solid state grafting with BPO as initiator was of the order 50:10:1 (reactivities per hydrogen atom) though details on how these numbers were obtained were not given. According to De Roover *et al.* **[95,177]**, the first step in the grafting process is abstraction of a methine hydrogen from the PP chain. The backbone

radical produced partitions between β-scission and addition of MA (and other processes). This conclusion was based on **[95,177]**:

(a) Correspondence between the FTIR of the grafted product and that of poly-MA.
(b) A statistical correlation between the degree of molecular weight reduction observed under their reaction conditions and the peroxide concentration.
(c) The observation that the aforementioned molecular weight reduction is independent on the MA concentration.

The authors **[95,177,178]** have proposed (on the basis of studies of model compounds **[95]** by FTIR analysis) that under conditions of melt processing all grafting occurs by reaction of $PP^{\bullet}$ radicals formed following β-scission with MA (refer to **Rn-4** followed by **Rn-6** and **Rn-7,** then followed by **Rn-12** and **Rn-13** in **Scheme 5.6**). A consequence of this hypothesis is that the grafted MA appears only at the chain ends as structures **(6)**. The free radical homopolymerisation of maleic anhydride can occur in molten polypropylene under the experimental conditions used for the functionalisation of polypropylene **[95,177,178]**. They proposed that a substantial fraction of grafts were of oligomeric nature with a chain length of five to six units (*structure 6*). They have also demonstrated that MA oligomerisation can occur in molten PP at 190°C under conditions similar to those used in the grafting experiments of this work. This group have also analysed a range of commercial MA–PP samples by FTIR and reported that all contained predominantly oligo- or poly-MA grafts **[177]**. They also reported that most (all those studied) commercial grades of PP–MA contained a significant amount of ungrafted MA present as either MA or poly-MA **[178]**.

The proposal, that most MA appears at chain ends as oligomer MA, has been challenged by Heinen *et al.* **[93,179]** and Zhang *et al.* **[158,180]**.These authors **[93,158,179,180]** provided NMR evidence to indicate that very little, if any, MA appeared at chain ends or indeed as oligo-MA and indicated that the principal graft sites are methine carbons and that MA is distributed along the chain as isolated succinic anhydride units (*structure-1*). Different reaction conditions were employed in these two studies: Heinen *et al.* **[93,179]** at 170°C melt, mini extruder, 5 min residence, 100 rpm, DCP initiator, whereas De Roover *et al.* **[95,177]** at 190°C melt, Brabender Plasticorder, 4 min residence, 75 rpm, DIPB initiator. It

is worth noting that the unimolecular β-scission process is likely to be favoured over addition of MA by one or more of the following factors: higher temperatures, lower pressures, lower MA concentrations, and poorer mixing. Another explanation lies with the ambiguity of the FTIR assignments. Further work is required to resolve this issue. These authors also proposed a further β-chain scission reaction of the MA-grafted PP to a lower molecular product (see **Rn-9** and **Rn-10** in **Scheme 5.6**). The NMR spectra showed **[158,180]** that the signals of MA attached to the tertiary carbons of the PP chains increased considerably with increasing MA content, whereas the signals of MA on the radical chain ends (with a single bond) arising from β-scission tended to decrease with increasing MA content. Moreover, the signals of MA on the radical chain ends with double bonds increased markedly with increasing MA content, and this indicated that β-scission occurred extensively after MA attached to the tertiary carbons. The authors have employed NMR spectroscopy to investigate the structure of the graft precise and unambiguous assignment of the carbon nuclear magnetic resonance (^{13}C NMR) signals of grafted MA structures. *Structure 7*, identified by ^{13}C NMR, and was proposed to arise from further reaction of *Structure 4* under the grafting conditions (see **Rn-9** and **Rn-10** followed by **Rn-11** in **Scheme 5.6**) **[93,179]**. This process seems unlikely, given the low concentration of graft MA units, even allowing for an enhanced reactivity of the methine (*Structure-1*) methylene (*structure-2*) or methyl hydrogen (*structure-3*) in **Scheme 5.5** and **Rn-8 in Scheme 5.6**). The importance of these two processes depends on the local MA concentration and the reaction temperature. Further grafting reactions include:

(a) Attack of PP radical on MA (**Rn-5** and **Rn-6** in **Scheme 5.6**)
(b) Hydrogen transfer from some donor molecule, e.g. PP backbone (**Rn-8**).
(c) Chain transfer of PP-g-MA, H-abstraction followed by β-scission (**Rn-9**)
(d) Intra-molecular abstraction, backbiting followed by β-scission (**Rn-10, Rn-11**).
(e) Combination PP-MA radical and PP radical or MA to give an oligomeric graft (**Rn-12, Rn-13** in **Scheme 5.6**), and
(f) Ene reaction (**Rn-14** and **Rn-15** in **Scheme 5.6**) [346].

In this work, the intensities of the C=C bands at 888 cm^{-1} and at 1648 cm^{-1} (1600–1700 cm^{-1}) as shown in **Fig. 5.5** is very small suggesting a very low yield of *structure-7* (see **Rn-9** and **Rn-11** in **Scheme 5.6**). Based on the different variables examined in this work, it is

clear that the only way to increase the extent of MA conversion to MA grafted on PP in conventional system would be to increase the initial concentration of the peroxide. Since the structural unit of polypropylene contains a more reactive hydrogen at the methyne site (see **Scheme 5.5** *Structure-1')* and due to the structure of MA which has low reactivity of its double bond, thus lower extent of homopolymerisation is expected, it is suggested that predominantly only one MA unit becomes bound on PP during the MA grafting reaction. This means that the probability of the homopolymerisation of MA in grafted PP system (see **Rn-13** in **Scheme 5.6**) is very low, due to the rapid transfer of the tertiary hydrogen to the succinyl free maleic anhydride radical (see **Rn-8** in **Scheme 5.6**). The effect of the initial maleic anhydride concentration on the percent of reacted maleic anhydride and on the degradation of polypropylene is an issue that has most divided authors who have been investigating this reaction. In this work, it has been shown that the grafted MA degree in the modified PP under all conditions examined, depends on the molar ratio of the peroxide to the anhydride ([peroxide]/[MA]) (see **Fig. 5.16**). It is clear from **Fig. 5.16** that at a constant molar ratio of [T-101]/[MA]I (e.g. 0.005 and 0.002] increasing the initial concentration of MA lead to a continuous increase in the level of MA grafting on PP. This is because the amount of peroxide available in this system is in direct proportionality with each of the different amounts of initial MA used. In contrast, when a constant weight level (e.g. 0.5 phr) of the same peroxide was used, the grafting level went through a maxima upon increase in the initial MA concentration, but on further increase, the grafting level decreased (see **Fig. 5.17)** with results that are in agreement with literature **[1,51,90,158,181,182]**. Increasing the concentration of [MA]i in this system, where the phr level of the peroxide is constant, means that the molar ratio of [peroxide] to [MA]i becomes smaller, thus, the amount of peroxide available to affect grafting is drastically reduced (see **Table 5.1,** p.256) thereby giving rise to the observed decrease in the grafting level. It is also clear from **Fig. 5.15** that MFI of the modified PP is also a function of the MA content, and it increases very significantly when the MA content is increased. This is most likely due to chain scissions, which is more profound when the MA content of the medium is high because of the increased availability of MA molecules during the formation of macroradicals. Higher MA concentration in a system containing constant molar ratio of [peroxide]/[MA] means that the weight percent of the peroxide is higher, thus more primary radicals are generated from the peroxide resulting in an amount of macroradicals that would undergo β-scission reaction (see **Rn-4** in **Scheme 5.6**) then attack the monomer MA (see

Rn-6 and **Rn-7** in **Scheme 5.6**) or would follow an alternative route (see **Rn-9** and **Rn-10** in **Scheme 5.6**) hence giving rise to an increase in MFI and reduction in the molecular weight. Consequently, the higher the initial MA content, the more the degradation of PP-g-MA chains via β-scissions and the higher MFI values as shown in **Fig. 5.15**.

5.3.2 Effect of Coagents on MA Grafting Reaction

The above discussion shows that the overall grafting efficiency (conversion) of MA on PP in the conventional system is low and that much higher concentration of peroxide (see **Fig. 5.14**), and higher temperature (see **Fig. 5.13**), are needed to achieve higher conversion rates, at the expense of degradation of the polymer. Generally, a limited grafting degree and severe degradation of PP during the melt grafting of MA onto PP are caused by the low reactivity of MA towards free radicals and its low solubility in the PP melt. The low free-radical reactivity of MA is inherently due to its structural symmetry and deficiency of electron density around the double bond [79,170,411,420]. As discussed in **Section 1.3.4**, Chapter 1 (p.48), the use of a highly reactive comonomer can significantly enhance the desired grafting and reduce the undesired side reaction. The much higher torque peak (torque-maximum) and final torque values during processing of PP with the coagents TRIS (PP-g-TRIS), and DVB (PP-g-DVB), in the presence of Trigonox-101 compared to conventional system in absence of coagents, suggest that the coagents are more reactive toward PP than MA (see **Fig. 5.28**). The high final torque (higher than in conventional system) when either of the two coagents is used, see **Fig. 5.28**, indicates that the coagents themselves undergo some degree of homopolymerisation and/or crosslinking reactions. However, the results show that optimising the conditions in a grafting system containing MA with TRIS or DVB, leads to a significant improvement in MA grafting yield with higher grafting efficiency achieved at much lower peroxide concentrations, thus resulting in negligible extent of degradation of the polymer matrix (see MFI values at 0.002 molar ratio peroxide in **Fig. 5.21**). As shown in **Fig. 5.19** and **5.21**, the level of MA-grafted PP was also affected by the type and concentration of peroxide used. The grafting degree increased initially with the initiator concentration reaching a maximum, and then levelled off. The higher the peroxide concentration in the reaction medium, the more primary radicals are formed and the higher the concentration of the PP macroradicals and that of DVB or TRIS radicals that would be available for the reaction with MA, thus the initial increase in MA

grafting level. A further increase in peroxide concentration results in no further increase in grafting level because of more reaction competition from side reaction and faster termination rate of the free radicals at higher free-radical concentration **[408,410]**.

One of the features of grafting MA onto PP in the presence of a coagent is that only a small amount of peroxide is required at any fixed concentration of the coagent. The level of MA-grafted PP in the processing of conventional PP/MA system using T-101 0.01 molar ratio to MA (≈0.28 phr) ([MA]i = 8 %, temp.180°C, 65 rpm, 10 min) was only 0.9 % (grafting efficiency ~ 11 %). In contrast in the coagent system, when the concentration of MA 8% and weight ratio of DVB to MA 2/8 w/w, ≈ 2 phr, it was enough to use only 0.001 molar ratio of T-101 to MA+DVB (≈0.14 phr) to achieve 3.4 % grafting degree (grafting efficiency more than 40 %). Interestingly, a further increase of T-101 concentration did not give rise to a significant increase in the grafting level (see **Fig. 5.21**). Moreover, the MFI of the processed PP in the presence of coagents TRIS or DVB was much lower than that in the absence of the coagent (see **Fig. 5.21**). This indicates that a certain level of peroxide is needed not only to initiate the grafting reaction, but also to assist branching/crosslinking reaction. If the peroxide concentration is above this level, the increase in peroxide concentration would only lead to more coagent assisted chain scission or branching/crosslinking of the polymer. Furthermore, the higher the DVB concentration, the less peroxide concentration was needed. The optimal grafting in the presence of DVB (in term of achieving high MA grafting with minimum chain scission or branching/crosslinking) can be achieved with a delicate balance between the molar ratios of the reagents (monomer, coagent, and initiator) and the process variables (e.g. temperature, processing time). The improvement in MA conversion to grafted-MA on PP in the presence of the coagents was due to the high reactivity of DVB or TRIS and its polyfunctional groups that can act as a linker for the MA through some extent of branching or crosslinking of the polymer chains. It is interesting to note that the extent of MA-grafted and the rate of MA-grafting in the presence of DVB were higher than that in the case of TRIS (see **Fig. 5.28**). The different reactivity of the two coagents and their effect on the extent of improvement in the grafting degree and in minimising the level of degradation of PP will be discussed in **Section 5.3.6** (p.287). Increasing DVB concentration and its ratio to MA from 1/9 to 4/6 resulted in increasing level of MA grafting (see **Fig. 5.25**). This agrees with the content of DVB in the processed PP as shown by the increase in the infrared peak area

index of aromatic peak at 711 cm^{-1}/2722 cm^{-1} (see **Fig. 5.26**). The presence of the coagents in the grafting system leads not only to higher MA grafting yield but also to lower extent of competition form side reactions. High concentration of peroxide may give rise to fast and high grafting of the coagents onto polymer chains, resulting in high branching/crosslinking of PP indicated by low MFI value, especially in the case of DVB (see **Fig. 5.26**). The kinetics of the grafting reaction in the presence of DVB or TRIS clearly showed that samples processed in the presence of the coagents did not contain measurable amount of either the free MA-co-DVB (MA-co-TRIS) copolymer or the poly DVB (poly TRIS). It was shown that the rate of MA-grafting is higher in the presence of the coagents compared to their absence with a higher rate of grafting with coagents (see **Fig. 5.27**). Moreover, it was observed that the presence of DVB or TRIS lead to complete grafting reaction in a much shorter time compared to conventional system processed in the absence of the coagents (see **Fig. 5.27**).

5.3.3. Mechanism of Free Radical Grafting of MA onto PP in the Presence of Coagent

The incorporation of a small concentration of the highly reactive coagent DVB or TRIS in the MA grafting system brings about an important change dominated by a clear improvement in the grafting yield (see **Fig. 5.21, 5.24, 5.25**) which is achieved at a faster rate (see **Fig. 5.27**) and with a substantial reduction in the main competing side reactions. First of all, the high reactivity of DVB or TRIS towards PP-macroradicals was clearly illustrated from the distinct torque behaviour during the reactive processing (see **Fig. 5.28**). The presence of DVB or TRIS in PP resulted in a torque peak under both shear initiation and free radical-initiation in the absence and presence of the monomer MA indicating the occurrence of a reaction which leads to an initial increase in polymer melt viscosity. It is also interesting to note that the addition of MA to a PP system containing the coagent DVB or TRIS results in a drastic reduction of the final torque (after the initial torque peak) compared to PP processed with the coagent only (i.e. without MA), see **Fig. 5.28**. This suggests that at the end of the reaction, the coagent-initiated side reaction, e.g. DVB-assisted branching of PP, are drastically reduced resulting in much higher extent of DVB-assisted MA-grafting reaction when compared to conventional MA-grafting system containing no coagent. This much higher MA-grafting level in the presence of the coagent was clearly illustrated under all conditions examined including different processing

temperatures (see **Fig. 5.19**), peroxide (see **Fig.5.21**) and MA concentrations (see **Fig. 5.24**). The mechanism of grafting of MA in the presence of DVB or TRIS is presented in **Schemes 5.7** and **5.8**.

Under the grafting conditions used, the extent of formation of a free MA-co-DVB or MA-co-TRIS copolymer and poly-DVB or poly-TRIS was found to be very small (present as a white insoluble fraction in xylene), most probability it was a 'free' copolymer (after purification of the grafted polymer product) at the end of the grafting reaction. In fact, it is almost certain (based on reactivities) that this reaction does occur during the initial stages of the grafting reaction, but the propagating MA-DVB or MA-TRIS copolymer radical (see **Rn-7** in **Scheme 5.6** or **Rn-7a** and **7b** in **Scheme 5.7**) would further react, on further processing, with PP, DVB or TRIS-containing-branched macroradical giving rise to further grafting (see **Rn-8** in **Scheme 5.7** and **5.8**). On further high temperature processing of the polymer melt, chain scission of the polypropylene (**Rn-5**) and the graft PP-DVB-co-MA or PP-TRIS-co-MA copolymer chains (see **Rn-6** and **Rn-9** in **Scheme 5.7** and **5.8**) or branching/crosslinking the PP-DVB or PP-TRIS copolymer with PP macroradicals (see **Rn-10** in **Scheme 5.7** and **5.8**) might take place giving rise to restructuring of branching/crosslinked graft copolymer.

In a separate study of grafting of antioxidants onto PP in the presence of TRIS, examined of the reaction mechanism suggested that the branching/crosslinking took place in the initial stage of processing [96,97]. Therefore, the grafting degree of MA can be significantly improved and part of the DVB monomer could preferentially react with PP macroradicals to produce relatively stable PP-DVB• macroradicals, thus contributing to a drastic decrease in the extent of β-scission reaction of the PP• macroradicals, this combined with the fact that much lower initial peroxide concentration is needed in the presence of the coagent, give rise to an overall much lower change in the molecular weight of the reactivity processed polymer (closer MFI values to that of PP control) compared to the conventional system, see **Fig. 5.21**.

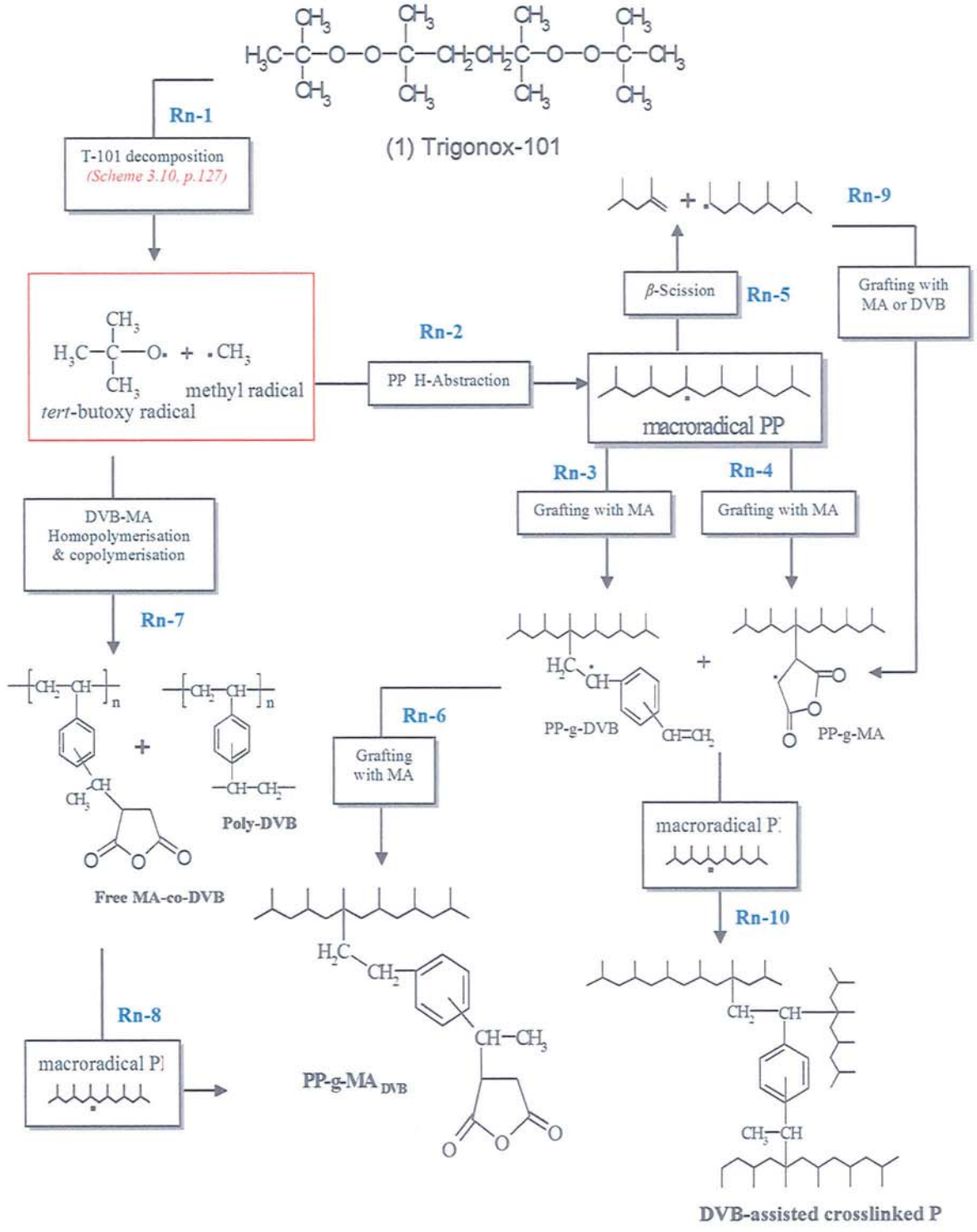

Scheme 5.7 The reaction mechanism of MA-grafting reaction of PP by peroxide initiation in the presence of DVB.

Scheme 5.8 The reaction mechanism of MA-grafting reaction of PP by peroxide initiation in the presence of TRIS (cont.)

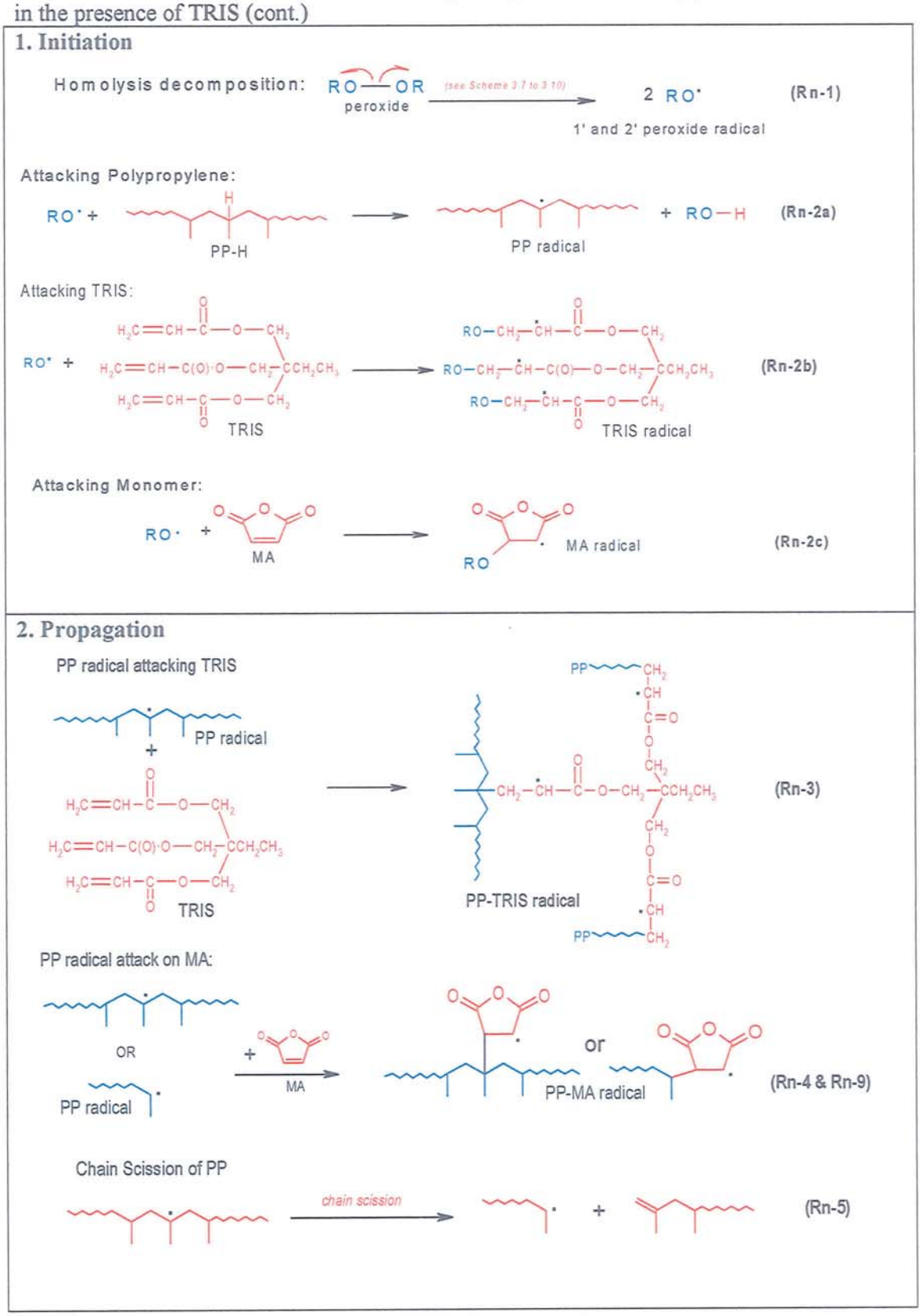

Scheme 5.8 The reaction mechanism of MA-grafting reaction of PP by peroxide initiation in the presence of TRIS (cont.)

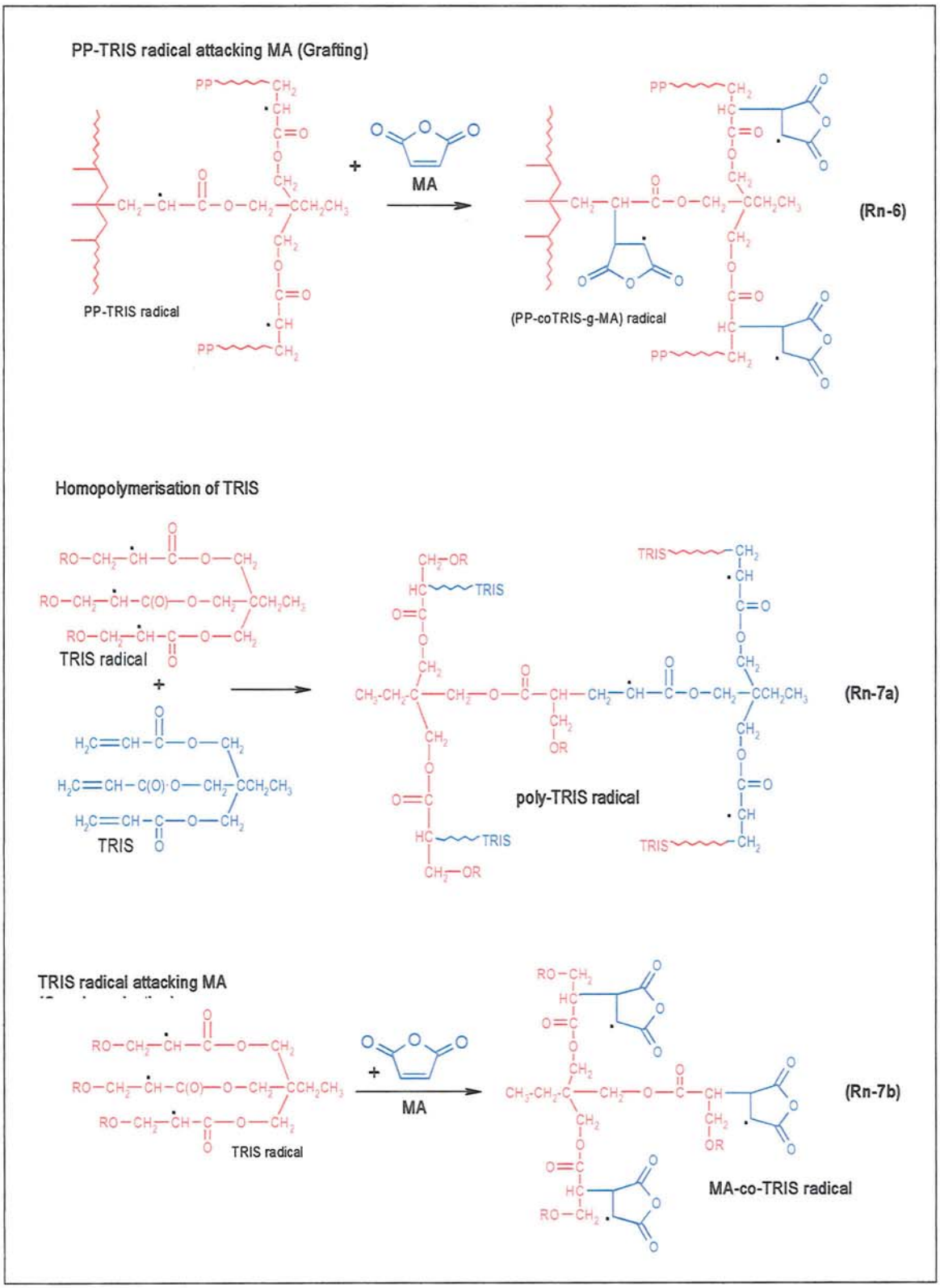

Scheme 5.8 The reaction mechanism of MA-grafting reaction of PP by peroxide initiation in the presence of TRIS (cont.)

3. Termination

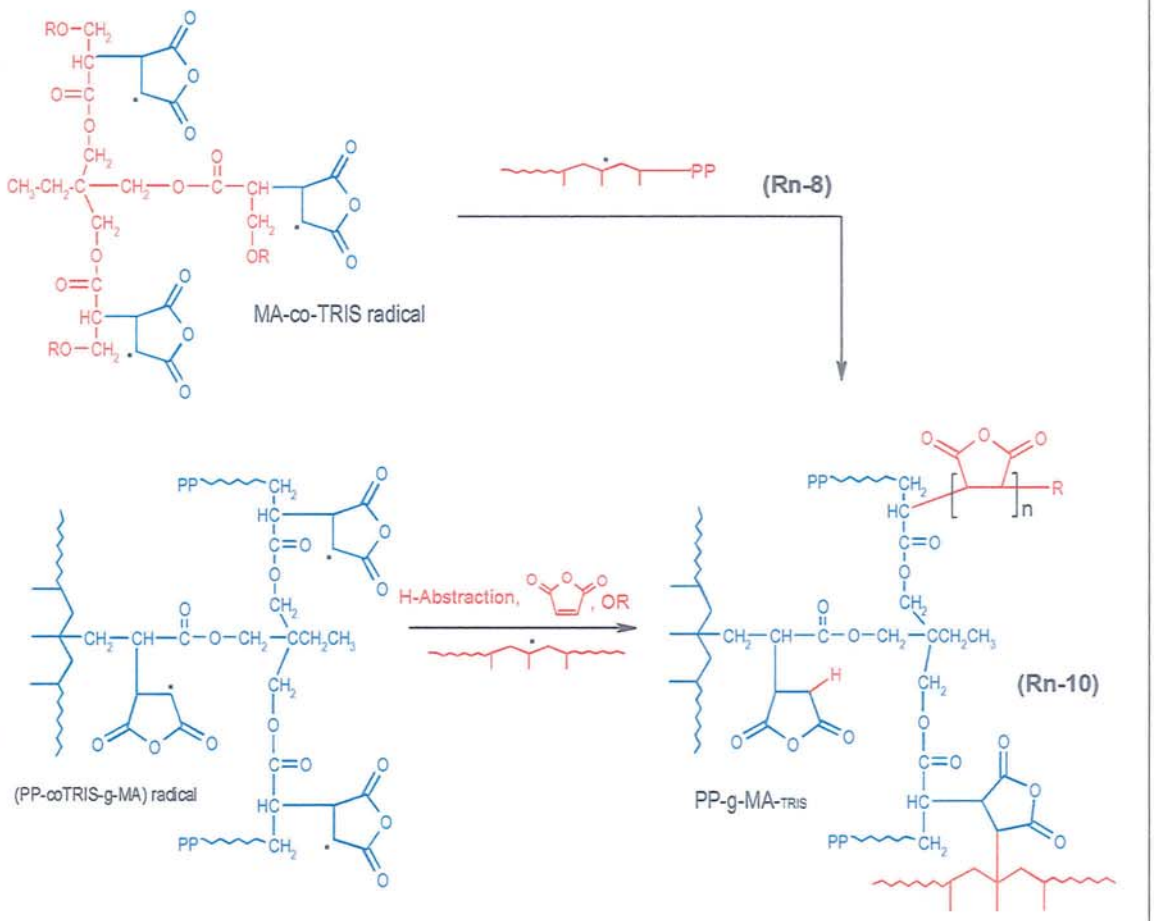

5.3.4 Comparison of Reactivity of Peroxides

It is reasonable to assume that competition between the grafting and side reaction processes, which determine the chemical structure of the product, will largely depend on the nature and concentration of the peroxide used. The difference in the rates of decomposition of various initiators are related to difference in the structures of the initiators and of the radicals produced. The effects of structure on initiator reactivity have been discussed by Moad *et.al.* [3,35,65,83,104]. During rapid processes typical of reactive extrusion, the reactivity of the peroxide initiator and its dissolution in the components of the grafting reaction blend, i.e. polymer and monomer, can markedly influence the course of grafting reactions and concomitant conversions [3,53,59]. During the free radical

grafting process of PP with GMA or MA in the presence of DVB, the β-scission of PP-chains may decrease because of PP branching/crosslinking with the coagent. It is well known that polypropylene is very sensitive to the attack of hydrogen-abstracting free radicals to form PP• macroradical, the sites of the grafting reaction as well as chain scission. Thus, it could be possible to differentiate the hydrogen-abstracting capability of the four peroxides used by observing the torque values recorded and possibly correlate this to the grafting degree and MFI.

Figures 5.31 and **5.32** show the torque value and the grafting degree of GMA and MA (in the presence of DVB) as well as the extent of MFI change for the functionalised PP. It was learned that the nature of peroxide initiators is decisive for grafting efficiency and degree of macromolecular degradation. To ensure a high yield of grafted product, it is advisable to use peroxides, which have thermodynamic affinity with PP and the temperature range of decomposition of which corresponds to the thermal regime of reactive extrusion. The grafting efficiency of the different peroxides used was evaluated and in general the results show that T-101 > DCP > T29B90 > BPO. The higher efficiency of the T-101 and DCP could be attributed to the longer time of the rate of their decomposition ($t_{1/2}$) at high temperatures (160-200°C). Also probability the nature of the radicals formed during their homolysis reaction whereby T-101 decomposes to generate *tert*-butoxyl and methyl radicals whereas DCP gives rise to cumyloxyl, phenyl and methyl radicals, see **Scheme 3.7** to **3.10** in Chapter 3 (pp.126,127).

Table 5.3 presents the Gibbs free energy changes (ΔG^{o}) of the homolysis reactions involving the free radicals of interest. From the viewpoint of thermodynamics, the capability of free radicals to abstract a hydrogen atom from PP chains increase from tertiary carbon radical to the phenyl radical (from the bottom to the top in **Table 5.3**). According to (ΔG^{o}) values in **Table 5.3**, phenyl free radicals (generated from DCP and BPO) should have even higher hydrogen abstraction capability than that of methyl or *tert*-butoxyl (T-101 and T-29B90) radical. However, it is very difficult to show a relationship between the torques values and the degree of H-abstraction due to the complex nature of the grafting system in the presence of a monomer and a comonomer.

Table 5.3 Free energy changes (ΔG^{o}) of some homolysis reaction **[421]**

Reaction	ΔG^{o} (kJ/mol)
$Ph\text{-}H \longrightarrow H^{\bullet} + Ph^{\bullet}$	508
$RO\text{-}H \longrightarrow H^{\bullet} + RO^{\bullet}$	473
$CH_4 \longrightarrow H^{\bullet} + CH_3^{\bullet}$	451
$RCH_3 \longrightarrow H^{\bullet} + RCH_2^{\bullet}$	444
$(R)_2CH_2 \longrightarrow H^{\bullet} + (R)_2CH^{\bullet}$	431
$(R)_3CH \longrightarrow H^{\bullet} + (R)_3C^{\bullet}$	415

5.3.5 Comparison of Reactivity of Monomers MA and GMA

The optimum melt reaction conditions required to achieve enhanced grafting level of GMA and MA on PP with minimum degradation of PP have been established using the peroxides Trigonox-101 (T-101) and Trigonox-29B90 (T-29B90) as free radical initiators (in all cases T-101 gave better results). Comparison of the grafting results for GMA and MA in the absence of coagent (conventional) system (see **Fig. 5.33** to **5.36**) under most conditions, showed that GMA grafts to a higher level suggesting that the reactivity of GMA is higher than that of MA.

One of the most important aspects of the study of copolymerization is the relationship between the composition of the monomer feed (i.e., the relative monomer concentrations, best expressed as molar ratio) and that of the resulting copolymer. It was already made clear (see **Section 1.3.1**, pp.31-37) that glycidyl methacrylate (GMA), for example, undergo homopolymerisation **[119-122,125]** would also readily engage in copolymerization with styrene **[123,126,424]**, whereas other monomer maleic anhydride (MA) (see **Section 1.3.2**, pp.37-43) would not homopolymerise to any appreciable extent **[93,158,179,180]**

would copolymerise without difficulty with styrene [1,187]. The monomer reactivity ratio for glycidyl methacrylate (GMA), maleic anhydride (MA), and oxazoline (OXA) in radical copolymerisation with styrene (St) and acrylonitrile (AN), are shown in **Table 5.4**. It is important to note that the monomer reactivity ratios depend on the system used for their determination and must be determined for each monomer pair of interest.

Table 5.4 Monomer Reactivity ratio in radical copolymerisation

Monomer 1	Monomer 2	T (°C)	r_1	r_2	Refs.
Styrene	Glycidyl methacrylate **(GMA)**	110	0.200	0.638	**[424]**
		135	0.262	0.681	**[424]**
		160	0.288	0.732	**[424]**
		170	0.316	0.750	**[424]**
		190	0.356	0.785	**[424]**
		230	0.438	0.852	**[424]**
		65	0.34	0.63	**[430]**
			0.44	0.56	**[431]**
			0.48	0.60	**[431]**
	Maleic anhydride **(MA)**	80	0.042	0	**[426]**
		50	0.097	0.002	**[426]**
		60	0.02	0	**[432]**
		25	0.09	0.04	**[433]**
		25	0.10	0.11	**[433]**
		25	0.10	0.23	**[433]**
	Oxazoline 2-isopropenyl **(OXA)**		0.67	0.64	**[434]**
Acrylonitrile	Glycidyl methacrylate **(GMA)**		0.95	0.85	**[435]**
		100	0.22	1.44	**[436]**
	Maleic anhydride **(MA)**	60	6	0	**[437]**
	Oxazoline 2-isopropenyl (OXA)		0.13	0.52	**[434]**
NOTE: r_1 = reactivity ratio of monomer 1 r_2 = reactivity ratio of monomer 2					

The reactivity ratios, deduced from copolymerisation, have been widely used for comparison of the reactivities of monomers grafting copolymerisation towards reference polymer radical. When a vinyl monomer (M_1) is copolymerised with a second monomer (M_2), the monomers reactivity ratio, r_1 and r_2, for any monomer pairs are the ratios of the rate constant of the different propagation reactions **[423,424]**:

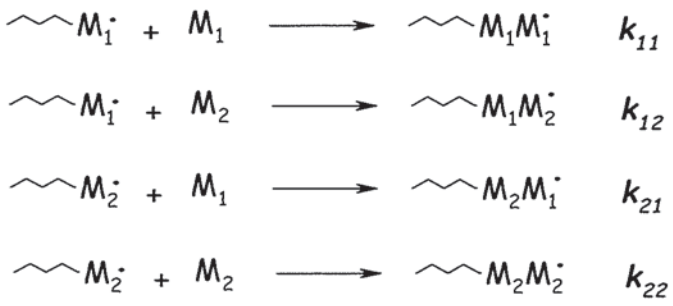

The relative rates of consumption of monomers M_1 and M_2 are given by Mayo-Lewis equation **[425,426]**:

$$\frac{-d[M_1]}{-d[M_2]} = \frac{[M_1]\{r_1[M_1] + M_2]\}}{[M_2]\{r_2[M_2] + M_1]\}} \qquad \text{Eq. 5.1}$$

where $r_1 = k_{11}/k_{12}$ and $r_2 = k_{22}/k_{21}$. Fineman and Ross **[427]** rearranged **Eq.5.1** to

$$G = r_1 F - r_2 \qquad \textbf{Eq.5.2}$$

where $G = X(Y-1)/Y$, $F = X^2/Y$, $X = [M_1]/[M_2]$, and $Y = d[M_1]/d[M_2]$. When G is plotted against F a straight line is produced having a slope r_1 and intercept r_2. Kelen and Tudos **[428]** refined the linearisation method in the form

$$\eta = [r_1 + r_2/a]\,\xi - r_2/a \qquad \textbf{Eq.5.3}$$

where $\eta = G/(a+F)$, $\xi = F/(a+F)$ thus plotting η against ξ gives a straight line that yields $-r_2/\alpha$ and r_1 as intercepts on extrapolation to $\xi = 0$ and $\xi = 1$, respectively. The value of $\alpha = (F_m F_M)^{1/2}$ where F_m and F_M are the lowest and highest F values, respectively. There is a real problem here in that the accuracy of r values is often insufficient to allow one to reasonably

conclude whether r_1 and r_2 varies with changes in reaction media variation and with temperature in activation energy for propagation reactions according to Arrhenius relation [408,424]

$$ln\ r_1 = ln\ k_{11}/k_{12} - \Delta E_{A1}/RT \qquad \textbf{Eq.5.4a}$$

$$ln\ r_2 = ln\ k_{22}/k_{21} - \Delta E_{A2}/RT \qquad \textbf{Eq.5.4b}$$

where ΔE_{A1} and ΔE_{A2} are the differences of the propagation activation energy.

As mentioned in the **Section 4.3.1** (p.179) and **Section 5.3.1** (262), the first step in the melt grafting process via the free radical mechanism is the abstraction of hydrogen atoms by initiating free radical (*tert*-butoxyl) from PP chain to create PP macroradicals. Since changes in the polymer molecular weight have a direct influence on the viscosity of the polymer melt **[1,3,35]**, the torque exerted by the motor on the polymer melt will vary accordingly to maintain a constant rotor speed. Therefore, the reactivity of a monomer may be indirectly extrapolated from the torque traces recorded during the grafting reaction. **Figure 5.33** compares the torque variation with time during the processing of PP alone (as a control), with PP/MA/T-101 (MA 8%), and PP/GMA/T-101 (GMA 12 %) under the same conditions (T-101 0.005 molar ratio to monomer, temp. 180°C, rotor speed 65 rpm). It can be observed that the torque values in the case of MA are much lower than for GMA, indicating that the ability of MA molecules to trap the PP macroradical to be lower than for GMA. The observed lower torque max and final torque during the reactive processing of MA in PP and the lower grafting level at different temperatures (see **Figure 5.33** and **5.34**), peroxide concentration (see **Fig. 5.35**), and monomer concentration (see **Fig. 5.36**) supports a lower reactivity of MA compared to GMA. These results are further supported by the data of **Table 5.4** which show clearly that the reactivity ratio of monomers 2 (r_2) in the copolymerisation of the reactive monomers with styrene and acrylonitrile decreases in the order of GMA > OXA > MA. Furthermore, the double bond in MA has lower reactivity than that in GMA due to the presence of two adjacent electron-attracting carbonyl groups and because of its symmetrical nature **[79,411,419,420]**.

In order to get a high level of grafting of GMA or MA and a low incidence of side reactions, it is required that the PP• macroradical is efficiently transformed to the graft sites. The monomers act to trap radicals that would otherwise undergo chain scission in PP. Thus, the use of a higher monomer concentration may result in less degradation of the polyolefin substrate. However, in the case of GMA and MA, the trapping of the radical by increasing the monomer concentration does not, in itself, prevent degradation of PP by β-chain scission. **Figure 5.36** shows that increasing the monomer concentration has resulted in a higher grafting level but at the same time it worsened the PP degradation as indicated by the increase in MFI. Even in the case of MA/T-29B90 (conventional) system, the increase in MA concentration was only worsening the degree of degradation of PP without improving its grafting level (see **Fig.5.35**).

As described in **Section 3.4.2** (p.111), the differences in the decomposition rates of various initiators can be conveniently expressed in terms of the initiator half-life times ($t_{1/2}$) defined as the time for the concentration of peroxide ***(I)*** to decrease to one half its original value. The rates of initiator disappearance of $I \rightarrow 2R^{\cdot}$ is [408]:

$$-(d[I]/dt = k_d.[I] \qquad \textbf{Eq.5.5a}$$

which on integration yields:

$$ln\,[I]_o/[I] = k_d.t \qquad \textbf{Eq.5.5b}$$

where $[I]_o$ is the initiator concentration at the start of graft copolymerisation. By setting $[I] = [Io]/2$, the integration yields $ln\ 2 = k_d.\ t_{1/2}$ the half-life times ($t_{1/2}$) is obtained as:

$$t_{1/2} = 0.693/k_d \qquad \textbf{Eq.5.5c}$$

Due to the differences of the half-life time ($t_{1/2}$) of T-29B90 and T-T-101 (at temp. 160°C, $t_{1/2}$ T29B90 = 0.83 min and T101 = 2.1 min, see **Table 2.3** in Chapter 2, p.63), it can be expected that at the first seconds of the grafting process of PP/GMA/T-29B90 and PP/MA/T-29B90 systems, the T-29B90 peroxide would produce initially a higher

concentration of transient *tert*-butoxyl radicals (see **Scheme 3.9** and **3.10**, pp.126,127) thus resulting in more PP• macroradical compared to the system where T-101 is used under the same concentration and temperature (of 160°C) (see **Rn.1** and **Rn.2** in **Scheme 4.5** (p.182) and **Scheme 5.7**, p.275). However, because of the lower reactivity of MA compared to GMA, the macroradicals produced would react to a lower extent (with MA) and free macroradicals (those which have not reacted with MA) would result in an increased level of degradation by chain scission (higher MFI), see **Fig. 5.35**.

Similar to the classical copolymerisation principles, involving reactivity ratios, monomer graft copolymerisation onto polyolefins also depends on the initiation and termination steps as well as on the propagation steps. As discussed in **Section 5.3.4** the rate of graft copolymerisation of GMA and MA onto PP also depends on the reactivity of the monomer with peroxide radicals and PP macroradicals. Dokolas *et al.* **[55,71,422]** studied grafting competition reactions of various monomers, namely, maleic anhydride (MA), methyl methacrylate (MMA), 2-hydroxyethyl methacrylate (HEMA), 2-dimethylamino ethyl methacrylate (DMAEMA), allyl methacrylate (AMA), methyl acrylate (MAc), methacrylonitrile (MAN), styrene (St), 4-vinylpyridine (4VP), and vinyl acetate (VA) towards *tert*-butoxyl radicals (in the presence of a radical trap) on PP, PE, and PET or their model compounds, 3-methyl pentane (for PP), 2,4-dimethyl pentane (for PE), and ethylene glycol dibenzoate (for PET). The authors concluded that experiments with HEMA, AMA, and MMA would give higher grafting level than the monomers of vinyl pyridine, styrene, and maleic anhydride. Based on this data, the expected reactivity of *tert*-butoxyl radicals towards these monomers was expected to decrease in the following order ***styrene > vinyl pyridine > alkyl methacrylate > vinyl acetate > maleic anhydride***. However, the amount of grafting was also dependent on the rates of propagation and termination. The more likely reason for a higher grafting level of methyl methacrylate (MMA) compared to the others was that the electrophilic nature of methyl acrylate did not favour attack from the electrophilic *tert*-butoxyl radicals **[422]**, and therefore, hydrogen atom abstraction from the hydrocarbon substrate was the more competitive reaction. The rate of reaction of *tert*-butoxyl radicals toward a series of alkyl methacrylates remained essentially constant. In contrast, *tert*-butoxyl radicals do not attack maleic anhydride (MA). Similar with the above study, the results on this study suggest that experiments with GMA gave higher graft

formation, compared to MA, because of the greater reactivity of GMA compared to MA. The extent of electron-attracting effect of the two carbonyl groups in MA makes the π electrons of the C=C less available, whereas this attraction is less pronounced in glycidyl methacrylate, thus the C=C π bond in this case is comparatively more localised and can react more easily during the melt graft reaction. However, the reactivity of GMA can also be limited by its relatively bulky size, which could reduce the extent of the reaction of PP macroradicals with the monomer. Other competing reactions such as homopolymerisation of the monomer and chain scission of the polymer (PP) backbone would also affect the final level of grafting. The reaction schemes illustrated in **Scheme 4.5** in **Chapter 4** (p.182) and **Scheme 5.6** indicate clearly that the success of any free radical grafting process will depend on the level of competition between the grafting and side reactions (polymerisation and chain crosslinking or fragmentation), which in turn is associated with the rate of formation of the primary radicals that can abstract a hydrogen from PP as well as the reactivity of the monomer towards the macroradical PP. The stability of the macroradicals (recombination between, or fragmentation of, macroradicals) is also very important. Typically, the reactivity of macroradicals in polymer melts toward a vinyl monomer is usually low as its accessibility is much reduced due to the bulkiness of the macromolecular chains surrounding it, as well as their restricted mobility due to the high polymer melt viscosity. Due to the higher reactivity of GMA (compared to MA) with the PP macroradical, a higher GMA grafting degree was found at lower temperatures (<160°C), see **Fig. 5.34**, and lower peroxide concentration (0.002 to 0,005 molar ratio to GMA), see **Fig 5.35**. By contrast, in the case of MA, the grafting degree was higher at higher temperatures (180° to 200°C) and higher peroxide concentrations (0.01 molar ratio to MA).

Furthermore, it is important to note that high grafting degree would not only depend on the properties of the radicals formed to produce macroradical PP, but also the solubility of the monomer in PP melt and the reactivity of the monomer with the PP macroradicals. The different reactivities and extent of grafting would also depend on differences in polarity, molecular size, chemical nature, and the extent of their solubility in the polymer **[1,3]**. It is clear that the levelling off the degree of grafting of MA on PP with increasing concentration of the initial MA used (see **Fig. 5.36**) suggest that the solubility of MA in PP is limited, whereas the observed continuous increase in the amount of grafted GMA at higher initial GMA concentration implies a higher solubility.

5.3.6 Comparison of the Reactivity of Comonomers DVB and TRIS The Q-e Scheme and Pattern Reactivity

One of the objectives of this study was to examine the efficiency of comonomers TRIS and DVB for the free radical grafting of GMA or MA onto PP. The efficiency of using the coagents TRIS or DVB for the GMA or MA/peroxide systems is expected to depend on whether or not the reactivity of the coagents towards PP macroradicals is greater than that of GMA or MA and its ability to copolymerise with the monomer. A comparison of the effect of the coagents on changes in the torque characteristic, grafting yield and MFI can be seen in **Fig. 5.45** to **5.49**. It should be noted that addition of a comonomer is efficient only when the comonomer activates the free radical reactivity of the monomer in question by some specific interaction (e.g. as in the St/MA system) or makes the reactivity ratio of copolymerisation favourable for the free radical grafting (e.g. as in the St/GMA system). As discussed in **Section 4.3.1** (p.179) and **Section 5.3.1** (262), the first step in the melt grafting is the abstraction of hydrogen atoms from PP-chain and formation of PP-macroradicals. It is assumed that the initial amount of PP-macroradicals formed in the presence of both coagents is the same since the grafting process is compared in the presence of the same concentration of the peroxide initiator (T-101). During the free radical grafting process of PP with the monomers in the presence of either TRIS or DVB, the extent of PP chain scission may decrease since the comonomer would trap the PP macroradical or may become branched and eventually crosslink with PP (for their mechanism reaction in the presence of the comonomer, see **Schemes 4.6** and **4.7** (pp.191,192) for GMA and **Schemes 5.7** and **5.8** for MA. When branching and/or crosslinking occur, there would be an increase in viscosity of the PP melt resulting in a torque increase. Therefore, the reactivity of the GMA and MA systems can also be observed when they are processed using the same composition and processing conditions (GMA 12 %, MA 8%, T-101 0.005 molar ratio to monomer, weight ratio coagent to monomer 2/8, temp 180°C, 65 rpm, 10 min). **Figures 5.37** and **5.40** show the evolution of the torque as a function of time for PP processing with the monomers in the absence and presence of the comonomers, as well as, PP alone used as a control. It can be seen from **Fig. 5.37** that the final torque values of MA in the presence of either TRIS or DVB is lower than that of GMA with DVB. It is also found that the grafting degree of MA was always lower compared to that of GMA for all examined variables;

temperature (see **Fig.5.38**), peroxide concentration (**Fig. 5.39**), monomer concentration (see **Fig. 5.40** and **5.41**), and coagent concentration (see **Fig. 5.42** and **5.43**), as well as processing time (see **Fig. 5.44**).

Various attempts have been made to place the radical-monomer reaction on a quantitative basis in terms of correlating structure with reactivity. A useful semi empirical relationship, the ***Q–e scheme***, has been proposed that the rate constant for radical-monomer reaction, for example, for the reaction of $M_1^{\bullet}$ radical with M_2 monomer, be written as [439]:

$$k_{12} = P_1 Q_2 \exp(-e_1 e_2) \qquad \textbf{Eq.5.6}$$

where $\mathbf{P_1}$ represents the intrinsic reactivity of $M_1^{\bullet}$ radical, Q_2 represents the intrinsic reactivity of M_2 monomer, e_1 represents the polarity of $M_1^{\bullet}$ radical, and e_2 represents the polarity of M_2 monomer. By assuming that the same e value applies to both a monomer and its corresponding radical (i.e. e_1 defines the polarities of M_1 and $M_1^{\bullet}$ radical, while e_2 defines the polarities of M_2 and $M_2^{\bullet}$ radical), and **Eq. 5.6** can be appropriately expressed to yield the monomer reactivity ratio in the forms:

$$r_1 = (Q_1/Q_2) \exp.[-e_1 (e_1 - e_2)] \qquad \textbf{Eq.5.7a}$$

$$r_2 = (Q_2/Q_1) \exp.[-e_2 (e_2 - e_1)] \qquad \textbf{Eq.5.7b}$$

where $r_1 = k_{11}/k_{12}$ and $r_2 = k_{22}/k_{21}$ which correlate monomer-radical reactivity with the parameter Q_1, Q_2, e_1, and e_2. Here, monomer reactivity is separated into the parameter Q, which describes the resonance factor (and to a slight extent the steric factor) present in the monomer, and the parameter e, which describe the polar factor. For example

$$\{[\ln(Q_1/r_1)] - e_1^2\} = -e_2 e_1 + \ln Q_2 \qquad \textbf{Eq. 5.8}$$

Table 5.5 lists important monomers designation, the Q and e values, and the correlation coefficient (***r***) for the regression.

Table 5.5 *Q-e Scheme* of monomers **[404]**

	AN	OXA	MA	GMA	BA	MMA	EVE	S	VA
Q	0.48	0.59	0.86	0.96	0.38	0.78	0.018	1	0.026
e	1.23	-0.64	3.69	0.20	0.85	0.40	-1.80	-0.80	-0.88
r	0.56	0.54	0.98	0.92	0.94	1.5	0.90	-	0.87

AN = Acrylonitrile; **OXA** = oxazoline-2-isopropenyl; **MA** = Maleic anhydride; **GMA** = Glycidyl methacrylate; **BA** = Butyl acrylate; **MMA** = methyl methacrylate; **EVE** = ethyl vinyl ether; **S** = styrene; **VA** = vinyl acetate

For example in the case of the decomposition of *tert*-butoxyl peroxide, the *tert*-butoxyl radicals are found initially and those would decompose further to methyl (and acetone), see **Scheme 3.9** and **3.10** in Chapter 3 (pp. 126,127). Using *tert*-butoxyl peroxide, Jenkins *et al.* **[439-441]** described the competitive reactions of acrylonitrile (AN) (strongly electron accepting, e = +1.23 in the ***Q-e schemes***) and ethyl vinyl ether (EVE) (strongly electron donating, e = – 1.17, see **Table 5.4**) with the *tert*-butoxyl radicals and with secondary methyl radicals using a nitroxide radical trapping technique. It was found that *tert*-butoxyl radicals reacted three to six times faster with the electron rich ethyl vinyl ether (EVE) than with the electron deficient acrylonitrile (AN), in agreement with previous findings that *tert*-butoxyl radicals are generally believed to behave in an electrophilic manner **[64]**. In marked contrast, it was proposed **[64]** that methyl radicals behave more as nucleophilies, for example, in the above system, methyl radicals, which are present in low concentrations as a result of some β-fragmentation of *tert*-butoxyl radicals, were only shown to react with acrylonitrile (AN) and not with ethylene vinyl ether (EVE). In addition, any carbon-based radical that may form by addition or abstraction reactions of *tert*-butoxyl radicals with ethyl vinyl ether (EVE) would react so fast with acrylonitrile (AN) that the reaction competes effectively with nitroxyl radical trapping. This leads to useful information on the process of second monomer addition in copolymerization.

It is likely that PP• macroradicals have a preference to react with electron donating monomers such as styrene (e value = -0.80) and oxazoline (e value = -0.64) compared to electron accepting monomer GMA (e = +0.20) and MA (e = +3.69) which is even stronger electron accepting. It is clear from results of this work that in presence of peroxide T-101, the observed levelling off of the degree of grafting in the case of MA on PP with increasing concentration of initial MA used (see **Fig. 5.36**) suggests that the reactivity and solubility

of MA in PP is only limited, whereas in comparison the observed continuous increase in the amount of grafted GMA at higher initial GMA concentration implies a higher reactivity and solubility. There are reports in the literature that show grafts consisting of single maleic anhydride units because the PP graft-MA radical undergoes intramolecular hydrogen abstraction [93,151,189]. Therefore, MA grafts on PP here may also be expected to be composed of single monomer units in length. Regardless of the origin of the radical site on the polymer backbone, the ability of this site to participate in a grafting reaction is dependent on the monomer reactivity.

As mentioned in the introduction, the best way to favour grafting against side reactions (homopolymerisation of GMA and degradation of PP by β-scission) is to promote the reactivity between the monomer and the macroradicals so that the latter, once formed, will react with the monomer before they undergo fragmentation. One way of doing so is to add a second monomer (coagent) which has a high reactivity towards the macroradicals, and the resulting macroradicals should be capable of reacting (or copolymerising) with the monomer GMA or MA. It is likely that the ideal graft copolymerisation is more suitable between monomers of similar $\boldsymbol{Q}$ values and with $\boldsymbol{e}$ values of opposite signs, preferably larger different in $\boldsymbol{e}$ values [420]. For example, styrene is capable for promoting the free radical grafting of MA onto PP since the $\boldsymbol{Q}$ and $\boldsymbol{e}$ values of styrene ($\boldsymbol{Q}$ = 1, $\boldsymbol{e}$ = – 0.80) and MA ($\boldsymbol{Q}$ = 0.86, $\boldsymbol{e}$ = 3.69). In case of the grafting of oxazoline in presence of styrene where their Q values are quite different ($Q_{styrene}$ = 1 and Q_{OXA} = 0.56) and their $\boldsymbol{e}$ value are quite close ($\boldsymbol{e}$ styrene = -0.80 and $\boldsymbol{e}$ oxazoline = -0.64), the presence of styrene would reduce the grafting efficiency [136,137,188]. Indeed, the St/OXA pair was shown to have no-favourable reactivity ratios [1] as well as the unfavourable $\boldsymbol{Q}$-$\boldsymbol{e}$ values of both monomers as mentioned above.

The generally accepted radical facilitated graft copolymerisation mechanism involves the reactions of (1) peroxide decomposition, (2) H-abstraction by the formed peroxide radical, (3) grafting polymer radical (PP) and monomer (M) to form PP-M$^{\cdot}$ macroradical, and (4) peroxide radical reactivity towards the monomer (homopolymerisation). The relative rates of the reactions of H-abstraction and monomer grafting to PP$^{\cdot}$ macroradical in competition with homopolymerisation are of critical importance for any successful graft

copolymerisation. The effectiveness of the comonomers to enhance grafting degree of GMA or MA on PP depend on the comonomer reactivity towards PP• macroradical and reactivity the PP•-comonomer macroradicals to the monomers GMA or MA. These two ability factors would probability depend on (1) resonance and substituents effect, (2) polarity, and (3) steric hindrance of the monomer and PP-comonomer macroradical. Electron-donating substituent such as phenyl in the DVB molecule increases the electron density on C=C π bond and facilitates its bonding thus it is more reactive and prone to be attacked by the PP macroradical. The order of monomer reactivities corresponds to the order of increased resonance stabilisation by the particular substituents of the radical formed from that monomer [408]:

$-\phi, -CH=CH_2 > -CN, -COR > -COOH, -COOR > Cl > -OCOR, -R > -OR, H$

Substituents composed of unsaturated linkages are most effective in stabilising the radical because of the loosely held π-electrons, which are available for resonance stabilisation (see **Scheme 5.9**). The order of substituents in enhancing radical reactivity is the opposite of their order in enhancing monomer reactivity. A substituent that increases monomer reactivity does so because it stabilises and decreases the reactivity of the corresponding radicals.

Based on the above argument, the kinetic results shown in **Fig. 44** for TRIS and DVB can be explained. It can be seen clearly from **Fig 5.44** that the level of grafting of GMA in the TRIS/GMA system is higher than in DVB/GMA system with the grafting by complete in the first 2 minutes of the TRIS/GMA reaction, whereas the reaction is completed at much higher time of 7 minutes in the DVB/GMA system and results in much higher grafting level. The reason for this is that the TRIS with has three reactive acrylate groups results very rapidly, but the DVB with two styrenic double bonds that are more resonance stabilised will react slower taking longer time for completion of the grafting process but at the same time would give rise to higher grafting level due to its higher reactivity, as discussed above.

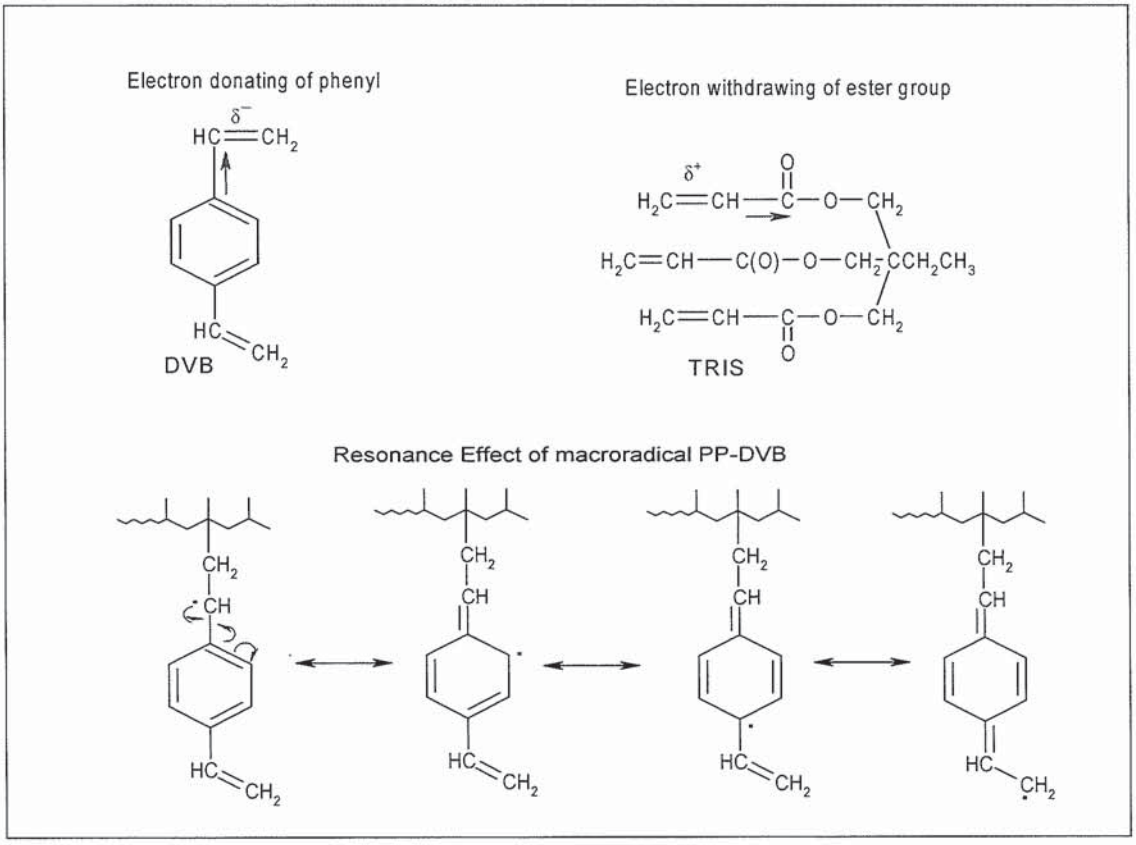

Scheme 5.9 Electron donating/withdrawing at DVB and TRIS and resonance effect of PP-DVB macroradical **[408]**

These findings are further supported by the higher torque maximum in DVB compared to that of TRIS (see **Fig. 5.46**) and the lower extent of MFI in the DVB system compared to the TRIS (see **Fig. 5.45**) this is therefore most probability because of DVB's ability to trap effectively the PP• macroradical which otherwise would undergo β-scission. However, PP-DVB• macroradicals are more stable (resonance effect) compared to the PP-TRIS• macroradicals. It is likely that graft copolymerisation of the monomers GMA or MA with the PP-DVB• macroradicals would be slower than is the case for PP-TRIS. The reaction rate constant of PP-TRIS• macroradical with the monomers GMA and MA can be expected therefore to be higher than that of the stabilised PP-DVB• macroradical (see **Fig. 5.44**). The comonomers DVB or TRIS are effective for increasing grafting level and suppressing the PP degradation (by β-scission reaction) in the presence of either GMA or MA when examined under all reaction parameter studied, i.e. temperatures and peroxide concentration (**Fig. 5.45**), coagent concentration (**Fig. 5.46 to 5.48**), and the monomer concentration (**Fig. 5.49**).

5.3.7 Compatibilisation of PBT/PP Blends with PP-g-GMA and PP-g-MA

Due to the significant difference between PBT and PP in terms of both physical and chemical properties, the polymer pairs are completely incompatible. If these polymers are blended directly, the high interfacial tension and lack of interfacial adhesion will lead to coarse, unstable morphology and poor overall physical and mechanical performance. Compatibilisation can be achieved through reactive blending where the desired copolymers are produced through interfacial reaction between reactive functionalities in the two polymers. Such graft copolymers strengthen the interface between domains, but perhaps more importantly they provide steric stabilization to reduce rate of coalescence all of which shift the balance between drop break up and coalescence to give a finer dispersion and more stable morphology **[321]**. Compatibilisation of PBT and PP with functionalised PP is expected to occur via reaction between the end groups of PBT and the GMA grafted on PP or MA grafted on PP. The blends of PBT/PP showed a sharp interface and poor adhesion between the dispersed phase and the matrix (see **Fig. 5.29**). However, in the reactive blends of both PBT/PP/PP-g-GMA and PBT/PP/PP-g-MA, as expected, the minor phase was hardly distinguishable as a result of the improvement of dispersibility, especially using PP-g-GMA_{TRIS} or PP-g-GMA_{DVB}. SEM suggests that the PBT/PP/*f*-PP blends have reduced interfacial tension resulting in the observed extremely fine dispersion of PBT in PP phase. The functionalised PP would also increase the adhesion at phase boundaries, giving improved stress transfer and stabiliser the dispersed phase by modifying the phase boundaries interface. Due to time limitation, very limited amount of work was done in this area but the SEM micrograph show clearly that the use of only 2.5 % of both PP-g-GMA_{DVB} and PP-g-GMA_{TRIS} result in very fine dispersion of the PBT phase indicating very good level of compatibilisation. The possible reaction between the epoxy group (GMA) in PP and the end groups (-OH and –COOH) of PBT is presented in the **Scheme 5.10**. The strong polarisation of the O-H bond of carboxylic acids end groups ensures fast reaction between epoxy and carboxylic acids groups (see **Rn-1** in **Scheme 5.10**). Other possible reactions are the esterification (see **Rn-2** in **Scheme 5.10**) of secondary hydroxyl groups and hydrolysis of the epoxy group In PBT/PP/PP-g-GMA blends, two competitive reactions take place during the melt blending viz. **(1)** compatibilisation due to interfacial reaction between PBT chains end functionalised-PP epoxide, resulting in the formation of

PBT-GMA-PP graft copolymer and **(2)** rapid crosslinking of the PP-PBT phase due to the simultaneous presence of hydroxyl and epoxide groups on PBT-GMA-PP chains (see **Rn-3** and **Rn-4** in **Scheme 5.10**). The compatibilisation efficiency is directly related to ratio of the epoxide in functionalised-PP and ester groups in PBT and is maximum when this ratio is PBT/PP/PP-g-GMA 80/10/10 and 80/5/15.

Scheme 5.10 Possible interfacial reactions of GMA grafted PP with end groups of PBT [442].

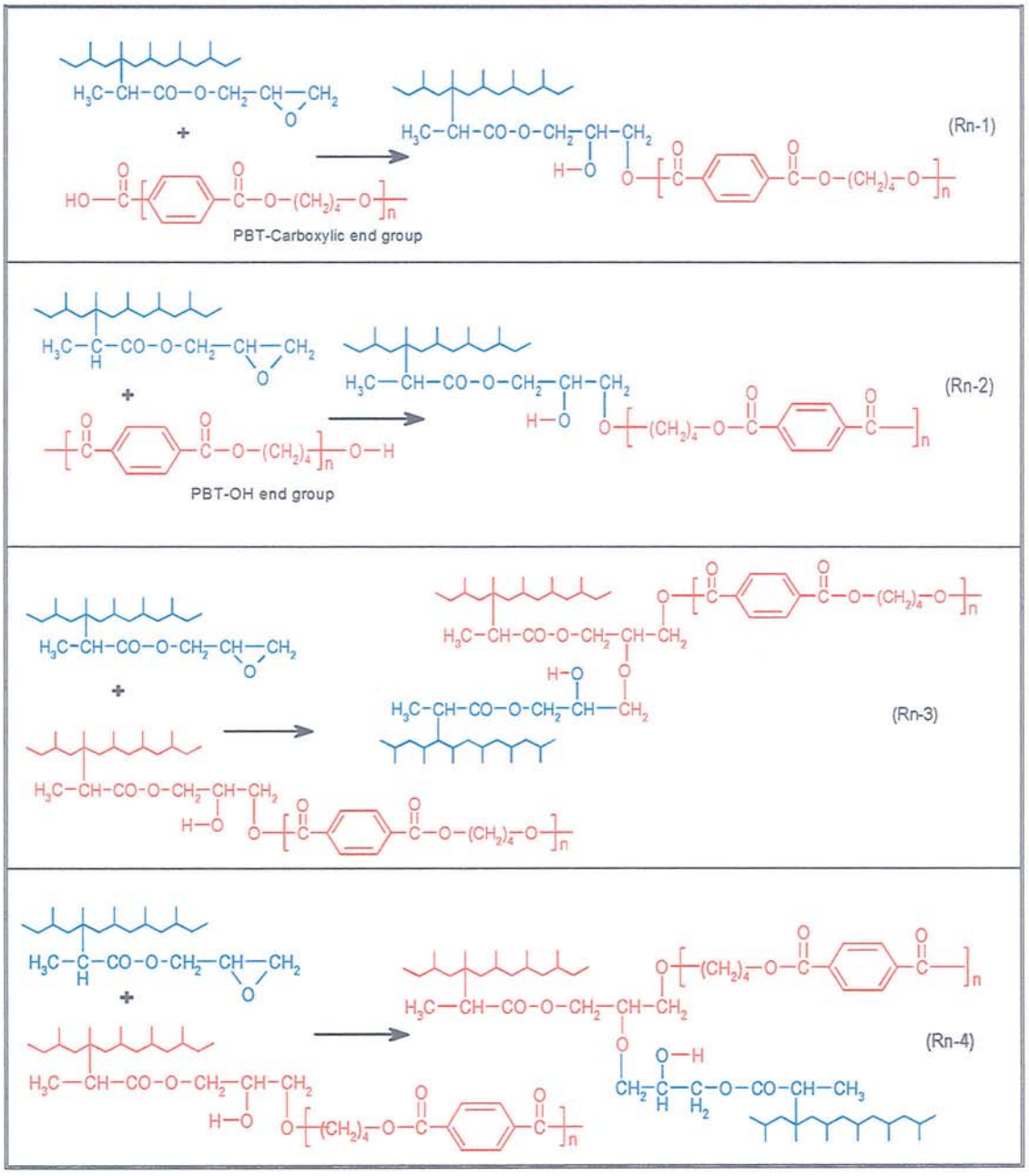

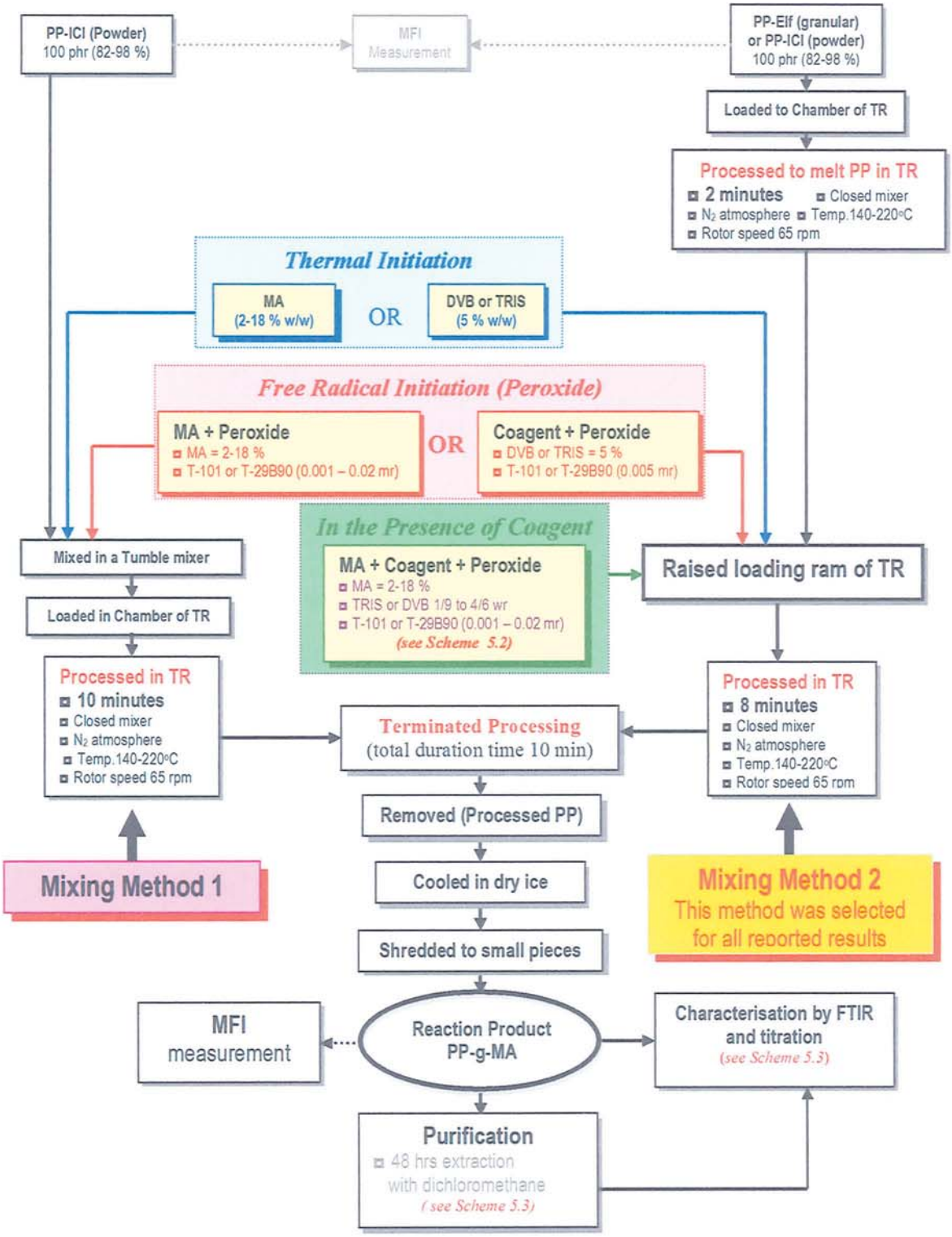

Scheme 5.1 Flow chart for reactive processing of PP with MA by thermal, free radical initiation using peroxide T-101 or T-29B90.

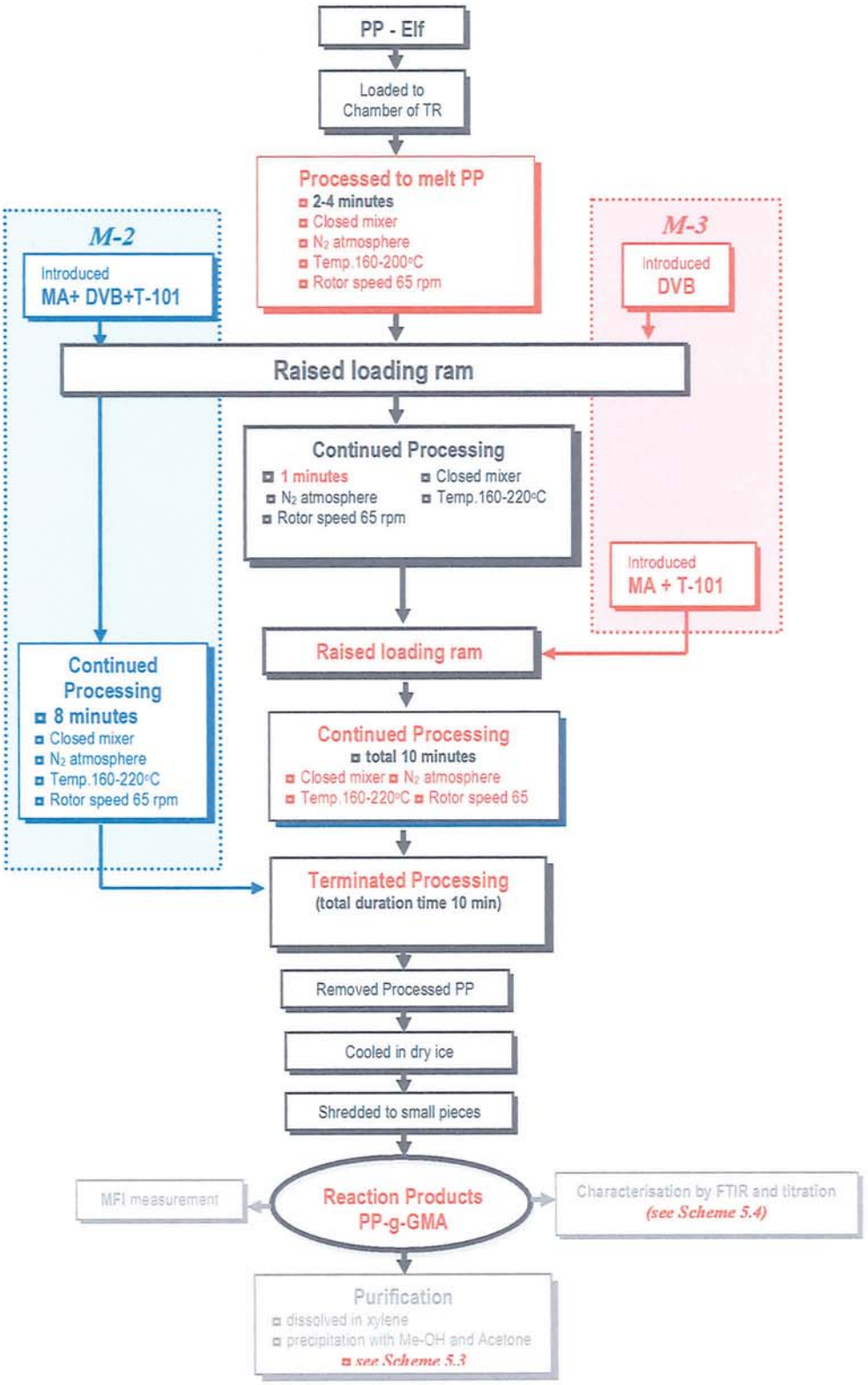

Scheme 5.2 Flow chart for reactive processing of PP with MA in the presence of coagent TRIS or DVB

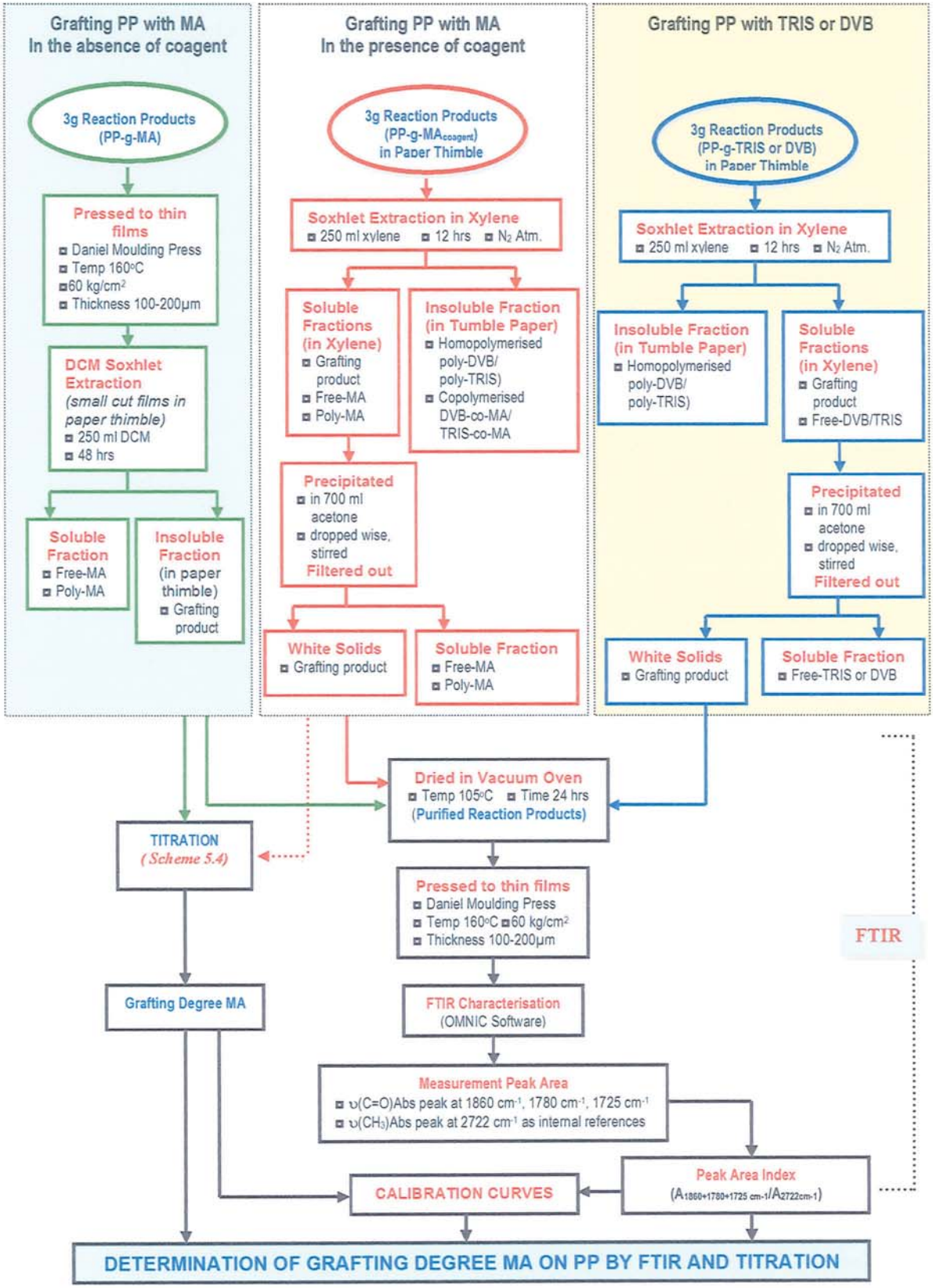

Scheme 5.3 Flow chart for purification methods and determination of grafting result

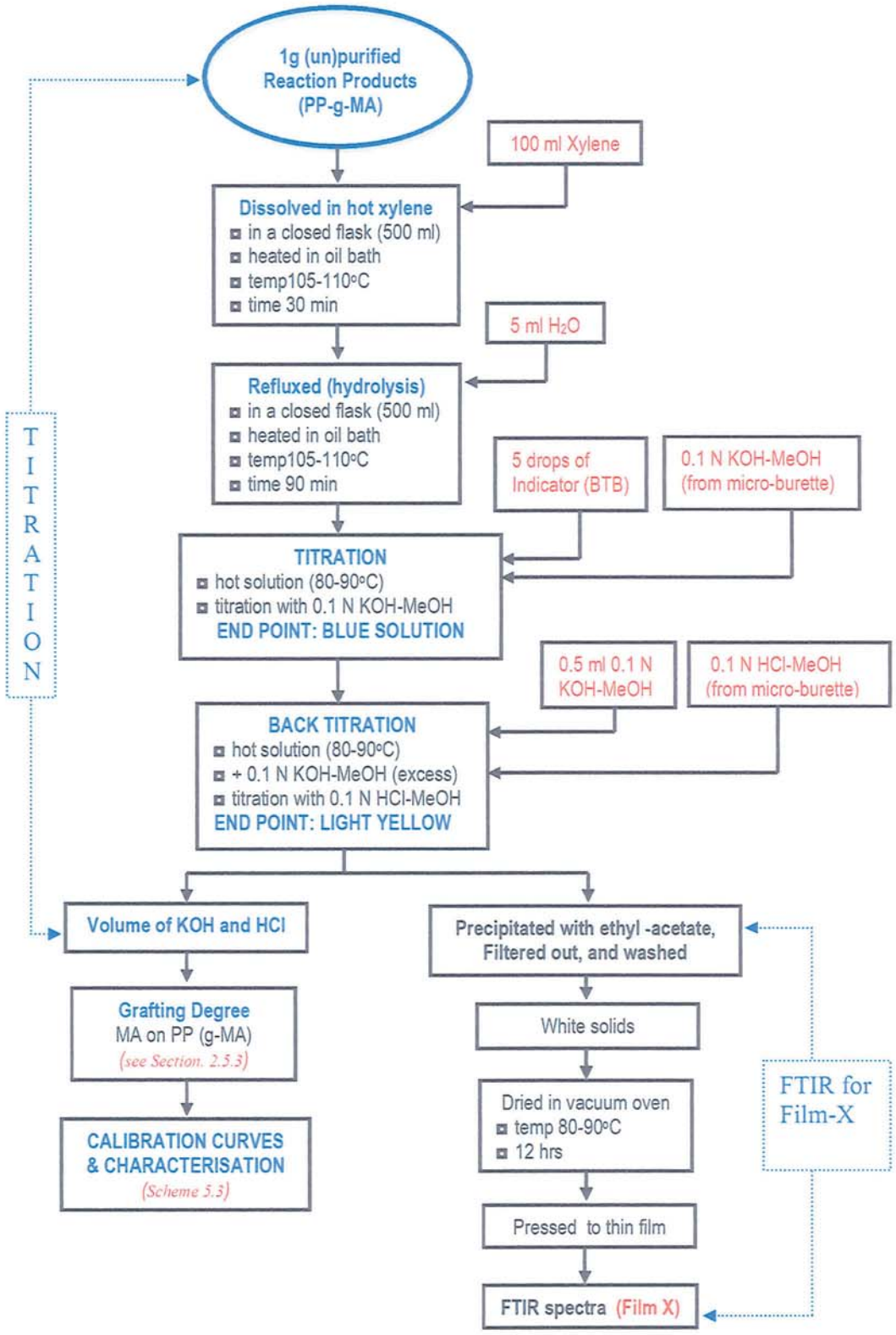

Scheme 5.4 Flow chart for determination of grafting MA on PP by Titration

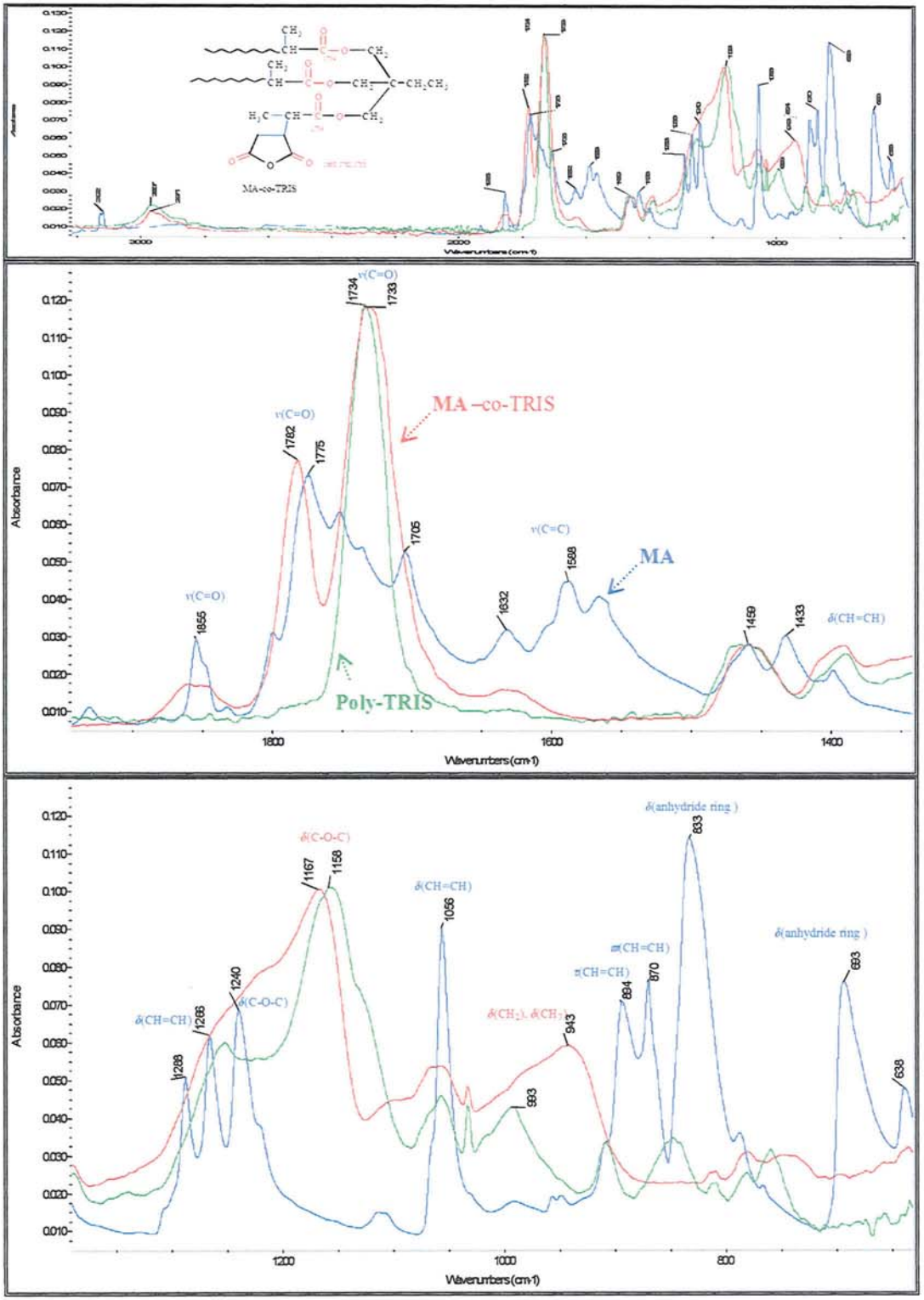

Figure 5.1 Comparison of ATR-FTIR spectra of synthesised of **MA-co-TRIS** film (red), poly-TRIS films (thickness ~100μm) (green), and neat of MA in KBr disc (blue).

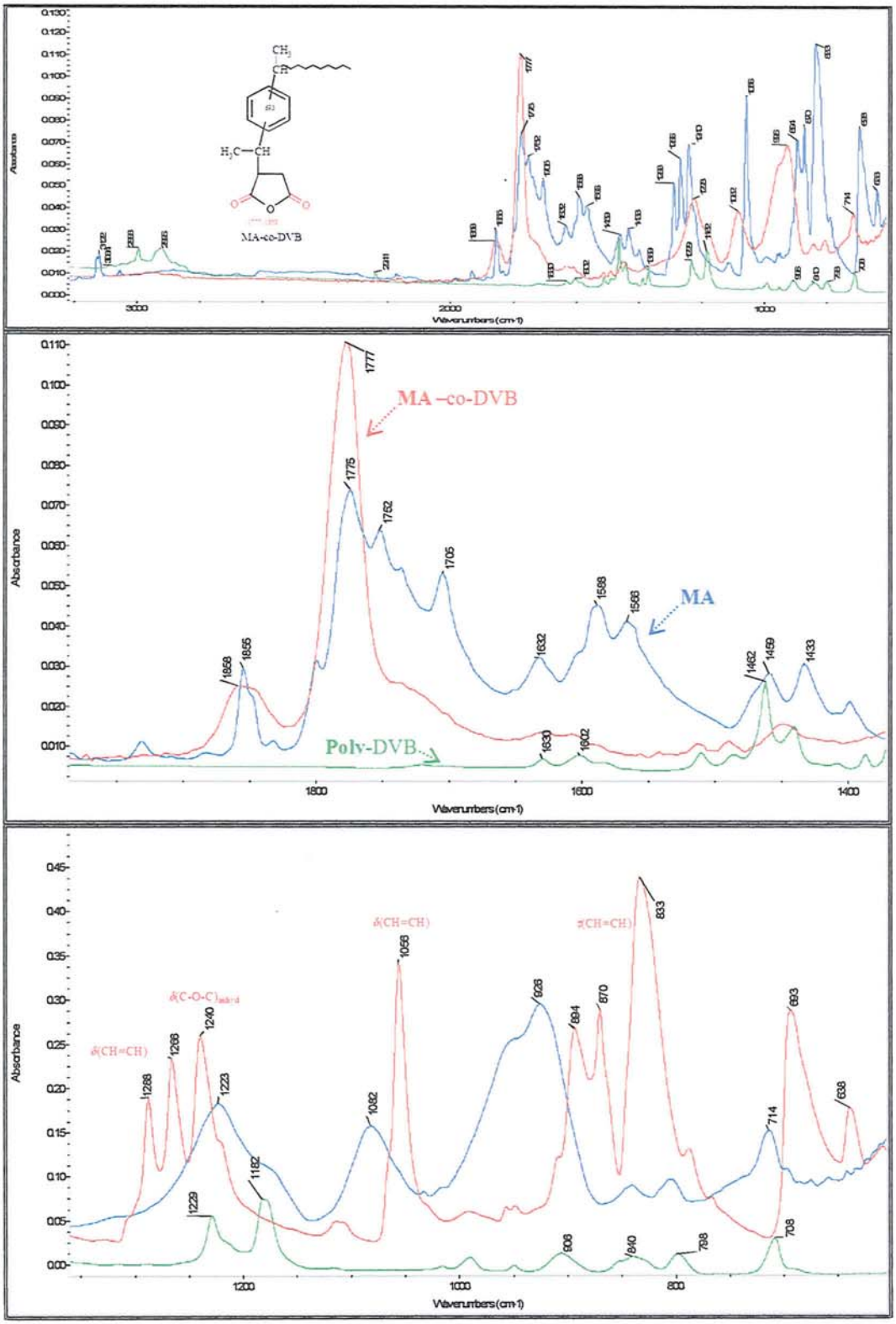

Figure 5.2 Comparison of ATR-FTIR spectra of synthesised MA-co-DVB (red), poly-DVB films (thickness ~100μm) (green), and neat of MA in KBr disc (blue).

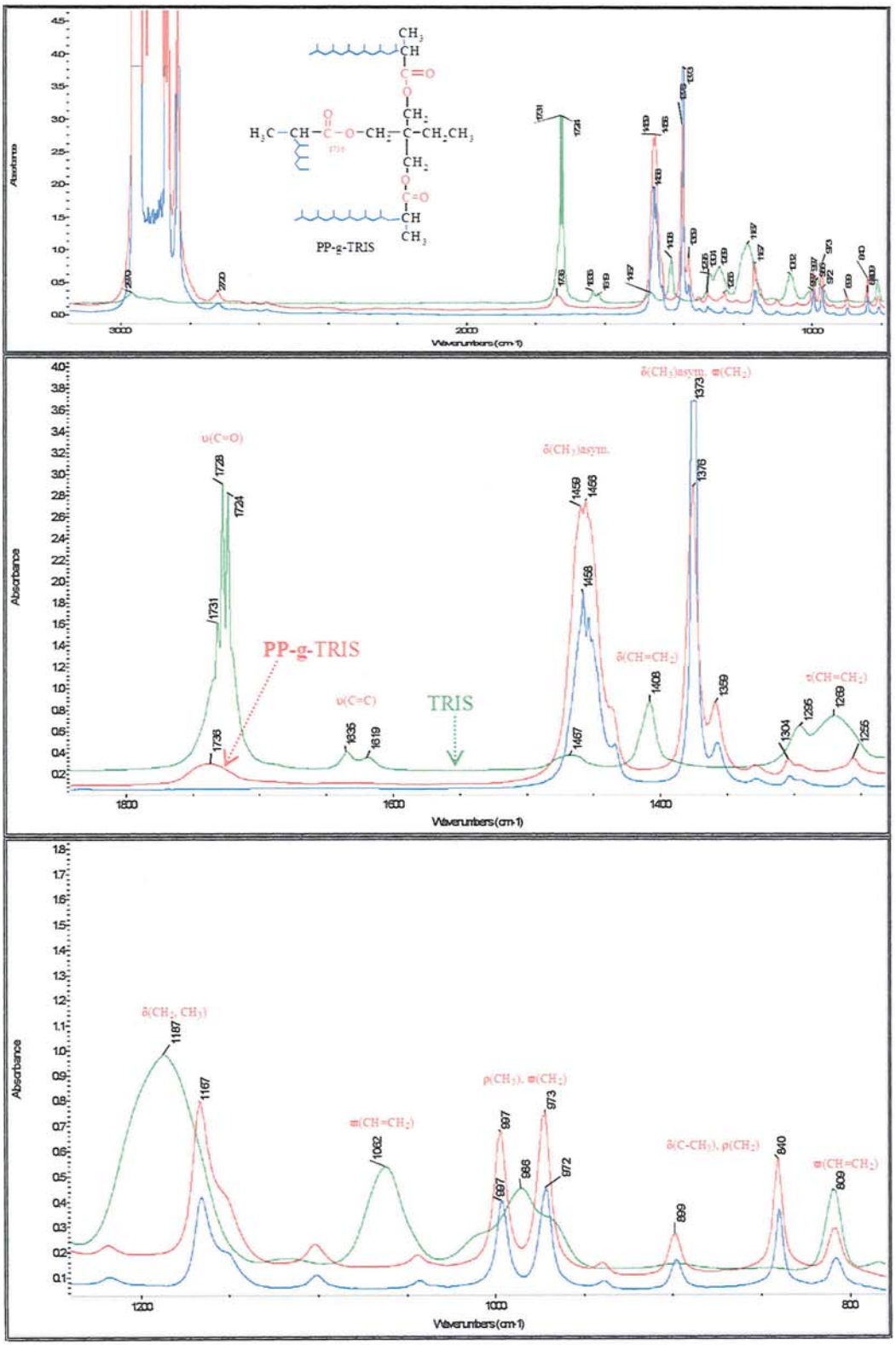

Figure 5.3 Comparison of FTIR spectra of the PP-g-TRIS film (red), PP alone films (thickness ~100μm) (blue) and neat of TRIS in KBr disc (green).

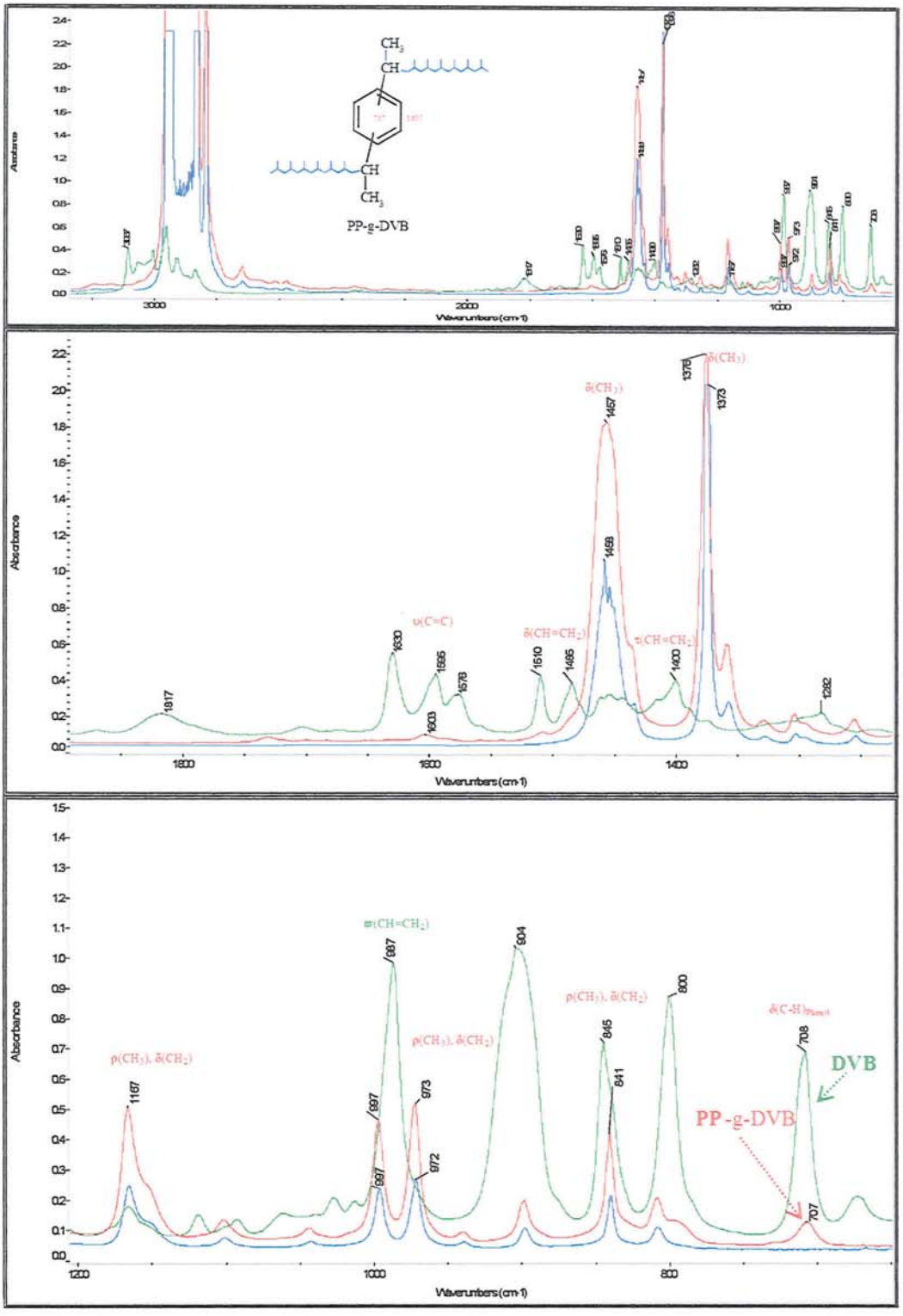

Figure 5.4 Comparison of infrared spectra of the purified PP-g-DVB film (red) with PP (alone) films (thickness ~100μm) (blue), and neat of DVB in KBr disc (green).

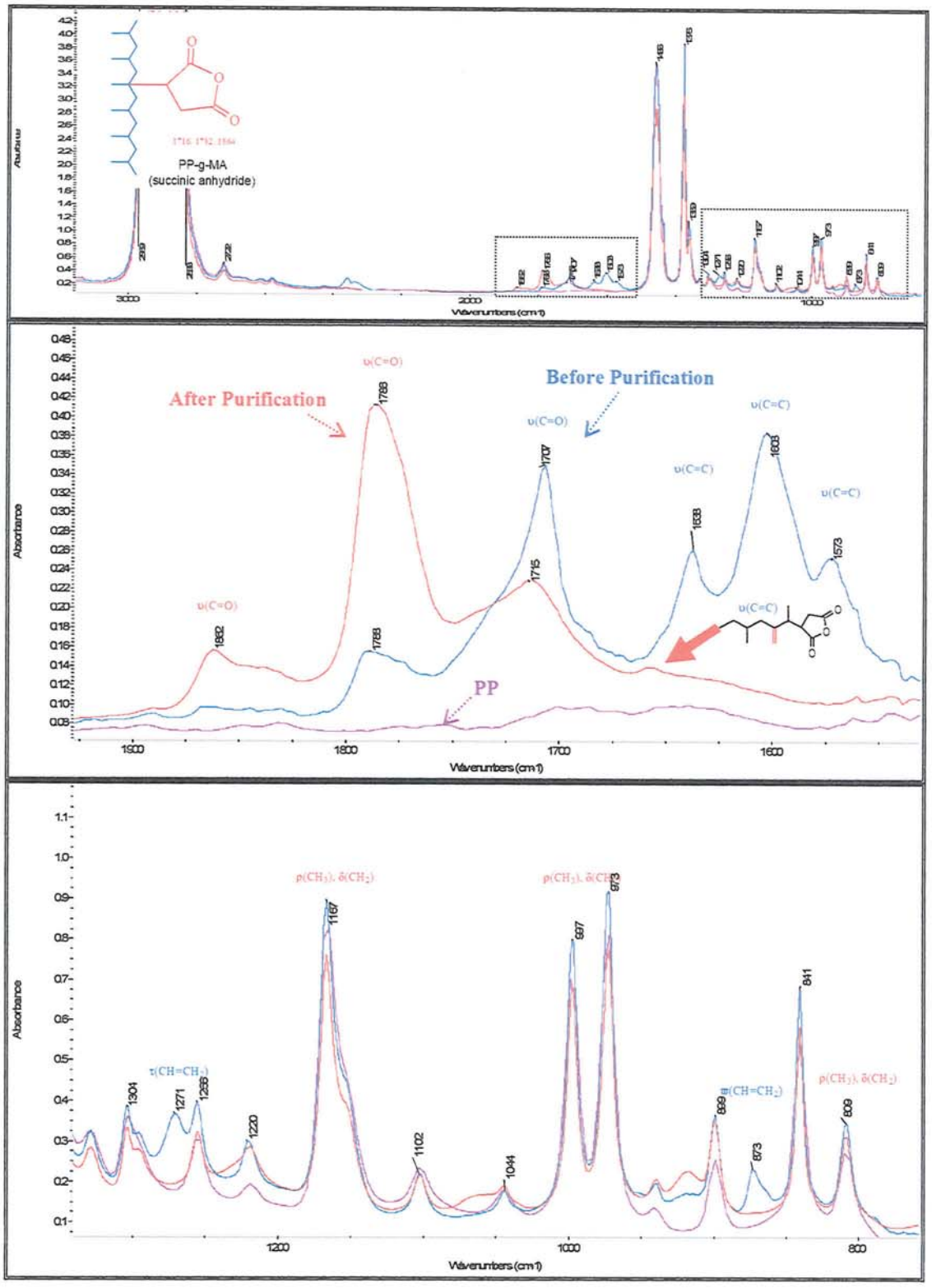

Figure 5.5 The comparison of infrared spectra of the virgin PP (purple) and the reaction product PP-g-MA films (thickness ~100μm), before (blue) and after purification (red).

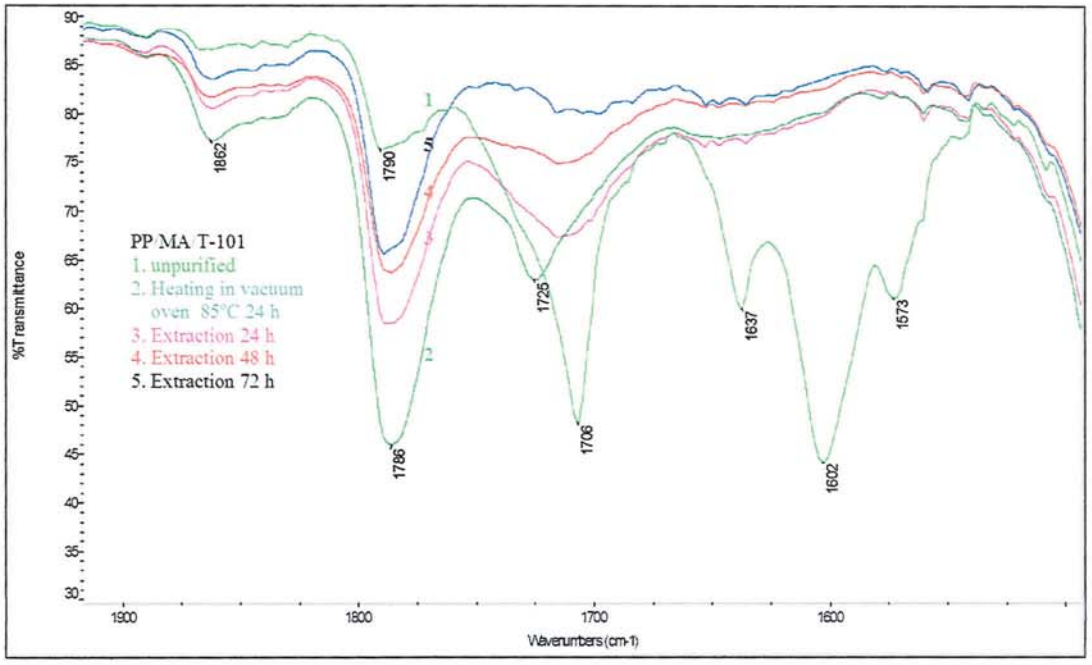

Figure 5.6 FTIR spectra of pressed films of PP/MA/T-101 in the different purification methods (1) unpurified, (2) Heating in 85°C for 24 h, and extraction in DCM (3) 24 h, (4) 48 h, and (5) 72 h.

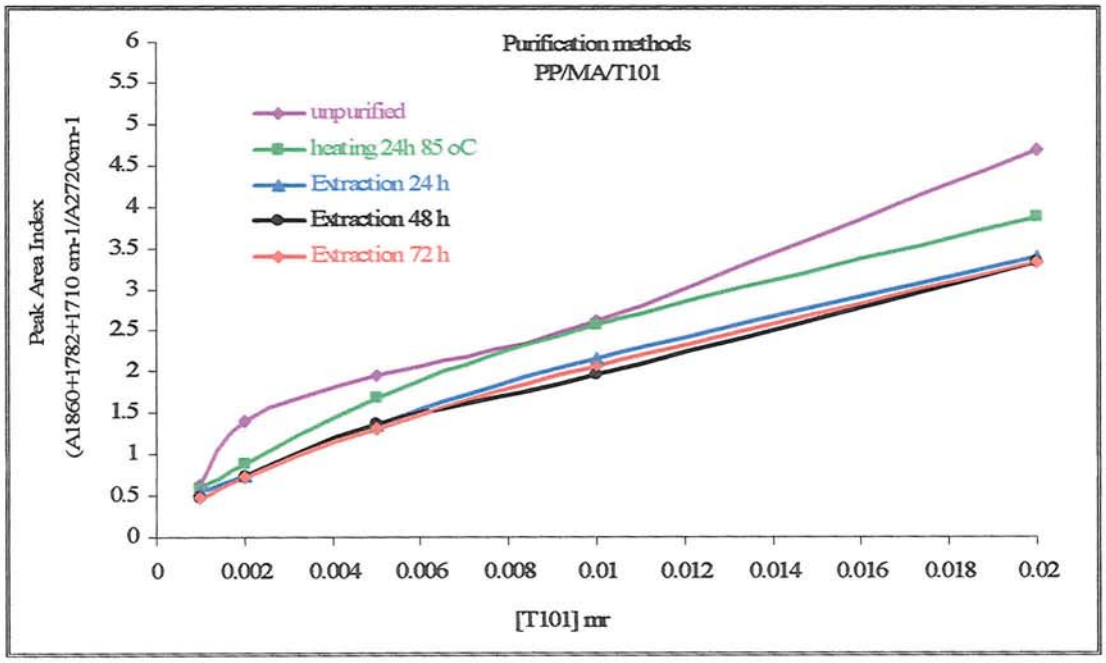

Figure 5.7 The comparison of MA-grafted on PP by the different of purification methods and the duration of extraction by DCM. Samples PP-Elf, MA 8 %, various [T-101], 180°C, 65 rpm, 10 min.

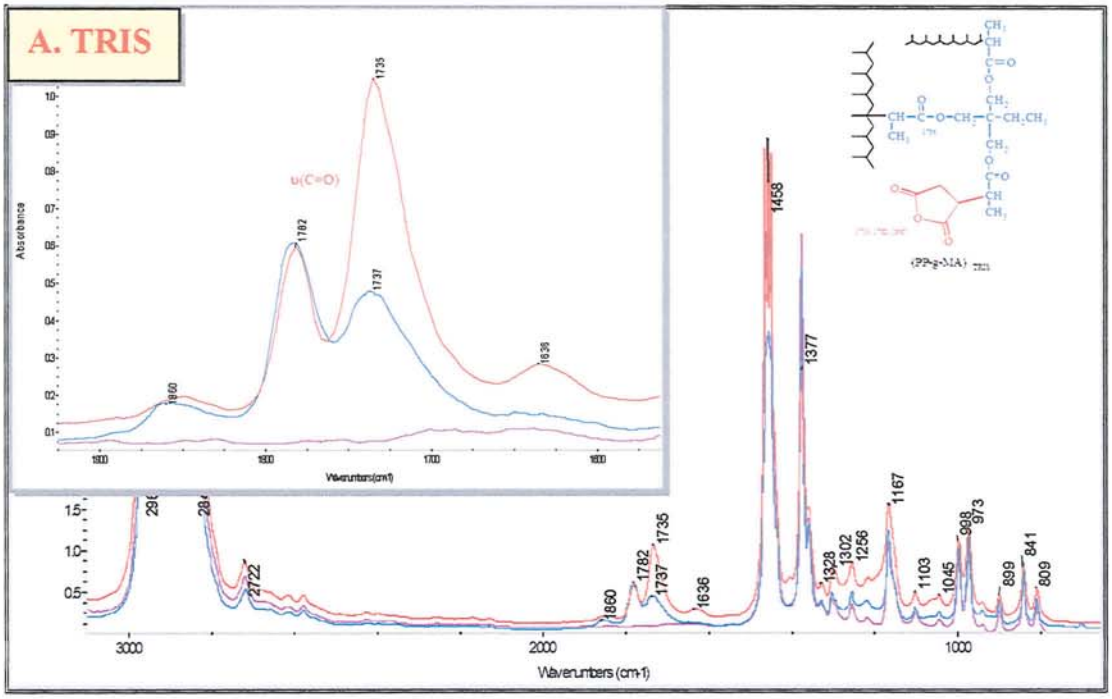

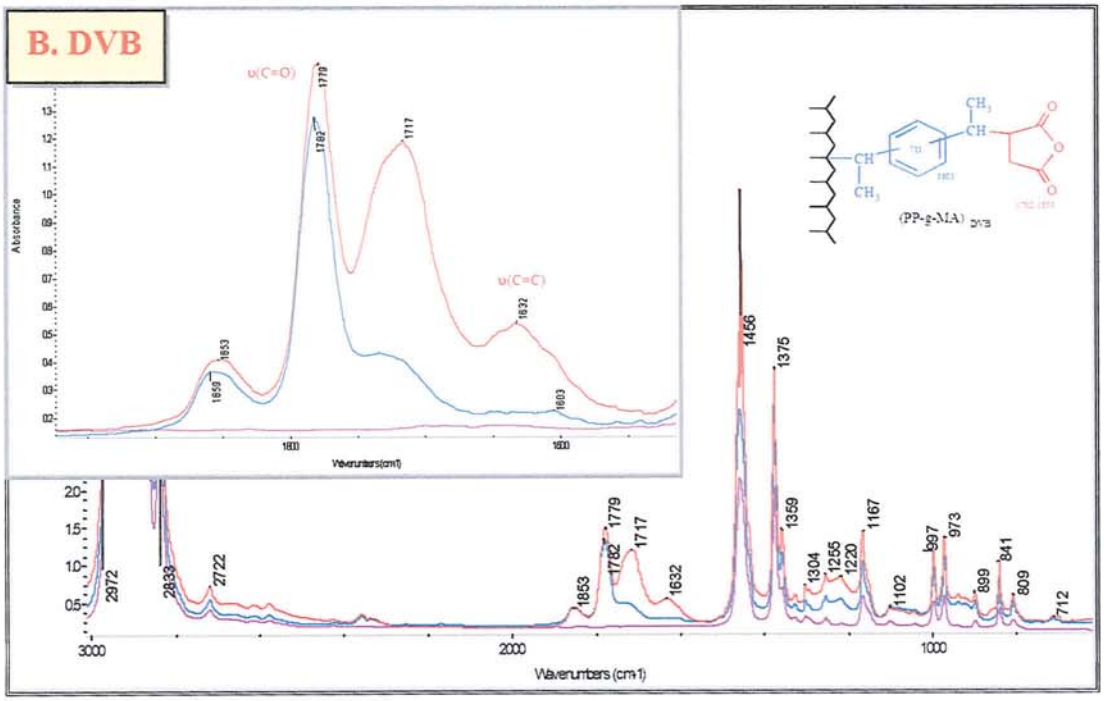

Figure 5.8 The comparison of infrared spectra of the virgin PP films (purple) with the reaction products (A) PP-g-MA_{TRIS} and (B) PP-g-MA_{DVB} films (thickness ~100μm) before (red) and after purification (blue) by Soxhlet extraction-precipitation (see **Scheme 5.3**)

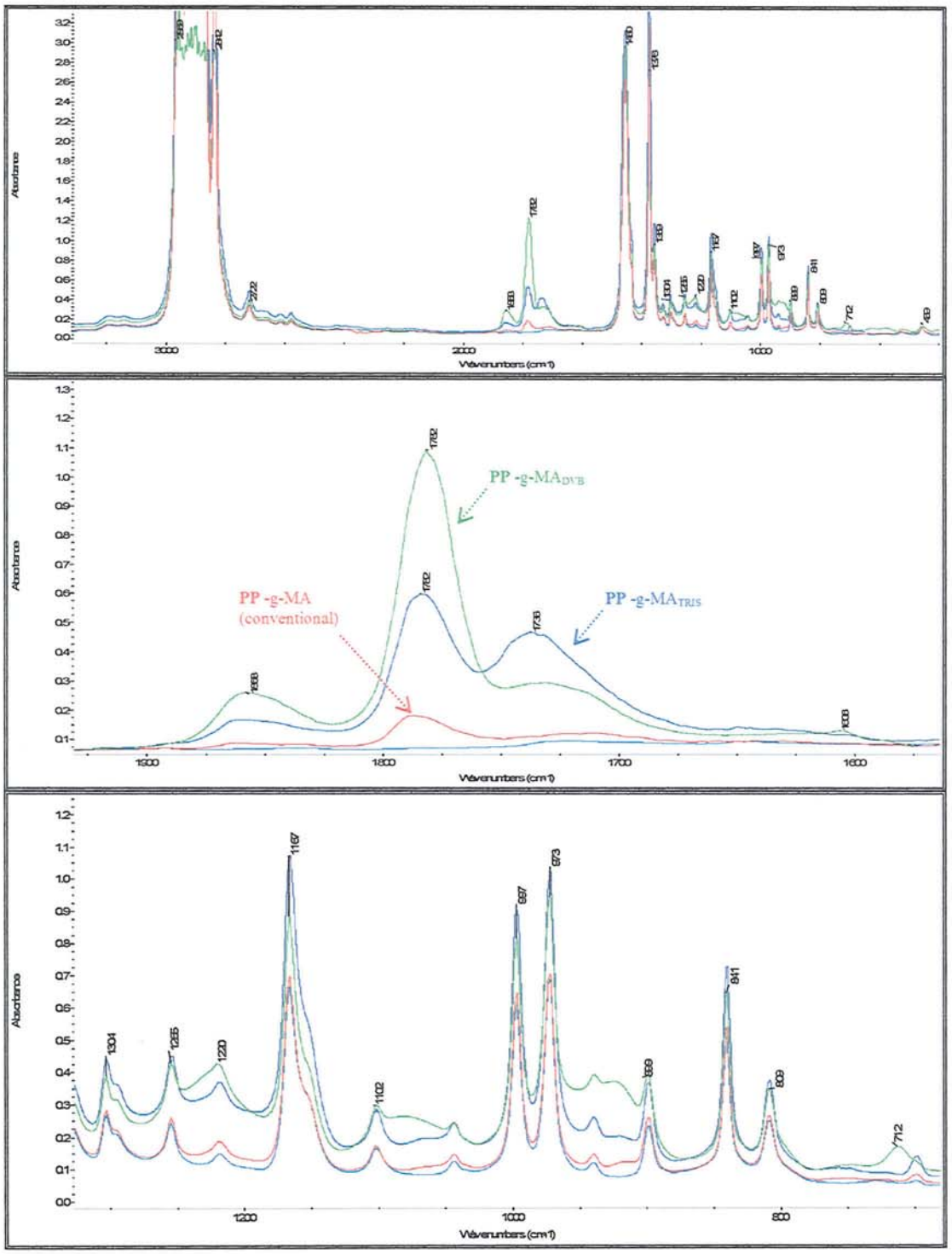

Figure 5.9 Comparison of IR spectra of thin films (all with thickness ~100μm) of PP alone (blue), purified films of PP-g-MA (DCM extraction of PP-MA in the absence of coagent) (red), purified (extraction-precipitation) PP-g-MA$_{TRIS}$ (in the presence of TRIS) (dark blue), and PP-g-MA$_{DVB}$ (in the presence of DVB) (green).

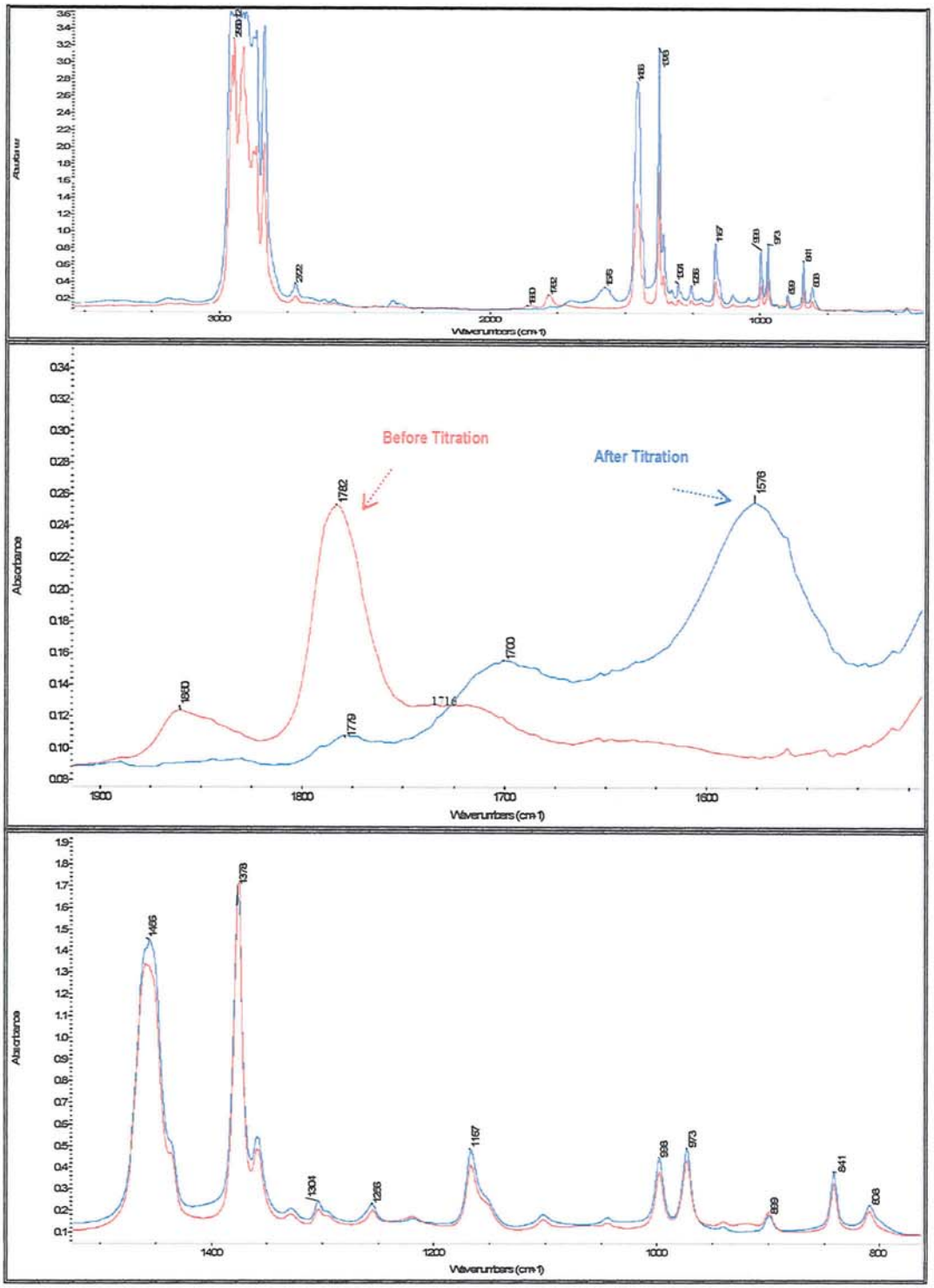

Figure 5.10 Comparison of FTIR spectra of grafted-MA on PP (Film X) processed in the presence of DVB (DVB+MA+T101 system before (red) and after (blue) titration (see **Scheme 5.4**, p.298).

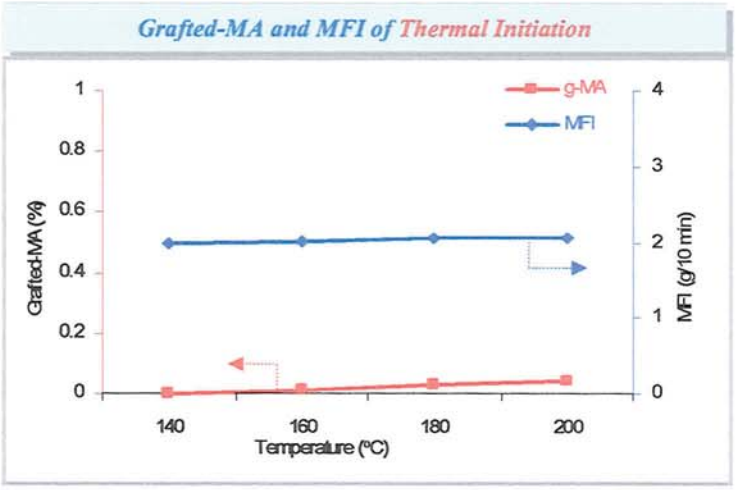

Figure 5.11 Effect of temperature on MA grafting level and MFI of processed PP/MA by thermal initiation (in the absence of peroxide) system (Samples T1-1 to T1-4 in Table D5.1 Appendix A; PP-Elf, MA 8 %, temp. 160-200°C, 65 rpm, 10 min, Method M-2).

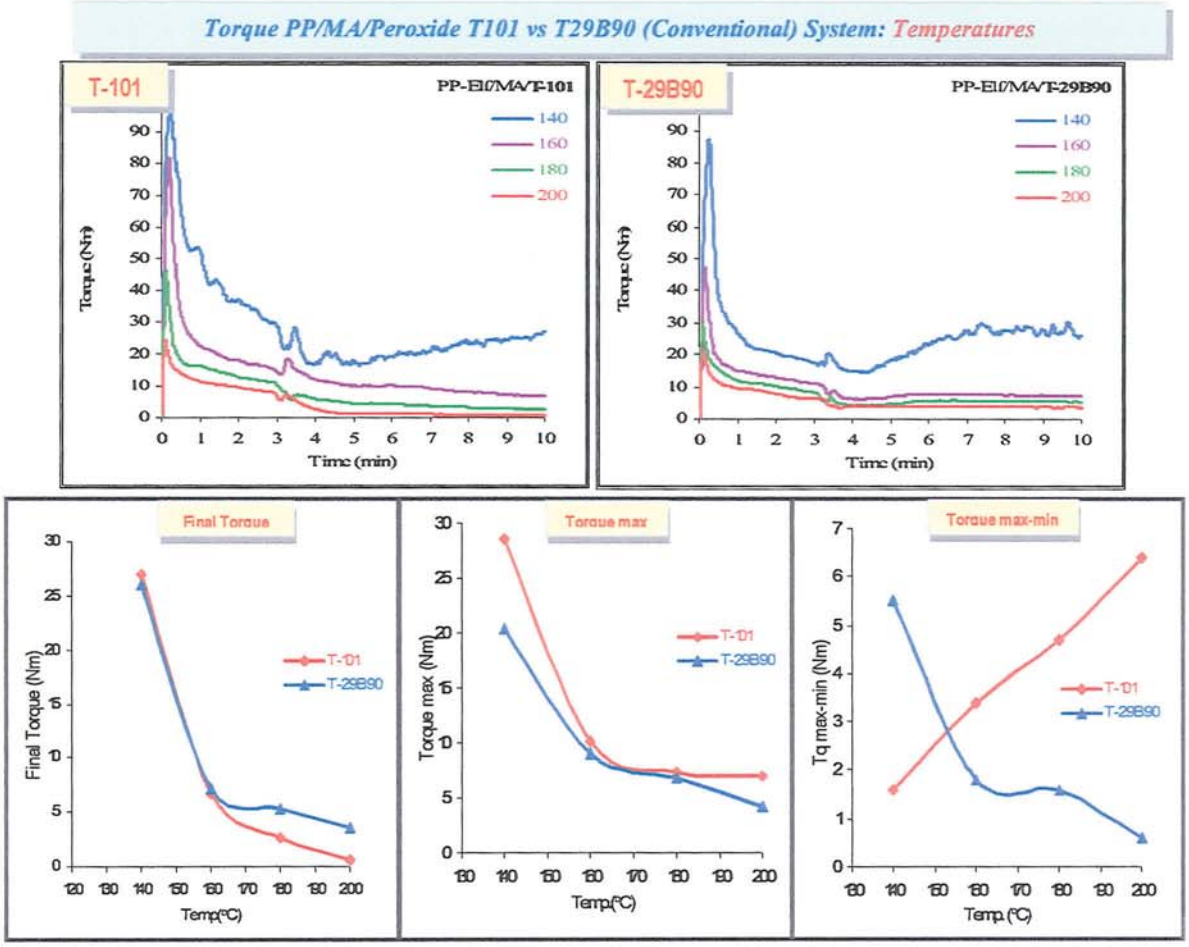

Figure 5.12 Effect of temperature on torque-time curves and torque characteristics of processed PP/MA/T-101 and PP/MA/T-29B90 system. (T-101 (samples M1-1 to M1-6 in Table D5.3) and T-29B90 (samples M14-1 to M14-6 in Table D5.4 Appendix D); PP-Elf, MA 8 %, [peroxide] 0.005 molar ratio to MA, 65rpm, 10min, mixing method M-2).

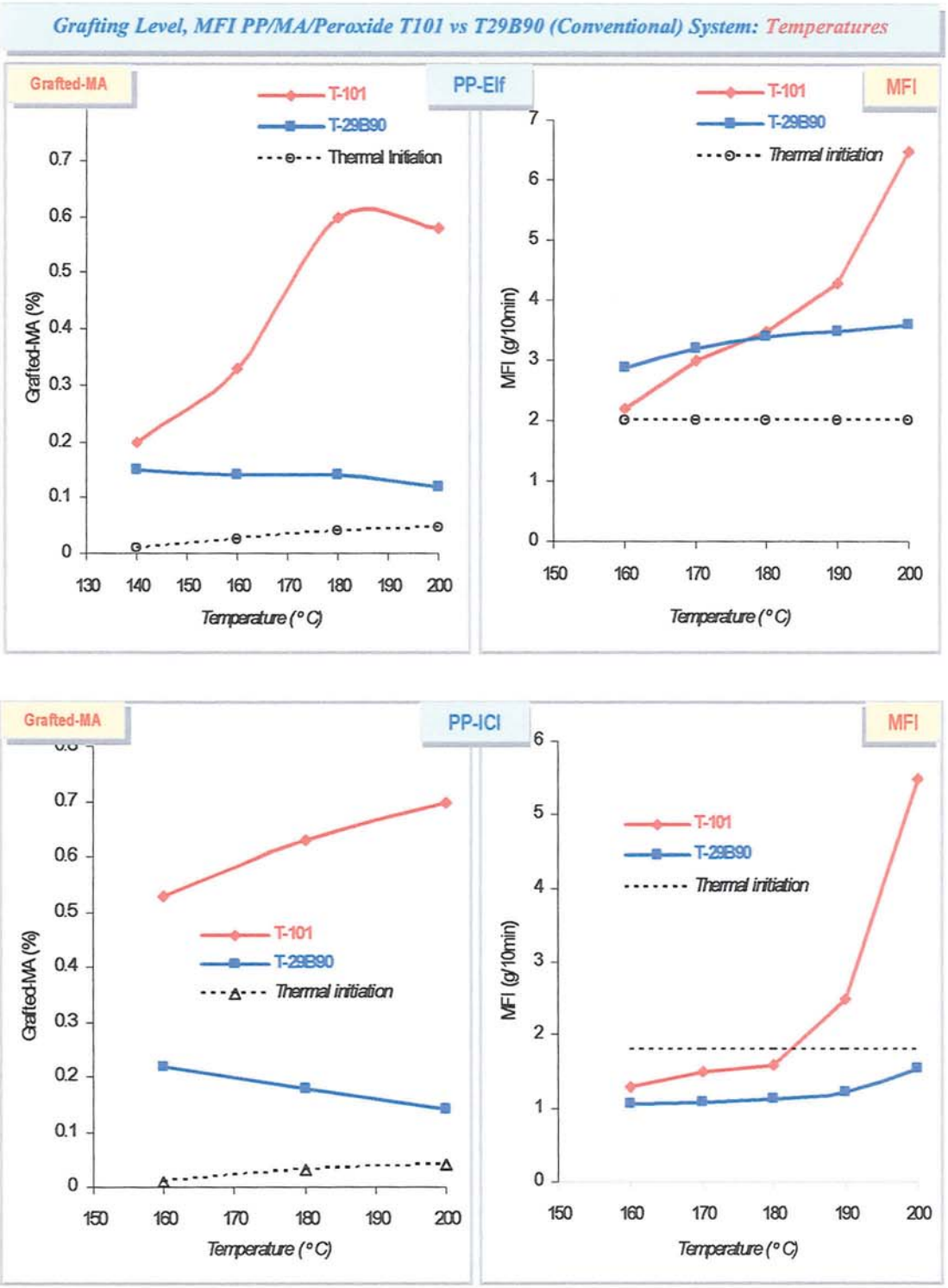

Figure 5.13 Effect of temperature on MA grafting level and MFI of processed *PP*/MA/peroxide (different peroxide, T-101 and T-29B90 and different types of PP, PP-Elf and PP-ICI). ([MA]i = 8 %, [peroxide] = 0.005 molar ratio to MA, 65rpm, 10min, mixing method M-2).

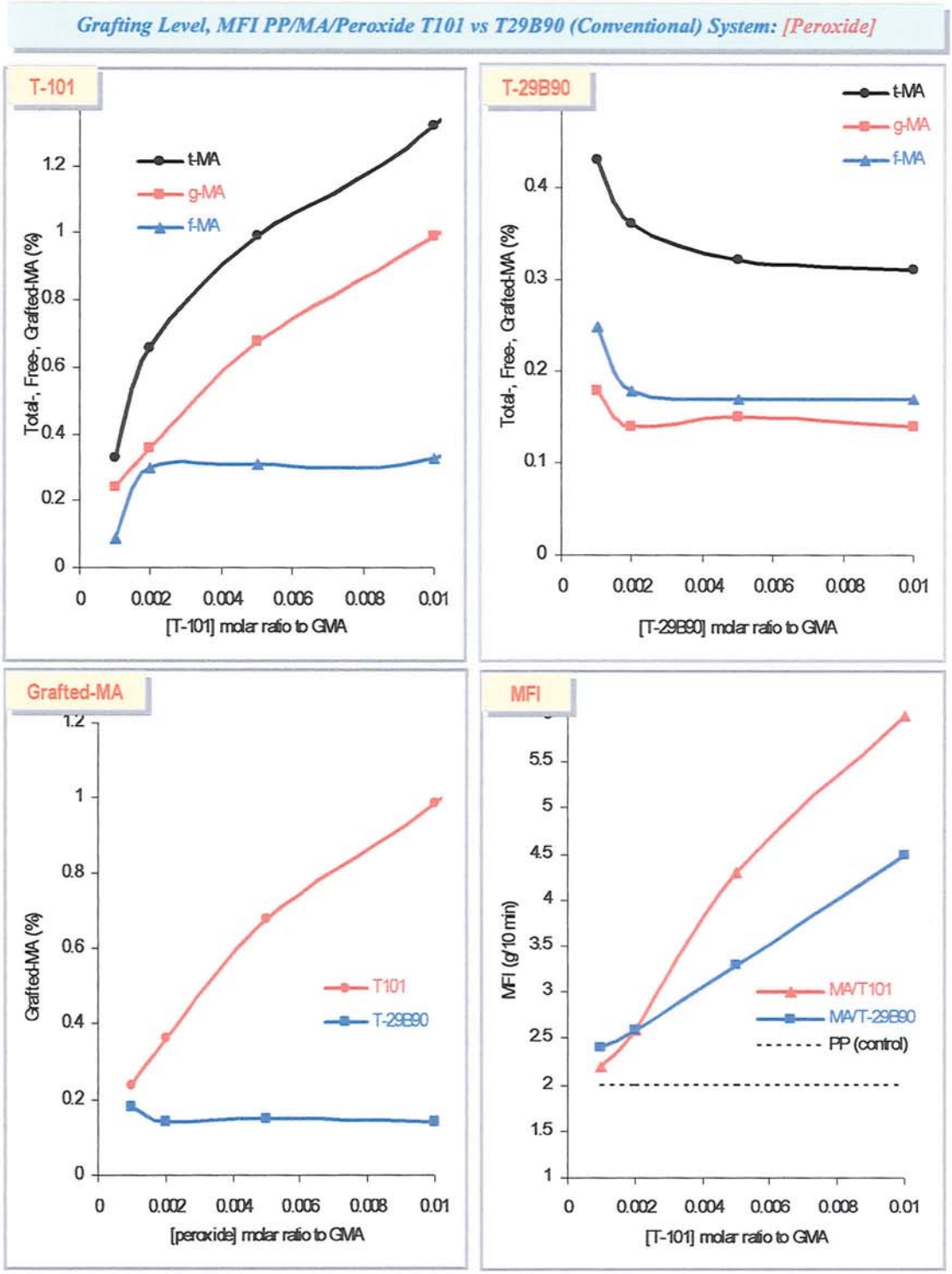

Figure 5.14 Effect of peroxide concentration on MA grafting level and MFI of processed PP/MA/peroxide (different peroxide T-101 and T-29B90) system (PP-Elf, [MA]i = 8%, [peroxide] = 0.001-0.01molar ratio to MA, temp. 160°C for T-29B90 and 180°C for T-101, 65rpm, 10min, mixing method M-2).

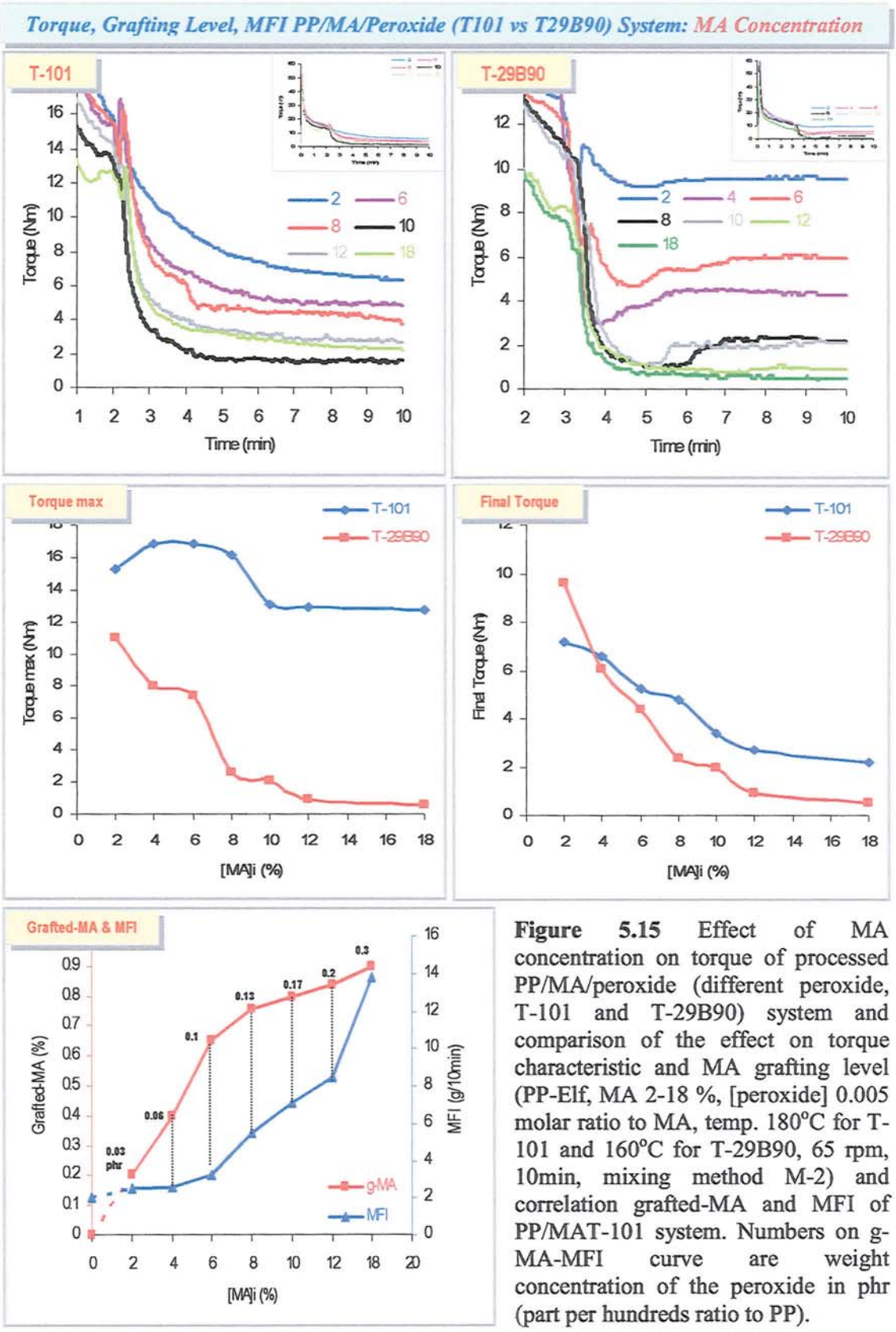

Figure 5.15 Effect of MA concentration on torque of processed PP/MA/peroxide (different peroxide, T-101 and T-29B90) system and comparison of the effect on torque characteristic and MA grafting level (PP-Elf, MA 2-18 %, [peroxide] 0.005 molar ratio to MA, temp. 180°C for T-101 and 160°C for T-29B90, 65 rpm, 10min, mixing method M-2) and correlation grafted-MA and MFI of PP/MAT-101 system. Numbers on g-MA-MFI curve are weight concentration of the peroxide in phr (part per hundreds ratio to PP).

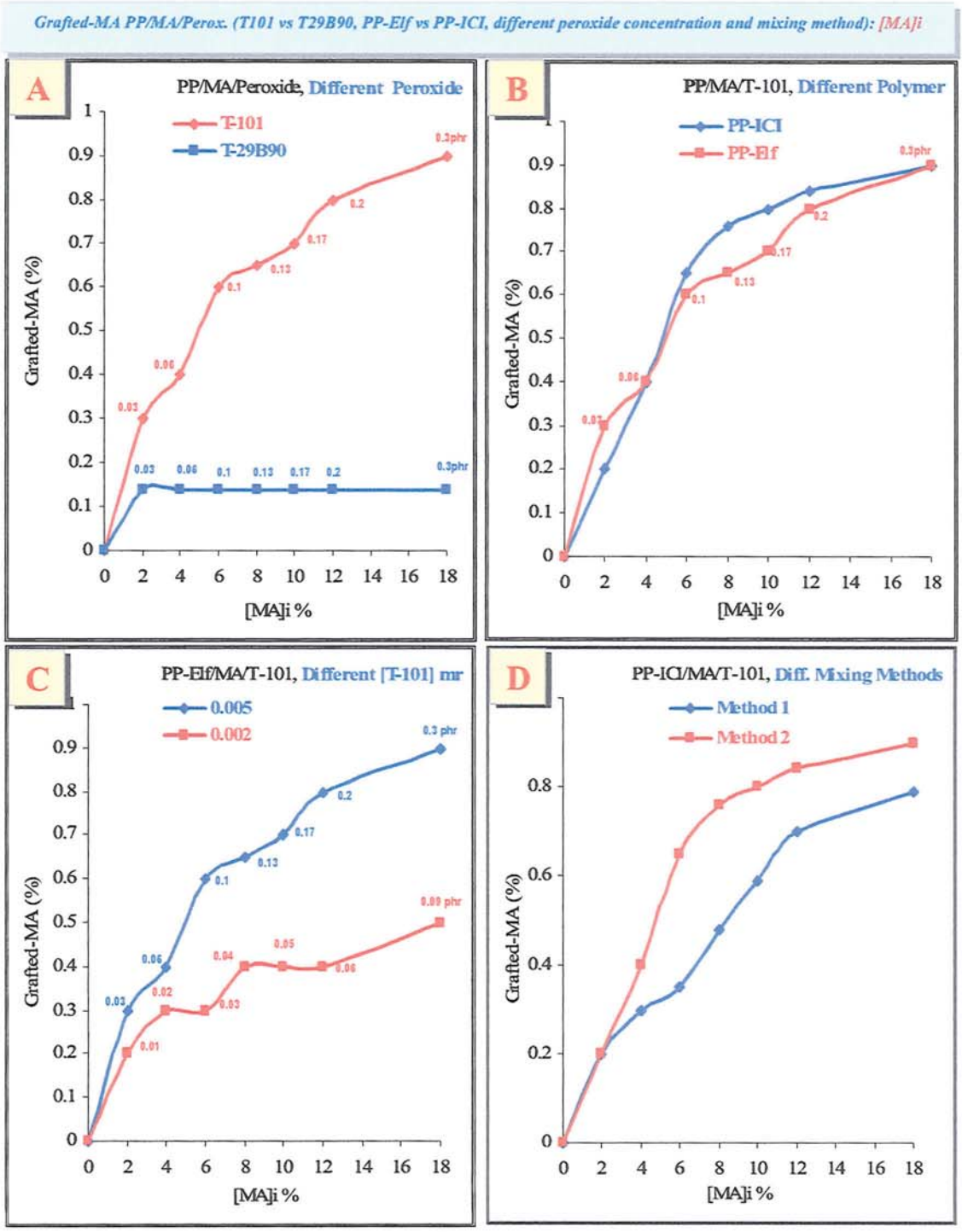

Figure 5.16 Comparison effects of MA initial concentration on MA grafting level of processed PP/MA/peroxide system in (A) different peroxide, T-101 and T-29B90, (B) different PP, PP-Elf (granular) and PP-ICI (powder) (C) different T-101 concentration, and (D) different mixing methods (see **Scheme 5.1**, p.295). (otherwise stated peroxide concentration = 0.005 molar ratio to MA, temp. 160°C for T-29B90 and 180°C for T-101, 65 rpm, 10min, otherwise stated mixing method M-2) (*Numbers in curves are weight concentration in phr of the peroxide used*).

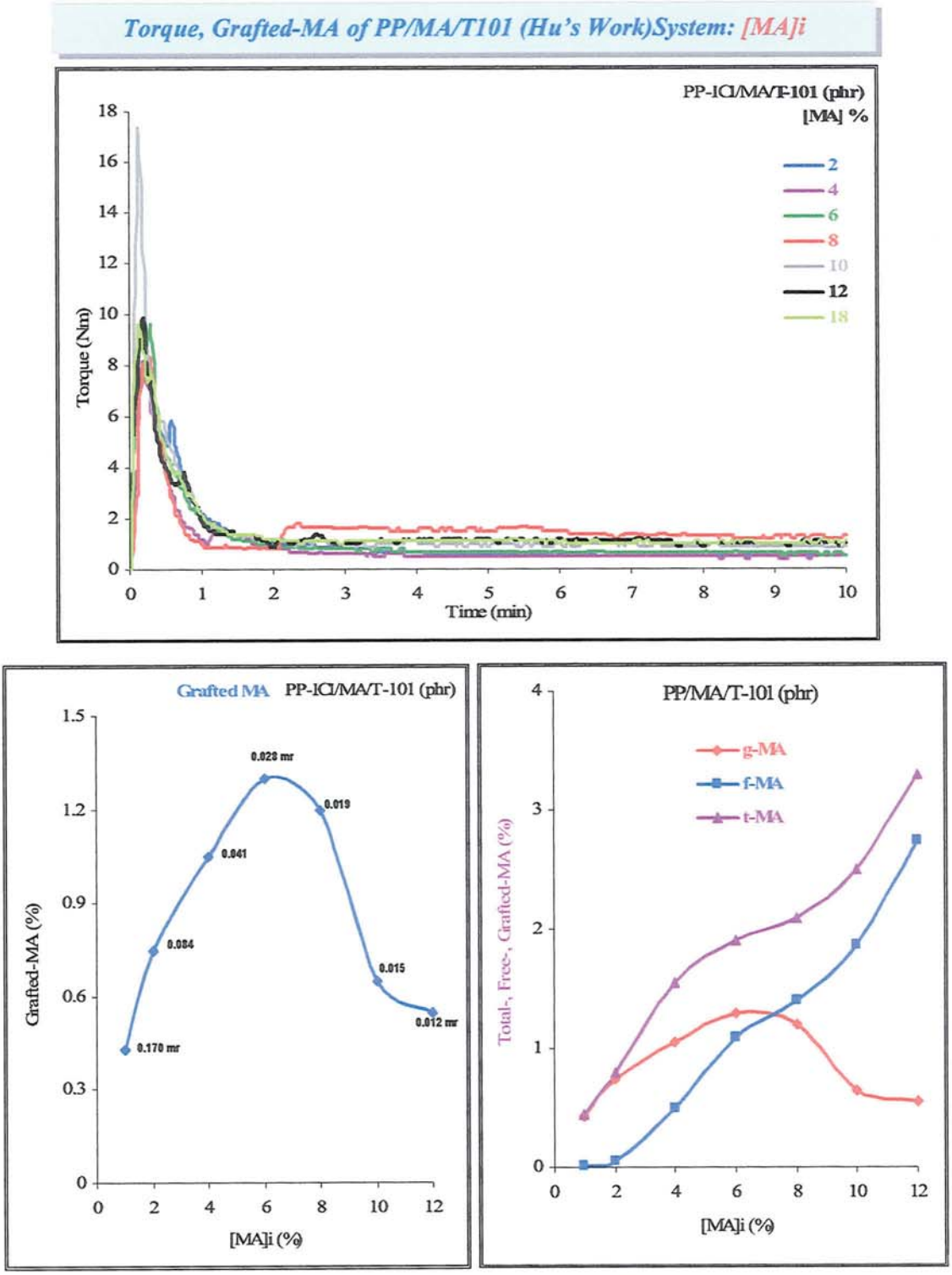

Figure 5.17 Effect of initial MA concentration on torque and MA grafting level of processed PP/MA/T-101 (Hu's Work) system. (Samples: M9-1 to M9-7 in Table C5.3 Appendix D; PP-ICI, [MA] = 2-18 %, [T-101] = 0.5 part weight of hundreds ratio of PP, **phr**, temp. 220°C, 75 rpm, 15min, mixing method M-1 (see **Scheme 5.1**, p.295) (*Numbers on 'Grafted-MA' curves are peroxide concentration in molar ratio (mr) of [T-101]/[MA]i*).

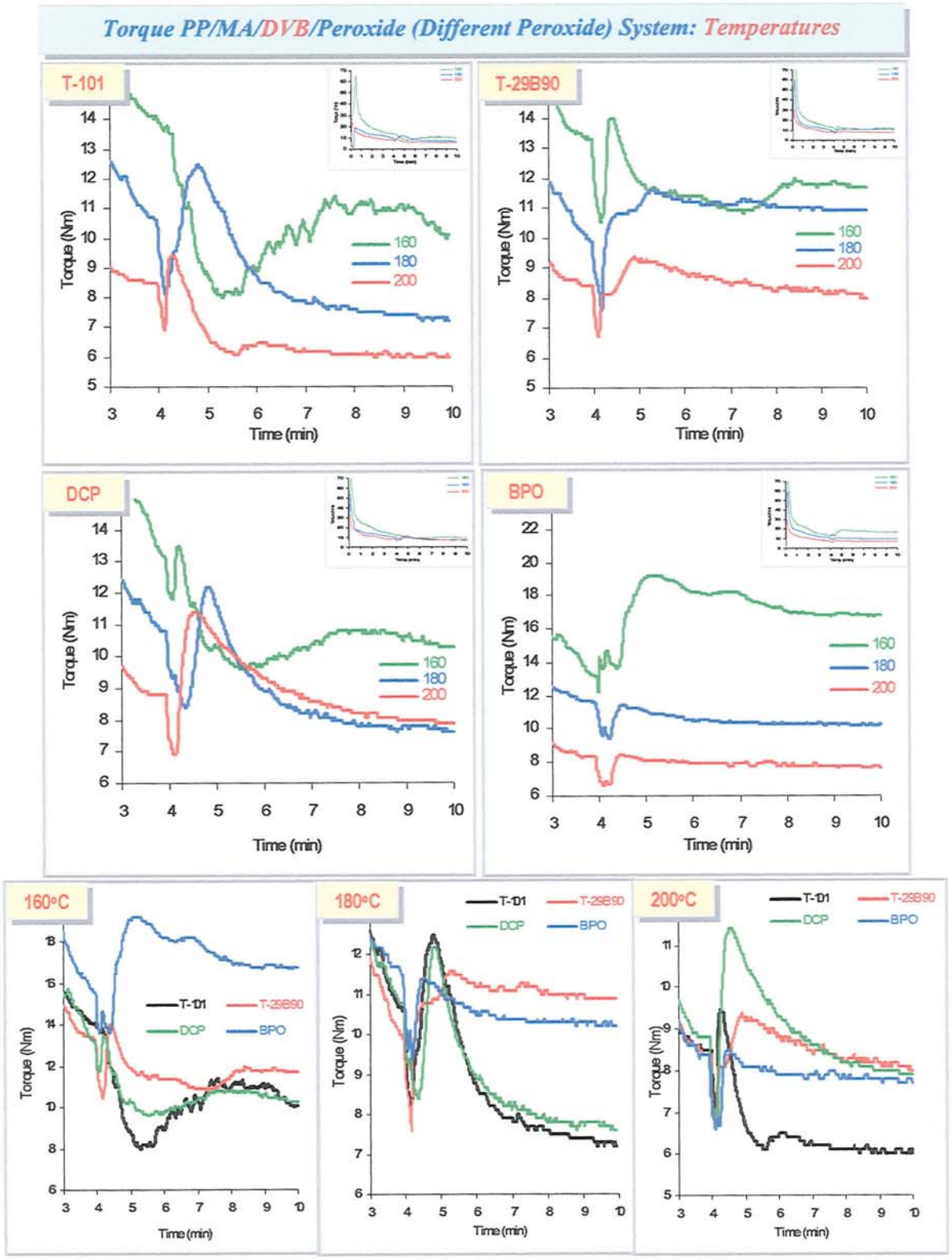

Figure 5.18 Effect of temperature on torque of processed PP/DVB/MA/peroxide (different peroxides) system. (Samples PP-Elf, [MA]i = 12 %, [DVB] = 2/8 weight ratio to MA, [peroxide] 0.005 molar ratio to MA+DVB, temp. 160-200°C, 65 rpm, 10min, mixing method **M-2**)

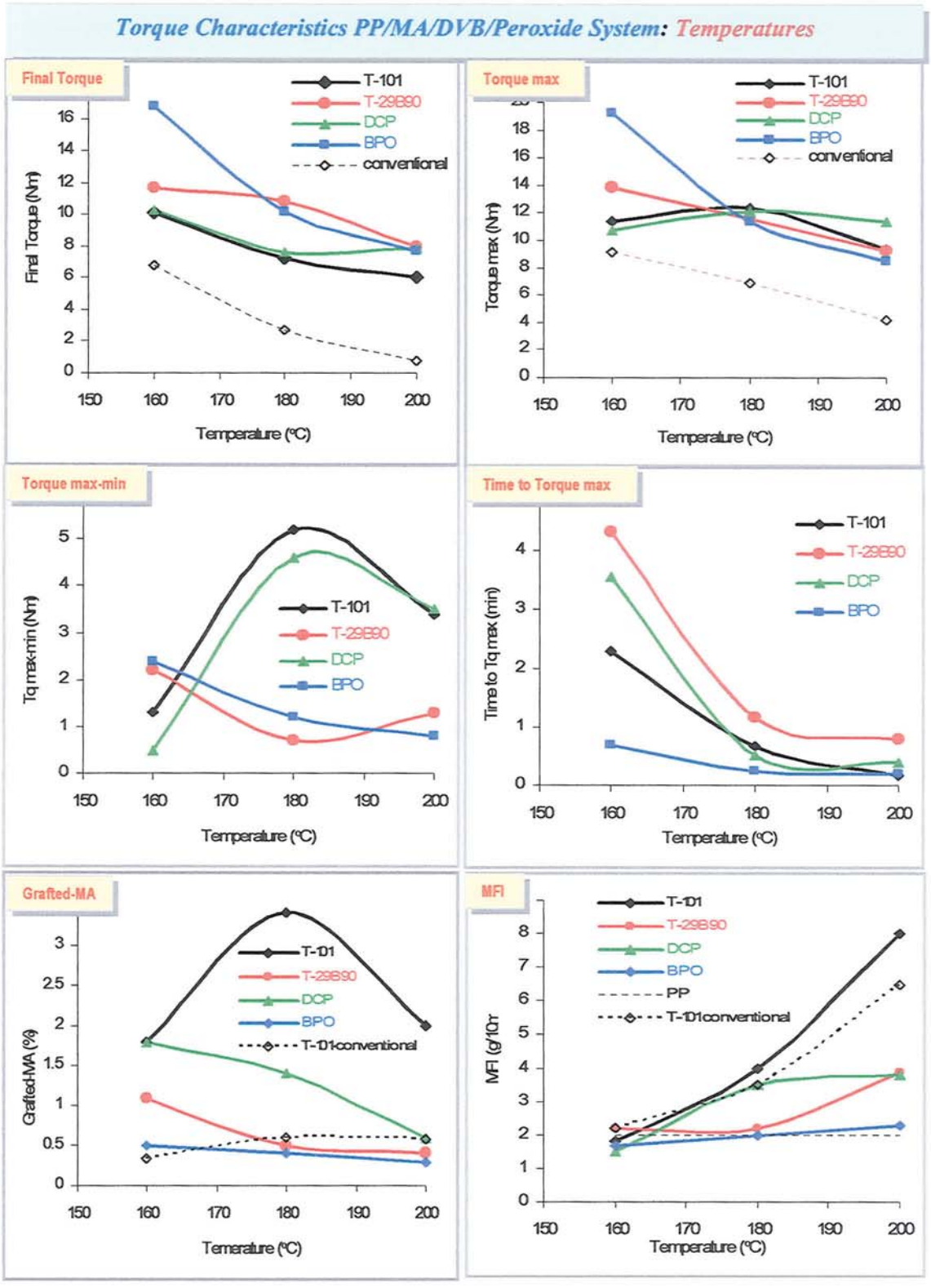

Figure 5.19 Effect of temperature on torque characteristics, grafting level and MFI of processed PP/DVB/MA/peroxide (different peroxides) system. (Samples PP-Elf, [MA]i = 8 %, [DVB] = 2/8 weight ratio to MA, [peroxide] = 0.005 molar ratio to MA+DVB, temp. 160-200°C, 65 rpm, 10min, mixing method **M-2**)

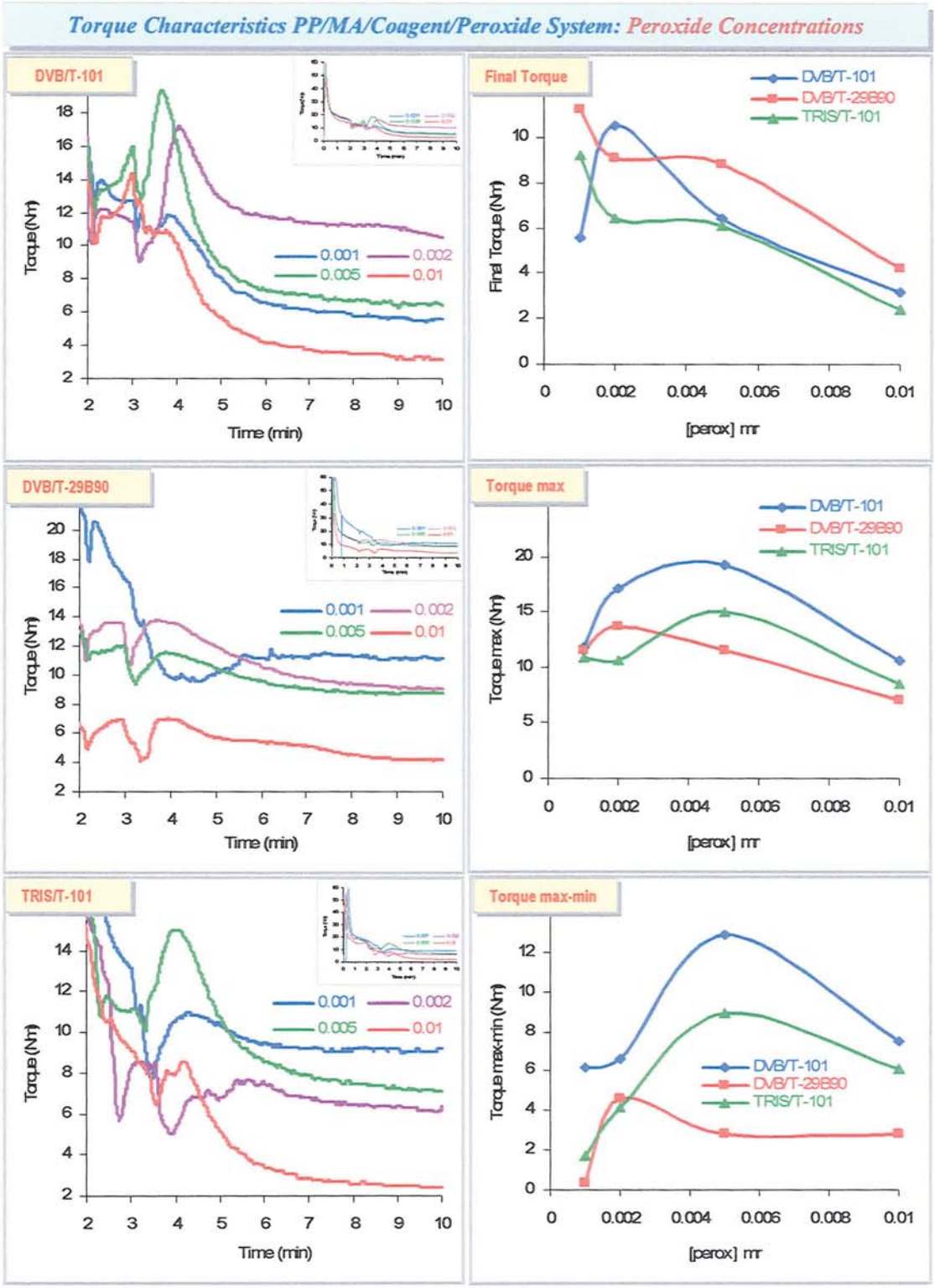

Figure 5.20 Effect of peroxide concentration on torque characteristics of processed PP/coagent/MA/peroxide (different coagents, DVB or TRIS, and different peroxides, T-101 or T-29B90) system. (Samples: PP-Elf, [MA] = 8 %, [coagent] = 2/8 weight ratio to MA, [peroxide] = 0.001-0.01 molar ratio to MA+DVB, temp. 180°C for T-101 and 160°C for T-29B90, 65 rpm, 10min, mixing method **M-3**)

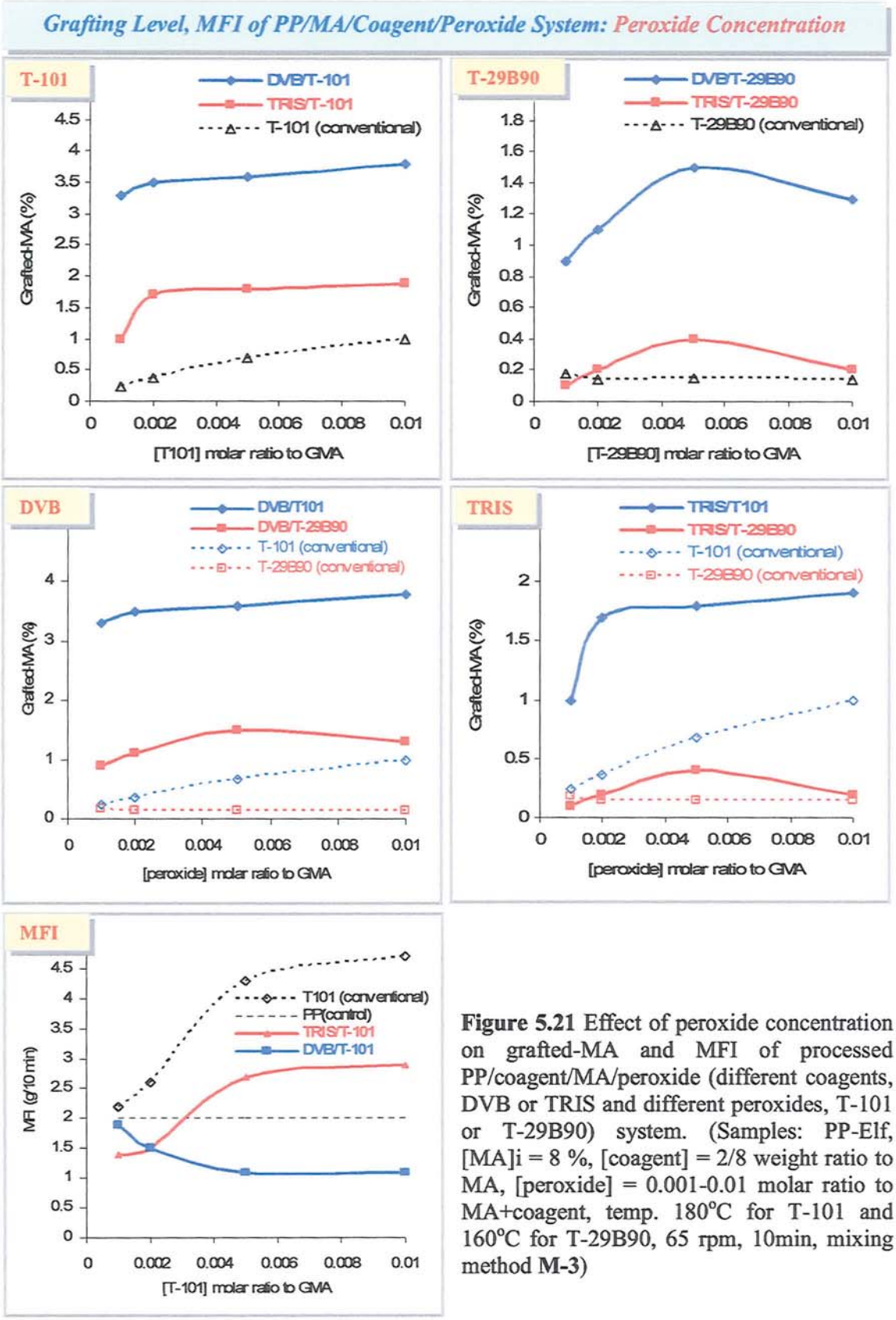

Figure 5.21 Effect of peroxide concentration on grafted-MA and MFI of processed PP/coagent/MA/peroxide (different coagents, DVB or TRIS and different peroxides, T-101 or T-29B90) system. (Samples: PP-Elf, [MA]i = 8 %, [coagent] = 2/8 weight ratio to MA, [peroxide] = 0.001-0.01 molar ratio to MA+coagent, temp. 180°C for T-101 and 160°C for T-29B90, 65 rpm, 10min, mixing method **M-3**)

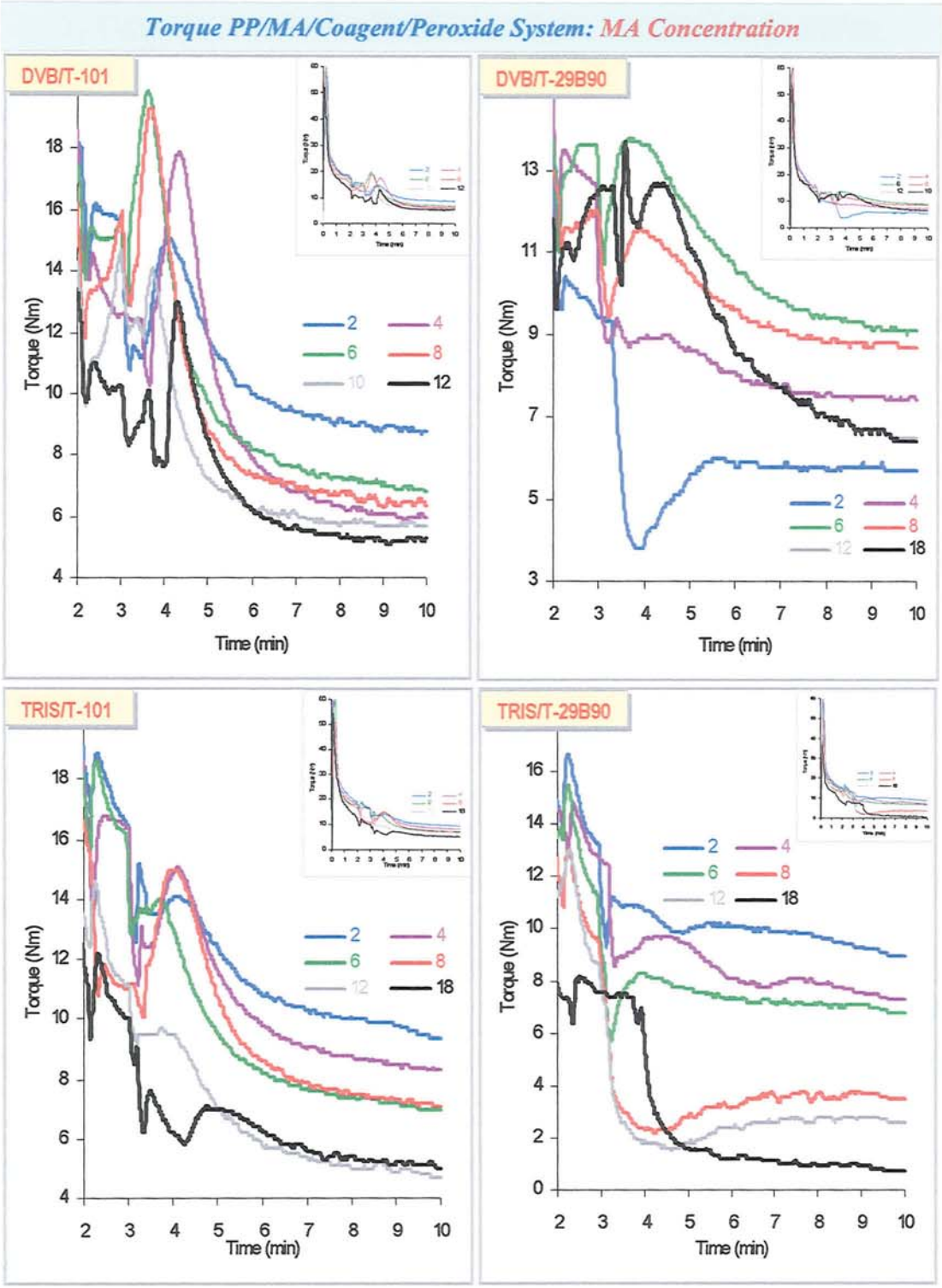

Figure 5.22 Effect of initial MA concentration on torque of processed PP/coagent/MA/peroxide (different coagents, DVB or TRIS, and different peroxides, T-101 or T-29B90) system. (Samples: PP-Elf, [coagent] = 2/8 weight ratio to MA, [peroxide] = 0.005 molar ratio to MA+coagent, temp. 180°C for T-101 and 160°C for T-29B90, 65 rpm, 10min, mixing method **M-3**)

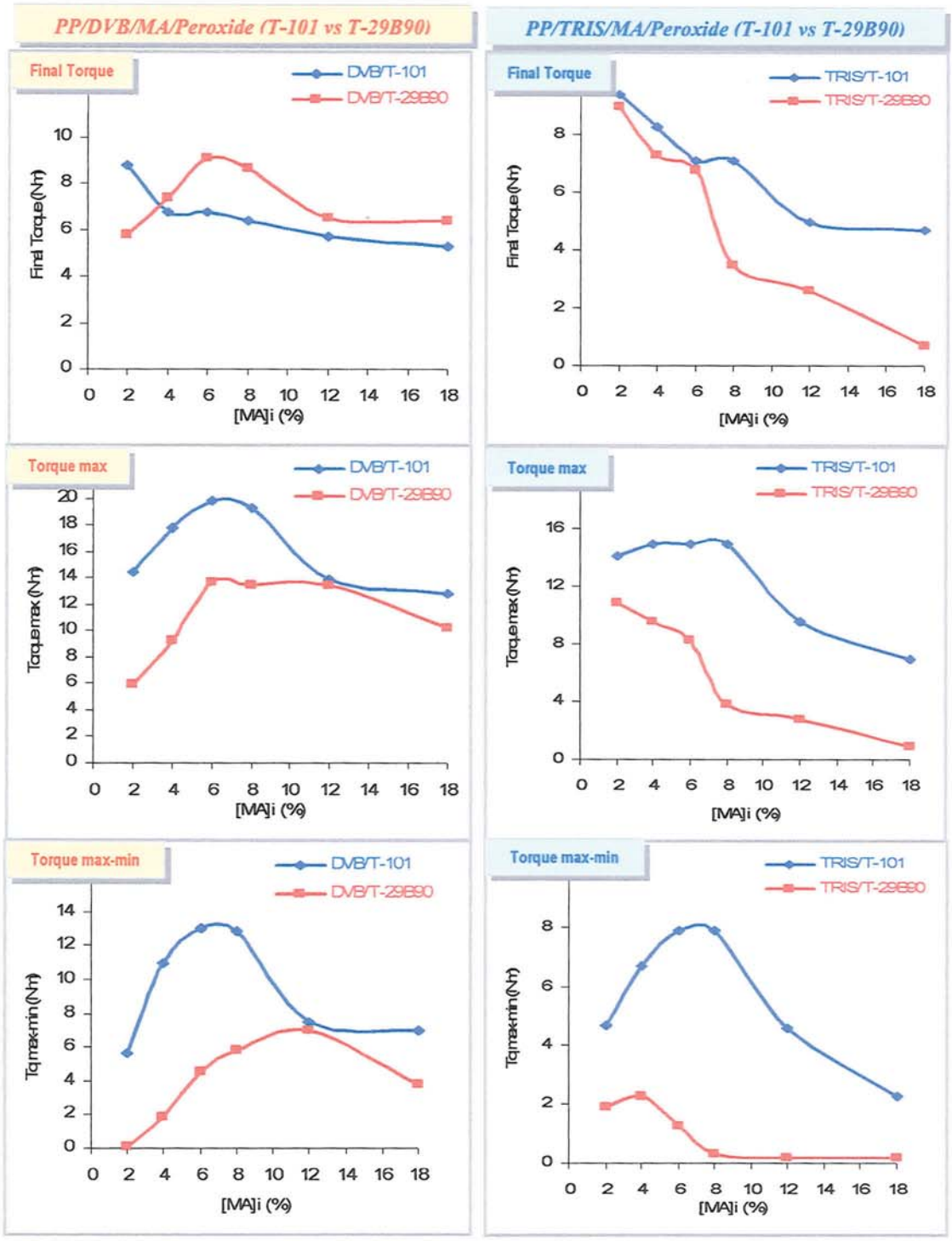

Figure 5.23A Comparison effect of initial MA concentration on torque characteristic of processed PP-Elf/coagent/MA/peroxide (T-101 vs T-29B90 in different coagents DVB and TRIS) system. (Samples: PP-Elf, [MA]i = 8 %, [coagent] = 2/8 weight ratio to MA, [peroxide] = 0.005 molar ratio to MA+coagent, temp. 180°C for T-101 and 160°C for T-29B90, 65 rpm, 10 min, mixing method **M-3**)

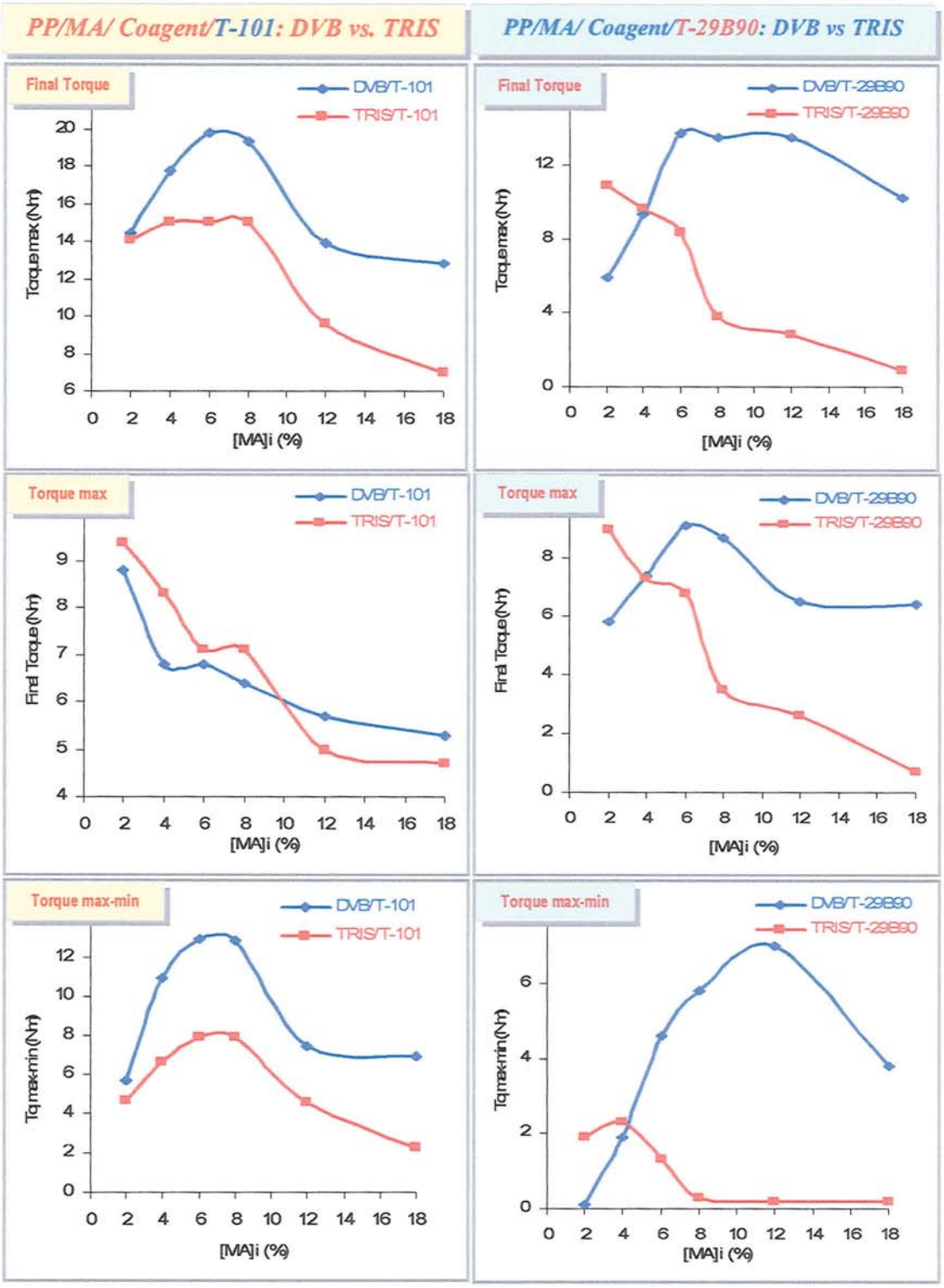

Figure 5.23B Comparison effect of initial MA concentration on torque characteristic of processed PP-Elf/coagent/MA/peroxide (DVB vs TRIS in different peroxides,T-101 or T-29B90) system. (Samples: PP-Elf, [MA]i = 8 %, [coagent] = 2/8 weight ratio to MA, [peroxide] = 0.005 molar ratio to MA+coagent, temp. 180°C for T-101 and 160°C for T-29B90, 65 rpm, 10 min, mixing method M-3)

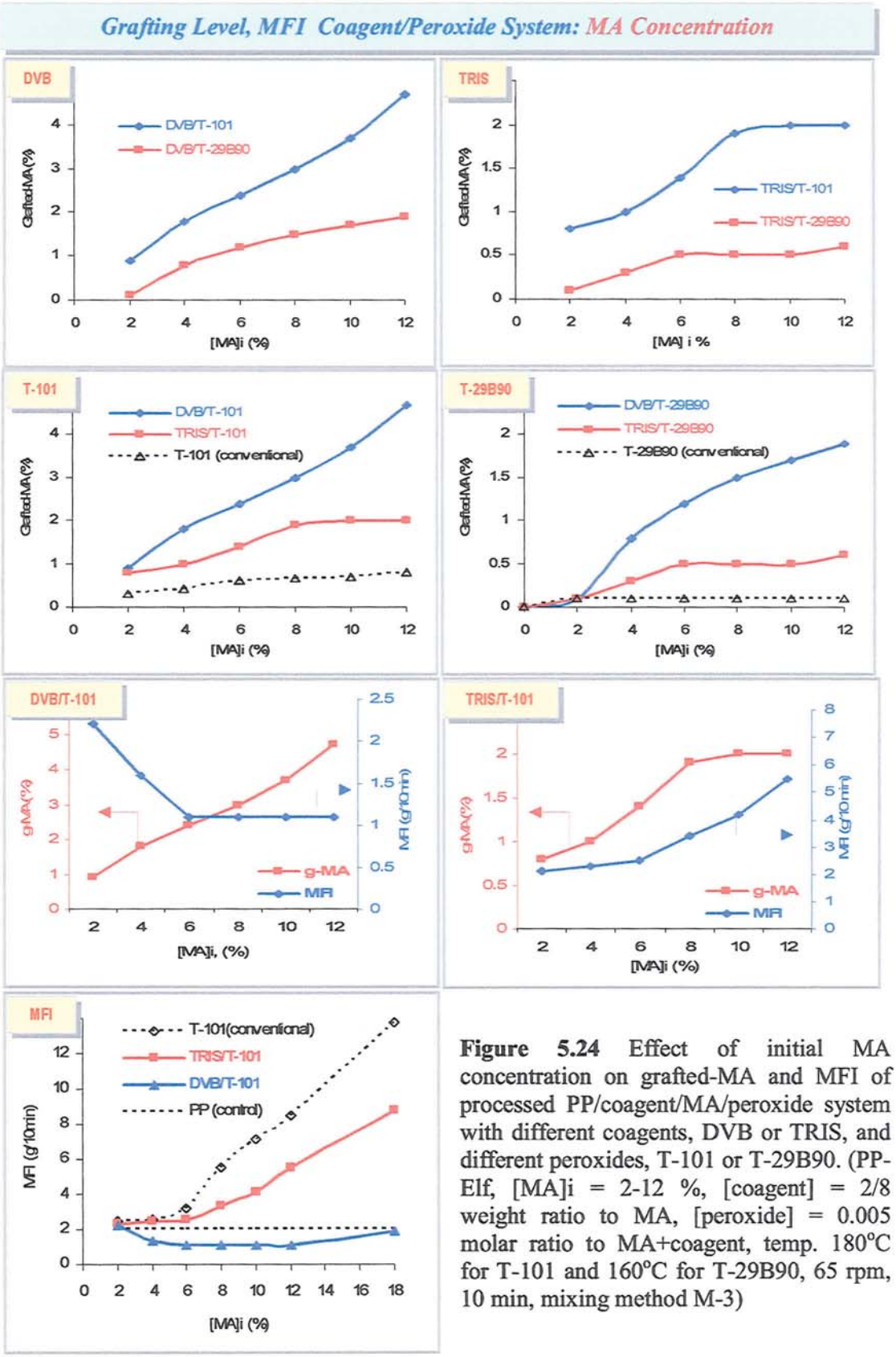

Figure 5.24 Effect of initial MA concentration on grafted-MA and MFI of processed PP/coagent/MA/peroxide system with different coagents, DVB or TRIS, and different peroxides, T-101 or T-29B90. (PP-Elf, [MA]i = 2-12 %, [coagent] = 2/8 weight ratio to MA, [peroxide] = 0.005 molar ratio to MA+coagent, temp. 180°C for T-101 and 160°C for T-29B90, 65 rpm, 10 min, mixing method M-3)

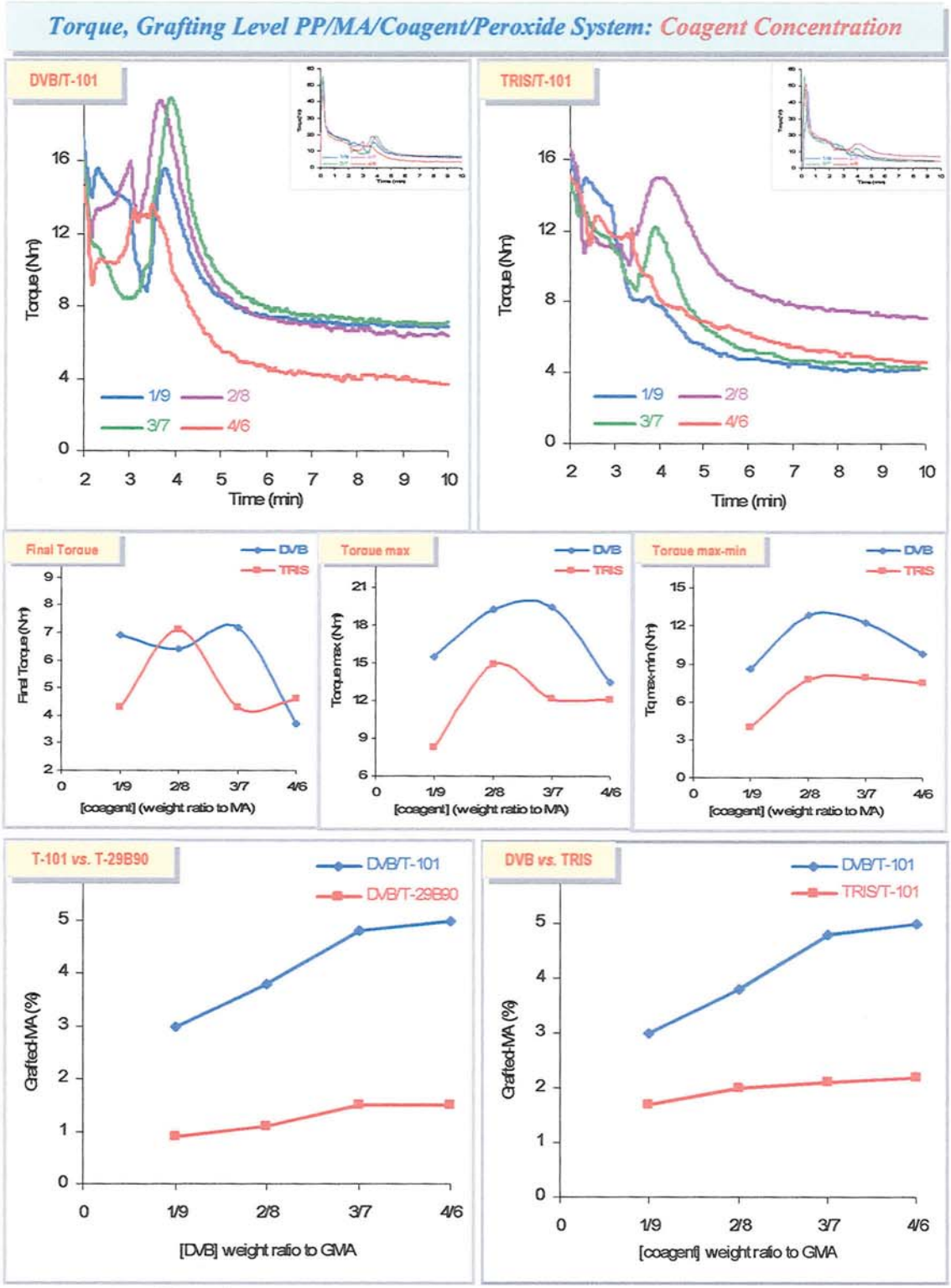

Figure 5.25 Effect of coagent concentration on torque characteristic and MA grafting level of processed PP/coagent/MA/peroxide (different coagent, TRIS or DVB, and different peroxide, T-101 and T-29B90) system. (Samples: PP-Elf, [MA]i = 8 %, [coagent] = 1/9 to 4/6 weight ratio to MA, [peroxide] = 0.005 molar ratio to MA+coagent, temp. 180°C, 65 rpm, 10 min, mixing method M-3).

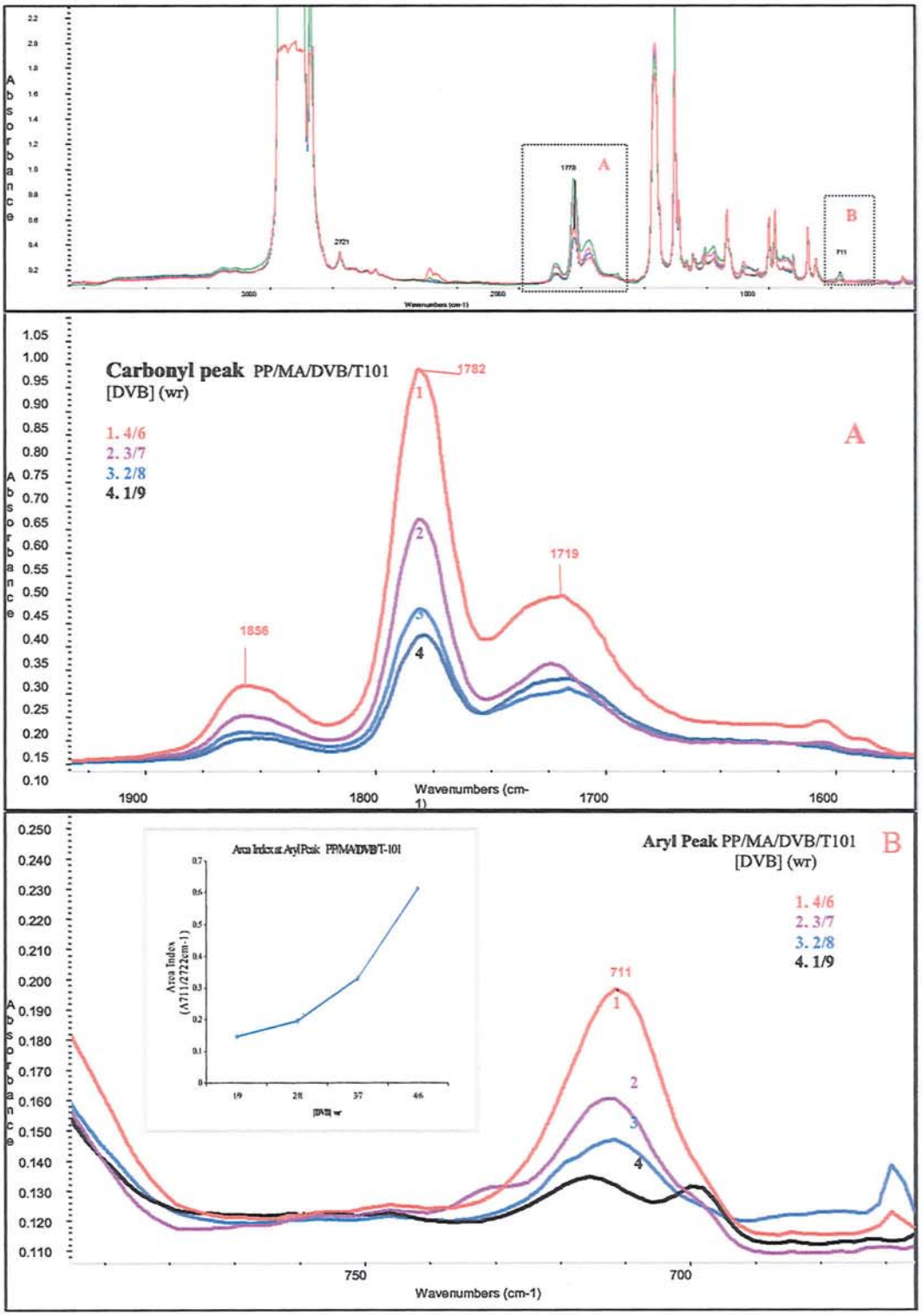

Figure 5.26 Comparison of FTIR spectra of purified processed PP/MA/DVB/T-101 films (in various DVB concentrations). All films are purified by Soxhlet extraction and precipitation (see **Scheme 5.3**) and of similar thickness (~100nm) (Samples: PP-Elf, [MA]i = 8 %, [coagent] = 1/9 to 4/6 weight ratio to MA, [T-101] = 0.005 molar ratio to MA+coagent), temp. 180°C, 65 rpm, 10 min, mixing method M-3).

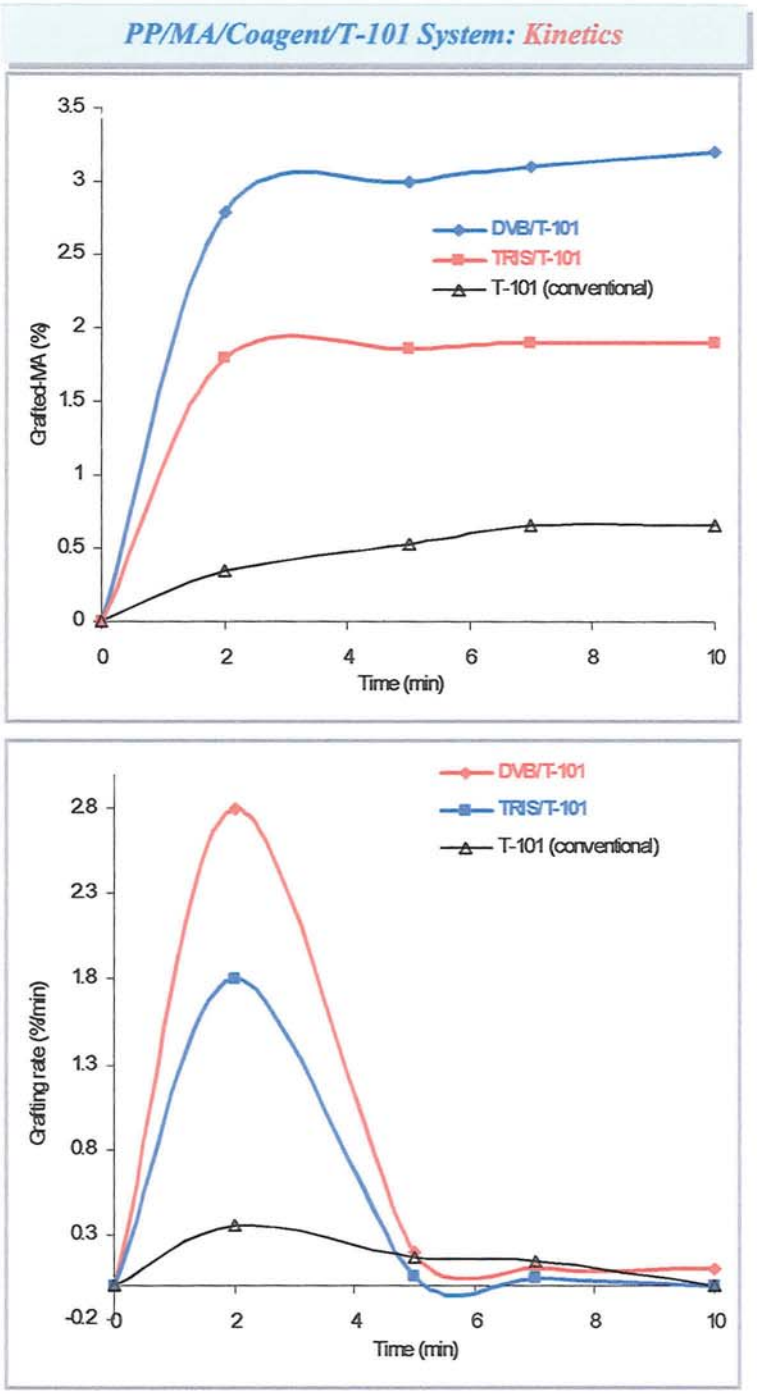

Figure 5.27 Comparison effect of processing time on grafted-MA and the grafting rate of processed PP with MA and T-101 in the absence (conventional) and the presence of coagents, DVB or TRIS) system. (Samples: PP-Elf, [MA]i = 8 %, [coagent] = 2/8 weight ratio to MA, [T-101] = 0.005 molar ratio to MA+coagent, temp. 180°C, 65 rpm, 10 min, mixing method M-2)

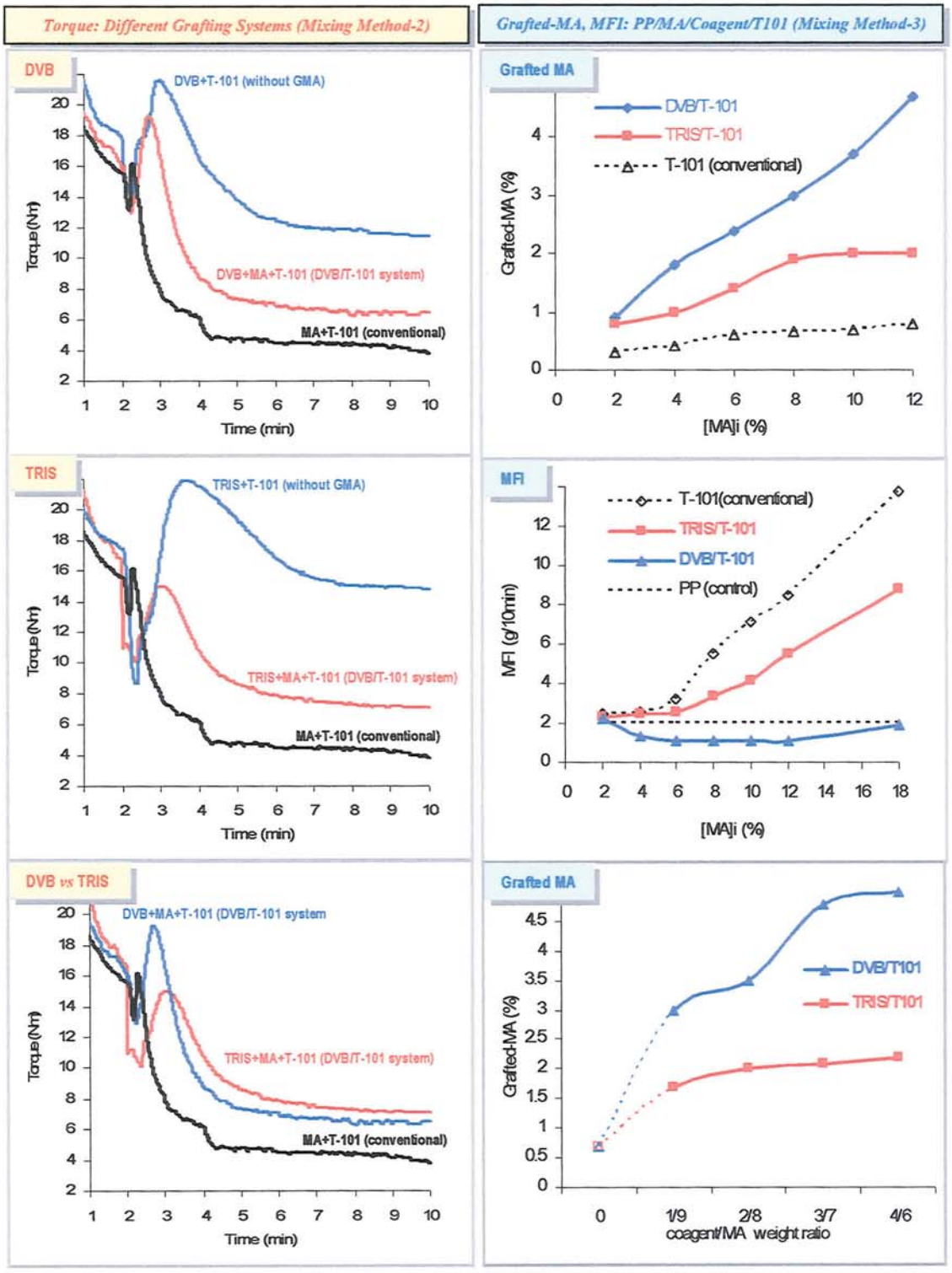

Figure 5.28 Comparison of the effectiveness of two coagents DVB and TRIS in the PP/MA/coagent/T-101 system (Temp. 180°C, 65 rpm, 10 min, mixing method M-3, [T-101] = 0.005 molar ratio to MA or MA+DVB or MA+TRIS) (Otherwise stated [MA]i = 8 %, [coagent] = 2/8 weight ratio to MA)

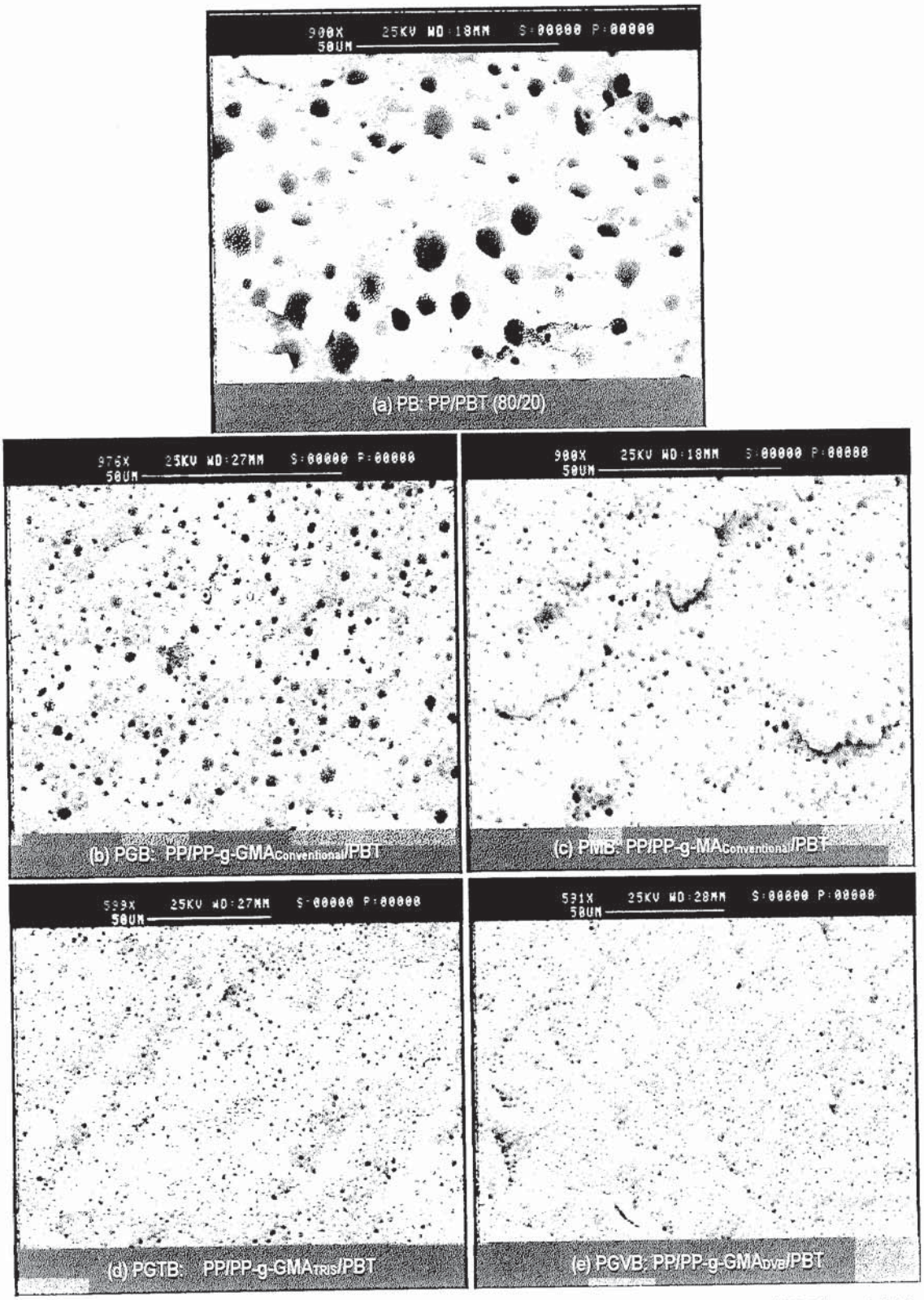

Figure 5.29 SEM of PP/*f*-PP/PBT (77.5/2.5/20): Effect of functionalised-PP (GMA or MA) and different GMA grafting system (conventional, TRIS or DVB system)

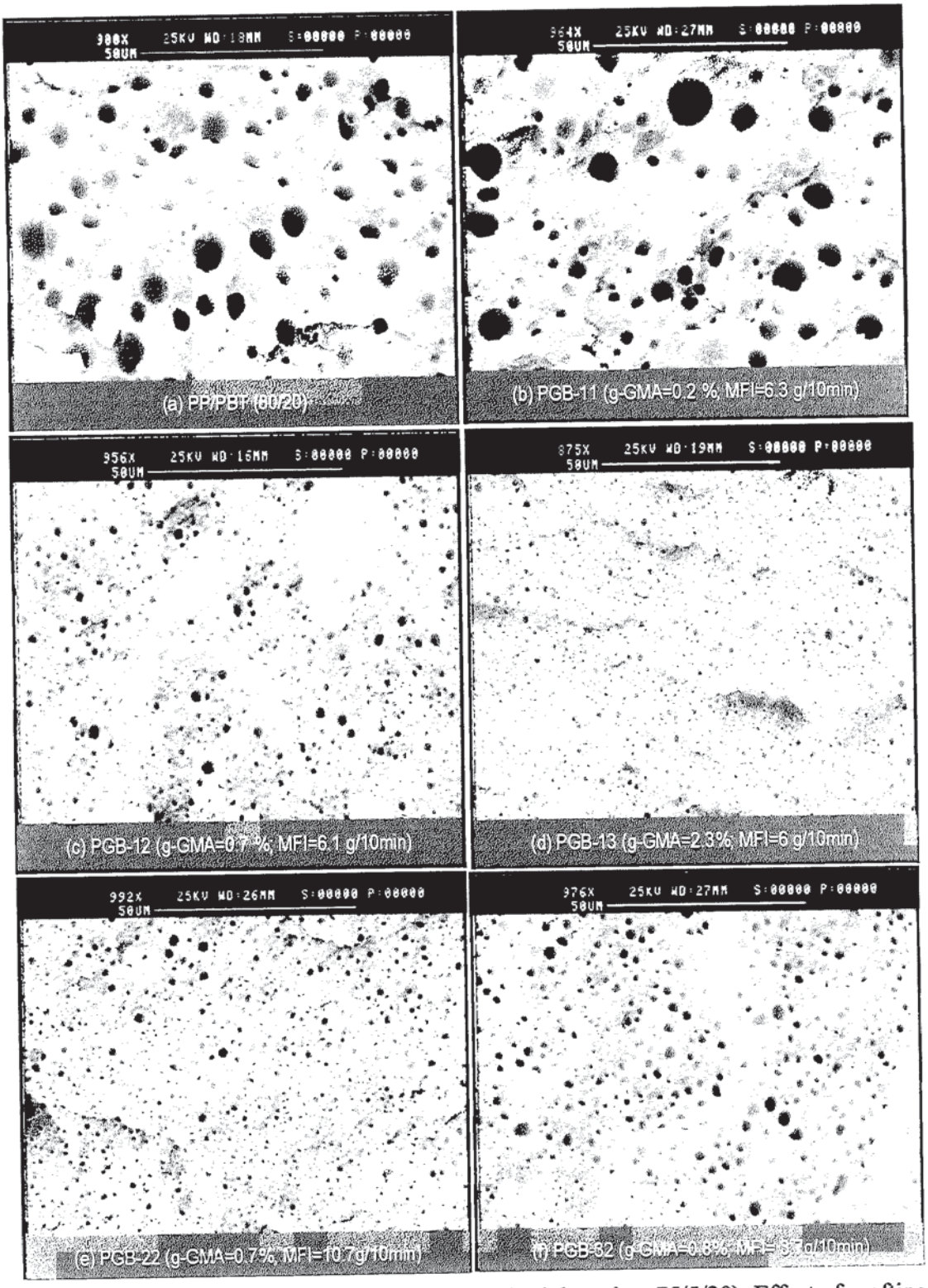

Figure 5.30 SEM of PP/PP-g-GMA/PBT blends (weight ratios: 75/5/20): Effect of grafting degree and MFI of PP-g-GMA (PGB-11, PGB-12, PGB-13 have similar MFI, ≈ 6 g/10min and PGB-12, PGB-22, PGB-23 have similar grafting degree, ≈ 0.7 %) (240°C, 65 rpm, 10 min).

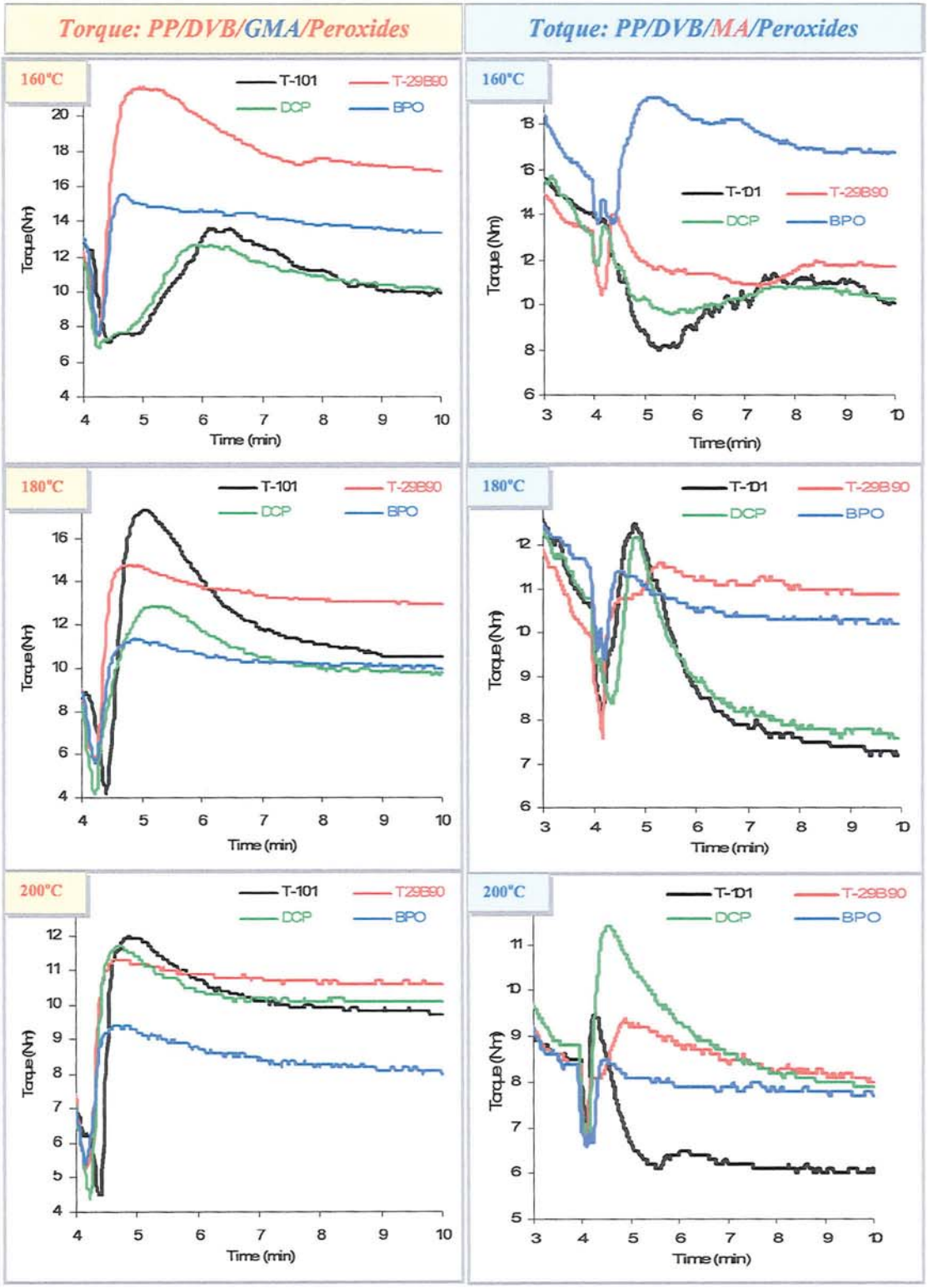

Figure 5.31 Comparison of the effect of different peroxides on torque of processed PP/DVB/**GMA**/peroxide and PP/DVB/**MA**/peroxide (different temperatures) system ([GMA] = 12%, [MA] = 8 %, [peroxide] = 0.005 molar ratio to monomer, temp.160-200°C, 65 rpm, 10min, mixing method M-2).

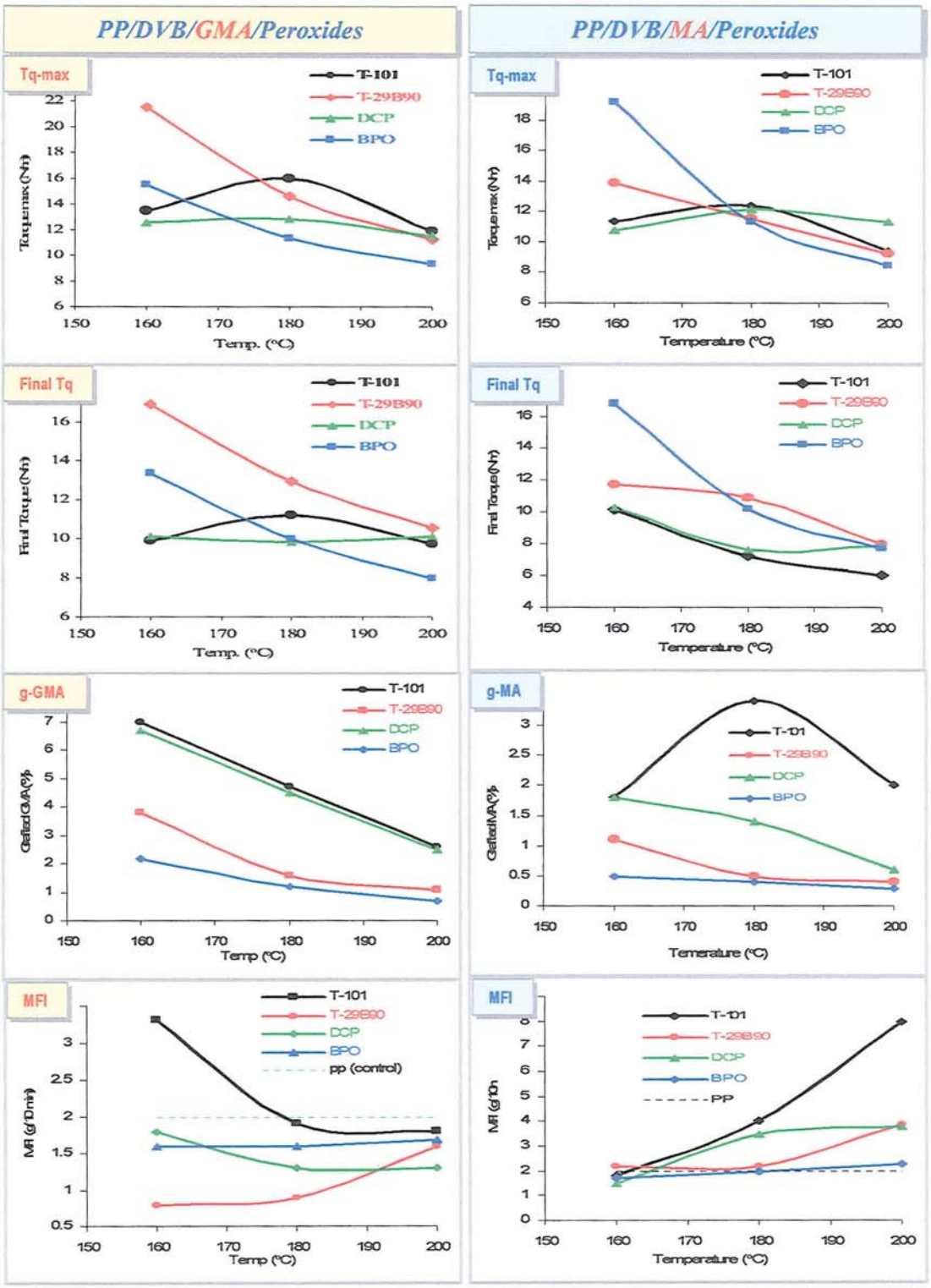

Figure 5.32 Comparison of the effect of different peroxide on torque characteristic, grafting level, and MFI of processed PP/DVB/**GMA**/peroxide and PP/DVB/**MA**/peroxide (different peroxides, BPO, DCP,T-101, T-29B90) system. (Samples: PP-Elf, [GMA]i = 12%, [MA] = 8 %, [peroxide] = 0.005 molar ratio to monomer, 65 rpm, 10min, mixing method M-2 (see **Scheme 4.1** for GMA and **Scheme 5.1** for MA)).

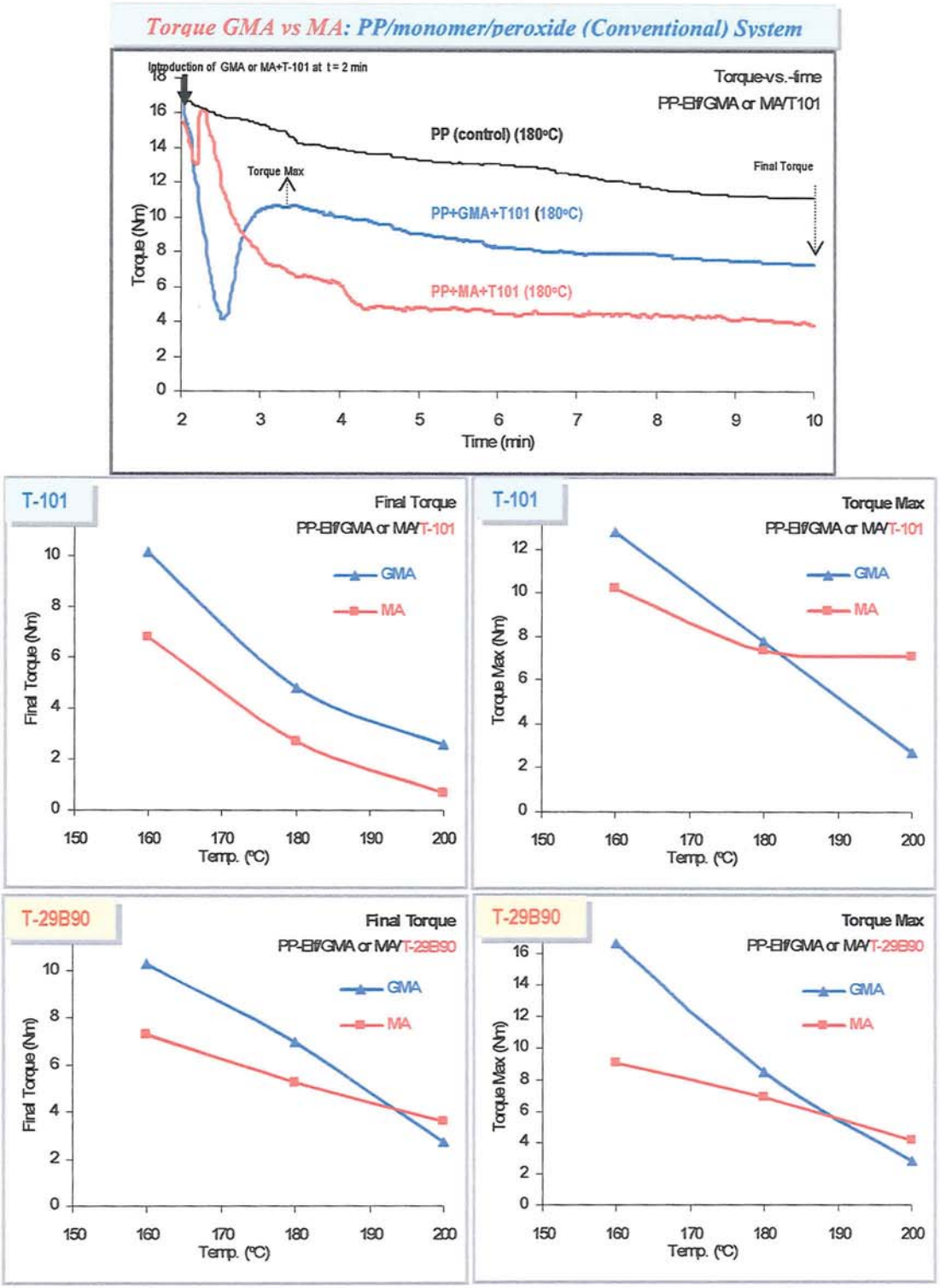

Figure 5.33 Comparison of the effect of temperature on torque characteristic of processed PP/GMA/peroxide and PP/MA/peroxide (different peroxide) system. (Samples: PP-Elf, [GMA] = 12%, [MA] = 8 %, [peroxide] = 0.005 molar ratio to monomer, temp. 160-200°C, 65 rpm, 10min, mixing method M-2 (see **Scheme 4.1** for GMA and **Scheme 5.1** for MA)).

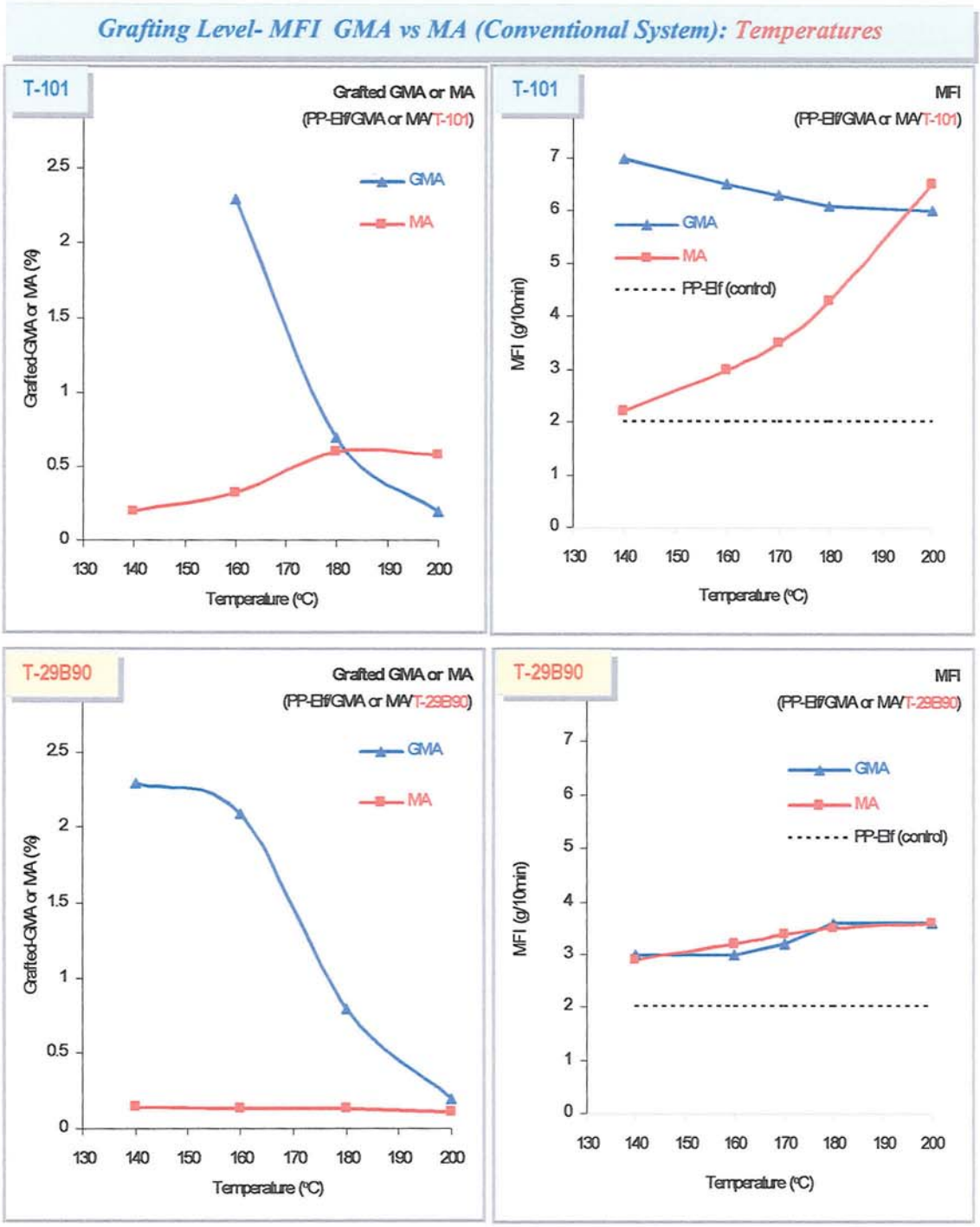

Figure 5.34 Comparison of the effect of temperature on grafting level and MFI of processed PP/GMA/peroxide and PP/MA/peroxide (different peroxide) system ([GMA] = 12%, [MA] = 8 %, [peroxide] = 0.005 molar ratio to monomer, temp. 160-200°C, 65 rpm, 10min, mixing method M-2, see **Scheme 4.1** for GMA and **Scheme 5.1** for MA).

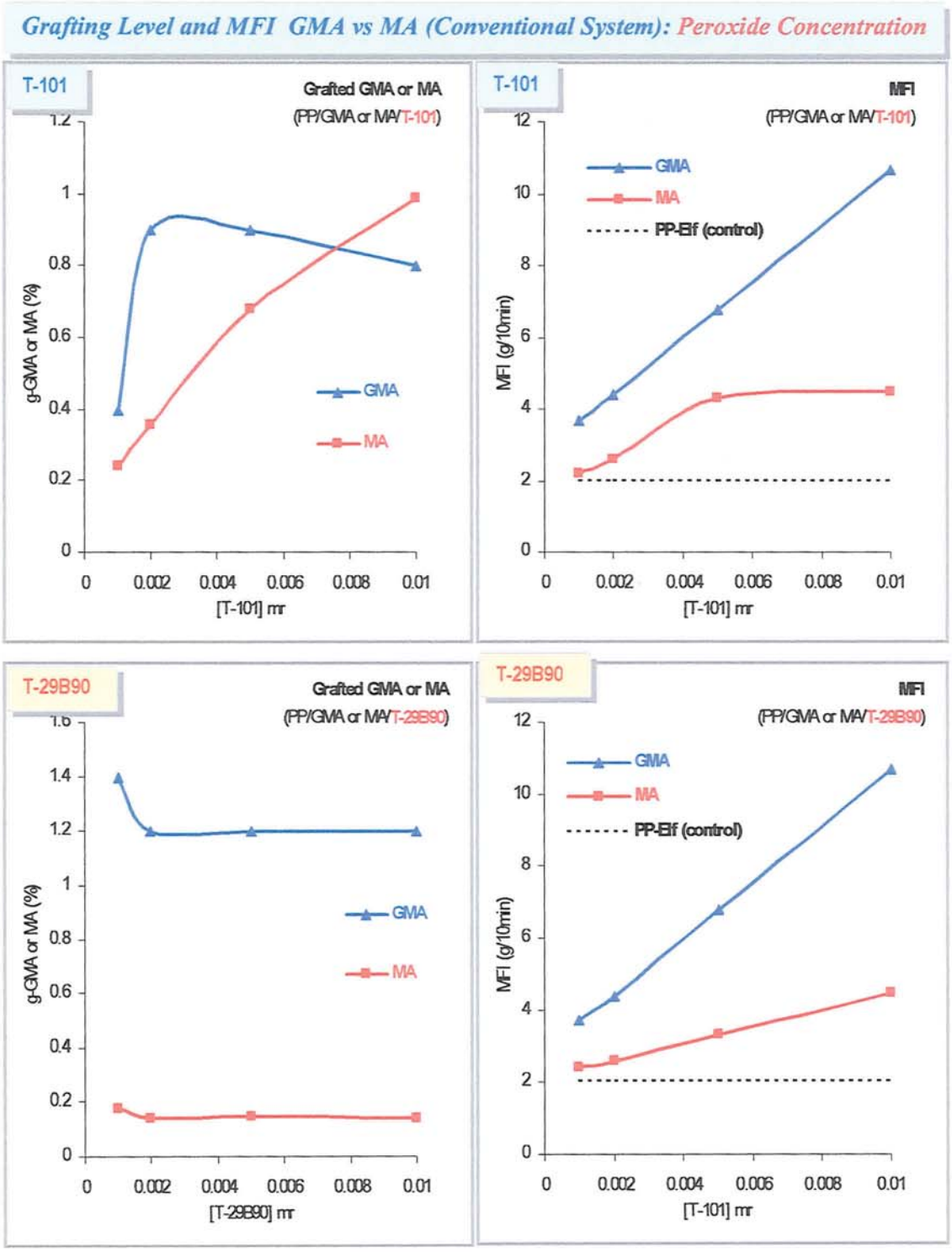

Figure 5.35 Comparison of the effect of peroxide concentration on grafting level and MFI of processed PP/GMA/peroxide and PP/MA/peroxide (different peroxide) system ([GMA] = 12%, [MA] = 8 %, [peroxide] = 0.001-0.01 molar ratio to monomer, **temp. 180°C for T-101** and **160°C for T-29B90**, 65 rpm, 10min, mixing method M-2, see Scheme 4.1 (p.198) for GMA and Scheme 5.1 for MA).

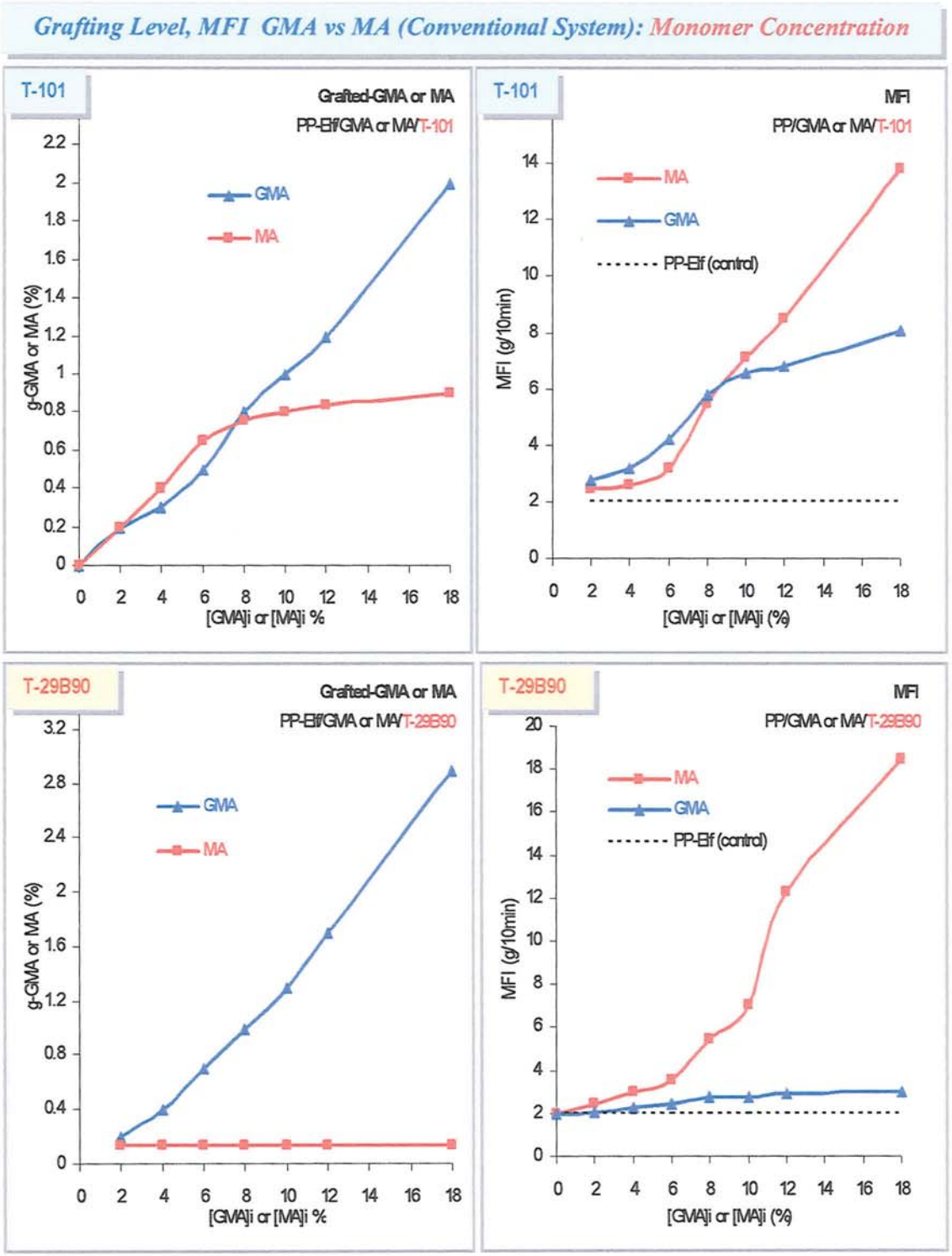

Figure 5.36 Comparison of the effect of initial monomer concentration on grafting level and MFI of processed PP/GMA/peroxide and PP/MA/monomer (different peroxide) system (Samples: PP-Elf, [GMA] = 12%, [MA] = 8 %, [peroxide] = 0.005 molar ratio to monomer, **temp. 180°C for T-101** and **160°C for T-29B90**, 65 rpm, 10min, mixing method M-2, see Scheme 4.1 for GMA and Scheme 5.1 for MA).

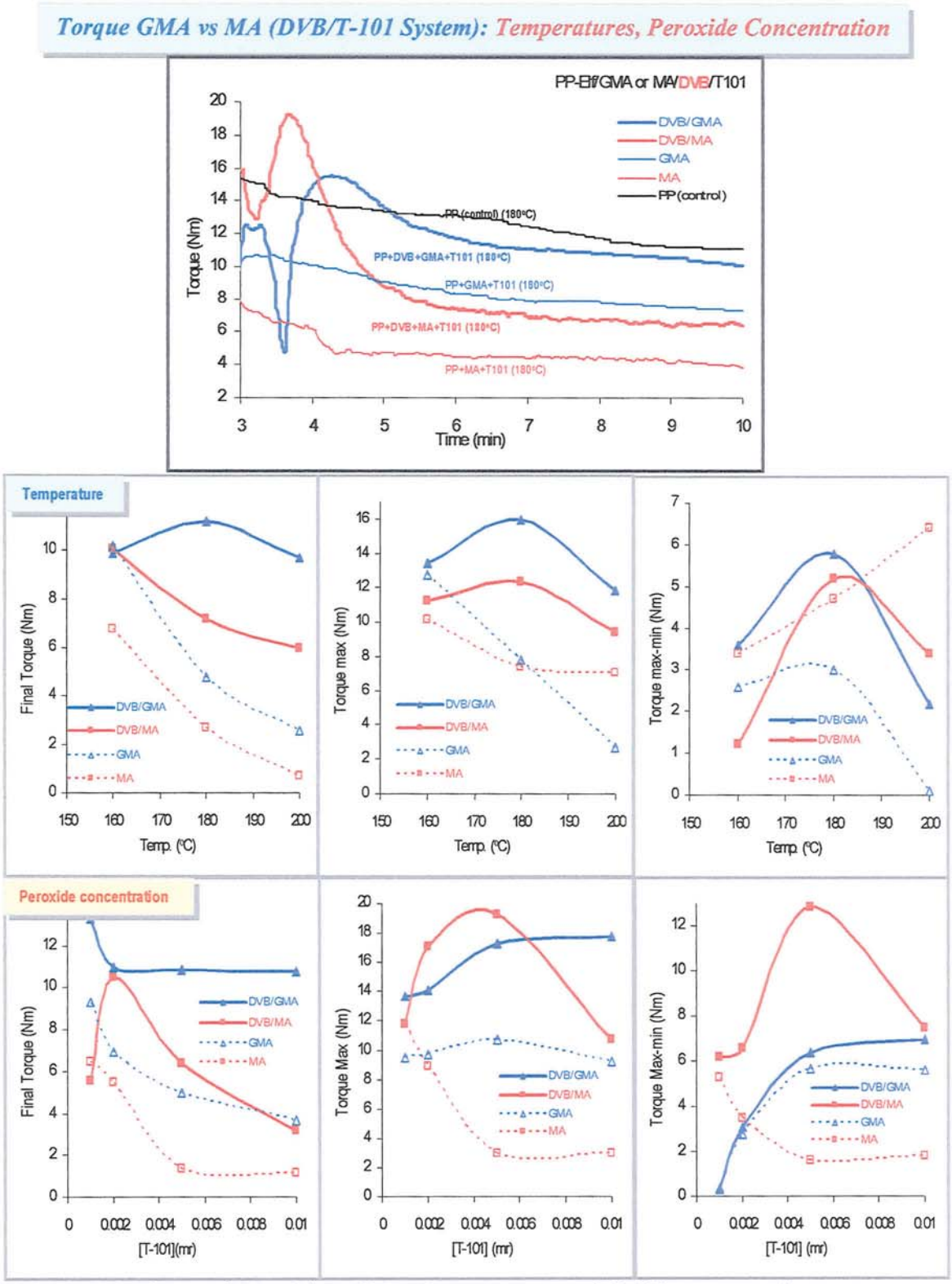

Figure 5.37 Comparison of the effect of temperature and T-101 concentration on torque characteristic of processed PP/DVB/monomer/T-101 system ([GMA] = 12%, [MA] = 8 %, [T-101] = 0.001-0.01 molar ratio to monomer, temp. 180°C, 65 rpm, 10min, mixing method M-3, see Scheme 4.2 (p.199) for GMA and Scheme 5.2 for MA).

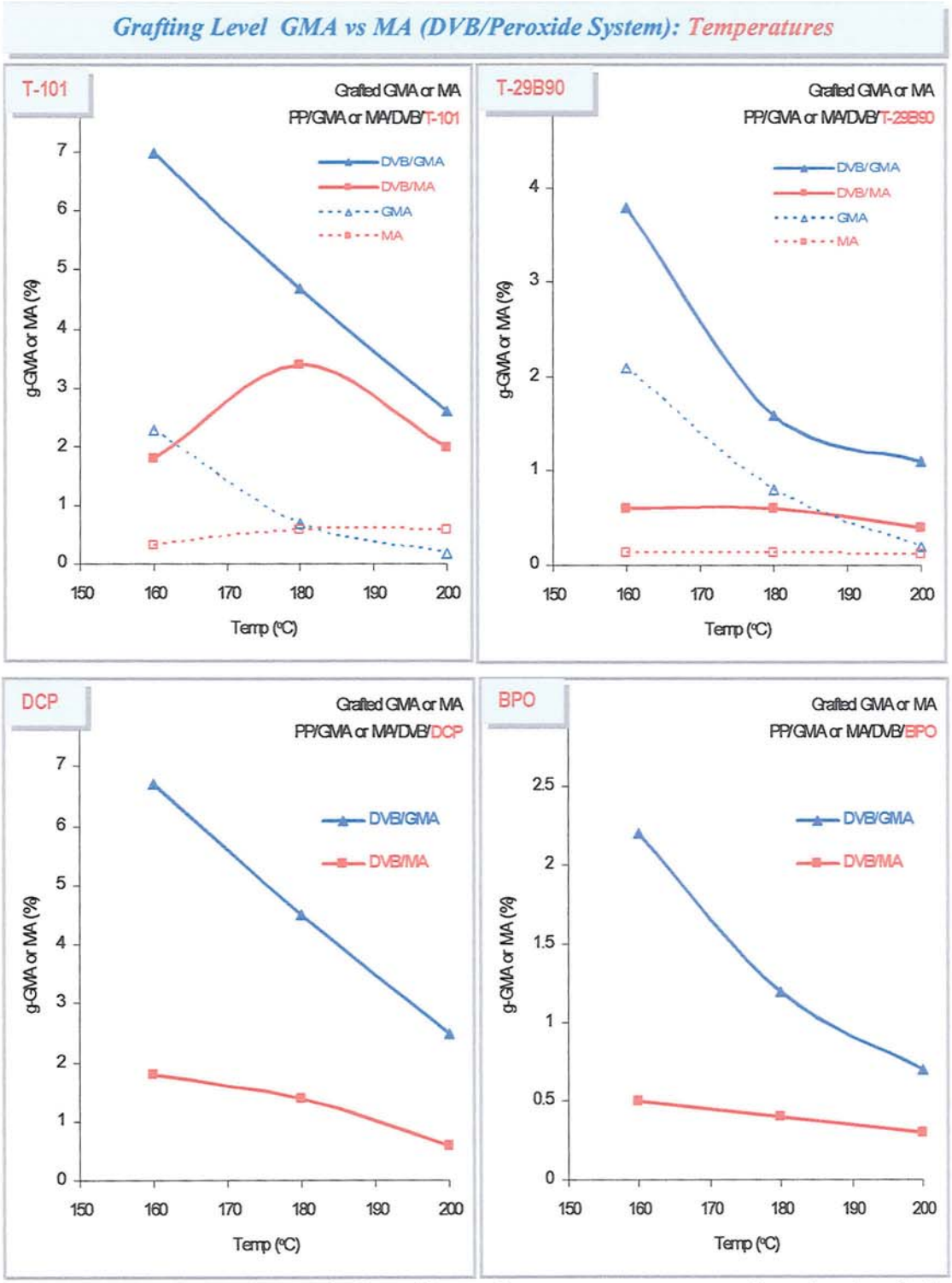

Figure 5.38 Comparison of the effect of temperature on grafting level of the PP/DVB/monomer/peroxide (different peroxides) system (PP-Elf, [GMA]i = 12%, [MA]i = 8%, [DVB] = 2/8 weight ratio to monomer, [perox] = 0.005 molar ratio to monomer, temp. 180-200°C, 65 rpm, 10min, mixing method M-3, see Scheme 4.2 for GMA and Scheme 5.2 for MA).

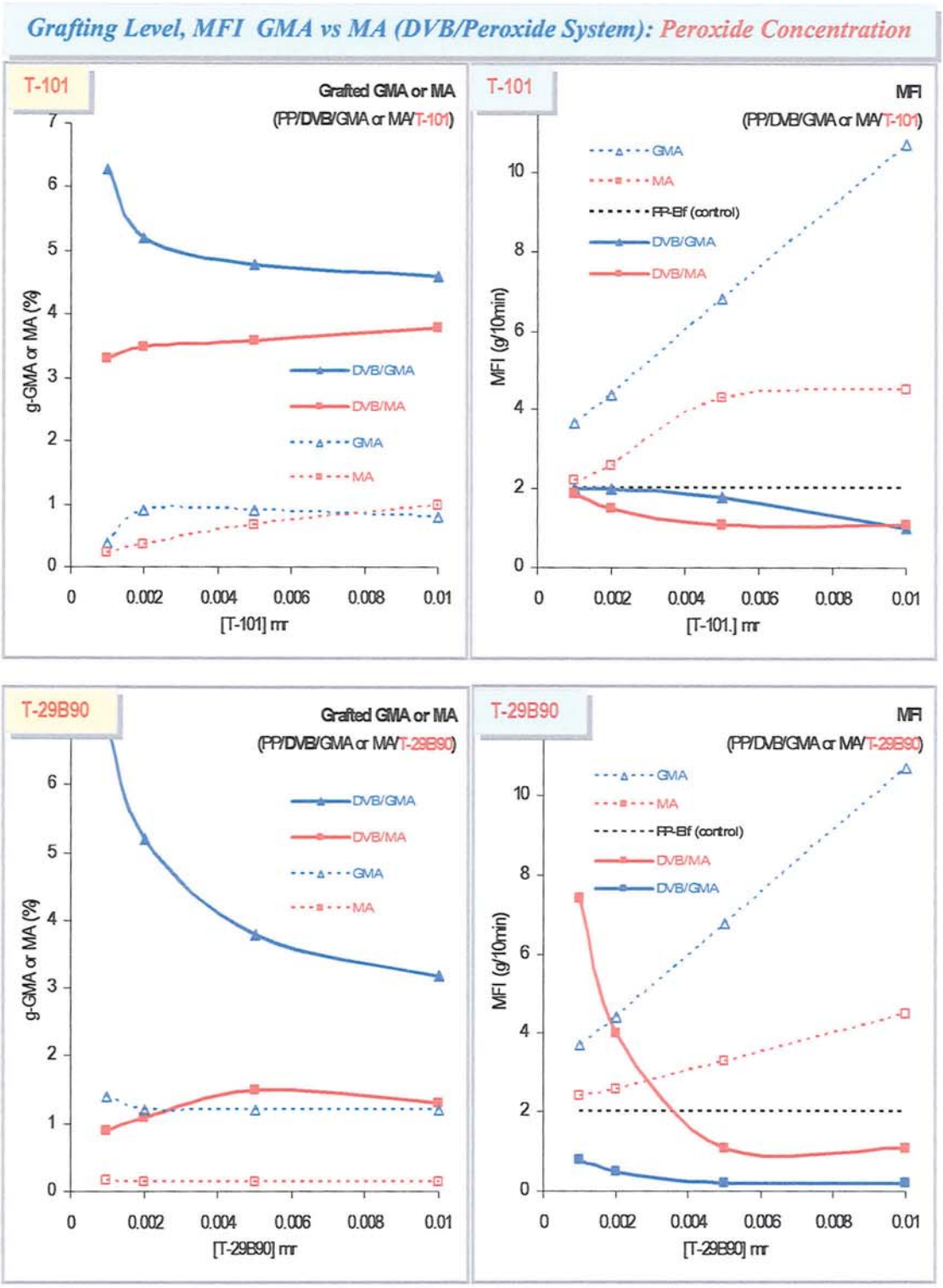

Figure 5.39 Comparison of the effect of peroxide concentration on grafting level and MFI of processed PP/DVB/GMA/peroxide and PP/DVB/MA/peroxide (different peroxide) system (PP-Elf, [GMA]i = 12%, [MA]i = 8%, [perox] = 0.001-0.01 molar ratio to monomer, **temp. 180°C for T-101** and **160°C for T-29B90**, 65 rpm, 10min, mixing method M-3, see Scheme 4.2 for GMA and Scheme 5.2 for MA).

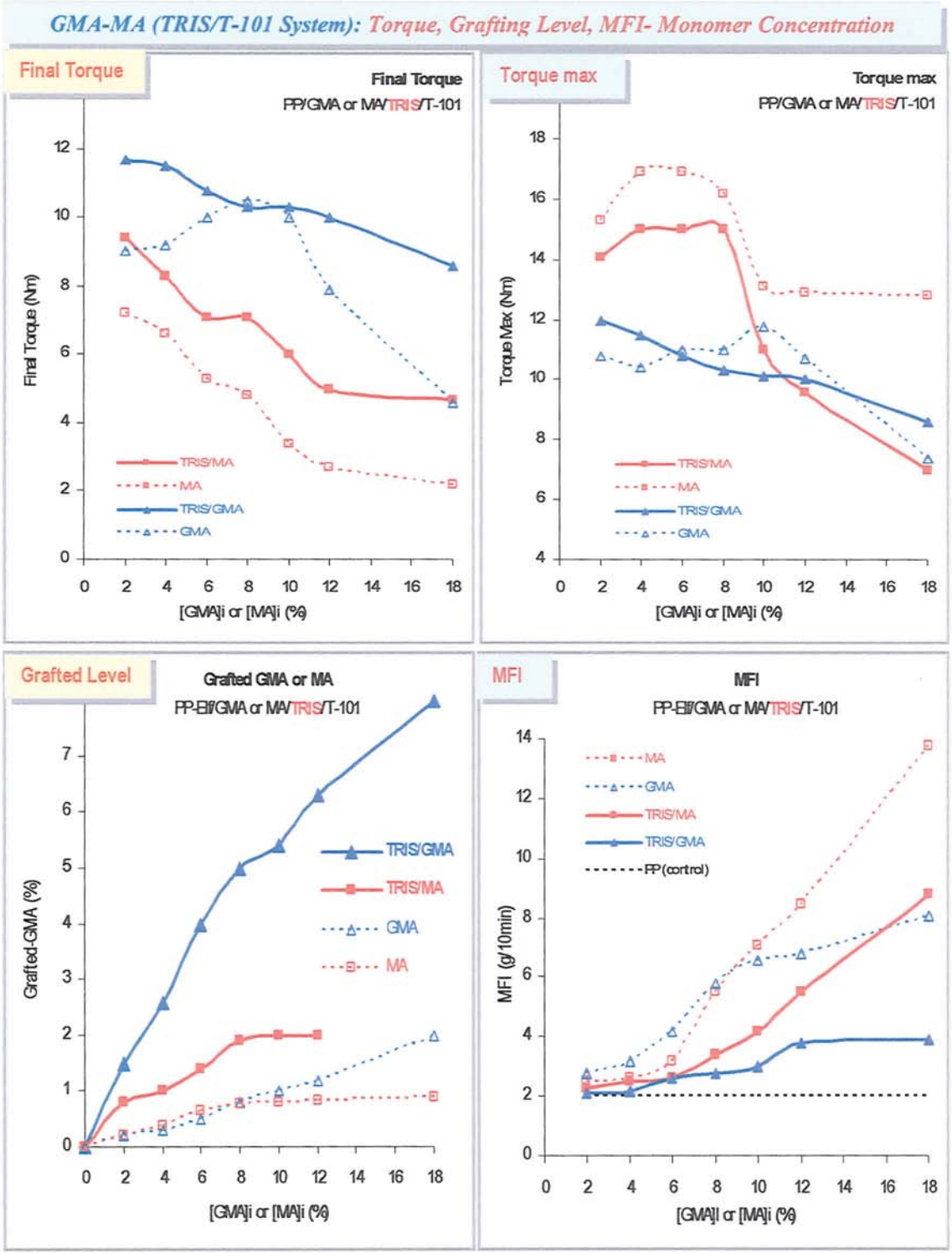

Figure 5.40 Comparison of the effect of initial monomer concentration on torque characteristic, grafting level, and MFI of the PP/TRIS/GMA/T-101 and PP/TRIS/MA/T-101 system (PP-Elf, [GMA]i = 12%, [MA]i = 8%, [TRIS] = 2/8 weight ratio to monomer, [T-101] = 0.005 molar ratio to monomer, temp. 180°C, 65 rpm, 10min, mixing method M-3, see Scheme 4.2 (p.199) for GMA and Scheme 5.2 for MA).

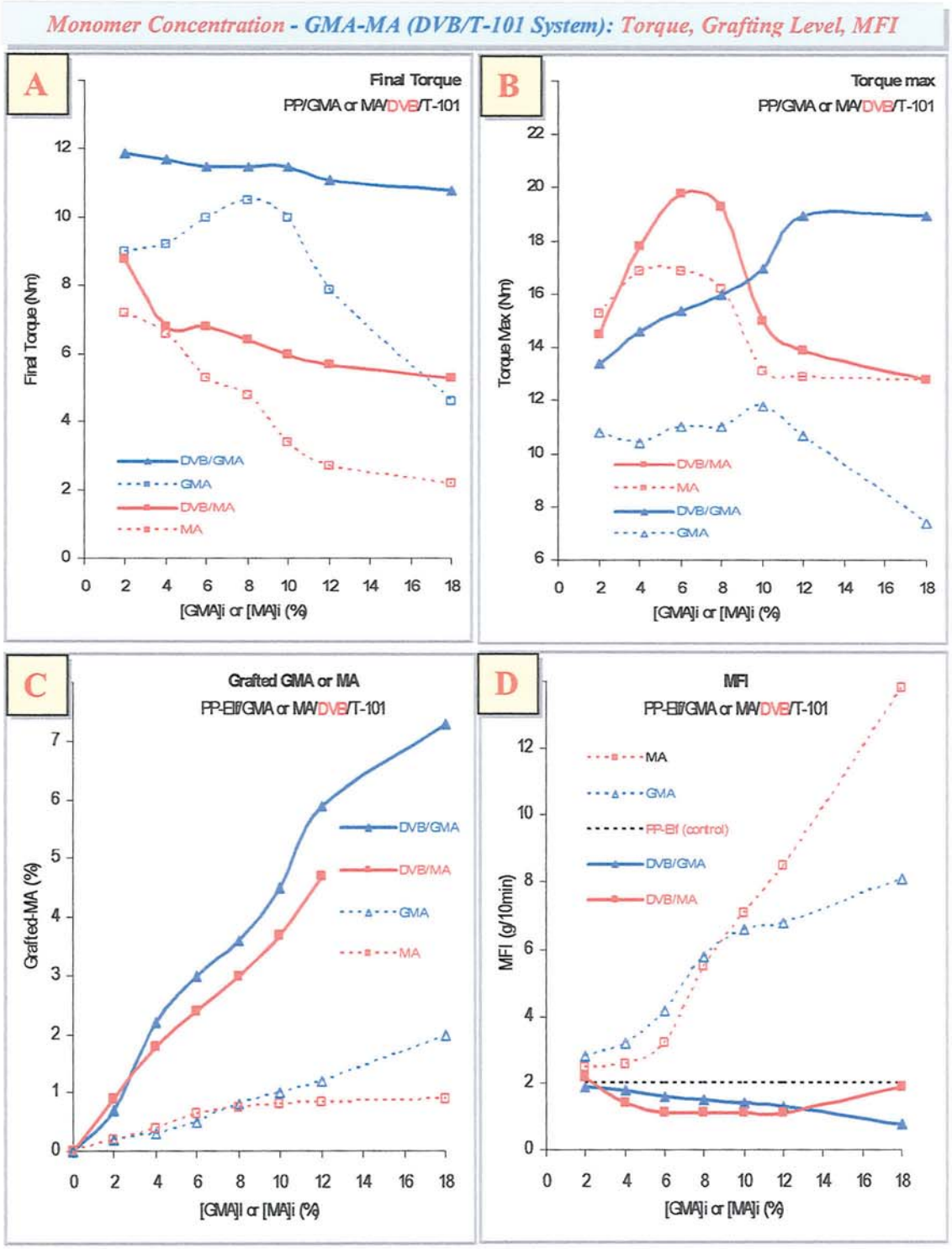

Figure 5.41 Comparison of the effect of initial monomer concentration on torque characteristics, grafting level and MFI of the PP/DVB/GMA/T-101 and PP/DVB/MA/T-101 system (PP-Elf, [GMA]i = 12%, [MA]i = 8%, [DVB] = 2/8 weight ratio to monomer, [T-101] = 0.005 molar ratio to monomer, temp. 180°C, 65 rpm, 10min, mixing method M-3, see Scheme 4.2 (p.199) for GMA and Scheme 5.2 for MA).

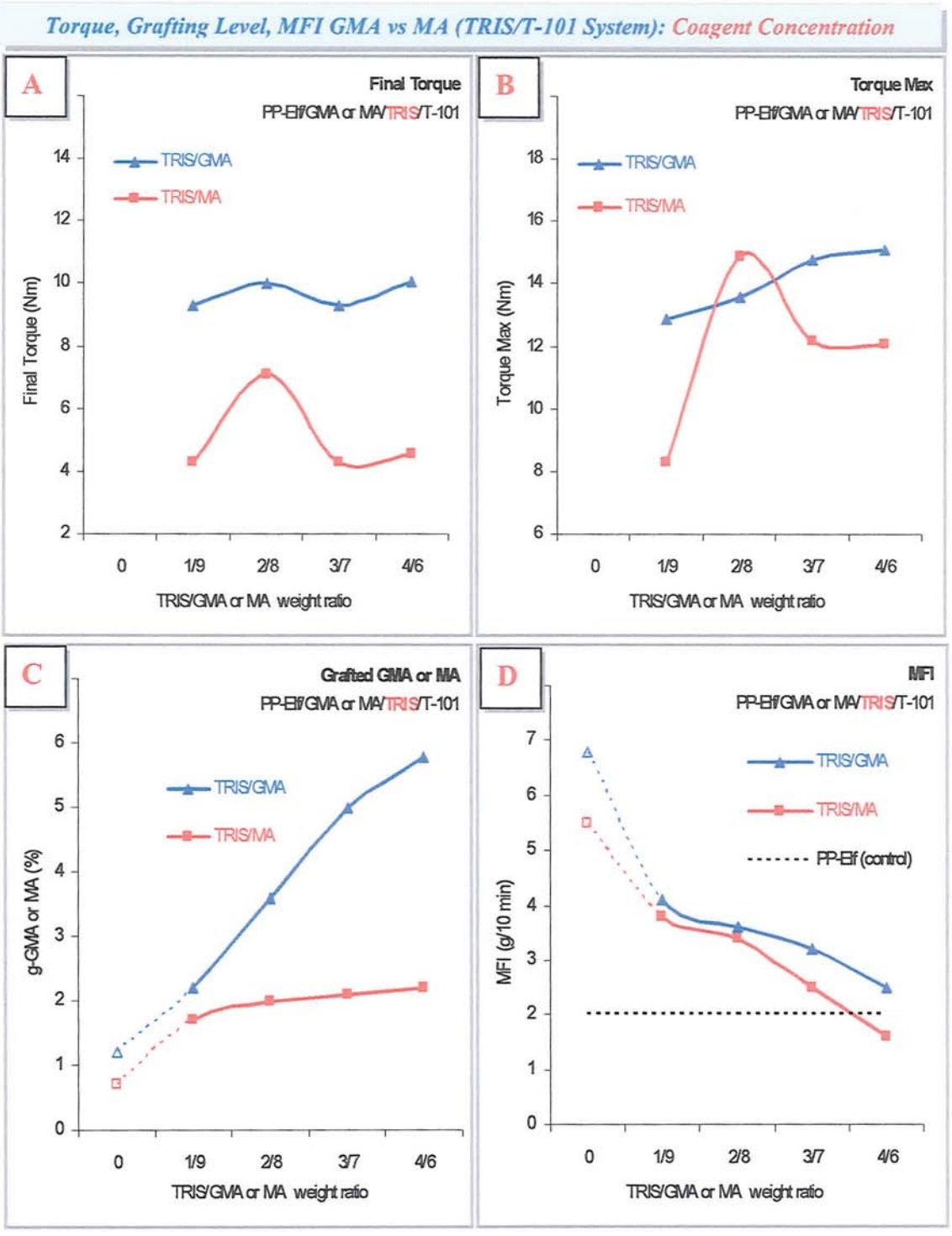

Figure 5.42 Comparison of the effect of coagent concentration on torque characteristic, grafting level and MFI of the PP/TRIS/GMA/T-101 and PP/TRIS/MA/T-101 system (PP-Elf, [GMA]i = 12%, [MA]i = 8%, [TRIS] = 1/9 to 4/6 weight ratio to monomer, [T-101] = 0.005 molar ratio to monomer, temp. 180°C, 65 rpm, 10min, mixing method M-2 (see Scheme 4.2) for GMA and M-3 (see Scheme 5.2) for MA).

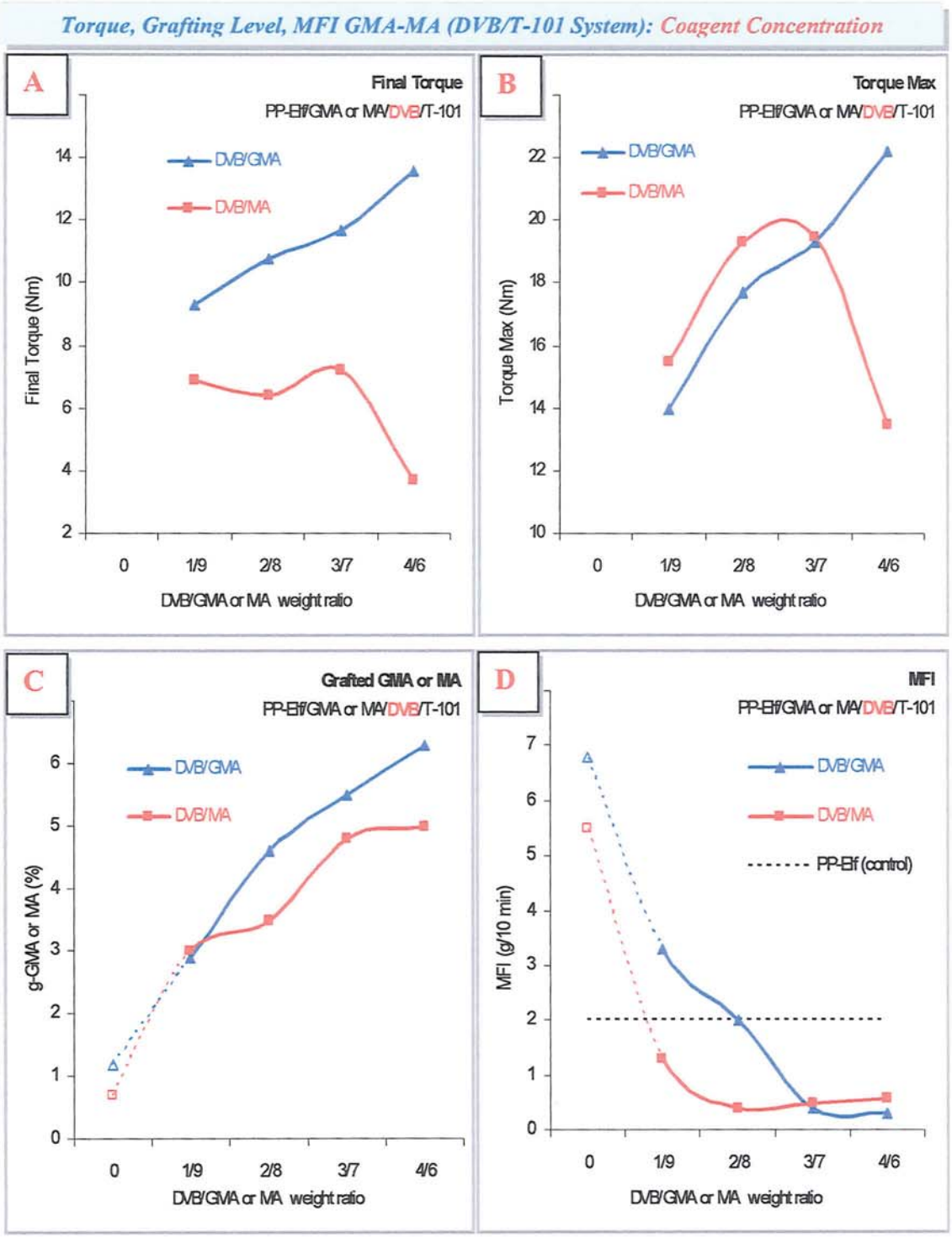

Figure 5.43 Comparison of the effect of DVB concentration on torque characteristic, grafting level and MFI of the PP/DVB/GMA/T-101 and PP/DVB/MA/T-101 system (PP-Elf, [GMA]i = 12%, [MA]i = 8%, [DVB] = 1/9 to 4/6 weight ratio to monomer, [T-101] = 0.005 molar ratio to monomer, temp. 180°C, 65 rpm, 10min, mixing method M-2 (see Scheme 4.2) for GMA and M-3 (see Scheme 5.2) for MA).

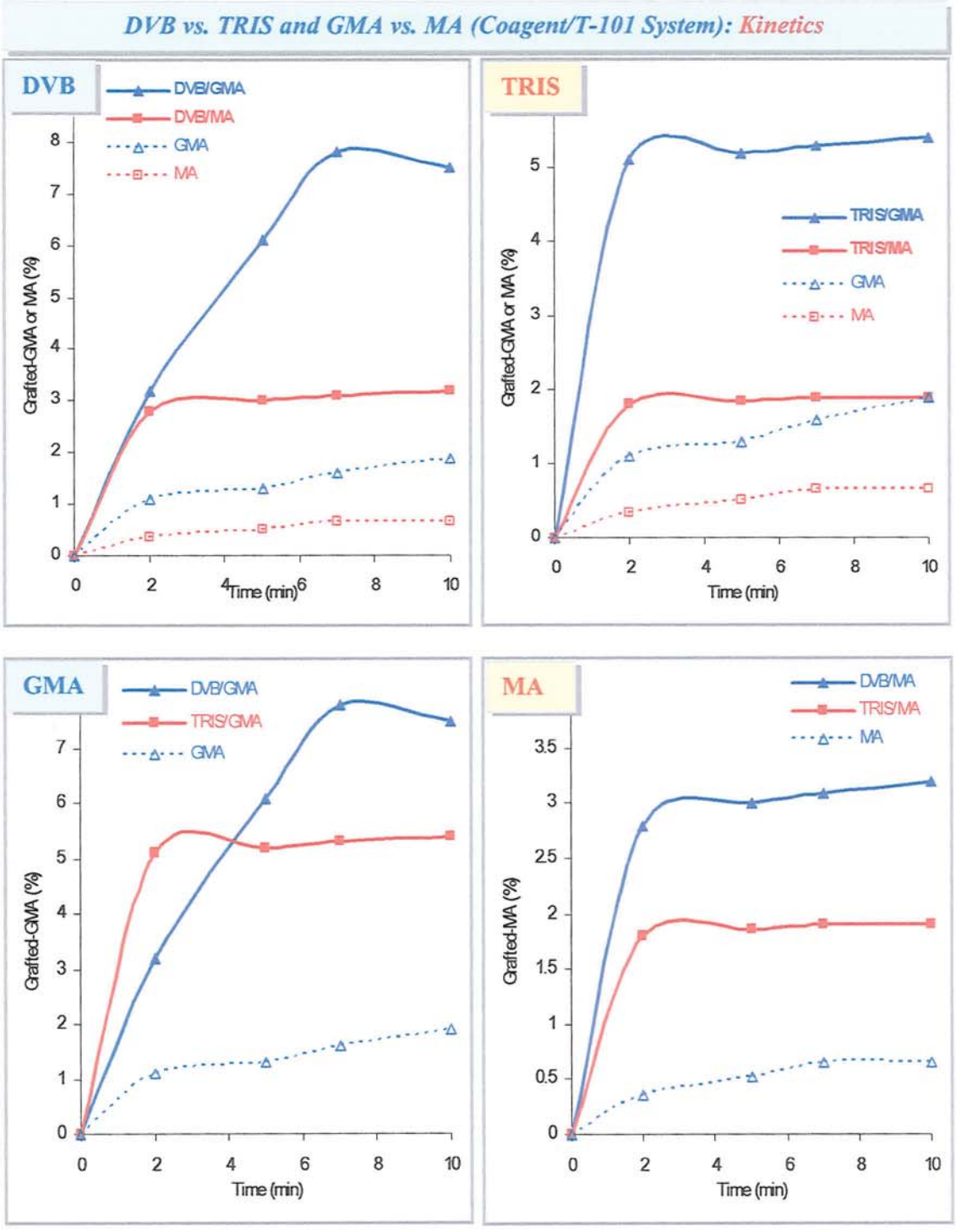

Figure 5.44 Comparison of the effect of processing time on grafting level of the PP/coagent/GMA/T-101 and PP/coagent/MA/T-101 (different coagents, TRIS and DVB) system. Samples: PP-Elf, [GMA]i = 12%, [MA]i = 8%, [TRIS] or [DVB] = 2/8 weight ratio to monomer, [T-101] = 0.005 molar ratio to monomer, temp. 160°C, 65 rpm, mixing method M-2 (see Scheme 4.2 and Scheme 5.2).

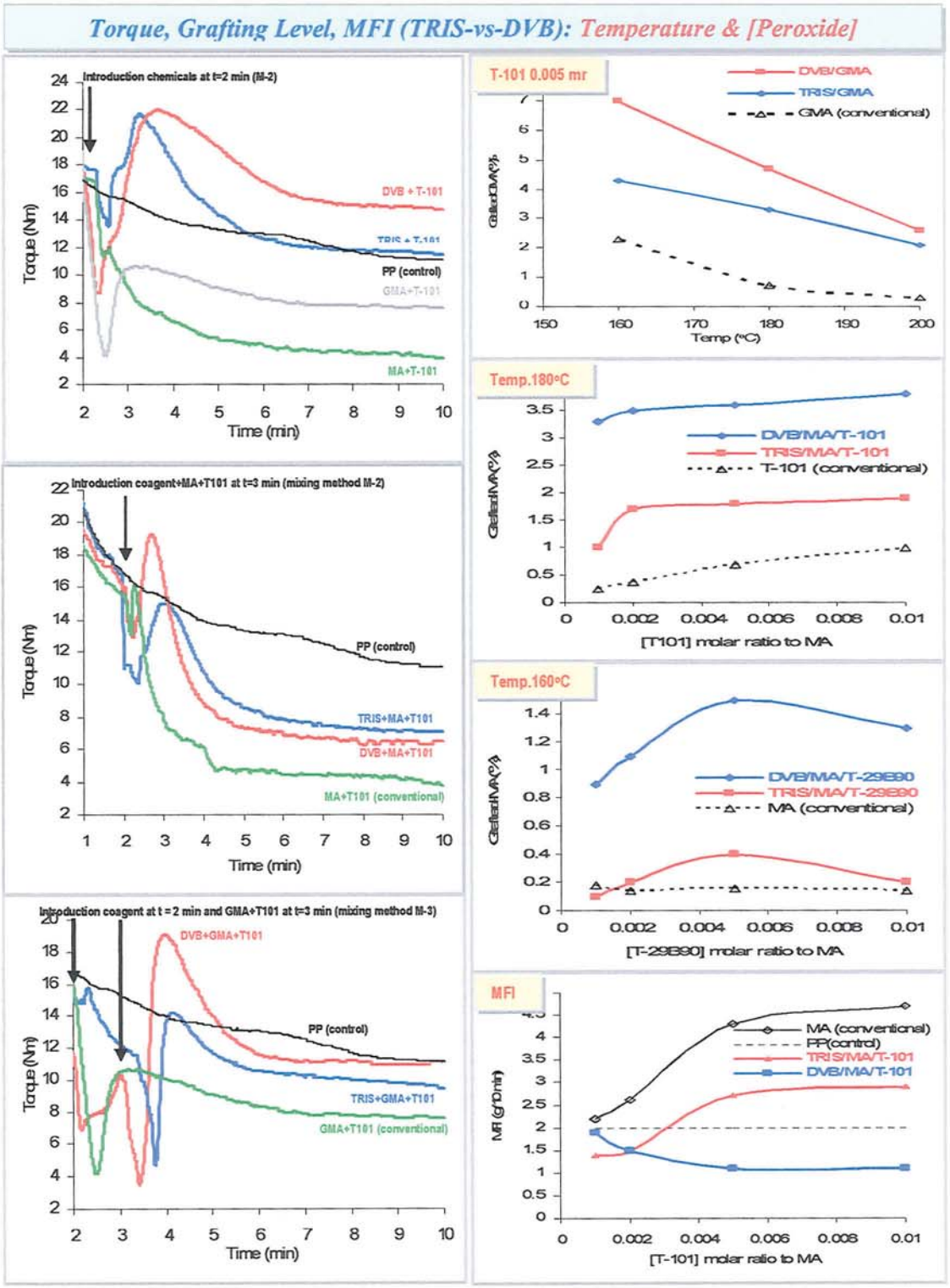

Figure 5.45 Comparison of the effect of DVB and TRIS on torque, grafting level and the change of MFI of processed PP/coagent/MA/T101 and PP/coagent/GMA/T-101 system at various temperatures and peroxide concentrations (different peroxide) (Samples: PP-Elf, [GMA]i = 12%, [MA]i = 8%, [coagent] = 2/8 wr, [T-101] = 0.001-0.01 mr, temp. 160-200°C, 65 rpm, mixing method M-2 for MA and M-3 for GMA.

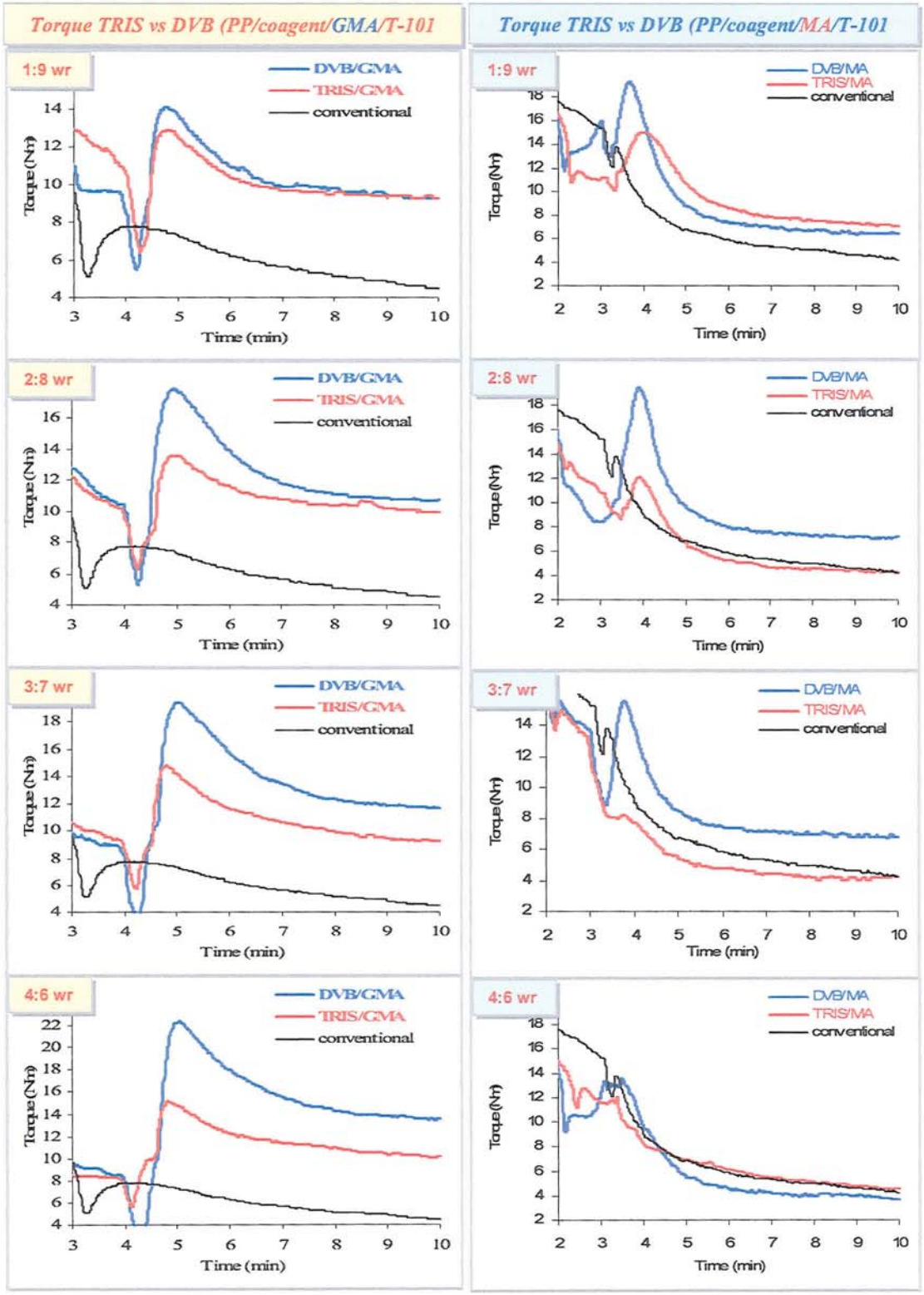

Figure 5.46 Comparison of torque of processed PP/coagent/GMA/T101 and PP/coagent/MA/T101 (different types and concentration of coagent) system. Samples: PP-Elf, [GMA]i = 12%, [MA]i = 8%, [coagent] = 1/9 to 2/8 wr, [T-101] = 0.005 mr, 180°C, 65 rpm, mixing method M-2 for GMA and M-3 for MA (see **Scheme 4.2** and **5.2**)

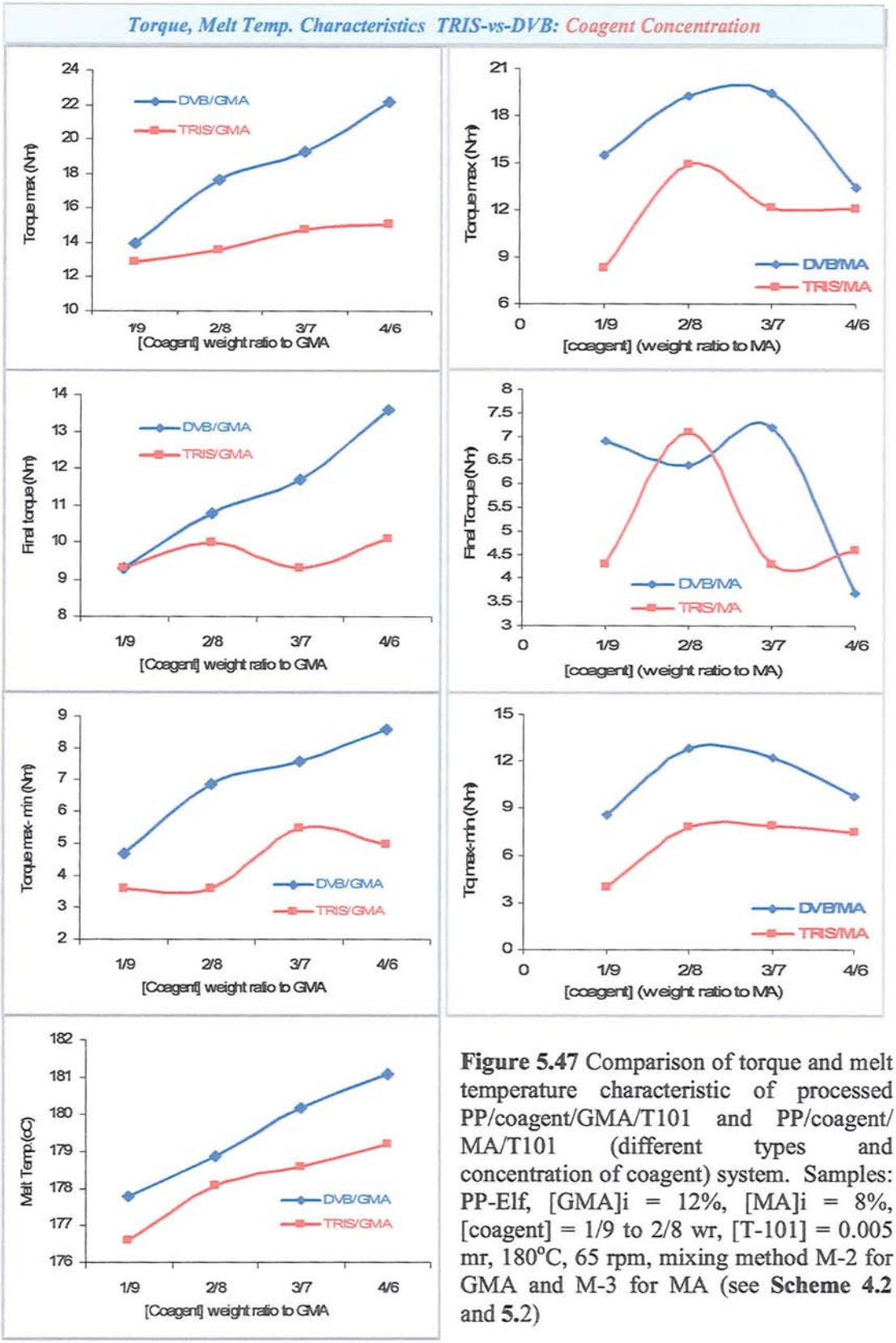

Figure 5.47 Comparison of torque and melt temperature characteristic of processed PP/coagent/GMA/T101 and PP/coagent/MA/T101 (different types and concentration of coagent) system. Samples: PP-Elf, [GMA]i = 12%, [MA]i = 8%, [coagent] = 1/9 to 2/8 wr, [T-101] = 0.005 mr, 180°C, 65 rpm, mixing method M-2 for GMA and M-3 for MA (see **Scheme 4.2** and **5.2**)

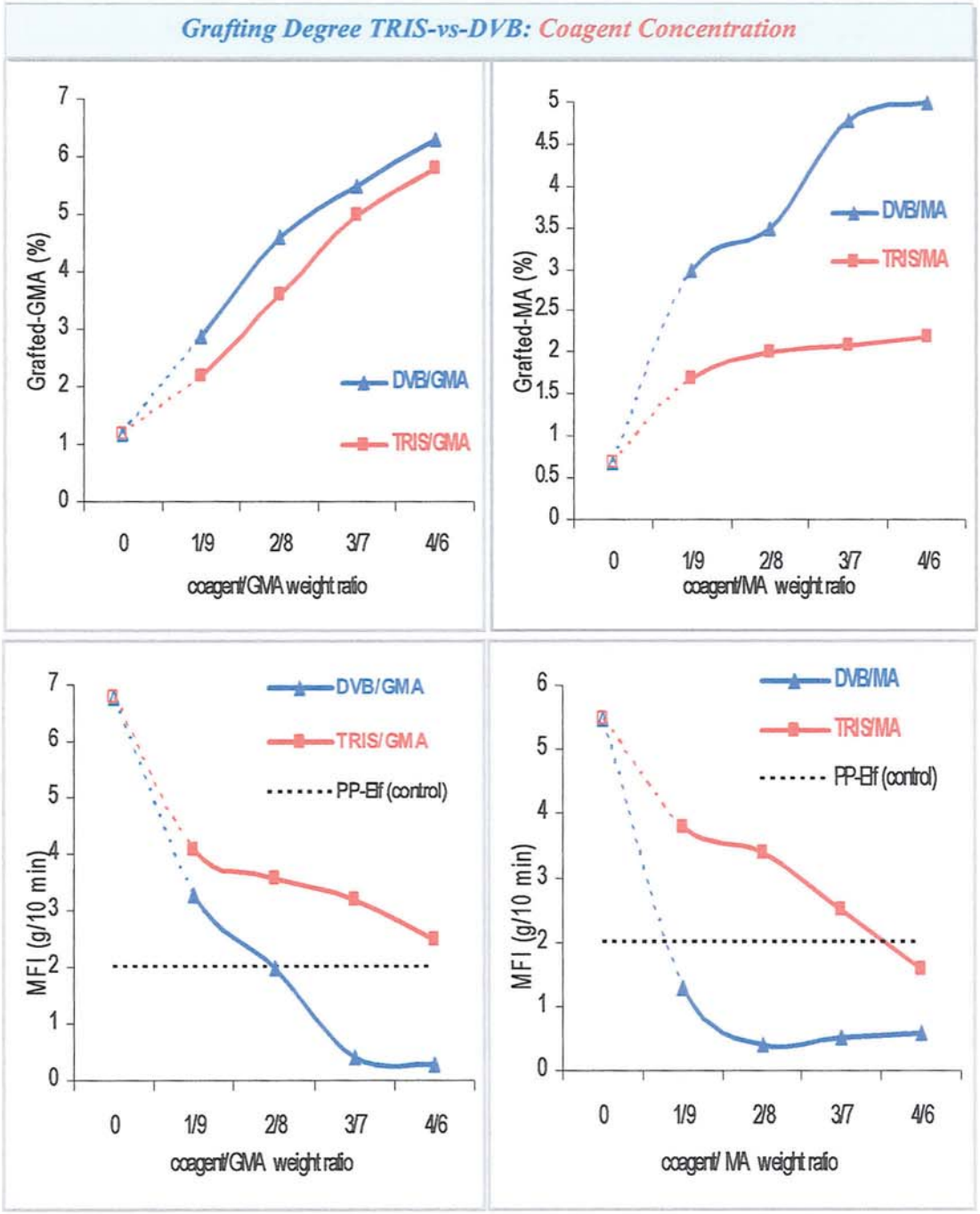

Figure 5.48 Comparison of effectiveness of the coagents DVB and TRIS in PP processed with GMA or MA with different concentrations of coagent: ([GMA]i = 12%, [MA]i = 8%, [TRIS] or [DVB] = 1/9 to 2/8 wr (eight ratio to monomer), [T-101] = 0.005 mr, temp. 180°C, 65 rpm, mixing method M-2 (Scheme 4.2 p.199) for GMA and M-3 (Scheme 5.2) for MA).

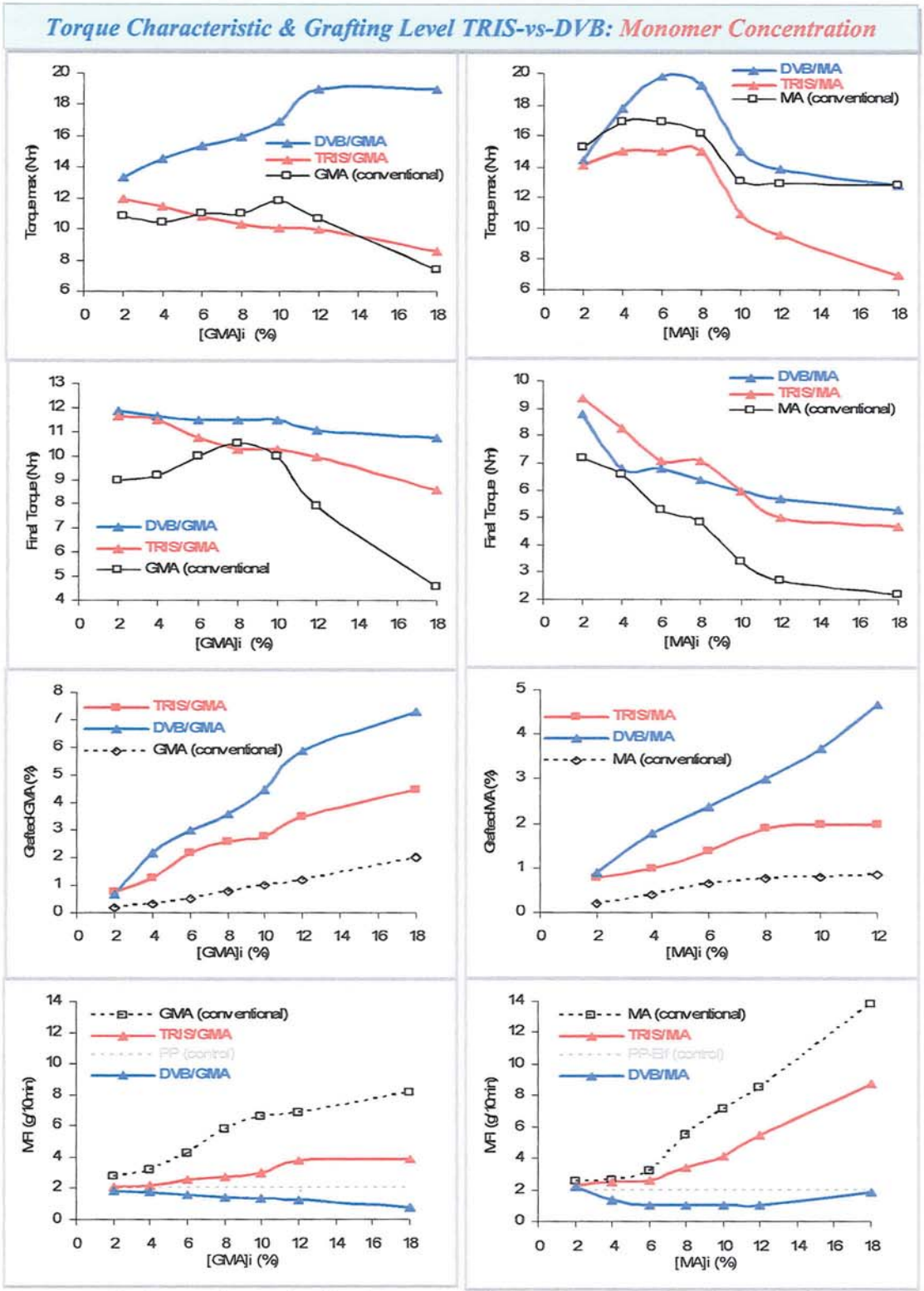

Figure 5.49 Comparison of effectiveness of the coagents DVB and TRIS of processed PP/coagent/GMA/T101 and PP/coagent/MA/T101 (various monomer concentrations) system. Samples: PP-Elf, [monomer]i = 2-18%, [coagent] = 2/8 weight ratio to monomer, [T-101] = 0.005 molar ratio to monomer+coagent, 180°C, 65 rpm, mixing method M-3.

CHAPTER 6

CONCLUSIONS AND RECOMMENDATION FOR FURTHER WORKS

6.1 Conclusions

The following conclusions can be drawn from the results discussed in **Chapter 3 to 5**:

6.1.1 In the reactive processing of natural rubber (NR) with glycidyl methacrylate (GMA), it was found that the grafting reaction could be initiated both thermally (**Fig.3.10**, p.133) and via free radicals initiation, BPO (**Fig.3.16**, p.139), DCP (**Fig.3.20**, p.143), T-101 (**Fig. 3.24**, p.147), and T-29B90 (**Fig. 3.30**, p.153). The high extent of GMA grafting onto NR is attributed to the relative reactivity of GMA with the C=C double bond of *cis*-1,4-polyisoprene. The main parameters which influenced the grafting level of GMA on NR were found to be in the order: processing temperature > type and concentration of peroxide > GMA concentration > addition sequence > rotor speeds (see **Fig 3.34, 3.36, 3.31, 3,11,** and **3.14**, respectively).

6.1.2 The effectiveness of peroxides in initiating the grafting reaction of GMA on NR was found to be in the order T-29B90 > T-101 > DCP > BPO. The GMA grafting degree increased constantly with increasing peroxide concentration, DCP (**Fig. 3.21-E**, p.144) and T-101 (**Fig. 3.26**, p.149), and GMA initial concentration (**Fig.3.31**, p.154). However at high peroxide concentration (>0.05 molar ratio to GMA) branch/crosslinking reaction became dominant and unacceptable. The crosslinking reaction of NR resulted through coupling

(without involving the diene double bond, step **C-1** in **Scheme 3.11**, p.118) and addition (which involving the diene double bond, step **C-2** in **Scheme 3.11**) reactions. The former occurs more intensely at higher peroxide concentrations, whereas the latter occurs predominantly at higher temperatures (decrease in C=C peak area index at 1662 cm^{-1}, **Figure 3.38**, p.161). The addition of a coagent such as TRIS to the system NR/GMA/T-101 resulted in excessive crosslinking because of the very high reactivity of the coagent and the presence of C=C in natural rubber. Therefore, any multifunctional and highly reactive coagents could not be used successfully in the grafting of GMA onto natural rubber.

6.1.3 Free radical-initiated grafting reactions of GMA on PP in the absence of coagent (conventional) system lead to GMA grafting (PP-g-GMA) as well as the formation of poly-GMA and radical-induced PP degradation (chain scission). The relative contribution of these reactions depended on both the chemical composition and the processing conditions. It was shown that in the conventional system poly-GMA formation competed strongly with the desired grafting reaction resulting in higher poly-GMA compared to grafted-GMA (see **Fig. 4.14**, p.215). This was further supported by kinetic study that showed the rate of homopolymerisation at the initial stages of the reaction to be faster than that of the grafting reaction (**Fig. 4.37**, p.238) with poly-GMA concentration becoming 10 times higher than grafted-GMA at higher (e.g. 200°C) temperatures, whereas the grafted-GMA level dropped to 4 times lower than its level at lower temperature of 160°C.

6.1.4 Only at the lower processing temperatures (<160°C), lower peroxide concentrations (<0.001 molar ratio to GMA ≅ 0.03 phr), and higher GMA concentrations (12 %) could the grafting degree exceed the poly-GMA level (**Fig.4.14**, p.215). The processing temperature was found to have a negative effect on the GMA grafting level (**Fig. 4.15**, p.216), but peroxide concentration had a positive effect (**Fig. 4.15**). However, at the higher peroxide concentrations, the extent of degradation was very dominant and intolerable, e.g. when the peroxide concentration was increased from 0.001 to 0.01 mr (160°C), the GMA grafting degree doubled (from 0.7 to 1.8 %) but the MFI rocketed almost to 400 % change compared to that of the PP (see **Fig. 4.18**, p.219). The peroxide T-29B90 which has a shorter half-life gave comparable grafting efficiencies and

lower MFI than values observed with the initiator T-101 (**Fig. 4.18**). In both peroxides T-101 and T-29B90 (conventional) system, an increase of GMA initial concentration led to higher GMA grafting degree as well as to an increase in the extent of the homopolymerisation reaction (**Fig. 4.19**, p.220).

6.1.5 The addition of DVB or TRIS as reactive comonomers in melt free radical grafting of GMA onto PP enhanced greatly the level of grafting reaction and reduced the extent of side reaction which was achieved at much lower peroxide concentration and consequently resulting in a negligible extent of PP degradation with very small amount of poly-GMA formation (see **Fig.4.27A** and **4.27B**, p.228). This was shown to be due to the high reactivity of the coagents towards PP macroradicals and GMA which is supported by a distinct torque behaviour during the reactive processing (**Fig.4.20**, p221). Further, high reactivity of the coagents towards GMA was demonstrated from the formation of comonomer of GMA-coagent when GMA+coagent+T-101 were added together during the melt grafting, method M-2 (**Fig. 4.39**, p.240). As a result, it is suggested that the coagent is both effective in trapping the PP macroradicals formed (by H-abstraction) such that the propagating radicals formed are highly reactive toward the desired monomer.

6.1.6 In the presence of the coagent DVB using different peroxides (T-101, T-29B90, DCP, and BPO), a very small amount of poly GMA and small extent of PP-degradation was measured over the whole temperature range (160°C – 200°C) (**Fig. 4.27A**, p.228). The GMA grafting degree for the peroxides used was high, even with the peroxide BPO which has a short half-life time, and this is due to the high rate of reaction in the DVB system. The effectiveness of peroxides in initiating the grafting reaction of GMA on PP in the presence of DVB was found to be especially at higher peroxide concentration in the order T-101 > DCP > T-29B90 > BPO, **Fig. 4.27A** (p.228) and **4.31** (p.232). When the weight ratio of DVB was fixed at 2/8 with respect to GMA (GMA = 12 %) (≅ 3.4 phr), the grafting degree decreased with increasing temperature (**Fig.4.27A**, p.229) and peroxide concentration for all peroxides **(Fig. 4.31**, p.232) used. Grafting in the presence of DVB was achieved at very low concentration of peroxides, but the use of higher concentrations (e.g. T-101) resulted not only in lower grafting levels **(Fig. 4.31)** but also higher level of DVB assisted crosslinking of PP (PP-

DVB-PP) reflected in lower MFI values than PP control and this became a dominant and unacceptable reaction (**Fig 4.29**, p.230) that should be avoided or minimised.

6.1.7 Examination of the kinetics of the grafting reaction in the presence of the coagents demonstrated that the rate of GMA-grafting in the coagent system was higher when compared to the grafting rate in their absence (**Fig. 4.38**, p.239). It was also observed that the presence of TRIS led to complete grafting reaction in shorter times compared to DVB. Almost 100 % of the GMA grafting in the TRIS system was achieved during the first two minutes of processing whereas, for the same time in the GMA/DVB system, the grafted-GMA was less than 40 %. Furthermore, the MFI of the processed PP in the GMA/DVB system decreased with processing time down to 70 % less than the virgin PP indicating a severe branching/crosslinking reaction (**Fig. 4.38**, p.239). This support the suggestion that DVB is more reactive towards PP macroradicals and formation of PP-DVB grafts or/and PP-DVB-PP crosslinks which occurs before the copolymerisation with GMA. In contrast, in the GMA/TRIS system, TRIS appears to be less reactive towards the PP-macroradicals but more reactive towards GMA and copolymerise with GMA before causing TRIS assisted PP cross linking.

6.1.8 The GMA grafting level in the presence of DVB or TRIS increased persistently with increasing of the initial GMA concentration (**Fig. 4.33**, p.234) and concentration of the coagent (**Fig. 4.35**, p. 236) but without any adverse effect on the formation of poly-GMA (poly-GMA level stayed very low). Although the concentration of poly-GMA formed is very small, it does increase slightly with processing time up to a maximum value of only 0.1 % (**Fig. 4.37**, p.238), whereas the poly-GMA concentration decreased to over 2 % in the conventional (without coagent) GMA grafting system.

6.1.9 Maleic anhydride (MA) could also be successfully grafted onto PP via melt free radical (peroxide) initiation and the results demonstrated that the effect of processing temperature in the PP/MA/T-101 (conventional) system was opposite with the PP/GMA/T-101 grafting system, i.e. for MA, increasing the temperature (160-200°C) resulted in a proportional increase in the grafting yield

(**Fig 5.13**, p.309) even though the overall grafting level was very low (grafting efficiency less than 8 %) and the desired grafting reaction was also accompanied by clear degradation of PP by chain scission (**Fig. 5.13**, p.309). Increasing the peroxide (T-101) concentration in the conventional system led to a proportional increase in the grafting level but with a parallel and significant increase in PP degradation via chain scission (**Fig. 5.14**, p.310). Even at a high concentration of the peroxide 0.01 molar ratio to MA (≈ 0.24 phr), the MA grafting degree did not exceed 1.3 % - that is less than 17 % of initial MA added ([MA]i = 8 %) due to low reactivity of MA towards PP with the MFI reaching to a value 6 g/10 min – that is 200 % change relative to MFI of the original PP illustrating the profound extent of polymer degradation (by chain scission) under these condition. Furthermore, an increase in the maleic anhydride initial concentration also resulted in a higher degree of chain scission indicated by the observed increased in MFI of the functionalised polypropylene (see **Fig. 5.15**, p.311). It was found that the peroxide T-29B90 has a negative effect under conditions of increase processing temperature (**Fig. 5.13,** p.309), higher concentration of peroxide (**Fig.5.14**, p.310) and initial MA level (**Fig. 5.16A**, p.312).

6.1.10 The addition of coagents (TRIS or DVB) to the system (PP+MA+coagent+ peroxide); using different peroxides (T-101, T-29B90, DCP, and BPO) resulted in higher grafting level and less polymer degradation (**Fig 5.19**, p.315). It was found that the use of peroxides with a shorter half life time ($t_{1/2}$) (e.g. T-29B90 and BPO) in the DVB grafting system resulted in lower grafting degree (even lower than the conventional system) especially at a higher temperature (200°C) (**Fig. 5.19**, p.315). The peroxide T-101 was found to be superior compared to the other peroxides examined here at all processing temperatures and the highest grafting degree was achieved at a temperature of 180°C. However, at 180°C the degradation of PP by chain scission occurred to a high extent as evidenced from a very high increase in MFI (**Fig. 5.19**, p.315). Similar trend with the conventional (PP/MA/T-101) system, the level of grafted-MA on PP in the coagent systems increased with increasing peroxide concentration (**Fig. 5.21**, p.317). Similar with the GMA grafting system in PP, the coagents DVB was superior to TRIS in enhancing the MA grafting level in the PP/DVB/MA/T-101 system the crosslinking reaction was more dominant as shown by its much lower MFI values (**Fig.5.21**, p.317).

6.1.11 The morphology, examined by SEM, of physical blend of PBT and PP at 20:80 w/w ratio showed that the disposed PBT phase was characterised by large spherical domains with clear and sharp interfacial boundaries (see **Fig.5.29a** and **5.30a**, pp. 326,327). When GMA and MA grafted PP was blended with PP in PP/*f*-PP/PBT blends (75:5:20 w/w %), a significant improvement in the dispersion of PBT phase was observed as shown from a much finer morphology which was attributed to the formation of a copolymer of PP-co-PBT through interfacial reactions of the grafted GMA (**Fig. 5.29b**) or MA groups (**Fig.5.29c**) in the PP phase with the carboxylic and hydroxyl end groups of PBT. The formation of such copolymer would then act to reduce the interfacial tension leading to the observed fine dispersion of PBT phase in the PP phase. The preliminary results also showed, based on morphology observation, that the PP-g-GMA_{TRIS} (prepared in the GMA+TRIS+T-101) and PP-g-GMA_{DVB} (prepared in the GMA+DVB+T-101) gave even more efficient compatibilising effect in PP-PBT blends compared to the effect of the corresponding PP-g-$GMA_{conventional}$ system (GMA+T-101, in the absence of coagent) (see **Fig. 5.29d** and **5.29e**). It was also found from SEM that the higher the GMA grafting level in the PP phase the finer was the dispersion of the PBT phase in PP (**Fig. 5.30 b,c,d**), which is much likely to be due to the higher extent of reaction between PP and PBT phases that took place during the reactive blending resulting in more PP-co-PBT copolymer formation at the interface. It was also found that the higher viscosity (lower MFI) of GMA functionalised PP, the more difficult was the dispersion of PBT in the higher viscosity polymer matrix (see **Fig. 5.30 c, e,** and **f**) resulting in coarse morphology.

6.2. Recommendations for Further Work

6.2.1 In this work, the use of reactive comonomers for promoting the otherwise very weak melt free radical grafting reactivity of glycidyl methacrylate (GMA) and maleic anhydride (MA) onto polypropylene (PP) was discussed. However, adding a reactive comonomer to a polymer–monomer grafting system will be beneficial only if it is capable of reacting more easily with the polymer free radicals and the resulting free radicals are able to copolymerize readily with the grafting monomer. TRIS or DVB were shown to be highly effective comonomers for grafting GMA and MA in PP. Other functional monomers on PP and other hydrocarbon polymers can be examined in the presence of these multifunctional comonomers and their effect on the balance between the grafting and the unwanted side reaction can be investigated.

6.2.2 Result from this work have shown that the GMA grafting reaction on NR and PP when using the peroxide T-29B90 were better than other peroxides (T-101, DCP, and BPO) at lower temperatures (<160°C). Whereas for the same chemical composition and processing conditions, grafting of MA on these polymer with T-29B90 resulted in more inferior grafting levels compared to other peroxides. Though the effect of the processing conditions and chemical composition on the grafting level and melt viscosity (MFI) has been investigated in some detail in this work and the characterisation of the GMA or MA modified polymers has been conducted using FTIR and differential solvent extraction, more work on the grafting mechanisms, microstructure of the grafts and the alteration of polymers need to be done to have a better understanding of the melt free radical grafting chemistry involved. The recommended work includes study of monomer reactivity ratio (r) of GMA and MA in copolymerisation with coagents DVB and TRIS, structural analysis of GMA or MA modified polymers in terms of grafting sequence of the monomer and the coagents, grafting structure, grafts distribution and mechanistic studies using model compounds in the absence (conventional) and presence of the coagents. This study would require the utilisation of high sensitivity analytical techniques, such as FT-NMR, DSC-XRD, and fluorescence spectroscopy to identify the length and the distribution of the grafts and their microstructure.

6.2.3 Due to time limitations, only a very preliminary work was conducted to examine the effect of the *f*-PP produced in this study in presence and absence of coagents on extent of compatibilising PP/*f*-PP/PBT blends by examining the morphology by SEM. The SEM results showed clearly the benefits in the blends in the presence of a small concentration (2.5 %) of the GMA modified polymer studied (in the order PP-g-GMA_{DVB} > PP-g-GMA_{TRIS} >> PP-g-$GMA_{conventional}$) (see **Fig. 5.29**, p.326). It would be important to examine in more detail the differences in compatibilising effect of the GMA functionalised PP without and with different coagents in PP-PBT blends and the differences such modification will impart on the thermal and mechanical properties using wide range of techniques including thermal analysis particularly by DMA. A further study on the relationship between the grafting structure of GMA modified PP and the compatibilisation effect with PBT will be very useful to screen the most suitable GMA or MA modified polymers for reactive blending and to get a better understanding of the nature of the interfacial reaction that occurs during the reactive blending step.

6.2.4 In this work the functionalisation of NR and PP with GMA and MA was carried out in a batch internal mixer. Due to its particular structure, the mixing chamber is not perfectly sealed. This may bring about complication when adding volatile liquid monomer such as GMA into the mixing chamber. The loss of GMA and MA during the reactive processing may be a reason for the overall low grafting efficiency. A further difficulty experienced when using the internal mixer for the compatibilisation of PBT with functionalised PP was due to the high processing temperatures (temperature setting 240°C) needed for PBT blending that the oxidation of the polymers can not be avoided at such a high temperature. It is suggested that both the melt grafting of GMA onto polymers and reactive blending of the functionalised-polymer with immiscible polymer blends is carried out in a twin screw extruder, which would be ideally suited for continuous production of reactively processed material and has a better handling of liquid reactants with specially designed barrel segment configuration that could provide better processing control.

References

1. G.H. Hu, J.J. Flat, and M. Lambla, *Chapter 1. Free-radical Grafting of Monomers onto Polymers by Reactive Extrusion: Principle and Applications*, in **Reactive Modifiers for Polymers**, Ed. S. Al-Malaika, Blackie Academic Professional, London (1997), 1-83.

2. J.M.J. Frechet, *Functional polymers: from plastic electronics to polymer-assisted therapeutics*, Prog. Polym. Sci., **30** (2005), 844–857.

3. G. Moad, *The synthesis of polyolefin graft copolymers by reactive extrusion*, Prog. Polym. Sci., **24** (1999), 81-142.

4. M. J. Yanjarappa and S. Sivaram, *Recent Development in the synthesis of functional poly(olefin)s*, Prog. Polym. Sci., **27** (2002), 1347-1398.

5. L.M. Robeson, Chapter 17: *Perspective in Polymer Blend Technology*, in **Polymer Blends Handbook**, Eds. L.A. Utracki, Kluwer Academic Publisher, London (2002), 1167-1200.

6. A. Ehrhardt, K. Miyazaki, Y. Sato, T. Hori, *Modified polypropylene fabrics and their metal ion sorption role in aqueous solution*, Appl. Surf. Sci., **252** (2005) 1070–1075

7. Y. Bondar, H. J. Kim, S. H. Yoon, Y. J. Lim, *Synthesis of cation-exchange adsorbent for anchoring metal ions by modification of poly(glycidyl methacrylate) chains grafted onto polypropylene fabric*, Rctv. Funct. Polym., **58** (2004), 43–51

8. M.R. Thomson, C. Tzoganakis, and G.L. Rempel, *Terminal Functionalisation of polypropylene via The Alder Ene Reaction*, Polym., **39** (1998), 327-334.

9. J. C. Brosse, I. Campistron, D. Derouet, A. EL Hamdaoi, S. Houdayer, D. Reyk, S. R. Gillier, *Chemical Modifications of Polydiene Elastomers: A Survey and Some Recent Results.* J. Appl. Polym. Sci., **78** (2000), 1461–1477.

10. R. Ohnishi, T. Fujimura, R. Tsunori, Y. Sugita, *A New Method for Producing High Melt Strength Poly(propylene) with a Reactive Extrusion*, Macromol. Mat. Eng., **290** (2005), 1227–1234.

11. Z. Jiruo, F. Ying, and C. Xinfang, *A new kind of material obtained by the mechanochemistry reaction modified CPE with maleic anhydride and styrene*, Mat. Let., **56** (2002), 543-545.

12. S. Zhang, A. R. Horrocks, *A review of flame retardant polypropylene fibres*, Prog. Polym. Sci. **28** (2003), 1517–1538

13. D. W. Jenkins and S.M. Hudson, *Review of Vinyl Graft Copolymerization Featuring Recent Advances toward Controlled Radical-Based Reactions and Illustrated with Chitin/Chitosan Trunk Polymers*, Chem. Rev. **101** (2001), 3245-3273

14. S. Krause, *Chapter 2 Polymer-Polymer Compatibility*, in **Polymer Blend**, vol.1 (eds. D.R. Paul and S. Newman), New York (1978), 15-113.

15. M. Weber, *Engineering Polymer Alloys by Reactive Extrusion*, Macromol. Symp. **181** (2002), 189–200

16. S. B. Brown, Chapter-5: *Reactive compatibilisation of polymer blends*, in **Polymer Blend Handbook**, Ed. L.A. Utracki, Kluwer Academic Publisher, London (2002), 339-415.

17. M. Xanthos, *Interfacial agents for multiphase polymer systems: Recent advances*, Polym. Eng. Sci., **28** (1988), 1392-1400.

18. M. Xanthos, M.W. Young, G. P. Kafwyannidis, D. N. Bikiaris, *Reactive Modification of Polyethylene Terephthalate With Polyepoxides*, Polym. Eng. Sci., **41** (2001), 543-555.

19. G.H. Hu, H. Cartier, L.F. Feng, B.G. Li, *Kinetics of the In Situ Polymerization and In Situ Compatibilization of Poly(propylene) and Polyamide 6 Blends*, J. Appl. Polym. Sci., **91** (2004), 1498–1504

20. T.K. Kang, Y. Kim, W.K. Lee, H.D. Park, W.J. Cho, and C.S. Ha, *Properties of Uncompatibilized and Compatibilized Poly(butylene terephthalate)–LLDPE Blends*, J. Appl. Polym. Sci., **72** (1999), 989–997.

21. J.K. Kim, S. Kim, and C.E. Park, *Compatibilisation mechanism of polymer blends with in situ compatibiliser*, *Polym.*, **38** (1997), 2155-2164.

22. Y.T. Shieh, T. N. Liao, F.C. Chang, *Reactive Compatibilization of PP/PBT Blends by a Mixture of PP- g-MA and Epoxy Resin*, J. Appl. Polym. Sci., **79** (2001), 2272–2285.

23. G.Hu, Y.Sun, and M. Lambla, *Effects of Processing Parameters on the in situ Compatibilisation of Polypropylene and Poly (Butylene Terephthalate) Blends by One-Step Reactive Extrusion*, J. Appl. Polym Sci., **61** (1996), 1039-1047.

24. X.H. Wang, H.X. Zhang, Z.G. Wang, and B.Z. Jiang, *Toughening of poly(butyleneterephthalate) with epoxidized ethylene propylenediene rubber*, Polym., **38** (1997), 1569-1572.

25. K. L. Borve, H. K. KotlarR, C.-G. Gustafson, *Polypropylene–Phenol Formaldehyde-Based Compatibilizers. I. Preparation and Characterization*, J. Appl. Polym. Sci., **75** (2000) 347–354.

26. K. L. Borve, H. K. KotlarR, C.-G. Gustafson, *Polypropylene–Phenol Formaldehyde-Based Compatibilizers. III. Application in PP/PBT and PP/PPE Blends*, J. Appl. Polym. Sci. **75** (2000), 361–370.

27. T. Vainio, H. Jukarainen, and J. Seppalla, *Compatibilization of Polypropylene/Poly(n-butylacrylate) Blend: Functionalization of the Poly(n-butylacrylate) Phase by Copolymerization*, J. Appl. Polym. Sci., **59** (1996), 2095-2105.

28. Y. Zhihui, Z. Yajie, Z. Xiaomin, Y. Jinghua, *Effect of compatibiliser PP-g-GMA on morphology and mechanical properties of PP/PC blends*, Polym., **39** (1998), 547-551.

29. M.J.Chung, L.W. Jang, J. H. Shim, J-S Yoon, *Preparation and Characterization of Maleic Anhydride-g-Polypropylene/Diamine-Modified Clay Nanocomposites*, J. Appl. Polym. Sci., **95** (2005), 307–311.

30. L. W. Jang, E. S. Kim, H. S. Kim, J-S.Yoon, *Preparation and Characterization of Polypropylene/Clay Nanocomposites with Polypropylene-graft-Maleic Anhydride*, J. Appl. Polym. Sci., **98** (2005), 1229–1234.

31. C. H. Hong, Y. B. Lee, J. W. Bae, J. Y. Jho,1 B. U. Nam, T. W. Hwang, *Preparation and Mechanical Properties of Polypropylene/Clay Nanocomposites for Automotive Parts Application*, J. Appl. Polym. Sci., **98** (2005), 427–433.

32. M. Diagne, M. Gueye, L. Vidal, A. Tidjani, *Thermal stability and fire retardant performance of photo-oxidized nanocomposites of polypropylene-graft-maleic anhydride/clay*, Polym. Deg. Stability, **89** (2005) 418-426.

33. E. Borsig, *Polypropylene derivatives*, J. Mat. Sci. Pure Appl. Chem., **A36** (1999), 1699-1715

34. A. Bhattacharyaa, B.N. Misra, *Grafting: a versatile means to modify polymers Techniques, factors and applications*, Prog. Polym. Sci., **29** (2004), 767–814.

35. G. Moad, D.H. Solomon, In **Comprehensive Polymer Science**: Eds. G.C. Eastmond, A. Ledwith, S. Russo, P. Sigwalt, London: Pergamon, 1989. p. 97.

36. Y. Minoura, M. Ueda, S. Mizunuma, M. Oba, *The reaction of polypropylene with maleic anhydride*, J. Appl. Polym. Sci., **13** (1969),1625–1640.

37. M. Lazár, L. Hrcková, U. Schulze, J. Pionteck, E. Borsig, *Grafting and Degradation Reactions at the Synthesis of Interpenetrating Polymer Networks in Situ from Polyethylene and Butyl Methacrylate*, J.Macromol. Sci. A:

Pure Appl. Chem. **A33** (1996), 261-273

38. L. Tan, J. Deng and W. Yang, *A facile approach to surface graft vinyl acetate onto polyolefin articles*, Polym. Adv. Technol., **15** (2004), 523–527

39. W. Yang, D. Yang, J. Hu, C. wang, S. Fu, *Dispersion copolymerisation of styrene and other vinyl monomers in polar solvents*, J. Polym. Sci. A: Polym. Chem., **39** (2001), 555-561.

40. Z.F. Zhou, N.C. Liu, H. Huang, *Reactivity of acrylonitrile-butadiene-styrene terpolymer grafted with long-chain unsaturated carboxylic acids*, Polymer (2004), 1-8

41. J. Zhao, J. Li, Y. Feng and J. Yin, *A novel approach to synthesis of functional CPVC and CPE or graft copolymers—in situ chlorinating graft*, Polym. Adv. Technol. **18** (2007), 822–828

42. C. Rosales, R. Perera, M. Ichaco, J. Gonzales, H. Rojas, A. Sanchez, A. D. Barios, *Grafting of polyethylenes by reactive extrusion I. Influence on the molecular structure*, J. Appl. Polym. Sci., **70** (1998), 161-176.

43. G. S. S. Rao, M. S. Choudhary, M. K. Naqvi and K. V. RAO, *Functionalisation of isotatctic Polypropylene with Acrylic acid in the melt Synthesis, Characterisation and Evaluation of Thermomechanical Properties*, Eur. Polym. J., **32** (1996), 695-700.

44. M. K. Razavi Aghjeh, H. Nazockdast, H. Assempour, *Parameters Affecting the Free-Radical Melt Grafting of Maleic Anhydride onto Linear Low-Density Polyethylene in an Internal Mixer*, J. Appl. Polym. Sci., **99** (2006), 141–149.

45. H. Cartier *and* G.H. Hu, *Plastification or Melting: A Critical Process for Free Radical Grafting in Screw Extruders*, Polym. Eng. Sci., **38** (1998), 177-185.

46. X.M. Xie, N.H. Chen, B.H. Guo, and S. Li, *Study of multi monomer melt grafting onto polypropylene in an extruder*, Polym. Inter., **49** (2000), 1677-1683.

47. J.M.G. Martinez, A.G. Cofrades, O. Laguna, S. Areso, E.P. Collar, *Influence of reactant concentration and reaction time in the chemical modification process of polypropylene by p-phenylen-bis-maleamic acid in the melt*, Eur. Polym. J., **36** (2000) 2253-2263.

48. H. R. Z. Sheshkali, H. Assempour, H. Nazockdast, *Parameters Affecting the Grafting Reaction and Side Reactions Involved in the Free-Radical Melt Grafting of Maleic Anhydride onto High-Density Polyethylene*, J. Appl. Polym. Sci., **105** (2007), 1869–1881

49. J.M.G. Martinez, O.Laguna, E.P. Collar, *Role of reaction time in batch process modification of atactic polypropylene by anhydride in melt*, J. Appl. Polym. Sci., **65** (1997), 1333-1 347.

50. Y. Guldogan, S. Egri, Z. M. O. Rzaev, E. Piskin, *Comparison of Maleic Anhydride Grafting onto Powder and Granular Polypropylene in the Melt by Reactive Extrusion*, J. Appl. Polym. Sci., **92** (2004), 3675–3684.

51. D.Shi, J. Yang, Z. Yao, Y. wang, H. Huang, W. Jing, J. Yin. G. Costa, *Functionalisation of isotactic polypropylene with maleic anhydride by reactive extrusion: Mechanism of melt grafting*, Polym., **42** (2001), 5549-5557.

52. M. Ratzsch, M.Arnold, E. Borsig, H. Bukha, N. Reichelt, *Radical Reaction on Polypropylene in the Solid State*, Prog. Polym. Sci., **27** (2002), 1195-1285.

53. A.H. Hogt, J. Meijer and J. Jelenic, *Modification of polypropylene by organic peroxides*, in **Reactive Modifiers for Polymer**, Ed. S.Al-Malaika, Blackie Academic & Professional, London (1997), 84-132.

54. O.L. Magelli and C.S. Sheppard, in: **Organic Peroxide**, Ed. S. Daniel, Wiley Interscience, Newyork, Chapter I, Volume I, 1-104

55. P. Dokolas, G. G. Qiao, D. H. Solomon, *Graft Copolymerization Studies. III. Methyl Methacrylate onto*

Polypropylene and Polyethylene Terephthalate, J. Appl. Polym. Sci., **83** (2002), 898–915.

56. S. Ranganathan, W. E. Baker, K. E. Russel, R. A. Whitney, *Peroxide Initiated Maleic Anhydride Grafting: Structural Studies on an Ester-Containing Copolymer and Related Substrates*, J. Polym. Sci.: Part A: Polym. Chem., **37** (1999), 1609–1618.

57. S. Knaus, L. S. Lukacic , Robert Liska, R. Saf, *Peroxide-initiated grafting of maleimides onto hydrocarbon substrates*, Eur. Polym. J., **41** (2005) 2240–2254.

58. H. Xie, M. Seay, K. Oliphant, and W.E. Baker, *Search for nonoxidative, hydrogen abstraction initiators useful for melt grafting process*, J. Appl. Polym Sci., **48** (1993), 1199-1208.

59. S.S. Pesetski, B. Jurkowski, Y.M. Krivoguz, and K. Kelar, *Free radical itaconic acid onto LDPE by reactive extrusion: I. Effect of initiator solubility*, Polym., **42** (2001) 469-475.

60. J.S. Parent, M. Tripp, and J. Dupont, *Selectivity of Peroxide-Initiated Graft Modification of Ethylene Copolymers*, Polym. Eng. Sci., **43** (2003), 234-242.

61. M. Saule, L. Moine, M. D. Castaing, B. Maillard, *Polymer Communication: Induced decomposition of an acrylic peroxide for chemical modification of polypropylene*, Polym., **45** (2004) 5749–5754.

62. S. S. Pesetskii, B. Jurkowski, O. A. Makarenko, *Free Radical Grafting of Itaconic Acid and Glycidyl Methacrylate onto PP Initiated by Organic Peroxides*, J. Appl. Polym. Sci., **86** (2002), 64–72.

63. G. David, J.J. Robin, and B. Boutevin, *Synthesis of carboxy-telechelic oligostyrene by dead-end polymerization: Evaluation of primary radical termination by kinetic study and kinetic simulation model*, J. Polym. Sci: Polym. Chem., **39** (2001), 2740.

64. W.K Busfield, I.D. Jenkins, M.J. Monteiro, *Initiation mechanism in copolymerisation: Reaction of tert-butoxyl radicals with comonomers ethyl vinyl ether and methyl methacrylate*, J. Polymer. Sci. A. Polym. Chem., **35** (1997) 263-270.

65. D. Bednarek, G. Moad, E. Rizzardo, D.H. Solomon, *End groups of poly(methyl methacrylate-co-styrene) prepared with tert-butoxy, methyl and/or phenyl radical initiation; effects of solvent, monomer composition and conversion*, Macromol., **21** (1988), 1522-1528.

66. S. Knaus, L. Spoljaric-Lukacic, R. Liska, R. Saf, *Peroxide-initiated grafting of maleimides onto hydrocarbon substrates*, Eur. Polym. J., **41** (2005), 2240–2254

67. E.S. Huyser and C.J. Bredeweg, *Induced decomposition of di-tert-butyl peroxide in primary and secondary alcohols*, J. Am. Chem. Soc., **86** (1964), 2401-2405.

68. S. Beuenman, M. Buback, T.P. Davies, R.G. Gilbert, R.A. Hutchinson, O.F. Olaj, G.T. Russel, J. Schweer, A.M. van Herk, *Critically evaluated rate coefficient for free radical polymerisation. 2. Propagation rate coefficient for methyl methacrylate*, Macromol Chem Phys, **198** (1997), 1545-1560.

69. S. Ranganathan, W. E. Baker, K. E. Russel, R. A. Whitney, *Peroxide-Initiated Grafting of Maleic Anhydride onto Linear and Branched Hydrocarbons*, J. Polym. Sci. A: Polym. Chem., **37** (1999), 3817–3825

70. J.B. Wong Sing, W.E. Baker, K.E. Russell, *Kinetics and mechanism of grafting of 2-(dimethylamino)ethyl methacrylate onto hydrocarbon substrates*, J. Polym. Sci. A: Polym. Chem., **33** (1995) 633-642.

71. P. Dokolas, M.G. Looney, S. Musgrave, S. Poon, D.H. Solomon, *Graft copolymerisation studies Part 1. Model related to polyolefins*, Polymer **41** (2000), 3137-3145.

72. M. Aglietto, R. Bertani, G. Ruggeri: and A. L. Segreg, *Functionalization of Polyolefins. Determination of the Structure of Functional Groups Attached to Polyethylene by Free Radical Reactions*, Macromole., **23** (1990), 1928-1933.

73. A.V. Machado, M. van Duin, J.A. Covas, *Monitoring polyolefin modification along the axis of twin screw extruder. II. Maleic anhydride grafting*, J. Polym. Sci. A: Polym. Chem., **38** (2000), 3919-3932.

74. A.V. Machado, J.A. Covas, M. van Duin, *Effect of polyolefin structure on maleic anhydride grafting*, Polym., **42** (2001), 3649-3655

75. A. V. Machado, J. A. Covas, M. V. Duin, *A Study of Grafting Reactions During Processing of Polyolefins*, Adv. Polym. Techn., **23** (2004), 196-210.

76. H.L. Huang, Z.H. Yao, Y. Wang, D.A. Shi, J.H. Yin, *Morphology, structure and rheological property of linear low density polyethylene grafted with acrylic acid*, J. Appl. Polym. Sci., **80** (2001), 2538-2544.

77. D. C. Clark, W. E. Baker, K. E. Russell, R. A. Whitney, *Dual Monomer Grafting of Styrene and Maleic Anhydride onto Model Hydrocarbon Substrates*, J. Polym. Sci. A: Polym. Chem., **38** (2000), 2456–2468.

78. J. H. Trivedi, N. K. Patel, and H. C. Trivedi, *Grafting of Vinyl Monomers onto Sodium Salt of Partially Carboxymethylated Guar Gum: Comparison of Their Reactivity*, Polym. Plast. Tech. Eng., **44** (2005), 407–425

79. P. Chandranupap, S. Bhattacharya, *Reactive Processing of Polyolefins with MAH and GMA in the Presence of Various Additives*, J. Appl. Polym. Sci. **78** (2000) 2405–2415.

80. S.S. Sengupta, J. S. Parent, J. K. Mclean, *Radical-Mediated Modification of Polypropylene: Selective Grafting via Polyallyl Coagents*, J. Polym. Sci. A: Polym. Chem., **43** (2005), 4882–4893

81. A. M. Atta, R. A. M. El-Ghazawy, *Effect of chemical crosslinking of swelling parameters of modified poly(vynil alcohol) hydrogel*, Int. J. Polym. Mat., 52 (2003), 623–636

82. A. C. Patel, R. B. Brahmbhatt, P.V.C. Rao, K.V. Rao, S. Devi, *Solid phase grafting of various monomers on hydroperoxidized Polypropylene*, Eur. Polym. J., 36 (2000), 2477-2484

83. G. Moad and D.H. Solomon, ***The chemistry of free radical polymerisation***, Oxford, Pergamon Press (1995).

84. M. Buback, H. Frautndorf, P. Vana, *Initiation of Free-Radical Polymerization by Peroxypivalates Studied by Electrospray Ionization Mass Spectrometry*, J. Polym. Sci. A: Polym. Chem. **42** (2004), 4266–4275

85. G. S. Srinivasa Rao and R. C. Jain, *Graft Copolymerisation of Polypropylene Copolymer with Maleic Anhydride: Effect of Grafting on Thermal, Mechanical Properties, and Paintability*, Polym. Plast. Techn. Eng., **41** (2002), 933–950

86. S. Camara, B.C. Gilbert, R. J. Meier, M. van Duin, A. C. Whitwood, *EPR studies of peroxide decomposition, radical formation and reactions relevant to cross-linking and grafting in polyolefins*, Polymer **47** (2006) 4683–4693

87. A. Sipos, J. McCarthy, K.E. Russell, *Kinetic study of grafting of maleic anhydride to hydrocarbon substrates*, J. Polym. Sci. A: Polym. Chem., **27** (1989), 3353–3362.

88. J.B. Wong Shing, W.E. Baker, K.E. Russell, and R.A. Whitney, *Effect of reaction condition on the grafting of 2-(dimethylamino) ethyl methacrylate onto hydrocarbon substrates*, J. Polym. Sci. A: Polym. Chem., **32** (1994), 1691-1702.

89. S.H.P. Bettini and J.A.M. Agnelli, *Grafting of maleic anhydride onto poly propylene by reactive processing. I. Effect of rotor speed and reaction time*, J. Appl. Polym. Sci., **74** (1999), 256-263.

90. D. Chang and J. L. White, *Experimental Study of Maleation of Polypropylene in Various Twin-Screw Extruder Systems*, J. Appl. Polym. Sci., **90** (2003), 1755–1764

91. R. Greco, G. Manglio, P.V. Musto, *Bulk Functionalization of Ethylene–Propylene Copolymer. 1. Influence of Temperature and Processing on the Reaction Kinetics*. J. Appl. Polym. Sci., **33** (1987), 2513–2527.

92. H.E.H. Meijer, L. E. Govaert, *Mechanical performance of polymer systems: The relation between structure and properties*, Prog. Polym. Sci. 30 (2005) 915–938

93. W. Heinen, H.W. Rossenmoller, C.B. Wenzel, H.J.M. de Groot, J. Lugtenburg, and M. van Duin, *^{13}C NMR study of the grafting of maleic anhydride onto polyethylene, polypropylene, and ethylene-propylene copolymers*, Macromolecules, **29** (1996), 1151-1157.

94. E. Niki and Y. Kamiya, *Reactivity of polystyrene and polypropylene toward tert-butoxy radical*, J. Org. Chem., **38** (1973) 1403-1406.

95. B. De Roover, M. Sclavons, V. Carlier, J. Devaux, R. Legras, A. Momtaz, *Molecular characterization of maleic anhydride functionalized polypropylene*. J. Polym. Sci. A: Polym. Chem., **33** (1995), 829-842.

96. S. Al-Malaika, *Chapter 6: Reactive antioxidant for polymers*, in **Reactive Modifiers for Polymers** (Ed. S. Al-Malaika), Blackie Academy &Proffesional, London (1997), 266-302.

97. S. Al-Malaika and N. Suharty, *Reactive processing of polymers: mechanism of grafting reactions of functional antioxidants on polyolefins in the presence of coagent*, Polymer degradation & Stability, **49** (1995), 77-89.

98. **Al-Malaika Polymer in Advance**

99. W.K. Busfield In: J. Brandrup, E.H. Immergut, editors. Polymer Handbook, 3rd edition. New York: Wiley, 1989. p. 295.

100. K.E. Russell, *Grafting of maleic anhydride to hydrocarbons below the ceiling temperature*, J. Polym. Sci., A: Polym. Chem., **33** (1995), 555-561.

101. K.E. Oliphant, K.E. Russell, W.E. Baker, *Melt grafting of a basic monomer onto polyethylene in a twin screw extruder: reaction kinetics*, Polymer, **36** (1995), 1597-1603.

102. K.E. Russel, *Free radical graft polymerization and copolymerisation at higher temperature*, Prog. Polym. Sci., **27** (2002), 1007-1038.

103. F. Tang, E.S. Huyser, *Thermal decomposition of bifunctional peroxides*, J. Org. Chem., **42** (1977), 2160–2163.

104. G. Moad, E. Rizzardo, D.H. Solomon, A.L.J. Beckwith, *absolute rate constants for radical-monomer reactions. The nitroxide method*, Polym. Bull., **29** (1992), 647-652.

105. T. Zytowski and H. Fischer, *Absolute rate constant and Arrhenius parameter for the addition of methyl radical to unsaturated compounds: The methyl affinities revisited*, J. Am. Chem. Soc., **119** (1997), 12869–12878.

106. D.V. Avila, C.E. Brown, K.U. Ingold, J. Lusztyk, *Solvent effect on the competitive β-scission and hydrogen atom abstraction reaction of the cumyloxyl radical. Resolution of a long-standing problem*, J. Am. Chem. Soc., **115** (1993), 466-470.

107. S. Al-Malaika, *Chapter 1. The Good, The Bad and The Ugly in The Science and Technology of Antioxidant Grafting on Polymer*, in **Chemistry and Technology of Polymer Additives**, Eds. S. Al-Malaika, A. Golovay, C.A. Wilkie, 1-20.

108. N.G. Gaylord, M. Mehta, *Role of homopolymerisation in the peroxide-catalysed reaction of maleic anhydride and polyethylene in the absence of solvent*, J. Polym. Sci. Lett. Ed., **20** (1982), 481-486.

109. M. Y. Pedram, H. Vega, and R. Quijada, *Melt functionalisation with methyl esters of itaconic acid*, Polymer **42** (2001), 4751-4758.

110. Q. Shi, L. Zhu, C. Cai, J. Yin, G. Costa, *Kinetics Study on Melt Grafting Copolymerization of LLDPE with Acid Monomers Using Reactive Extrusion Method*, J. Appl. Polym. Sci., 101 (2006), 4301–4312

111. E. T. Kang, K. G. Neoh, J. L. Shi, K. L. Tan, D. J. Liaw, *Surface Modification of Polymers for Adhesion*

Enhancement, Polym. Adv. Technol. 10 (1999), 20-29

112. N. C. Liu, H.Q. Xie, and W.E. Baker, *Comparison of the effectiveness of different basic functional groups for the reactive compatibilisation of polymer blends*, Polym., **34** (1993), 4680-4687.

113. N.C. Liu and W.E. Baker, *Basic Functionalisation of Polypropylene and The Role of Interfacial Chemical Bonding in Its Toughening*, Polym., **35** (1994), 988-994.

114. Alain Guyot, *Direct and Indirect Functionalization of Polypropylene*, Polym. Adv. Tech., 7 (1996), 61-66

115. B. Lu and T. C. Chung, *Synthesis of Maleic Anhydride Grafted Polyethylene and Polypropylene, with Controlled Molecular Structures*, J. Polym. Sci. A: Polym. Chem., **38** (2000), 1337–1343.

116. T.C. Chung, *Maleic Anhydride Modified Polypropylene with Controllable Molecular Structure: New Synthetic Route via Borane-Terminated Polypropylene*, Macromol., **31** (1998), 5943–5946.

117. B. Lu and T. C. Chung, *New Maleic Anhydride Modified PP Copolymers with Block Structure: Synthesis and Application in PP/Polyamide Reactive Blends*, Macromol., **32** (1999), 2525-2533.

118. H. Huang, N. C. Liu, *Nondegradative Melt Functionalization of Polypropylene with Glycidyl Methacrylate*, J. Appl. Polym. Sci., **67** (1998), 1957–1963.

119. Y.J. Sun, G.H. Hu and M. Lambla, *Free radical grafting of glycidyl methacrylate onto polypropylene*, Angew. Macromol. Chem., **229** (1995), 1-13.

120. Y.J. Sun, G.H. Hu and M. Lambla, *Free radical grafting of glycidyl methacrylate onto polypropylene in a Co-Rotating Twin Screw Extruder*, J. Appl. Polym. Sci., **57** (1995), 1043–1054.

121. Z. Yin, Y. Zhang, X. Zhang, J. Yin, *Isothermal Crystallization of PP-g-GMA Copolymer*, J. Appl. Polym. Sci., **63** (1997), 1565–1569.

122. Y. Pan, J. Ruan and D Zhou, *Solid-Phase Grafting of Glycidyl Methacrylate onto Polypropylene*, J. Appl. Polym. Sci, **65** (1997), 1905–1912.

123. G.H. Hu and H. Cartier, *Styrene-Assisted melt free radical grafting of glycidyl methacrylate onto propylene*, J. Polym. Sci. A: Polym. Chem., **36** (1998), 1053-1063.

124. Hanwen Xiao, Fengyuan Yu, Ying Yu, Shiqiang Huang, *Grafting of Glycidyl Methylacrylate onto Chlorinated Polypropylene and its Bonding to Aluminum Flake*, J. Appl. Polym. Sci., 104 (2007), 2515–2521

125. R.R. Galluci, R.C. Going, *Preparation and reaction of epoxy-modified polyethylene*, J. Appl. Polym. Sci., **27** (1982), 425-437.

126. H. Cartier and G.H. Hu, *Styrene-assisted free radical grafting of glycidyl methacrylate onto polyethylene in the melt*, J. Polym. Sci. Part A: Polym. Chem., **36** (1998), 2763-2774.

127. X. Zhang, Z. Yin, L. Li, J. Yin, *Grafting of glycidyl methacrylate onto ethylene-propylene copolymer: preparation and characterisation*, J. Appl. Polym Sci., **61** (1996), 2253-2257.

128. G.H. Hu and H. Cartier, *Styrene-Assisted melt free radical grafting of glycidyl methacrylate onto an ethylene and propylene rubber*, J. Appl. Polym. Sci., **71** (1999), 125-133.

129. S. Al-Malaika and W. Kong, *Reactive processing of polymers: Melt Grafting of glycidyl methacrylate on ethylene-propylene copolymer in the presence of a coagent*, J. Appl. Polym Sci., **79** (2001), 1401-1415.

130. S. Al-Malaika and W. Kong, *Reactive processing of polymers: Functionalisation of ethylene-propylene diene terpolymer (EPDM) in the presence an absence of coagent and effect of functionalised EPDM on compatibilisation of poly (ethylene terephathalate)/EPDM blends*, Polym. Degrad. Stab., **90** (2005), 197-210.

131. C. D. Cordella, N. S. M. Cardozo, R.B. Neto, R.S. Mauler, *Functionalization of Styrene–Butadiene–Styrene (SBS) Triblock Copolymer with Glycidyl Methacrylate (GMA)*, J. Appl. Polym. Sci., **87** (2003), 2074–2079.

132. B. Wong and W.E. Baker, *Melt rheology of graft modified polypropylene*, Polym., **38** (1997), 2781-2789.

133. G.H. Hu, Y-J. Sun, M. Lambla, *Devolatilisation: A critical sequential operation for in-situ compatibilisation of immiscible polymer blends by one step reactive extrusion*, Polym. Eng. Sci., **36** (1996), 676–684.

134. W. Kong, *Reactive processing methods for functionalisation of polymers and in-situ compatibilisation of poly (ethylene terephthalate) based blends*, PhD Thesis, Aston University, 2001.

135. L.F. Chen, B. Wong, W.E. Baker, *Melt grafting of glycidyl methacrylate onto propylene and reactive compatibilisation of rubber toughened polypropylene*, Polym. Eng. Sci., **36** (1996), 1594-1607.

136. T. Vainio, G. H. Hu, M. Lambla, and J. seppala, *Functionalised Polypropylene Prepared by Melt Free Radical Grafting of Low Volatile Oxazoline and Its Potential in Compatibilisation of PP/PBT Blends*, J. Appl. Polym. Sci., **61** (1996), 843-852.

137. T. Vainio, G.H. Hu, M. Lambla, J. Seppala, *Functionalization of Polypropylene with Oxazoline and Reactive Blending of PP with PBT in a Corotating Twin-Screw Extruder*, J. Appl. Polym. Sci., **63** (1997), 883–894.

138. S. AL-Malaika and K. Artus, *Chemical Modification of Polymer Blends by Reactive Processing: In Situ Reactions of Interlinking Agents in PS/EPDM Blends Polymer*, J. Appl. Polym. Sci., **69** (1998), 1933–1951.

139. D. Graebling, *Synthesis of Branched Polypropylene by a Reactive Extrusion Process*, Macromol., **35** (2002), 4602-4610

140. S. Buniran, *Compatibilisation and Stabilisation of Immiscible Polymer Blends by Reactive Processing*, PhD Thesis, Aston University (1998).

141. F. Pazzagli and M. Pracella, *Reactive compatibilisation of polyolefin/PET blends by grafting with glycidyl methacrylate*, Macromol. Symp. **149** (2000), 225–230.

142. N. Torres, J. J. Robin, and B. Boutevin, *Functionalization of high-density polyethylene in the molten state by glycidyl methacrylate grafting*, J. Appl. Polym. Sci., **81** (2001), 581-590.

143. Q. Wei, D.Chionna, E. Galoppini, Mariano Pracella, *Functionalization of LDPE by Melt Grafting with Glycidyl Methacrylate and Reactive Blending with Polyamide-6*, Macromol. Chem. Phys., **204** (2003), 1123-1133.

144. I. Pesneau, M. F. Champagne, M. A. Huneault, *Glycidyl Methacrylate–Grafted Linear Low-Density Polyethylene Fabrication and Application for Polyester/Polyethylene Bonding*, J. Appl. Polym. Sci., **91** (2004), 3180–3191

145. B.C. Trivedi, B.M. Culbertson, *Chapter 11 Graft Copolymers*, in **Maleic Anhydride**, Plenum Press, New York (1982), 459–476.

146. G. Samay, T. Nagy, J.L. White, *Grafting maleic anhydride and comonomers onto polyethylene*, J. Appl Polym Sci **56** (1995), 1423

147. M. van Duin, *Grafting of Polyolefins with Maleic Anhydride: Alchemy or Technology?*, Macromol. Symp., **202** (2003), 1-10.

148. D. C. Clark, W. E. Baker and R. A. Whitney, *Maleic Anhydride onto Polyethylene: Effect of Polyethylene Microstructure*, J. Appl. Polym.Sci., **79** (2001), 96–107.

149. C. Li, Y. Zhang, Y.Zhang, *Melt grafting of maleic anhydride onto low density polyethelene/polypropylene blends*, Polym. Test., **22** (2003), 191-195.

150. N.G. Gaylord and R. Mehta, V. Kumar, and M. Tazi, *High density polyethylene-g-maleic anhydride*

preparation in presence of electron donors, J. Appl. Polym. Sci., **38** (1989), 359-371.

151. N.G. Gaylord and R. Mehta, *Radical catalyst homopolymerisation of maleic anhydride in the presence of polar organic compounds*, J. Polym. Sci. Part A Polym Chem., **26** (1988), 1189-1198.

152. N.G. Gaylord, R. Mehta, D.R. Mohan, V. Kumar, *Maleation of linear low-density polyethylene by reactive processing*, J. Appl. Polym. Sci., **44** (1992), 1941–1949.

153. N.G. Gaylord, R. Mehta, N. Mehta. *Degradation and cross linking ethylene-propylene copolymer rubber on reaction with maleic anhydride and/or peroxides*, J. Appl. Polym. Sci., **33** (1987), 2549–2558.

154. C.H. Wu, A.C. Su, *Suppresion of side reactions during melt functionalisation of ethylene-propylene rubber*, Polym., **33** (1992), 1987–1992.

155. N.G. Gaylord, M.K. Mishra, *Non degradative reaction of maleic anhydride and molten polypropylene in the presence of peroxides*, J. Polym. Sci. Polym. Lett. Ed., **23** (1983), 23–30.

156. A. R. Oromehie, S. A. Hashemi, I. G. Meldrum and D. N. Waters, *Functionalisation of Polypropylene with Maleic Anhydride and Acrylic Acid for Compatibilising Blends of Polypropylene with Poly(ethylene terephthalate)*, Polym. Int. **42** (1997) 117-120

157. E. Passaglia, S. Ghetti, F. Picchiconi and G. Ruggeri, *Grafting of diethyl maleate and maleic anhydride onto styrene-b-(ethylene-co-1-butene)-b-styren triblock copolymer (SEBS)*, Polymer **41** (2000), 4389-4400.

158. R. Zhang, Y. Zhu, J. Zhang, W. Jiang, J. Yin, *Effect of the Initial Maleic Anhydride Content on the Grafting of Maleic Anhydride onto Isotactic Polypropylene*, J. Polym. Sci. A: Polym. Chem., **43** (2005) 5529–5534.

159. W. Qiu, T. Endo, T. Hirotsu, *A novel technique for preparing of maleic anhydride grafted polyolefins*, Eur. Polym. J., **41** (2005), 1979-1984.

160. W. Qiu and T. Hirotsu, *A New Method to Prepare Maleic Anhydride Grafted Poly(propylene)*, Macromol. Chem. Phys., **206** (2005), 2470–2482.

161. Q. Dong, Y. Liu, *Styrene-Assisted Free-Radical Graft Copolymerization of Maleic Anhydride onto Polypropylene in Supercritical Carbon Dioxide*, J. Appl. Polym. Sci. **90** (2003), 853–860.

162. B. G. Soares, R. S. C. Colombaretti, *Melt Functionalization of EVA Copolymers with Maleic Anhydride*, J. Appl. Polym. Sci., **72** (1999) 1799–1806.

163. S.J. Kim, C.J. Kang, S.R. Chowdhury, W.J. Cho, C.S. Ha, *Reactive Compatibilization of the Poly(butyleneterephtalate) –EVA Blend by Maleic Anhydride. II. Correlations Among Gel Contents, Grafting Yields, and Mechanical Properties*, J. Appl. Polym. Sci. **89** (2003) 1305–1310.

164. O.P. Grigoryepa, J.K. Korcis, *Melt grafting of maleic anhydride onto an ethylene propylene diene terpolymer (EPDM)*, Eur. Polym. J., **36** (2000), 1419-1429.

165. R. Qi, J. Qian, Z. Chen, X. Jin, C. Zhou, *Modification of Acrylonitrile–Butadiene–Styrene Terpolymer by Graft Copolymerization with Maleic Anhydride in the Melt. II. Properties and Phase Behavior*, J. Appl. Polym. Sci., **91** (2004), 2834–2839.

166. H. M. Wilhelm, M. I. Felisberti, *Bulk Modification of Styrene–Butadiene–Styrene Triblock Copolymer with Maleic Anhydride*, J. Appl. Polym. Sci., **83** (2002), 2953–2960.

167. C. Nanakson, A. Kaesaman, and P. Supasanthitikul, *The grafting of maleic anhydride onto natural rubber*, Polym. Test., **23** (2004), 35-41

168. J. Saelao and P. Phinyocheep, *Influence of Styrene on Grafting Efficiency of Maleic Anhydride onto Natural Rubber*, J. Appl. Polym. Sci., **95** (2005), 28–38.

169. A. K. Naskar, S. K. De, A. K. Bhowmick, *Thermoplastic Elastomeric Composition based on Maleic Anhydride–Grafted Ground Rubber Tyre*, J. Appl. Polym. Sci., **84** (2002), 370–378.

170. B.C. Trivedi, B.M. Culbertson, *Chapter 3 Reactions of Functional Groups*, in **Maleic Anhydride**, Plenum Press, New York (1982), 41–146.

171. Y. Zhang, Y. Huang, K. Mai, *Crystallization and Dynamic Mechanical Properties of Polypropylene/Polystyrene Blends Modified with Maleic Anhydride and Styrene*, J. Appl. Polym. Sci., **96** (2005), 2038–2045.

172. C.P. Papadopoulou and N.K. Kalfoglou, *Comparison of compatibilizer effectiveness for PET/PP blends: their mechanical, thermal and morphology characterization*, Polym., **41** (2000), 2543–2555.

173. J. D. Tucker, S. Lee *and* R. L. Einsporn, *A Study of the Effect of PP-g-MA and SEBS-g-MA on the Mechanical and Morphological Properties of Polypropylene/Nylon 6 Blends*, Polym. Eng. Sci., **40** (2000), 2577-2589.

174. D. Wang, C. A. Wilkie, *In-situ reactive blending to prepare polystyrene–clay and polypropylene–clay nanocomposites*, Polym. Degrad. Stab. **80** (2003) 171–182.

175. S. Su, D.D. Jiang, C.A. Wilkie, *Poly(methyl methacrylate), polypropylene and polyethylene nanocomposite formation by melt blending using novel polymerically-modified clays*, Polym. Degrad. Stab., **83** (2004) 321–331.

176. J. Zhang, P. J. Cole, U. Nagpal, C. W. Macosko, *Direct correlation between adhesion promotion and coupling reaction at immiscible polymer-polymer interfaces*, J. Adhes., **82** (2006), 887–902

177. B. De Roover, J. Devaux, and R. Legras, *Maleic Anhydride Homopolymerization during Melt Functionalization of Isotactic Polypropylene*, J. Polym. Sci. A Polym. Chem., **34** (1996), 1195-1202.

178. M. Sclavons, V. Carlier, B. De Roover, P. Fanquinet, J. Devaux,R. Legras, *The anhydride content of some commercial PP-g-MA: FTIR and titration*, J. Appl. Polym. Sci., **62** (1996), 1205-1210.

179. W. Heinen, S.W. Erkens, M. van Duin, J. Lugtenburg, *Model Compounds and ^{13}C NMR Increments for the Characterization of Maleic Anhydride-Grafted Polyolefins*, J. Polym. Sci: A Polym. Chem., **37**(1999), 4368-4385

180. L. Yang, F. Zhang, T. Endo, T. Hirotsu, *Structural characterisation of maleic anhydride grafted polyethylene by ^{13}C NMR spectroscopy*, Polym., **43** (2002), 2591-2594.

181. J.M.G. Martinez, O. Laguna, E.P. Collar., *Chemical modification of polypropylene by maleic anhydride: Influence of stereospecificity and process condition*, J. Appl. Polym Sci., **68** (1997), 483-495.

182. S.H.P. Bettini and J.A.M. Agnelli, *Grafting of maleic anhydride onto poly propylene by reactive processing. I. Effect of maleic anhydride concentration on the reaction*, J. Appl. Polym. Sci., **74** (1999), 247-255.

183. S. H. P. Bettini, J. A. M. Agnelli, *Grafting of Maleic Anhydride onto Polypropylene by Reactive Extrusion*, J. Appl. Polym. Sci., **85** (2002), 2706–2717.

184. N.G. Gaylord, M. Martan, A.B. Deshpande, *Donor-acceptor in copolymerisation. LVIII. Alternating diene-dienophile copolymers. 12. Structure of Furan-maleic anhydride copolymer prepared from the monomer and the Diels-Alder*, J. Polym. Sci. Polym. Chem., **16** (1978) 1527-1537.

185. Z. Song and W.E. Baker, *Melt grafting of tert-Butylaminoethyl methacrylate onto polyethylene*, Polymer, **33** (1992), 3266-3273.

186. G.H. Hu, J.J. Flat, M. Lambla, *Concept of nano reactor for the control of the selectivity of the free radical grafting of maleic anhydride onto polypropylene in the melt*, Makromol. Chem. Macromol. Symp., **75** (1993), 137–157.

187. Y. Li, X.M. Xie and B.H. Guo, *Study on styrene-assisted melt free-radical grafting of maleic anhydride onto polypropylene*, Polymer, **42** (2001), 3419-3425

188. N.C. Liu and W.E. Baker, Chapter 4; *Modification of polymer melts by oxazolines and their use for interfacial coupling reactions with other functional polymers*, in **Reactive modifiers for Polymers** (Ed. S. Al-Malaika), Blackie Academic & Professional, London (1997), 163-193.

189. N.C. Liu, W.E. Baker, and K.E. Russel, *Functionalisation of polyethylene and their use in reactive blending*, J. Appl. Polym. Sci., **41** (1990), 2285-2300.

190. M. G. Oliveira, A. C. O. Gomes, M. S. M. Almeida, B.G. Soares, *Reactive Compatibilization of NBR/EPDM Blends by the Combination of Mercapto and Oxazoline Groups*, Macromol. Chem. Phys., **205** (2004), 465–475

191. U. Antilla, C. Vocke and J. Seppala, *Functionalisation of polyolefins and elastomer with oxazoline compound*, J. Appl. Polym. Sci., **72** (1999), 877-885.

192. C. Vocke, U. Anttila, M. Heino, P. Hietaoja, J. Seppala, *Use of Oxazoline Functionalized Polyolefins and Elastomers as Compatibilizers for Thermoplastic Blends*, J. Appl. Polym. Sci., **70** (1998), 1923–1930.

193. B. G. Soares, M.S.M. Almeida, P.I.C. Guimaraes, *The reactive compatibilization of NBR/EVA blends with oxazoline-modified nitrile rubber*, Eur. Polym. J., **40** (2004), 2185–2194

194. J. Piglowski, I. Gancarz, M. Wlazlak, *Oxazoline-functionalized hydrogenated nitrile rubber as impact modifier for polyamide-6*, Polym., **41** (2000), 3671–3681

195. C. Worner, P. Muller, R. Mulhaupt, *Toughened Poly (Butylene Terephthalate) and Blends Prepared by Simultaneous Chain Extension, Interfacial Coupling, and Dynamic Vulcanization Using Oxazoline Intermediates*, J. Appl. Polym. Sci., **66** (1997), 633–642.

196. J.B. Jun, J.G. Park, D.H. Kim, K.D. Suh, *Blends of Poly (Butylene Terephthalate) With Ethylene Propylene Elastomer Containing Isocyanate Functional Group*, Eur. Polym. J., **37** (2001), 597-602.

197. S.H. Park, K.Y. Park, K.D. Suh, *Compatibilising effect of isocyanate functional groups on polyethylene terephthalate/low density polyethylene blends*, J. Polym. Sci. B: Polym. Phys., **36** (1998), 447-453

198. S.H. Park, J.S. Lee, K.D. Suh, *Low density polyethelene with an isocyanate functional group*, J. Mater. Sci., **33** (1998), 5145-5148.

199. W.C. Jung, K.Y. Park, J.Y. Kim, K.D. Suh, *Evaluation of Isocyanate Functional Groups as a Reactive Group in the Reactive Compatibilizer*, J. Appl. Polym. Sci., **88** (2003), 2622–2629

200. W. Wang, L. Wang, X. Chen, Q. Yang, T. Sun, J. Zhou, *Study on the Graft Reaction of Polypropylene Fiber with Acrylic Acid*, Macromol. Mater. Eng., **291** (2006), 173–180.

201. P. Ghosh, B. Chattapadhyay and A.K. Sen, *Modification of low density polyethylene (LDPE) by graft copolymerisation with some acrylic monomers*, Polym., **39** (1998), 193-201.

202. R.A. Tan, W. Wang, G.H. Hu, A. de Souza Gomes, *Functionalisation of polypropylene with fluorinated acrylic monomers in the molten state*, Eur. Polym. J., **35** (1999), 1979-1984.

203. N. Yurtseven and L. Aras, *The compatibilization of methyl methacrylate-methacrylic acid copolymer and polystyrene through the functionalization of polystyrene*, Polym., **36** (1995), 3355-3358.

204. B.R. de Gascue, B. Mendez, J.L. Manosalva, J. Lopez, V.R.S. Quiteria, A.J. Muller, *Experimental analysis of the grafting products of diethyl maleate onto linear and branched polyethylene*, Polym., **43** (2002), 2151-2159.

205. C. Rosales, L. Marques, J. Gonzales, R. Perera, B. Rojas, M. Vivas, *Free radical grafting of diethylmaleate on linear low-density polyethylenes*, Polym. Eng. Sci, **36** (1996), 2247-2252.

206. D. Munteanu, *Chapter 5: Moisture cross-linkable silane-modified polyolefins,* in **Reactive Modifiers for Polymers**, (Ed. S. Al-Malaika), Blackie Academic & Professional, London (1997), 196-265.

207. Y.T. Shieh and T.H. Tsai, *Silane Grafting Reactions of Low-Density Polyethylene*, J. Appl. Polym. Sci. **69** (1998), 255–261.

208. Z. Wang, X. Wu, Z. Gui, Y. Hu, W. Fan, *Thermal and crystallization behaviour of silane-crosslinked polypropylene*, Polym. Int., 54 (2005), 442–447

209. T.Y. Bae, K.Y. Park, D.H. Kim, K.D. Suh, *Poly (ethylene terephthalate)/ polypropylene reactive blends through isocyanate functional group,* J. Appl. Polym. Sci., **81** (2001), 1056-1062

210. J.S. Lee, K.Y. Park, D. Yoo, K.D. Suh, *In situ Compatibilising of PET/PS blends through carbamate functionalised reactive copolymers*, J. Polym. Sci. B. Polym. Phys., **38** (2000), 1396-1404.

211. S.S. Pesetskii, B. Jurkowski, Y.M. Krivogu, R. Urbanowicz, *Itaconic acid grafting on LDPE blended in molten state*, J. Appl. Polym. Sci., **65** (1997),1493–1502.

212. R. Anbarasan, O. Babot, B. Maillard, *Crosslinking of high-density polyethelene in the presence of organic peroxides*, J. Appl. Polym. Sci., 93 (2004), 75-81

213. J. C. Forsyth, W. E. Baker, K. E. Russel, R. A. Whitney, *Peroxide-Initiated Vinylsilane Grafting: Structural Studies on a Hydrocarbon Substrate*, J. Polym. Sci. A: Polym. Chem., **35** (1997), 3517–3525.

214. P.S. Hope and M.J. Folkes, *Chapter 1 Introduction*, in **Polymer Blends and Alloys** (eds. M.J. Folkes and P.S. Hope, Blackie and Professional, London (1993), 1-6.

215. H. Li, G.-H. Hu, *The Early Stage of the Morphology Development of Immiscible Polymer Blends during Melt Blending: Compatibilized vs. Uncompatibilized Blends*, J. Polym. Sci. B: Polym. Phys., **39** (2001), 601–610

216. Y. W. Cheung and M.J. Guest, *A study of blending of ethylene-styrene copolymers differing in the copolymer styrene content: miscibility considering*, J. Polym. Sci. B: Polym. Phys., **38** (2000), 2976-2987.

217. C. Coning, M.V. Duin, C. Pagnoulle, and R. Jerome, *Strategies for compatibilisation of polymer blends*, Prog. Polym. Sci., **23** (1998), 707-757.

218. A.D. Litmanovich, N.A. Plate, Y.V. Kudryavtsev, *Reaction in polymer blends: Interchain effects and theoretical problems*, Prog. Polym. Sci., **27** (2002), 915-970.

219. M.Muller, *Miscibility Behaviour and Single Chain Properties in Polymer Blends: A Bond Fluctuation Model Study*, Macromol. Theory Simul, **8** (1999), 343-374.

220. Y. He, B. Zhu, and Y. Inoue, *Hydrogen bonds in polymer blends*, Prog. Polym. Sci., **29** (2004), 1021-1051.

221. C.W. Macosko, H.K. Jeon, T.R. Hoye, *Reactions at Polymer-Polymer Interfaces for Blend Compatibilisation*, Prog. Polym. Sci., **30** (2005), 939-947.

222. G.H. Hu and I. Kadri, *Modeling Reactive Blending: An Experimental Approach*, J. Polym. Sci. B: Polym. Phys. **36** (1998), 2153–2163.

223. S.H. Zhang, X. Jin, P.C. Painter, J. Runt, *Composition-dependent dynamics in miscible polymer blends: influence of intermolecular hydrogen bonding*, Polym., **45** (2004), 3933–3942

224. P. Charoensirisomboon, T. Chiba, K. Torikai, H. Saito, T. Ougizawa, T. Inoue, M. Weber, *Morphology-interface-toughness relationship in polyamide/polysulfone blends by reactive processing*, Polym.,**40** (1999), 6965–6975

225. J. Teng, J.U. Otaigbe and E.P. Taylor, *Reactive Blending of Functionalized Polypropylene and Polyamide 6: In situ Polymerization and In situ Compatibilization*, Polym. Eng. Sci. **44** (2004), 648–659.

226. H. Li, T.Chiba, N. Higashida, Y. Yang and T. Inoue, *Polymer-polymer interface in Polypropylene/polyamide blends by reactive processing*, Polym., **38** (1997), 3921-3925.

227. S. Jose, S. V. Nair, S. Thomas, J. Karger-Kocsis, *Effect of Reactive Compatibilisation on the Phase Morphology and Tensile Properties of PA12/PP Blends*, J. Appl. Polym. Sci., **99** (2006), 2640–2660.

228. F. Ide and A. Hasegawa, *Studies on polymer blend of nylon 6 and PP or nylon 6 and PPs using the reaction of polymer*, J. Appl. Polym. Sci., **18** (1974), 963-974.

229. J. Roeder, R.V.B. Oliveira, D. Becker, M.W. Gonzalves, V. Soldi, A.T.N. Pires, *Compatibility effect on the thermal degradation behaviour of polypropylene blends with polyamide 6, ethylene propylene diene rubber and polyurethane*, Polym. Degrad. Stab., **90** (2005), 481-487.

230. C. Marco, G. Ellis, M.A. Gomez, J.G. Fatou, J.M. Arribas, I. Campoy, and A. Fontecha, *Rheological properties, crystallisation, and morphology of compatibilised blends of isotactic polypropylene and polyamide*, J. Appl. Polym. Sci., **65** (1997), 2665-2677.

231. N Zeng, SL Bai, C.G Sell, J.M Hiver and YW Mai, *Study on the microstructures and mechanical behaviour of compatibilized polypropylene/polyamide-6 blends*, Polym. Int., **51** (2002), 1439–1447

232. J. Roeder, R.V.B. Oliveira, M.C. Goncalves, V. Soldi, A.T.N. Pires, *Polypropylene/ polyamide-6 blends: influence of compatibilizing agent on interface domains*, Polym. Test., **21** (2002), 815–821.

233. L. Pan, T. Chiba, and T. Inoue, *Reactive Blending of Polyamide with Polyethylene: Pull-Out of In Situ-Formed Graft Copolymers*, Polym., **42** (2001), 8825-8831.

234. C. Jiang, S. Filippi, P. Magagnini, *Reactive compatibilizer precursors for LDPE/PA6 blends. II: maleic anhydride grafted polyethylenes*, Polym., **44** (2003) 2411–2422

235. S. Filippi, L. Minkova, N. Dintcheva, P. Narducci, P. Magagnini, *Comparative study of different maleic anhydride grafted compatibilizer precursors towards LDPE/PA6 blends: Morphology and mechanical properties*, Polym., **46** (2005), 8054–8061.

236. L. Pan, T. Inoue, H. Hayami, S. Nishikawa, *Reactive Blending of Polyamide with Polyethylene: Pull-Out of In Situ-Formed Graft Copolymers and Its Application For High-Temperature Materials*, Polym., **43** (2002), 337-343.

237. M.V.Duin, M.v.Gurp, L. Leemans, M. Walet, M. Aussems, P. Martin, R. Legras, A.V. Machado, J.A Copas, *Interfacial Chemistry and Morphology of In-Situ Compatibilised PA-6 and PBT Based Blends*, Macromol. Symp., **198** (2003), 135-145.

238. L. Minkova, Hr. Yordanov, S. Fillippi, N. Grizzuti, *Interfacial tension of compatibilised blends of LDPE and PA6: the breaking thread method*, Polym., **44** (2003), 7925-7932.

239. K. Kelar and B. Jurkowki, *Preparation of functionalisation low density polyethylene by reactive extrusion and its blend with polyamide-6*, Polym., **41** (2000),1055-1062

240. M.B. Coltelli, E. Passaglia, and F.Ciardelli, *One-step functionalization and reactive blending of polyolefin/polyamide mixtures (EPM/PA6)*, Polym., **47** (2006), 85–97.

241. A.R. Bhattacharyya, A.K. Ghosh, A. Misra, *Reactivity Compatibilised Polymer Blends. A Case Study on PA-6/EVA*, Polym., **42** (2001), 9143-9154.

242. G. Chen, J. Yang, and J. Liu, *Preparation of HIPS/MA graft copolymer and its compatibilisation in HIPS/PA1010 blends*, J. Appl. Polym. Sci., **71** (1999), 2017-2025.

243. E. Carone Jr, U. Kopcak, M.C. Goncalves, S.P. Nunes, *In situ compatibilization of polyamide 6/natural rubber blends with maleic anhydride*, Polym., **41** (2000), 5929–5935

244. K. H. Yoon, H.W. Lee, O. O. Park, *Properties of Poly(ethylene terephthalate) and Maleic Anhydride-Grafted Polypropylene Blends by Reactive Processing*, J. Appl. Polym. Sci., **70** (1998), 389–395.

245. J. M. Lusinchi, B. Boutevin, N. Torres,1 J. J. Robin, *In Situ Compatibilization of HDPE/PET Blends*, J. Appl. Polym. Sci., **79** (2001), 874–880.

246. S. H. Lee, Jung K. Park, J. H. Han and K. S. Suh, *Space charge behaviour in maleic anhydride grafted polyethylene/ethylene–vinyl–acetate copolymer laminates*, J. Phys. D: Appl. Phys. 30 (1997) 1–4.

247. S. J. Kim, B.S. Shin, J.L. Hong, W.J. Cho, and C.S. Ha, *Reactive compatibilisation of PBT/EVA blend by maleic anhydride*, Polym., **42** (2001), 4073-4080.

248. V. Tanrattanakul, A. Hiltnert and E. Baer, W. G. Perkins and F. L. Massey, A. Moet, *Effect of elastomer functionality on toughened PET*, Polym., **38** (1997), 4117-4125.

249. H. T. Oyama, T. Kitagawa, T. Ougizawa, T. Inoue, M. Weber, *Novel Application of Reactive Blending: Tailoring morphology of PBT/SAN blends*, Polym., **45** (2004), 1033-1043.

250. S. Balakrishnan, R. Neelakantan, S.N. Jainsankar, *Effect of functionality levels and compatibility of polycarbonate blend with maleic anhydride grafted ABS*, J. Appl. Polym. Sci., **74** (1999), 2102-2110.

251. N. Torres, J. J. Robin, B. Boutevin, *Study of Compatibilization of HDPE–PET Blends by Adding Grafted or Statistical Copolymer*, J. Appl. Polym. Sci., **81** (2001), 2377–2386.

252. Y.X. Pang, D.M. Ji, H.J. Hu, D.J. Hourston, M. Song, *Effects of a compatibilizing agent on the morphology, interface and mechanical behaviour of polypropylene/poly(ethylene terephthalate) blends*, Polym., **41** (2000), 357–365.

253. A. Tedesco, R.V. Barbosa, S.M.B. Nachtigall, and R.S. Mauler, *Comparative study of PP-MA and PP-GMA as compatibilizing agents on polypropylene/nylon 6 blends*, Polym. Test., **21** (2002), 11–15.

254. Y.Tang, Y. Hu, L. Song, R. Zong, Z. Gui, W. Fan, *Preparation and combustion properties of flame retarded polypropylene polyamide-6 alloys*, Polym. Degrad. Stab., **91** (2006), 234-241

255. X. Zhang and J. Yin, *The characterisation of the interfacial reaction in polyamide 1010/poly(propylene-g-glycidyl methacrylate) blends*, Macromol. Chem. Phys., **199** (1998), 2631-2634.

256. X. Zhang, X.L. Li, D. Wang, Z. Yin, and J. Yin, *Morphology, Thermal Behavior, and Mechanical Properties of PA1010/PP and PA1010/PP- g-GMA Blends*, J. Appl. Polym. Sci., **64** (1997), 1489–1498.

257. Z. Xiaomin, Y. Zhihui, N. Tainhai and Y. Jinghua, Morphology, *Mechanical properties and Interfacial Behaviour of PA1010/PP/PP-g-GMA Ternary Blends*, Polym., **38** (1997), 5905-5912

258. Q. Wei, D. Chionna and M. Pracella, *Reactive Compatibilization of PA6/LDPE Blends with Glycidyl Methacrylate Functionalized Polyolefins*, Macromol. Chem. Phys., **206** (2005), 777–786.

259. E. G. Koulouri, A. X. Georgaki and J. K. Kallitsis, *Reactive compatibilization of aliphatic polyamides with functionalized polyethylenes*, Polym., **38** (1997), 4185-4192.

260. G. Gao, J. Wang, J. Yin, X. Yu, R. Ma, X. tang, Z. Yin, X. Zhang, *Rheological, thermal, and morphological properties of ABS-PA1010 blends*, J. Appl. Polym. Sci., **72** (1999), 683-688.

261. S. L. Sun, Z. Y. Tan, X. F. Xu, C. Zhou, Y. H. Ao, H. X. Zhang, *Toughening of Nylon-6 with Epoxy-Functionalized Acrylonitrile-Butadiene-Styrene Copolymer*, J. Polym. Sci. B: Polym. Phys., **43** (2005), 2170–2180.

262. Y.J. Sun, G.H. Hu, and M. Lambla, *In-situ Compatibilisation of Polypropylene and Poly (Butylene Terephthalate) Polymer Blends by One-Step Reactive Extrusion*, Polym., **37** (1996), 4119-4127.

263. H. Cartier and G.H. Hu, *Compatibilisation of Polypropylene and Poly (Butylene Terephthalate) Blends by Reactive Extrusion, Effect of the Molecular Structure of a Reactive Compatibiliser*, J. Mater. Sci., **35** (2000), 1985.

264. M. Pracella and D. Chionna, *Reactive compatibilisation of blends of PET and PP modified by GMA grafting*, Macromol. Symp., **198** (2003), 161-172.

265. M.F. Champagne, M.A. Huneault, C. Row, W. Peyrell, *Reactive Compatibilization of Polypropylene/Polyethylene Terephthalate Blends*, Polym. Eng. Sci., **39** (1999), 976-984.

266. X. Xu, J. Qiao, J. Yin, Y. Gao, X. Zhang, Y. Ding, Y. Liu, Z. Xin, J. Gao, F. Huang, and Z. Song , *Preparation of fully cross-linked CNBR/PP-g-GMA and CNBR/PP/PP-g-GMA thermoplastic elastomers and their morphology, structure and properties*, J. Polym. Sci. B: Polym. Phys., **42** (2004), 1042-1052.

267. Loyens and G. Groeninckx, *Phase Morphology Development in Reactively Compatibilised Polyethylene Terephthalate/Elastomer Blends*, Macromol. Chem. Phys., 203 (2002), 1702–1714.

268. H.Yang, M. Lai, W. Liu, C. Sun, J. Liu, *Morphology and Thermal and Mechanical Properties of PBT/HIPS and PBT/HIPS-G-GMA Blends*, J. Appl. Polym. Sci., **85** (2002), 2600–2608.

269. J.K. Kim and H. Lee, *The Effect of PS-GMA as An In-Situ Compatibilizer on The Morphology and Rheological Properties of The Immiscible PBT/PS Blends*, Polym., **37** (1996), 305-311.

270. S.L. Sun, X.Y. Xu, H.D. Yang, H.X. Zhang, *Toughening of poly(butylene terephthalate) with epoxy-functionalized acrylonitrile–butadiene–styrene*, Polym., **46** (2005), 7632–7643

271. S. Lee and O.O. Park, *Preparation of Poly (Butylene Terephthalate)/Oxazoline Containing Polystyrene Graft Copolymer through Melt Blending And Their Application As A Compatibilizer in Polycarbonate/Polystyrene*, Polym., **42** (2001), 6661-6668.

272. M.W. Fowler and W.E. Baker, *Rubber toughening of polystyrene through reactive blending*, Polym. Eng. Sci., 28 (1988), 1427-1433.

273. W.Y. Su, Y. Wang, K. Mina, R.P. Quirk, *In situ copolymerization and compatibilization of polyester and polystyrene blends. I. Synthesis of functionalized polystyrenes and the reactions with polyester*, Polym., **42** (2001), 5107-5119.

274. W.Y. Su, Y. Wang, K. Min, R.P. Quirk, *In situ copolymerization and compatibilization of polyester and polystyrene blends. II. Thermally and chemically induced reaction and mechanical properties*, Polym., **42** (2001), 5121-5134.

275. K.G. Gravalos, J.K.Kallitsis , N.K. Kalfoglou, *In situ compatibilization of poly(ethyleneterephthalate)/poly(ethylene-co-ethylacrylate) blends*, Polym., **36** (1995),1393-1399.

276. V. N. Ignatov, C. Carraro, V. Tartarit, R. Pippa, F. Pilati, C. Berti, M. Toselli, M. Fiorini, *Reactive blending of commercial PET and PC, with freshly added catalysts*, Polym., **37** (1996), 5883-5887

277. M. Fiorini, F. Pilati, C. Berti and M. Toselli, and V. Ignatov, *Reactive blending of poly(ethylene terephthalate) and bisphenol-A polycarbonate: effect of various catalysts and mixing time on the extent of exchange reactions*, Polym., **38** (1997), 413-419.

278. V. N. Ignatov, C. Carraro, V. Tartari, R. Pippa and M. Scapin, F. Pilati, C. Berti, M.Toselli, M. Fiorini, *PET/PC blends and copolymers by one-step extrusion: 1. Chemical structure and physical properties of 50/50 blends*, Polym., **38** (1997), 195- 200.

279. V. N. Ignatov, C. Carraro, V. Tartari, R. Pippa and M. Scapin, F. Pilati, C. Berti, M.Toselli, M. Fiorini, *PET/PC blends and copolymers by one-step extrusion: 2. Influence of the initial polymer composition and type of catalyst*, Polym., **38** (1997), 201-205.

280. Z. Zhang, Y. Xie and D. Ma, *Relationship between miscibility and chemical structures in reactive blending of poly(bisphenol A carbonate) and poly(ethylene terephthalate)*, Eur. Polym. J., **37** (2001), 1961-1966.

281. A. Molnar and A. Eisenberg, *Miscibility of Polyamide-6 with Lithium or Sodium Sulfonated Polystyrene Ionomers*, Macromol., **25** (1992), 5774-5782.

282. H.M. Li, Z.G. Shen, F.M. Zhu, S.A.Lin, *Polymer blends of sPS/PA6 compatibilized by sulfonated syndiotactic polystyrene*, Europ. Polym. J., **38** (2002), 1255–1263.

283. T. L. Boykin *and* R.T. B. Moore, *The Role of Specific Interactions and Transreactions on the Compatibility of Polyester Ionomers With Poly(Ethylene Terephthalate) and Nylon 6,6*, Polym. Eng. Sci., **38** (1998), 1658-1663.

284. J.W. Lee, C.H. Kim, J.K Park,T.S. Hwang, *Study on the Microphase Structure and Mechanical Properties of the Blends of Acrylonitrile Butadiene Styrene and Sodium Sulphonated Styrene Acrylonitrile Ionomer*, Polym. Intern., **45** (1998), 47-54

285. X. Wang, X. Cui, *Effect of ionomers on mechanical properties, morphology,and rheology of polyoxymethylene and its blends with methyl methacrylate–styrene–butadiene copolymer*, Eur. Polym. J., **41** (2005), 871–880.

286. S. Xu, T. Tang, B. Chen, B. Huang, *Compatibilisation of blends of polystyrene and zinc salt of sulfonated polystyrene by poly(styrene-b-4-vinylpyridine) diblock copolymer*, Polym., **40** (1999), 2239-2247.

287. S. Filippi, H. Yordanov, L. Minkova, G. Polacco, M. Talarico, *Reactive Compatibilizer Precursors for LDPE/PA6 Blends, 4. Maleic Anhydride and Glycidyl Methacrylate Grafted SEBS*, Macromol. Mater. Eng. **289** (2004), 512–523.

288. A.N. Wilkinson, L. Laugel, M.L. Clemens, V.M. Harding, M. Marin, *Phase Structure in Polypropylene/PA6/SEBS Blends*, Polym., **40** (1999), 4971–4975.

289. A.N. Wilkinson, M.L. Clemens, V.M. Harding, *The effects of SEBS-g-maleic anhydride reaction on the morphology and properties of polypropylene/PA6/SEBS ternary blends*, Polym., **45** (2004), 5239–5249.

290. B. Ohlsson, H. Hassander, and B. Tornell, *Improved Compatibility Between Polyamide and Polypropylene By The Use of Maleic Anhydride Grafted SEBS*, Polym., **39** (1998), 6705-6714.

291. K. Dedecker and G. Groeninckx, *Reactive compatibilisation of A/(B/C) polymer blends Part 1. Investigation of the phase morphology development and stabilisation*, Polym., **39** (1998), 4985-4992.

292. K. Dedecker and G. Groeninckx, *Reactive compatibilisation of A/(B/C) polymer blends Part 2. Analysis of the phase inversion region and the co-continuous phase morphology*, Polym., **39** (1998), 4993-5000.

293. H. Liu,T. Xie, L. Hou,1,3 Y. Ou, G. Yang, *Toughening and Compatibilization of Polypropylene/Polyamide-6 Blends with a Maleated–Grafted Ethylene-co-vinyl Acetate*, J. Appl. Polym. Sci., **99** (2006), 3300–3307.

294. Y. Ou, Y. Lei, X. Fang and Guisheng Yang, *Maleic Anhydride Grafted Thermoplastic Elastomer as an Interfacial Modifier for Polypropylene/Polyamide 6 Blends*, J. Appl. Polym. Sci., **91** (2004), 1806–1815.

295. J.C. Lepers, B.D. Favis, C. Lacroix, *The Influence of Partial Emulsification on Coalescence Suppression and Interfacial Tension Reduction in PP/PET Blends*, J. Polym. Sci. B: Polym. Phys., **37** (1999), 939–951.

296. M. Heino, J. Kirjava, P. Hietaoja, and J. Seppala, *Compatibilisation of Poly (Ethylene Terephthalate)/Polypropylene Blends with Styrene-Ethylene/Butylene-Styrene (SEBS) Block copolymer*, J. Appl. Polym. Sci., **65** (1997), 241-249.

297. M. Pracella, L. Rolla, D. Chionna, A. Galeski, *Compatibilization and Properties of Poly(ethylene terephthalate)/Polyethylene Blends Based on Recycled Materials*, Macromol. Chem. Phys., **203** (2002),1473–1485.

298. E. M. Araujo, E. Hage Jr., A. J. F. Carvalho, *Acrylonitrile–Butadiene–Styrene Toughened Nylon 6: The Influences of Compatibilizer on Morphology and Impact Properties*, J. Appl. Polym. Sci. **87** (2003), 842–847.

299. E. M. Araujo, E. Hage, Jr., A. J. F. Carvalho, *Effect of Compatibilizer in Acrylonitrile-Butadiene-Styrene Toughened Nylon 6 Blends: Ductile–Brittle Transition Temperature*, J. Appl. Polym. Sci., **90** (2003), 2643–2647.

300. V. Chiono, S. Filippi, H. Yordanov, L. Minkova and P. Magagnini, *Reactive compatibilizer precursors for LDPE/PA6 blends. III: ethylene–glycidyl methacrylate copolymer*, Polym., **44** (2003), 2423-2432.

301. G.L. Mantovani, L.B. Canto, E.H. Junior, L.A. Pessan, *Toughening of PBT by ABS, SBS, and HIPS systems and the effect of reactive functionalised copolymers*, Macromol. Symp., **176** (2001), 167–180.

302. N. M. Larocca, E. Hage JR., L. A. Pessan, *Effect of Reactive Compatibilization on the Properties of Poly(butylene terephthalate)/Acrylonitrile–Ethylene–Propylene–Diene Styrene Blends*, J. Polym. Sci. B: Polym. Phys., **43** (2005), 1244–1259

303. N.K. Kalfoglou, D.S. Skafidas, J.K. Kallitsis, J.C. Lambert, L.Van der Stappen, *Comparison of compatibiliser effectiveness for PET/HDPE blends*, Polym., **36** (1995), 4453-4462.

304. Y. Pietrasanta, J.J. Robin, N. Torresl, and B. Boutevin, *Reactive compatibilization of HDPE/PET blends by glycidyl methacrylate functionalized polyolefins*, Macromol. Chem. Phys., **200** (1999), 142–149

305. K. Wang, J.Wu, H. Zeng, *Microstructures and fracture behavior of glass fiber reinforced PBT/PC/E-GMA elastomer blends—1:microstructures*, Comp. Sci. Tech., **61** (2001), 1529–1538.

306. P. Martin , C. Maquet , R. Legras , C. Bailly , L. Leemans , M. van Gurp and M. van Duin , *Particle-in-particle morphology in reactively compatibilized poly(butylene terephthalate)/epoxide-containing rubber blends*, Polym., **45** (2004), 3277-3284.

307. P. Martin, C. Gallez, J. Devaux, R. Legras, L. Leemans, M. van Gurp, M. van Duin, *Reactive compatibilization of blends of polybutyleneterephthalate with epoxide-containing rubber. The effect of the concentrations in reactive functions*, Polym., **44** (2003), 5251–5262.

308. W. Hale, H. Keskkula, D.R. Paul, *Compatibilisation of PBT/ABS Blends by Methyl Methacrylate-Glycidyl Methacrylate-Ethyl Acrylate Terpolymer*, Polym.,, **40** (1999), 365-377.

309. K. Friedrich, M. Evstatiev, S. Fakirov, O. Evstatiev, M. Ishii, M. Harrass, *Microfibrillar reinforced composites from PET/PP blends: processing, morphology and mechanical properties*, Comp. Sci. Tech., **65** (2005), 107–116.

310. C.H. Tsai and F.C. Chang, *Polymer blend of PBT and PP compatibilised by ethylene-co-glycidyl methacrylate copolymers*, J. Appl. Polym. Sci., **61** (1996), 321-332.

311. M. Pracella, D. Chionna, A. Pawlak and A. Galeski, *Reactive Mixing of PET and PET/PP Blends with Glycidyl Methacrylate–Modified Styrene-b-(Ethylene-co-Olefin) Block Copolymers*, J. Appl. Polym. Sci., **98** (2005), 2201–2211.

312. J.C. Lepers, B.D. Favis, S.L. Kent, *Interface–property relationships in biaxially stretched PP–PET blends*, Polym., **41** (2000),1937–1946.

313. W. Loyens, G. Groeninckx, *Ultimate mechanical properties of rubber toughened semicrystalline PET at room temperature*, Polym., **43** (2002), 5679–5691

314. N. Napke and J. Karger-Kocsis, *Thermoplastic elastomer based on compatibilised poly(ethylene terephthalate) blends: Effect of rubber type and dynamic curing*, Polym., **42** (2001), 1109-1120.

315. R. Scaffaro, F. P. L. Mantia, *Evolution of the Morphology and Characterization of Compatibilized PBT/EVA Blends Prepared by Reactive Extrusion*, Macromol. Chem. Phys., **207** (2006), 265–272.

316. R. Scaffaro, F. P. L. Mantia, C. Castronovo, Reactive Compatibilization of PBT/EVABlends with an Ethylene-Acrylic Acid Copolymer and a Low Molar Mass Bis-Oxazoline, Macromol. Chem. Phys.,**205** (2004), 1402–1409.

317. R. Scaffaro, F. P. La Mantia, L. Canfora, G. Polacco, S. Filippi, and P. Magagnini, *Reactive compatibilization of PA6/LDPE blends with an ethylene–acrylic acid copolymer and a low molar mass bis-oxazoline*, Polym., **44** (2003), 6951–6957.

318. S. Voronov, V. Samaryk, Y. Roiter, J. Pionteck, P. Potschke, S. Minko, I. Tokarev, S. Varvarenko, N. Nosova, *Compatibilization of Polymer Blends with High-Molecular-Weight Peroxides*, J. Appl. Polym. Sci., **96** (2005), 232–242.

319. Z. Fang, M. Zeng, G. Cai, C. Xu, *Application of Phase Dispersion–Crosslinking Synergism on Recycling Commingled Plastic Wastes*, J. Appl. Polym. Sci., **82** (2001), 2947–2952.

320. Y. Roiter, V. Samaryk, S. Varvarenko, N. Nosova, I. Tarnavchyk, J. Pionteck, P. Potsche, S. Voronov, *Peroxide-containing compatibiliser for polypropylene blends with other polymers*, Macromol. Symp., **210** (2004), 209-217.

321. H. Ismail, Supri, A.M.M. Yusof, *Blend of waste poly(vinylchloride) (PVCw)/acrylonitrilebutadiene-rubber (NBR): the efect of maleic anhydride (MAH,)* Polym.Test., **23** (2004), 675–683.

322. S.C. Jana, N.Patel, and D.Dharaiya, *Compatibilisation of PBT-PPE Blends Using Low Molecular Weight Epoxy*, Polym., **42** (2001), 8681-8693.

323. H. X. Zang, D. J. Hourston, *Reactive Compatibilization of Poly(butylene terephthalate)/Low-Density Polyethylene and Poly(butylene terephthalate)/Ethylene Propylene Diene Rubber Blends with a Bismaleimide*, J. Appl. Polym. Sci. **71** (1999), 2049–2057.

324. N.K. Gupta, A.K. Jain, R. Singhal, A.K. Nagpal, *Effect of Dynamic Crosslinking on Tensile Yield Behaviour of Polypropylene/Ethylene-Propylene-Diene Rubber Blends*, J. Appl. Polym. Sci., **78** (2000), 2104-2121.

325. A. Hassan, M.U. Wahit, C.Y. Chee, *Mechanical and Morphological Properties of PP/NR/LLDPE Ternary Blend – Effect of HVA-2*, Polym.Test., **22** (2003), 281-290.

326. I. Pesneau, M.F. Llauro, M. Gregoire, A. Michel, *Morphology Control of Polyester–Polyolefin Blends by Transesterification during Processing Operations in the Presence of Dibutyltin Oxide*, J. Appl. Polym. Sci., **65** (1997), 2457-2469.

327. A. Jha and A.K. Bhowmick, *Mechanical and Dynamic Mechanical Thermal Properties of Heat- and Oil-Resistant Thermoplastic Elastomeric Blends of Poly (Butylene Terephthalate) and Acrylate Rubber*, J. Appl. Polym. Sci, **78** (2000), 1001-1008.

328. Y.J. Sun, R.J.G. Willemse, T.M. Liu, and W.E. Baker, *In situ compatibilisation of polyolefin and polystyrene using Friedel-Crafts alkylation through reactive extrusion*, Polym., **39** (1998), 2201-2208.

329. Y.J. Sun, W.E. Baker, *Polyolefin/Polystyrene In Situ Compatibilization Using Friedel–Crafts Alkylation*, J. Appl. Polym. Sci., **65** (1997), 1385–1393.

330. M. F. Diaz, S. E. Barbosa, Numa J. Capiati, *Addition Compatibilization of PP/PS Blends by Tailor-Made Copolymers*, Polym. Eng. Sci., **46** (2006), 329–336.

331. S.S.Raya, S. Pouliota, M. Bousminaa, L.A. Utracki, *Role of organically modified layered silicate as an active interfacial modifier in immiscible polystyrene/polypropylene blends*, Polym., **45** (2004), 8403–8413.

332. G.H. Hu, S. Lorek, Y. Holl, M. Lambla, *Catalytic aminolysis of acrylic copolymers in solution and in the melt. II. Comparison between styrenic and ethylenic copolymers*, J. Polym. Sci. A: Polym. Chem., **30** (1992), 635–641.

333. G.H. Hu, S. Triouleyre, M. Lambla, *Kinetic behaviour of chemical reactions in homogeneous and heterogeneous polymer melts*, Polym., **38** (1997), 545-550.

334. S. B. Brown, *Reactive Extrusion* , in Encyclopedia of Polymer Science and Engineering (Eds. H.F. Mark, N.M. Bikales, C.G. Overberger and G. Menges, J.I. Kroschwitz, 2nd Edition, Vol. 14, 169 (1988).

335. A. Marquez, J. Quijano, M. Gaulin, *A Calibration technique to evaluate the power law parameters of polymer melts using a torque rheometer*, Polym. Eng. Sci., **36** (1996), 2556-2583.

336. B. Cheng, C. Zhou, W. Yu, X. Sun, *Evaluation of rheological parameters of polymer melts in torque rheometers*, Polym. Test., **20** (2001), 811-818.

337. J. G. Mallette, R.R. Soberanis, *Evaluation of rheological properties of non-newtonian fluids in internal mixers: an alternative methods based on the power law model*, Polym. Eng. Sci., **38** (1998), 1436-1442.

338. A. Zhang, L. Wang, Y. Zhou, *A study on rheological properties of carbon black extended powdered SBR using a torque rheometer*, Polym.Test., **22** (2003), 133–141.

339. J.E. Goodrich and R.S. Porter, *A rheological interpretation of torque-rheometer data*, Polymer Eng. Sci., **7** (1967), 45-51.

340. A.K. Maity, S.F. Xavier, *Rheological properties of ethylene-propylene block copolymer and EPDM rubber blends using a torque rheometer*, Eur. Polym. J., **35** (1999), 173-181.

341. L.B. Canto, L.A. Pessan, *Determination of the composition of styrene-glycidyl methacrylate copolymers by FTIR and titration*, Polym. Test., **21** (2002), 35-38.

342. N. Papke and J. Karger-Kocsis, *Determination methods of the grafting yield in glycidyl methacrylate-grafted ethylene/propylene/diene rubber (EPDM-g-GMA): Correlation between FTIR and ^{1}H-NMR analysis*, J. Appl. Polym. Sci., **74** (1999), 2616-2624.

343. E. Andreassen, *Infrared and Raman spectroscopy of polypropylene*, in **Polypropylene: An A-Z Reference** (Ed. J. Karger-Kocsis), Kluwer Publisher (1999), 320-328.

344. K.J. Ganzeveld, L.P.B. Janssen, *The grafting of maleic anhydride on high density polyethelene in an extruder*, Polym. Eng. Sci., **32** (1992), 467-474.

345. M. Sclavons, P.Franquinet, V.Carlier, G.Verfaillie, I.Fallais, R.legras, M.laurent, and F.C.Thyrion, *Quantification of the Maleic anhydride grafted onto Polypropylene by Chemical and Viscosimetric Titrations, and FTIR spectroscopy*, Polym., **41** (2000), 1989 -1999.

346. M. Sclavons, M. Laurent, J. Devaux, V. Carlier, *Maleic anhydride-grafted polypropylene: FTIR study of a model polymer grafted by ene-reaction*, Polym., **46** (2005), 8062–8067.

347. X. Zhu, D. yan, *In Situ FTIR study on the melting process of isotactic polypropylene*, Macromol. Chem. Phys., **202** (2001), 1109-1113

348. A. M. Healey, P. J. Hendra, Y. D. West, *A Fourier-transform Raman study of the strain-induced crystallization and cold crystallization of natural rubber*, Polym., 37 (1996), 4009 4024

349. J. Samran, P. Phinyocheep, P. Daniel, D. Derouet, J.-Y. Buzare, *Raman spectroscopic study of non-catalytic hydrogenation of unsaturated rubbers*, J. Raman Spectrosc. **35** (2004), 1073–1080

350. Noury Initiator, **Akzo technical sheet**, Akzo Chemie bv, May 1982.

351. A.D. Robert, **Natural Rubber Science and Technology**, Oxford (1988), Oxford University Press;

352. F. Ngolemasango, E. Ehabe, C. Aymard, J. S.-Beuve,. B. Nkouonkam, F Bonfils, *Role of short polyisoprene*

chains in storage hardening of natural rubber, Polym. Int. 52 (2003),1365–1369

353. F.H. Larsen, T. Rasmussen, W.B. Pedersen, N.C. Nielsen, H.J. Jakobsen, *Observation of immobile regions in natural rubber at ambient temperature by solid-state 13C CP/MAS NMR spectroscopy*, Polymer **40** (1999), 7013–7017

354. A.Y. Coran and R.P. Patel, *Chapter 9: Thermoplastic Elastomers Based on Elastomer/Thermoplastic Blends Dinamically Vulcanized*, in **Reactive Modifiers for Polymers** (Ed. S. Al-Malaika), Blackie Academic & Professional, London (1997), 349-394.

355. C. Nakason, W. Pechurai, K. Sahakaro, A. Kaesaman, *Rheological, Thermal, and Curing Properties of Natural Rubber-g-Poly(methyl methacrylate)*, J. Appl. Polym. Sci., **99** (2006), 1600–1614.

356. G. J. Lake, in ***Handbook of Adhesion***, D. E. Packwhich, Ed., Longman, Harlow, UK, 1992.

357. P. S. Achary, C. Gouri, R. Ramaswamy, *Reactive Bonding of Natural Rubber to Metal by a Nitrile–Phenolic Adhesive*, J. Appl. Polym. Sci., **81** (2001), 2597–2608.

358. J. W. Cook, S. Edge, D. E. Pacham, A. S. Thompson,*Thermal Behavior of Natural Rubber and Chlorinated Rubber Blends*, J. Appl. Polym. Sci., 65 (1997), 1379–1384.

359. P.Suriyachi, S.Kiatkamjonwong, P.Prasassarakich, *Natural rubber-g-glycidyl methacrylate/styrene as a compatibiliser in natural rubber/PMMA blends*, Rub. Chem. Techn., **77** (2004), 914-930.

360. T. Xavier, J. Samuel, T. Kurian, *Synthesis and Characterization of Novel Melt Processable Ionomers based on Radiation Induced Styrene Grafted Natural Rubber*, Macromol. Mater. Eng., **286** (2001), 507-512.

361. H. Ismail, A. Rusli and A.A. Rashid, *Maleated natural rubber as a coupling agent for paper sludge filled natural rubber composites*, Polym. Test., **24** (2005), 856–862

362. S.H. El-Sabbagh, *Compatibility Study of Natural Rubber and Ethylene–Propylene Diene Rubber Blends*, Polym. Test., **22** (2003), 93–100.

363. C. Nakason, A. Kaesman, S. Homsin, S. Kiatkamjornwong, *Rheological and Curing Behavior of Reactive Blending. I. Maleated Natural Rubber–Cassava Starch*, J. Appl. Polym. Sci., **81** (2001), 2803–2813.

364. C. Nakason, S. Saiwari, A. Kaesaman, *Thermoplastic Vulcanizates Based on Maleated Natural Rubber/Polypropylene Blends: Effect of Blend Ratios on Rheological, Mechanical, and Morphological Properties*, Polym. Eng. Sci., **46** (2006), 594-600.

365. W. Arayapranee, P. Prasassarakich, G. L. Rempel, *Process Variables and Their Effects on Grafting Reactions of Styrene and Methyl Methacrylate onto Natural Rubber*, J. Appl. Polym. Sci., **89** (2003), 63–74.

366. D.-Y. Lee, N. Subramaniam, C. M. Fellows, R. G. Gilbert, *Structure–Property Relationships in Modified Natural Rubber Latexes Grafted with Methyl Methacrylate and Vinyl neo-Decanoate*, J. Polym. Sci. A: Polym. Chem., 40 (2002), 809–822

367. V. George, I. J. Britto, M. S. Sebastian, *Studies on radiation grafting of methyl methacrylate onto natural rubber for improving modulus of latex film*, Rad. Phys. Chem., **66** (2003), 367–372.

368. R. S. Lehrle, S. L. Willist, *Modification of natural rubber: a study to assess the effect of vinyl acetate on the efficiency of grafting methyl methacrylate on rubber in latex form, in the presence of azo-bis-isobutyronitrile*, Polymer, **38** (1997), 5937 5946.

369. L. Thiraphattaraphun, S. Kiatkamjornwong, P. Prasassarakich and S. Damronglerd, *Natural rubber-g-methyl methacrylate/poly(methyl methacrylate) blends*, J. Appl. Polym. Sci., **81** (2001), 428-439.

370. P.Wang, K.L. Tan, C.C. Ho and M.C. Khew, E.T. Kang, *Surface modification of natural rubber latex films by graft copolymerization*, Eur. Polym. J., **36** (2000) 1323-1331.

371. P.C.Oliveira, A.Guimaraesa, J.Y.Cavaille, L. Chazeau, R.G. Gilbert and A.M. Santos, *Poly(dimethylaminoethyl methacrylate) grafted natural rubber from seeded emulsion polymerization*, Polym., **46** (2005), 1105–1111.

372. W. Kangwansupamonkon, R. G. Gilbert, S. Kiatkamjornwong, *Modification of Natural Rubber by Grafting with Hydrophilic Vinyl Monomers*, Macromol. Chem. Phys., **206** (2005), 2450–2460

373. Z. Peng, S.D. Li, M.F. Huang, K. Xu, C. WANG, P.W. Li, X.G. Chen, *Thermogravimetric Analysis of Methyl Methacrylate-Graft-Natural Rubber*, J. Appl. Polym. Sci., **85** (2002), 2952–2955.

374. S.D. Li, C.Wang, K. Xu and Z. Peng, *Thermooxidative Degradation of Methyl Methacrylategraft-Natural Rubber*, J. Appl. Polym. Sci., **90** (2003), 1227–1232.

375. M. H. Zhou, T. Hoang, I.G. Kim, C. S. Ha, W.J. Cho, *Synthesis and Properties of Natural Rubber Modified with Stearyl Methacrylate and Divinylbenzene by Graft Polymerization*, J. Appl. Polym. Sci., **79** (2001), 2464–2470.

376. W. Arayapranee and G. L. Rempel, *Factorial experimental design for grafting of vinyl monomers onto natural rubber latex*, J. Appl. Polym. Sci., **93** (2004), 455-463.

377. W. Arayapranee and P. Prasassarakich, G. L. Rempel, *Synthesis of graft copolymers from natural rubber using cumene hydroperoxide redox initiator*, J. Appl. Polym. Sci., **83** (2002), 2993-3001.

378. P. A. Nelson and S. K. N. Kutty, *Cure Characteristics and Mechanical Properties of Maleic Anhydride Grafted Reclaimed Rubber/Styrene Butadiene Rubber Blends*, Polym. Plast. Technol. Eng. 43 (2004), 245–260

379. S. Chuayjuljit, P. Siridamrong, V. Pimpan, *Grafting of Natural Rubber for Preparation of Natural Rubber/Unsaturated Polyester Resin Miscible Blends*, J. Appl. Polym. Sci., **94** (2004), 1496–1503.

380. A. Mounir, N. A. Darwish and A. *Shehata, Effect of maleic anhydride and liquid natural rubber as compatibilizers on the mechanical properties and impact resistance of the NR-NBR blend*, Polym. Adv. Technol., **15** (2004), 209–213.

381. P. L. Teh, Z. A. M. Ishak, A. S. Hashim, J. Karger-Kocsis, U. S. Ishiaku, *Physical Properties of Natural Rubber/Organoclay Nanocomposites Compatibilized with Epoxidized Natural Rubber*, J. Appl. Polym. Sci. **100** (2006), 1083–1092.

382. M. Schneider, T. Pith, and M. Lambla, *Toughening of polystyrene by natural rubber-based composite particles, Part III: Fracture mechanism*, J. Materials Sci., **32** (1997), 5191-5204.

383. Z. Oommen, S. Thomas, C. K. Premalatha and B. Kuriakose, *Melt rheological behaviour of natural rubber/poly(methylmethacrylate)/natural rubber-g-poly(methyl methacrylate) blends*, Polym, **38** (1997), 5611-5621.

384. S. B. Neoh, A.S. Hashim, *Highly Grafted Polystyrene-Modified Natural Rubber as Toughener for Polystyrene*, J. Appl. Polym. Sci., **93** (2004), 1660–1665.

385. A. Asaletha, G. Groeninckx, M.G. Kumaran, S. Thomas, *Melt rheology and morphology of physically compatibilised natural rubber-polystyrene blends by the addition of natural rubber-g-polystyrene*, J. Appl. Polym. Sci., **69** (1998), 2673-2690.

386. S. Chuayjuljit, S. Moolsin, P. Potiyaraj, *Use of Natural Rubber-g-Polystyrene as a Compatibilizer in Casting Natural Rubber/Polystyrene Blend Films*, J. Appl.Polym. Sci., **95** (2005), 826–831.

387. A. S. Hashim and S.K. Ong, *Study on polypropylene/natural rubber blend with polystyrene-modified natural rubber as compatibiliser*, Polym. Int., **51** (2002), 611-616.

388. S. Kawahara, W.Klinklai, H. Kuroda and Y. Isono, *Removal of proteins from natural rubber with urea*, Polym. Adv. Tech., **15** (2004), 181–184.

389. K. Suchiva, T. Kowitteerawut, L. Srichantamit, *Structure Properties of Purified Natural Rubber*, J. Appl. Polym. Sci., 78 (2000), 1495–1504

390. N. Rattanasom and K. Suchiva, *Rheological and Processing Properties of Purified Natural Rubber*, J. Appl. Polym. Sci., **98** (2005), 456–465.

391. C. Nanakson, A. Kaesaman, Z. Samoh, S. Homsin, and S. Kiatkamjornwong, *Rheological of maleated natural rubber and natural rubber blends*, Polym. Test., **21** (2002), 449-455.

392. M.P. Merkel, V.L. Dimonie, M.S. El-Aasser, J.W. Vanderhoff, E.S. Daneils, *Morphology and grafting reaction in core/sell latexes*, J. Polym. Sci. Polym. A. Polym Chem., **25** (1987), 1219-1233.

393. Lenka, S.; Nayak, P. L.; Das, A. P., *Graft copolymerisation onto rubber. VII. Graft copolymerisation of methyl methacrylate onto rubber using potassium peroxydisulfate catalised by siver ion*, J Appl Polym Sci., **30** (1985), 2753-2759.

394. Z. Yao, B-G. Li, K. Cao, Z.R. Pan, *Semicontinuous thermal bulk copolymerization of styrene and maleic anhydride: Experiments and reactor model*, **J. Appl. Polym. Sci., 67 (1998), 1905.**

395. E. Borsig, A. Fiedlerova, M. Lazar, *Efficiency of chemical cross-linking of polypropylene*, J. Macromol. Sci. Chem., **16** (1981), 513-528.

396. M. Lazar, L. Hrckova, E. Borsig, N. Reichelt, M. Ratzsch, *Course of degradation and build-up reaction in isotactic polypropylene during peroxide decomposition*, J. Appl. Polym. Sci., **78** (2000), 886-893.

397. E. Borsig, L. Hrckova, A. Fiedlerova, M. Lazard, *Degradation of polypropylene under the effect of the low molecular mass organic peroxide below the melting temperature of the polymer*, J. Macromol. Sci.- Pure Appl. Chem., **A35** (1998), 1313-1326

398. M. Lazar, A. Kleinova, A. Fiedlerova, I Janigova, E. Borsig, *Role of minority structure and mechanism of peroxide crosslinking of polyethylene*, J. Polym. Sci. A: Polym. Chem., **42** (2004), 675-688

399. P. G. Mekarbane and B.J. Tabner, *ESR spin-trap study of the radicals present during the thermolysis of some novel alkyl peroxy esters*, Magn. Reson. Chem., 38 (2000), 845–852

400. I. Chodak, *Properties of crosslinked polyolefin-based material*, Prog. Polym. Sci., 20 (1995), 1165-1199

401. I. Chodak, E. Zimanyiove, *The effect of temperature on peroxide initiated crosslinking of polypropylene*, Eur. Polym. J., 20 (1984), 81-84

402. S. J. Oh, J. L. Koenig, *Solid-State NMR Studies of cis-1,4-polyisoprene Crosslinked with Dicumyl Peroxide in the Presence of Triallyl Cyanurate*, J. Polym. Sci. B: Polym. Phys., **38** (2000), 1417–1423

403. F. E. Okieimen and I. N. Urhoghide *Graft copolymerization of acrylonitrile and methyl methacrylate monomer mixtures on crumb natural rubber*, J.Appl. Polym. Sci., 84 (2002), 1872-1877.

404. R.Z. Greenley, *Q and e values for free radical copolymerisations of vinyl monomers and telogens*, in **Polymer Handbook**, 4th Edition, Eds: J. Brandrup, E.H. Immergut, E.A. Grulke, John Wiley & Sons, Inc., New York (1999), 309-337

405. S. Toki, T. Fujimaki, M. Okuyama, *Strain-induced crystallization of natural rubber as detected real-time by wide-angle X-ray diffraction technique*, Polym., **41** (2000) 5423–5429

406. R. Anbarasan, O. Babot, B. Maillard, *Crosslinking of high-density polyethelene in the presence of organic peroxides*, J. Appl. Polym. Sci., **93** (2004), 75-81

407. K.J. Ivin, *Thermodynamics of addition polymerisation*, J. Polym. Sci. A: Polym. Chem., **38** (2000), 2137.

408. G. Odian, *Radical Chain Polymerisation,* in ***Principles in polymerisation***, Fourth Edition, John Wiley & Son, Inc., New Jersey (2004), 198-349

409. H. Yamazaoe, P.B. Zetterland, B. Yamada, D.J. Hill, P.J. Pomery, *Free-Radical Bulk Polymerization of Styrene: ESR and Near-Infrared Spectroscopic Study of the Entire Conversion Range*, Macromol. Chem. Phys., **202** (2001), 824-829

410. J. L. White, A. Sasaki, *Free Radical Graft Polymerization*, Polym. Plast. Tech. Eng., 42 (2003), 711–735

411. V. Pallassana and M. Neurock, *First-Principles Periodic Density Functional Study of the Hydrogenation of Maleic, Anhydride to Succinic Anhydride over Palladium(111)*, J. Phys. Chem. **B104** (2004), 9449-9459

412. H.A. Stretz, D.R. Paul, *Properties and morphology of nanocomposites based on styrenic polymers, Part II: Effects of maleic anhydride units*, Polym., **47** (2006) 8527-8535.

413. F. Zafar, E. Sharmin, S. M. Ashraf, S. Ahmad, *Studies on Poly(Styrene-co-Maleic Anhydride)-Modified Polyesteramide-Based Anticorrosive Coatings Synthesized from a Sustainable Resource*, J. Appl. Polym. Sci., **92** (2004) 2538–2544

414. J.B. Faisant, A. A'it-Kadi, M. Bousmina and L. Deschenes, *Morphology, thermomechanical and barrier properties of polypropylene-ethylene vinyl alcohol blends*, Polym., **39** (1998), 533-545.

415. Qi Wang, H. Chen, and Y. Liu, *LDPE-g-MA prepared throught solid-phase mechanochemistry and its compatibilising effects on HDPE/CaCO3*, Polym. Plast. Technol. Eng., **41** (2002), 215–228

416. K. Clark *and* S. Lee, *Removal of Ungrafted Monomer from Polypropylene-Graft-Maleic Anhydride via Supercritical Carbon Dioxide Extraction*, Polym. Eng. Sci., **44** (2004), 1636-1641.

417. S. Augier, S. Coiai, T. Gragnoli, E. Passaglia, J.-L. Pradel, J.-J. Flat, *Coagent assisted polypropylene radical functionalization: monomer grafting modulation and molecular weight conservation*, Polymer **47** (2006), 5243–5252.

418. E. Borsig, A. Fiedlerova, and L. Hrckova, *Influence of maleic anhydride on the molecular polypropylene at the functionalisation reaction*, J.M.S.-Pure Appl. Chem., **A32** (1995), 2017-2024.

419. M. E. Ryan, A. M. Hynes, and J. P. S. Badyal, *Pulsed Plasma Polymerization of Maleic Anhydride*, ACS Chem. Mater., **8** (1996), 37-42.

420. S. Schiller, J. Hu, A. T. A. Jenkins, R. B. Timmons, F. S. Sanchez-Estrada, W. Knoll, and R. Forch, *Chemical Structure and Properties of Plasma-Polymerized Maleic Anhydride Films*, Amer. Chem. Soc., Chem. Mater., **14** (2002), 235-242

421. T.L. Hill, An Introduction to statistical thermodynamics, Dover, New York, 1986.

422. P. Dokolas, D.H. Solomon, *Graft copolymerization studies Part II. Models related to polyethylene terephthalate*, Polymer, **41** (2000), 3523.

423. K. B. Wiles, V. A. Bhanu, A. J. Pasquale, T. E. Long, J. E. MCGrath, *Monomer Reactivity Ratios for Acrylonitrile–Methyl Acrylate Free-Radical Copolymerization*, J. Polym. Sci. A: Polym. Chem., 42 (2004), 2994–3001

424. A. Wolf, F. Bandermann, C. Schwede, *Batch and Continuous Thermal Free-Radical Copolymerization of Styrene with Glycidyl Methacrylate at High Reaction Temperatures*, Macromol. Chem. Phys., 203 (2002), 393-400

425. F.R. Mayo and F.M. Lewis, *Copolymerization. I. A Basis for Comparing the Behavior of Monomers in Copolymerization; The Copolymerization of Styrene and Methyl Methacrylate,* J. Am. Chem. Soc., 66 (1944), 1594-1601.

426. R.Z. Greenley, *Free Radical Copolymerisation Reactivity Ratio,* in **Polymer Handbook**, 4th Edition, Eds: J. Brandrup, E.H. Immergut, E.A. Grulke, John Wiley & Sons, Inc., New York (1999), 181-308

427. M. Fineman and S.D. Ross, *Linear method for determining monomer reactivity ratios in copolymerization* ,J. Polym Sci., 5 (1950), 259-262.

428. T. Kelen and F. Tudos, "New improved linear graphical method for detemining copolymerization reactivity ratios" *React. Kinet. Catal. Lett* **1**, 487-492 (1974)

429. X.-D. Zhong, M. Ishifune, N.Yamashita, *Study on copolymerisation of acrylamide with styrene initiated by methyl ethyl ketone and its derivatives in comparison with conventional radical initiator* , J.M.S. Pure Appl.Chem., A37(2000), 49-63

430. J. A. Simms, *Epoxide-substituted vinyl and acrylate copolymers*, J. Appl. Polym. Sci. **13** (1961), 58-63.

431. A. S. Brar, A. Yadav, S. Hooda, *Characterization of glycidyl methacrylate/styrene copolymers by one- and two-dimensional NMR spectroscopy*, Eur. Polym. J., **38** (2002), 1683-1690

432. C.B Chapman, L. Valentine, *The preparation and properties of grafts of polycaprolactam on vinyl copolymers*, J. Polym. Sci., **34** (1959), 319

433. A. Zerroukhi, C. Cincu, J. P. Montheard, *Substituted Styrenes–Maleic Anhydride Copolymers—Measurements of the Reactivity Ratios with High Conversions and Relations between Molecular Masses and Viscosity*, J. Appl. Polym. Sci., **71**: (1999),1447–1454

434. D.M. Dibona, R.F. Fibiger, E.F. Gurnee, J.E. Suhuetz, *Copolymerization kinetics for 2-isopropenyl-2-oxazoline (methods and results)*, J. Appl. Polym. Sci., **31** (1986), 1509-1514

435. Y. Iwakura, T. Kurosaki, N. Nakabayashi, Macromol. Chem., 46 (1961), 570.

436. A. S. Brar, K.Dutta, *Acrylonitrile and Glycidyl Methacrylate Copolymers: Nuclear Magnetic Resonance Characterization*, Macromolecules 1998, *31*, 4695-4702

437. F.R. Mayo, F.M. Lewis, C. Walling, *Copolymerization. VIII. The Relation Between Structure and Reactivity of Monomers in Copolymerization*, J. Am. Chem. Soc., **70** (1948), 1529

438. B.C. Trivedi, B.M. Culbertson, *Chapter 9 Random Addition Copolymerisations*, in **Maleic Anhydride**, Plenum Press, New York (1982), 269–305.

439. A. D. Jenkins, *Reactivity in Radical Polymerization: Beyond the Q-e Scheme*, J. Polym. Sci. A: Polym.Chem., **34** (1996), 3495-3510

440. A.D. Jenkins, *Interpretation of reactivity in radical polymerisation-radicals, monomers and transfer agents: beyond the Q-e scheme*, J. Polym. Sci. A: Polym. Chem., **37** (1999), 113-126.

441. A. D. Jenkins, *The revised patterns of reactivity scheme. Part 6. A general formulation of the scheme and the 'alternating tendency'*, J.M.S.—Pure Appl. Chem., **A37** (2000), 1547–1569

442. P. Martin, J. Devaux, R. Legras, M. van Gurp, M. van Duin, *Competitive reactions during compatibilization of blends of polybutyleneterephthalate with epoxide-containing rubber*, Polym., , **42** (2001), 2463-2478.

Appendix-A

Table A2.1 Major FTIR absorbtion bands and their assignment of polymers [310,345-349].

Name	Figure	Peak (cm-1)	Intensity	Assignment
NR	Fig.A.2.1	3285	Broad-weak	υ(O-H) of protein/non rubber component
		3036	Broad weak	υ(=CH) in C(CH3)=CH)
		2834-2996	very strong	υ(CH2, CH3) sym. and asym
		2725	weak	υ(C-CH3)
		1742	weak	υ(C=O of protein/non rubber component)
		1662	medium	υ(C=C)
		1430-1456	very strong	δ(CH3), υ(CH3), δ(CH2)
		1374	strong	δ(CH2)
		1309	medium	τ(CH2)
		1287	weak	δ(CH)
		1239	medium	τ(CH)
		1127	medium	ν(C-C)cis
		1089	medium	ϖ(CH2)
		1037	medium	τ(CH3)
		1010	weak	υ(C-CH2)
		958	weak	υ(C-CH3)
		888	medium	ϖ(CH), υ(CH=CCH3)
		827-843	strong	υ(CH2-CH2), C-H out of plane cis C(CH3)=CH
		742	medium	ρ(CH2)
		574	medium	τ(=C-C-C)
PP	Fig. A2.2	2967	very strong	υ(CH3)
		2836	very strong.	υ(CH2)
		2720	weak	υ(C-CH3)
		1459	strong	δ(CH3)asym., δ(CH2)
		1376	strong	δ(CH3)sym., ω(CH2), δ(CH), υ(C-C)b
		1359	medium	υ(CH3)sym, δ(CH)
		1325	weak	δ(CH), τ(CH2)
		1304	weak	ω(CH2), τ(CH2)
		1255	weak	δ(CH), τ(CH2), ρ(CH2)
		1167	medium	υ(C-C)b, ρ(CH3), δ(CH)
		1105	very weak	υ(C-C)b, ρ(CH3), ω(CH2), τ(CH), δ(CH)
		1045	very weak	υ(C-CH3), υ(C-C)b, δ(CH)
		997	medium	ρ(CH3), δ(CH), ω(CH2)
		971	medium	ρ(CH3), υ(C-C)b
		940	very weak	ρ(CH3), υ(C-C)b
		899	weak	ρ(CH3), ρ(CH2), δ(C-H), δ(CH3)sym., ω(CH2)
		841	medium	ρ(CH2), υ(C-C)b, υ(C-CH3)b , ρ(CH3)
		809	weak	ρ(CH2), υ(C-C)b, υ(C-CH3)b
		966	strong	υ(C-C)
PBT	Fig.A.2.3	3440	weak	υ(aromatic ring)
		2962	medium	υ(CH2)
		1731	strong	υ(C=O)
		1409	strong	δ(CH2)
		1269	very strong	ϖ(CH2)
		1117	very strong	δ (aromatic ring)
		730	strong	out-of-plane of aromatic ring

Abreviation: b = backbone, δ = bending, υ = stretching, ρ = rocking, τ = twisting, ϖ = wagging

Table A2.2 Major absorbtion bands and probable assignment in the FTIR spectra of **monomers and coagents** (Cont.)

Name	Figure	Peak (cm^{-1})	Intensity	Assignment
GMA	Fig. 2.5	2958	weak	$\upsilon(CH_2,CH_3)$
		1720	very strong	υ(C=O)
		1638	medium	υ(C=C)
		1454	medium	$\delta(CH_3)$*asym*, $\delta(CH_2)$
		1379	weak	$\delta(CH_3)$, δ(CH), $\tau(CH_2)$
		1349	medium	$\delta(CH_3)$, δ(CH), $\tau(CH_2)$
		1317	strong	$\delta(CH{=}CH_2)$
		1296	very strong	$\tau(CH_2)$, $\varpi(CH_2)$, δ(CH)
		1255	weak	δ (CH), $\tau(CH_2)$, $\rho(CH_3)$
		1171	very strong	δ(C-O), $\rho(CH_3)$, $\upsilon(C\text{-}C)_b$, δ(CH)
		1018	medium	$\upsilon(C\text{-}CH_3)$, $\upsilon(C\text{-}C)_b$, δ(CH)
		944	medium	$\tau(CH{=}CH_2)$
		908	medium	υ(epoxy ring)
		843	medium	$\rho(CH_2)$, υ(epoxy ring), $\rho(CH_3)$
		815	medium	$\varpi(CH{=}CH_2)$
		762	medium	$\rho(CH_2)$,$\upsilon(C\text{-}CH_3)$, υ(epoxy ring)
MA	Fig. 2.6	3122	medium	υ(C-H)
		1855	medium	υ(C=O) asym.
		1775	strong	υ(C=O) sym.
		1752	strong	υ(C=O) asym.
		1705	strong	υ(C=O) sym.
		1632	medium	δ(C=C)
		1588	strong	δ(C=C)
		1566	strong	δ(C=C)
		1459	medium	δC-H in CH=CH
		1433	medium	δC-H in CH=CH
		1288	strong	δ(C-O)
		1266	strong	δ(C-O)
		1240	strong	δ (CH), δ(C=O in anhydride)
		1056	medium	δ (CH) in plane
		894	medium	υ(C-C)
		870	strong	δ(C-H) out of plane
		833	strong	δ (C-H)
		693	strong	δ (maleic anhydride ring)
		639	strong	δ (maleic anhydride ring)
		609	medium	δ (maleic anhydride ring)
		561	medium	δ(C=O)

Abreviation: b = backbone, δ = bending, υ = stretching, ρ = rocking, τ = twisting, ϖ = wagging

Table A2.2 (Cont.) Major absorbtion bands and probable assignment in the FTIR spectra of **monomers and coagents.**

Name	Figure	Peak (cm^{-1})	Intensity	Assignment
TRIS	Fig. 2.7	2970	medium	$\upsilon(CH_2,CH_3)$
		1728	strong	υ(>C=O)
		1635	medium	υ(C=C)
		1466	medium	$\delta(CH_3)$*asymmetric* $\delta(CH_2)$
		1408	strong	$\delta(CH{=}CH_2)$
		1295	medium	$\tau(CH_2)$, $\varpi(CH_2)$, δ(CH)
		1270	strong	$\tau(CH_2)$, $\varpi(CH_2)$, δ(CH)
		1188	strong	δ(CH) in plane, δ(C-O)
		1062	strong	$\rho(CH_3)$
		986	strong	υ(C-C), $\upsilon(C\text{-}CH_3)$, $\rho(CH_3)$, τ(CH)
		809	strong	υ(C-C), $\upsilon(C\text{-}CH_3)$, $\rho(CH_3)$, ϖ (CH)
DVB	Fig. 2.8	3087	strong	υ(CH)Aromatic
		2965	strong	υ(CH)aliphatic
		2872	strong	$\upsilon(CH_2)$aliphatic
		1817	medium	-
		1630	strong	$\upsilon(C{=}CH_2)$
		1596	strong	υ(C=C)Ar
		1510	strong	δ(CH) aromatic ring
		1485	strong	$\upsilon(CH{=}CH_2)$
		1454	medium	$\upsilon(CH{=}CH_2)$
		1400	strong	$\delta(CH{=}CH_2)$
		1282	weak	$\delta(CH{=}CH_2)$
		1210	weak	$\delta(CH{=}CH_2)$
		1167	weak	$\delta(CH{=}CH_2)$
		987	strong	$\tau(CH_2{=}C\text{-}H)$,$\rho(CH_3)$, $\rho(CH_2)$,υ(C-C)Ar
		945	weak	$\tau(CH_2{=}C\text{-}H)$,$\rho(CH_3)$, $\rho(CH_2)$,υ(C-C)Ar
		903	strong	$\tau(CH_2{=}C\text{-}H)$,$\rho(CH_3)$, $\rho(CH_2)$,υ(C-C)Ar
		845	strong	δ(CH) Aromatic ring
		800	strong	δ(=CH)
		708	strong	δ(CH) Aromatic ring
		673	weak	$\varpi(CH{=}CH_2)$
		617	weak	ϖ(=CH) phenyl ring

Abreviation: δ = bending, υ = stretching, ρ = rocking, τ = twisting, ϖ = wagging

Table A2.3 Major absorbtion bands and probable assignment in the FTIR spectra of **peroxides** (Continued)

Name	Figure	Peak (cm^{-1})	Intensity	Assignment
T-101	Fig. 2.9	2976	very strong	$\upsilon(CH_3)$
		2932	strong	$\upsilon(CH_2)$
		1472	medium	$\tau(CH_2)$
		1379	medium	$\delta(CH_3)$, $\varpi(CH_3)$, $\upsilon(C\text{-}C)_b$
		1363	weak	$\delta(CH_3)$, $\upsilon(C\text{-}H)$
		1239	medium	$\upsilon(C\text{-}O\text{-}O\text{-}C\text{-})$, $\delta(CH)$,$\rho(CH_3)$
		1200	medium	$\tau(CH_2)$, $\delta(CH)$, $\upsilon(C\text{-}C)_b$
		1144	medium	$\upsilon(C\text{-}C)_b$, $\upsilon(C\text{-}CH_3)$, $\delta(CH)$
		1103	weak	$\upsilon(C\text{-}C)_b$, $\varpi(CH_3)$, $\tau(CH)$
		881	strong	$\upsilon(C_3C\text{-}O)$
		753	medium	$\upsilon(C\text{-}O\text{-}O\text{-}C)$
T-29B90	Fig. 2.10	2976	very strong	$\upsilon(CH_3)$asym.
		2954	very strong	$\upsilon(CH_2)$asym.
		2926	very strong	$\upsilon(CH_3)$sym
		2869	strong	$\upsilon(CH_2)$sym
		2838	strong	$\upsilon(CH_2)$sym
		1732	strong	υ(C=O) of dibutyl phthalate (impurity)
		1473	strong	$\delta(CH_3)$asym.
		1456	medium	$\delta(CH_2)$
		1386	strong	$\varpi(CH_2)$
		1362	very strong	$\tau(CH_2)$
		1288	strong	$\varpi(CH_2)$, $\delta(CH_2)$, $\tau(CH_2)$
		1242	strong	$\upsilon(C\text{-}O\text{-}O\text{-}C\text{-})$, $\varpi(CH_2)$, $\delta(CH_2)$
		1192	very strong	$\delta(CH)$, $\tau(CH_2)$, $\rho(CH_2)$
		1152	strong	$\upsilon(C\text{-}C)$, $\upsilon(C\text{-}CH_3)$, $\delta(CH)$
		976	strong	$\upsilon(C\text{-}C)$, $\upsilon(C\text{-}CH_3)$, $\delta(CH)$
		952	medium	$\rho(CH_3)$, $\rho(CH_2)$, $\delta(CH)$
		921	medium	$\rho(CH_3)$, $\upsilon(C\text{-}C)$
		885	strong	$\rho(CH_3)$, $\upsilon(C\text{-}C)$
		860	strong	$\upsilon(C_3\text{-}C\text{-}O)$
		823	medium	$\upsilon(C_3\text{-}C\text{-}O)$
		760	strong	$\upsilon(\text{-}C\text{-}O\text{-}O\text{-}C\text{-})$
		668	medium	$\delta(C\text{-}O)$

Abreviation: b = backbone, δ = bending, υ = stretching, ρ = rocking, τ = twisting, ϖ = wagging

Table A2.3 (Cont.) Major absorbtion bands and probable assignment in the FTIR spectra of **peroxides.**

Name	Figure	Peak (cm^{-1})	Intensity	Assignment
DCP	Fig.2.11	3061, 3004	medium	υ(CH)ar.
		2988, 2973	medium	$\upsilon(CH_3)$asym.
		2927, 2855	medium	$\upsilon(CH_3)$sym.
		1493,1448	medium	$\delta(CH_3)$, $\delta(CH_2)$
		1375, 1360	medium	$\delta(CH_3)$, τ(CH)
		1262	strong	υ(C-C), $\rho(CH_3)$
		1158, 1102	strong	$\upsilon(C\text{-}CH_3)$, δ(CH)
		1073,1028	strong	$\upsilon(C_3\text{-}C\text{-}O)$
		933, 914	strong	υ(-C-O-O-C-)
		859	strong	δ(-C-O-O-C-)
		769, 702	very strong	$\delta\ (CH)_{Ar}$
BPO	Fig. 2.12	1780	strong	υ(>C=O) asym
		1762	strong	υ(>C=O) sym.
		1596	medium	υ(=CH aromatic)
		1446	medium	(C-O)
		1232	strong	δ(CH), τ(CH), ρ(CH)
		1180	strong	aryl C-O stretching
		999	strong	υ(O-O)
		845	medium	δ(CH)
		706	strong	δ phenylene ring.
AIBN	Fig. 2.13	2997	medium	$\upsilon(CH_3)$
		2243	small	υ(C≡N)
		1459	medium	υ(N=N)
		1381	medium	$\upsilon(C\text{-}CH_3)$
		1365	medium	$\upsilon(C\text{-}CH_3)$
		1229	strong	υ(C-N)
		1176	strong	$\upsilon(C\text{-}CH_3)$
		950	medium	-
		851	medium	υ(C-N=N-C)
		706	medium	δ(C-N=N-C)
Abreviation: b = backbone, δ = bending, υ = stretching, ρ = rocking, τ = twisting, ϖ = wagging				

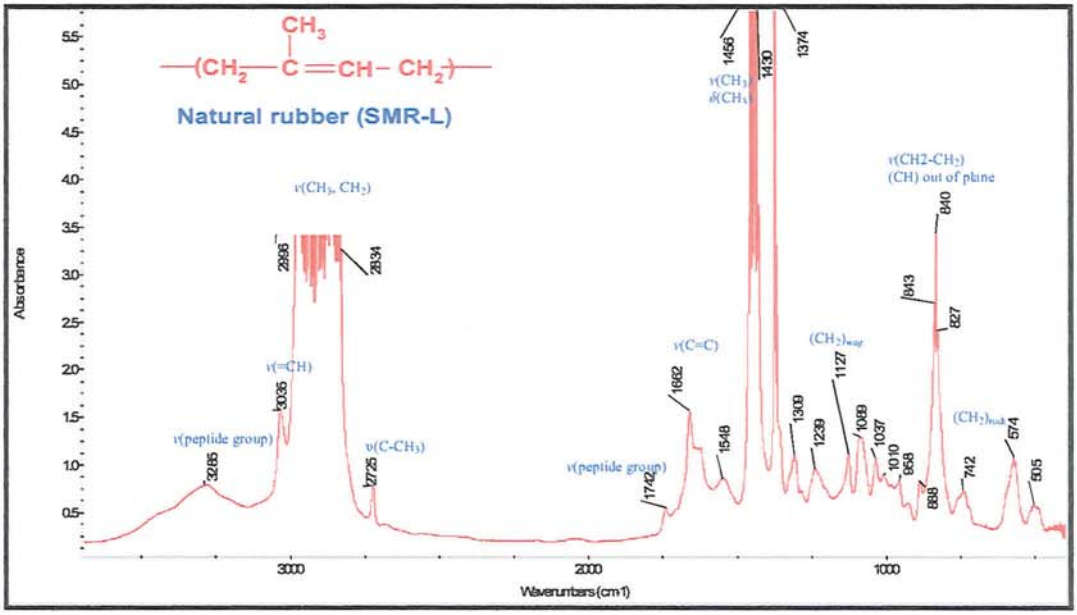

Figure A2.1 FTIR spectrum of cured natural rubber film **(SMR-L)**, thickness ~ 0.1 mm, (samples unpurified raw natural rubber).

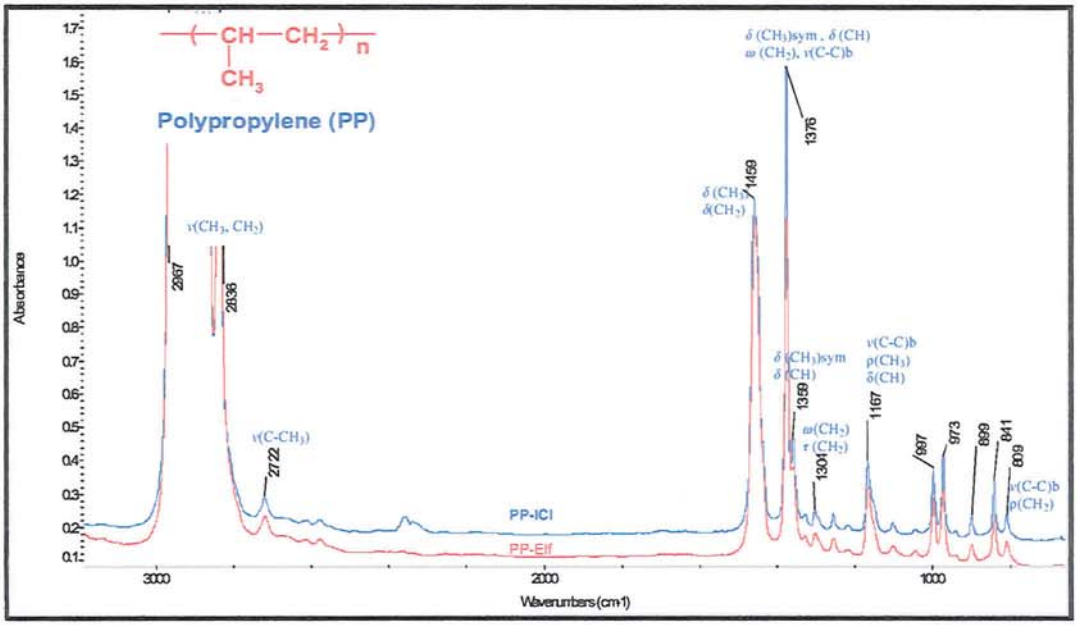

Figure A2.2 FTIR spectrum of pressed film of unprocessed polypropylene (PP), PP-ICI (blue) and PP-Elf (red), thickness ~ 0.1 mm, pressed in Daniel Press at 160°C, 2 min.

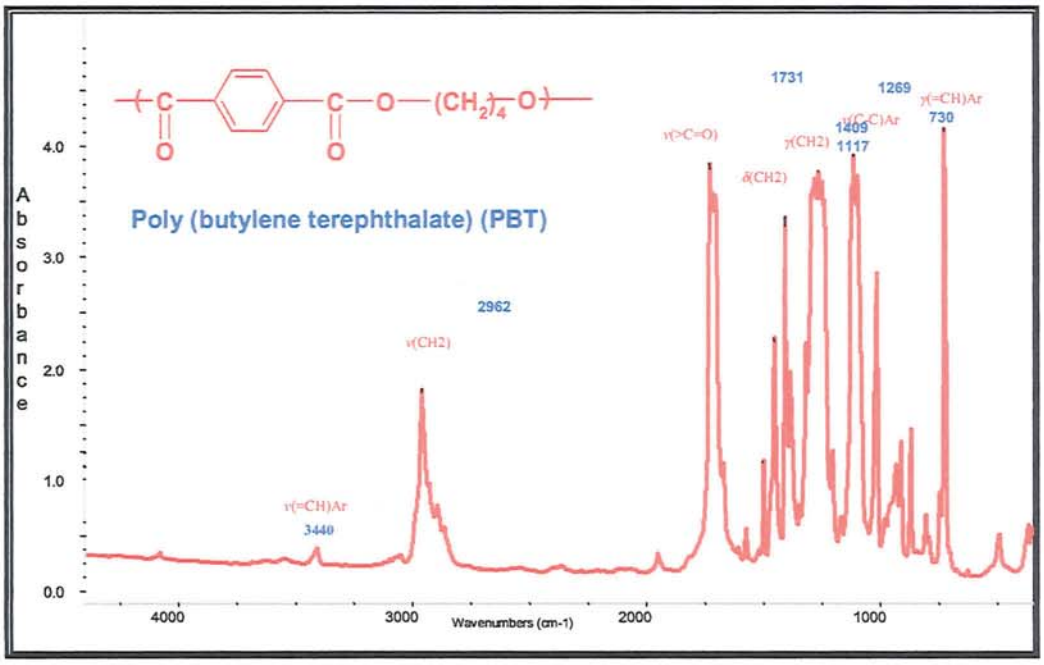

Figure A2.3 FTIR spectrum of pressed film of PBT (thickness ~0.1 mm), Sample PBT Arnite T0820 pressed in Daniel Press 265°C, 60 kg/cm^2, 1 min.

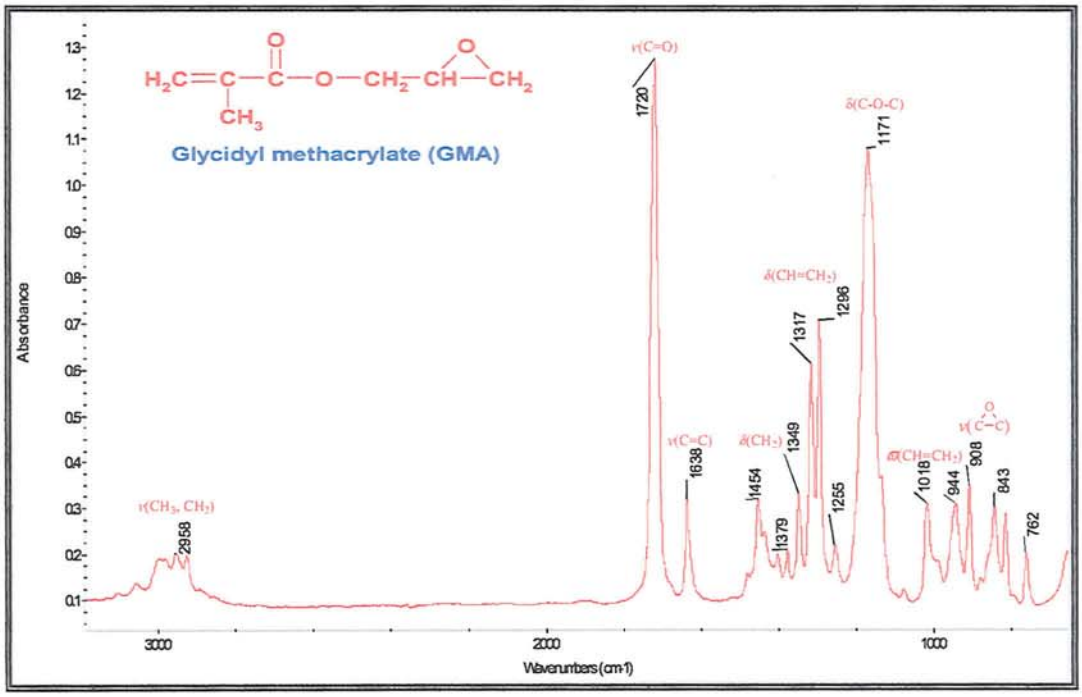

Figure A2.4 FTIR spectrum of neat **GMA** film between KBR cells.

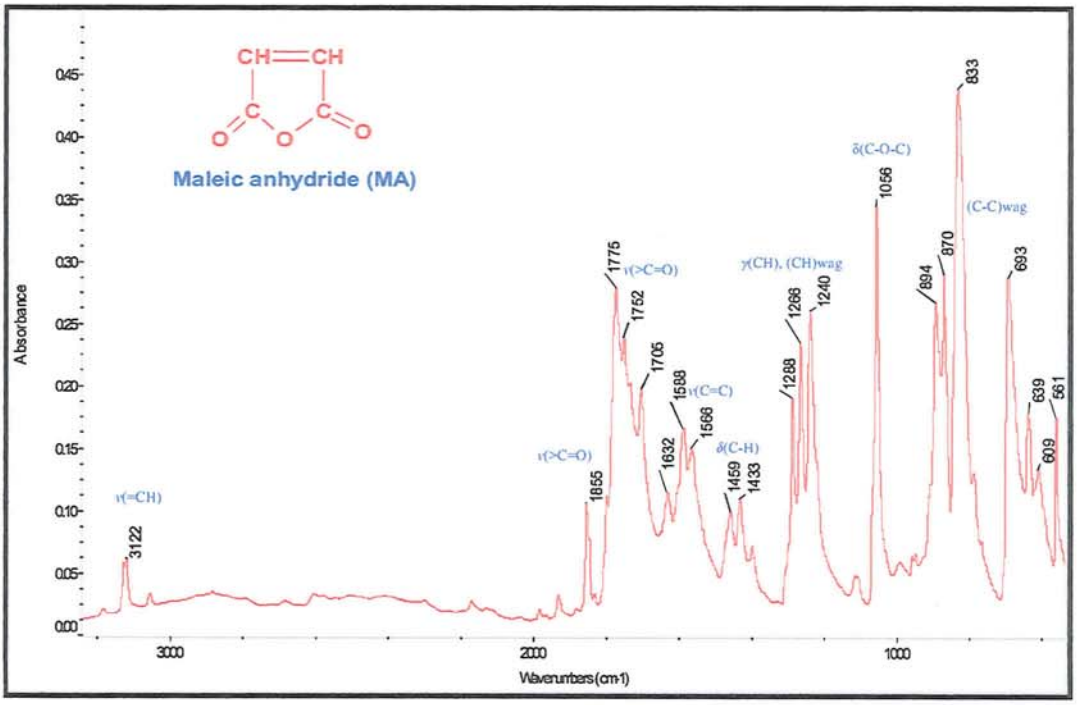

Figure A2.5 FTIR spectrum of MA (ATR-FTIR)

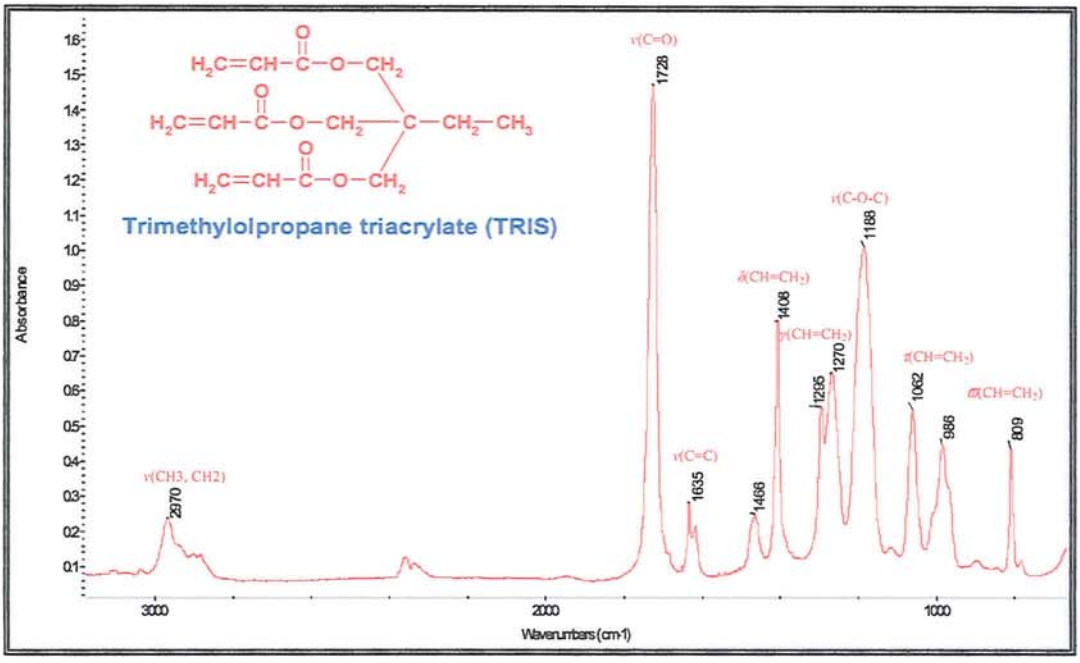

Figure A2.6 FTIR spectrum of neat **TRIS** film between KBR cells

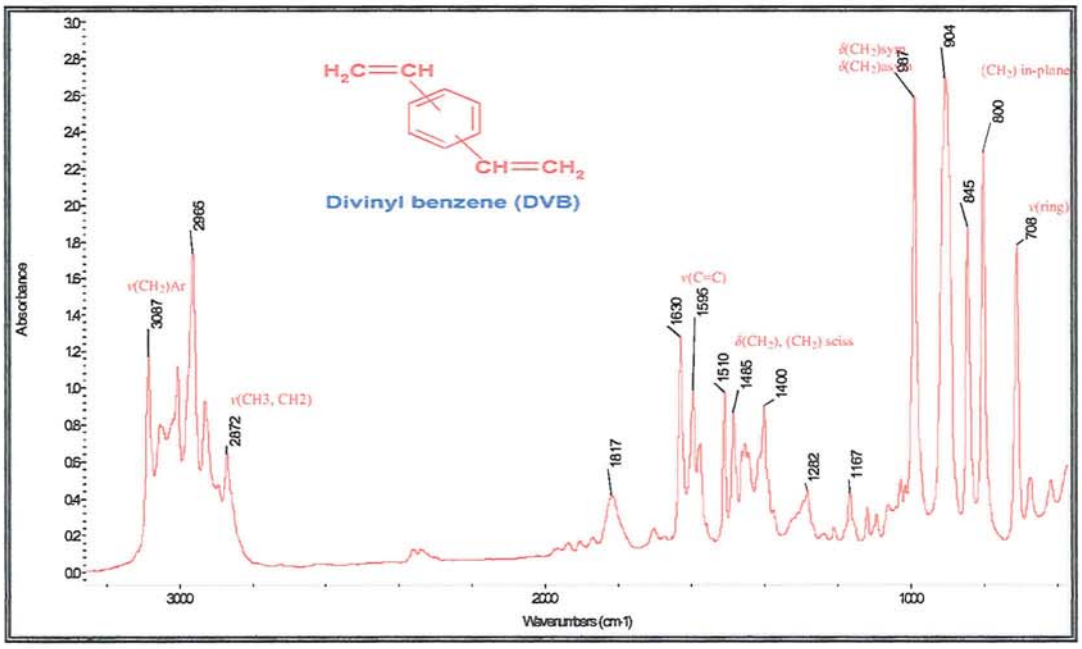

Figure A2.7 FTIR spectrum of neat DVB film between KBR cells

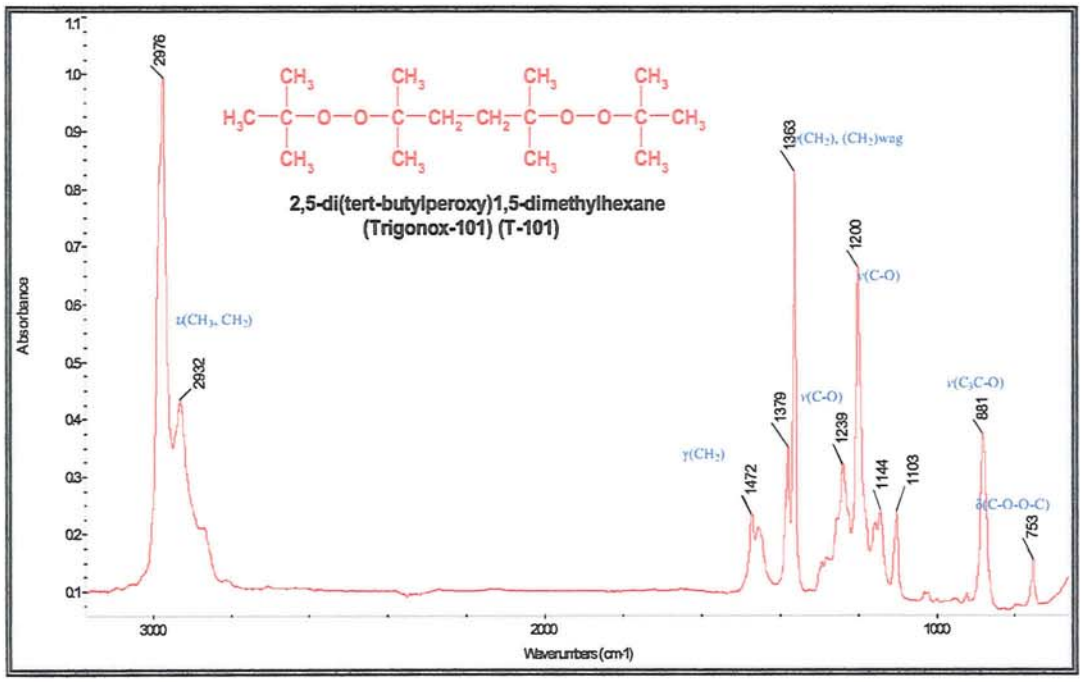

Figure A2.8 FTIR Spectrum of neat **Trigonox-101** between KBR cells

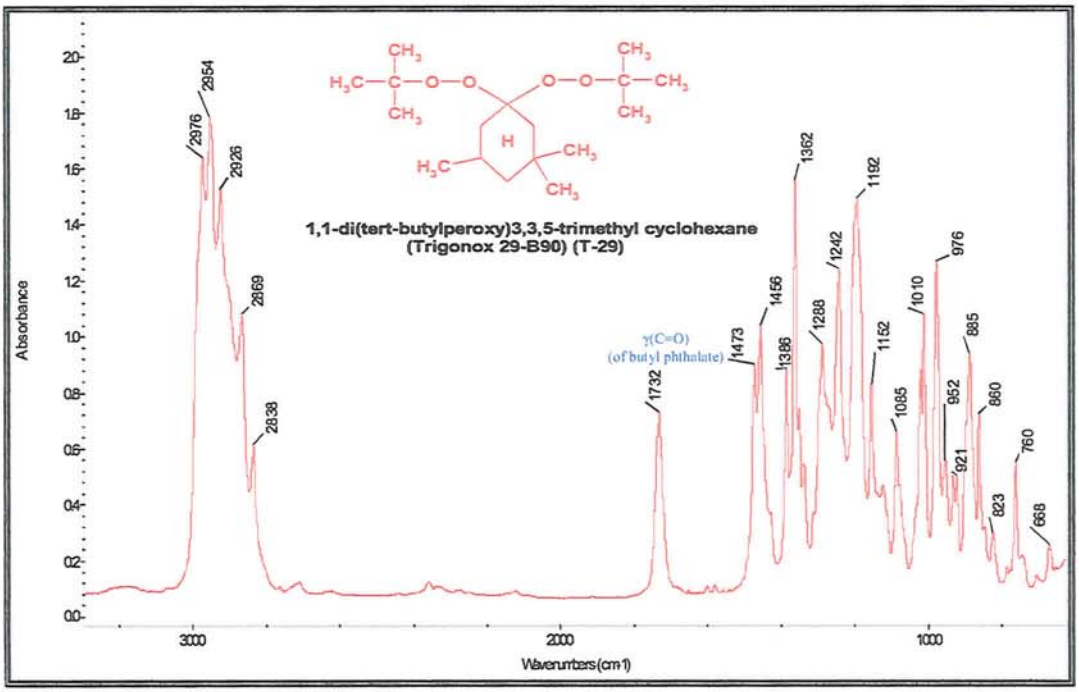

Figure A2.9 FTIR Spectrum of neat **Trigonox-29B90** between KBR cells

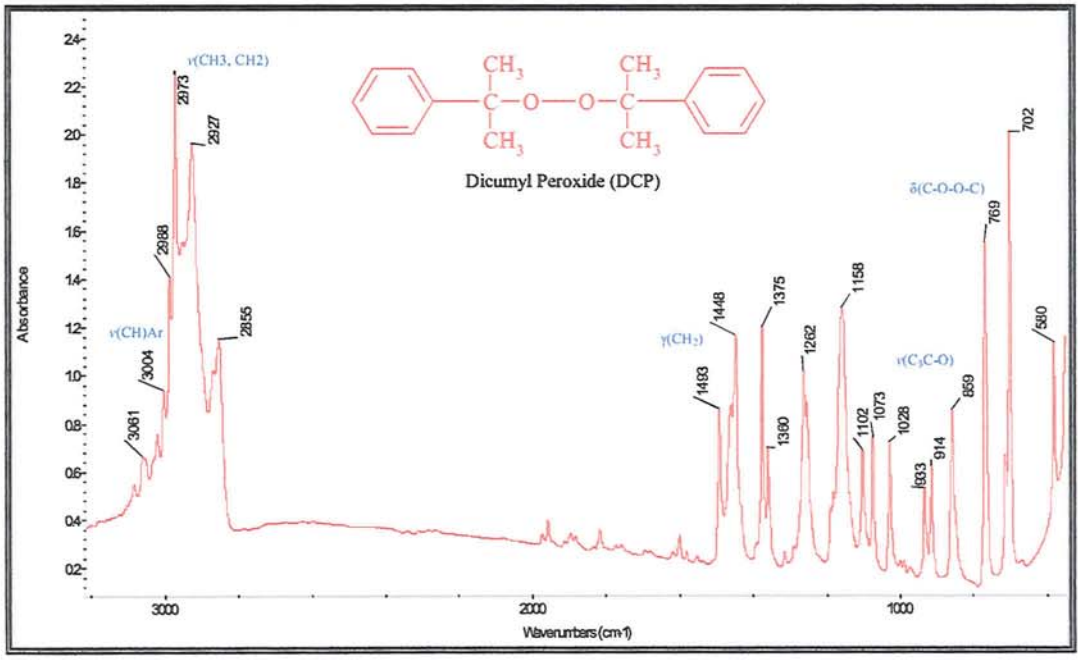

Figure A2.10 FTIR Spectrum of neat dicumyl **peroxide (DCP)** between KBR cells.

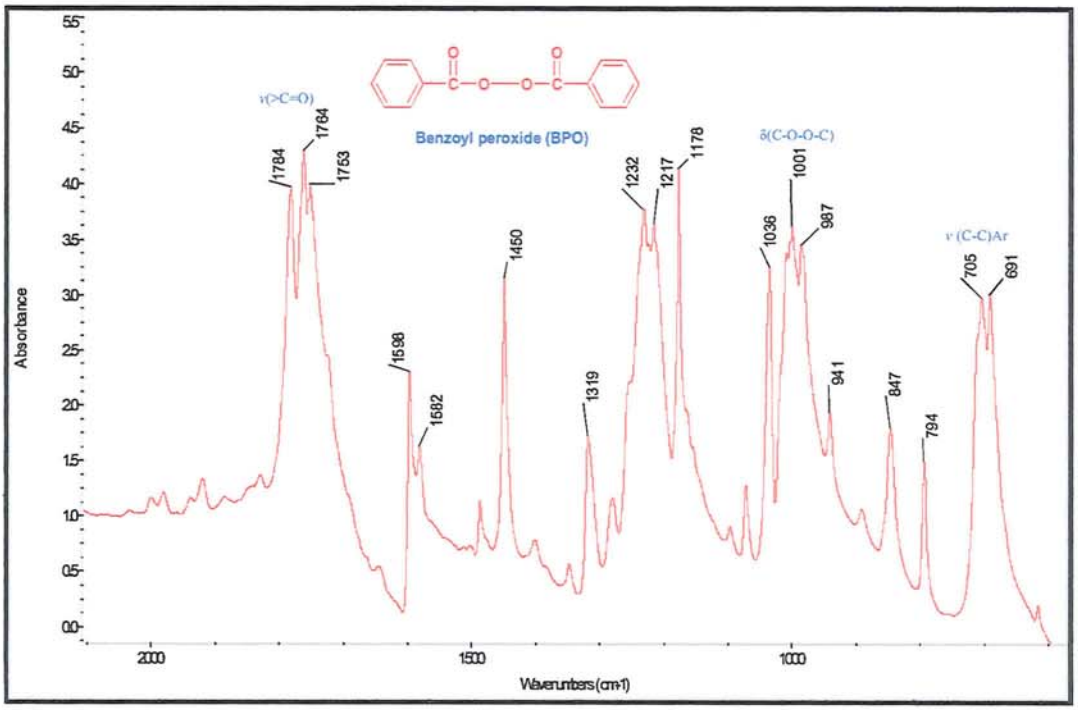

Figure A2.11 FTIR Spectrum of neat benzoyl **peroxide (BPO)** between KBR cells.

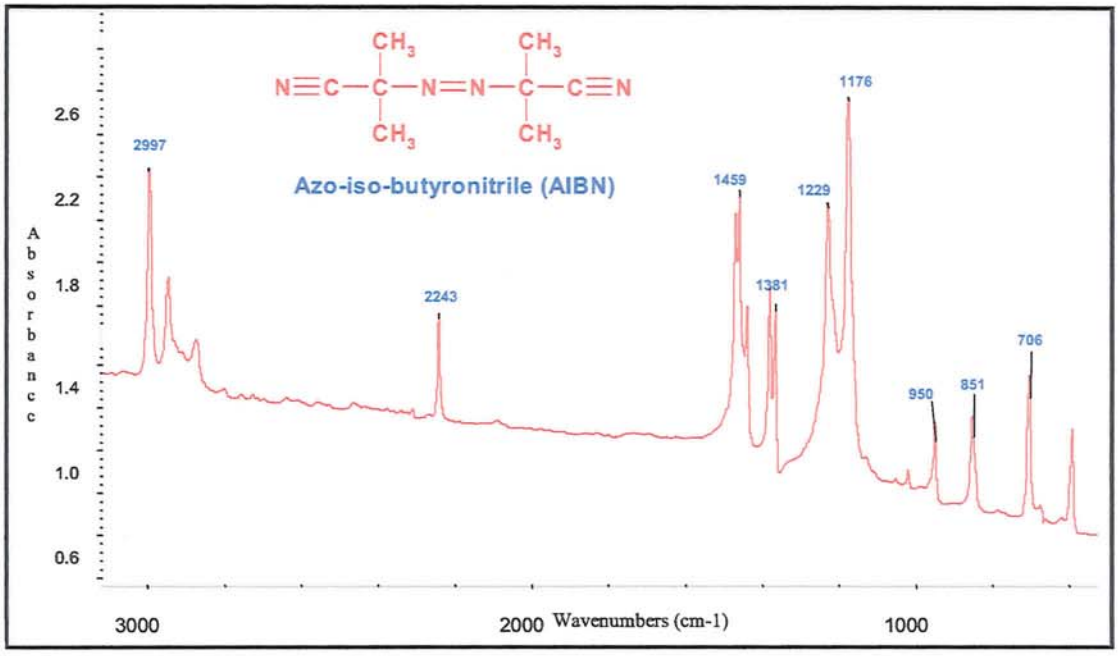

Figure A2.12 FTIR Spectrum of neat **azoisobutyronitrile (AIBN)** between KBR cells

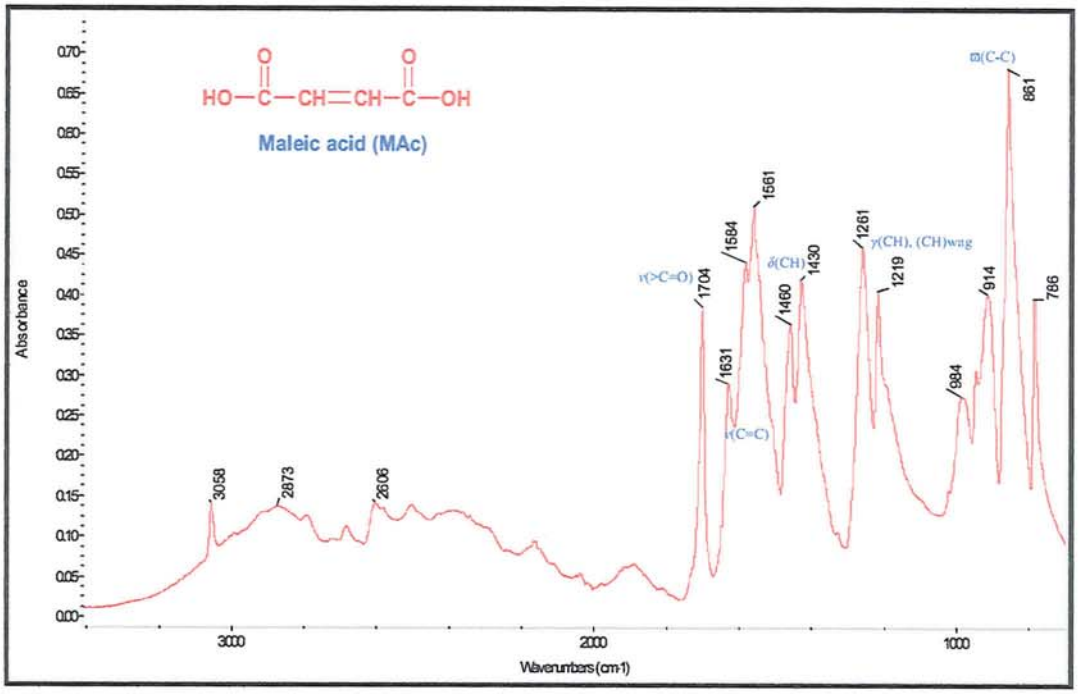

Figure A2.13 FTIR spectrum of Maleic acid (FTIR-ATR)

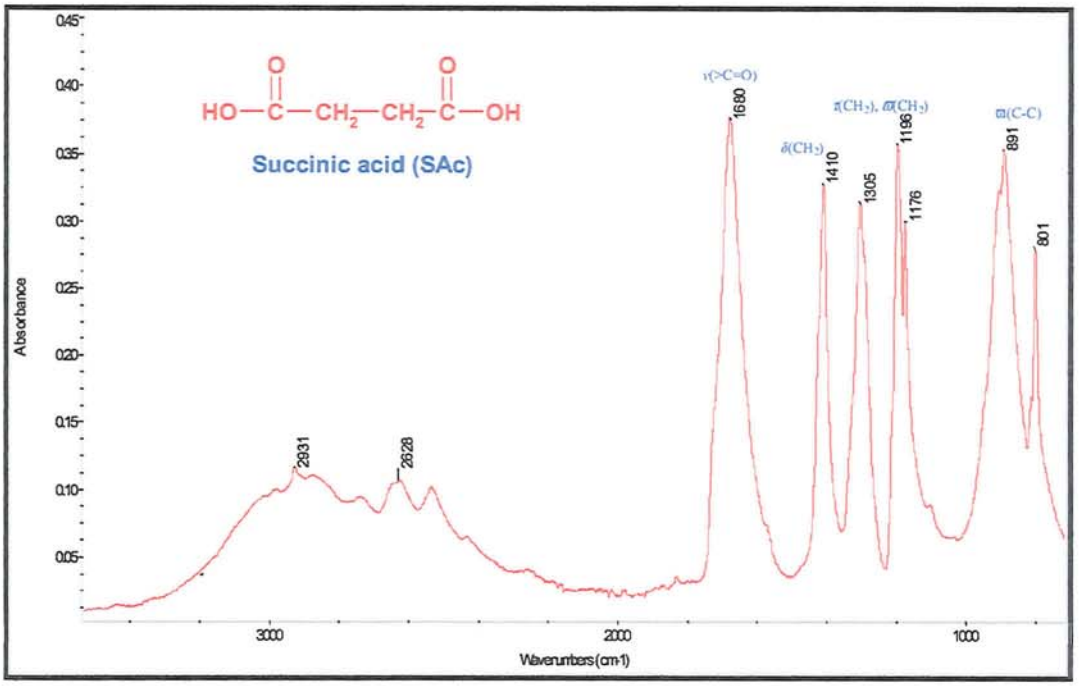

Figure A2.14 FTIR spectrum of succinic acid (FTIR-ATR)

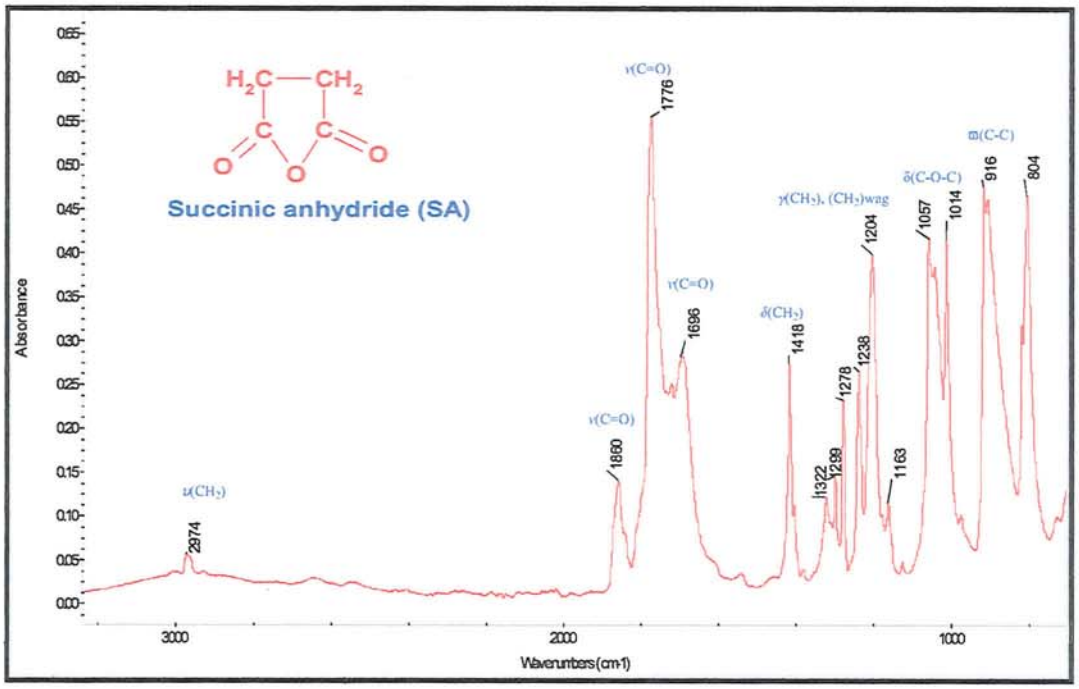

Figure A2.15 FTIR spectrum of succinic anhydride (FTIR-ATR)

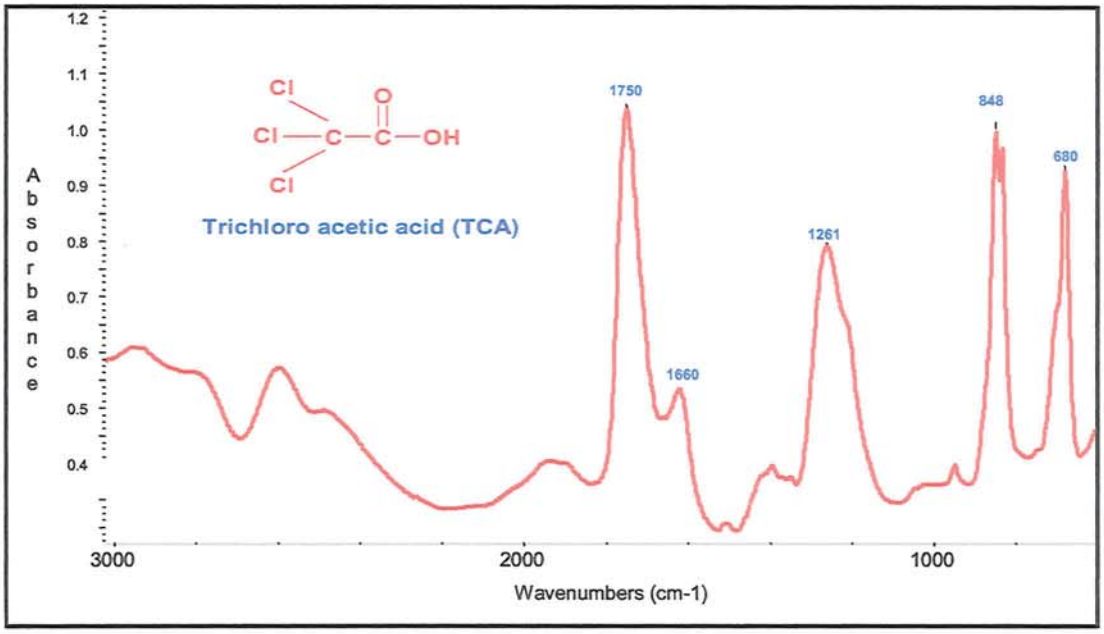

Figure A2.16 FTIR Spectrum of neat **tricholoro acetic acid (TCA)** between KBR cells

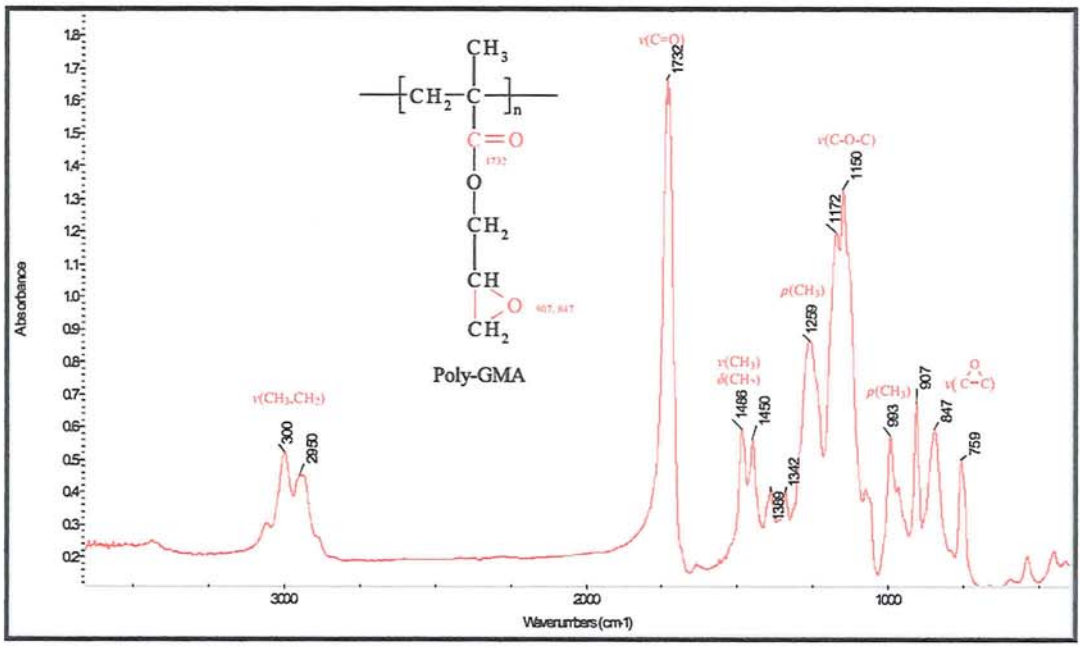

Figure A2.17 FTIR-ATR spectrum **Poly-GMA** (diamond ATR attachment).

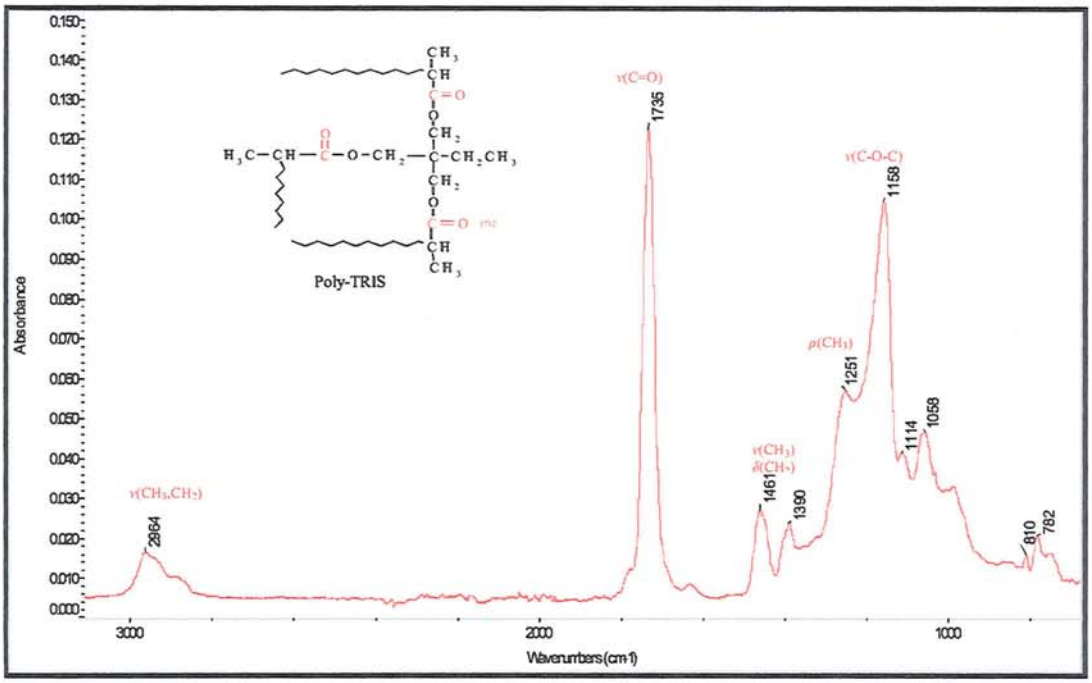

Figure A2.18 FTIR-ATR spectrum of **poly-TRIS** (diamond ATR attachment)

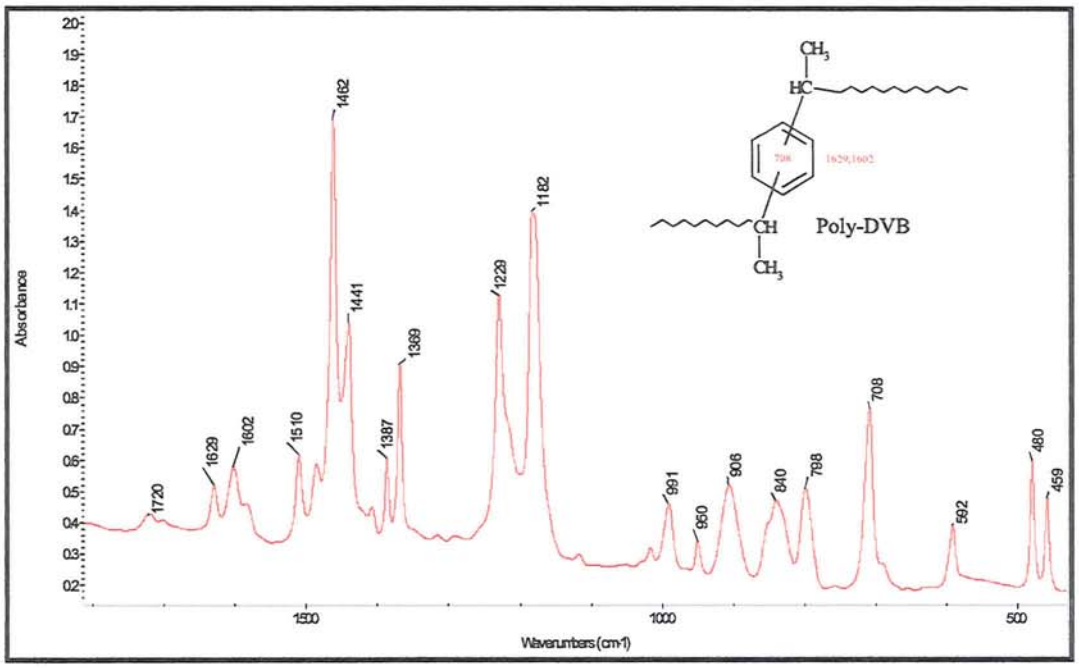

Figure A2.19 FTIR-ATR spectrum of **Poly-DVB** (diamond ATR attachment).

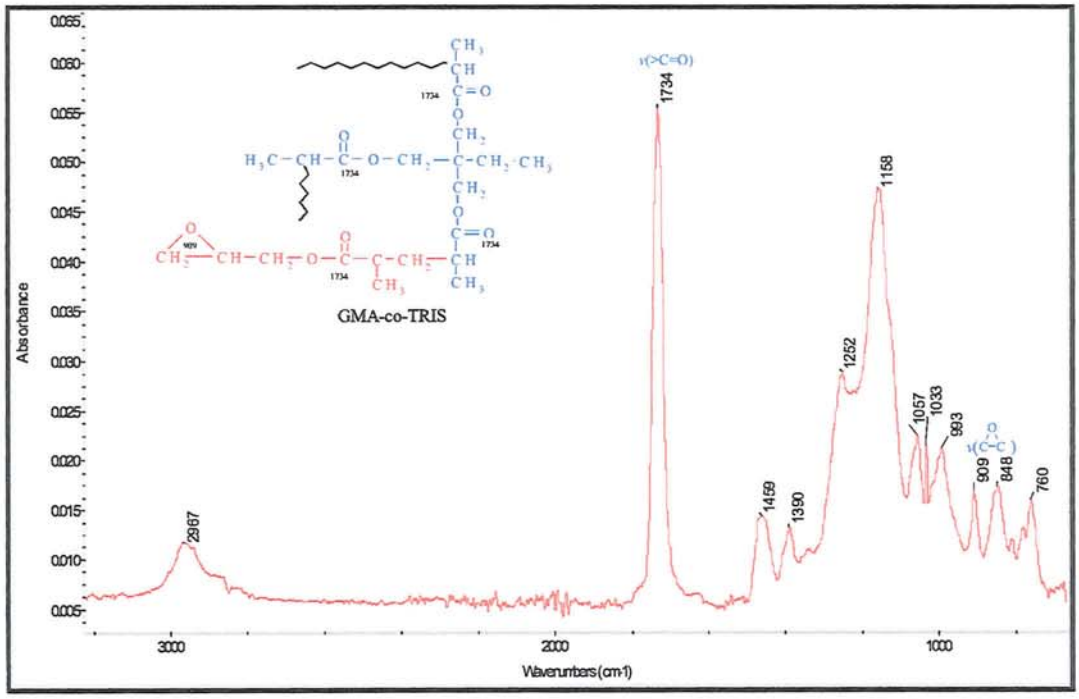

Figure A2.20 FTIR-ATR spectrum of **GMA-*co*-TRIS** (diamond ATR attachment).

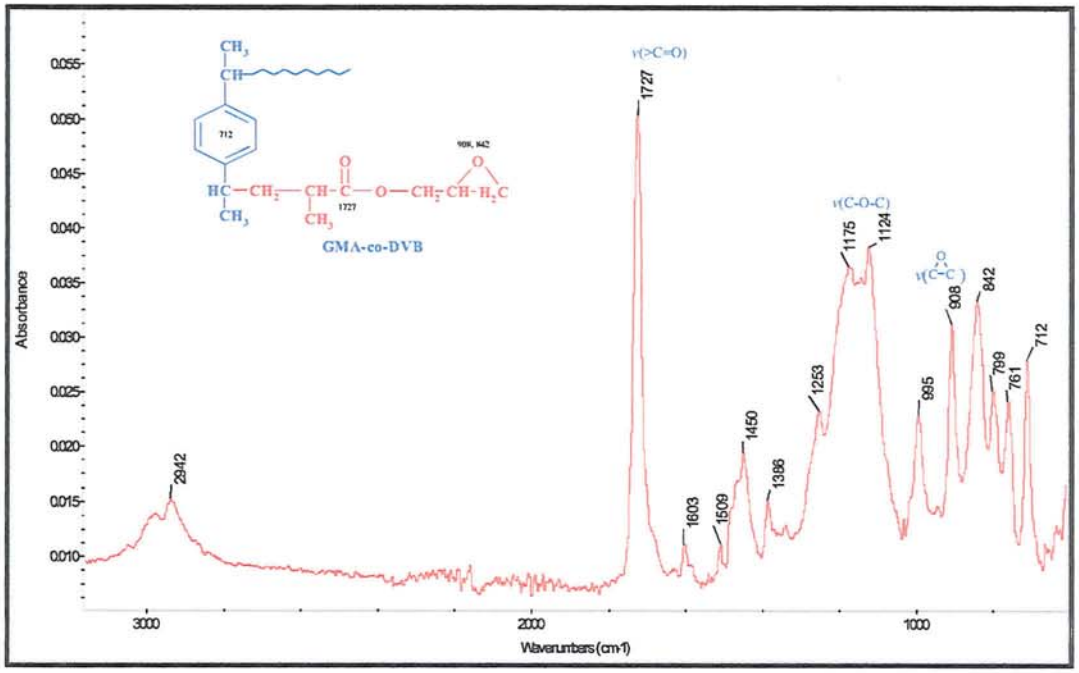

Figure A2.21 FTIR-ATR spectrum of **GMA-*co*-DVB** (diamond ATR attachment).

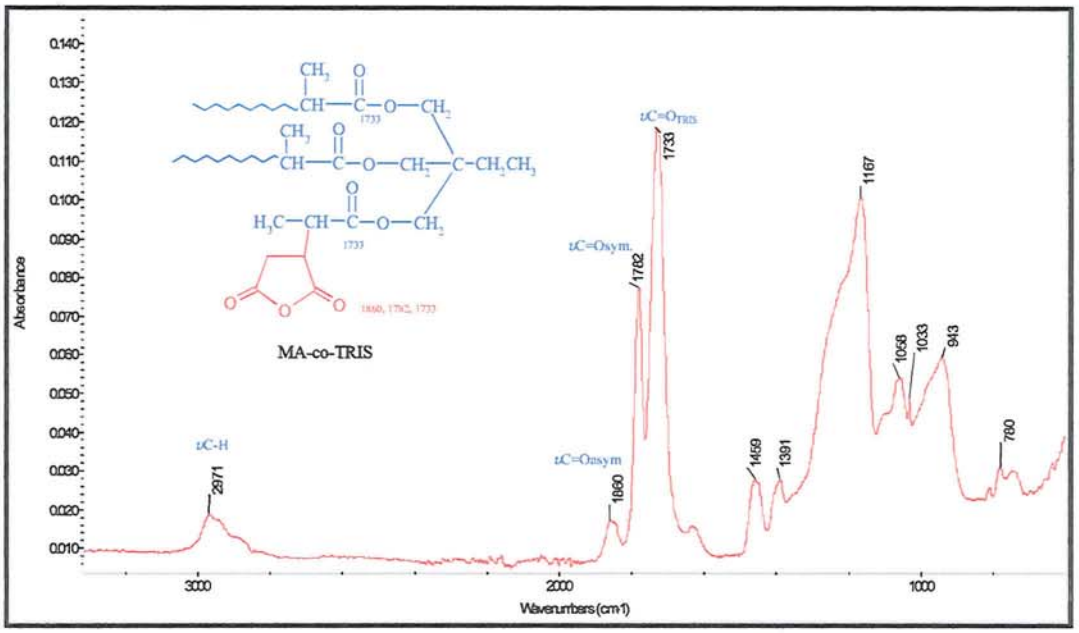

Figure A2.22 FTIR-ATR spectrum of copolymer **MA-*co*-TRIS** (diamond ATR attachment)

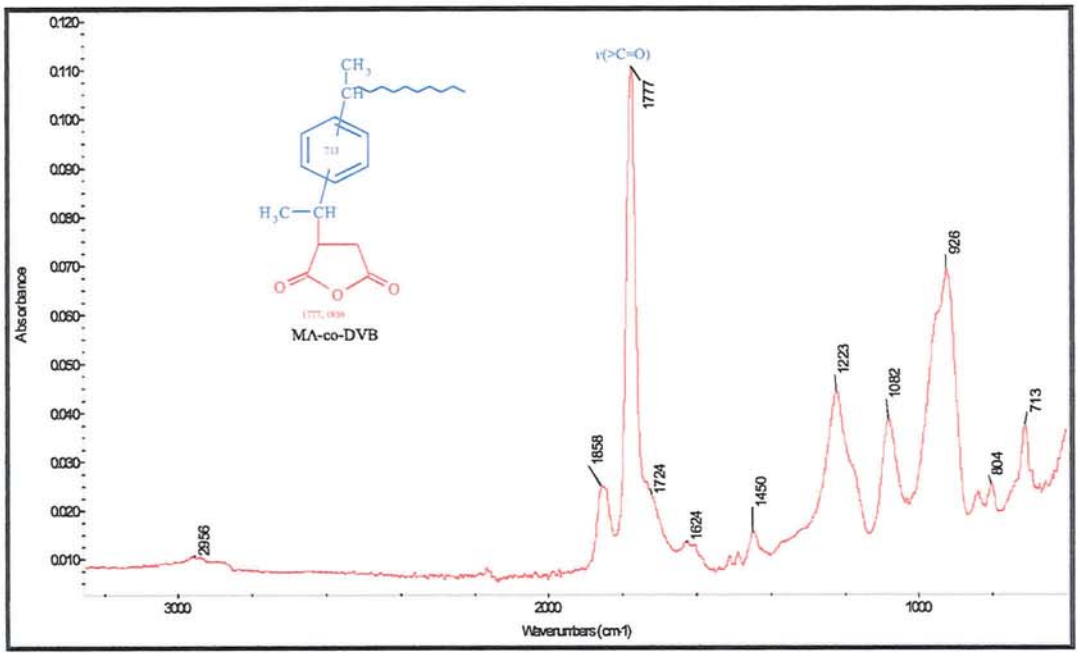

Figure A2.23 FTIR-ATR spectrum of copolymer **MA-*co*-DVB** (diamond ATR attachment).

Appendix B

Table B.3.1 Chemical compositions and processing conditions for NR/GMA **(Thermal Initiation)** system and calculated grafting yields.

Sample Code		Processing Composition			Processing Condition				Analysis		
		SMR-L (phr)	GMA (%)	[T-101] (mr)	Rotor speed (rpm)	Oil Temp (°C)	Mixing Time (minutes)	Atmos-phere	Grafting Degree (%)	Grafting Effcn. (%)	method
C1-n	C1-0	100	-	-	-	-	-	-	-	-	-
	C1-1	100	0	0	65	120	15	'Air'	-	-	IR
	C1-2	100	0	0	65	160	15	'Air'	-	-	IR
	C1-3	100	0	0	65	170	15	'Air'	-	-	IR
	C1-4	100	0	0	65	180	15	'Air'	-	-	IR
	C1-5	100	0	0	65	200	15	'Air'	-	-	IR
G0-n	G0-1	100	3	0	65	160	10	Nitrogen	0.3	10	IR
	G0-2	100	6	0	65	160	10	Nitrogen	0.7	12	IR
	G0-3	100	9	0	65	160	10	Nitrogen	1.0	11	IR
	G0-4	100	12	0	65	160	10	Nitrogen	1.1	9	IR
	G0-5	100	15	0	65	160	10	Nitrogen	1.3	9	IR
	G0-6	100	18	0	65	160	10	Nitrogen	1.5	8	IR
T1-n	T1-1	100	6	0	65	100	15	'Air'	0.1	1.7	IR
	T1-2	100	6	0	65	120	15	'Air'	0.2	3.3	IR
	T1-3	100	6	0	65	140	15	'Air'	0.5	8.3	IR
	T1-4	100	6	0	65	160	15	'Air'	0.7	11.7	IR
	T1-5	100	6	0	65	170	15	'Air'	0.6	10	IR
	T1-6	100	6	0	65	180	15	'Air'	0.5	8.3	IR
	T1-7	100	6	0	65	200	15	'Air'	0.4	6.7	IR
T2-n	T2-1	100	15	0	65	150	15	Nitrogen	0.4	2.7	Tr
	T2-2	100	15	0	65	170	15	Nitrogen	0.8	5.3	Tr
	T2-3	100	15	0	65	190	15	Nitrogen	2.0	13.3	Tr
	T3-4	100	15	0	65	210	15	Nitrogen	1.8	12	Tr
t1-n	t1-1	100	6	0.0	65	200	2.5	Nitrogen	0.3	5	IR
	t1-2	100	6	0.0	65	200	5	Nitrogen	0.6	10	IR
	t1-3	100	6	0.0	65	200	10	Nitrogen	0.8	13.3	IR
	t1-4	100	6	0.0	65	200	15	Nitrogen	0.8	13.3	IR
t2-n	t2-1	100	15	0.0	65	170	2.5	Nitrogen	0.2	1.3	Tr
	t2-2	100	15	0.0	65	170	5	Nitrogen	0.6	4	Tr
	t2-3	100	15	0.0	65	170	10	Nitrogen	0.9	6	Tr
	t2-4	100	15	0.0	65	170	15	Nitrogen	0.85	5.7	Tr
t3-n	t3-1	100	15	0.0	65	200	2.5	Nitrogen	0.4	2.7	Tr
	t3-2	100	15	0.0	65	200	5	Nitrogen	0.7	4.7	Tr
	t3-3	100	15	0.0	65	200	10	Nitrogen	1.3	8.7	Tr
	t3-4	100	15	0.0	65	200	15	Nitrogen	1.5	10	Tr

Abreviation: **C1-n** = control NR (no GMA and peroxide) in different temperatures; **G0-n** = NR + GMA in different [GMA] (no peroxide); **T1-n** and **T2-n** = NR + GMA (no peroxide) in different temperature; **t1-n, t2-n, t3-n =**: NR + GMA (no peroxide) in different in processing time ; **phr** = per hundreds (weight) rubber; **mr** = molar ratio to GMA; **IR** = infra red measurement; **Tr** = Titration method

Table B.3.2 Chemical compositions and processing conditions for **NR/GMA/T-101** system and calculated grafting yields (cont.)

Sample Code		Processing Composition				Processing condition				Analysis		
		SMR-L (phr)	GMA (%)	[T-101] (mr)		r.speed (rpm)	Temp (°C)	Time (minutes)	Atmos-phere	g-GMA (%)	Graft. Effic n	method
M1	M-1	100	12	0.02		75	160	15	Nitrogen	3.7	30.8	IR
M2-n	M2-1	100	12	0.004	+0.016	75	160	15	Nitrogen	3.5	29.2	IR
	M2-2	100	12	0.01	+0.01	75	160	15	Nitrogen	3.7	30.8	IR
	M2-3	100	12	0.016	+0.004	75	160	15	Nitrogen	4	33.3	IR
M2-2n	M2-21	100	12	0.005	+0.005	65	160	10	Nitrogen	3.5	29.2	IR
	M2-22	100	12	0.01	+0.01	65	160	10	Nitrogen	4.4	36.7	IR
	M2-23	100	12	0.015	+0.015	65	160	10	Nitrogen	5.2	43.3	IR
	M2-24	100	12	0.02	+0.02	65	160	10	Nitrogen	5.4	45	IR
M2-4n	M2-41	100	12	0.000	0.04	65	160	15	Nitrogen	3.1	25.8	IR
	M2-42	100	12	0.005	0.035	65	160	15	Nitrogen	3.8	31.7	IR
	M2-43	100	12	0.010	0.030	65	160	15	Nitrogen	4	33.3	IR
	M2-44	100	12	0.015	0.025	65	160	15	Nitrogen	4.4	36.7	IR
	M2-45	100	12	0.020	0.020	65	160	15	Nitrogen	4.6	38.3	IR
	M2-46	100	12	0.025	0.015	65	160	15	Nitrogen	4.6	38.3	IR
	M2-47	100	12	0.030	0.010	65	160	15	Nitrogen	4.7	39.2	IR
	M2-48	100	12	0.035	0.005	65	160	15	Nitrogen	4.8	40	IR
M-3	M-3	100	12	0.02		75	160	15	Nitrogen	3.3	27.5	IR
M3-n	M3-1	100	12	0.01		65	160	10	Nitrogen	2.6	21.7	IR
	M3-2	100	12	0.02		65	160	10	Nitrogen	3.3	27.5	IR
	M3-3	100	12	0.03		65	160	10	Nitrogen	3.3	27.5	IR
M4-1n	M4-11	100	12	0.005	0.015	75	160	15	Nitrogen	4.2	35	IR
	M4 -12	100	12	0.01	0.01	75	160	15	Nitrogen	3.5	29.2	IR
	M4 -13	100	12	0.015	0.005	75	160	15	Nitrogen	2.9	24.2	IR
M4-2n	M4-21	100	12	0.005	0.005	65	160	10	Nitrogen	3.9	32.5	IR
	M4 -22	100	12	0.01	0.01	65	160	10	Nitrogen	4	33.3	IR
	M4 -23	100	12	0.015	0.015	65	160	10	Nitrogen	4.6	38.3	IR
M4-3n	M4-31	100	12	0.002	0.018	75	160	15	Nitrogen	3.8	31.7	IR
	M4-32	100	12	0.004	0.016	75	160	15	Nitrogen	3.7	30.8	IR
	M4-33	100	12	0.006	0.014	75	160	15	Nitrogen	3.6	30	IR
	M4-34	100	12	0.008	0.012	75	160	15	Nitrogen	3.4	28.3	IR
	M4-35	100	12	0.01	0.010	75	160	15	Nitrogen	3.4	28.3	IR
	M4-36	100	12	0.012	0.008	75	160	15	Nitrogen	3.2	26.7	IR
	M4-37	100	12	0.014	0.006	75	160	15	Nitrogen	2.8	23.3	IR
	M4-38	100	12	0.016	0.004	75	160	15	Nitrogen	2.7	22.5	IR
	M4-39	100	12	0.018	0.002	75	160	15	Nitrogen	2.3	19.2	IR
T3-n	T3-1	100	12	0.02		75	140	15	Nitrogen	3.3	27.5	IR
	T3-2	100	12	0.02		75	160	15	Nitrogen	3.7	30.8	IR
	T3-3	100	12	0.02		75	180	15	Nitrogen	4.4	36.7	IR
	T3-4	100	12	0.02		75	200	15	Nitrogen	4	33.3	IR
T4-n	T4-1	100	15	0.02		65	150	15	Nitrogen	3.7	24.7	Tr
	T4-2	100	15	0.02		65	170	15	Nitrogen	4.2	28	Tr
	T4-3	100	15	0.02		65	190	15	Nitrogen	-	-	Tr
	T4-4	100	15	0.02		65	210	15	Nitrogen	-	-	Tr
T5-n	T5-1	100	6	0.04		65	100	15	'Air'	0.8	13.3	IR
	T5-2	100	6	0.04		65	120	15	'Air'	1.3	21.7	IR
	T5-3	100	6	0.04		65	140	15	'Air'	2.0	33.3	IR
	T5-4	100	6	0.04		65	160	15	'Air'	2.4	40	IR
	T5-5	100	6	0.04		65	170	15	'Air'	2.4	40	IR
	T5-6	100	6	0.04		65	180	15	'Air'	1.9	31.7	IR
	T5-7	100	6	0.04		65	200	15	'Air'	1.7	28.3	IR

Abreviation: **M1, M2-n, M3-n, M4-n** = NR+GMA+T-101 in different addition sequence method; **T3-n, T4-n , T5-n** = NR+GMA+T-101 in different temperature; **phr** = per hundreds (weight) rubber; **mr** = molar ratio to GMA; **IR** = infra red measurement; **Tr** = Titration method; All samples (NR/GMA/T-101) were processed using method-1 **(M1)** except **M2, M3, M4** (see Scheme 3-2).

Table B.3.2 (cont.) Chemical compositions and processing conditions for **NR/GMA/T-101** system and calculated grafting yields.

Sample Code		Processing Composition			Processing condition				Analysis		
		SMR-L (phr)	[GMA] (%)	[T101] (mr)	Rotor speed (rpm)	Oil Temp (°C)	Mixing Time (minutes)	Atmos-phere	Grafting Degree (%)	Grafting Effcn. (%)	method
T6-n	T5-1	100	6	0.04	65	100	15	Nitrogen	0.9	15.0	IR
	T5-2	100	6	0.04	65	120	15	Nitrogen	1.7	28.3	IR
	T5-3	100	6	0.04	65	140	15	Nitrogen	2.3	38.3	IR
	T5-4	100	6	0.04	65	160	15	Nitrogen	2.2	36.7	IR
	T5-5	100	6	0.04	65	170	15	Nitrogen	2.2	36.7	IR
	T5-6	100	6	0.04	65	180	15	Nitrogen	2	33.3	IR
	T5-7	100	6	0.04	65	200	15	Nitrogen	2	33.3	IR
T7-n	T6-1	100	6	0.04	75	100	15	Nitrogen	1	16.6	IR
	T6-2	100	6	0.04	75	120	15	Nitrogen	1.8	30.0	IR
	T6-3	100	6	0.04	75	140	15	Nitrogen	2.2	36.7	IR
	T6-4	100	6	0.04	75	160	15	Nitrogen	2.2	36.7	IR
	T6-5	100	6	0.04	75	170	15	Nitrogen	2.2	36.7	IR
	T6-6	100	6	0.04	75	180	15	Nitrogen	2.2	36.7	IR
	T6-7	100	6	0.04	75	200	15	Nitrogen	1.7	28.3	IR
S1-n	S1-1	100	6	0.04	50	160	10	Nitrogen	2.2	36.7	IR
	S1-2	100	6	0.04	65	160	10	Nitrogen	2.1	35.0	IR
	S1-3	100	6	0.04	75	160	10	Nitrogen	2	33.3	IR
	S1-4	100	6	0.04	85	160	10	Nitrogen	1.9	33.3	IR
S2-n	S2-1	100	12	0.02	50	160	10	Nitrogen	4	33.3	IR
	S2-2	100	12	0.02	65	160	10	Nitrogen	3.9	32.5	IR
	S2-3	100	12	0.02	75	160	10	Nitrogen	3.9	32.5	IR
	S2-4	100	12	0.02	85	160	10	Nitrogen	3.8	31.7	IR
S3-n	S3-1	100	12	0.03	40	170	15	'Air'	4.8	40.0	IR
	S3-2	100	12	0.03	50	170	15	'Air'	4.9	40.8	IR
	S3-3	100	12	0.03	60	170	15	'Air'	4.85	40.4	IR
	S3-4	100	12	0.03	70	170	15	'Air'	4.9	40.8	IR
	S3-5	100	12	0.03	80	170	15	'Air'	4.8	40.0	IR
	S3-6	100	12	0.03	100	170	15	'Air'	4.8	40.0	IR
S4-n	S4-1	100	12	0.03	40	170	15	Nitrogen	5.4	45.0	IR
	S4-2	100	12	0.03	50	170	15	Nitrogen	5.1	42.5	IR
	S4-3	100	12	0.03	60	170	15	Nitrogen	4.9	40.8	IR
	S4-4	100	12	0.03	70	170	15	Nitrogen	4.7	39.2	IR
	S4-5	100	12	0.03	80	170	15	Nitrogen	4.4	36.7	IR
	S4-6	100	12	0.03	100	170	15	Nitrogen	4.3	35.8	IR
t4-n	t4-1	100	15	0.02	65	150	2.5	Nitrogen	2	13.3	Tr
	t4-2	100	15	0.02	65	150	5	Nitrogen	3	20.0	Tr
	t4-3	100	15	0.02	65	150	10	Nitrogen	3.3	22.0	Tr
	t4-4	100	15	0.02	65	150	15	Nitrogen	3.8	25.3	Tr
t5-n	t5-1	100	15	0.02	65	170	2.5	Nitrogen	4	26.7	Tr
	t5-2	100	15	0.02	65	170	5	Nitrogen	4.1	27.3	Tr
	t5-3	100	15	0.02	65	170	10	Nitrogen	4.6	30.7	Tr
	t5-4	100	15	0.02	65	170	15	Nitrogen	4.8	32.0	Tr
t6-n	t6-1	100	6	0.02	65	150	5	Nitrogen	2.0	33.3	IR
	t6-2	100	6	0.02	65	150	10	Nitrogen	2.1	35.0	IR
	t6-3	100	6	0.02	65	150	15	Nitrogen	2.3	38.3	IR
	t6-4	100	6	0.02	65	150	20	Nitrogen	2.3	38.3	IR

Abreviation: T5-n, T6-n = NR+GMA+T-101 in different temperature; **S1-n,S2-n, S3-n, S4-n** = NR+GMA+T101 in different rotor speed; **t4-n, t5-n, t6-n** = NR+GMA+T-101 in different processing time; **phr** = per hundreds (weight) rubber; **mr** = molar ratio to GMA; **IR** = infra red measurement; **Tr** = Titration method; All samples (NR/GMA/T-101) were processed using method-1 **(M1)** (see Scheme 3-2).

Table B.3.2 (cont.) Chemical compositions and processing conditions for **NR/GMA/T-101** system and calculated grafting yields.

Sample Code		Processing Composition				Processing condition				Analysis		
		SMR-L (phr)	[GMA] (%)	[T101] (mr)		Rotor speed (rpm)	Oil Temp (°C)	Mixing Time (minutes)	Atmos-phere	Grafting Degree (%)	Grafting Effcn. (%)	method
G-n	G1	100	3	0.02		65	170	10	Nitrogen	0.9	30.0	Tr
	G2	100	6	0.02		65	170	10	Nitrogen	1.5	25.0	Tr
	G3	100	9	0.02		65	170	10	Nitrogen	2.9	32.2	Tr
	G4	100	12	0.02		65	170	10	Nitrogen	4.1	34.2	Tr
	G5	100	15	0.02		65	170	10	Nitrogen	4.6	30.1	Tr
	G6	100	18	0.02		65	170	10	Nitrogen	5	27.8	Tr
G1-n	G1-1	100	3	0.01		65	160	10	Nitrogen	0.4	13.3	IR
	G1-2	100	3	0.02		65	160	10	Nitrogen	0.7	23.3	T
	G1-3	100	3	0.03		65	160	10	Nitrogen	0.8	26.7	IR
	G1-4	100	3	0.04		65	160	10	Nitrogen	0.9	30.0	IR
	G1-5	100	3	0.05		65	160	10	Nitrogen	0.9	30.0	IR
	G1-6	100	3	0.10		65	160	10	Nitrogen	1.1	36.7	IR
G2-n	G2-1	100	6	0.01		65	160	10	Nitrogen	1.3	21.7	IR
	G2-2	100	6	0.02		65	160	10	Nitrogen	1.6	26.7	Tr
	G2-3	100	6	0.03		65	160	10	Nitrogen	2	33.3	IR
	G2-4	100	6	0.04		65	160	10	Nitrogen	2.2	36.7	IR
	G2-5	100	6	0.05		65	160	10	Nitrogen	2.5	41.7	IR
G3-n	G3-1	100	9	0.01		65	160	10	Nitrogen	2.1	23.3	IR
	G3-2	100	9	0.02		65	160	10	Nitrogen	2.7	30.0	Tr
	G3-3	100	9	0.03		65	160	10	Nitrogen	3.4	37.8	IR
	G3-4	100	9	0.04		65	160	10	Nitrogen	3.5	38.9	IR
	G3-5	100	9	0.05		65	160	10	Nitrogen	4	44.4	IR
G4-n	G4-1	100	12	0.01		65	160	10	Nitrogen	3.2	26.7	IR
	G4-2	100	12	0.02		65	160	10	Nitrogen	4.1	34.2	IR
	G4-3	100	12	0.03		65	160	10	Nitrogen	5.1	42.5	IR
G5-n	G5-1	100	15	0.01		65	160	10	Nitrogen	3.1	20.7	IR
	G5-2	100	15	0.02		65	160	10	Nitrogen	4.7	31.3	Tr
	G5-3	100	15	0.03		65	160	10	Nitrogen	6.4	42.7	IR
G6-n	G6-1	100	18	0.01		65	160	10	Nitrogen	5.9	32.7	IR
	G6-2	100	18	0.02		65	160	10	Nitrogen	6.8	37.8	Tr
	G6-3	100	18	0.03		65	160	10	Nitrogen	7.1	39.4	IR
2G1-n	2G1-1	100	12	0.01	0.02	75	160	15	Nitrogen	4	33.3	IR
	2G1-2	100	12	0.02	0.01	75	160	15	Nitrogen	4.1	34.2	IR
2G2-n	2G2-1	100	12	0.0075	0.0025	65	160	15	Nitrogen	3.5	29.2	IR
	2G2-2	100	12	0.015	0.005	65	160	15	Nitrogen	4.4	36.7	IR
	2G2-3	100	12	0.0225	0.0075	65	160	15	Nitrogen	5.2	43.3	IR
	2G2-4	100	12	0.03	0.01	65	160	15	Nitrogen	5.4	45.0	IR
3G1-n	3G1-1	100	12	0.01		65	160	15	Nitrogen	2.2	18.3	IR
	3G1-2	100	12	0.02		65	160	15	Nitrogen	2.8	23.3	IR
	3G1-3	100	12	0.03		65	160	15	Nitrogen	2.8	23.3	IR
4G1-n	4G1-1	100	12	0.01	0.02	75	160	15	Nitrogen	3.4	28.3	IR
	4G1-2	100	12	0.02	0.01	75	160	15	Nitrogen	3	25.0	IR
4G2-n	4G2-1	100	12	0.0025	0.0075	65	160	15	Nitrogen	1.8	15	IR
	4G2-2	100	12	0.005	0.015	65	160	15	Nitrogen	3.5	29.2	IR
	4G2-3	100	12	0.0075	0.0225	65	160	15	Nitrogen	3.7	30.8	IR
	4G2-4	100	12	0.01	0.03	65	160	15	Nitrogen	4.1	34.2	IR
4G3-n	4G3-1	100	3	0.005	0.015	65	160	15	Nitrogen	0.4	13.3	IR
	4G3-2	100	6	0.005	0.015	65	160	15	Nitrogen	1.3	21.7	IR
	4G3-3	100	10	0.005	0.015	65	160	15	Nitrogen	2.8	28.0	IR
	4G3-4	100	12	0.005	0.015	65	160	15	Nitrogen	3.5	29.2	IR
	4G3-5	100	15	0.005	0.015	65	160	15	Nitrogen	4.8	32.0	IR

Abreviation: Gn, G1-n, G2-n, G3-n, G4-n, G5-n, G6-n = NR+GMA+T101 in different [GMA] using addition seq.method-1 **(M1)** (see Scheme 3-2). ; **2G1-n, 2G2-n** = NR + GMA + T101 in different [GMA] using addition seq. method-2; **3G1-n** = NR + GMA + T101 in different [GMA] using addition seq. method-3; 4G1-n,4G2n, 4G3-n = NR + GMA + T101 in different [GMA] using addition seq. method-2; **phr** = part per hundreds (weight) rubber; **mr** = molar ratio to GMA; **IR** = infra red measurement; **Tr** = Titration method

Table B.3.3 Chemical compositions and processing conditions for **NR/GMA/BPO** system and calculated grafting yields.

Sample Code		PROCESSING COMPOSITION			PROCESSING CONDITION				ANALYSIS		
		SMR-L (phr)	GMA (phr)	BPO (mr)	Rotor speed (rpm)	Temp (°C)	Mixing Time (min.)	Atmos-phere	Grafting Degree (%)	Grafting Efficiency (%)	Method
B1-n	B1-1	100	6	0.01	65	120	15	Nitrogen	0.5	8.3	IR
	B1-2	100	6	0.02	65	120	15	Nitrogen	0.5	8.3	IR
B2-n	B2-1	100	6	0.01	65	140	15	Nitrogen	0.4	6.7	IR
	B2-2	100	6	0.02	65	140	15	Nitrogen	0.4	6.7	IR
	B2-3	100	6	0.03	65	140	15	Nitrogen	0.3	5.0	IR
	B2-4	100	6	0.04	65	140	15	Nitrogen	0.3	5.0	IR
	B2-5	100	6	0.05	65	140	15	Nitrogen	0.3	5.0	IR
	B2-6	100	6	0.1	65	140	15	Nitrogen	0.3	5.0	IR
B3-n	B3-1	100	6	0.01	65	160	15	Nitrogen	0.3	5.0	IR
	B3-2	100	6	0.02	65	160	15	Nitrogen	0.3	5.0	IR
	B3-3	100	6	0.03	65	160	15	Nitrogen	0.3	5.0	IR
	B3-4	100	6	0.04	65	160	15	Nitrogen	0.3	5.0	IR
	B3-5	100	6	0.05	65	160	15	Nitrogen	0.3	5.0	IR
	B3-6	100	6	0.1	65	160	15	Nitrogen	0.3	5.0	IR
B4-n	B4-1	100	3	0.03	65	140	15	Nitrogen	0.2	6.7	IR
	B4-2	100	6	0.03	65	140	15	Nitrogen	0.4	6.7	IR
	B4-3	100	9	0.03	65	140	15	Nitrogen	1.3	14.4	IR
	B4-4	100	12	0.03	65	140	15	Nitrogen	1.8	13.0	IR
	B4-5	100	15	0.03	65	140	15	Nitrogen	2.9	19.3	IR
	B4-6	100	18	0.03	65	140	15	Nitrogen	3.1	17.2	IR
B5-n	B5-1	100	9	0.04	65	140	15	Nitrogen	1.3	14.4	IR
	B5-2	100	12	0.04	65	140	15	Nitrogen	1.9	15.8	IR

Notes: * All (NR/GMA/BPO) samples were processed using method-1
phr = per hundreds (weight) rubber; **mr** = molar ratio to GMA; **IR** = FTIR (Calibration Curve) method

Table B.3.4 Chemical compositions and processing conditions for **NR/GMA/DCP** system and calculated grafting yields.

Sample Code		PROCESSING COMPOSITION			PROCESSING CONDITION				ANALYSIS		
		SMR-L (phr)	GMA (phr)	[DCP] (mr)	Rotor speed (rpm)	Temp (°C)	Mixing Time (min.)	Atmos-phere	Grafting Degree (%)	Grafting Efficiency (%)	Method
D1-n	D1-1	100	6	0.04	65	120	15	Nitrogen	1.2	20.0	IR
	D1-2	100	6	0.04	65	140	15	Nitrogen	1.2	20.0	IR
	D1-3	100	6	0.04	65	160	15	Nitrogen	1.6	23.3	IR
	D1-4	100	6	0.04	65	180	15	Nitrogen	1.1	18.3	IR
	D1-5	100	6	0.04	65	200	15	Nitrogen	1.0	16.6	IR
D2-n	D2-1	100	6	0.01	65	160	15	Nitrogen	0.6	10	IR
	D2-2	100	6	0.02	65	160	15	Nitrogen	0.8	13.3	IR
	D2-3	100	6	0.03	65	160	15	Nitrogen	1.2	20.0	IR
	D2-4	100	6	0.04	65	160	15	Nitrogen	1.2	20.0	IR
	D2-5	100	6	0.05	65	160	15	Nitrogen	1.4	23.3	IR
	D2-6	100	6	0.10	65	160	15	Nitrogen	2.1	35.0	IR
D3-n	D3-1	100	3	0.03	65	160	15	Nitrogen	0.4	13.3	IR
	D3-2	100	6	0.03	65	160	15	Nitrogen	1.2	20.0	IR
	D3-3	100	9	0.03	65	160	15	Nitrogen	2.0	22.2	IR
	D3-4	100	12	0.03	65	160	15	Nitrogen	3.4	28.3	IR
	D3-5	100	15	0.03	65	160	15	Nitrogen	4.8	32.0	IR
	D3-6	100	18	0.03	65	160	15	Nitrogen	6.2	34.4	IR

Notes: * All samples were processed using method-1
phr = per hundreds (weight) rubber; **mr** = molar ratio to GMA; **IR** = FTIR (Calibration Curve) method

Table B.3.5 Chemical compositions and processing conditions for **NR/GMA/T-29B90** system and calculated grafting yields.

Sample Code		PROCESSING COMPOSITION			PROCESSING CONDITION				ANALYSIS	
		SMR-L (phr)	GMA (phr)	T-29B90 (mr)	Rotor speed (rpm)	Temp (°C)	Mixing Time (min.)	Atmosphere	Grafting Degree (%)	Gel (%)
G29-n	G29-1	100	6	0.002	65	150	15	Nitrogen	3.2	48
	G29-2	100	6	0.002	65	160	15	Nitrogen	2.2	47
	G29-3	100	6	0.002	65	170	15	Nitrogen	1.6	47
	G29-4	100	6	0.002	65	180	15	Nitrogen	1.6	46
	G29-5	100	6	0.002	65	200	15	Nitrogen	1.6	45

Notes: * All (NR/GMA/T-29B90) samples were processed using method-1
phr = per hundreds (weight) rubber; **mr** = molar ratio to GMA

Table B.3.6 Chemical compositions and processing conditions for **NR/GMA/TRIS/T-101** system and calculated grafting yields and % gel.

Sample Code		PROCESSING COMPOSITION					PROCESSING CONDITION				ANALYSIS		
		NR (phr)	GMA (%)	TRIS		T-101 mr	Rotor speed (rpm)	Temp (°C)	Mixing Time (min.)	Atmos-phere	Grafting Degree (%)	Method	Gel (%)
				wr	mr								
GT1-n	GT1-0	100	9	0	0	0.002	60	170	15	Nitrogen	0.7	Tr	2
	GT1-1	100	9	1:9	0.005	0.002	60	170	15	Nitrogen	2.7	Tr	66
	GT1-2	100	8	2:8	0.01	0.002	60	170	15	Nitrogen	4.3	Tr	76
	GT1-3	100	7	3:7	0.02	0.002	60	170	15	Nitrogen	3.9	Tr	80
GT2-n	GT2-0	100	9	0	0	0.01	65	170	15	Nitrogen	2.3	Tr	49
	GT2-1	100	9	1:9	0.005	0.01	65	170	15	Nitrogen	3.4	Tr	94
	GT2-2	100	8	2:8	0.01	0.01	65	170	15	Nitrogen	5.1	Tr	98
	GT2-3	100	7	3:7	0.02	0.01	65	170	15	Nitrogen	4.8	Tr	98
	GT2-4	100	6	4:7	0.03	0.01	65	170	15	Nitrogen	2.6	Tr	99
GT3-n	GT3-1	100	9	1:9	0.005	0.01	65	170	15	Nitrogen	3.4	Tr	94
	GT3-2	100	9	1:9	0.005	0.02	65	170	15	Nitrogen	3.4	Tr	96
	GT3-3	100	9	1:9	0.005	0.03	65	170	15	Nitrogen	3.4	Tr	97

Notes: * All (NR/GMA/TRIS/T-101) samples were processed using method-1 (addition of GMA+TRIS+T101 at t=2min **phr** = per hundreds (weight) rubber; wr= weight ratio to GMA; **mr** = molar ratio to GMA(+TRIS); T = Titration method

Table B.3.7 Chemical compositions and processing conditions for **NR/GMA/TRIS/T-101** in the presence and absence of coagent TRIS system and calculated grafting yields and % gel.

Sample Code	PROCESSING COMPOSITION					PROCESSING CONDITION				ANALYSIS	
	NR (phr)	GMA (%)	TRIS		T-101 mr	Rotor speed (rpm)	Temp (°C)	Mixing Time (min.)	Atmos-phere	Grafting Degree (%)	Gel (%)
			wr	mr							
C1-2	100	-	-	-	-	65	160	15	Air	-	1
G6-02	100	6	-	-	0.002	60	160	15	Air	0.7(Tr)	0.8
G6-2	100	6	-	-	0.02	60	160	15	Air	1.5 (Tr)	59
GT91-1	100	9	1:9	0.005	0.01	60	160	15	Air	3.4 (Tr)	96
GT91-3	100	9	1:9	0.005	0.03	60	160	15	Air	3.4 (Tr)	96
GT82-1	100	8	2:8	0.01	0.01	60	160	15	Air	3.3 (Tr)	96

Notes: * All (NR/GMA/TRIS/T-101) samples were processed using method-1 (addition of GMA+TRIS+T101at t=2min) **phr** = per hundreds (weight) rubber; wr = weight ratio to GMA; **mr** = molar ratio of T-101 to GMA +TRIS; **Tr** = Titration method

Appendix-C

Table C.4.1 The experimental Composition and Conditions and Result of PP/GMA **(Thermal Initiation)** System.

CODE		COMPOSITION				PROCESSING CONDITION			ANALYSIS RESULT				
		PP (phr)	GMA (%)	T-101		Temp. (°C)	Rotor speed (rpm)	Time (min)	Graft GMA (%)	Free-GMA (%)	Poly-GMA (%)	Method	MFI (g/10min)
				phr	mr								
PP1		100	-	-	-	180	65	10	-	-	-		2
PP2		100	-	0.03	-	180	65	10	-	-	-		2
PP3		100	-	0.03	-	200	65	10	-	-	-		2
PP4		100	-	0.03	-	220	65	10	-	-	-		2
T1-n	T1-1	88	12	0	0	160	65	10	0.04	-	-	Tr	2.1
	T1-2	88	12	0	0	180	65	10	0.1	-	-	Tr	2.1
	T1-3	88	12	0	0	200	65	10	0.1	-	-	Tr	2.1
	T1-4	88	12	0	0	220	65	10	0.1	-	-	Tr	2.1
T2-n	T2-1	88	12	0	0	180	65	2	0.12	1.2	0.04	IR	2.1
	T2-2	88	12	0	0	180	65	5	0.13	1.2	0.1	IR	2.1
	T2-3	88	12	0	0	180	65	7	0.16	1.3	0.12	IR	2.1
	T2-4	88	12	0	0	180	65	10	0.14	1.1	0.1	IR	2.1

Notes: Total weight of samples = 35 gr; phr = per hundreds resin; mr = molar ratio to GMA; MFI = Melt Flow Index
IR = measured from FTIR and calibration curves.

Table C.4.2 The experimental Composition and Result of **PP/GMA/T101** System

CODE		COMPOSITION				PROCESSING CONDITION			RESULTS/ANALYSIS				
		PP (%)	GMA (%)	T-101		Temp. (°C)	Rotor speed (rpm)	Time (min)	g-GMA (%)	f-GMA (%)	p-GMA (%)	Method	MFI (g/10min)
				phr	mr								
G1-n	G1-1	88	12	0.03	0.001	160	65	10	0.8	0.5	0.1	IR	5.4
	G1-2	88	12	0.03	0.001	180	65	10	0.3	1.2	0.8	IR	3.9
	G1-3	88	12	0.03	0.001	200	65	10	0.2	1.5	1.7	IR	3.8
G2-n	G2-1	88	12	0.15	0.005	160	65	10	2.0	0.4	3.6	IR	7
	G2-2	88	12	0.15	0.005	170	65	10	0.8	0.5	1.9	IR	6.5
	G2-3	88	12	0.15	0.005	180	65	10	0.7	0.5	1.5	IR	6.3
	G2-4	88	12	0.15	0.005	190	65	10	0.6	1.0	1.5	IR	6
	G2-5	88	12	0.15	0.005	200	65	10	0.2	1.7	1	IR	6
G3-n	G3-1	88	12	0.3	0.01	160	65	10	1.2	0.1	3.2	IR	12
	G3-2	88	12	0.3	0.01	180	65	10	0.7	1.9	2	IR	10
	G3-3	88	12	0.3	0.01	200	65	10	0.3	5.1	1.6	IR	8.8
G4-n	G4-1	100	9	0.3	0.016	120	65	10	2.0	-	-	Tr	-
	G4-2	100	9	0.3	0.016	130	65	10	1.9	-	-	Tr	-
	G4-3	100	9	0.3	0.016	140	65	10	1.8	-	-	Tr	-
	G4-4	100	9	0.3	0.016	150	65	10	1.6	-	-	Tr	-
	G4-5	100	9	0.3	0.016	160	65	10	0.9	-	-	Tr	-
	G4-6	100	9	0.3	0.016	180	65	10	0.9	-	-	Tr	-
	G4-7	100	9	0.3	0.016	200	65	10	0.7	-	-	Tr	-
G5-n	G5-1	88	12	0.03	0.001	180	65	10	0.4	2.4	1.6	IR	3.7
	G5-2	88	12	0.06	0.002	180	65	10	0.9	2.6	1.6	IR	4.4
	G5-3	88	12	0.15	0.005	180	65	10	0.9	2.6	2.8	IR	6.8
	G5-4	88	12	0.3	0.01	180	65	10	0.8	3.1	2.8	IR	10.7
G6-n	G6-1	100	6	0.075	0.005	180	65	10	0.3	-	0.2	Tr	5
	G6-2	100	6	0.15	0.01	180	65	10	0.5	-	0.5	Tr	7.7
	G6-3	100	6	0.3	0.02	180	65	10	0.6	-	0.6	Tr	11.1
G7-n	G7-1	100	9	0.1	0.005	180	65	10	0.8	-	-	Tr	-
	G7-2	100	9	0.3	0.02	180	65	10	1.7	-	-	Tr	-
	G7-3	100	9	0.5	0.03	180	65	10	2.3	-	-	Tr	-
	G7-4	100	9	0.7	0.04	180	65	10	2.7	-	-	Tr	-
	G7-5	100	9	1.0	0.05	180	65	10	2.4	-	-	Tr	-
G8-n	G8-1	98	2	0.02	0.005	180	65	10	0.2	0.5	0	IR	2.8
	G8-2	96	4	0.04	0.005	180	65	10	0.3	0.5	0	IR	3.2
	G8-3	94	6	0.06	0.005	180	65	10	0.5	0.7	0.1	IR	4.2
	G8-4	92	8	0.08	0.005	180	65	10	0.8	1.5	0.4	IR	5.8
	G8-5	90	10	0.11	0.005	180	65	10	1.0	1.5	0.6	IR	6.6
	G8-6	88	12	0.14	0.005	180	65	10	1.2	2.5	1.1	IR	6.8
	G8-7	88	18	0.19	0.005	180	65	10	2.0	3	6.1	IR	8.1
G9-n	G9-1	100	3	0.3	0.05	180	65	10	0.7	-	-	Tr	-
	G9-2	100	6	0.3	0.024	180	65	10	1.2	-	-	Tr	-
	G9-3	100	9	0.3	0.016	180	65	10	1.5	-	-	Tr	-
	G9-4	100	12	0.3	0.012	180	65	10	1.6	-	-	Tr	-
	G9-5	100	15	0.3	0.008	180	65	10	1.6	-	-	Tr	-
	G9-6	100	18	0.3	0.004	180	65	10	1.7	-	-	Tr	-
G10-n	G10-1	88	12	0.14	0.005	180	65	2	1.1	2.8	3.4	IR	6.6
	G10-2	88	12	0.14	0.005	180	65	5	1.2	2.1	3.2	IR	6.5
	G10-3	88	12	0.14	0.005	180	65	7	1.8	2	2.6	IR	6.1
	G10-4	88	12	0.14	0.005	180	65	10	1.8	0.6	2.6	IR	6.2
G11-n	G11-1	100	9	0.18	0.01	180	65	2	0.1	-	0.7	Tr	10.6
	G11-2	100	9	0.18	0.01	180	65	5	0.4	-	0.8	Tr	10.5
	G11-3	100	9	0.18	0.01	180	65	7	0.5	-	0.8	Tr	10.2
	G11-4	100	9	0.18	0.01	180	65	10	0.7	-	0.8	Tr	10.1
G12-n	G12-1	100	9	0.3	0.016	180	65	2	0.5	-	-	Tr	-
	G12-2	100	9	0.3	0.016	180	65	5	0.7	-	-	Tr	-
	G12-3	100	9	0.3	0.016	180	65	10	1.1	-	-	Tr	-
	G12-4	100	9	0.3	0.016	180	65	20	1.2	-	-	Tr	-
	G12-5	100	9	0.3	0.016	180	65	20	1.0	-	-	Tr	-

Notes: Total weight of samples = 35 gr; phr = per hundreds resin; mr = molar ratio to GMA; MFI = Melt Flow Index
IR = measured from FTIR and calibration curves; Tr = measured of grafted GMA by titration.

Table C.4.3 The experimental Composition and Result of **PP/GMA/T-29B90** system.

CODE		COMPOSITION				PROCESSING CONDITION			ANALYSIS RESULTS				
		PP (%)	GMA (%)	T-29B90		Temp. (°C)	Rotor speed (rpm)	Time (min)	Grafted-GMA (%)	Free-GMA (%)	Poly-GMA (%)	Method	MFI (g/10min)
				phr	mr								
G13-n	G13-1	88	12	0.14	0.005	160	65	10	2.1	1.5	2.9	IR	3
	G13-2	88	12	0.14	0.005	170	65	10	1.7	1.9	2.4	IR	3
	G13-3	88	12	0.14	0.005	180	65	10	0.8	3.2	1.5	IR	3.2
	G13-4	88	12	0.14	0.005	190	65	10	0.3	3.6	1.6	IR	3.6
	G13-5	88	12	0.14	0.005	200	65	10	0.2	4	1.6	IR	3.6
G14-n	G14-1	88	12	0.3	0.01	160	65	10	1.7	3.7	2.9	IR	3.8
	G14-2	88	12	0.3	0.01	180	65	10	0.4	3.3	3.4	IR	3.6
	G14-3	88	12	0.3	0.01	200	65	10	0.3	4.2	1.7	IR	3.4
G15-n	G15-1	100	9	0.3	0.015	160	65	10	1.3	-	-	Tr	-
	G15-2	100	9	0.3	0.015	180	65	10	0.4	-	-	Tr	-
	G15-3	100	9	0.3	0.015	200	65	10	0.2	-	-	Tr	-
G16-n	G16-1	88	12	0.03	0.001	160	65	10	1.4	2.6	2	IR	2.8
	G16-2	88	12	0.06	0.002	160	65	10	1.2	3.1	2.4	IR	2.8
	G16-3	88	12	0.14	0.005	160	65	10	1.2	3.5	2	IR	2.8
	G16-4	88	12	0.28	0.01	160	65	10	1.2	4.5	2	IR	3.2
G17-n	G17-1	98	2	0.02	0.005	160	65	10	0.2	0.1	0.1	IR	2.1
	G17-2	96	4	0.04	0.005	160	65	10	0.4	0.2	0.2	IR	2.3
	G17-3	94	6	0.07	0.005	160	65	10	0.7	0.2	0.8	IR	2.5
	G17-4	92	8	0.09	0.005	160	65	10	1.0	0.5	1	IR	2.9
	G17-5	90	10	0.12	0.005	160	65	10	1.3	0.7	1.8	IR	2.8
	G17-6	88	12	0.14	0.005	160	65	10	1.7	0.9	2.6	IR	2.8
	G17-7	82	18	0.23	0.005	160	65	10	2.9	2.6	7	IR	2.8

Notes:
Total weight of samples = 35 gr; **phr** = per hundreds of resin; **wr** = weight ratio to GMA; **mr** = molar ratio to GMA+DVB;
IR = measured of GMA content by FTIR and calibration curves; Tr = measured of grafted GMA by titration.

Table C.4.4 The experimental Composition and Result of **PP/GMA/TRIS/T-101** system

CODE		COMPOSITION						PROCESS. CONDTN			ANALYSIS RESULT				
		PP (%)	GMA (%)	TRIS		T-101		Temp (°C)	Rotor speed (rpm)	Time (min)	Graft-GMA (%)	Free GMA (%)	Poly-GMA (%)	Method	MFI (g/10min)
				phr	wr	phr	mr								
GT 1-n	GT1-1	100	12	3.5	2/8	0.16	0.005						0.4	Tr	4
	GT1-2	100	12	3.5	2/8	0.16	0.005	180	65	10	3.3	0.5	0.3	Tr	3.7
	GT1-3	100	12	3.5	2/8	0.16	0.005	200	65	10	2.1	1.7	0.1	Tr	3.3
GT 2-n	GT2-1	100	9	1.0	1/9	0.1	0.005	180	65	10	1.4	-	-	Tr	-
	GT2-2	100	9	1.0	1/9	0.2	0.01	180	65	10	2.2	-	-	Tr	-
	GT2-3	100	9	1.0	1/9	0.4	0.02	180	65	10	3.0	-	-	Tr	-
	GT2-4	100	9	1.0	1/9	0.6	0.03	180	65	10	3.4	-	-	Tr	-
	GT2-5	100	9	1.0	1/9	0.9	0.05	180	65	10	4.4	-	-	Tr	-
GT 3-n	GT3-1	100	3	0.3	1/9	0.032	0.005	180	65	10	0.4	-	-	Tr	3.2
	GT3-2	100	6	0.6	1/9	0.064	0.005	180	65	10	0.8	-	-	Tr	3.2
	GT3-3	100	9	1.0	1/9	0.097	0.005	180	65	10	1.4	-	-	Tr	3.1
	GT3-4	100	12	1.3	1/9	0.137	0.005	180	65	10	1.8	-	-	Tr	3.0
GT 4-n	GT4-1	100	3	0.3	1/9	0.13	0.02	180	65	10	1.5	-	-	Tr	3.3
	GT4-2	100	6	0.6	1/9	0.25	0.02	180	65	10	2.8	-	-	Tr	5.1
	GT4-3	100	9	1.0	1/9	0.38	0.02	180	65	10	3.1	-	-	Tr	7.3
	GT4-4	100	12	1.3	1/9	0.50	0.02	180	65	10	4.2	-	-	Tr	7.5
	GT4-5	100	15	1.6	1/9	0.63	0.02	180	65	10	4.5	-	-	Tr	7.7
	GT4-6	100	18	1.9	1/9	0.75	0.02	180	65	10	4.5	-	-	Tr	11.4
GT 5-n	GT5-1	98	2	0.5	2/8	0.13	0.005	180	65	10	1.5	1.2	0	Tr	2.1
	GT5-2	96	4	1.1	2/8	0.14	0.005	180	65	10	2.6	1.4	0	Tr	2.2
	GT5-3	94	6	1.6	2/8	0.15	0.005	180	65	10	4.6	1.6	0.1	Tr	2.6
	GT5-4	92	8	2.2	2/8	0.16	0.005	180	65	10	4.9	2.2	0.1	Tr	2.8
	GT5-5	90	10	2.8	2/8	0.17	0.005	180	65	10	5.4	2.5	0.2	Tr	3
	GT5-6	88	12	3.4	2/8	0.18	0.005	180	65	10	6.3	3.0	0.3	Tr	3.8
	GT5-7	82	18	5.5	2/8	0.21	0.005	180	65	10	8.4	5.0	0.3	Tr	3.9
GT 6-n	GT6-1	100	12	1.6	1/9	0.3	0.01	180	65	10	2.2	1.9	0.2	Tr	7.1
	GT6-2	100	12	3.6	2/8	0.33	0.01	180	65	10	3.6	2	0	Tr	5.6
	GT6-3	100	12	6.4	3/7	0.44	0.01	180	65	10	5.0	2.6	0	Tr	5.3
	GT6-3	100	12	10.3	4/6	0.54	0.01	180	65	10	5.8	2.1	0	Tr	4
GT 7-n	GT7-1	100	3	0.344	1/9	0.194	0.03	180	65	10	0.5	0.1		Tr	9.5
	GT7-2	100	3	0.750	2/8	0.206	0.03	180	65	10	0.6	0.1		Tr	9.0
	GT7-3	100	3	1.281	3/7	0.222	0.03	180	65	10	0.6	0.1		Tr	8.4
GT 8-n	GT8-2	100	6	0.7	1/9	0.064	0.005	180	65	10	1.8	-	-	Tr	4.0
	GT8-3	100	6	1.5	2/8	0.069	0.005	180	65	10	2.2	-	-	Tr	3.3
	GT8-4	100	6	2.6	3/7	0.074	0.005	180	65	10	2.7	-	-	Tr	2.5
GT 9-n	GT9-1	100	6	0.7	1/9	0.129	0.01	180	65	10	2.2	0.2		Tr	5.4
	GT9-2	100	6	1.5	2/8	0.138	0.01	180	65	10	1.8	0.1		Tr	3.8
	GT9-3	100	6	2.6	3/7	0.150	0.01	180	65	10	1.8	0.1		Tr	3.8
GT 10-n	GT10-1	100	6	0.7	1/9	0.256	0.02	180	65	10	2.6	0.2		Tr	10.5
	GT10-2	100	6	1.5	2/8	0.278	0.02	180	65	10	2.2	0.1		Tr	9.5
	GT10-3	100	6	2.6	3/7	0.300	0.02	180	65	10	2.2	0.1		Tr	9.5
GT 11-n	GT11-1	100	9	1	1/9	0.097	0.005	180	65	10	2.8	0.1		Tr	3.1
	GT11-2	100	9	2.2	2/8	0.103	0.005	180	65	10	2.6	0.2		Tr	2.6
	GT11-3	100	9	3.7	3/7	0.113	0.005	180	65	10	2.8	0.2		Tr	2.2
GT 12-n	GT12-1	100	9	1	1/9	0.4	0.02	180	65	10	3.1	-	-	Tr	14
	GT12-2	100	9	2.2	2/8	0.42	0.02	180	65	10	3.1	-	-	Tr	13
	GT12-3	100	9	3.7	3/7	0.45	0.02	180	65	10	3.2	-	-	Tr	12
GT 13-n	GT13-1	88	12	1.3	1/9	0.15	0.005	180	65	10	1.7	-	-	Tr	4.1
	GT13-2	88	12	2.9	2/8	0.16	0.005	180	65	10	2.8	-	-	Tr	3.1
	GT13-3	88	12	5.0	3/7	0.17	0.005	180	65	10	3.6	-	-	Tr	2.5
GT 14-n	GT14-1	100	9	1.0	1/9	0.2	0.01	180	65	2	0.7	-	0.6	Tr	5.9
	GT14-2	100	9	1.0	1/9	0.2	0.01	180	65	5	1.1	-	0.24	Tr	6.3
	GT14-3	100	9	1.0	1/9	0.2	0.01	180	65	7	1.4	-	0.1	Tr	6.3
	GT14-4	100	9	1.0	1/9	0.2	0.01	180	65	10	1.4	-	0.1	Tr	6.4
GT 15-n	GT15-1	88	12	3.5	2/8	0.16	0.005	180	65	2	5.2	1.6	0.2	Tr	3.9
	GT15-2	88	12	3.5	2/8	0.16	0.005	180	65	5	5.9	1.2	0.4	Tr	3.8
	GT15-3	88	12	3.5	2/8	0.16	0.005	180	65	7	5.9	1.2	0.6	Tr	3.8
	GT15-4	88	12	3.5	2/8	0.16	0.005	180	65	10	6	1.2	0.6	Tr	3.8

Notes: Total weight of samples = 35 gr; phr = per hundreds resin; wr = weight ratio to GMA; mr = molar ratio to GMA+DVB;
IR = measured from FTIR and calibration curves; Tr = measured of grafted GMA by titration.

Table C.4.5 The experimental Composition and Result of **PP/GMA/DVB/T-101** System

CODE		COMPOSITION						PROCESSING CONDITION			ANALYSIS RESULT				
		PP (%)	GMA (%)	DVB		T-101		Temp. (°C)	Rotor speed (rpm)	Time (min)	Graft GMA (%)	Free-GMA (%)	Poly-GMA (%)	Method	MFI (g/10min)
				phr	wr	phr	mr								
GV-M1		88	12	3.4	2/8	0.18	0.005	180	65	10	7.6		0.1	IR	-
GV-M2		88	12	3.4	2/8	0.18	0.005	180	65	10	8.5		0	IR	-
GV-M3		88	12	3.4	2/8	0.18	0.005	180	65	10	5.7		0	IR	-
GV-M4		88	12	3.4	2/8	0.18	0.005	180	65	10	5.9		0	IR	-
GV-M5		88	12	3.4	2/8	0.18	0.005	180	65	10	7		0	IR	-
GV-M6		88	12	3.4	2/8	0.18	0.005	180	65	10	7.6		0.1	IR	-
GV1-n	GV1-1	88	12	3.4	2/8	0.18	0.005	160	65	10	7	1.7	0	IR	3.3
	GV1-2	88	12	3.4	2/8	0.18	0.005	180	65	10	4.7	1.8	0.1	IR	1.9
	GV1-3	88	12	3.4	2/8	0.18	0.005	200	65	10	2.6	2.1	0.1	IR	1.8
GV2-n	GV2-1	88	12	3.5	2/8	0.04	0.001	180	65	10	6.3	0.6	0.1	IR	2
	GV2-2	88	12	3.5	2/8	0.07	0.002	180	65	10	5.2	1	0.1	IR	1.8
	GV2-3	88	12	3.5	2/8	0.18	0.005	180	65	10	4.8	1.6	0.2	IR	1.8
	GV2-4	88	12	3.5	2/8	0.37	0.01	180	65	10	4.6	2	0.2	IR	1
GV3-n	GV3-1	100	9	1	1/9	0.3	0.016	140	65	10	4.4	-	-	Tr	-
	GV3-2	100	9	1	1/9	0.5	0.026	140	65	10	4.5	-	-	Tr	-
	GV3-3	100	9	1	1/9	0.7	0.038	140	65	10	5.2	-	-	Tr	-
	GV3-4	100	9	1	1/9	1	0.054	140	65	10	5.2	-	-	Tr	-
GV4-n	GV4-1	98	2	0.5	2/8	0.13	0.005	180	65	10	0.7	0.5	0.1	IR	1.9
	GV4-2	96	4	1.1	2/8	0.14	0.005	180	65	10	2.2	0.9	0.1	IR	1.8
	GV4-3	94	6	1.6	2/8	0.15	0.005	180	65	10	3.6	1.5	0.2	IR	1.8
	GV4-4	92	8	2.2	2/8	0.16	0.005	180	65	10	4.1	1.8	0.2	IR	1.6
	GV4-5	90	10	2.8	2/8	0.17	0.005	180	65	10	5.5	3.1	0.3	IR	1.3
	GV4-6	82	12	3.4	2/8	0.18	0.005	180	65	10	5.8	3.1	0.3	IR	1.1
	GV4-7	82	18	5.5	2/8	0.21	0.005	180	65	10	7.3	6.8	0.3	IR	0.8
GV5-n	GV5-1	100	9	3.0	1/3	0.3	0.016	180	65	10	4.4	-	-	Tr	-
	GV5-2	100	9	6.0	2/3	0.3	0.016	180	65	10	4.6	-	-	Tr	-
	GV5-3	100	9	9.0	3/3	0.3	0.016	180	65	10	4.6	-	-	Tr	-
	GV5-4	100	9	18	6/3	0.3	0.016	180	65	10	4.2	-	-	Tr	-
GV6-n	GV6-1	100	9	1	1/9	0.3	0.016	180	65	10	1.7	-	-	Tr	-
	GV6-2	100	9	2.25	2/8	0.3	0.016	180	65	10	2.4	-	-	Tr	-
	GV6-3	100	9	3.9	3/7	0.3	0.016	180	65	10	2.9	-	-	Tr	-
	GV6-4	100	9	6	4/6	0.3	0.016	180	65	10	4.2	-	-	Tr	-
GV7-n	GV7-1	88	12	1.6	1/9	0.32	0.01	180	65	10	2.9	2	0.3	IR	4.1
	GV7-2	88	12	3.5	2/8	0.37	0.01	180	65	10	4.6	2.5	0	IR	2.5
	GV7-3	88	12	6.1	3/7	0.42	0.01	180	65	10	5.5	2.1	0	IR	1.6
	GV7-4	88	12	9.4	4/6	0.50	0.01	180	65	10	6.3	1.7	0	IR	1.0
GV8-n	GV8-1	88	12	3.5	2/8	0.18	0.005	180	65	2	3.2	4	0.15	IR	0.4
	GV8-2	88	12	3.5	2/8	0.18	0.005	180	65	5	6.1	2	0	IR	0.4
	GV8-3	88	12	3.5	2/8	0.18	0.005	180	65	7	7.8	1.5	0	IR	0.5
	GV8-4	88	12	3.5	2/8	0.18	0.005	180	65	10	7.5	1.3	0	IR	0.5

Notes: Total weight of samples = 35 gr; phr = per hundreds resin; wr = weight ratio to GMA; mr = molar ratio to GMA+DVB;
IR = measured from FTIR and calibration curves; T = measured of grafted GMA by titration

Table C.4.6 The experimental Composition and Result of **PP/GMA/DVB/T-29B90** System

CODE		COMPOSITION						PROCESSING CONDITION			ANALYSIS RESULTS				
		PP (%)	GMA (%)	DVB		T-29B90		Temp. (°C)	Rotor speed (rpm)	Time (min)	Grafting Degree (%)	Free-GMA (%)	Poly-GMA (%)	Method	MFI (g/10min)
				phr	wr	phr	mr								
GV 9-n	GV9-1	88	12	3.4	2/8	0.18	0.005						0.1	IR	0.8
	GV9-2	88	12	3.4	2/8	0.18	0.005	180	65	10	1.6	0.9	0.3	IR	0.9
	GV9-3	88	12	3.4	2/8	0.18	0.005	200	65	10	1.1	0.8	0.3	IR	1.6
GV 10-n	GV10-1	88	12	3.4	2/8	0.04	0.001	160	65	10	6.9	1	0	IR	1.6
	GV10-2	88	12	3.4	2/8	0.08	0.002	160	65	10	5.2	1	0	IR	1.2
	GV10-3	88	12	3.4	2/8	0.2	0.005	160	65	10	3.8	1.2	0.1	IR	1
	GV10-4	88	12	3.4	2/8	0.4	0.01	160	65	10	3.2	1.5	0.4	IR	1
GV 11-n	GV11-1	100	12	1.4	1/9	0.3	0.004	160	65	10	6.5	-	-	Tr	-
	GV11-2	100	12	1.4	1/9	0.5	0.019	160	65	10	6.6	-	-	Tr	-
	GV11-3	100	12	1.4	1/9	0.7	0.027	160	65	10	6.8	-	-	Tr	-
	GV11-4	100	12	1.4	1/9	1	0.038	160	65	10	6.9	-	-	Tr	-
GV 12-n	GV12-1	87	12	1.6	1/9	0.3	0.01	160	65	10	2.6	1.6	0	Tr	2.4
	GV12-2	85	12	3.5	2/8	0.4	0.01	160	65	10	3.2	1.4	0.5	Tr	1.4
	GV12-3	83	12	6.3	3/7	0.5	0.01	160	65	10	2.5	1.3	1.1	Tr	0.4
	GV12-4	80	12	10	4/6	0.6	0.01	160	65	10	1.9	1.1	0	Tr	0.4
GV 13-n	GV13-1	87	12	1.6	1/9	0.16	0.005	170	65	10	2.2	-	0	IR	3.5
	GV13-2	85	12	3.5	2/8	0.18	0.005	170	65	10	3.2	-	0	IR	3.3
	GV13-3	83	12	6.3	3/7	0.22	0.005	170	65	10	4.0	-	0.1	IR	2.3
	GV13-4	80	12	10	4/6	0.26	0.005	170	65	10	4.0	-	0.1	IR	1.7
GV 14-n	GV14-1	88	12	3.4	2/8	0.18	0.005	180	65	2	2.7	-	0	IR	
	GV14-2	88	12	3.4	2/8	0.18	0.005	180	65	5	3.9	-	0	IR	-
	GV14-3	88	12	3.4	2/8	0.18	0.005	180	65	7	4.5	-	0	IR	-
	GV14-4	88	12	3.4	2/8	0.18	0.005	180	65	10	4.6	-	0	IR	-

Notes: Total weight of samples = 35 gr; phr = per hundreds resin; wr = weight ratio to GMA; mr = molar ratio to GMA+DVB;
IR = measured from FTIR and calibration curves.

Table C.4.7 The experimental Composition and Result of **PP/GMA/DVB/DCP** System.

CODE		COMPOSITION						PROCESSING CONDITION			ANALYSIS RESULTS				
		PP (%)	GMA (%)	DVB		DCP		Temp. (°C)	Rotor speed (rpm)	Time (min)	Grafting Degree (%)	Free-GMA (%)	Poly-GMA (%)	Method	MFI (g/10min)
				phr	wr	phr	mr								
GV 15-n	GV15-1	88	12	3.4	2/8	0.18	0.005						0	IR	1.8
	GV15-2	88	12	3.4	2/8	0.18	0.005	180	65	10	4.5	0.7	0.3	IR	1.3
	GV15-3	88	12	3.4	2/8	0.18	0.005	200	65	10	2.5	0.9	0.3	IR	1.3
GV 16-n	GV16-1	88	12	3.4	2/8	0.02	0.001	180	65	10	7.6	1.1	0	IR	1.5
	GV16-2	88	12	3.4	2/8	0.18	0.005	180	65	10	4.5	1	0.3	IR	1.2
	GV16-3	88	12	3.4	2/8	0.24	0.01	180	65	10	4.1	1.8	0.2	IR	1

Notes: Total weight of samples = 35 gr; phr = per hundreds resin; wr = weight ratio to GMA; mr = molar ratio to GMA+DVB;
IR = measured from FTIR and calibration curves.

Table C.4.8 The experimental Composition and Result of **PP/GMA/DVB/BPO** System.

CODE		COMPOSITION						PROCESSING CONDITION			ANALYSIS RESULTS				
		PP (%)	GMA (%)	DVB		T-101		Temp. (°C)	Rotor speed (rpm)	Time (min)	Graft-GMA (%)	Free-GMA (%)	Poly-GMA (%)	Methods	MFI (g/10min)
				phr	wr	phr	mr								
GV 17-n	GV17-1	88	12	3.4	2/8	0.18	0.005	160	65	10	2.2	0.7	0	IR	1.6
	GV17-2	88	12	3.4	2/8	0.18	0.005	180	65	10	1.2	0.6	0	IR	1.6
	GV17-3	88	12	3.4	2/8	0.18	0.005	200	65	10	0.7	0.3	1	IR	1.7
GV 18-n	GV18-1	88	12	3.4	2/8	0.03	0.001	160	65	10	5.3	-	-	IR	3
	GV18-2	88	12	3.4	2/8	0.16	0.005	160	65	10	2.3	-	-	IR	1.7
	GV18-3	88	12	3.4	2/8	0.3	0.01	160	65	10	2.2	-	-	IR	1.1

Notes: Total weight of samples = 35 gr; phr = per hundreds resin; wr = weight ratio to GMA; mr = molar ratio to GMA+DVB;
IR = measured from FTIR and calibration curves.

Table C.4.9 Major absorbtion bands and probable assignment in the FTIR spectra of poly- GMA, poly-TRIS, poly-DVB, GMA-co-TRIS, and GMA-co-DVB (cont.).

Name	Figure	Peak(cm^{-1})	Intensity	Assignment
Poly GMA	Fig. 2.10 & Fig. 4.1	3001	Medium	$\upsilon(CH_2,CH_3)$
		2958	medium	$\upsilon(CH_2,CH_3)$
		1732	very strong	υ(>C=O)
		1486	Medium	$\delta(CH_3)$, $\delta(CH_2)$
		1450	medium	$\delta(CH_3)$, $\delta(CH_2)$
		1389	Weak	$\delta(CH_3)$, δ(CH), $\tau(CH_2)$
		1342	weak	$\delta(CH_3)$, δ(CH), $\tau(CH_2)$
		1259	broad & strong	δ(CH), $\tau(CH_2)$, $\rho(CH_3)$
		1172	strong	δ(C-O)
		1150	strong	$\upsilon(C\text{-}C)_b$, $\upsilon(C\text{-}CH_3)$, δ(CH), $\rho(CH_3)$
		993	Medium	$\rho(CH_3)$, δ(CH), $\omega(CH_2)$
		907	Medium	υ(epoxy ring)
		847	Medium	$\rho(CH_2)$, $\upsilon(C\text{-}C)_b$, $\upsilon(C\text{-}CH_3)_b$, $\rho(CH_3)$
		759	medium	υ(epoxy ring)
Poly TRIS	Fig. 2.11 & Fig. 4.2	2968	medium	$\upsilon(CH_2,CH_3)$
		1740	strong	υ(>C=O)
		1461	medium	$\delta(CH_3)$, $\delta(CH_2)$
		1390	medium	$\delta(CH_3)$, δ(CH), $\tau(CH_2)$
		1251	medium	$\upsilon(C\text{-}CH_3)$,
		1158	strong	δ(C-O-C)
		986	medium	$\rho(CH_3)$
		809	weak	$\rho(C\text{-}CH_3)$, υ(C-C)
Poly DVB	Fig.2.12 & Fig. 4.3	1720	weak	-
		1629	medium	υ(C=C) Aromatic ring
		1601	medium	υ(C=C) Aromatic ring
		1510	medium	δ(CH)Ar para substitution
		1485	medium	δ(CH)Ar, $\delta(CH_2)$
		1462	strong	$\delta(CH_3)$ asym, $\delta(CH_2)$
		1441	strong	$\delta(CH_3)$ asym
		1387	medium	$\delta(CH_3)$
		1369	strong	$\delta(CH_3)$
		1229	strong	$\rho(CH_3)$
		1183	strong	$\rho(CH_3)$
		991	medium	$\rho(CH_3)$, υ(C-C)
		950	medium	$\rho(CH_3)$, υ(C-C)
		905	medium	$\rho(CH_3)$, $\rho(CH_2)$, δ(CH)
		840	medium	$\rho(CH_2)$, υ(C-C), $\upsilon(C\text{-}CH_3)$, $\rho(CH_3)$
		798	medium	$\rho(CH_2)$, δ(CH), υ(C-C)Ar
		708	strong	υ(CH)Ar
		592	medium	$\varpi(CH_2)$
		480	medium	$\varpi(CH_2)$
		459	medium	$\varpi(CH_2)$

Abreviation: δ = bending or deformation , υ = stretching, ρ = rocking, τ = twisting or scissoring , ϖ = wagging

Table C.4.9 (cont.) Major absorbtion bands and probable assignment in the FTIR spectra of poly- GMA, poly-TRIS, poly-DVB, GMA-co-TRIS, and GMA-co-DVB.

Name	Figure	Peak (cm^{-1})	Intensity	Assignment
GMA-co-TRIS	Fig. 2.13 & Fig. 4.4	2967	medium	$\upsilon(CH_2,CH_3)$
		1734	very strong	υ(>C=O)
		1459	medium	$\delta(CH_3)$, $\delta(CH_2)$
		1390	medium	$\delta(CH_3)$, δ(CH), $\tau(CH_2)$
		1252	strong	δ(C-O)
		1158	very strong	υ(C-C)$_a$, $\upsilon(C\text{-}CH_3)$, δ(CH), $\rho(CH_3)$
		1057	medium	$\delta(CH_3)$, δ(CH), $\tau(CH_2)$
		1033	sharp-medium	δ(CH), $\tau(CH_2)$, $\rho(CH_3)$
		993	medium	δ(C-O)
		909	medium	υ(epoxy ring)
		848	medium	υ(epoxy ring)
		760	medium	υ(epoxy ring)
GMA-co-DVB	Fig. 2.14 & Fig. 4.5	2942	medium	$\upsilon(CH_2,CH_3)$
		1727	strong	υ(>C=O)
		1603	weak	$\delta(CH_3)$, $\delta(CH_2)$
		1509	weak	$\delta(CH_3)$, δ(CH), $\tau(CH_2)$
		1450	medium	δ(CH), $\tau(CH_2)$, $\rho(CH_3)$
		1386	weak	$\delta(CH_3)$, δ(CH), $\tau(CH_2)$
		1253	medium	δ(C-O)
		1175	strong	υ(C-C), $\upsilon(C\text{-}CH_3)$, δ(CH), $\rho(CH_3)$
		1124	strong	δ(C-O-C)
		995	medium	δ(C-O)
		908	medium	υ(epoxy ring)
		842	medium	υ(epoxy ring)
		799	medium	υ(C-C)Ar
		761	medium	υ(epoxy ring)
		712	medium	$\rho(CH_2)$, υ(C-C), $\upsilon(C\text{-}CH_3)$
Abreviation: δ = bending or deformation , υ = stretching, ρ = rocking, τ = twisting or scissoring , ϖ = wagging				

Appendix D

Table D5.1 The experimental Composition and Result **PP/MA (Thermal Initiation)**

CODE	COMPOSITION				PROCESSING CONDITION			ANALYSIS RESULT		
	PP (%)	MA (%)	T-101		Temp. (°C)	Rotor speed (rpm)	Time (min)	g-MA (%)	Method	MFI (g/10min)
			phr	mr						
PP-1	100 (E)	-	-	-	180	65	10	-	IR	2.1
PP-2	100 (E)	-	0.02	-	180	65	10	-	IR	22.5
T1-1	100 (E)	8	-	-	140	65	10	0	IR	2
T1-2	100 (E)	8	-	-	160	65	10	0.025	IR	2.02
T1-3	100 (E)	8	-	-	180	65	10	0.040	IR	2.05
T1-4	100 (E)	8	-	-	200	65	10	0.045	IR	2.05
T2-1	100 (I)	8	-	-	140	65	10	-	-	-
T2-2	100 (I)	8	-	-	160	65	10	0.01	IR	1.8
T2-3	100 (I)	8	-	-	180	65	10	0.03	IR	1.8
T2-4	100 (I)	8	-	-	200	65	10	0.04	IR	1.8

Notes: **Total weight of samples = 35 gr; E = PP-Elf (granular); (I) = PP-ICI (powder); phr = per hundreds resin; MFI = Melt Flow Index IR = measured from FTIR and calibration curves.**

Table D5.2 The experimental Composition and Result **PP/DVB or TRIS/T-101 system**

CODE	COMPOSITION				PROCESSING CONDITION			MFI (g/10min)
	PP (%)	DVB or TRIS (%)	T-101		Temp. (°C)	Rotor speed (rpm)	Time (min)	
			phr	mr				
Tris042	100	Tris (6%)	0.07	0.005	180	65	10	3.7
DVB042	100	DVB (6%)	0.04	0.005	180	65	10	1.0

Notes: **Total weight of samples = 35 gr; phr = per hundreds resin; mr = molar ratio to MA; MFI = Melt Flow Index IR = measured from FTIR and calibration curves.**

Table D5.3 The experimental Composition and Result of **PP/MA/T-101** system.

CODE	COMPOSITION				PROCESSING CONDITION			RESULTS/ANALYSIS				
	PP (%)	MA (%)	T-101		Temp. (°C)	Rotor speed (rpm)	Time (min)	t-MA	g-MA (%)	Grafting Efficiency (%)	MFI (g/10min)	Method
			phr	mr								
M1-1	100 (E)	8	0.12	0.005	**140**	65	10	-	0.2	**2.5**	**2**	FTIR
M1-2	100 (E)	8	0.12	0.005	**160**	65	10	-	0.3	**3.8**	**2.2**	FTIR
M1-3	100 (E)	8	0.12	0.005	**170**	65	10	-	-		**3**	FTIR
M1-4	100 (E)	8	0.12	0.005	**180**	65	10	-	0.6	**7.5**	**3.5**	FTIR
M1-5	100 (E)	8	0.12	0.005	**190**	65	10	-	-		**4.3**	FTIR
M1-6	100 (E)	8	0.12	0.005	**200**	65	10	-	0.58	**7.3**	**6.5**	FTIR
M2-1	100 (I)	8	0.12	0.005	**160**	65	10	-	0.53	6.6	**1.3**	FTIR
M2-2	100 (I)	8	0.12	0.005	**170**	65	10	-	-		**1.5**	FTIR
M2-3	100 (I)	8	0.12	0.005	**180**	65	10	-	0.63	7.9	**1.6**	FTIR
M2-4	100 (I)	8	0.12	0.005	**190**	65	10	-	0.63	7.9	**2.5**	FTIR
M2-5	100 (I)	8	0.12	0.005	**200**	65	10	-	0.7	8.7	**5.5**	FTIR
M3-1	100 (I)	8	0.12	0.005	180	65	**2**	-	0.3	3.7	-	FTIR
M3-2	100 (I)	8	0.12	0.005	180	65	**5**	-	0.42	5.2	-	FTIR
M3-3	100 (I)	8	0.12	0.005	180	65	**7**	-	0.66	8.3	-	FTIR
M3-4	100 (I)	8	0.12	0.005	180	65	**10**	-	0.6	7.5	-	FTIR
M4-1	100 (E)	8	0.024	**0.001**	180	65	10	0.33	0.24	3	-	FTIR
M4-2	100 (E)	8	0.048	**0.002**	180	65	10	0.66	0.36	4.5	-	FTIR
M4-3	100 (E)	8	0.12	**0.005**	180	65	10	0.99	0.68	8.5	-	FTIR
M4-4	100 (E)	8	0.24	**0.01**	180	65	10	1.32	0.99	16.5	-	FTIR
M4-5	100 (E)	8	0.48	**0.02**	180	65	10	2.37	1.68	21	-	FTIR
M5-1	100 (E)	**2**	0.01	0.002	180	65	10	-	0.2	2.5	-	FTIR
M5-2	100 (E)	**4**	0.02	0.002	180	65	10	-	0.3	3.7	-	FTIR
M5-3	100 (E)	**6**	0.03	0.002	180	65	10	-	0.3	3.7	-	FTIR
M5-4	100 (E)	**8**	0.04	0.002	180	65	10	-	0.4	5	-	FTIR
M5-5	100 (E)	**10**	0.05	0.002	180	65	10	-	0.4	5	-	FTIR
M5-6	100 (E)	**12**	0.06	0.002	180	65	10	-	0.4	5	-	FTIR
M5-7	100 (E)	**18**	0.09	0.002	180	65	10	-	0.5	5	-	FTIR
M6-1	100 (E)	**2**	0.03	0.005	180	65	10	-	0.3	3.7	2.5	FTIR
M6-2	100 (E)	**4**	0.06	0.005	180	65	10	-	0.4	5	2.6	FTIR
M6-3	100 (E)	**6**	0.08	0.005	180	65	10	-	0.6	7.5	3.2	FTIR
M6-4	100 (E)	**8**	0.12	0.005	180	65	10	-	0.65	8.1	5.5	FTIR
M6-5	100 (E)	**10**	0.14	0.005	180	65	10	-	0.7	8.7	7.1	FTIR
M6-6	100 (E)	**12**	0.17	0.005	180	65	10	-	0.8	10	8.5	FTIR
M6-7	100 (E)	**18**	0.26	0.005	180	65	10	-	0.9	11	13.8	FTIR

Notes: Total weight of samples = 35 gr; **Abbreviation** : E = PP-Elf (granular); I = PP-ICI (powder); phr = per hundreds resin; mr = molar ratio
MFI = Melt Flow Index **IR** = measured from FTIR and calibration curves; **Tr** = titration; **t-MA** = total-MA (unpurified samples); **g-MA** = grafted-MA; **f-MA** = free-MA (unreacted MA

Table D5.3 (cont.) The experimental Composition and Result of **PP/MA/T-101** system

CODE	COMPOSITION				PROCESSING CONDITION			RESULTS/ANALYSIS				
	PP (%)	MA (%)	T-101		Temp. (°C)	Rotor speed (rpm)	Time (min)	t-MA	g-MA (%)	f-MA	MFI (g/10min)	Method
			phr	mr								
M7-1	100 (I)	2	0.03	0.005	160	60	10	0.3	0.2	-	-	FTIR
M7-2	100 (I)	4	0.06	0.005	160	60	10	0.65	0.4	-	-	FTIR
M7-3	100 (I)	6	0.08	0.005	160	60	10	1.35	0.7	-	-	FTIR
M7-4	100 (I)	8	0.11	0.005	160	60	10	1.52	0.76	-	-	FTIR
M7-5	100 (I)	10	0.14	0.005	160	60	10	1.6	0.8	-	-	FTIR
M7-6	100 (I)	12	0.17	0.005	160	60	10	1.65	0.84	-	-	FTIR
M7-7	100 (I)	18	0.26	0.005	160	60	10	1.3	0.9	-	-	FTIR
M8-1	100 (I) (A)	2	0.03	0.005	160	60	10	0.3	0.2	-	-	FTIR
M8-2	100 (I) (A)	4	0.06	0.005	160	60	10	0.66	0.3	-	-	FTIR
M8-3	100 (I) (A)	6	0.08	0.005	160	60	10	1.4	0.35	-	-	FTIR
M8-4	100 (I) (A)	8	0.11	0.005	160	60	10	1.58	0.48	-	-	FTIR
M8-5	100 (I) (A)	10	0.14	0.005	160	60	10	1.78	0.59	-	-	FTIR
M8-6	100 (I) (A)	12	0.17	0.005	160	60	10	1.9	0.7	-	-	FTIR
M8-7	100 (I) (A)	18	0.26	0.005	160	60	10	1.76	0.79	-	-	FTIR
M9-1	100 (I) (A)	1	0.5	0.170	200	60	10	0.45	0.43	0.02	-	FTIR
M9-2	100 (I) (A)	2	0.5	0.083	200	60	10	0.8	0.75	0.05	-	FTIR
M9-3	100 (I) (A)	4	0.5	0.041	200	60	10	1.55	1.05	0.5	-	FTIR
M9-4	100 (I) (A)	6	0.5	0.026	200	60	10	1.9	1.3	1.1	-	FTIR
M9-5	100 (I) (A)	8	0.5	0.019	200	60	10	2.1	1.2	1.4	-	FTIR
M9-6	100 (I) (A)	10	0.5	0.015	200	60	10	2.5	0.65	1.87	-	FTIR
M9-7	100 (I) (A)	12	0.5	0.012	200	60	10	3.3	0.55	2.75	-	FTIR

Notes: Total weight of samples = 35 gr; **Abbreviation :** E = PP-Elf (granular); I = PP-ICI (powder); phr = per hundreds resin; mr = molar ratio
MFI = Melt Flow Index **IR** = measured from FTIR and calibration curves; **Tr** = titration; **t-MA** = total-MA (unpurified samples); **g-MA** = grafted-MA; **f-MA** = free-MA (unreacted MA

Table D5.4 The experimental Composition and Result of **PP/MA/T-29B90** system.

CODE	COMPOSITION				PROCESSING CONDITION			RESULTS/ANALYSIS				
	PP (%)	MA (%)	T-101		Temp. (°C)	Rotor speed (rpm)	Time (min)	t-MA	g-MA (%)	f-MA	MFI (g/10min)	Method
			phr	mr								
M14-1	100 (E)	8	0.1	0.005	**140**	65	10	-	0.15	-	-	FTIR
M14-2	100 (E)	8	0.1	0.005	**160**	65	10	-	0.14	-	**2.9**	FTIR
M14-3	100 (E)	8	0.1	0.005	**170**	65	10	-		-	**3.2**	FTIR
M14-4	100 (E)	8	0.1	0.005	**180**	65	10	-	0.13	-	**3.4**	FTIR
M14-5	100 (E)	8	0.1	0.005	**190**	65	10	-		-	**3.5**	FTIR
M14-6	100 (E)	8	0.1	0.005	**200**	65	10	-	0.12	-	**3.6**	FTIR
M15-1	100 (I)	8	0.1	0.005	**160**	65	10	-	0.22	-	**1.06**	FTIR
M15-2	100 (I)	8	0.1	0.005	**170**	65	10	-	-	-	**1.08**	FTIR
M15-3	100 (I)	8	0.1	0.005	**180**	65	10	-	0.18	-	**1.12**	FTIR
M15-4	100 (I)	8	0.1	0.005	**190**	65	10	-	-	-	**1.22**	FTIR
M15-5	100 (I)	8	0.1	0.005	**200**	65	10	-	0.14	-	**1.54**	FTIR
M16-1	100 (E)	8	0.024	**0.001**	180	65	10	0.43	0.18	0.25	-	FTIR
M16-2	100 (E)	8	0.048	**0.002**	180	65	10	0.36	0.14	0.18	-	FTIR
M16-3	100 (E)	8	0.12	**0.005**	180	65	10	0.32	0.15	0.17	-	FTIR
M16-4	100 (E)	8	0.24	**0.01**	180	65	10	0.31	0.14	0.17	-	FTIR
M17-1	100 (E)	**2**	0.03	0.005	160	60	10	-	0.14	-	-	FTIR
M17-2	100 (E)	**4**	0.06	0.005	160	60	10	-	0.14	-	-	FTIR
M17-3	100 (E)	**6**	0.08	0.005	160	60	10	-	0.14	-	-	FTIR
M17-4	100 (E)	**8**	0.11	0.005	160	60	10	-	0.14	-	-	FTIR
M17-5	100 (E)	**10**	0.14	0.005	160	60	10	-	0.14	-	-	FTIR
M17-6	100 (E)	**12**	0.17	0.005	160	60	10	-	0.14	-	-	FTIR
M17-7	100 (E)	**18**	0.20	0.005	160	60	10	-	0.14	-	-	FTIR

Notes: Total weight of samples = 35 gr; **Abbreviation :** E = PP-Elf (granular); I = PP-ICI (powder); phr = per hundreds resin; mr = molar ratio
MFI = Melt Flow Index **IR** = measured from FTIR and calibration curves; **Tr** = titration; **t-MA** = total-MA (unpurified samples); **g-MA** = grafted-MA; **f-MA** = free-MA (unreacted MA

Table D5.5 The experimental Composition and Result of **PP/MA/DVB/T-101** system.

CODE	COMPOSITION						PROCESSING CONDITION			RESULTS/ANALYSIS		
	PP (%)	MA (%)	DVB		T-101		Temp. (°C)	Rotor speed (rpm)	Time (min)	g-GMA (%)	MFI (g/10min)	Method
			phr	wr	phr	mr						
M10-1	100 (E)	8	2	2/8	0.14	0.005	160	65	10	1.8	1.8	FTIR
M10-2	100 (E)	8	2	2/8	0.14	0.005	180	65	10	3.4	4.2	FTIR
M10-3	100 (E)	8	2	2/8	0.14	0.005	200	65	10	3.2	8.5	FTIR
M10-1	100 (E)	8	2	2/8	0.03	0.001	180	65	10	3.3	-	FTIR
M10-2	100 (E)	8	2	2/8	0.06	0.002	180	65	10	3.5	1.5	FTIR
M10-3	100 (E)	8	2	2/8	0.14	0.005	180	65	10	3.6	1.1	FTIR
M10-4	100 (E)	8	2	2/8	0.28	0.01	180	65	10	3.8	1.1	FTIR
M11-1	100 (E)	2	0.5	2/8	0.14	0.005	180	65	10	0.9	2.2	FTIR
M11-2	100 (E)	4	1	2/8	0.14	0.005	180	65	10	1.8	1.4	FTIR
M11-3	100 (E)	6	1.5	2/8	0.14	0.005	180	65	10	2.4	1.1	FTIR
M11-4	100 (E)	8	2	2/8	0.14	0.005	180	65	10	3	1.1	FTIR
M11-5	100 (E)	10	2.5	2/8	0.14	0.005	180	65	10	3.7	1.1	FTIR
M11-6	100 (E)	12	3	2/8	0.14	0.005	180	65	10	4.7	1.1	FTIR
M11-7	100 (E)	18	4.5	2/8	0.14	0.005	180	65	10	-	1.9	FTIR

Notes: Total weight of samples = 35 gr; **Abbreviation :** **E** = PP-Elf (granular); I = PP-ICI (powder); phr = per hundreds resin; mr = molar ratio
MFI = Melt Flow Index **IR** = measured from FTIR and calibration curves; **Tr** = titration; **t-MA** = total-MA (unpurified samples); **g-MA** = grafted-MA; **f-MA** = free-MA (unreacted MA

Table D5.6 The experimental Composition and Result of **PP/MA/TRIS/T-101** system.

CODE	COMPOSITION						PROCESSING CONDITION			RESULTS/ANALYSIS		
	PP (%)	MA (%)	TRIS		T-101		Temp. (°C)	Rotor speed (rpm)	Time (min)	g-GMA (%)	MFI (g/10min)	Method
			phr	wr	phr	mr						
M12-1	100 (E)	8	2	2/8	0.14	0.001	180	65	10	1	-	FTIR
M12-2	100 (E)	8	2	2/8	0.14	0.002	180	65	10	1.7	1.5	FTIR
M12-3	100 (E)	8	2	2/8	0.14	0.005	180	65	10	1.8	2.7	FTIR
M12-4	100 (E)	8	2	2/8	0.14	0.01	180	65	10	1.9	2.9	FTIR
M13-1	100 (E)	2	0.5	2/8	0.14	0.005	180	65	10	0.8	2.3	FTIR
M13-2	100 (E)	4	1	2/8	0.14	0.005	180	65	10	1	2.5	FTIR
M13-3	100 (E)	6	1.5	2/8	0.14	0.005	180	65	10	1.4	2.6	FTIR
M13-4	100 (E)	8	2	2/8	0.14	0.005	180	65	10	1.9	3.4	FTIR
M13-5	100 (E)	10	2.5	2/8	0.14	0.005	180	65	10	2	4.2	FTIR
M13-6	100 (E)	12	3	2/8	0.14	0.005	180	65	10	2	5.5	FTIR
M13-7	100 (E)	18	4.5	2/8	0.14	0.005	180	65	10	-	8.8	FTIR

Notes: Total weight of samples = 35 gr; **Abbreviation :** **E** = PP-Elf (granular); I = PP-ICI (powder); phr = per hundreds resin; mr = molar ratio
MFI = Melt Flow Index **IR** = measured from FTIR and calibration curves; **Tr** = titration; **t-MA** = total-MA (unpurified samples); **g-MA** = grafted-MA; **f-MA** = free-MA (unreacted MA

Table D5.7 The experimental Composition and Result of **PP/MA/DVB/T-29B90** system.

CODE	COMPOSITION						PROCESSING CONDITION			RESULTS/ANALYSIS		
	PP (%)	MA (%)	DVB		T-29B90		Temp. (°C)	Rotor speed (rpm)	Time (min)	g-GMA (%)	MFI (g/10min)	Method
			phr	wr	phr	mr						
M18-1	100 (E)	8	2	2/8	0.14	0.005	160	65	10	1.1	2.2	FTIR
M18-2	100 (E)	8	2	2/8	0.14	0.005	180	65	10	1	2.2	FTIR
M18-3	100 (E)	8	2	2/8	0.14	0.005	200	65	10	0.8	3.9	FTIR
M19-1	100 (E)	8	2	2/8	0.14	0.001	180	65	10	0.9	-	FTIR
M19-2	100 (E)	8	2	2/8	0.14	0.002	180	65	10	1.1	-	FTIR
M19-3	100 (E)	8	2	2/8	0.14	0.005	180	65	10	1.5	-	FTIR
M19-4	100 (E)	8	2	2/8	0.14	0.01	180	65	10	1.3	-	FTIR
M20-1	100 (E)	2	0.5	2/8	0.14	0.005	180	65	10	0.1	-	FTIR
M20-2	100 (E)	4	1	2/8	0.14	0.005	180	65	10	0.8	-	FTIR
M20-3	100 (E)	6	1.5	2/8	0.14	0.005	180	65	10	1.2	-	FTIR
M20-4	100 (E)	8	2	2/8	0.14	0.005	180	65	10	1.5	-	FTIR
M20-5	100 (E)	10	2.5	2/8	0.14	0.005	180	65	10	1.7	-	FTIR
M20-6	100 (E)	12	3	2/8	0.14	0.005	180	65	10	1.9	-	FTIR
M20-7	100 (E)	18	4.5	2/8	0.14	0.005	180	65	10	-	-	FTIR

Notes: Total weight of samples = 35 gr; **Abbreviation :** **E** = PP-Elf (granular); I = PP-ICI (powder); phr = per hundreds resin; mr = molar ratio
MFI = Melt Flow Index **IR** = measured from FTIR and calibration curves; **Tr** = titration; **t-MA** = total-MA (unpurified samples); **g-MA** = grafted-MA; **f-MA** = free-MA (unreacted MA

Table D5.8 The experimental Composition and Result of **PP/MA/TRIS/T-29B90** system.

CODE	COMPOSITION						PROCESSING CONDITION			RESULTS/ANALYSIS		
	PP (%)	MA (%)	TRIS		T-29B90		Temp. (°C)	Rotor speed (rpm)	Time (min)	g-GMA (%)	MFI (g/10min)	Method
			phr	wr	phr	mr						
M21-1	100 (E)	8	2	2/8	0.14	0.001	180	65	10	0.1	-	FTIR
M21-2	100 (E)	8	2	2/8	0.14	0.002	180	65	10	0.2	-	FTIR
M21-3	100 (E)	8	2	2/8	0.14	0.005	180	65	10	0.4	-	FTIR
M21-4	100 (E)	8	2	2/8	0.14	0.01	180	65	10	0.2	-	FTIR
M22-1	100 (E)	2	0.5	2/8	0.14	0.005	180	65	10	0.1	-	FTIR
M22-2	100 (E)	4	1	2/8	0.14	0.005	180	65	10	0.3	-	FTIR
M22-3	100 (E)	6	1.5	2/8	0.14	0.005	180	65	10	0.5	-	FTIR
M22-4	100 (E)	8	2	2/8	0.14	0.005	180	65	10	0.5	-	FTIR
M22-5	100 (E)	10	2.5	2/8	0.14	0.005	180	65	10	0.5	-	FTIR
M22-6	100 (E)	12	3	2/8	0.14	0.005	180	65	10	0.6	-	FTIR
M22-7	100 (E)	18	4.5	2/8	0.14	0.005	180	65	10	-	-	FTIR

Notes: Total weight of samples = 35 gr; **Abbreviation :** **E** = PP-Elf (granular); I = PP-ICI (powder); phr = per hundreds resin; mr = molar ratio
MFI = Melt Flow Index **IR** = measured from FTIR and calibration curves; **Tr** = titration; **t-MA** = total-MA (unpurified samples); **g-MA** = grafted-MA; **f-MA** = free-MA (unreacted MA

Table D5.9 The experimental Composition and Result of **PP/MA/DVB/DCP** system.

CODE	COMPOSITION						PROCESSING CONDITION			RESULTS/ANALYSIS		
	PP (%)	MA (%)	DVB		DCP		Temp. (°C)	Rotor speed (rpm)	Time (min)	g-GMA (%)	MFI (g/10min)	Method
			phr	wr	phr	mr						
M23-1	100 (E)	8	2	8	0.14	0.005	160	65	10	1.8	1.5	FTIR
M23-2	100 (E)	8	2	8	0.14	0.005	180	65	10	1.4	3.5	FTIR
M23-3	100 (E)	8	2	8	0.14	0.005	200	65	10	0.8	3.8	FTIR

Notes: Total weight of samples = 35 gr; **Abbreviation :** **E** = PP-Elf (granular); **I** = PP-ICI (powder); phr = per hundreds resin; mr = molar ratio
MFI = Melt Flow Index **IR** = measured from FTIR and calibration curves; **Tr** = titration; **t-MA** = total-MA (unpurified samples); **g-MA** = grafted-MA; **f-MA** = free-MA (unreacted MA

Table D5.10 The experimental Composition and Result of **PP/MA/DVB/BPO** system.

CODE	COMPOSITION						PROCESSING CONDITION			RESULTS/ANALYSIS		
	PP (%)	MA (%)	DVB		T-101		Temp. (°C)	Rotor speed (rpm)	Time (min)	g-GMA (%)	MFI (g/10min)	Method
			phr	wr	phr	mr						
M24-1	100 (E)	8	2	8	0.14	0.005	160	65	10	0.5	1.7	FTIR
M24-2	100 (E)	8	2	8	0.14	0.005	180	65	10	0.4	2	FTIR
M24-3	100 (E)	8	2	8	0.14	0.005	200	65	10	0.3	2.3	FTIR

Notes: Total weight of samples = 35 gr; **Abbreviation :** **E** = PP-Elf (granular); **I** = PP-ICI (powder); phr = per hundreds resin; mr = molar ratio
MFI = Melt Flow Index **IR** = measured from FTIR and calibration curves; **Tr** = titration; **t-MA** = total-MA (unpurified samples); **g-MA** = grafted-MA; **f-MA** = free-MA (unreacted MA

Table D5.11 FTIR assignment MA-co-TRIS and MA-co-DVB

Name	Figure	Peak (cm^{-1})	Intensity	Assignment
MA-co-TRIS	Fig. 2.32 & Fig. 5.1	2971	medium	$\upsilon(CH_2,CH_3)$
		1860	medium	υ(>C=O)
		1782	strong	υ(>C=O)
		1733	very strong	υ(>C=O)
		1459	medium	$\delta(CH_3)$, δ(CH), $\tau(CH_2)$
		1391	medium	$\upsilon(C\text{-}CH_3)$, $\rho(CH_3)$
		1167	very strong	δ(C-O)
		1058	medium	δ(CH), $\tau(CH_2)$, $\rho(CH_3)$
		1033	small	δ(C-O)
		943	strong	υ(anhydride)
		780	small	υ(anhydride)
MA-co-DVB	Fig. 2.33 & Fig. 5.2	2956	medium	$\upsilon(CH_2,CH_3)$
		1858	strong	υ(>C=O)
		1777	weak	υ(>C=O)
		1724	weak	υ(>C=O)
		1624	medium	$\upsilon(C=C)_{phenyl}$
		1450	weak	$\delta(CH_3)$, δ(CH), $\tau(CH_2)$
		1223	medium	δ(C-O)
		1082	strong	υ(C-C), $\upsilon(C\text{-}CH_3)$, δ(CH), $\rho(CH_3)$
		926	strong	δ(C-O-C)
		804	medium	δ(C-O)
		713	medium	υ(anhydride)

Abreviation:
δ = bending or deformation , υ = stretching, ρ = rocking, τ = twisting or scissoring , ϖ = wagging